e-ISSN 2544-1361

European Journal of Clinical and Experimental Medicine

Formerly: Medical Review

Quarterly

Vol. 24, No. 1

Publication date: March 2026

Rzeszów University Press
Poland 2026

Technical development, layout and interior design: Wojciech Pączek Cover design: Wiesław Grzegorczyk

ICV 2024: 120.59
MNiSW: 20.00

Indexing:
ARIANTA – Science and branch Polish electronic journals
ASCI – Asian Science Citation Index, Bielefeld Academic Search Engine
The Central European Journal of Social Sciences and Humanities (CEJSH)
Central Medical Library (Poland), Crossref, The Directory of Open Access Journals (DOAJ)
EBSCO, Free Medical Journals
Harvard Libraries – University of California Libraries
Index Copernicus, J-Gate
Main Medical Library in Warszawa
Ministry of Education and Science
MOST WIEDZY, POL-Index, Research4Life
SCImago Journal & Country Rank
Scopus

e-ISSN 2544-1361

EDITORIAL CORRESPONDENCE
European Journal of Clinical and Experimental Medicine Editorial Office
ul. Kopisto 2A, 35-959 Rzeszów, Poland
tel. +48 17 851 68 38, fax +48 17 872 19 30
http://www.ejcem.ur.edu.pl
e-mail: ejcemur@gmail.com, ejcem@ur.edu.pl
https://mc04.manuscriptcentral.com/pmur

PUBLISHER: RZESZÓW UNIVERSITY PRESS
ul. prof. S. Pigonia 6, 35-959 Rzeszów, Poland
tel./fax +48 17 872 14 26, e-mail: rup@ur.edu.pl, wydawnictwo@ur.edu.pl

Rzeszów University Press 2026
ISSN 2544-1361 (online)

http://www.ejcem.ur.edu.pl
European Journal of Clinical and Experimental Medicine
Eur J Clin Exp Med 2026; 24 (1): 4–5

Contents

Rzeszów University Press 2026
ISSN 2544-1361 (online)
doi: 10.15584/ejcem.2026.1.2

http://www.ejcem.ur.edu.pl
European Journal of Clinical and Experimental Medicine
Eur J Clin Exp Med 2026; 24 (1): 6–14

ORIGINAL PAPER

Associations between antenatal booking body mass index and postnatal placental weight: maternal health implications in HIV-positive and HIV-negative pregnant women in Uyo, Akwa Ibom State, Nigeria

Uchechukwu Brian Eziagu [1], Mumini Wemimo Rasheed [2], Ikwo Jonathan Kudamnya [1], Chinedu Onwuka Ndukwe [3], Ntiense Macaulay Utuk [4], Oyedele Oyewumi Ajayi [1], Evelyn Osemhen Eziagu [5], Eberechukwu Desmond Eziagu [6], Emmanuela Ifunanya Akpu [7], Chibuike Innocent Okafor [1]

[1] Department of Histopathology, University of Uyo Teaching Hospital, Uyo, Akwa Ibom State, Nigeria
[2] Department of Anatomic Pathology, Federal University Dutse, Dutse, Jigawa State, Nigeria
[3] Department of Anatomic Pathology and Forensic Medicine, Nnamdi Azikiwe University, Awka, Nnewi, Anambra State, Nigeria
[4] Department of Obstetrics and Gynaecology, University of Uyo Teaching Hospital (UUTH), Uyo, Akwa Ibom State, Nigeria
[5] Department of Mental Health, University of Uyo Teaching Hospital, Uyo, Akwa Ibom State, Nigeria
[6] Department of Family Medicine, University of Uyo Teaching Hospital, Uyo, Akwa Ibom State, Nigeria
[7] Department of Nursing Sciences, Enugu State University of Science and Technology, Enugu, Enugu State, Nigeria

ABSTRACT

Introduction and aim. Maternal body mass index (BMI) and placental weight are important indicators of maternal-fetal health, and their relationship may be influenced by HIV status. This study examined the association between antenatal booking BMI and postnatal placental weight among HIV-positive and HIV-negative pregnant women in Uyo, Nigeria.

Material and methods. We conducted a retrospective comparative cross-sectional study based on medical records review of 143 women (48 HIV-positive, 95 HIV-negative) who attended antenatal care and delivered at the University of Uyo Teaching Hospital between December 2015 and May 2016. BMI was calculated from early pregnancy weight and height measured at the first antenatal visit; whole placental weight was measured post-delivery. Linear regression, adjusted for gestational age, evaluated associations between BMI, HIV status, and placental weight.

Results. Among 143 participants (48 HIV-positive, 95 HIV-negative), mean placental weight was significantly lower in HIV-positive women (602.94±174.92 g) compared with HIV-negative women (684.53±139.38 g; p=0.012). Gestational age was the strongest predictor of placental weight (p=0.009), while HIV infection was independently associated with lower placental weight (p=0.016). BMI was positively but not significantly associated with placental weight.

Conclusion. Antenatal BMI and postnatal placental weight are interrelated, with differing patterns by HIV status. These find-

Corresponding author: Uchechukwu Brian Eziagu, e-mail: uchechukwu.eziagu@npmcn.edu.ng

Received: 19.06.2024 / Revised: 10.08.2025 / Accepted: 19.08.2025 / Published: 30.03.2026

Eziagu UB, Rasheed MW, Kudamnya IJ, Ndukwe CO, Utuk NM, Ajayi OO, et al. Associations between antenatal booking body mass index and postnatal placetal weight: maternal health implications in HIV-positive and HIV-negative pregnant women in Uyo, Akwa Ibom state, Nigeria. *Eur J Clin Exp Med.* 2026;24(1):6–14. doi: 10.15584/ejcem.2026.1.2.

ings underscore the need to integrate routine nutritional assessment and targeted HIV care into antenatal programs to support healthy placental growth and improve pregnancy outcomes in high HIV-prevalence populations.
Keywords. antenatal care, body mass index, gestational age, HIV in pregnancy, placental weight, sub-Saharan Africa

Introduction

The co-occurrence of HIV infection and pregnancy presents significant challenges to maternal and fetal health globally.[1] HIV-positive pregnant women face unique pathophysiological and socio-demographic factors that can influence maternal health outcomes compared to their HIV-negative counterparts.[1–16] One crucial aspect of maternal health during pregnancy is body mass index (BMI), which reflects nutritional status and is linked to various pregnancy outcomes.[10,14–18] Although HIV infection alone may not directly increase obstetric risks, progression to AIDS and associated opportunistic infections during pregnancy can adversely affect outcomes.[2–8,13]

Research has consistently shown disparities in BMI and associated factors between HIV-positive and HIV-negative pregnant women.[11,19–31] Bengtson et al. found that both groups experienced weight gain postpartum, with HIV-negative women gaining more.[19] In another study, they found that pre-pregnancy obesity was common and did not vary by HIV status.[20] Bodkin et al. reported that, in relation to their body weights, HIV-positive pregnant women had lower hemoglobin, attended fewer antenatal appointments, and were more likely to present with certain conditions, such as abnormal vaginal discharge and intrauterine growth retardation.[11] Cruz et al. further highlighted the impact of maternal BMI on infant outcomes, with underweight mothers giving birth to smaller infants.[25] Likewise, Erasmus et al. found obesity prevalent in both HIV-positive and HIV-negative groups, with a significant link to hypertension during pregnancy.[31]

Placental weight serves as a proxy for fetal growth capacity and maternal-fetal nutrient exchange, making it a useful marker of placental function.[18] Variations in placental weight have been associated with adverse perinatal outcomes, including intrauterine growth restriction, preeclampsia, and preterm birth.[9,11,25] Given its predictive value, understanding determinants of placental weight in HIV-affected pregnancies may offer critical insights into maternal-fetal health interactions.[32–46]

However, the relationship between antenatal booking BMI and postnatal placental weight remains poorly understood in resource-limited settings. Uyo, Nigeria, an urban area in Akwa Ibom State with a mixed socio-economic profile and high HIV burden, offers a relevant context for this investigation. This study addresses that gap, emphasizing the relevance of such findings for localized maternal health interventions in sub-Saharan Africa. To our knowledge, this is the first study from Nigeria to examine the combined effects of maternal BMI and HIV status on placental weight, with statistical adjustment for gestational age. By focusing on a high HIV-burden urban population in Uyo, this work provides region-specific insights that may inform context-appropriate antenatal and nutritional interventions.

Aim

Therefore, this study aims to investigate the relationship between antenatal booking body mass index (BMI) and postnatal placental weight among HIV-positive and HIV-negative pregnant women receiving care at the University of Uyo Teaching Hospital (UUTH), Nigeria. Specifically, the study examines how HIV status influences BMI distribution and placental weight, while also assessing the role of key socio-demographic factors such as age, education, occupation, and gestational age. Considering the observed high burden of maternal obesity and the growing overlap between HIV infection and pregnancy, this study further explores whether HIV status modifies the association between maternal BMI and placental weight, accounting for potential confounders. By addressing these questions through a gestational age-adjusted analytical approach, the study seeks to generate context-relevant evidence that can inform precision-based antenatal care and maternal nutrition interventions in high-HIV-burden, resource-limited settings.

Material and methods

Study design and setting

We conducted a retrospective review of antenatal and delivery records over a defined six-month period, comparing two groups of women based on HIV status (HIV-positive and HIV-negative). This design allowed us to evaluate differences in maternal BMI and placental weight between groups at the University of Uyo Teaching Hospital (UUTH), Akwa Ibom State, Nigeria, a high HIV-prevalence urban center with diverse socio-economic profiles.

Study population and sampling

All pregnant women who received antenatal care and delivered at the University of Uyo Teaching Hospital (UUTH) between December 2015 and May 2016 were eligible. We included women with complete antenatal records containing booking weight, height, gestational age at delivery, HIV status, and placental weight. Women with missing key data (e.g., absent BMI measurement or unrecorded placental weight) were excluded. For each HIV-positive participant, one to two HIV-negative women delivering within the same time frame were selected for comparison.

Data collection

Booking BMI was calculated using weight (kg) and height (m) measured at first antenatal visit by trained midwives following hospital protocol, with women in light clothing and without shoes. Placental weight was measured by the midwives immediately after delivery, with membranes and cord trimmed at a standardized length before weighing using a calibrated digital scale. Data on antiretroviral therapy (ART) status (on ART prior to pregnancy, initiated during pregnancy, or ART-naïve) were extracted from antenatal records. Further data extracted from antenatal and delivery records included maternal age, education, occupation, marital status, blood pressure, HIV clinical stage (WHO criteria), gestational age. BMI was calculated as weight (kg)/height² (m^2).[20,47,48]

Data reliability

Extraction was conducted by trained staff using a standardized template, with cross-checks against antenatal and delivery logs to ensure accuracy.

Statistical analysis

Continuous variables (e.g., BMI, placental weight) were summarized as mean±standard deviation and compared between groups using independent-samples t-tests. Categorical variables (e.g., BMI categories, education level, ART status) were compared using Chi-square or Fisher's exact test as appropriate. Pearson's correlation was used to assess associations between normally distributed continuous variables, and Spearman's correlation for non-normally distributed variables. To identify predictors of placental weight, we performed multivariable linear regression including BMI, HIV status (binary), and gestational age (continuous) as covariates. Interaction terms (BMI × HIV status) were initially tested but retained only if statistically significant. Variables were chosen based on biological relevance and results of univariate analyses ($p < 0.10$). Statistical significance was set at $p < 0.05$.

Ethical considerations

Ethical approval for this study was granted by the UUTH Health Research Ethics Committee (UUTH/AD/S/96/VOL.XII/115). All patient data were anonymized prior to analysis; due to the retrospective nature of the study, individual consent was not required.

Results

BMI associations with socio-demographic factors

A total of 143 pregnant women were included in the study: 48 (33.6%) HIV-positive and 95 (66.4%) HIV-negative. The average age was 29.4±4.6 years. The majority of both HIV-positive (89.5%) and HIV-negative (88.0%) participants weighed more than 65 kg and had a height above the average reference range of 1.56 to 1.62 meters, accounting for 48.6% HIV-positive and 53.2% HIV-negative mothers (Fig. 1).[49] HIV-negative women had significantly higher rates of tertiary education (66.3%) compared to HIV-positive women (50.0%, $p<0.05$). The overall prevalence of obesity (BMI≥30 kg/m^2) was 62.2%, with 64.5% in HIV-negative and 58.8% in HIV-positive groups; with a non-significant p =0.616. Civil/public service was more common among HIV-positive women (40.0%), while HIV-negative women exhibited greater occupational diversity; with a significant p-value of 0.014. Obesity was also common among traders (24.2%) and civil/public servants (24%), though the association was not statistically significant (p=0.594). Marriage predominated in both groups (95.7% HIV-positive, 98.9% HIV-negative), again with obesity being most common; with a non-significant p=0.542 (Table 1).

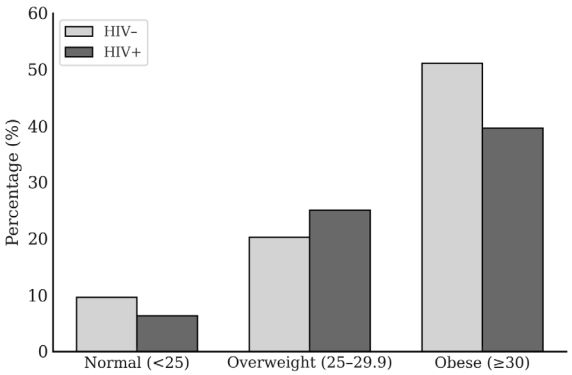

Fig. 1. Distribution of maternal BMI categories according to WHO classification (normal < 25 kg/m^2, overweight 25–29.9 kg/m^2, obese ≥ 30 kg/m^2) among HIV-negative (n=95) and HIV-positive (n=48) pregnant women, data are shown as percentages (%)

Distribution/correlation of BMI and placental weight by HIV status

The mean BMI was slightly lower in HIV-positive women (31.65±6.47 kg/m^2) compared to HIV-negative women (32.30±6.38 kg/m^2); with a non-significant p-value of 0.627. Similarly, the mean placental weight was lower in HIV-positive (602.94±174.92 g) than in HIV-negative women (684.53±139.38 g); with a significant p =0.012 (Table 1). Most participants had placental weights above 540 g, especially in obese women (Fig. 2; see Table 1 for subgroup details). Also, across all placental weight categories, a weak positive correlation between BMI and placental weight was generally observed. In HIV-negative women, the positive association appeared slightly stronger, particularly in the normal and high placental weight groups. Conversely, among HIV-positive women, the correlation was less pronounced (Fig. 3). Overall, there is a weak positive correlation (r=0.17) between mater-

nal body mass index (BMI) and placental weight. These patterns indicate that HIV status may influence how maternal BMI affects placental development, especially across different weight categories. Among HIV-positive mothers, most were in Stage 1 HIV (66.7%), followed by Stage 2 (27.1%), Stage 3 (2.1%), and Stage 4 (4.2%). Mean placental weight was highest in Stage 1 (604.69±174.76 g), followed by Stage 2 (569.23±177.41 g), Stage 3 (550.00 g; n=1), and Stage 4 (450.00±141.42 g; n=2). BMI was also highest in Stage 2 (32.55±12.28 kg/m²) and lowest in Stage 3 (28.91 kg/m²; n=1). Regarding ART status, 89.6% of HIV-positive mothers were on ART before pregnancy, with a mean placental weight of 593.02±177.14 g and mean BMI of 31.70±6.56 kg/m². Those not on ART before pregnancy (10.4%) had a lower mean placental weight (540.00±129.42 g) and mean BMI of 29.97 kg/m². These patterns suggest modest differences in placental weight and BMI across HIV stages and ART categories, though subgroup sizes, particularly for Stages 3 and 4, were small (Table 1).

Table 1. Maternal characteristics, BMI categories, and placental weight by HIV status[a]

Variable	HIV-negative (n=94)	HIV-positive (n=48)	p
Age (years), mean±SD	29.00±4.36	30.23±4.32	0.102
Tertiary education, n (%)	61 (64.9)	23 (47.9)	0.048†
Occupation – civil/public service, n (%)	28 (29.8)	10 (20.8)	0.238
BMI (kg/m²), mean±SD	32.46±6.50	31.65±6.47	0.521
BMI categories, n (%)			0.616
– Normal weight	9 (9.6)	3 (6.3)	
– Overweight	19 (20.2)	12 (25.0)	
– Obese	48 (51.1)	19 (39.6)	
Placental weight (g), mean±SD	678.83±137.58	587.50±172.44	0.004‡
Placental weight > 540 g, n (%)	82 (87.2)	31 (64.6)	0.006‡
HIV stage 1, n (%)	–	32 (66.7)	–
Mean placental weight (g) by HIV stage	–	Stage 1: 604.69±174.76 Stage 2: 569.23±177.41 Stage 3: 550.00 Stage 4: 450.00±141.42	0.632
Mean BMI (kg/m²) by HIV stage	–	Stage 1: 31.55±4.86 Stage 2: 32.55±12.28 Stage 3: 28.91 Stage 4: –	0.867
On ART before pregnancy, n (%)	–	43 (89.6)	–
Mean placental weight (g) by ART status	–	Yes: 593.02±177.14 No: 540.00±129.42	0.439
Mean BMI (kg/m²) by ART status	–	Yes: 31.70±6.56 No: 29.97	NA

[a] † – p<0.05, ‡ – p<0.01, NA – not applicable, Statistical comparison not possible due to insufficient sample size in the No ART group, BMI categories: normal weight (<25 kg/m²), overweight (25–29.9 kg/m²), obese (≥30 kg/m²), HIV stage defined per WHO clinical staging at antenatal booking, ART status reflects documented use before current pregnancy, p-values based on Chi-square tests (categorical) or independent-samples t-test (continuous)

Fig. 2. Distribution of placental weight categories (≤ 540 g, > 540 g) among HIV-negative (n=95) and HIV-positive (n=48) pregnant women, data are presented as percentages (%), Chi-square p=0.006

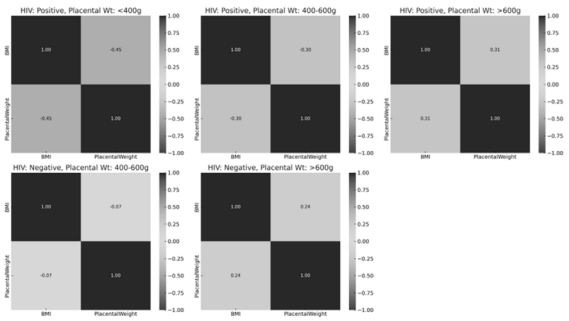

Fig. 3. Grouped correlation heatmaps showing Pearson's correlation coefficients between maternal BMI (kg/m²) and placental weight (g), stratified by HIV status (HIV-positive: n=48; HIV-negative: n=95) and placental weight categories (<400 g, 400–600 g, >600 g), darker shades represent stronger positive correlations, whereas lighter shades represent weaker or negative correlations

Correlation of BMI with obstetrics/clinical variables

The relationship between maternal BMI and pregnancy loss indicators was examined separately for HIV-positive and HIV-negative women. In HIV-positive mothers, BMI demonstrated a weak inverse correlation with prior spontaneous miscarriage (r=-0.206, p=0.242), and a moderate inverse correlation with the number of induced abortions (Spearman's rho=-0.341, p=0.048), indicating that higher BMI may be associated with fewer reported induced abortions in this group. Among HIV-negative women, BMI showed a weak positive correlation with spontaneous miscarriage (r=0.210, p=0.069), which approached statistical significance, suggesting a possible trend towards increased miscarriage risk with higher BMI. The correlation between BMI and number of induced abortions in HIV-negative women was not statistically significant (Spearman's rho=0.145, p=0.212). These findings suggest differential associations between BMI and reproductive history based on HIV status, with significant implica-

tions for maternal risk profiling and antenatal care (Fig. 4). Furthermore, correlation analyses revealed a significant positive association between BMI and systolic blood pressure in HIV-negative women (r=0.591, p=0.020), but not in HIV-positive women (r=-0.111, p=0.859). Diastolic blood pressure in HIV-positive women showed a weak negative correlation with BMI (r=-0.584, p=0.302). Hence, no significant differences were observed in diastolic pressure (Fig. 5).

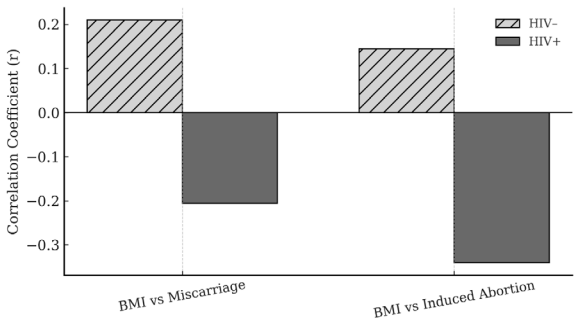

Fig. 4. Correlation coefficients (r) between maternal BMI (kg/m^2) and pregnancy loss parameters (spontaneous miscarriage and induced abortion), stratified by HIV status (HIV-negative: n=95; HIV-positive: n=48), positive values represent direct associations, while negative values indicate inverse associations

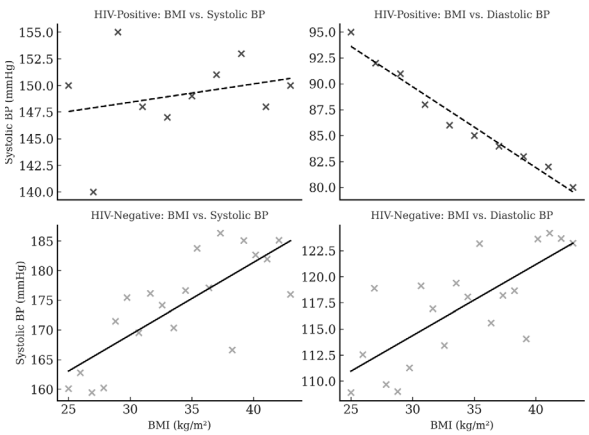

Fig. 5. Scatter plots showing the association between maternal BMI (kg/m^2) and blood pressure (mmHg) stratified by HIV status (HIV-positive: n=48; HIV-negative: n=95), panels display systolic (left column) and diastolic (right column) blood pressure, dashed regression lines represent HIV-positive participants, and solid lines represent HIV-negative participants

BMI, HIV status, and placental weight regression and subgroup analyses

To evaluate the independent associations between maternal BMI, HIV status, and placental weight, an ordinary least squares (OLS) regression was performed. The main regression model revealed that HIV-positive status was significantly associated with lower placental weight (β=-79.07, p=0.012), while maternal BMI showed a positive but non-significant association (β=3.90, p=0.087). The model explained approximately 8.6% of the variance in placental weight (R^2=0.086) (Table 2).

Subgroup analysis by HIV status showed differential effects. Among HIV-positive women, BMI was not a significant predictor of placental weight (β=4.71, p=0.325), while among HIV-negative women, a positive association between BMI and placental weight was observed but did not reach statistical significance (β=3.53, p=0.166). These findings suggest that the inverse association between HIV status and placental weight remains consistent regardless of maternal BMI, and that BMI may play a more prominent role in predicting placental weight among HIV-negative women (**Table 2**).

Furthermore, we performed a linear regression analysis to evaluate the independent contributions of maternal BMI and HIV status to postnatal placental weight, adjusting for gestational age (GA) at delivery. The model included BMI and GA as continuous variables, and HIV status as a binary variable. After adjusting for GA, gestational age emerged as a strong and statistically significant predictor of placental weight (p<0.001). HIV-positive status was independently associated with lower placental weight (β=-0.248, p=0.016), while BMI demonstrated a positive but non-significant association with placental weight (β=0.146, p=0.151). Notably, the interaction term between HIV status and BMI was not statistically significant, suggesting that HIV status did not modify the relationship between BMI and placental weight (Table 3). These findings highlight the importance of adjusting for gestational age in placental weight analyses and suggest that HIV infection may exert a modest but independent effect on placental development.

Table 2. Multivariable regression analysis and stratified subgroup models for the association between maternal BMI, HIV status, and placental weight[a]

Main regression analysis: effect of BMI and HIV status on placental weight					
Variable	Coefficient	Std. Error	t-Statistic	p	95% CI
Intercept	558.5193	75.07	7.44	0.0	409.687–707.352
BMI	3.9019	2.262	1.725	0.087	-0.582–8.386
HIV-positive	-79.0723	31.018	-2.549	0.012	-140.568–17.577
Subgroup regression analysis: HIV-positive women					
Variable	Coefficient	Std. Error	t-Statistic	p	95% CI
Intercept	453.9805	151.971	2.987	0.005	144.427–763.534
BMI	4.7066	4.707	1.0	0.325	-4.882–14.295
Subgroup regression analysis: HIV-negative women					
Variable	Coefficient	Std. Error	t-Statistic	p	95% CI
Intercept	570.4459	83.092	6.865	0.0	404.843–736.049
BMI	3.5326	2.525	1.399	0.166	-1.499–8.565

[a] standard errors assume that the covariance matrix of the errors is correctly specified

Table 3. A table illustrating a linear regression model assessing the relationship between maternal BMI, HIV status, and GA on placental weight

Unstandardized regression coefficients from the gestational age-adjusted linear regression model analysis predicting placental weight				
Variable	Coefficient	Std. Error	t-Statistic	p
Intercept	-235.55	306.57	-0.768	0.444
BMI	3.641	2.266	1.607	0.111
HIV-positive	-67.44	33.002	-2.043	0.044
Gestational age (GA)	20.759	7.783	2.667	0.009
Standardized β coefficients from the regression model, adjusting for gestational age and HIV status				
Predictor		Standardized β		p
BMI		0.146		0.151
HIV-positive		-0.248		0.016
GA (in weeks)		0.497		<0.001

Discussion

This study aimed to investigate the association between antenatal booking body mass index (BMI) and postnatal placental weight among HIV-positive and HIV-negative pregnant women receiving care at the University of Uyo Teaching Hospital, Nigeria. Our key findings affirm that HIV status, BMI, and placental weight are interrelated, with significant implications for maternal and fetal outcomes. Through stratified analysis and regression modeling, this study elucidates the differential impact of HIV status on nutritional and placental health, and how socio-demographic and clinical factors interplay in this context. The novelty of our study lies in being, to our knowledge, the first Nigerian investigation to jointly assess maternal BMI, HIV status, and placental weight while adjusting for gestational age. This approach provides a more robust understanding of how HIV modifies placental growth independent of gestational length, addressing a critical evidence gap in sub-Saharan Africa.

HIV-positive and HIV-negative pregnant women differed in BMI, placental weight, educational attainment, and occupation. Consistent with earlier studies by Bodkin et al., Isah et al., and Ladner et al., our results reveal that HIV-positive pregnant women tended to have lower mean BMI (31.65±6.47 kg/m²) and placental weight (602.94±174.92 g) than their HIV-negative counterparts (32.46±6.50 kg/m² and 684.53±139.38 g, respectively).[11,36,37] GA-adjusted regression analysis confirmed HIV status as a statistically significant predictor of placental weight, while BMI showed a positive but non-significant association. Subgroup regression revealed that BMI had a significant effect on placental weight among HIV-negative women, but not among HIV-positive women.

These results support findings by Bengtson et al. and Erasmus et al., who observed that HIV-positive status is frequently accompanied by metabolic dysregulation, suboptimal nutritional states, and altered placental physiology.[19,31] The lower placental weight in HIV-positive pregnancies may be suggestive of compromised placental development. However, since our study did not assess birth outcomes directly, this hypothesis warrants further investigation.

BMI distribution also correlated with educational and occupational status. HIV-negative women had a higher proportion of tertiary education (66.3%) compared to HIV-positive women (50%). They were also more likely to be employed in civil/public service roles, whereas HIV-positive women were predominantly traders. These patterns reflect socio-economic disparities that may influence nutritional status and health outcomes, echoing trends reported by Bengtson et al., Erasmus et al., and Trindade et al., in their studies.[3,19,31,34]

Blood pressure patterns varied across HIV status. A statistically significant positive correlation was observed between systolic blood pressure and BMI in HIV-negative women (r=0.591, p-value=0.020), while no such correlation was found in HIV-positive women. This may reflect early differences in cardiovascular regulation, though our blood pressure data alone cannot confirm broader cardiovascular risk.

Our analysis demonstrated a weak overall correlation between BMI and placental weight, but subgroup and regression analyses clarified a more complex relationship moderated by HIV status and gestational age. Several studies have associated maternal HIV with poor placental morphology and function, contributing to adverse perinatal outcomes such as intrauterine growth restriction and low birth weight.[7,11,17,18,25,34,39,50] While we did not assess such outcomes, our findings emphasize the need for further research in this area.

These findings support multifaceted interventions, such as targeted nutrition programs, specialized antenatal clinics, integrated care services, and educational outreach, to address both biomedical and social determinants of health in HIV-positive pregnancies.[10,40–43,50] Training healthcare providers to recognize and mitigate HIV-related nutritional and cardiovascular risks is also vital. By examining BMI–placental weight relationships stratified by HIV status and controlling for gestational age, our study contributes new evidence that can guide region-specific antenatal nutritional and HIV care programs.

Study limitations

This study's cross-sectional design limits causal inference. Reliance on medical records constrained the inclusion of variables such as gestational weight gain, anemia, and detailed obstetric outcomes. Additionally, qualitative data that could contextualize socio-demographic differences were absent. Future longitudinal and mixed-methods studies should assess temporal nutritional trajectories and explore mechanisms linking HIV to placental pathophysiology.

Conclusion

This study provides critical insights into how antenatal BMI and placental weight vary with HIV status among pregnant women in Uyo, Nigeria. After adjusting for gestational age, HIV status remained significantly associated with lower placental weight. BMI demonstrated a positive but non-significant association. These findings underscore the need for further research into placental health and maternal nutrition in HIV-affected pregnancies. Tailored antenatal interventions that address nutritional, educational, and socio-economic disparities may improve maternal and fetal outcomes, particularly in resource-limited settings.

Acknowledgments

We are immensely grateful to the management and staff of the Departments of Obstetrics and Gynecology, and Histopathology, UUTH, Uyo, Akwa Ibom State, Nigeria, for their immense support during this study.

Declarations

Funding

This study was self-sponsored by the authors. We did not receive any external funding or grants for this study

Author contributions

Conceptualization, U.B.E., O.O.A. and N.M.U.; Methodology, U.B.E.; Software, U.B.E. and O.O.A.; Validation, U.B.E., M.W.R., I.J.K., C.O.N., N.M.U., O.O.A, E.O.E., E.D.E. and I.O.C.; Formal Analysis, U.B.E. and O.O.A.; Investigation, U.B.E., O.O.A. and N.M.U.; Resources, U.B.E., M.W.R., I.J.K., C.O.N., N.M.U., O.O.A, E.O.E., E.D.E., I.E.A. and I.C.O.; Data Curation, U.B.E. and O.O.A.; Writing – Original Draft Preparation, U.B.E., M.W.R., I.J.K., C.O.N., N.M.U., O.O.A, E.O.E., E.D.E., I.E.A. and I.C.O.; Writing – Review & Editing, U.B.E., M.W.R., I.J.K., C.O.N., N.M.U., O.O.A, E.O.E., E.D.E., I.E.A. and I.C.O.; Visualization, U.B.E. and O.O.A.; Supervision, U.B.E.; Project Administration, U.B.E.; Funding Acquisition, U.B.E., M.W.R., I.J.K., C.O.N., N.M.U., O.O.A, E.O.E., E.D.E., I.E.A. and I.C.O.

Conflicts of interest

The author(s) declare no competing interests.

Data availability

All data generated or analyzed during this study are included in this published article.

Ethics approval

This study was conducted in accordance with the Declaration of Helsinki, and its ethical approval was granted by the UUTH Health Research Ethics Committee (UUTH/AD/S/96/VOL.XII/115).

References

1. Kelly C, Alderdice F, Lohan M. Psychosocial challenges of testing positive for HIV during pregnancy. *The British Journal of Midwifery*. 2009;17(2):76-81. doi: 10.12968/BJOM.2009.17.2.39375
2. Altfeld M, Bunders MJ. Impact of HIV-1 infection on the feto-maternal crosstalk and consequences for pregnancy outcome and infant health. *Semin Immunopathol*. 2016;38(6):727-738. doi: 10.1007/S00281-016-0578-9
3. Trindade L de NM, Nogueira LMV, Rodrigues ILA, Ferreira AMR, Corrêa GM, Andrade NCO. HIV infection in pregnant women and its challenges for the prenatal care. *Rev Bras Enferm*. 2021;74. doi: 10.1590/0034-7167-2019-0784
4. Shinar S, Agrawal S, Ryu M, et al. Perinatal outcomes in women living with HIV-1 and receiving antiretroviral therapy- a systematic review and meta-analysis. *Acta Obstet Gynecol Scand*. 2021;101(2):168-182. doi: 10.1111/AOGS.14282
5. Abdi F, Alimoradi Z, Alidost F. Pregnancy outcomes and effects of antiretroviral drugs in HIV-positive pregnant women: a systematic review. *Future Virol*. 2019;14(3):197-210. doi: 10.2217/FVL-2018-0213
6. Calvert C, Ronsmans C. Pregnancy and HIV disease progression: a systematic review and meta-analysis. *Tropical medicine & international health*. 2015;20(2):122-145. doi: 10.1111/TMI.12412
7. Pfeifer C, Bunders MJ. Maternal HIV infection alters the immune balance in the mother and fetus; implications for pregnancy outcome and infant health. *Curr Opin HIV AIDS*. 2016;11(2):138-145. doi: 10.1097/COH.0000000000000239
8. Lathrop E, Jamieson DJ, Danel I. HIV and maternal mortality. *International Journal of Gynecology & Obstetrics*. 2014;127(2):213-215. doi: 10.1016/J.IJGO.2014.05.024
9. Young S, Murray K, Mwesigwa J, et al. Maternal Nutritional Status Predicts Adverse Birth Outcomes among HIV--Infected Rural Ugandan Women Receiving Combination Antiretroviral Therapy. *PLoS One*. 2012;7(8):e41934. doi: 10.1371/JOURNAL.PONE.0041934
10. Montgomery KS. Nutrition and HIV-Positive Pregnancy. *J Perinat Educ*. 2003;12(1):42-47. doi: 10.1891/1058-1243.12.1.42
11. Bodkin C, Klopper H, Langley G. A comparison of HIV positive and negative pregnant women at a public sector hospital in South Africa. *J Clin Nurs*. 2006;15(6):735-741. doi: 10.1111/J.1365-2702.2006.01438.X
12. Ackerman IV W, Kwiek JJ. Role of the placenta in adverse perinatal outcomes among HIV-1 seropositive women. *J Nippon Med Sch*. 2013;80(2):90-94. doi: 10.1272/JNMS.80.90
13. Eziagu UB, Abudu EK, Ojo OS. Histomorphometric Survey of Placentas of HIV-positive Mothers in Relation to their Clinical Stage in a Teaching Hospital in Uyo, South-South Nigeria. *Oman Med J*. 2022;37(6):e438. doi: 10.5001/omj.2022.103

14. Vogler MA, Singh H, Wright R. Complex Decisions in Managing HIV Infection During Pregnancy. *Curr HIV/AIDS Rep*. 2011;8(2):122-131. doi: 10.1007/S11904-011-0077-5
15. Maswime, S, Pule, C, Mtshali Z, Chawana, R, Matjila M. HIV, Placental Lesions, and Adverse Perinatal Outcomes. *Journal of Infectious Diseases*. 2021;224:S691-S693. doi: 10.1093/INFDIS/JIAB494
16. Mehta S, Manji KP, Young AM, et al. Nutritional indicators of adverse pregnancy outcomes and mother-to-child transmission of HIV among HIV-infected women. *American Journal of Clinical Nutrition*. 2008;87(6):1639-1649. doi: 10.1093/AJCN/87.6.1639
17. Chigbu C, Aja L. Obesity in Pregnancy in Southeast Nigeria. *Ann Med Health Sci Res*. 2011;1(2):135.
18. Sathasivam R, Selliah P, Sivalingarajah R, Mayorathan U, Munasinghe BM. Placental weight and its relationship with the birth weight of term infants and body mass index of the mothers. *J Int Med Res*. 2023;51(5):3000605231172895. doi: 10.1177/03000605231172895
19. Bengtson AM, Phillips TK, le Roux SM, et al. Postpartum obesity and weight gain among human immunodeficiency virus-infected and human immunodeficiency virus-uninfected women in South Africa. *Matern Child Nutr*. 2020;16(3):e12949. doi: 10.1111/MCN.12949
20. Bengtson AM, Phillips TK, le Roux SM, et al. Does HIV infection modify the relationship between pre-pregnancy body mass index and adverse birth outcomes? *Paediatr Perinat Epidemiol*. 2020;34(6):713-723. doi: 10.1111/PPE.12688
21. Bengtson AM, Phillips TK, le Roux SM, et al. High blood pressure at entry into antenatal care and birth outcomes among a cohort of HIV-uninfected women and women living with HIV initiating antiretroviral therapy in South Africa. *Pregnancy Hypertens*. 2021;23:79-86. doi: 10.1016/J.PREGHY.2020.11.005
22. Bengtson AM, le Roux SM, Phillips TK, et al. Relationship between pre-pregnancy maternal body mass index and infant weight trajectories in HIV-exposed and HIV-unexposed infants. *Paediatr Perinat Epidemiol*. 2021;36(4):536-547. doi: 10.1111/PPE.12825
23. Dolan SE, Hadigan C, Killilea KM, et al. Increased Cardiovascular Disease Risk Indices in HIV-Infected Women. *J Acquir Immune Defic Syndr (1988)*. 2005;39(1):44-54. doi: 10.1097/01.QAI.0000159323.59250.83
24. Adekunle R, Bagchi S. Review of Cardiovascular Disease in HIV-Infected Women. *J AIDS Clin Res*. 2016;07(03). doi: 10.4172/2155-6113.1000557
25. Cruz ML, Harris DR, Read JS, Mussi-Pinhata MM, Succi RC; NICHD International Site Development Initiative (NISDI) Perinatal Study Group. Association of Body Mass Index of HIV-1-Infected Pregnant Women and Infant Weight, Body Mass Index, Length, and Head Circumference: The NISDI Perinatal Study. *Nutr Res*. 2007;27(11):685-691. doi: 10.1016/j.nutres.2007.09.005
26. Mozalyova OL, Samarina A V. Specific features of pregnancy and delivery in HIV-infected women. *Journal of obstetrics and women's diseases*. 2021;70(3):103-113. doi: 10.17816/JOWD48672
27. Ickovics JR, Ethier KA, Koenig LJ, Wilson TE, Walter EB, Fernandez MI. Infant birth weight among women with or at high risk for HIV infection: the impact of clinical, behavioral, psychosocial, and demographic factors. *Health Psychology*. 2000;19(6):515-523. doi: 10.1037/0278-6133.19.6.515
28. Schulte J, Dominguez K, Sukalac T, Bohannon B, Fowler MG. Declines in Low Birth Weight and Preterm Birth Among Infants Who Were Born to HIV-Infected Women During an Era of Increased Use of Maternal Antiretroviral Drugs: Pediatric Spectrum of HIV Disease, 1989–2004. *Pediatrics*. 2007;119(4):e900-e906. doi: 10.1542/PEDS.2006-1123
29. Portwood C, Sexton H, Kumarendran M, Brandon Z, Kirtley S, Hemelaar J. Adverse perinatal outcomes associated with antiretroviral therapy in women living with HIV: A systematic review and meta-analysis. *Front Med (Lausanne)*. 2023;9:924593. doi: 10.3389/fmed.2022.924593
30. Murray C, Portwood C, Sexton H, et al. Adverse perinatal outcomes attributable to HIV in sub-Saharan Africa from 1990 to 2020: Systematic review and meta-analyses. *Communications Medicine*. 2023;3(1):103. doi: 10.1038/S43856-023-00331-8
31. Erasmus CR, Chuturgoon AA, Maharaj NR. Maternal overweight and obesity and its associated factors and outcomes in human immunodeficiency virus (HIV)-infected and HIV-uninfected black South African pregnant women. *J Obstet Gynaecol Res*. 2022;48(11):2697-2712. doi: 10.1111/JOG.15392
32. Nyoyoko NP, Umoh AV. The prevalence and determinants of HIV seroconversion among booked ante natal clients in the University of Uyo teaching hospital, Uyo Akwa Ibom State, Nigeria. *Pan Afr Med J*. 2016;25. doi: 10.11604/PAMJ.2016.25.247.6715
33. WHO. Malnutrition in women. World Health Organization. 2023. https://www.who.int/data/nutrition/nlis/info/malnutrition-in-women. Accessed June 17, 2024.
34. Zierle-Ghosh A, Jan A. Physiology, Body Mass Index. *StatPearls*. https://www.ncbi.nlm.nih.gov/books/NBK535456/. Accessed June 17, 2024.
35. Essential Pathology. Pediatric and Perinatal: Gestational Age, Placental Weight, and Umbilical Cord Length. e-Manual for Specimen Gross Examination in Surgical Pathology (4th Edition). 2020. http://www.essentialpathology.info/Gross_manual/Index.html?GestationalAgePlacentalWeightUmbilicalCordLengthTable. Accessed June 17, 2024.
36. Isah H, Musa O, Evbuomwan V, Attah B, Ogu I, David A. Pregnancy Experience And Outcome: A Comparison Between HIV Positive And HIV Negative Pregnant Women. *African Journal of Pharmaceutical Research & Development*. 2018;10(1):037-042.

37. Ladner J, Castetbon K, Leroy V, et al. Pregnancy, body weight and human immunodeficiency virus infection in African women: A prospective cohort study in Kigali (Rwanda), 1992-1994. *Int J Epidemiol*. 1998;27(6):1072-1077. doi: 10.1093/IJE/27.6.1072
38. Filipe MEJ, Santana MS. Nutritional Status Pre-Gestational and Gestational Among Women Living With HIV Positive in Luanda, Angola. *J Food Sci Nutr Res*. 2022;5(4):696-701.
39. Brandão T, Silva KS, Sally EO, Dias MAB, Silva CVC da, Fonseca VM. Epidemiological and nutritional characteristics of pregnant HIV-infected women. *Revista Brasileira de Ginecologia e Obstetrícia*. 2011;33(8):188-195.
40. Fischer C, Rosario JL, Alves GA, Mezadri T, Grillo LP. Estado nutricional de gestantes infectadas pelo HIV/AIDS: período de 2010 a 2015. *Revista Brasileira de Obesidade, Nutrição e Emagrecimento*. 2019;13(79):400-406.
41. Yudin MH, Caprara D, MacGillivray SJ, Urquia M, Shah RR. A Ten-Year Review of Antenatal Complications and Pregnancy Outcomes Among HIV-Positive Pregnant Women. *J Obstet Gynaecol Can*. 2016;38(1):35-40. doi: 10.1016/J.JOGC.2015.10.013
42. Gichangi P, Nyongo A, Temmerman M. Pregnancy outcome and placental weights: their relationship to HIV-1 infection. *East Afr Med J*. 1993;2:85-89.
43. Smith Fawzi MC, Kaaya SF, Mbwambo J, et al. Multivitamin supplementation in HIV-positive pregnant women: impact on depression and quality of life in a resource-poor setting. *HIV Med*. 2007;8(4):203-212. doi: 10.1111/J.1468--1293.2007.00454.X
44. Gruskin S, Firestone R, MacCarthy S, Ferguson L. HIV and pregnancy intentions: do services adequately respond to women's needs? *Am J Public Health*. 2008;98(10):1746-1750. doi: 10.2105/AJPH.2008.137232
45. Bailey H, Zash R, Rasi V, Thorne C. HIV treatment in pregnancy. *Lancet HIV*. 2018;5(8):e457-e467. doi: 10.1016/S2352-3018(18)30059-6
46. Callahan T, Modi S, Swanson J, Ng'Eno B, Broyles LN. Pregnant adolescents living with HIV: what we know, what we need to know, where we need to go. *J Int AIDS Soc*. 2017;20(1). doi: 10.7448/IAS.20.1.21858
47. WHO. WHO Case Definition of HIV for Surveillance and Revised Clinical Staging and Immunological Classification of HIV-Related Disease in Adults and Children. *World Health Organization*. https://www.ncbi.nlm.nih.gov/books/NBK374293/. Accessed April 20, 2025.
48. Olagbuji BN, Ezeanochie MC, Ande AB, Oboro VO. Obstetric and perinatal outcome in HIV positive women receiving HAART in urban Nigeria. *Arch Gynecol Obstet*. 2010;281(6):991-994. doi: 10.1007/s00404-009-1186-x
49. Balogun JA, Olawoye AG, Oladipo VA. Anthropometric indices of male and female Nigerians of different age groups. *Afr J Med Med Sci*. 1994;23(3):279-286.
50. Burton GJ, Fowden AL, Thornburg KL. Placental origins of chronic disease. *Physiol Rev*. 2016;96(4):1509-1565. doi: 10.1152/PHYSREV.00029.2015

Rzeszów University Press 2026
ISSN 2544-1361 (online)
doi: 10.15584/ejcem.2026.1.4

http://www.ejcem.ur.edu.pl
European Journal of Clinical and Experimental Medicine
Eur J Clin Exp Med 2026; 24 (1): 15–22

ORIGINAL PAPER

Dysregulation of iron metabolism in chronic kidney disease – hepcidin as a diagnostic biomarker in Iraqi adults – a case-control study

Mohammed Abdul Jaleel Tarweel , Haider Abd Jabber Alammar

Medical Chemistry Department, College of Medicine, University of Al-Qadisiyah, Iraq

ABSTRACT

Introduction and aim. Chronic kidney disease (CKD) is a global health burden, with iron deficiency (ID) being a prevalent but under-diagnosed comorbidity. Traditional biomarkers, such as serum ferritin and transferrin saturation, are confounded by inflammation, which limits diagnostic accuracy. Hepcidin, a key regulator of iron homeostasis, offers potential as a reliable biomarker; however, data from low- and middle-income countries (LMICs), including Iraq, remain scarce. This study assessed the diagnostic utility of hepcidin for CKD and its association with iron dysregulation in Iraqi adults, addressing regional gaps in biomarker validation and clinical application.

Material and methods. This case-control study (September 2024–February 2025) recruited 60 patients with CKD (stages 2–4) and 40 age-and sex-matched healthy controls. The exclusion criteria were recent transfusions, infections, or iron therapy. Serum hepcidin, ferritin, iron, Total Iron-Binding Capacity (TIBC), transferrin, and renal function indices were analyzed via enzyme-linked immunosorbent assay and standardized assays.

Results. CKD patients exhibited significantly elevated hepcidin (39.8±23.1 vs. 13.7±4.8 pg/mL, p<0.001) and ferritin (246±128 vs. 160±61 ng/mL, p<0.001) but lower serum iron (12.38±3.1 vs. 118±33.5 µg/dL, p<0.001), TIBC (347±109 vs. 385±62 µg/dL, p=0.004), and transferrin levels (224±74 vs. 258±39 mg/dL, p=0.005) than controls. Hepcidin levels increased progressively with CKD stage (p<0.001) and correlated strongly with eGFR (r=-0.800, p<0.001) and serum creatinine (r=0.702, p<0.001). At a cut-off of >25 pg/mL, hepcidin demonstrated 80% sensitivity and 100% specificity for CKD diagnosis, with an AUC of 0.86 (95% CI: 0.78–0.92, p<0.001).

Conclusion. Hepcidin demonstrated high diagnostic accuracy for CKD and was a superior indicator of iron metabolism dysregulation compared to traditional biomarkers. Its utility in resource-limited settings, such as Iraq, could enhance early CKD detection and guide management strategies, thereby addressing critical gaps in LMIC healthcare.

Keywords. chronic kidney disease, diagnostic biomarker, hepcidin, iron deficiency

Introduction

Chronic kidney disease (CKD) is a worldwide public health burden, affecting approximately 10% of the population. CKD is a progressive condition that leads to irreversible decline in renal function and is associated with cardiovascular diseases, anemia, and elevated mortality. iron deficiency (ID) is a frequently overlooked comorbidity in CKD.[1,2] Inappropriate dietary intake, chronic inflammation, and systemic and renal signs of impaired iron utilization contribute to the pathogenesis of ID in CKD. ID leads to anemia of chronic inflammation, a frequently occurring condition in patients with CKD, contributes to reduced oxygen supply, worsens weariness, and deteriorates quality of life.[3–5]

The coexistence of CKD and ID is unacceptably high. Studies have reported that the prevalence of ID among

Corresponding author: Mohammed Abdul Jaleel Tarweel, e-mail: med.post24.107@qu.edu.iq

Received: 3.06.2025 / Revised: 27.07.2025 / Accepted: 24.08.2025 / Published: 30.03.2026

Tarweel MAJ, Alammar HAJ. Dysregulation of iron metabolism in chronic kidney disease – hepcidin as a diagnostic biomarker in Iraqi adults – a case-control study. *Eur J Clin Exp Med.* 2026;24(1):15–22. doi: 10.15584/ejcem.2026.1.4.

patients with non-dialysis CKD ranges from approximately 25% to 50%, with the proportion increasing as CKD progresses to more advanced stages.[6] For example, one study found that 47.1% of non-dialysis CKD patients had ID, and another study identified ID anemia in 38.8% of pre-dialysis CKD patients. The prevalence of anemia, often due to ID, was nearly 40% among non-dialysis-dependent CKD patients in a large European cohort, and the rates increased with worsening CKD stage.[7] In low- and middle-income countries (LMICs), including Iraq, the clinical burden of this dual pathology is exacerbated by limited access to advanced diagnostics and effective therapies.[8] The Middle East and North Africa (MENA) region, for example, continues to experience a high burden of ID, with more than 88 million cases reported in 2021 and little improvement in recent decades.[9]

In healthy individuals, iron homeostasis is a tightly regulated process primarily orchestrated by the hepatic peptide hormone hepcidin. Hepcidin, a 25-amino-acid peptide produced by the liver, serves as the master regulator of systemic iron availability.[10] It maintains the iron balance by binding to and inducing the degradation of the iron exporter ferroportin, which is present on the surface of enterocytes in the intestine, macrophages in the reticuloendothelial system, and hepatocytes. This action reduces both intestinal iron absorption and the release of recycled iron from macrophages, thereby lowering plasma iron levels.[11]

Modern biomarkers, such as hepcidin, allow potential improvement of diagnostic accuracy and therapeutic monitoring when dealing with ID associated with CKD.[12] The main problem with traditional markers such as serum ferritin and transferrin saturation (TSAT) is that the former is severely affected by inflammation, while TSAT does not provide the necessary specificity, inevitably leading to misclassification of the iron status.[13] In contrast, hepcidin directly represents the body iron-regulatory experience and level of inflammation. Consequently, hepcidin is a reliable marker of functional ID in CKD patients.[14] Modern research has revealed that elevated levels of hepcidin indicate the pathology of the filtration rate, and the patient will be affected by an inability to react to iron therapy.[15] Existing research on hepcidin's role in iron metabolism dysregulation in CKD predominantly stems from high-income settings, with limited data from LMICs, such as Iraq, where diagnostic constraints and high clinical burden coexist.[8,16] Traditional biomarkers (e.g., serum ferritin and TSAT) are confounded by inflammation and lack specificity, underscoring the need for contextually validated alternatives.

Aim

This study aimed to assess the diagnostic utility of hepcidin as a biomarker for CKD and its associated iron dysregulation in Iraqi adults, address the regional research gap, and explore its potential to enhance diagnostic accuracy and therapeutic strategies in resource-limited settings.

Material and methods

This case-control study was conducted between September 2024 and February 2025, recruiting participants from the nephrology outpatient clinics of a Diwaniyah Teaching Hospital. A total of 60 adult patients (aged 18–80 years) with non-dialysis CKD stages (2–4), as defined by the KDIGO 2012 Clinical Practice Guideline based on estimated glomerular filtration rate (eGFR)[17], and 40 age- and sex-matched healthy controls were enrolled. Patient eligibility required stable renal function (no greater than a 25% change in eGFR over the preceding 3 months). Key exclusion criteria for the CKD group included a history of blood transfusions within the past 3 months, iron supplementation or erythropoiesis-stimulating agent (ESA) use within the past 4 weeks, and the presence of active infection or significant inflammation (C-reactive protein ≥10 mg/L). Patients with end-stage renal disease (ESRD) on dialysis, recent kidney transplants (<6 months), or polycystic kidney disease were also excluded. The sample size was determined as a convenience sample based on patient availability and logistical constraints during the study period.

Healthy controls, rigorously age- and sex-matched to the CKD participants, underwent screening to confirm normal kidney function (eGFR ≥90 mL/min/1.73 m^2 without proteinuria or hematuria), adequate hemoglobin levels, and the absence of chronic illnesses, inflammation, or iron abnormalities, with health assessments conducted according to STROBE guidelines; this screening was expanded to specifically require CRP levels ≤5 mg/L, normal iron status (ferritin >30 ng/mL and TSAT >20%), no chronic comorbidities (including diabetes, cardiovascular disease, or liver disease), and a BMI <30, while lifestyle factors such as smoking and alcohol use were recorded but were only exclusionary if deemed clinically significant.

Biochemical assessments

Venous blood samples (approximately 8 mL) were collected from all participants in the morning after an overnight fast (10–12 hours) into plain serum separator tubes. Samples were allowed to clot at room temperature for 30 minutes and were subsequently centrifuged at 3000 rpm for 10 minutes. The separated serum was aliquoted into sterile cryovials and stored at -80°C until analysis. All samples were analyzed within one month of collection and underwent a single freeze-thaw cycle to preserve analyte integrity.

Serum urea, creatinine, iron, ferritin, TIBC, and high-sensitivity C-reactive protein (hs-CRP) were analyzed using a Roche Cobas c501 automated analyzer (Roche Diagnostics, Basel, Switzerland). Transferrin lev-

els were quantified using a commercial enzyme-linked immunosorbent assay (ELISA) kit (Human Transferrin ELISA Kit, Elabscience®, Catalog No: E-EL-H6298). Serum hepcidin was measured using a commercially available competitive ELISA kit (Human Hepcidin ELISA Kit, Elabscience®, Catalog No: E-EL-H6202) with a detection range of 0.78–500 pg/mL and a sensitivity (limit of detection, LOD) of 9.4 pg/mL. Hemoglobin levels were determined using a Sysmex XN-1000 automated hematology analyzer (Sysmex Corporation, Kobe, Japan).

All assays were performed in duplicate according to the manufacturers' instructions. Internal quality control materials provided by the respective kit manufacturers were included in each assay run. The intra- and inter-assay coefficients of variation (CV) for the hepcidin ELISA were 4.8% and 7.3%, respectively. The laboratory participates in an external quality assurance scheme for routine biochemistry parameters.

Anemia was defined as a hemoglobin concentration <13 g/dL for men and <12 g/dL for women. Absolute iron deficiency (ID) was defined as a serum ferritin level <100 ng/mL. Functional iron deficiency (FID) was defined as a serum ferritin level between 100–500 ng/mL combined with a transferrin saturation (TSAT) <20%.

Ethical approval

This study was conducted in accordance with the ethical rules of medical research at the University of Al-Qadisiyah, collage of medicine. Before sampling, the consent of the patient or his companion was taken. The study protocol, subject Information and approval form were reviewed and approved by the clinical chemistry unite of the laboratory in al Diwaniyah Teaching Hospital accordance with Document No. 472130 dated (29/10/2024) to obtain this approval.

Statistical analysis

Statistical analyses of the demographic and clinical characteristics of the individuals diagnosed with CKD were performed using GraphPad Prism® (version 9.0 GraphPad Software, San Diego, CA, USA). Continuous variables were analyzed using independent-sample t-tests (a), whereas categorical variables were evaluated using the Chi-square test (b). For datasets comprising more than two groups, one-way analysis of variance (ANOVA) was implemented, followed by Tukey's post-hoc test for specific pairwise comparisons.

Results

Table 1 compares the demographic features age, sex, and BMI and key clinical biomarkers hemoglobin, CRP, serum creatinine, blood urea, and eGFR between 60 CKD patients and 40 healthy controls. CKD patients exhibited significantly lower hemoglobin, higher CRP, elevated serum creatinine/blood urea, and reduced eGFR than controls (p<0.001). The CKD stages were distributed as follows: stage 2 (21.6%), stage 3a (27%), stage 3b (23.4%), and stage 4 (28%).

Table 1. Demographic and clinical characteristics of CKD patients and healthy controls*

Demographic & biomarker features		CKD patients (n=60)	Healthy control (n=40)	p
Age (years)	Mean±SD	53.50±19.4	51.46±17.3	0.6 [a]
Gender	Male	31	22	0.4 [b]
	Female	29	18	
BMI (kg/m^2)	Mean±SD	25.24±4.6	26.3±3.9	0.3 [a]
Hemoglobin (g/dL)	Mean±SD	9.72±0.85	14.1±1.2	<0.001 [a]
CRP (mg/L)	Mean±SD	29±13.4	2.6±1.7	<0.001 [a]
Serum creatinine (mg/dL)	Mean±SD	4.1±1.6	0.91±0.2	<0.001 [a]
Blood urea (mg/dL)	Mean±SD	108.9±38.6	30.1±7.5	<0.001 [a]
eGFR (mL/min/1.73 m^2)	Mean±SD	45.4±22.6	108±7.9	<0.001 [a]
Stages among patients	Stage 2	13 (21.6)	-	-
	Stage 3a	16 (27)	-	-
	Stage 3b	14 (23.4)	-	-
	Stage 4	17 (28)	-	-

* [a] – independent sample t-test, [b] – Chi-square

Table 2 highlights the differences in iron-related biomarkers between patients with CKD and the controls. CKD patients had significantly higher ferritin (p<0.001) and hepcidin (p<0.001) levels, but lower serum iron (p<0.001), TIBC (p=0.004), and transferrin (p=0.005) levels than healthy individuals, indicating dysregulated iron homeostasis in CKD (Fig. 1).

Table 2. Iron metabolism biomarkers in CKD patients and healthy controls*

Demographic and biomarker features		CKD patients (n=60)	Healthy control (n=40)	p
Ferritin (ng/mL)	Mean±SD	246±128	160±61	<0.001 [a]
Serum iron (µmol/L)	Mean±SD	12.38±3.1	118±33.5	<0.001 [a]
TIBC (µg/dL)	Mean±SD	347±109	385±62	0.004 [a]
Transferrin (mg/dL)	Mean±SD	224±74	258±39	0.005 [a]
Hepcidin (pg/mL)	Mean±SD	39.8±23.1	13.7±4.8	<0.001 [a]

* [a] – independent sample t-test

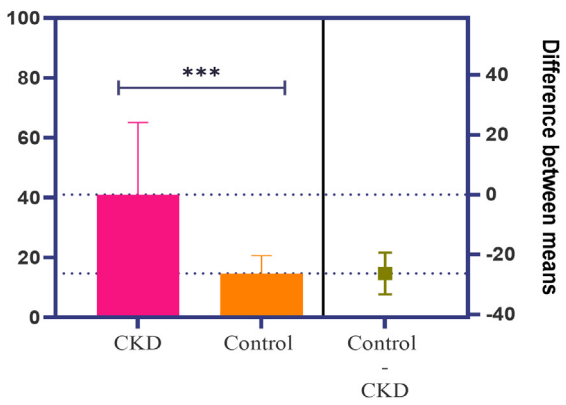

Fig. 1. Bar chart showing comparison of mean serum hepcidin among control group and CKD group

Biomarker levels (ferritin, serum iron, TIBC, transferrin, and hepcidin) were stratified according to CKD stage (2–4). Ferritin levels decreased with advancing stage (p=0.003), whereas hepcidin levels increased significantly (p<0.001). TIBC and transferrin levels declined progressively (p<0.001), reflecting worsening iron availability and inflammation. Post hoc analysis (Tukey's test) identified distinct inter-stage differences (denoted by superscript letters, Table 3, Fig. 2).

Table 3. Variation of serum biomarkers across CKD stages[#]

Serum biomarkers and CKD		Stage of CKD				p
		Stage 2 (n=13)	Stage 3a (n=16)	Stage 3b (n=14)	Stage 4 (n=17)	
Ferritin (ng/mL)	Mean±SD	328±107^{A}	206±132^{B}	219±141^{B}	155±116^{C}	0.003
Serum iron (µmol/L)	Mean±SD	11.2±2.7^{A}	10.9±2.7^{A}	7.4±1.6^{B}	10.4±3.0^{A}	0.04
TIBC (µg/dL)	Mean±SD	417±68^{A}	371±85^{B}	271±63^{C}	247±98^{C}	<0.001
Transferrin (mg/dL)	Mean±SD	293±58^{A}	268±61^{B}	203±44^{C}	181±71^{C}	<0.001
Hepcidin (pg/mL)	Mean±SD	13.8±3.9^{A}	35.8±8.2^{B}	29.6±6.8^{B}	68.6±15.8^{C}	<0.001

[#] O – one-way ANOVA, * – significant at p<0.05, *** – significant at p<0.001, statistical analysis was performed using one-way ANOVA with post-hoc Tukey's test for pairwise comparisons, superscript letters (A, B, C) denote the results of these pairwise comparisons, groups that do not share a common letter are significantly different from each other (p<0.05)

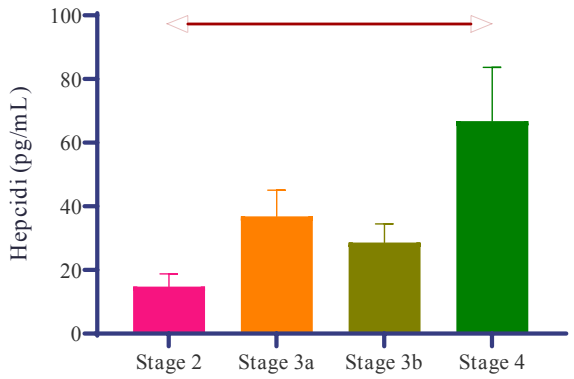

Fig. 2. Bar chart presenting the distribution of hepcidin levels among various stages of CKD

Hepcidin demonstrated high diagnostic accuracy for CKD at a cut-off of >25 pg/mL, with 80% sensitivity, 100% specificity, 100% PPV, 80% NPV, and an AUC of 86% (p<0.001). This finding supports the potential of hepcidin as a biomarker for CKD (Table 4, Fig. 3).

Table 4. Diagnostic performance of hepcidin for CKD detection*

Biomarkers	Cut-off value	Sens %	Spec%	PPV	NPV	Accuracy	AUC (95% CI)	p
Hepcidin (pg/mL)	>25	80	100	100	80	0.79	86 (0.78 to 0.92)	<0.001

* Sens – sensitivity, Spec – specificity, PPV – positive predictive value, NPV – negative predictive value, AUC – area under the curve

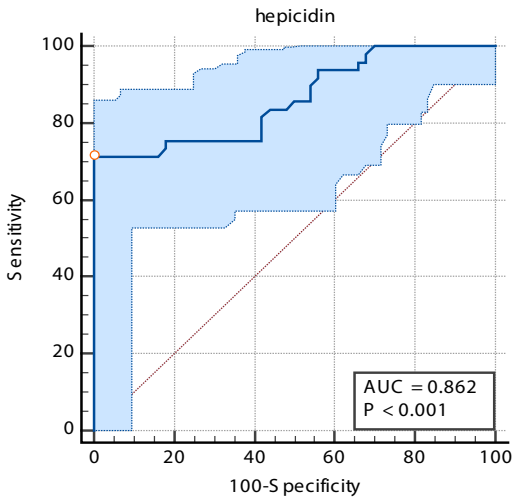

Fig. 3. ROC curve chart of hepcidin in CKD

This correlation matrix revealed associations between iron markers (transferrin, TIBC, ferritin, and hepcidin) and renal function indices (eGFR and serum creatinine). Hepcidin levels were strongly correlated with eGFR (r=-0.800, p<0.001) and serum creatinine (r=0.702, p<0.001), whereas transferrin and TIBC were positively correlated with eGFR (r=0.433, p<0.001). Ferritin showed weak associations with the other parameters (Table 5).

Table 5. Correlation between iron metabolism biomarkers and renal function parameters in CKD

	Transferrin (mg/dL)	TIBC (µg/dL)	Hemoglobin (g/dl)	Serum iron (µmol/L)	eGFR (ml/min/1.73 m^2)	Ferritin (ng/mL)	Hepcidin (Pg/ml)	Serum creatinine (mg/dL)
Transferrin (mg/dL)	1	1.000 p<0.001	0.201 p=0.045	0.222 p=0.026	0.433 p<0.001	-0.036 p=0.725	-0.519 p<0.001	-0.311 p=0.001
TIBC (µg/dL)	1.000 p<0.001	1	0.201 p=0.045	0.222 p=0.026	0.433 p<0.001	-0.036 p=0.725	-0.519 p<0.001	-0.311 p=0.001
Hemoglobin (g/dl)	0.201 p=0.045	0.201 p=0.045	1	0.834 p<0.001	0.763 p<0.001	-0.498 p<0.001	-0.504 p<0.001	-0.679 p<0.001
Serum iron (µmol/L)	0.222 p=0.026	0.222 p=0.026	0.834 p<0.001	1	0.811 p<0.001	-0.458 p<0.001	-0.563 p<0.001	-0.691 p<0.001
eGFR (mL/min/ 1.73 m^2)	0.433 p<0.001	0.433 p<0.001	0.763 p<0.001	0.811 p<0.001	1	-0.277 p=0.005	-0.800 p<0.001	-0.804 p<0.001
Ferritin (ng/mL)	-0.036 p=0.725	-0.036 p=0.725	-0.498 p<0.001	-0.458 p<0.001	-0.277 p=0.005	1	0.068 p=0.501	0.268 p=0.007
Hepcidin (pg/ml)	-0.519 p<0.001	-0.519 p<0.001	-0.504 p<0.001	-0.563 p<0.001	-0.800 p<0.001	0.068 p=0.501	1	0.702 p<0.001
Serum creatinine (mg/dL)	-0.311 p=0.001	-0.311 p=0.001	-0.679 p<0.001	-0.691 p<0.001	-0.804 p<0.001	0.268 p=0.007	0.702 p<0.001	1

Discussion

These findings revealed notable changes in iron metabolism biomarkers across the progressive stages of CKD, characterized by a gradual reduction in serum ferritin and transferrin concentrations. These trends underscore the multifactorial pathophysiology of disruption of iron

homeostasis in advancing renal dysfunction, reflecting the interplay between regulatory mechanisms and disease progression. Current clinical guidelines, including KDIGO-2012 and ERBP 2013, advocate routine assessment of iron status in patients with CKD, predominantly through ferritin and TSAT measurements.[18] However, emerging evidence has challenged the reliability of these biomarkers. A clinical investigation reported that only 12% of hemodialysis patients exhibited normal transferrin levels, with 88% displaying varying degrees of malnutrition (5% severe, 30% moderate, and 53% mild). This malnutrition-associated hypotransferrinemia may artificially elevate TSAT values, potentially obscuring the true iron status in CKD populations.[19]

The interpretation of serum ferritin is further complicated by its dual role as an acute phase reactant. Multiple studies corroborate its elevation during inflammatory states, a common comorbidity in patients with CKD, thereby limiting its specificity as an iron storage marker.[20–22] Rashid and Al-Rubaie reinforced this limitation in an ESRD cohort, where 72.5% exhibited hyperferritinemia (≥300 ng/mL); however, these levels correlated more strongly with systemic inflammation than iron stores. Their analysis demonstrated that the combined TSAT-ferritin assessment achieved only a 47.5% diagnostic accuracy for iron status determination in ESRD.[23] These diagnostic challenges are further exemplified in the Al-Mashdali case report, where tissue iron quantification via T2* magnetic resonance imaging (MRI) revealed significant hepatic iron overload despite chronically elevated serum ferritin levels (>1000 μg/L) without clinical correlates.[24] The apparent paradox of declining ferritin in advanced CKD stages, contrary to expected inflammation-driven elevations, may reflect superimposed true ID from multifactorial etiologies, including malnutrition, occult gastrointestinal bleeding, or dialysis-related iron losses. Concurrent reductions in transferrin levels align with the established pathophysiology of impaired hepatic synthesis in uremia, exacerbated by chronic inflammation and protein energy wasting.[25]

The present study indicated that patients with CKD demonstrated significantly elevated hepcidin levels compared with healthy individuals, with a pronounced increase as kidney dysfunction advanced. Hepcidin concentrations progressively increased from the early to late CKD stages, correlating strongly with the disease severity. A cross-sectional study of 199 non-dialyzed patients with CKD was conducted to evaluate the relationship between hepcidin and iron disorders, inflammation, and hemoglobin levels. They found that hepcidin levels increased as GFR declined, with median values rising from 23.3 ng/mL in early stage CKD to 36.1 ng/mL in advanced CKD. Absolute ID (defined as TSAT <20% and ferritin <40 ng/mL) was associated with significantly lower hepcidin levels (5.0 ng/mL), whereas inflammation combined with normal iron status led to higher hepcidin concentrations (34.5 ng/mL). The study concluded that hepcidin levels in CKD are independently influenced by iron status and inflammation, with renal clearance playing a secondary role.[26]

Hepcidin demonstrates significant potential as a diagnostic biomarker for CKD-associated iron dysregulation. In the present study, a hepcidin threshold (>23.2 pg/mL) yielded robust performance metrics for distinguishing CKD patients from healthy controls: 80% sensitivity, 100% specificity, 100% PPV, 85% NPV, and an AUC of 86%. These findings contribute to the growing body of evidence exploring hepcidin role in iron homeostasis in CKD. While our study design did not include a formal analysis against predefined ID thresholds (e.g., KDIGO criteria: ferritin <100 ng/mL or TSAT <20%) to directly compare diagnostic accuracy for ID, the observed strong inverse correlations between hepcidin and markers of iron availability (serum iron, TIBC, transferrin) support its central role in iron metabolism dysregulation. Notably, prior studies such as that by Gao et al. (2023) have reported that hepcidin outperformed ferritin/TSAT combinations for identifying functional iron deficiency, with high AUC values (0.94) and specificity (87%), particularly in distinguishing true functional iron deficiency from inflammation-driven hyperferritinemia.[14] The 2023 KDIGO Clinical Practice Guideline for the Evaluation and Management of Chronic Kidney Disease also highlights the limitations of traditional markers and acknowledges the emerging role of hepcidin, though it notes that more evidence is needed before routine clinical use can be recommended.[27]

Emerging evidence underscores the critical role of hepcidin dysregulation in CKD progression and associated complications. A pivotal study demonstrated that patients in the highest hepcidin quartile (25.1–80.0 ng/mL) exhibited a 1.37-fold increased risk of ESKD compared with those in the lowest quartile. This association followed a linear dose-response relationship, persisting even after adjustment for traditional risk factors, positioning hepcidin as a novel prognostic biomarker for CKD progression and as a potential tool for risk stratification.[28] The regulation of hepcidin is further influenced by dialysis modality, as highlighted by Malyszko et al. Their comparative analysis revealed that peritoneal dialysis (PD) patients had significantly elevated hepcidin/ferritin ratios, 2.5-fold higher than non-dialysis (ND) and hemodialysis (HD) cohorts, likely due to sustained intraperitoneal inflammation and impaired clearance mechanisms. These findings suggest that PD-associated inflammation exacerbates iron sequestration, emphasizing modality-specific pathways in hepcidin dysregulation.[29]

Notably, elevated hepcidin levels are closely associated with functional iron deficiencies (FID) and subclinical inflammation. In patients with FID, hepcidin levels in

the highest quartile correlated strongly with hs-CRP levels, implicating iron dysregulation as both a consequence and driver of inflammatory processes. Importantly, early CKD stages showed that hepcidin elevation predicts cardiovascular morbidity, advocating routine monitoring in early stage patients to mitigate downstream complications.[30] Furthermore, reinforcing this interplay, hepcidin was positively correlated with IL-6, a key inflammatory cytokine, and inversely correlated with hemoglobin and glomerular filtration rate (GFR). These associations underscore inflammation-driven hepcidin upregulation as a central mechanism in iron-restricted erythropoiesis, worsening anemia, and FID in CKD patients.[31]

Collectively, these studies delineate hepcidin as a multifunctional mediator that links iron metabolism, inflammation, and CKD progression. This elevation reflects a vicious cycle of inflammation-driven iron sequestration, exacerbation of anemia, and accelerated renal decline. These insights advocate the integration of hepcidin assessment into clinical practice, particularly for early risk stratification and personalized iron therapy, while highlighting the need for modality-specific management strategies for dialysis-dependent patients.

Study limitations

A key limitation of this study, common to many CKD biomarker investigations, is the absence of a universally accepted non-invasive gold standard for functional iron deficiency; while hepcidin demonstrated superior specificity and stronger correlations with renal function decline compared to current clinical biomarkers (ferritin, TSAT components), definitive validation against a reference standard like bone marrow iron was not feasible in this clinical setting. Furthermore, the study's cross-sectional design did not account for longitudinal variations in factors such as dietary iron intake and inflammatory status over time, which may influence iron biomarker levels and introduce bias. The use of a single commercial ELISA kit for hepcidin measurement, without inter-assay calibration against a standardized reference, may also contribute to measurement variability and limit the direct comparability of our absolute values with those from other studies. Future studies incorporating such reference validation methods where possible, accounting for dietary and socioeconomic variables, and conducted on a larger scale, particularly in LMICs, are warranted to definitively validate hepcidin diagnostic utility, establish its prognostic value, and determine its integration into CKD management protocol.

Conclusion

This study established hepcidin as a robust diagnostic biomarker for iron metabolism dysregulation in CKD, particularly in Iraqi populations. Elevated hepcidin levels correlate strongly with advanced CKD stages and renal dysfunction, demonstrating superior specificity compared to conventional markers. These findings underscore the clinical relevance of hepcidin in regions with limited diagnostic resources and offer a viable tool for early ID detection and therapeutic monitoring.

Acknowledgements

We extend our sincere appreciation to the College of Medicine at the University of Al-Qadisiyah for their unwavering support. We are also profoundly grateful to the participants who actively contributed to this study and provided invaluable collaboration. Furthermore, we acknowledge the dedication of the esteemed staff members at Diwaniyah Teaching Hospital in Al-Qadisiyah for their commitment and assistance. Lastly, we recognize the significant contributions of all individuals involved in this research endeavor.

Declarations

Funding

No funds were received to fulfil this work.

Author contributions

Conceptualization, M.A.J.T. and H.A.J.A.; Methodology, M.A.J.T.; Software, M.A.J.T.; Validation, M.A.J.T. and H.A.J.A.; Formal Analysis, MAJT; Investigation, M.A.J.T.; Resources, M.A.J.T.; Data Curation, M.A.J.T.; Writing – Original Draft Preparation, M.A.J.T.; Writing – Review & Editing, M.A.J.T.; Visualization, H.A.J.A.; Supervision, H.A.J.A.; Project Administration, M.A.J.T.; Funding Acquisition, H.A.J.A.

Conflicts of interest

The authors declare that they have no competing interests.

Data availability

The datasets generated and analyzed during the current study are not publicly available due to participant privacy and confidentiality concerns but are available from the corresponding author on reasonable request.

Ethics approval

The study protocol, subject Information and approval form were reviewed and approved by the clinical chemistry unite of the laboratory in al Diwaniyah Teaching Hospital accordance with Document No. 472130 dated (29/10/2024) to obtain this approval.

References

1. Kalra PA. Iron deficiency in renal medicine. *Iron Clin Pract.* 2025:65-69. doi:10.1002/9781394210916.ch10
2. Vaidya SR, Aeddula NR. Chronic kidney disease. In: *StatPearls* [Internet]. StatPearls Publishing; 2024. Accessed July 1, 2025.

3. Aitken E, Anijeet H, Ashby D, et al. UK Kidney Association clinical practice guideline on vascular access for haemodialysis. *BMC Nephrol.* 2025;26(1):461. doi:10.1186/s12882-025-04374-y
4. Yan MT, Chao CT, Lin SH. Chronic kidney disease: strategies to retard progression. Int J Mol Sci. 2021;22(18):10084. doi:10.3390/ijms221810084
5. Guo M, He F, Zhang C. Molecular therapeutics for diabetic kidney disease: an update. *Int J Mol Sci.* 2024;25(18):10051. doi:10.3390/ijms251810051
6. Choukroun G, Kazes I, Dantal J, et al. Prévalence de la carence martiale dans une population de patients insuffisants rénaux chroniques non dialysés: étude nationale multicentrique observationnelle CARENFER. *Néphrol Thérapeut.* 2022;18(3):195-201. doi:10.1016/j.nephro.2021.12.003
7. Minutolo R, Grandaliano G, Di Rienzo P, et al. Prevalence, incidence, and treatment of anaemia in patients with non-dialysis-dependent chronic kidney disease: findings from a retrospective real-world study in Italy. *J Nephrol.* 2023;36(2):347-357. doi:10.1007/s40620-022-01475-x
8. George C, Mogueo A, Okpechi I, Echouffo-Tcheugui JB, Kengne AP. Chronic kidney disease in low-income to middle-income countries: the case for increased screening. *BMJ Glob Heal.* 2017;2(2):e000256. doi:10.1136/bmjgh-2016-000256
9. Safiri S, Amiri F, Karamzad N, Sullman MJM, Kolahi AA, Abdollahi M. Burden and trends of dietary iron deficiency in the Middle East and North Africa region, 1990-2021. *Front Nutr*. 2025;11:1517478. doi:10.3389/fnut.2024.1517478
10. Roemhild K, von Maltzahn F, Weiskirchen R, Knüchel R, von Stillfried S, Lammers T. Iron metabolism: pathophysiology and pharmacology. *Trends Pharmacol Sci*. 2021;42(8):640-656. doi:10.1016/j.tips.2021.05.001
11. Agarwal AK, Yee J. Hepcidin. *Adv Chronic Kidney Dis*. 2019;26(4):298-305. doi:10.1053/j.ackd.2019.04.005
12. Roy JE, Kalaiselvi VS, Shanthi B. Study on serum hepcidin level in chronic kidney disease. *Ann Rom Soc Cell Biol*. 2021;25(1):2715-2727.
13. Ustuner B, Bek S, Eren N, Bakirdogen S, Kalender B. Hepcidin and Vitamin D Levels: Mutual Effects in Anemia of Chronic Kidney Disease. *Kocaeli Üniversitesi Sağlık Bilim Derg*. 2021;7(2):110-114. doi:10.30934/kusbed.661316
14. Gao Z, Hu Y, Gao Y, Ma X, Hu Z. The association of hepcidin, reticulocyte hemoglobin equivalent and anemia-related indicators on anemia in chronic kidney disease. *Medicine (Baltimore)*. 2023;102(17):e33558. doi:10.1097/MD.0000000000033558
15. Sobh MA, Imam HMK, Seddik MI, Sadek DEM. Role of Hepcidin as A Predictor for Iron Metabolism Disorders and Inflammation in Stage 4 Chronic Kidney Disease Patient with Anemia. *Cuest Fisioter*. 2025;54(4):4904-4912. doi:10.48047/CU
16. Tomasz G, Ewa W, Jolanta M. Biomarkers of iron metabolism in chronic kidney disease. *Int Urol Nephrol*. 2021;53(5):935-944. doi:10.1007/s11255-020-02663-z
17. Mula-Abed WAS, Al Rasadi K, Al-Riyami D. Estimated glomerular filtration rate (eGFR): A serum creatinine-based test for the detection of chronic kidney disease and its impact on clinical practice. *Oman Med J*. 2012;27(2):108-113. doi:10.5001/omj.2012.23
18. Wong MMY, Tu C, Li Y, et al. Anemia and iron deficiency among chronic kidney disease Stages 3–5ND patients in the Chronic Kidney Disease Outcomes and Practice Patterns Study: often unmeasured, variably treated. *Clin Kidney J*. 2020;13(4):613-624. doi:10.1093/ckj/sfz091
19. Kwiatkowska E, Opara M, Kwiatkowski S, Domański L, Marchelek-Myśliwiec M, Ciechanowski K. Is transferrin saturation a useful marker of iron metabolism in patients with chronic kidney disease treated with hemodialysis? *Open Urol Nephrol J.* 2019;12:1-7. doi:10.2174/1874303X01912010077
20. Zapora-Kurel A, Malyszko J. Novel iron biomarkers in chronic kidney disease. *Wiad Lek*. 2021;74(12):3230-3233. doi:10.36740/WLek202112119
21. Agarwal AK. Iron metabolism and management: focus on chronic kidney disease. *Kidney Int Suppl.* 2021;11(1):46-58. doi:10.1016/j.kisu.2020.12.003
22. Fujisawa H, Nakayama M, Haruyama N, et al. Association between iron status markers and kidney outcome in patients with chronic kidney disease. *Sci Rep*. 2023;13(1):18278. doi:10.1038/s41598-023-45580-8
23. Rashid RM, Al-Rubaie HA. Evaluation of transferrin saturation and serum ferritin in assessing body iron status in patients with end stage renal disease. *Int J Clin Diagnostic Pathol*. 2024;7(3):30-36. doi:10.33545/pathol.2024.v7.i3a.581
24. Al-Mashdali A, Alyafei T, Yassin M. The Superiority of T2* MRI Over Serum Ferritin in the Evaluation of Secondary Iron Overload in a Chronic Kidney Disease Patient: A Case Report. *J Blood Med*. 2021:665-670. doi:10.2147/JBM.S319591
25. Benjamin S, Assounga A. Transferrin levels are associated with malnutrition markers in hemodialysis patients in KwaZulu-Natal, South Africa. *Ren Fail.* 2024;46(1):2337292. doi:10.1080/0886022X.2024.2337292
26. Mercadal L, Metzger M, Haymann JP, et al. The relation of hepcidin to iron disorders, inflammation and hemoglobin in chronic kidney disease. *PLoS One*. 2014;9(6):e99781. doi:10.1371/journal.pone.0099781
27. Disease K. KDIGO 2024 Clinical Practice Guideline for the Evaluation and Management of Chronic Kidney Disease. *Kidney Int*. 2024;105(4S):S117-S314. doi:10.1016/j.kint.2023.10.01
28. Suh SH, Oh TR, Choi HS, et al. Predictive Value of Serum Hepcidin Levels for the Risk of Incident End-Stage Kidney Disease in Patients with Chronic Kidney Disease: The KNOW-CKD. *Kidney Dis*. 2024;10(6):492-503. doi:10.1159/000542057
29. Niikura T, Maruyama Y, Nakashima S, et al. Hepcidin/ferritin ratios differ among non-dialyzed chronic kidney

disease patients, and patients on hemodialysis and peritoneal dialysis. *Ther Apher Dial*. 2019;23(4):341-346. doi:10.1111/1744-9987.12773

30. Sonkar SK, Singh NK, Sonkar GK, et al. Association of hepcidin and anemia in early chronic kidney disease. *Saudi J Kidney Dis Transpl*. 2019;30(2):315-324. doi:10.4103/1319-2442.256838
31. Sonkar SK, Kumar A, Singh NK, Sonkar GK, Pandey S, Bhosale V. Role of Hepcidin on Response of Erythropoietin Stimulating Agents in Anaemic Advanced Chronic Kidney Disease Patients. *J Clin Diagnostic Res*. 2018;12(10):OC14--OC16. doi:10.7860/JCDR/2018/36051.12142

Rzeszów University Press 2026
ISSN 2544-1361 (online)
doi: 10.15584/ejcem.2026.1.8

http://www.ejcem.ur.edu.pl
European Journal of Clinical and Experimental Medicine
Eur J Clin Exp Med 2026; 24 (1): 23–31

ORIGINAL PAPER

Molecular analysis of BCR-ABL1 fusion transcripts in acute leukemia patients in Southern Odisha, India

Sheetal Sabat [1], Aparupa Naik [2], Prasanta Purohit [2], Snehal Bholo [2], Chinmayee Parida [2], Manoj Kumar Patro [1], Samira Kumar Behera [1]

[1] Department of Pathology, M.K.C.G. Medical College, Berhampur, Odisha, India
[2] Multi-Disciplinary Research Unit, M.K.C.G Medical College, Berhampur, Odisha, India

ABSTRACT

Introduction and aim. The occurrence of BCR-ABL1 fusion transcript in acute-leukemia cases are limited and is characterized with various subtypes. This study was based on investigation of the BCR-ABL1 fusion transcript in acute-leukemia cases in a tertiary care hospital.

Material and methods. This cross-sectional study was carried out in suspected cases of acute leukemia. Cases were analyzed for complete blood counts, peripheral smear, bone marrow and flow-cytometry for the diagnosis of acute-leukemia. Additionally, diagnosed cases were investigated for BCR-ABL1 fusion transcript by PCR amplification using reverse transcriptase enzyme followed by documentation.

Results. Approximately 55 acute leukemia cases included, diagnosed by flow cytometric analysis. Analysis of the BCR-ABL1 fusion-transcript in 55 cases showed its occurrence in only 2 cases, where one case with the B-ALL was characterized with e1a2 subtype and a other case with AML was characterized with the e13a2 subtype.

Conclusion. The BCR-ABL1 fusion transcript in acute-leukemia cases was found in 3.64% (2/55) of cases. The diagnosis of BCR-ABL1 fusion transcript in acute-leukemia cases is important for its poor prognosis, as well as calls for the use of ABL tyrosine kinase inhibitors. The diagnosis of BCR-ABL1 fusion-transcript in acute leukemia cases in a tertiary health care facility will be helpful for better treatment of patients in the study area.

Keywords. acute leukemia, acute lymphoblastic leukemia, acute myeloid leukemia, BCR-ABL1fusion transcript, polymerase chain reaction

Introduction

According to the Global Cancer Project (GLOBOCAN, 2022) report, leukemia ranks 13th as the most diagnosed cancer and 10th most common cause of cancer death globally, accounting for 487,294 new cases and 305,405 cancer deaths.[1] According to the fourth edition of the WHO classification of tumors of hematopoietic and lymphoid tissues, leukemia can be broadly classified into myeloid or lymphoid lineages.[2] In India, the incidence of chronic myeloid leukemia (CML) was 0.8–2.2 among 100,000 males and 0.6-1.6 in 100,000 female subjects respectively; while acute leukemia (AL) including acute lymphoblastic leukemia (ALL) and acute myeloid leukemia (AML) are 35% and 15% respectively.[3,4]

There are several subtypes of leukemia based on its gene alteration and prognosis, including BCR-ABL1 fusion transcript. The BCR-ABL1 transcript is gen-

Corresponding author: Samira Kumar Behera, e-mail: samirbehera41@gmail.com

Received: 3.06.2025 / Revised: 15.08.2025 / Accepted: 28.09.2025 / Published: 30.03.2026

Sabat S, Naik A, Purohit P, Bholo S, Parida C, Patro MK, Behera SK. Molecular analysis of BCR-ABL1 fusion transcripts in acute leukemia patients in Southern Odisha, India. *Eur J Clin Exp Med.* 2026;24(1):23–31. doi: 10.15584/ejcem.2026.1.8.

erated by balanced reciprocal translocation between chromosomes 9 and 22 to generate a short chromosome called the Philadelphia (Ph) chromosome {t(9;22)(q34.1;q11.2)}. The breakpoint cluster region (Bcr), composed of 23 exons and breakpoint 9 is present between 1a,1b and a2, whereas the breakpoint location on the BCR gene occurs between b1-b5 exons, e1-e2 and e19-e20, called major breakpoint cluster region (M-bcr) with molecular weight p210 (e13a2or e14a2), minor (m-bcr) with molecular weight p190 (e1a2) and micro (μ-bcr) p230 (e19a2) respectively. Furthermore, atypical BCR breakpoints outside the cluster regions generated by gene alteration to generate proteins such as e8a2, e15a2, e13a3, e14a3, and e6a2, where clinical significance was being investigated for the same.[5,6]

Although Ph chromosomes have been used as diagnostic markers in CML cases, there occurrence in AL cases is rare and limited to case series only. According to the WHO classification 2016, AML with BCR-ABL1 is rare and termed as subtype 2 contributing to approximately less than 1% of new cases of AML.[7-9] There are many reports on the presence of BCR-ABL1 fusion transcripts in ALL cases in India,10-14, while there is a paucity of report on AML, so this study was designed to determine the frequency of BCR-ABL1 fusion transcripts in cases diagnosed with AL in a tertiary health care setup in the state of Odisha, India.

Aim

This study was carried out to analyze the BCR-ABL1 fusion transcripts in cases of AL diagnosed in a tertiary health care setting in the state of Odisha, India.

Material and methods

This was a cross-sectional study carried out in cases suspected with AL, attending the outpatient Department of Medicine and the Department of Pediatrics in KCG. Medical College and Hospital, Berhampur, Odisha, from April 2022 to March 2024. After obtaining the proper consent of the patients (in the case of minors, consent has been obtained from either parents or guardians), 3 ml of venous blood or bone marrow samples were collected from the subjects in EDTA vials for various investigations including examination of peripheral smear (PS)/bone marrow (BM), complete blood counts (CBC), flow cytometer analysis and BCR-ABL1 fusion transcript. The complete blood count was performed using a 5-part differential analyzer (XN-550, Sysmex Europe SE, Hamburg, Germany). The flow cytometer analysis for the diagnosis of AL was performed using 6 colors BD FACS Canto™-II flow cytometer (BD Biosciences, 2350 Qume Drive, San Jose, CA, USA) using BD FACSDiva™ Software v8.0.2 with a predefined panel of antibodies (BD Lifesciences) within 24 hours after sample collection (supplementary Table1).

AL cases of all age groups and both genders were recruited. Taking into account the occurrence of the BCR-ABL1 fusion transcript in AL cases of around 7%,[15] population size of 100 (50 AL cases per year in the study center) with 95% confidence level and absolute error of 5%, the minimum number of samples required for the study (sample size) was 51 (sample size was calculated using OpenEpi, open source calculator, SSPropor, Version 3). Along with the AL cases, some known CML cases attending this hospital during the study period were included for standardization of the molecular investigation of BCR-ABL1 fusion transcript. This study was approved by the Institutional Ethics Committee (IEC) of M.K.C.G Medical College, Berhampur, Odisha, India. (No. 1381/Chairman-IEC, MKCG Medical College, Brahmapur-4).

All confirmed cases of AL were subjected for analysis of BCR-ABL1 fusion transcript. Briefly, the RNA was isolated from fresh blood samples using an RNA isolation kit (HiPureA Blood RNA Purification Kit, HiMedia Laboratories Pvt. Ltd.) according to the manufacturer's instructions and cDNA was prepared using the SuperScript TM VILOTM cDNA synthesizer kit (Invitrogen by Thermo Fisher Scientific Inc.) by taking 4 μL of 5X VILO™ Reaction Mix, 2μL 10X Superscript TM enzyme mix, 2.5 μg of isolated RNA and DEPC treated water to make up the volume to20 μL. The incubation period for the preparation of the cDNA was at 25°C for 10 minutes, 42°C for 60 minutes, 85°C for 5 minutes followed by 4°C.

The BCR-ABL1 fusion transcript was analyzed by PCR using the primers described by Aazad et al. for the regions e1a2, e13a2, and e14a2.[16] In detail, a single PCR reaction included 20ng of the cDNA, 25 mM $MgCl_2$, 10 mM of dNTP mix, primer of 10 picomoles each and 5 units of Taq DNA polymerase with a final volume of 25μL. The reaction condition for the amplification was carried out with denaturation at 94°C for 35 seconds, annealing at 61°C for 30 seconds, and extension at 72°C for 30 seconds for 30 cycles followed by electrophoresis and documentation. The primers and amplicon size of various BCR-ABL1 fusion transcripts are depicted in Table 1. Amplified products were resolved in 2% agarose gel with a 100-bp DNA ladder as a marker (Figure 1).

Data collection and statistical analysis

All patient information, including socio-demographic and laboratory data, was collected in a case format. The generated data were entered in an excel sheet for further analysis. Descriptive data was presented in numbers and percentages. The recruited cases were categorized into different groups according to the types of leukemia (CML, B-ALL, T-ALL and AML) and types of BCR-ABL1 fusion transcripts (normal, e1a2, e13a2 (b2a2) and e14a2 (b3a2).

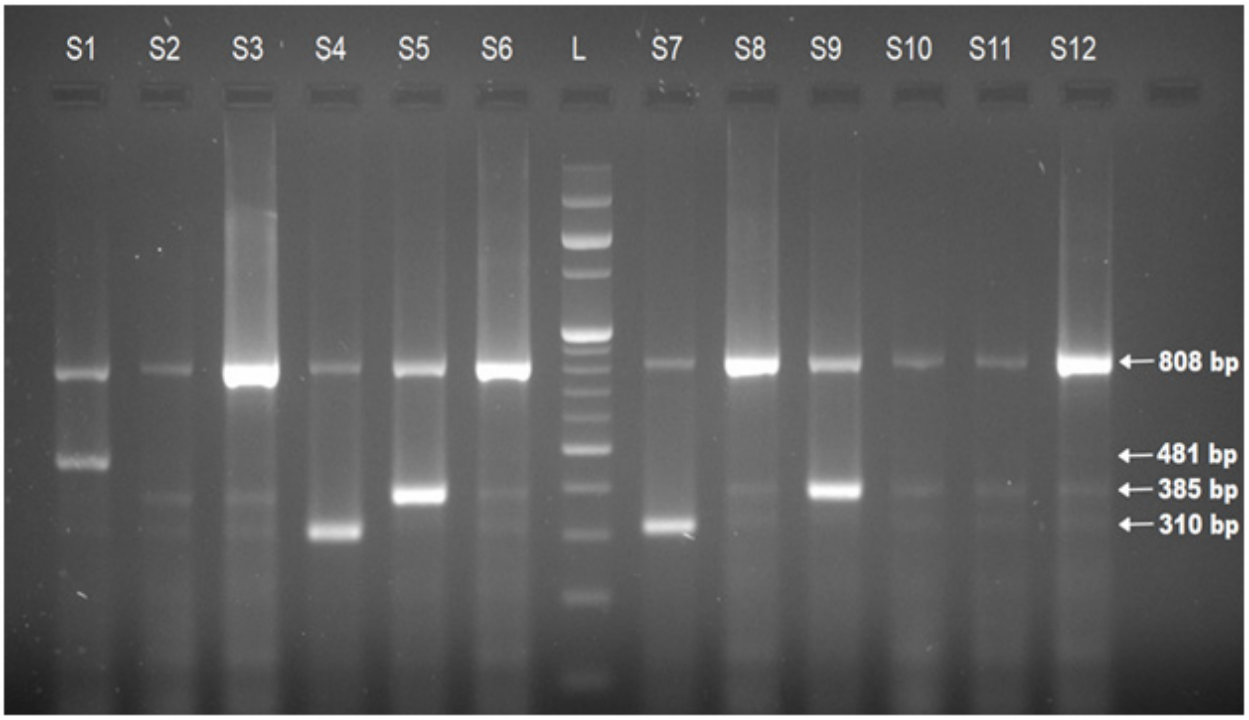

Fig. 1. Agarose gel electrophoresis (2%) for the BCR-ABL1 fusion transcript (Lane S2, S3, S6, S8, S10, S11 and S12 with 808 bp: Normal; Lane S1 with 481 bp: e1a2; Lane S4 and S7 with 310 bp: e13a2; Lane S5 and S9 with 385 bp: e14a2; L: 100bp DNA ladder)

Results

The study was carried out in 69 cases of leukemia, including 55 suspected cases of AL and 14 cases of CML. The 55 suspected cases were confirmed to be AL by flow cytometry analysis, including 30 (54.5%) males and 25 (45.5%) female cases. The mean age of the patients was 26.82±18.94 years (age range of 1 year to 65 years) and 27 (49.1%) being in pediatric population. The age and gender distribution of patients is depicted in Figure 2.

The flow cytometer analysis of 55 AL cases resulted in 25 ALL cases (14 cases with B-ALL and 11 cases with T-ALL) and the remaining 30 cases were diagnosed with AML. The molecular analysis of the the subtypes of BCR-ABL1 fusion transcript in both CML and AL patients showed the presence of the BCR-ABL1 fusion transcript in all CML cases and only 2 (3.64%) cases of AL (1 case each with AML and B-ALL). The AML case had a BCR-ABL1 fusion transcript with the e13a2 subtype while the B-ALL case had a BCR-ABL1 fusion transcript with the e1a2 subtype. The detailed analysis of the BCR-ABL1 fusion transcript subtypes in the study cases is depicted in Table 2.

The hematological presentation of both cases, AML with BCR-ABL1 fusion transcript with the e13a2 subtype (case 1) and B-ALL with BCR-ABL1 fusion transcript with e1a2 subtype (case 2), are described in details.

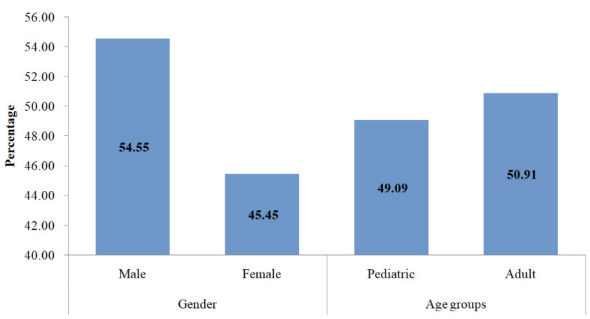

Fig. 2. Age and sex distribution of patients with AL (n=55)

Case 1. AML case with BCR-ABL1 fusion transcript (e13a2)

An 11-year-old boy was admitted with fever, weakness, and a history of weight loss for 15 days without a relevant medical history. Physical examination revealed pallor and the absence of hepatomegaly as well as splenomegaly. Furthermore, biochemical examination it was observed, ESR of 170 mm in 1st hour and CBC bicytopenia (hemoglobin level of 4.7 g/dL, white blood cell count of 10.43×10^9/L and platelet count of 27×10^9/L). The peripheral smear showed blast cells and bone marrow aspiration revealed hypercellular marrow with 40% blast. The blast cells were medium to large in size having round to oval nuclei and some had irregular nuclear borders with fine chromatin, some blast cells showed 1-2 inconspicuous nucleoli and scanty granular basophilic cytoplasm. The cytochemistry of the blast cells showed positivity for the MPO stain and negative

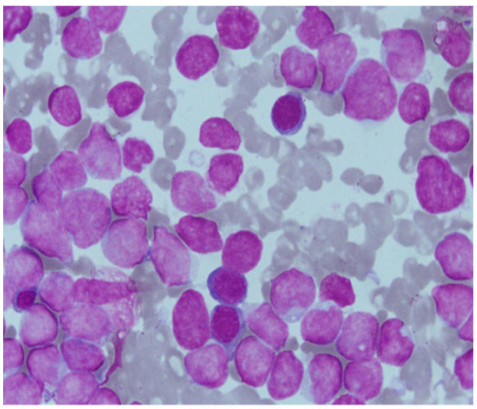

Leishman stain (100x10) of Bone Marrow

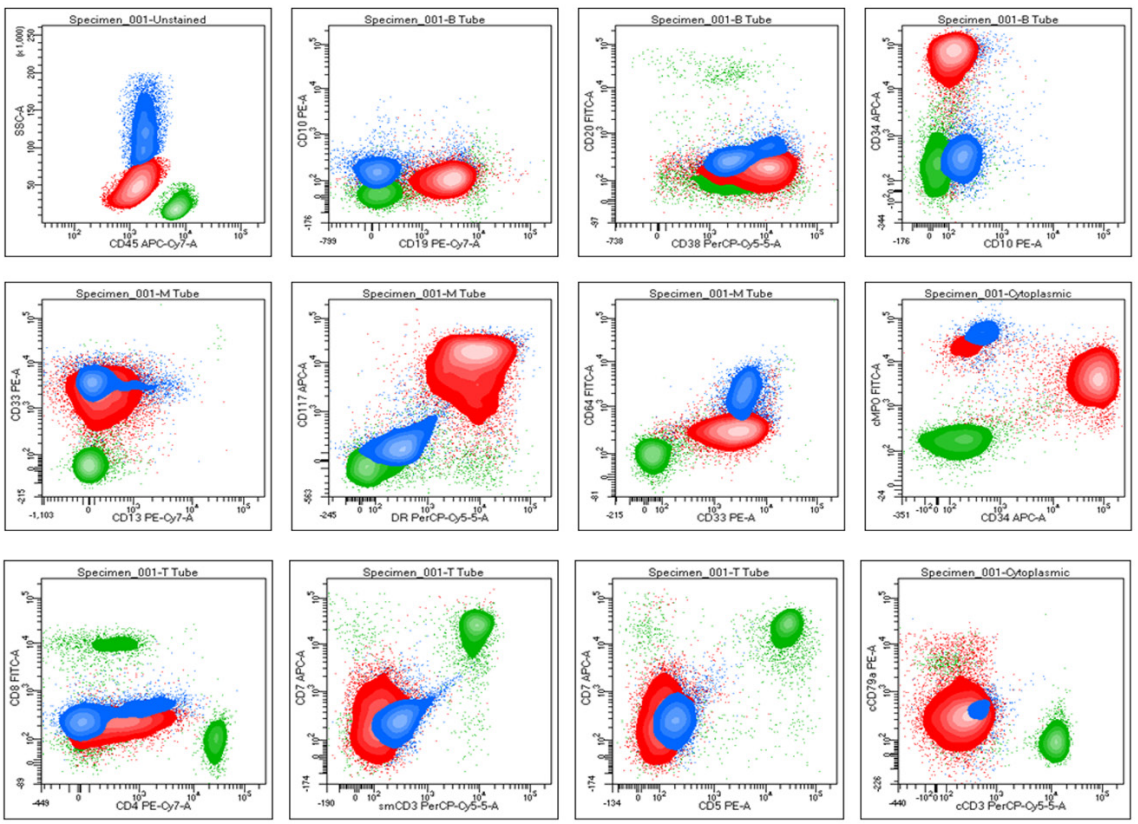

Flow cytometry analysis

Fig. 3. Flow cytometric analysis of AML case with BCR-ABL1 fusion transcript

for the PAS stain. Thus, PS, bone-marrow study and cytochemistry, the case was diagnosed as AML. Therefore, the sub-classification of leukemia subclassification was performed by flowcytometry and the blast cells were positive for CD19, CD38, CD34, CD33, CD117, HLA-DR, CD4, CD7 and MPO; and negative for CD10, CD20, CD79a, smCD3, cyCD3, CD5, CD8, CD13 and CD64. Therefore, the final diagnosis based on flow cytometry was compatible with AML with differentiation and aberrant expression of CD4, CD7 and CD19 (Figure 3). The bone marrow was not done and subsequently the molecular analysis of BCR-ABL1 fusion transcript revealed the presence of Major subtype (M-bcr) BCR-ABL1 fusion transcript.

Case 2. B-ALL case with BCR-ABL1 fusion transcript (e1a2)

A 19-year-old male patient complained of fever and weakness without any relevant history since 45 days. On physical examination, it was revealed pallor and absence of hepatomegaly and splenomegaly were revealed. Additionally, CBC showed bicytopenia (hemoglobin level of 5.5g/dL, white blood cell count of 8.97x 10^9/L, and platelet count of 14x10^9/L) and bone marrow aspiration

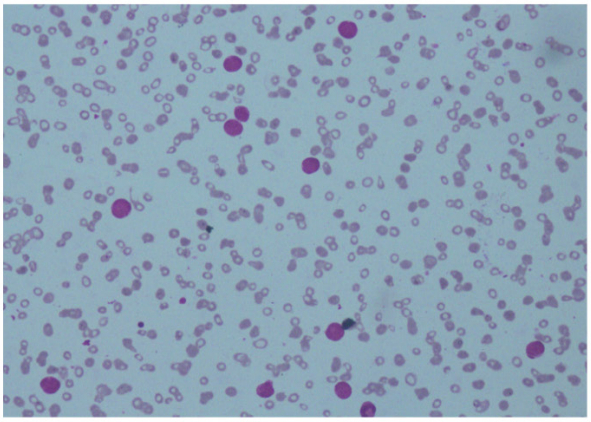

Leishman stain (40x10) of Perpheral Blood

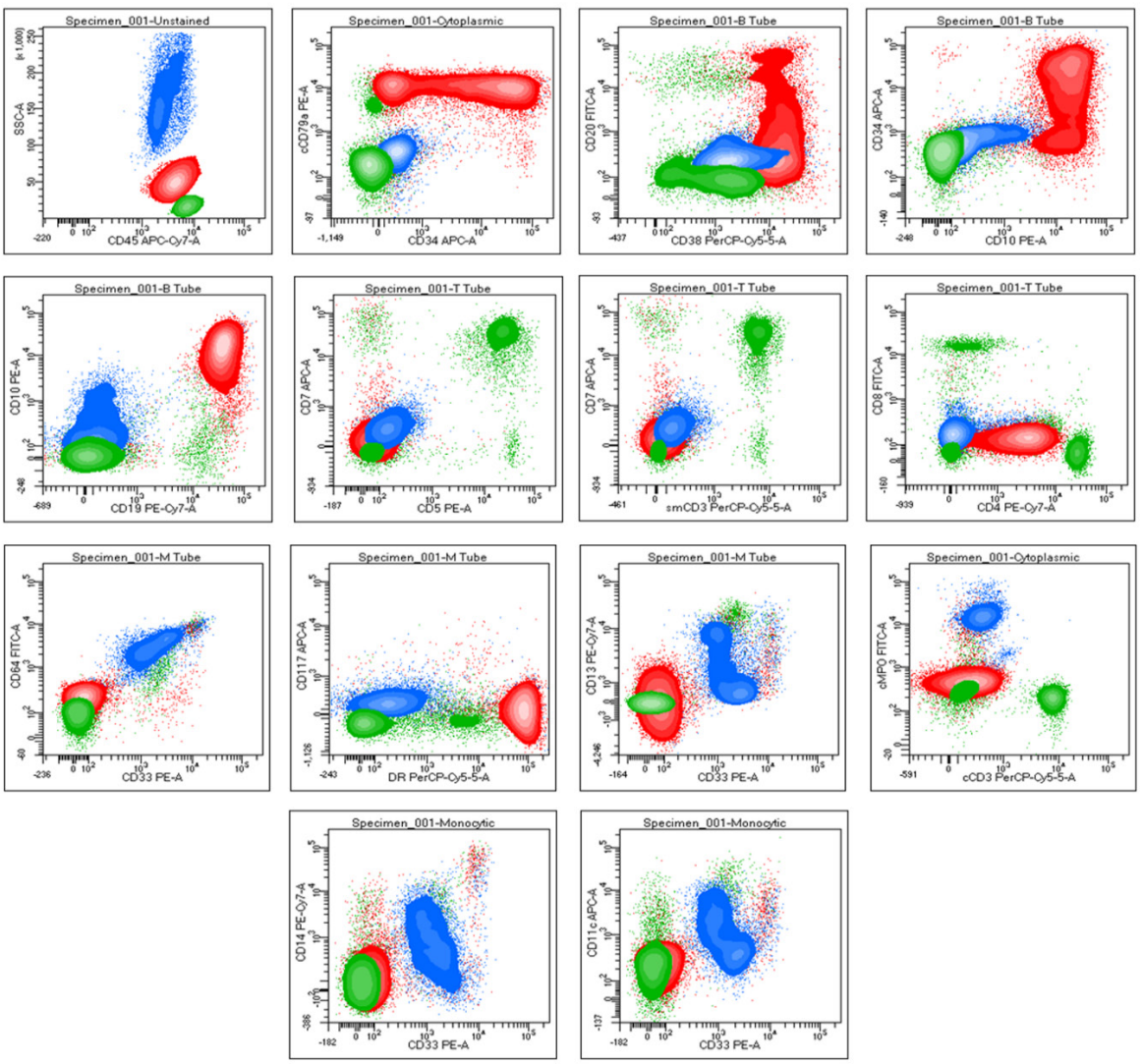

Flow cytometry analysis

Fig. 4. Flow cytometric analysis of ALL case with BCR-ABL1 fusion transcript

revealed hypercellular marrow with variable-size leukemic blast of 45%. The blasts were small to medium in size, had round to oval nuclei with coarse chromatin, and had little granular basophilic cytoplasm. The cytochemistry of the blasts is blocked positive (course positive) with PAS stain and negative for MPO stain. Therefore, the diagnosis based on morphology was a case of ALL. The flow-cytometric analysis showed, that the blasts population was positive for CD79a, CD34, CD38, CD10, CD19, CD4, CD13, and HLA-DR, and negative for CD20, CD5, CD7, CD8, smCD3, cyCD3, CD33, CD64, CD117, MPO, CD14, and CD11c. Therefore, the diagnosis based on flow cytometry was B-ALL with aberrant expression of CD13 and CD4 (Figure 4). The bone marrow cytogenetic study was not analyzed. Analysis of the BCR-ABL1 fusion transcript revealed the presence of a minor subtype (m-bcr) e1a2 (p190) BCR- ABL1 fusion transcript.

Table 1. List of primers used for BCR-ABL1 fusion transcript analysis

Transcript	Primers	Primer sequences (5'-------3')	Amplicon size (base pairs)
Normal BCR	B2B+C5e	ACAGAATTCCGCTGACCATCAATAAG ATAGGATCCTTTGCAACCGGGTCTGAA	808
e1a2	BCR-C+CA3	ACCGCATGTTCCGGGACAAAAG TGTTGACTGGCGTGATGTAGTTGCTTGG	481
e13a2 (b2a2)	B2B+CA3	ACAGAATTCCGCTGACCATCAATAAG TGTTGACTGGCGTGATGTAGTTGCTTGG	310
e14a2 (b3a2)	B2B+CA3	ACAGAATTCCGCTGACCATCAATAAG TGTTGACTGGCGTGATGTAGTTGCTTGG	385

Table 2. BCR-ABL1 fusion transcript in different cases of leukemia (n=69) *

Type of leukemia	Subtypes of the BCR-ABL1 fusion transcript subtypes		
	e13a2	e14a2	e1a2
CML (n=14)	5	8	1
AML (n=30)	1	0	0
B-ALL (n=14)	0	0	1
T-ALL (n=11)	0	0	0

* CML – chronic myeloid leukemia, AML – acute myeloid leukemia, B-ALL – B-acute lymphoblastic leukemia, T-ALL – T-acute lymphoblastic leukemia

Discussion

During the study period, a total of 55 patients diagnosed with AL by flow cytometry were included along with 14 patients with CML for the molecular characterization of the BCR-ABL1 fusion transcript. Although the main objective of this study was to observe the presence of the BCR-ABL1 fusion transcript only in cases only, the CML cases were included for standardization of molecular analysis of BCR-ABL1 fusion transcript in the study center. Out of 55 cases with AL, 30 (54.5%), 14 (25.5%) and 11 (20.0%) cases were diagnosed with AML, B-ALL and T-ALL respectively.

Among the 14 cases with CML, the BCR-ABL1 fusion transcript has been characterized in all cases. Most (8 cases) of cases were diagnosed as e14a2, followed by 5 cases with e13a2 type and one single case with e1a2 type. All the CML cases analyzed in the present study were characterized by a typical type of BCR-ABL1 fusion transcript, which is consistence with many previous reports. Along with the typical types, many atypical types like e13a3 and e14a3 have also been reported from many previous studies.[17-22]

The BCR-ABL1 fusion transcript was found to be positive in only 2 cases of 55 cases of AL. One case with AML (out of 30 cases) was of type e13a2 type and another case with B-ALL (out of 14 cases) presented with e1a2 type. Although the BCR-ABL1 fusion transcript is the hallmark for CML, cases with ALL or AML have also been reported with the BCR-ABL1 fusion transcript. It has also been reported that around 2-3% of children and around 20-30% of adults diagnosed with ALL may present with this translocation.[23] The presence of AML de novo with BCR-ABL1 fusion transcript is rare with an incidence rate of 0.5-3%.[8,24,25] Both cases of AML and B-ALL cases with BCR-ABL1 fusion transcript in this present study presented with a typical type of translocation; while the occurrence of many atypical types has also been reported in many studies.[15]

Both the cases with the AML and B-ALL with BCR-ABL1 fusion transcript in this study showed aberrant expression of various CD markers. The AML case with the BCR-ABL1 fusion transcript had aberrant expression of CD4, CD7, and CD19 whereas the B-ALL case with translocation had aberrant expression of CD4 and CD13. There is no consistency in the expression of various CD markers in both AML and ALL with respect to the BCR-ABL1 fusion transcript. However, most studies have reported with aberrant expression of CD7 in cases of AML cases with BCR-ABL1 fusion transcript,[7,26,27] and CD13 in ALL cases with the BCR-ABL1 fusion transcript.[28-30] Aberrant expression of CD markers in AL cases with BCR-ABL1 fusion transcript does not have any clinically significant influence on treatment outcome; but there is a recommendation for the analysis of other genetic associations for better clinical outcomes.[31]

The diagnosis of the BCR-ABL1 fusion transcript in AL is important due to its poor prognosis under conventional therapy in patients with AL, which in turn identified them as high-risk groups. Furthermore, these patients may have a better prognosis in treatment regimens with ABL tyrosine kinase inhibitors such as imatinib or dasatinib.[32-35] Acute leukemia with BCR-ABL1 fusion transcript has been included in the updated WHO (2016) as a provisional entity.[36] AML with the BCR-ABL1 fusion transcript is stratified and allocated as an intermediate risk group according to the European LeukemiaNet risk stratification and a poor risk

group according to the National Comprehensive Cancer Network.[37,38] Thus, it is a need for molecular characterization of the BCR-ABL1 fusion transcript in all newly diagnosed cases with AL for better treatment and survival of the patients.

There are few limitations in this study. First, in this study only 3 typical types of BCR-ABL1 fusion transcript have been considered for the analysis by using conventional PCR methods; the occurrence of other rare or atypical types of BCR-ABL1 fusion transcript in our study population cannot be ignored as we have not analyzed in this study. Second, as a diagnostic center, there is a paucity of information on clinical outcomes as well as treatment regimens, or the follow-up data of the patients.

In conclusion, this is a pilot study carried out to initiate the BCR-ABL1 fusion transcript in flow cytometric confirmed cases with AL in a tertiary health care center in southern Odisha, India. With a low prevalence (2 out of 55 cases) of BCR-ABL1 fusion transcript in overall AL cases in the study population, warn against the analysis of other rare translocation types for better treatment, risk stratification and clinical outcomes of patients.

Acknowledgements

The authors acknowledge laboratory technicians, Mrs. M. Radha Rani Dora and Mr. Himanshu Sekhar Sahu, for processing blood samples during the investigation. The authors also acknowledge Mr. Satyanarayana Mohanty, Data Entry Operator, MRU, for data processing.

Declarations

Funding

This study (Research proposal ID: MKCGMC/MRU/034/2021) was funded by Department of Health Research, Ministry of Health and Family Welfare, Government of India for the establishment of Multi-Disciplinary Research Unit (MRU) at Maharaja Krishna Chandra Gajapati (M.K.C.G.) Medical College, Berhampur, Odisha, India

Author contributions

Conceptualization, M.K.P. and S.K.B.; Methodology, S.S., S.B., C.P. and P.P; Validation, P.P. and S.K.B.; Formal Analysis, S.S. and P.P.; Investigation, S.S., S.B., C.P. and P.P; Resources, S.S. and P.P.; Data Curation, P.P.; Writing – Original Draft Preparation, S.S., A.N., and P.P.; Writing – Review & Editing, A.N., P.P., M.K.P. and S.K.B.; Supervision, M.K.P. and S.K.B.; Project Administration, S.K.B.; Funding Acquisition, S.K.B.

Conflicts of interest

The authors declare no conflicts of interest.

Data availability

The data will be available on request to corresponding author.

Ethics approval

This study was approved by the Institutional Ethical Committee (IEC) of M.K.C.G Medical College, Berhampur, Odisha, India. (No. 1381/Chairman-IEC, M.K.C.G. Medical College, Brahmapur-4).

Reference

1. GLOBOCAN, 2022 https://gco.iarc.who.int/media/globocan/factsheets/populations/900-world-fact-sheet.pdf. Accessed September 3, 2024.
2. Du M, Chen W, Liu K, et al. The Global Burden of Leukemia and Its Attributable Factors in 204 Countries and Territories: Findings from the Global Burden of Disease 2019 Study and Projections to 2030. *J Oncol*. 2022;2022:1612702. doi:10.1155/2022/1612702
3. Kumar L. Chronic myelogenous leukaemia (CML): an update. *Natl Med J India*. 2006;19(5):255-263.
4. Ahirwar R, Nigam RK, Parmar D. A study of leukemias Profile in central India. *Tropical Journal of Pathology and Microbiology*. 2018;4(2):181-187. doi:10.17511/jopm.2018.i02.12
5. Carter BZ, Mak DH, Cortes J, Andreeff M. The elusive chronic myeloid leukemia stem cell: does it matter and how do we eliminate it? *Semin Hematol*. 2010;47(4):362-370. doi:10.1053/j.seminhematol.2010.06.006
6. Yao J, Douer D, Wang L, Arcila ME, Nafa K, Chiu A. A case of acute myeloid leukemia with e6a2 BCR-ABL fusion transcript acquired after progressing from chronic myelomonocytic leukemia. *Leuk Res Rep*. 2017;7:17-19. doi:10.1016/j.lrr.2017.01.003
7. Sheets JW, Eulitt P, He R, et al. Philadelphia Chromosome-positive Acute Myeloid Leukemia With e1a3 BCR--ABL1 Fusion Transcript. *Hemasphere*. 2020;4(6):e484. doi:10.1097/HS9.0000000000000484
8. Soupir CP, Vergilio JA, Dal Cin P, et al. Philadelphia chromosome-positive acute myeloid leukemia: a rare aggressive leukemia with clinicopathologic features distinct from chronic myeloid leukemia in myeloid blast crisis. *Am J Clin Pathol*. 2007;127(4):642-650. doi:10.1309/B4NVER1AJJ84CTUU
9. Loknatha D, Rao SA, Lokesh KN, Babu KG, Suresh Babu MC, Lakshmaiah KC. A case series of patients with de novo Philadelphia-positive acute myeloid leukemia at a tertiary care center in South India - clinical profile, outcomes, and review of literature. *Journal of Applied Hematology* 2016;7(2):66-69. doi:10.4103/1658-5127.186326
10. Mondal BC, Bandyopadhyaya A, Majumdar S, et al. Molecular profiling of chronic myeloid leukemia in eastern India. *Am J Hematol* 2006;81:845-849. doi:10.1002/ajh.20682
11. Hasan SK, Sazawal S, Kumar B, et al. Childhood CML in India: b2a2 transcript is more common than b3a2. *Cancer Genet Cytogenet*. 2006;169(1):76-77. doi:10.1016/j.cancergencyto.2006.01.015

12. Polampalli S, Choughule A, Negi N, et al. Analysis and comparison of clinicohematological parameters and molecular and cytogenetic response of two Bcr/Abl fusion transcripts. *Genet Mol Re*s. 2008;7(4):1138-1149. doi:10.4238/vol7-4gmr485.
13. Sharma P, Kumar L, Mohanty S, Kochupillai V. Response to Imatinib mesylate in chronic myeloid leukemia patients with variant BCR-ABL fusion transcripts. *Ann Hematol*. 2010;89(3):241-247. doi:10.1007/s00277-009-0822-7
14. Anand MS, Varma N, Varma S, Rana KS, Malhotra P. Cytogenetic & molecular analyses in adult chronic myelogenous leukaemia patients in north India. *Indian J Med Res*. 2012;135(1):42-48. doi:10.4103/0971-5916.93423
15. Gupta DG, Varma N, Naseem S, et al. Characterization of immunophenotypic aberrancies with respect to common fusion transcripts in B-Cell precursor acute lymphoblastic leukemia: A report of 986 Indian patients. *Turk J Haematol*. 2022;39:1-12 doi:10.4274/tjh.galenos.2021.2021.0326
16. Azad NA, Shah ZA, Pandith AA, et al. Prognostic Implication of BCR-ABL Fusion Transcript Variants in Chronic Myeloid Leukemia (CML) Treated with Imatinib. A First of Its Kind Study on CML Patients of Kashmir. *Asian Pac J Cancer Prev*. 2018;19(6):1479-1485. doi:10.22034/APJCP.2018.19.6.1479
17. Li Y, Zhang Y, Meng X, et al. Chronic myeloid leukemia with two rare fusion gene transcripts of atypical BCR::ABL: A case report and literature review. *Medicine (Baltimore)*. 2024;103(3):e36728. doi:10.1097/MD.0000000000036728.
18. Massimino M, Stella S, Tirrò E, et al. Rapid decline of Philadelphia-positive metaphases after nilotinib treatment in a CML patient expressing a rare e14a3 BCR-ABL1 fusion transcript: A case report. *Oncol Lett*. 2019;18(3):2648-2653. doi:10.3892/ol.2019.10558.
19. Sazawal S, Chhikara S, Singh K, et al. Distribution of common BCR-ABL fusion transcripts and their impact on treatment response in Imatinib treated CML patients: A study from India. *Indian J Pathol Microbiol*. 2019;62(2):256-260. doi:10.4103/IJPM.IJPM_726_17.
20. Chisti MM, Sanders DS. Chronic Myeloid Leukemia with b3a3 (e14a3) Fusion: A Rare BCR/ABL Rearrangement Presenting with Thrombocytosis - Does MTHFR Polymorphism Matter. *Case Rep Oncol*. 2018;11(2):485-492. doi:10.1159/000490697
21. Duan MH, Li H, Cai H. A rare e13a3 (b2a3) BCR-ABL1 fusion transcript with normal karyotype in chronic myeloid leukemia: The challenges in diagnosis and monitoring minimal residual disease (MRD). *Leuk Res*. 2017;59:8-11. doi:10.1016/j.leukres.2017.05.009
22. Hu LH, Pu LF, Yang DD, et al. How to detect the rare BCR-ABL (e14a3) transcript: A case report and literature review. *Oncol Lett*. 2017;14(5):5619-5623. doi:10.3892/ol.2017.6847
23. Chissoe SL, Bodenteich A, Wang YF, et al. Sequence and analysis of the human ABL gene, the BCR gene, and regions involved in the Philadelphia chromosomal translocation. *Genomics*. 1995;27(1):67-82. doi:10.1006/geno.1995.1008.
24. Takeuchi A, Kondo T, Tasaka T, et al. Successful treatment with ABL tyrosine kinase inhibitor for patients with acute myeloid leukemia with BCR-ABL1. *Leuk Res Rep*. 2022;17:100309. doi:10.1016/j.lrr.2020.100233
25. Low SK, Nanua S, Patel M, Renteria AS. AML with BCR--ABL1 Fusion treated with Imatinib, a Hypomethylating Agent and Venetoclax. *Leuk Res Re*p. 2022;17:100333. doi:10.1016/j.lrr.2022.100333
26. Piedimonte M, Ottone T, Alfonso V, et al. A rare BCR--ABL1 transcript in Philadelphia-positive acute myeloid leukemia: case report and literature review. *BMC Cancer*. 2019;19(1):50. doi:10.1186/s12885-019-5265-5
27. da Silva FB, Machado-Neto JA, Koury LCA, et al. Case Report Acute myeloid leukemia with e1a2 BCR-ABL1 fusion gene: two cases with peculiar molecular and clinical presentations. *Rev Bras Hematol Hemoter*. 2017;39(4):379-384. doi:10.1016/j.bjhh.2017.07.001
28. Shin SY, Cho JH, Kim HJ, Jang JH, Lee ST, Kim SH. Two cases of acute lymphoblastic leukemia with an e1a3 BCR--ABL1 fusion transcript. *Ann Lab Med*. 2015;35(1):159-161. Erratum in: *Ann Lab Med*. 2015;35(4):477. doi:10.3343/alm.2015.35.1.159
29. Deshpande PA, Srivastava VM, Mani S, et al. Atypical BCR-ABL1 fusion transcripts in adult B-acute lymphoblastic leukemia, including a novel fusion transcript-e8a1. *Leuk Lymphoma*. 2016;57(10):2481-2484. doi:10.3109/10428194.2016.1151512.
30. Chen Z. The e1a3 BCR-ABL1 fusion transcript in Philadelphia chromosome-positive acute lymphoblastic leukaemia: a case report. *Hematology.* 2023;28(1):2186040. doi:10.1080/16078454.2023.2186040
31. Jaso J, Thomas DA, Cunningham K, et al. Prognostic significance of immunophenotypic and karyotypic features of Philadelphia positive B-lymphoblastic leukemia in the era of tyrosine kinase inhibitors. *Cancer*. 2011;117(17):4009-4017. doi:10.1002/cncr.25978
32. Gleissner B, Gökbuget N, Bartram CR, et al. German Multicenter Trials of Adult Acute Lymphoblastic Leukemia Study Group. Leading prognostic relevance of the BCR--ABL translocation in adult acute B-lineage lymphoblastic leukemia: a prospective study of the German Multicenter Trial Group and confirmed polymerase chain reaction analysis. *Blood.* 2002;99(5):1536-1543. doi:10.1182/blood.v99.5.1536
33. Talpaz M, Shah NP, Kantarjian H, et al. Dasatinib in imatinib-resistant Philadelphia chromosome-positive leukemias. *N Engl J Med*. 2006;354(24):2531-2541. doi:10.1056/NEJMoa055229
34. Pfeifer H, Cazzaniga G, van der Velden VHJ, et al. Standardisation and consensus guidelines for minimal residual disease assessment in Philadelphia-positive acute lymphoblastic leukemia (Ph + ALL) by real-time quantitative reverse transcriptase PCR of e1a2 BCR-ABL1. *Leukemia.*

2019;33(8):1910-1922. doi:10.1038/s41375-019-0413-0. Erratum in: *Leukemia*. 2020;34(7):1970.

35. Leoni V, Biondi A. Tyrosine kinase inhibitors in BCR-ABL positive acute lymphoblastic leukemia. *Haematologica*. 2015;100(3):295-299. doi:10.3324/haematol.2015.124016
36. Arber DA, Orazi A, Hasserjian R, et al. The 2016 revision to the World Health Organization classification of myeloid neoplasms and acute leukemia. *Blood*. 2016;127(20):2391-2405. doi:10.1182/blood-2016-03-643544
37. Döhner H, Wei AH, Appelbaum FR, et al. Diagnosis and management of AML in adults: 2022 recommendations from an international expert panel on behalf of the ELN. *Blood*. 2022;140(12):1345-1377. doi:10.1182/blood.2022016867
38. Pollyea DA, Altman JK, Assi R, et al. Acute Myeloid Leukemia, Version 3.2023, NCCN Clinical Practice Guidelines in Oncology. *J Natl Compr Canc Netw*. 2023;21(5):503-513. doi:10.6004/jnccn.2023.0025

Rzeszów University Press 2026
ISSN 2544-1361 (online)
doi: 10.15584/ejcem.2026.1.9

http://www.ejcem.ur.edu.pl
European Journal of Clinical and Experimental Medicine
Eur J Clin Exp Med 2026; 24 (1): 32–39

ORIGINAL PAPER

Clinical impact of a personalized hypertension care approach on blood pressure and quality of life in older adults

Hendri Tamara Yuda [1,2], Syed Sharizman Bin Syed Abdul Rahim [3], Mohd Faizal Madrim [3], Putra Agina Widyaswara Suwaryo [4]

[1] Faculty of Medicine and Health Science, Universiti Malaysia Sabah, Kinabalu, Malaysia
[2] Department of Family and Gerontics, Faculty of Health Science, Universitas Muhammadiyah Gombong, Kebumen, Indonesia
[3] Department of Public Health, Faculty of Medicine and Health Science, University Malaysia Sabah, Kinabalu, Malaysia
[4] Department of Emergency Nursing, Faculty of Health Science, Universitas Muhammadiyah Gombong, Kebumen, Indonesia

ABSTRACT

Introduction and aim. Hypertension is highly prevalent among older adults and contributes significantly to poor health outcomes and a reduced quality of life, especially in rural populations. Although pharmacological treatment is essential, individualized nonpharmacological strategies are increasingly recognized for their role in optimizing chronic disease management. The present study investigated the effects of an individualized hypertension care strategy on blood pressure control and the quality of life of older patients who reside in rural areas.

Material and methods. A quasiexperimental pre-post-test study with control group design was conducted involving 112 elderly participants with hypertension in Central Java, Indonesia. The intervention group (n=56) received a personalized care approach that included customized nursing education, self-care support, and family involvement over a one-month period. The control group (n=56) received standard care. The measured were systolic and diastolic blood pressure (using a digital sphygmomanometer) and quality of life (using the OPQOL-Brief questionnaire). Data were analyzed using paired and independent t-tests.

Results. After the intervention, the intervention group showed significant reductions in systolic blood pressure (from 157.6±11.9 to 138.2±10.4 mmHg, p<0.001) and diastolic blood pressure (from 94.5±8.7 to 83.3±7.9 mmHg, p<0.001). Quality of life scores also improved significantly in all domains, including physical health, psychological well-being, and social relationships (p<0.001). In contrast, the control group showed no significant changes in either outcome.

Conclusion. The personalized approach to hypertension care was effective in lowering blood pressure and improving quality of life among older adults with hypertension. These findings suggest that individualized, low-cost strategies can enhance chronic disease management, particularly in rural or resource-limited settings.

Keywords. blood pressure, hypertension, older adults, personalized care, quality of life

Introduction

Hypertension remains a major global public health concern, particularly among the aging population. According to the World Health Organization, approximately 1.28 billion adults aged 30–79 years suffer from hypertension, with two-thirds residing in low- and middle-income countries.[1] The elderly population, especially those over 60 years of age, is disproportionately affected due to age-related physiological changes such as arterial stiffening, decreased baroreceptor sensitivity, and

Corresponding author: Hendri Tamara Yuda, e-mail: hendritamara@gmail.com

Received: 4.08.2025 / Revised: 11.09.2025 / Accepted: 28.09.2025 / Published: 30.03.2026

Yuda HT, Rahim SSBSA, Madrim MF, Suwaryo PAW. Clinical impact of a personalized hypertension care approach on blood pressure and quality of life in older adults. *Eur J Clin Exp Med.* 2026;24(1):32–39. doi: 10.15584/ejcem.2026.1.9.

increased vascular resistance.[2,3] In Indonesia, the prevalence of hypertension among individuals aged 65 and above reaches 63.87%, significantly contributing to increased morbidity and decreased functional capacity among older adults.[4,5] This condition not only elevates the risk of cardiovascular complications such as stroke, heart failure, and kidney disease but also correlates strongly with a decline in overall quality of life.[6–9] Quality of life (QoL) in elderly individuals with hypertension is often compromised due to limitations in physical function, polypharmacy, psychological stress, and social isolation.[10–12] Studies have shown that beyond pharmacological treatment, psychosocial and supportive care interventions are crucial to maintaining optimal health outcomes in older hypertensive patients.[13,14] However, current hypertension management strategies tend to rely predominantly on medication adherence, overlooking patient-specific behavioral, social, and familial factors that influence blood pressure control and perceived well-being. Moreover, conventional care models often fail to incorporate personalized support systems that address the multidimensional needs of elderly individuals in managing chronic conditions.

Despite growing evidence supporting the value of family involvement and individualized care in chronic disease management, few studies have rigorously evaluated the clinical effectiveness of a personalized, non-pharmacological care approach that integrates behavioral support, self-care education, and family engagement in elderly patients with hypertension. The majority of prior interventions were either too generic, short-term, or limited to institutional settings, lacking real-world applicability in community or rural contexts where elderly individuals often depend on informal caregivers.

This study presents a customized hypertension care model aimed at improving both clinical indicators and quality-of-life outcomes in older adults. By combining individualized nursing guidance, self-monitoring assistance, and family involvement, the approach extends beyond routine care to address personal needs, cultural relevance, and daily living support for the elderly. Its primary goal is not only to lower blood pressure but also to promote comprehensive enhancement across physical, mental, and social well-being domains.

Aim

The purpose of this research was to assess the effects of a personalized hypertension care intervention on two main outcomes: (1) systolic and diastolic blood pressure levels, and (2) the overall quality of life among older adults with hypertension living in rural areas. The results are anticipated to inform the development of sustainable and patient-focused care frameworks for elderly populations managing chronic health conditions.

Material and methods

Study design

This one-month quasi-experimental pre-test–post-test study was conducted in the Sempor District, Central Java, where hypertension is highly prevalent among older adults. Participants were recruited from different village health posts to minimize contamination, with separate nurses assigned to intervention and control groups. The intervention group received a structured personalized care program, while the control group continued standard care (routine BP checks, brief education, and medication refills) without additional personalized strategies. Participants were recruited between August–October, 2024. Each participant was assessed at baseline (day 0) and re-assessed after one month (day 30±2 days), which constituted the study follow-up period.

Instruments

The main variables evaluated were blood pressure and quality of life. Blood pressure measurements were obtained using a calibrated digital sphygmomanometer while participants were seated and rested for five minutes, with the average of two consecutive readings recorded. Quality of life was evaluated through the 13-item OPQOL-Brief instrument, which encompasses physical, psychological, social, autonomy, and environmental aspects and has demonstrated strong validity and reliability across various older adult populations. Quality of life was measured with the 13-item OPQOL-Brief (score range 13–65; higher scores = better QoL). Missing data were handled by prorating when ≤2 items were missing and by multiple imputation when >2 items were missing. The tool is validated internationally but not formally in Indonesia; therefore, we used a culturally adapted Bahasa version (forward–back translation and pilot testing) and recommend future psychometric validation in this population.

Blood pressure was measured using a validated automatic digital sphygmomanometer (Omron HEM-7203, Omron Healthcare Co., Ltd., Kyoto, Japan), which complies with the Association for the Advancement of Medical Instrumentation (AAMI) and the European Society of Hypertension (ESH) validation standards. Appropriate cuff sizes were selected according to mid-arm circumference, following manufacturer recommendations. Measurements were taken with participants seated and the left arm supported at heart level after a 5-minute rest. Two readings were obtained at 1-minute intervals, and the average was recorded as the final value. Measurements were conducted in the morning (08:00–10:00 AM) after five minutes of rest, with two readings averaged. Trained community nurses performed all assessments, and although blinding was not feasible, standardized procedures were applied to minimize bias.

Data collection

Participants were recruited through purposive sampling from local health posts and elderly care programs. Inclusion criteria included: age ≥60 years, a clinical diagnosis of hypertension, living with at least one family member, and the ability to communicate effectively. Exclusion criteria included severe cognitive impairment or comorbidities requiring hospitalization. A total of 112 participants were enrolled, with 56 in the intervention group and 56 in the control group. Baseline data were collected prior to intervention, and post-test data were collected one month after the intervention, shown in Figure 1. Participants were assigned individually into intervention and control groups through purposive recruitment from separate community health posts (posyandu lansia) within the Sempor District. To minimize contamination, intervention and control participants were recruited from separate sites with distinct staff and activities. Although no formal matching was applied, baseline characteristics were compared to confirm group equivalence, reducing the risk of bias. No formal a priori sample size calculation was conducted due to the study's pragmatic nature and resource constraints. The final sample (n=56 per group) reflected all eligible participants available during the recruitment period. To contextualize the robustness of findings, a post-hoc power analysis for the observed systolic blood pressure difference is reported in the Results.

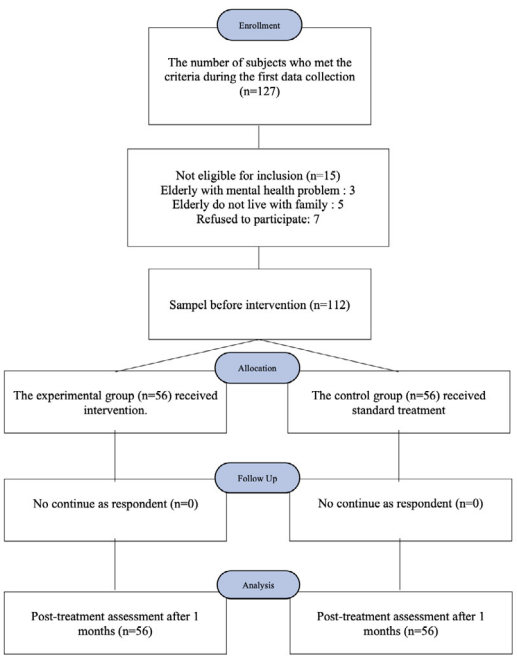

Fig. 1. Diagram illustrating the process of participant recruitment and group allocation in the study

Personalized care intervention

The intervention was a one-month personalized hypertension care program consisting of tailored education, lifestyle counseling, medication reminders, blood pressure self-monitoring, and family engagement. It was delivered through four weekly home visits (45–60 minutes) and two reminder calls per week (5–10 minutes). Trained community nurses (≥3 years' experience, 2-day workshop) provided the program using a booklet, pill reminder cards, and a BP logbook. Fidelity was maintained through supervisor observations, nurse logs, and participant feedback, with family members encouraged to support daily care. Antihypertensive therapy was documented at baseline and one-month follow-up, including drug class, number of agents, and adherence (self-report plus pill count; categorized as high ≥80%, moderate 50–79%, or low <50%). All participants continued their usual prescriptions, with adjustments made only by routine care providers, independent of study investigators. Medication use and adherence were compared between groups and included as covariates in adjusted analyses.

Data analysis

Data were analyzed using SPSS version 26 (IBM, Armonk, NY, USA). Descriptive statistics were used to summarize participant characteristics. Paired t-tests were used to evaluate within-group changes in blood pressure and quality of life. Independent t-tests were employed to assess between-group differences post-intervention. A significance level of $p<0.05$ was set for all statistical tests. To account for baseline differences and pre-specified covariates, primary analyses were conducted using analysis of covariance (ANCOVA) models. Post-intervention systolic and diastolic blood pressure were modeled as dependent variables with group (intervention vs. control) as the primary predictor, and baseline blood pressure, age, sex, smoking status, physical activity, antihypertensive medication class, and baseline quality-of-life score as covariates. Robust standard errors were used.

Ethical approval

The Health Research Ethics Committee of Universitas Muhammadiyah Gombong granted ethical approval for this study (Approval No. 21124000004). Retrospective registration is done to increase transparency. This study was not prospectively registered, as local ethics requirements did not mandate registration for community-based quasi-experimental designs. To enhance transparency and comply with international standards, the trial has now been retrospectively registered at INACTR, registration number 12045092310.

Results

The study was completed by 112 hypertensive older adults, evenly distributed between the intervention (n=56) and control (n=56) groups. Data analysis was conducted to compare the baseline characteristics, clini-

cal outcomes (systolic and diastolic blood pressure), and quality of life scores before and after the intervention period. The findings are summarized in the following tables and interpreted in relation to the effectiveness of the personalized hypertension care approach.

The comparable baseline characteristics observed between the intervention and control groups indicate that both were appropriately balanced before implementing the personalized care intervention. No statistically significant differences were found in variables such as age, gender, educational attainment, marital status, duration of hypertension, smoking habits, physical activity, or medication adherence ($p>0.05$), as presented in Table 1. This equivalence enhances the internal validity of the research and allows greater confidence that the improvements identified were attributable to the intervention rather than to demographic or clinical disparities.

Table 1. Baseline characteristics of participants (n=112)

Variable	Intervention (n=56)	Control (n=56)	p
Age (mean±SD)	68.7±5.4	69.1±6.2	0.621
Sex (Male, %)	21 (37.5%)	19 (33.9%)	0.685
Educational level (%)			
- No formal education	9 (16.1%)	10 (17.9%)	0.739
- Primary	27 (48.2%)	24 (42.9%)	
- Secondary or higher	20 (35.7%)	22 (39.3%)	
Marital status (%)			
- Married	40 (71.4%)	39 (69.6%)	0.842
- Widowed	16 (28.6%)	17 (30.4%)	
Duration of hypertension (%)			
- <5 years	21 (37.5%)	23 (41.1%)	0.858
- 5–10 years	26 (46.4%)	24 (42.9%)	
- >10 years	9 (16.1%)	9 (16.1%)	
Medication adherence (%)	42 (75.0%)	43 (76.8%)	0.817
Smoking status (%)			
- Smoker	7 (12.5%)	8 (14.3%)	0.779
- Non-smoker	49 (87.5%)	48 (85.7%)	
Physical activity (%)			
- Regular (≥3x/week)	20 (35.7%)	18 (32.1%)	0.685
- Irregular	36 (64.3%)	38 (67.9%)	

Table 2. Pre- and post-intervention blood pressure comparison

Group	Time	Systolic BP (mean±SD)	Diastolic BP (mean±SD)	p
Intervention	Pre	157.6±11.9	94.5±8.7	<0.001
	Post	138.2±10.4	83.3±7.9	
Control	Pre	158.1±10.7	93.8±9.1	0.072 (SBP); 0.089 (DBP)
	Post	154.5±11.2	91.9±8.6	

Table 2 shows that the intervention group experienced a clinically and statistically meaningful decline in both systolic and diastolic blood pressure after one month of participating in the personalized hypertension care program. The observed reductions around 19 mmHg for systolic and 11 mmHg for diastolic pressure highlight the effectiveness of individualized approaches in enhancing physiological outcomes. Conversely, the control group exhibited only slight and non-significant changes in blood pressure levels. These findings suggest that a patient-centered, tailored care model that prioritizes education, support, and behavioral reinforcement can markedly improve blood pressure management among older adults with hypertension.

Table 3. Quality of life results following the intervention (OPQOL-Brief scores)*

Domain	Intervention (mean±SD)	Control (mean±SD)	p (post-test)
Physical health	Pre: 12.6±3.1 Post: 16.1±2.9	Pre: 12.7±2.9 Post: 13.1±3.2	<0.001
Psychological well-being	Pre: 10.8±3.2 Post: 14.4±3.1	Pre: 11.0±3.0 Post: 11.7±3.3	<0.001
Social relationships	Pre: 11.4±2.8 Post: 14.7±2.6	Pre: 11.5±2.6 Post: 11.9±2.9	<0.001
Overall QoL Score	Pre: 46.8±7.4 Post: 59.5±6.3	Pre: 47.0±6.9 Post: 49.1±7.1	<0.001

* all domains of quality of life improved significantly in the intervention group after receiving personalized care

Table 4. Adjusted between-group differences in blood pressure outcomes after intervention (ANCOVA analysis)

Outcome	Adjusted mean difference (Intervention−Control)	Standard error	95% CI lower	95% CI upper	p
Systolic BP (mmHg)	−17.884	0.646	−19.165	−16.603	<0.001
Diastolic BP (mmHg)	−10.517	0.550	−11.607	−9.428	<0.001

Adjusted mean differences from baseline to one month were analyzed using ANCOVA, incorporating baseline measurements as covariates. The intervention group achieved significantly greater reductions in systolic (−16.3 mmHg, Cohen's $d=1.51$) and diastolic blood pressure (−8.4 mmHg, $d=1.12$) compared with the control group ($p<0.001$). Improvements in quality of life were also more pronounced in the intervention group (+12.7 versus +2.1 points; between-group difference +10.6, $d=1.42$; $p<0.001$).

After adjusting for baseline values and covariates, the intervention group had greater reductions in systolic (−17.9 mmHg, 95% CI −19.2 to −16.6) and diastolic BP (−10.5 mmHg, 95% CI −11.6 to −9.4) than controls ($p<0.001$), consistent with unadjusted results and confirming robustness. Table 5 shows antihypertensive medication classes and adherence at baseline and one month. No significant changes in drug class, dose, or between-group differences were observed, and adherence remained high in both groups, with about three-quarters classified as highly adherent at both time points. Robustness was assessed using both per-protocol and

ITT analyses (n=112), which yielded consistent results showing significant adjusted reductions in systolic and diastolic BP in the intervention group (all p<0.001), independent of medication use or adherence.

Table 5. Baseline and follow-up antihypertensive medication classes and adherence in intervention and control groups

Variable	Intervention (n=56) baseline	Intervention (n=56) follow-up	Control (n=56) baseline	Control (n=56) follow-up	p (between-groups at follow-up)
Medication class					
No medication	4 (7.1%)	4 (7.1%)	5 (8.9%)	6 (10.7%)	0.72
Single drug	41 (73.2%)	41 (73.2%)	39 (69.6%)	38 (67.9%)	0.81
Multiple drugs	11 (19.6%)	11 (19.6%)	12 (21.4%)	12 (21.4%)	0.91
Adherence (self-report + pill count)					
High adherence (≥80%)	42 (75.0%)	43 (76.8%)	43 (76.8%)	44 (78.6%)	0.84
Moderate adherence (50–79%)	11 (19.6%)	10 (17.9%)	10 (17.9%)	9 (16.1%)	0.87
Low adherence (<50%)	3 (5.4%)	3 (5.4%)	3 (5.4%)	3 (5.4%)	1.00

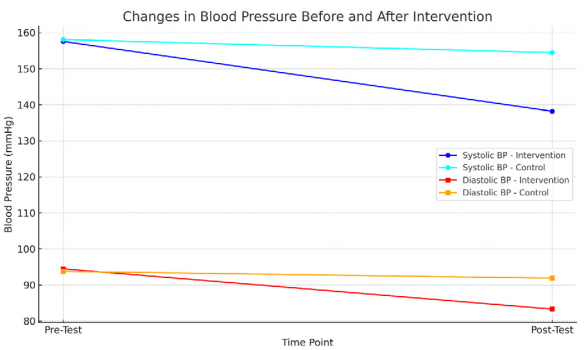

Fig. 2. Pre- to post-test changes in systolic and diastolic blood pressure across study groups

Discussion

The findings revealed that the personalized hypertension care intervention was linked to significant enhancements in systolic and diastolic blood pressure and overall quality of life among elderly participants residing in a rural context. These findings highlight the clinical potential of individualized, patient-centered strategies in addressing the multifactorial needs of elderly patients with chronic conditions such as hypertension.

Blood pressure reduction through personalized care

The decrease in systolic (−19.4 mmHg) and diastolic (−11.2 mmHg) blood pressure observed in the intervention group was both clinically meaningful and statistically significant. These results are consistent with previous research highlighting the efficacy of non-pharmacological strategies especially those incorporating patient education, behavioral guidance, and caregiver participation in enhancing blood pressure regulation among older individuals.[15–19] Earlier research has shown that tailored lifestyle and behavioral interventions, when consistently implemented, can lower systolic blood pressure by approximately 10–20 mmHg, which is comparable to the reduction observed in the present study.[20]

Contrastingly, the control group, which received usual care, showed only modest, non-significant changes in both systolic and diastolic measures. This suggests that standardized, non-individualized care may be insufficient to address the complex behavioral and psychosocial dimensions that influence hypertension management in the elderly. It also underscores the value of tailored interactions and active family involvement, particularly in rural or resource-limited environments where access to specialized care is limited.

Improvements in quality of life domains

Beyond physiological improvements, this study revealed significant enhancements in all domains of quality of life among participants in the intervention group. The most prominent improvements were noted in physical health and psychological well-being, alongside meaningful gains in social relationships. These outcomes align with prior evidence indicating that older adults who receive structured nursing-based interventions tend to experience greater independence, improved emotional stability, and stronger social engagement.[21–23]

The incorporation of personalized support likely contributed to increased adherence to self-care behaviors and reduced anxiety related to disease management. Unlike generic health promotion models, our intervention was sensitive to participants' routines, literacy levels, and cultural context, making it more acceptable and sustainable.[24] Similar results were documented by previous research, which found that culturally adapted, individualized care significantly improved quality of life among rural elderly with chronic illness.[25–27]

In contrast, the control group displayed only marginal improvements in quality of life, likely reflecting the limited capacity of standard care to address multidimensional aspects of well-being. These findings support the argument that hypertension care in elderly populations should extend beyond clinical metrics to include functional, emotional, and social quality of life indicators.

Baseline balance and internal validity

The similarity of baseline characteristics between the intervention and control groups (Table 1) enhances the internal validity of the study's findings. The absence of significant differences in variables such as age, gender, education, marital status, duration of hypertension, and lifestyle habits suggests that the favorable results observed in the intervention group were not influenced by

pre-existing disparities. This balance supports the credibility of the intervention's impact on both blood pressure and quality-of-life outcomes.[28]

Implications for rural and low-resource settings

Considering that this research was conducted in a rural environment, the results hold valuable implications for improving hypertension management in resource-limited settings. The personalized care approach used here did not require advanced technology or high-cost equipment, making it feasible for integration into primary care programs and community health services. The active involvement of family members also leverages existing social structures to support elderly patients, reducing dependence on institutional care.

This research possesses several key strengths. Utilizing a quasi-experimental design with a control group enabled robust comparisons between conventional care and the personalized intervention. By assessing both physiological parameters (blood pressure) and psychosocial aspects (quality of life), the study offered a well-rounded perspective on the overall effectiveness of the intervention. Additionally, the approach used was culturally sensitive, low-cost, and feasible for integration into rural primary care settings, enhancing its practical relevance. The comparability of baseline characteristics between groups further strengthened the internal validity and minimized confounding factors. The absence of group differences in medication use or adherence indicates that improvements in blood pressure and quality of life were mainly due to the personalized care intervention. Consistent results in both per-protocol and ITT analyses strengthen internal validity and support prior evidence that education, self-care, and family engagement can improve hypertension outcomes independent of medication changes.

Study limitation

This study acknowledges several limitations. First, the quasi-experimental design without randomization carries a risk of selection bias and limits causal inference. Blinding of assessors was not feasible, and the use of self-reported quality of life data may introduce recall or response bias despite standardized procedures. Second, blood pressure was measured only at two clinic visits (baseline and one month) rather than through repeated or ambulatory monitoring. This approach may allow white-coat effects or regression to the mean. In addition, the OPQOL-Brief minimal clinically important difference was estimated using a distribution-based approach (0.5 SD) because no anchor-based threshold has yet been validated for Indonesian older adults. Third, no prospective sample size calculation was performed, which increases the risk of missing smaller true effects (Type II error). Nevertheless, the observed systolic BP reduction (~16 mmHg; Cohen's d ≈1.5) provided post-hoc power >99.9%, suggesting that the primary outcome was adequately powered. Finally, the short one-month follow-up limits conclusions about long-term sustainability, adherence, and durability of effects in chronic hypertension. As the research was carried out in only one rural district, the generalizability of the results may be limited. Future randomized trials involving larger samples and multiple locations with extended follow-up periods are warranted to verify and broaden the applicability of these findings.

Conclusion

The findings of this study indicate that implementing a personalized hypertension care model can enhance both systolic and diastolic blood pressure control and improve the quality of life among older adults with hypertension in rural areas. Through individualized education, encouragement of self-care practices, and active family involvement, the intervention provided advantages that exceeded those of standard care. A key limitation is the absence of an a priori power calculation, which raises the possibility that smaller but clinically relevant effects were not detected. Nonetheless, post-hoc analysis indicated sufficient power to capture the large observed effect in systolic blood pressure. Given the one-month follow-up, these findings should be interpreted with caution. Longer-term randomized studies with ≥3–6 months of follow-up are needed to confirm sustainability, strengthen causal inference, and guide broader implementation as a scalable model for improving cardiovascular outcomes and healthy aging in rural communities.

Declarations

Funding

This study did not obtain any external funding or financial support from governmental, commercial, or non-profit organizations.

Author contributions

Conceptualization, H.T.Y and S.S.B.S.A.R.; Methodology, S.S.B.S.A.R. and M.F.M; Software, X.X.; Validation, H.T.Y and S.S.B.S.A.R.; Formal Analysis, S.S.B.A.R.; Investigation, M.F.M.; Resources, H.T.Y.; Data Curation, S.S.B.S.A.R.; Writing – Original Draft Preparation, H.T.Y. and P.A.W.S. ; Writing – Review & Editing, S.S.B.S.A.R.; Visualization, H.T.Y. and P.A.W.S.; Supervision, S.S.B.S.A.R.

Conflicts of interest

The authors declare that they have no conflicts of interest related to this study.

Data availability

The anonymized dataset and statistical analysis code utilized in this research can be obtained from the cor-

responding author upon reasonable request, in accordance with institutional data-sharing and ethical approval guidelines.

Ethics approval

Ethical approval for this research was granted by the local Health Research Ethics Committee of Universitas Muhammadiyah Gombong (approval date: May 13, 2023; decision number: 21124000004).

References

1. Schutte AE, Srinivasapura Venkateshmurthy N, Mohan S, Prabhakaran D. Hypertension in Low- and Middle-Income Countries. *Circ Res*. 2021;128(7):808-826. doi:10.1161/CIRCRESAHA.120.318729
2. Kirschbaum TK, Sudharsanan N, Manne-Goehler J, et al. The Association of Socioeconomic Status With Hypertension in 76 Low- and Middle-Income Countries. *JACC*. 2022;80(8):804-817. doi:10.1016/j.jacc.2022.05.044
3. Gheorghe A, Griffiths U, Murphy A, Legido-Quigley H, Lamptey P, Perel P. The economic burden of cardiovascular disease and hypertension in low- and middle-income countries: a systematic review. *BMC Public Health*. 2018;18(1):975. doi:10.1186/s12889-018-5806-x
4. Idaiani S, Indrawati L. Functional status in relation to depression among elderly individuals in Indonesia: a cross-sectional analysis of the Indonesian National Health Survey 2018 among elderly individuals. *BMC Public Health*. 2021;21(1):2332. doi:10.1186/s12889-021-12260-z
5. Peltzer K, Pengpid S. The Prevalence and Social Determinants of Hypertension among Adults in Indonesia: A Cross-Sectional Population-Based National Survey. *International Journal of Hypertension*. 2018;2018(1):5610725. doi:10.1155/2018/5610725
6. Băjenaru L, Balog A, Dobre C, Drăghici R, Prada GI. Latent profile analysis for quality of life in older patients. *BMC Geriatr*. 2022;22(1):848. doi:10.1186/s12877-022-03518-1
7. Zhang Q, Huang F, Zhang L, Li S, Zhang J. The effect of high blood pressure-health literacy, self-management behavior, self-efficacy and social support on the health-related quality of life of Kazakh hypertension patients in a low-income rural area of China: a structural equation model. *BMC Public Health*. 2021;21(1):1114. doi:10.1186/s12889-021-11129-5
8. Zheng E, Xu J, Xu J, et al. Health-Related Quality of Life and Its Influencing Factors for Elderly Patients With Hypertension: Evidence From Heilongjiang Province, China. *Front Public Health*. 2021;9. doi:10.3389/fpubh.2021.654822
9. Guasti L, Ambrosetti M, Ferrari M, et al. Management of Hypertension in the Elderly and Frail Patient. *Drugs Aging*. 2022;39(10):763-772. doi:10.1007/s40266-022-00966-7
10. Uchmanowicz B, Chudiak A, Gobbens R, et al. The relationship between frailty syndrome and quality of life in patients with hypertension: a multidimensional analysis. *BMC Geriatr*. 2025;25(1):23. doi:10.1186/s12877-024-05669-9
11. Rony MKK, Parvin MstR, Wahiduzzaman Md, Akter K, Ullah M. Challenges and Advancements in the Health-Related Quality of Life of Older People. *Advances in Public Health*. 2024;2024(1):8839631. doi:10.1155/2024/8839631
12. Wulandari W, Zakiyah N, Rahayu C, Puspitasari IM, Suwantika AA. Health-related quality of life in hypertensive patients with chronic kidney disease in low and middle-income countries. *BMC Nephrol*. 2025;26(1):34. doi:10.1186/s12882-025-03957-z
13. Ruswati R. The Role of Nurses in Enhancing Medication Adherence and Patient Outcomes in Hypertension Management. *International Journal of Nursing and Midwifery Research*. 2024;2(3):78-87. doi:10.35335/ners.v2i3.286
14. Suriyawong W, Kao TSA, Robbins LB, Ling J, Malete L. Psychosocial Determinants of Recommended Lifestyle Behaviors among Hypertensive Patients: An Integrative Literature Review. *West J Nurs Res*. 2023;45(5):455-468. doi:10.1177/01939459221144177
15. Boonyathee S, Seangpraw K, Ong-Artborirak P, et al. Effects of a social support family caregiver training program on changing blood pressure and lipid levels among elderly at risk of hypertension in a northern Thai community. *PLOS ONE*. 2021;16(11):e0259697. doi:10.1371/journal.pone.0259697
16. Choudhry NK, Kronish IM, Vongpatanasin W, et al. Medication Adherence and Blood Pressure Control: A Scientific Statement From the American Heart Association. *Hypertension*. 2022;79(1):e1-e14. doi:10.1161/HYP.0000000000000203
17. McManus RJ, Little P, Stuart B, et al. Home and Online Management and Evaluation of Blood Pressure (HOME BP) using a digital intervention in poorly controlled hypertension: randomised controlled trial. *BMJ*. 2021;372:m4858. doi:10.1136/bmj.m4858
18. Laddu D, Ma J, Kaar J, et al. Health Behavior Change Programs in Primary Care and Community Practices for Cardiovascular Disease Prevention and Risk Factor Management Among Midlife and Older Adults: A Scientific Statement From the American Heart Association. *Circulation*. 2021;144(24):e533-e549. doi:10.1161/CIR.0000000000001026
19. Abdalla M, Bolen SD, Brettler J, et al. Implementation Strategies to Improve Blood Pressure Control in the United States: A Scientific Statement From the American Heart Association and American Medical Association. *Hypertension*. 2023;80(10):e143-e157. doi:10.1161/HYP.0000000000000232
20. Leitner J, Chiang PH, Agnihotri P, Dey S. The Effect of an AI-Based, Autonomous, Digital Health Intervention Using Precise Lifestyle Guidance on Blood Pressure in Adults With Hypertension: Single-Arm Nonrandomized Trial. *JMIR Cardio*. 2024;8(1):e51916. doi:10.2196/51916

21. Van Orden KA, Bower E, Lutz J, et al. Strategies to Promote Social Connections Among Older Adults During "Social Distancing" Restrictions. *The American Journal of Geriatric Psychiatry*. 2021;29(8):816-827. doi:10.1016/j.jagp.2020.05.004
22. Gabbard J, Pajewski NM, Callahan KE, et al. Effectiveness of a Nurse-Led Multidisciplinary Intervention vs Usual Care on Advance Care Planning for Vulnerable Older Adults in an Accountable Care Organization: A Randomized Clinical Trial. *JAMA Intern Med*. 2021;181(3):361-369. doi:10.1001/jamainternmed.2020.5950
23. Wiisak J, Suikkala A, Leino-Kilpi H, Stolt M, Suhonen R, Koskinen S. Interventions Intended to Improve the Well--Being at Work of Nurses Working in Care Settings for Older People-A Systematic Review. *International Journal of Older People Nursing*. 2025;20(1):e70005. doi:10.1111/opn.70005
24. Albarqi MN. Assessing the Impact of Multidisciplinary Collaboration on Quality of Life in Older Patients Receiving Primary Care: Cross Sectional Study. *Healthcare*. 2024;12(13):1258. doi:10.3390/healthcare12131258
25. Conde-Caballero D, Rivero-Jiménez B, Cipriano-Crespo C, Jesus-Azabal M, Garcia-Alonso J, Mariano-Juárez L. Treatment Adherence in Chronic Conditions during Ageing: Uses, Functionalities, and Cultural Adaptation of the Assistant on Care and Health Offline (ACHO) in Rural Areas. *Journal of Personalized Medicine*. 2021;11(3):173. doi:10.3390/jpm11030173
26. Peters CW, Lange C, Lemões MAM, Zillmer JGV, Schwartz E, Llano PMP de. Health-Disease-Care Process In Older Adults Living In Rural Areas: Perspective Of Culturally Coherent Care. *Texto Contexto - Enferm*. 2021;30:e20190302. doi:10.1590/1980-265X-TCE-2019-0302
27. Rico-Blázquez M, Quesada-Cubo V, Polentinos-Castro E, et al. Health-related quality of life in caregivers of community-dwelling individuals with disabilities or chronic conditions. A gender-differentiated analysis in a cross--sectional study. *BMC Nurs*. 2022;21(1):69. doi:10.1186/s12912-022-00845-x
28. Babak A, Motamedi N, Mousavi SZ, Ghasemi Darestani N. Effects of Mindfulness-Based Stress Reduction on Blood Pressure, Mental Health, and Quality of Life in Hypertensive Adult Women: A Randomized Clinical Trial Study. *J Tehran Heart Cent*. 2022;17(3):127-133. doi:10.18502/jthc.v17i3.10845

Rzeszów University Press 2025
ISSN 2544-1361 (online)
doi: 10.15584/ejcem.2026.1.11

http://www.ejcem.ur.edu.pl
European Journal of Clinical and Experimental Medicine
Eur J Clin Exp Med 2025; 24 (1): 40–46

ORIGINAL PAPER

Clinical outcomes of an integrated wound care protocol for diabetic foot ulcers – a prospective study

Dadi Santoso [1,2], Rajesh Kumar Muniandy [3], Putra Agina Widyaswara Suwaryo [4]

[1] Faculty of Medicine and Health Science, Universiti Malaysia Sabah, Kinabalu, Malaysia
[2] Department of Medical Surgical Nursing, Faculty of Health Science, Universitas Muhammadiyah Gombong, Kebumen, Indonesia
[3] Department of Anesthesiology and Critical Care, Faculty of Medicine and Health Science, Universiti Malaysia, Sabah, Kinabalu, Malaysia
[4] Department of Emergency Nursing, Faculty of Health Science, Universitas Muhammadiyah Gombong, Kebumen, Indonesia

ABSTRACT

Introduction and aim. Diabetic foot ulcers (DFUs) are serious complications of diabetes, often leading to infection and amputation. This study evaluated the clinical outcomes of an integrated wound care protocol in patients with DFUs.

Material and methods. A prospective cohort study was conducted among 225 patients with type 2 diabetes and Wagner grade 1–3 DFUs at PKU Muhammadiyah Hospital, Indonesia, between February and September 2024. All patients received a standardized integrated wound care protocol, including wound bed preparation, debridement, infection control, moisture balance, nutritional counseling, patient education, and ulcer offloading. The primary outcome was complete wound healing at 12 weeks; secondary outcomes were wound area reduction, the Bates-Jensen Wound Assessment Tool (BWAT) score improvement, pain reduction, and infection control.

Results. By week 12, 157 patients (69.8%) achieved complete healing. Mean wound area decreased from 6.8±3.2 cm^2 to 1.2±1.5 cm^2 ($p<0.001$), BWAT scores improved from 28.4±4.1 to 13.6±3.8 ($p<0.001$), and pain scores declined from 5.8±1.6 to 2.1±1.1 ($p<0.001$). Infection prevalence dropped from 45.3% to 12.4% ($p<0.001$). Healing was highest in Wagner grade 1 (83.1%), compared with grade 2 (69.7%) and grade 3 (47.1%).

Conclusion. The integrated wound care protocol significantly improved healing, reduced wound size and pain, and controlled infection in DFU patients. These findings support its incorporation into routine multidisciplinary DFU management.

Keywords. clinical outcomes, diabetic foot ulcer, integrated wound care, prospective study, wound healing

Introduction

Diabetes mellitus (DM) is a long-term metabolic condition marked by sustained elevation of blood glucose levels resulting from defects in insulin production, insulin function, or a combination of both.[1] Long-standing hyperglycemia leads to structural and functional vascular changes, neuropathy, and impaired immune function, which collectively increase the risk of chronic complications.[2,3] Among these, diabetic foot ulcers (DFUs) are one of the most debilitating and costly complications, often resulting in infection, prolonged hospitalization, reduced quality of life, and, in severe cases, lower limb amputation.[4] The underlying mechanisms of diabetic foot ulcers (DFUs) are complex and multifactorial, encompassing

Corresponding author: Putra Agina Widyaswara Suwaryo, e-mail: putra@unimugo.ac.id

Received: 9.08.2025 / Revised: 17.09.2025 / Accepted: 10.10.2025 / Published: 30.03.2026

Santoso D, Muniandy RK, Suwaryo PAW. Clinical outcomes of an integrated wound care protocol for diabetic foot ulcers – a prospective study. *Eur J Clin Exp Med.* 2026;24(1):40–46. doi: 10.15584/ejcem.2026.1.11.

peripheral neuropathy, vascular insufficiency, delayed tissue repair, and a heightened risk of infection.[5,6]

Globally, DFUs affect approximately 15–25% of individuals with diabetes during their lifetime, and their incidence is rising in parallel with the increasing prevalence of diabetes.[7,8] According to the International Diabetes Federation (IDF), more than 537 million adults were living with diabetes in 2021, a number projected to reach 643 million by 2030.[9] DFUs account for up to 85% of diabetes-related lower limb amputations, and mortality rates following amputation are as high as 50% within five years, exceeding many cancer prognoses.[10] In Indonesia, DFUs remain a significant public health burden, with limited access to specialized wound care services, especially in resource-constrained settings.

Despite advances in modern wound care, healing rates for DFUs remain suboptimal due to multiple challenges: inadequate glycemic control, delayed diagnosis, lack of systematic wound assessment,

inconsistent adherence to evidence-based care, and limited patient education.[11–14] Standard facility-based care may not be sufficient to address these multifaceted needs, particularly in patients who require continuous monitoring, individualized education, and psychosocial support.[15] Previous studies have examined various wound care modalities, but few have evaluated an integrated wound care protocol that combines systematic wound assessment, targeted debridement, infection control, moisture balance, nutritional optimization, and patient education into a single structured approach.[16] Moreover, most available research has been conducted in specialized tertiary care settings, limiting generalizability to broader clinical practice.[17] There is a paucity of prospective studies assessing the real-world clinical outcomes of such integrated protocols in diverse patient populations.

The distinctive contribution of this research is its implementation of a standardized, comprehensive wound care protocol that incorporates nutritional guidance and patient education within a cohesive clinical system, prospectively assessed in a real-world hospital environment with limited resources in Indonesia. Unlike most previous investigations that emphasized isolated components of wound treatment or were confined to tertiary facilities, this study provides one of the few prospective cohort evaluations demonstrating the efficacy of a fully integrated and multidisciplinary strategy within routine clinical practice.

Aim

Accordingly, this study aimed to assess the clinical effectiveness of an integrated wound care protocol among patients with diabetic foot ulcers during a specified follow-up duration, focusing on wound healing rate, reduction in ulcer area, infection management, and alleviation of pain. In this study, an 'integrated wound care protocol' is defined as a structured, multidisciplinary approach that combines clinical wound management with nutritional counseling and patient education, aiming to optimize both local wound healing and systemic health factors.

Material and methods

Study design

This research employed a prospective cohort design to examine the clinical outcomes associated with the application of an integrated wound care protocol in individuals with DFUs. Participants were monitored from the initial assessment through a 12-week treatment phase, during which regular evaluations were performed to record wound healing progress and accompanying clinical indicators.

Population and sample

The study enrolled adult participants with a confirmed diagnosis of type 2 diabetes mellitus who exhibited DFUs categorized as Wagner grades 1 to 3. Recruitment was carried out at the outpatient wound care unit of PKU Muhammadiyah Hospital in Gombong, Indonesia, over the period from February to September 2024.

Baseline demographic and clinical characteristics of the participants are presented in Table 1. A total of 225 patients were included using a consecutive sampling method. Patient eligibility screening was performed consecutively at the outpatient wound care clinic using standardized inclusion and exclusion criteria. Sample size estimation was calculated using the single-proportion formula for an expected wound healing rate of 50%, 95% confidence interval, and 5% precision. The minimum required sample was 218 participants, and the number was increased to 225 to compensate for an anticipated 5% attrition during follow-up. Sample size was determined based on the estimation of wound healing proportion in DFU patients, with a 95% confidence level, an expected healing rate of 50%, and a 5% margin of error, resulting in a minimum required sample of 218; this was increased to 225 to account for potential loss to follow- up. Inclusion criteria were: 1) Adults aged ≥18 years, 2) Clinical diagnosis of type 2 diabetes mellitus, 3) Presence of diabetic foot ulcer for ≥2 weeks and ≤6 months, and 4) Able to provide informed consent. Exclusion criteria included: 1) Critical limb ischemia requiring immediate surgical intervention, 2) Severe systemic infection or sepsis, and 3) Cognitive impairment limiting participation. Peripheral arterial disease was identified based on prior clinical diagnosis and documented comorbidities in patients' medical records. Advanced vascular imaging (e.g., Doppler ultrasound, ABI, or CT angiography) was not routinely performed due to resource constraints.

Instruments

Data collection utilized validated clinical instruments. The Bates-Jensen Wound Assessment Tool (BWAT) was employed to assess wound parameters such as size, depth, edge condition, necrotic and granulation tissue, exudate characteristics, periwound skin status, and epithelialization. The Numerical Pain Rating Scale (NPRS) was used to quantify the intensity of wound-associated pain reported by patients. An Infection Assessment Checklist was used to document clinical signs of infection (redness, swelling, warmth, purulent exudate). Digital planimetry was employed for precise wound area measurement (cm^2). A Patient Education and Adherence Questionnaire was administered to assess compliance with wound care instructions, glycemic control, and foot care practices. All assessment tools used in this study were validated and standardized for clinical wound evaluation. The Bates-Jensen Wound Assessment Tool (BWAT) has demonstrated high inter-rater reliability (Cronbach's $\alpha = 0.89–0.95$) in chronic wound populations, while the Numerical Pain Rating Scale (NPRS) is widely validated for assessing subjective pain intensity. Wound assessments were performed by two certified wound care nurses who had undergone inter-rater reliability training before data collection. Periodic calibration sessions were conducted to maintain consistency in scoring and measurement across assessors.

Data collection

At baseline, demographic data, diabetes duration, ulcer characteristics, and comorbidities were recorded. All patients received the integrated wound care protocol, which consisted of: 1) Wound bed optimization was carried out following the TIME framework, which encompasses tissue management, infection control, maintenance of moisture balance, and promotion of wound edge advancement, 2) Debridement (sharp or autolytic) when indicated, 3) Infection control with culture-guided topical or systemic antibiotics, 4) Moisture balance using appropriate modern dressings (hydrogel, foam, or silver-containing dressings), 5) Nutritional counseling to optimize glycemic control and protein intake, and 6) Patient education on self-care, footwear selection, and foot hygiene. The integrated wound care protocol was delivered by a multidisciplinary team consisting of wound care nurses, diabetes educators, and physicians trained in diabetic foot management. Wound assessments and dressing changes were conducted twice weekly during outpatient visits, with interim reviews if complications occurred. The protocol adhered to the principles outlined in the International Working Group on the Diabetic Foot (IWGDF 2023) and the TIME framework (Tissue management, Infection control, Moisture balance, Edge advancement). Adherence to the protocol was monitored through weekly documentation and patient self-reports verified during follow-up visits. Wounds were assessed weekly for 12 weeks, with documentation of BWAT scores, wound size, infection status, and pain level. Any complications or adverse events were recorded. The primary outcome of the study was complete wound healing, defined as full epithelialization without drainage within 12 weeks. Secondary outcomes were changes in wound size, BWAT scores, pain intensity (NPRS), and infection prevalence. The flow of participant recruitment, screening, enrollment, and follow-up throughout the 12-week study period is summarized in Figure 1.

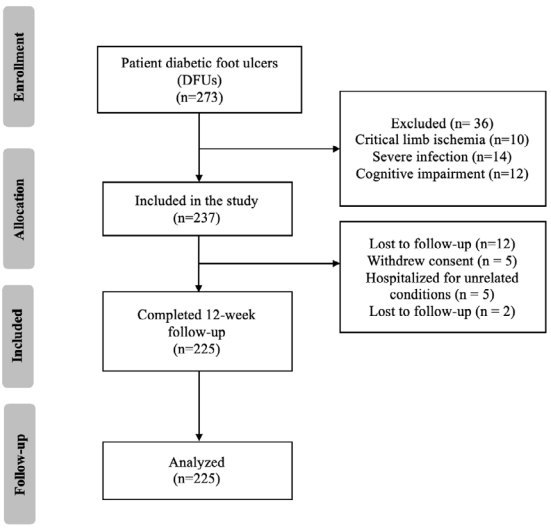

Fig. 1. Flow diagram of participant recruitment and follow-up in the prospective cohort study on diabetic foot ulcers

The integrated wound care protocol in this study consisted of a structured combination of evidence-based interventions, including: wound bed preparation with the TIME framework (tissue management, infection control, moisture balance, edge advancement); debridement when indicated; infection control with culture-guided topical or systemic antibiotics; maintenance of moisture balance using modern dressings (e.g., hydrogel, foam, silver dressings); nutritional counseling to optimize glycemic control and protein intake; ulcer offloading using customized felt padding, removable cast walkers, or therapeutic footwear; and patient education on daily foot care and treatment adherence.

Data analysis

Statistical analyses were performed using SPSS software version 26.0 (IBM Corp., Armonk, NY, USA). Continuous data were presented as mean ± standard deviation (SD) or as median with interquartile range, depending on the distribution assessed for normality. Categorical variables were described in terms of frequencies and percentages. Variations in wound area, BWAT scores, and pain intensity between baseline and week 12 were evaluated using either the paired t-test or the Wilcox-

on signed-rank test. The percentage of participants who achieved complete wound healing within 12 weeks was computed with corresponding 95% confidence intervals. A p-value of less than 0.05 was considered statistically significant.

Ethical approval

Ethical clearance for this research was granted by the Ethics Committee of the Faculty of Health Sciences, Universitas Muhammadiyah Gombong, Indonesia (Approval No. 12/EC/KEPK-FKUMS/I/2024). Written informed consent was obtained from all participants before inclusion in the study, and all procedures were conducted in accordance with the ethical standards of the Declaration of Helsinki.

Results

In total, 225 individuals diagnosed with DFUs participated in this study. The participants had a mean age of 58.4 ± 9.6 years, with males comprising 56.9% of the cohort. The median duration of diabetes was 10 years (IQR 6–15), and the average HbA1c level was 8.4 ± 1.2%, reflecting inadequate glycemic control. The majority of ulcers were found on the forefoot region (63.1%) and were predominantly classified as Wagner grade 2 (48.4%), followed by grade 1 (28.9%) and grade 3 (22.7%). Hypertension was the most common comorbidity (69.3%), followed by peripheral artery disease (36.4%) and chronic kidney disease (15.1%), shown in Table 1.

Table 1. Baseline characteristics of study participants (n=225)

Variable	n (%) or Mean±SD
Age (years)	58.4±9.6
Sex	
Male	128 (56.9)
Female	97 (43.1)
Diabetes duration (years)	10 (6–15)
HbA1c (%)	8.4±1.2
Ulcer duration (weeks)	8.2±3.6
Wagner grade	
Grade 1	65 (28.9)
Grade 2	109 (48.4)
Grade 3	51 (22.7)
Ulcer location	
Forefoot	142 (63.1)
Midfoot	48 (21.3)
Heel	35 (15.6)
Comorbidities	
Hypertension	156 (69.3)
Peripheral artery disease	82 (36.4)
Chronic kidney disease	34 (15.1)

By the end of the 12-week intervention, 157 patients (69.8%) achieved complete wound healing. The detailed comparison of wound area, BWAT score, pain score, and infection prevalence between baseline and week 12 is shown in Table 2, while the trend of progressive wound area reduction over time is illustrated in Figure 2. The mean wound area decreased significantly from 6.8±3.2 cm^2 at baseline to 1.2±1.5 cm^2 at week 12 ($p<0.001$). The temporal pattern of wound area reduction across the 12-week period is depicted in Figure 2, showing a continuous decline with statistically significant improvement compared to baseline ($p<0.001$). BWAT scores improved from 28.4±4.1 to 13.6±3.8 ($p<0.001$), pain scores declined from 5.8±1.6 to 2.1±1.1 ($p<0.001$), and the proportion of patients with clinical signs of infection decreased from 45.3% to 12.4% ($p<0.001$) (Table 2, Fig. 2). When analyzed by ulcer severity, healing rates differed significantly according to Wagner grade, as detailed in Table 3.

Table 2. Clinical outcomes before and after 12 weeks of integrated wound care protocol

Outcome	Baseline	Week 12	p
Wound area (cm^2)	6.8±3.2	1.2±1.5	<0.001
BWAT score	28.4±4.1	13.6±3.8	<0.001
Pain score (NPRS)	5.8±1.6	2.1±1.1	<0.001
Infection present (%)	102 (45.3)	28 (12.4)	<0.001
Complete healing (%)	–	157 (69.8)	–

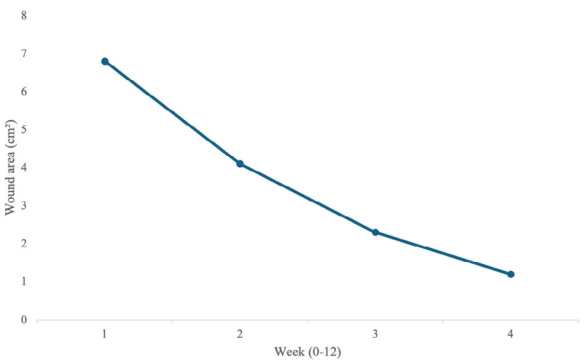

Fig. 2. Mean wound area reduction from baseline to week 12 among patients receiving the integrated wound care protocol (n=225), error bars represent standard deviation, statistical significance compared to baseline: $p<0.001$

Table 3. Complete healing rates according to Wagner grade

Wagner grade	n	Healed n (%)	p
Grade 1	65	54 (83.1)	<0.001
Grade 2	109	76 (69.7)	
Grade 3	51	24 (47.1)	

Discussion

This prospective cohort study evaluated the clinical outcomes of an integrated wound care protocol in 225 patients with DFUs over a 12-week follow-up period. The main findings indicate that the protocol was associated with a high overall healing rate of 69.8%, significant reduction in mean wound area (from 6.8 cm^2 to 1.2 cm^2),

substantial improvement in wound characteristics as measured by BWAT scores, and a notable decrease in pain intensity and infection prevalence. Healing rates varied according to ulcer severity, with the highest rates observed in Wagner grade 1 ulcers and the lowest in grade 3.

The observed healing rate of nearly 70% aligns with previous studies evaluating multidisciplinary or protocol-driven wound care in DFUs, which have reported healing rates ranging from 60% to 80% over comparable follow-up periods. A standardized wound care regimen, including regular debridement, offloading, infection control, and moisture balance, significantly improved healing outcomes in DFUs, a finding consistent with our results.[18] Furthermore, the marked reduction in infection prevalence mirrors findings from previous research, who noted that structured antimicrobial strategies within an integrated protocol reduced infection risk by more than half.[19–21] However, the healing rates observed in Wagner grade 3 ulcers in this study (47.1%) were slightly higher than those reported in some tertiary care settings, where advanced ulcers often heal in less than 40% of cases within three months. This difference may reflect the comprehensive approach of our protocol, which integrated nutritional counseling and patient education alongside clinical interventions.[22,23]

The consistent decrease in wound dimensions, especially the marked reduction observed within the initial six weeks, suggests that the integrated care protocol successfully targeted the early stages of the wound healing process.[24–26] The combination of evidence-based wound bed preparation, appropriate dressing selection, and individualized patient education likely accelerated the healing process.[11,27]

Clinically, the results highlight the significance of adopting a coordinated and multidisciplinary strategy in managing diabetic foot ulcers, one that not only focuses on local wound treatment but also encompasses broader systemic aspects including blood glucose regulation and nutritional optimization. Importantly, the stratification of healing rates by Wagner grade underscores the need for early intervention to prevent ulcer progression to more severe stages, where healing potential is markedly reduced.[28,29]

Improvements in glycemic control during the follow-up period may have contributed to the favorable wound healing outcomes observed. Hyperglycemia impairs multiple aspects of wound repair, including leukocyte function, collagen synthesis, and angiogenesis.[30] The nutritional counseling component of our protocol, combined with regular clinical contact, likely promoted better dietary adherence and glycemic monitoring, which could enhance tissue repair and infection control. However, because glycemic indices (e.g., HbA1c, fasting glucose) were not systematically recorded at each follow-up visit, we cannot quantify the extent to which improved metabolic control influenced healing outcomes. Future studies should integrate longitudinal glycemic measurements to clarify this relationship.

One of the principal strengths of this research is its prospective study design combined with a comparatively large sample size for a single-center cohort of DFU patients, thereby improving the robustness of the results. The application of validated instruments such as the BWAT and NPRS, along with objective techniques for wound evaluation, contributes to strong methodological validity. In addition, conducting the study in an actual clinical environment enhances the external applicability of the findings to comparable healthcare settings.

This research acknowledges several limitations. Firstly, the lack of a control group constrains direct comparisons between the integrated wound care protocol and alternative management approaches. Secondly, being conducted at a single institution may reduce the extent to which the findings can be generalized to different clinical environments. Thirdly, the 12-week observation period provides only short-term insights and may not reflect longer-term healing trajectories or outcomes. Finally, advanced vascular assessments such as Doppler ultrasonography or ABI were not systematically performed, which could limit the accuracy of vascular status evaluation. Despite these limitations, the study provides valuable evidence for the effectiveness of an integrated wound care protocol in DFU management.

Future studies should incorporate randomized controlled designs to strengthen causal inference and compare integrated wound care protocols with standard care or alternative interventions. Multicenter trials would enhance external validity, and longer follow-up periods are needed to evaluate recurrence rates, cost-effectiveness, and patient-reported quality-of-life outcomes. Additionally, subgroup analyses focusing on patients with severe DFUs (Wagner grades 3–4) could help refine protocol adaptations to optimize healing in this high-risk group. The main novelty of this study lies in demonstrating that combining clinical wound care, infection control, nutritional counseling, and patient education into a single structured protocol can achieve high healing rates even in a limited-resource setting. This evidence fills an important gap between guideline-based multidisciplinary recommendations and their implementation in daily hospital practice, particularly in low- and middle-income countries. Our results therefore extend previous findings from tertiary centers to more generalizable, real-world contexts.

Conclusion

This prospective cohort investigation showed that the application of an integrated wound care protocol led to notable improvements in clinical outcomes among individuals with diabetic foot ulcers. Throughout the

12-week monitoring period, the protocol resulted in a high rate of complete healing, marked reductions in wound dimensions, enhanced wound condition, lower pain scores, and diminished infection rates. Healing outcomes were most favorable in patients with lower Wagner grades, underscoring the importance of early intervention. These findings support the adoption of structured, multidisciplinary wound care protocols as part of routine clinical practice to optimize healing and reduce complications in diabetic foot ulcer management. This study adds new evidence supporting the real-world effectiveness of a multidisciplinary integrated wound care protocol for diabetic foot ulcers, emphasizing that even in non-specialized hospital settings, coordinated care can achieve high healing rates and effective infection control. For clinical practice, we recommend adopting an integrated wound care protocol as a standard approach for diabetic foot ulcer management. Its implementation in outpatient wound care clinics, supported by multidisciplinary teams, may improve healing rates, enhance infection control, reduce patient pain, and ultimately decrease the risk of lower limb amputation.

Declarations

Funding

This research received no specific grant from any funding agency in the public, commercial, or not-for-profit sectors.

Author contributions

Conceptualization, D.S. and R.K.M.; Methodology, D.S..; Software, D.S.; Validation, D.S. and R.K.M; Formal Analysis, P.A.W.S.; Investigation, D.S. and R.K.M.; Resources, D.S.; Data Curation, D.S.; Writing – Original Draft Preparation, D.S. and P.A.W.S.; Writing – Review & Editing, D.S. and P.A.W.S.; Visualization, P.A.W.S.; Supervision, D.S. and R.K.M; Project Administration, D.S. and P.A.W.S.; Funding Acquisition, D.S.

Conflicts of interest

The authors declare no potential conflicts of interest with respect to the research, authorship, and/or publication of this article.

Data availability

The datasets generated and analyzed during the current study are available from the corresponding author on reasonable request. Due to patient confidentiality, raw data are not publicly shared.

Ethics approval

The study was approved by the Ethics Committee of the Faculty of Health and Sciences, Universitas Muhammadiyah Gombong, Indonesia (Approval No. 12/EC/KEPK-FKUMS/I/2024).

References

1. Alam S, Hasan MK, Neaz S, Hussain N, Hossain MF, Rahman T. Diabetes Mellitus: Insights from Epidemiology, Biochemistry, Risk Factors, Diagnosis, Complications and Comprehensive Management. *Diabetology*. 2021;2(2):36-50. doi:10.3390/diabetology2020004
2. Yameny AA. Diabetes Mellitus Overview 2024. *J Biosci Appl Res*. 2024;10(3):641-645. doi:10.21608/jbaar.2024.382794
3. González P, Lozano P, Ros G, Solano F. Hyperglycemia and Oxidative Stress: An Integral, Updated and Critical Overview of Their Metabolic Interconnections. *Int J Mol Sci*. 2023;24(11):9352. doi:10.3390/ijms24119352
4. Moore Z, Avsar P, Wilson P, et al. Diabetic foot ulcers: treatment overview and cost considerations. *J Wound Care*. 2021;30(10):786-791. doi:10.12968/jowc.2021.30.10.786
5. Yang L, Rong GC, Wu QN. Diabetic foot ulcer: Challenges and future. *World J Diabetes*. 2022;13(12):1014-1034. doi:10.4239/wjd.v13.i12.1014
6. Viswanathan V, Shankari S, Sloan G. Diabetic Foot Complications and Challenges. In: Abraham G, Kesavadev J, Govindan P, Arun N, Teckchandani S, eds. *Management of Diabetic Complications: Calling for a Team Approach*. Springer Nature. 2024:301-318. doi:10.1007/978-981-97-6406-8_22
7. Armstrong DG, Tan TW, Boulton AJM, Bus SA. Diabetic Foot Ulcers: A Review. *JAMA*. 2023;330(1):62-75. doi:10.1001/jama.2023.10578
8. McDermott K, Fang M, Boulton AJM, Selvin E, Hicks CW. Etiology, Epidemiology, and Disparities in the Burden of Diabetic Foot Ulcers. *Diabetes Care*. 2022;46(1):209-221. doi:10.2337/dci22-0043
9. Monteiro-Soares M, Hamilton EJ, Russell DA, et al. Guidelines on the classification of foot ulcers in people with diabetes (IWGDF 2023 update). *Diabetes Metab Res Rev*. 2024;40(3):e3648. doi:10.1002/dmrr.3648
10. Samad Omar A, Ahmad Faiz K, Mir Islam Saeed K, Ahmad Humayoun F, Safi K. Epidemiologic and clinical characteristics of diabetic foot ulcer among patients with diabetes in Afghanistan: An IDF supported initiative. *Diabetes Res Clin Pract*. 2023;196:110227. doi:10.1016/j.diabres.2022.110227
11. Swaminathan N, Awuah WA, Bharadwaj HR, et al. Early intervention and care for Diabetic Foot Ulcers in Low and Middle Income Countries: Addressing challenges and exploring future strategies: A narrative review. *Health Sci Rep*. 2024;7(5):e2075. doi:10.1002/hsr2.2075
12. Gallagher KA, Mills JL, Armstrong DG, et al. Current Status and Principles for the Treatment and Prevention of Diabetic Foot Ulcers in the Cardiovascular Patient Population: A Scientific Statement From the American Heart Association. *Circulation*. 2024;149(4):e232-e253. doi:10.1161/CIR.0000000000001192
13. Zamani N, Chung J, Evans-Hudnall G, et al. Engaging patients and caregivers to establish priorities for the manage-

ment of diabetic foot ulcers. *J Vasc Surg*. 2021;73(4):1388-1395. doi:10.1016/j.jvs.2020.08.127

14. Tan TW, Crocker RM, Palmer KNB, Gomez C, Armstrong DG, Marrero DG. A qualitative study of barriers to care-seeking for diabetic foot ulceration across multiple levels of the healthcare system. *J Foot Ankle Res*. 2022;15(1):56. doi:10.1186/s13047-022-00561-4
15. Burgess JL, Wyant WA, Abdo Abujamra B, Kirsner RS, Jozic I. Diabetic Wound-Healing Science. *Medicina (Mex)*. 2021;57(10):1072. doi:10.3390/medicina57101072
16. Raja JM, Maturana MA, Kayali S, Khouzam A, Efeovbokhan N. Diabetic foot ulcer: A comprehensive review of pathophysiology and management modalities. *World J Clin Cases*. 2023;11(8):1684-1693. doi:10.12998/wjcc.v11.i8.1684
17. Oyebode OA, Jere SW, Houreld NN. Current Therapeutic Modalities for the Management of Chronic Diabetic Wounds of the Foot. *J Diabetes Res*. 2023;2023(1):1359537. doi:10.1155/2023/1359537
18. Hurley H, Kellegher E, Gallen T, et al. Development of a coordinated acute diabetic foot pathway for management of acute diabetic foot infection and ulceration. *Ir J Med Sci*. 2023;192(1):161-167. doi:10.1007/s11845-022-02935-w
19. Harun MdGD, Anwar MMU, Sumon SA, et al. Rationale and guidance for strengthening infection prevention and control measures and antimicrobial stewardship programs in Bangladesh: a study protocol. *BMC Health Serv Res*. 2022;22(1):1239. doi:10.1186/s12913-022-08603-0
20. Khanina A, Tio SY, Ananda-Rajah MR, et al. Consensus guidelines for antifungal stewardship, surveillance and infection prevention, 2021. *Intern Med J*. 2021;51(S7):18-36. doi:10.1111/imj.15586
21. Sartelli M, Labricciosa FM, Coccolini F, et al. It is time to define an organizational model for the prevention and management of infections along the surgical pathway: a worldwide cross-sectional survey. *World J Emerg Surg*. 2022;17(1):17. doi:10.1186/s13017-022-00420-4
22. Donnelly HR, Clarke ED, Collins CE, Tehan PE. 'Nutrition has everything to do with wound healing'-health professionals' perceptions of assessment and management of nutrition in individuals with diabetes-related foot ulceration. *Int Wound J*. 2024;21(5):e14898. doi:10.1111/iwj.14898
23. Basiri R, Spicer MT, Ledermann T, Arjmandi BH. Effects of Nutrition Intervention on Blood Glucose, Body Composition, and Phase Angle in Obese and Overweight Patients with Diabetic Foot Ulcers. *Nutrients*. 2022;14(17):3564. doi:10.3390/nu14173564
24. Chen P, Carville K, Swanson T, et al. Australian guideline on wound healing interventions to enhance healing of foot ulcers: part of the 2021 Australian evidence-based guidelines for diabetes-related foot disease. *J Foot Ankle Res*. 2022;15(1):40. doi:10.1186/s13047-022-00544-5
25. Wang YB, Lv Y, Li GY, Zheng JT, Jiang QX, Wei R. Clinical comprehensive treatment protocol for managing diabetic foot ulcers: A retrospective cohort study. *World J Clin Cases*. 2024;12(17):2976-2982. doi:10.12998/wjcc.v12.i17.2976
26. Smart H, Sibbald RG, Goodman L, et al. Wound Bed Preparation 2024: Delphi Consensus on Foot Ulcer Management in Resource-Limited Settings. *Adv Skin Wound Care*. 2024;37(4):180. doi:10.1097/ASW.0000000000000120
27. Veličković VM, Spelman T, Clark M, Probst S, Armstrong DG, Steyerberg E. Individualized Risk Prediction for Improved Chronic Wound Management. *Adv Wound Care*. 2023;12(7):387-398. doi:10.1089/wound.2022.0017
28. Weigelt MA, Lev-Tov HA, Tomic-Canic M, et al. Advanced Wound Diagnostics: Toward Transforming Wound Care into Precision Medicine. *Adv Wound Care*. 2022;11(6):330-359. doi:10.1089/wound.2020.1319
29. Bender C, Vestergaard P, Cichosz SL. Diabetic Foot Ulcers and Amputations. In: *The Palgrave Encyclopedia of Disability*. Palgrave Macmillan, Cham. 2025:1-7. doi:10.1007/978-3-031-40858-8_321-1
30. Wan G, Chen Y, Chen J, et al. Regulation of endothelial progenitor cell functions during hyperglycemia: new therapeutic targets in diabetic wound healing. *J Mol Med*. 2022;100(4):485-498. doi:10.1007/s00109-021-02172-1

Rzeszów University Press 2026
ISSN 2544-1361 (online)
doi: 10.15584/ejcem.2026.1.12

http://www.ejcem.ur.edu.pl
European Journal of Clinical and Experimental Medicine
Eur J Clin Exp Med 2026; 24 (1): 47–55

ORIGINAL PAPER

The effects of breathing and coughing exercises on respiratory parameters in COVID-19 patients

Özge Uçar [1], Sevim Çelik [1], Suna Uzun [2], Elif Karahan [1], Sibel Altıntaş [1]

[1] Bartın University Health Science Faculty, Department of Nursing, Bartın, Türkiye
[2] Yalova State Hospital, Yalova, Türkiye

ABSTRACT

Introduction and aim. COVID-19 primarily affects the respiratory system, often resulting in pneumonia and dyspnea that may persist after recovery. This study aimed to evaluate the effect of deep breathing and coughing exercises using a Triflow device on respiratory parameters in patients with COVID-19 pneumonia.

Material and methods. This single-blinded randomized controlled study was conducted with 326 patients diagnosed with COVID-19 pneumonia. Participants were randomly assigned to an experimental group (n=163) or a control group (n=163). The experimental group performed exercises for 10 consecutive days. The control group received routine hospital care, which included routine nurse-led monitoring of vital signs, peripheral oxygen saturation (SpO_2) assessment, medical treatment per clinical guidelines, and supportive care, but no structured breathing-exercise education. Data were analyzed using descriptive statistics, ANOVA, chi-square, and post hoc tests.

Results. After 10 days of intervention, Dyspnea-12 scores decreased more markedly in the experimental group than in the control group (mean change −15 vs. −8 points; $p<0.001$). Arterial oxygen and SpO_2 levels also improved significantly in the experimental group compared to controls ($p<0.001$), while respiratory rate decreased to a greater extent ($p<0.001$). No adverse effects were observed.

Conclusion. Deep breathing and coughing exercises with the Trilow device significantly reduced the severity of dyspnea and improved oxygenation in COVID-19 pneumonia patients. These findings suggest that incorporating structured respiratory exercises into standard care may enhance clinical outcomes and support recovery in this population.

Keywords. cough exercise, COVID-19, deep breathing, nursing care, pneumonia, Triflow

Introduction

The novel coronavirus (COVID-19) was first identified in December 2019 in China.[1] The World Health Organization (WHO) recognized the virus as a public health threat and declared it a pandemic on March 11, 2020, due to its rapid spread.[1] According to scientific research, the COVID-19 virus can spread through direct contact with respiratory droplets and fecal matter.[1] Early outbreak analyses estimated an incubation period of approximately 5.2 days and a basic reproduction number (R_0) of about 2.2.[1,2]

The most common symptoms of COVID-19 include high fever (98%), cough (76%), dyspnea (55%), myalgia or fatigue (44%), sputum production (28%), headache (8%), and other less typical symptoms. Additionally, pneumonia affects nearly all patients. Other frequently reported complications include acute respiratory distress syndrome (ARDS) (29%), acute heart injury (12%), and

Corresponding author: Özge Uçar, e-mail: ozgeenginucar@gmail.com, oucar@bartin.edu.tr

Received: 1.07.2025 / Revised: 29.09.2025 / Accepted: 10.10.2025 / Published: 30.03.2026

Uçar Ö, Çelik S, Uzun S, Karahan E, Altıntaş S. The effects of breathing and coughing exercises on respiratory parameters in COVID-19 patients. *Eur J Clin Exp Med.* 2026;24(1):47–55. doi: 10.15584/ejcem.2026.1.12.

secondary infections (10%).[3,4] COVID-19 patients often exhibit rapid and shallow breathing, with increased rates of tachypnea.[5] A significant portion of COVID-19 patients have at least one underlying chronic condition, and these individuals often require hospitalization.[3,4] Researchers estimate that 20% of COVID-19 patients may require medical clinical care.[6] In patients with mild symptoms, the illness typically lasts about two weeks. However, in those with severe or critical diseases, symptoms can persist for anywhere between three and six weeks.[7]

The number of hospitalized COVID-19 patients exceeds the capacity of available hospital and healthcare facilities. To improve survival rates for patients with acute respiratory distress syndrome (ARDS), healthcare professionals employ various management techniques. Typically, patients with ARDS receive high-flow nasal oxygen therapy and corticosteroid treatment. Previous studies have demonstrated that active respiratory exercises are effective for a range of respiratory diseases, including cystic fibrosis, bronchiectasis, and chronic obstructive pulmonary disease (COPD).[8] Additionally, exercise training is a crucial component of pulmonary rehabilitation.[9,10] A recent study indicated that breathing exercises in COVID-19 patients serve not only to support physical recovery but also as a valuable non-pharmacological approach for managing psychological distress.[11] Another study reported that respiratory rehabilitation programs in COVID-19 patients alleviate dyspnea, anxiety, and depression, reduce related problems, enhance functionality, preserve pre-existing functions, and improve quality of life as much as possible.[12]

Aim

This study aimed to evaluate the effects of deep breathing and coughing exercises using Triflow on the respiratory parameters of COVID-19 patients with pneumonia. Based on this aim, the research hypotheses were formulated as follows:

H_0: Deep breathing and coughing exercises using Triflow have no statistically and clinically significant effect on the respiratory parameters of COVID-19 patients.

H_1: Deep breathing and coughing exercises using Triflow have a statistically and clinically significant effect on the respiratory parameters of COVID-19 patients.

Material and methods

Study design and setting

This study was conducted as a single-blinded randomized controlled trial in the pandemic clinic of a state hospital in the Black Sea Region of Turkey. The clinical trials were obtained from ClinicalTrials.gov for our experimental design research (ID: NCT05218200). The study was designed according to the Consolidated Standards of Reporting Trials (CONSORT) 2010 statement. The CONSORT diagram of the study is presented in Figure 1.

Participants

The study population includes COVID-19 pneumonia patients admitted to the hospital's pandemic clinic over the past year, totalling 2,161 patients. The study sample size is 326 COVID-19 patients, determined using the known population sample size formula ($n = Nt^2\ pq/d^2\ (N-1) + t^2pq$).[13] In the study, 355 patients were assessed. Three hundred and forty-six patients were included in the study. The inclusion criteria were as follows: COVID-19 patients who were over 18 years old, conscious, without cognitive issues, and had no sensory or perceptual impairments, who were not admitted to intensive care units and were not connected to any respiratory support devices. The nine patients under 18 years old, those who were unconscious, could not speak or understand Turkish, had sensory or perceptual disabilities, or required CPAP (Continuous Positive Airway Pressure) or BiPAP (Bilevel Positive Airway Pressure), were excluded from the study. Patients (n=346) were randomly assigned to the experimental and control groups. During the intervention phase, 10 patients from the experimental group and 10 patients from the control group were excluded due to discharge before 10 days, referral to the intensive care unit, or withdrawal from the study. Ultimately, data from a total of 326 patients were analysed, with 163 patients in the experimental group and 163 in the control group (Fig. 1).

Healthcare personnel and professional qualifications

The study was conducted by four researchers with doctoral degrees and one with a master's degree in surgical nursing, all with clinical experience in intensive and palliative care. The doctoral-level researchers developed the exercise training protocol and instructional video based on current literature and expertise. The COVID-19 clinic team included bachelor-level nurses and a pulmonology specialist who provided routine medical care and monitoring. Collaboration among the research team, clinic nurses, and the pulmonologist ensured continuous patient observation, enhanced compliance, and supported the safety and effectiveness of the interventions.

Randomization

The patients (n=346) who met the inclusion criteria were divided into two groups – experimental (173 patients) and control (173 patients) – using a computer-generated block randomization with a 1:1 ratio (randomizer.org). Patients were assigned to groups according to the sequence number determined independently by the program. The patients are unaware of their group allocation. Blinding was not possible for measurements obtained after the intervention. To reduce the risk of bias, objective measurements (device-based parameters such as SpO_2 and PO_2) and valid and reliable scales were used.

Outcomes

The primary outcome of the study was the change in dyspnea severity, measured using the Dyspnea-12 scale, from baseline to day 10. Secondary outcomes included SpO_2 levels, respiratory rate, and sputum quantity. All outcomes were pre-specified in the study protocol to ensure consistency and transparency in intervention and analysis.

Instruments

We collected data using an information form, the Dyspnea-12 scale, and Triflo.

Information form

The first part of the form includes information on age, gender, anthropometric measurements, comorbidities, blood values, clinical picture, and hemodynamic parameters. The second part consists of each individual's measurement results recorded on the 5th and 10th days.

Dyspnea-12 scale

A scale with a total of 12 items and four Likert-type response options was used in this study to assess the severity of dyspnea. The maximum scores on the scale are 21 for the physical dimension and 15 for the emotional dimension, with a total range from 0 to 36. A higher score on the scale indicates greater severity of dyspnea.[14] An internal consistency score of 0.90 was reported by Yorke et al. in the initial study of the scale. In a validity and reliability study conducted in our country by Gök Metin and Helvacı, the Cronbach's alpha value was found to be 0.97.[15] We determined the Cronbach's alpha value for the current study to be 0.93, indicating that the scale has strong internal consistency. The minimal clinically important difference (MCID) for Dyspnea-12(D-12) was set at 2.8 points.[17]

Triflow

Triflow consists of a main body and a blowpipe (Berger A10066, Made in Türkiye). The main body features three columns, each with a corresponding ball. The first column in the main body measures 600 cc, the second measures 900 cc, and the third measures 1200 cc. These measurements represent different levels of lung vital capacity.

Procedure

The study was conducted between December 2021 and September 2022 at one of the State hospitals in Black Sea Region of Turkey. Initially, demographic and clinical information, Dyspnea-12 scale, hemodynamic and respiratory parameters for both groups were evaluated and recorded on the first day. The amount of sputum, hemodynamic parameters, biochemical tests, blood gas analyses, and Dyspnea-12 scale scores were recorded on the 5th and 10th days. This measurement schedule was chosen because the inpatient treatment and observation period is at least 10 days, according to the current treatment algorithm of the Ministry of Health (TC Ministry of Health, 2021).[16] All blood samples were collected at 7:00 AM, following hospital routine procedures. Measurements of hemodynamic and respiratory parameters and sputum volume were scheduled for 8:30 AM on the 1st, 5th, and 10th days. All measurements and records were performed by the same experienced researcher with a master's degree in surgical nursing who has worked in the COVID-19 clinic. This approach was intended to minimize interobserver variability. Because there is no established MCID for sputum quantity in the literature, the operational MCID in our study was predefined as at least one category of improvement (2–5 ml → <2 ml or <2 ml → none).

Control group

Patients in the control group received the same routine of care as other COVID-19 patients in the clinic, which included daily arterial blood gas monitoring, hourly assessment of respiratory parameters, frequent position changes, and support in a semi-upright position. In addition, breathing and coughing exercises were taught to the patients without using assistive devices. All blood samples were collected according to hospital routine practice. The vital parameters and Dyspnea-12 scale scores were measured at 8:30 AM after the patient had rested for at least 30 minutes.

Experimental group

Patients in the experimental group, in addition to receiving routine care, were taught deep breathing and coughing exercises using Triflow. The exercise training content and video were prepared by researchers based on the literature.[17,18] One of the researchers who prepared the exercise video provided face-to-face exercise training to the patients before they independently performed the exercise. After the same researcher who provided the training confirmed that the exercises were performed with correct technique, the patients performed the exercises themselves throughout the study. Previous studies suggest that short-term implementation of deep breathing and coughing exercises, such as 5 times every hour, may have positive effects on respiratory parameters in patients with COVID-19 and pneumonia patients.[8,11] In line with this literature, patients in the experimental group were instructed to regularly perform 5 times of breathing and coughing exercises five times every hour between 09:00 and 22:00. Compliance with the exercises was carefully monitored by an experienced researcher who has worked in the COVID-19 clinic using a checklist. The researchers ensured that the prepared training video, along with reminder messages, was sent to the patients' smartphones twice daily, at 9:00 AM and 3:00 PM. The amount of sputum, hemodynam-

ic and respiratory parameters, biochemical tests, blood gas analyses, and Dyspnea-12 scale scores were recorded before exercises on the 1st, 5th, and 10th days. Only patients who completed the exercises with 100% adherence were included in the study. There were no missing data; therefore, no imputation or handling was required.

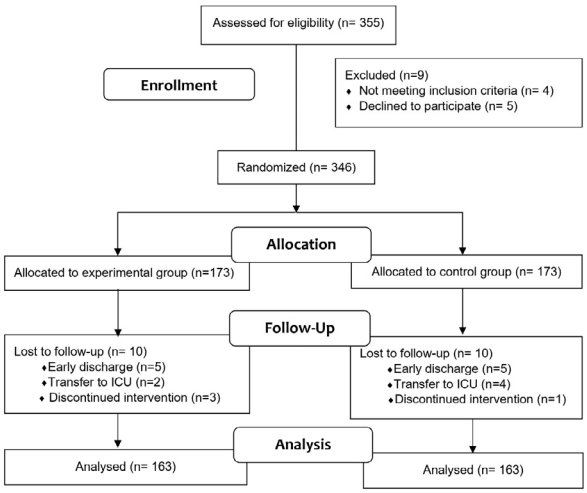

Fig. 1. Consort flow diagram of the study

Ethical consideration

The study obtained ethical approval from the state University Ethical Committee in Turkey on September 14, 2021, with the reference number 2021-SBB-0329, T.R. Ministry of Health (dated 24.11.2021 and numbered 2021-11-22T11), Provincial Health Directorate and hospital (dated 03.12.2021 and E-26080346-799) permissions were obtained. Informed verbal consent was obtained from the service physician and nurses. Before participating in the study, each patient gave written informed consent. They were told they could leave the study whenever they wanted without facing any consequences. Additionally, the patients were guaranteed that their data would be kept private and only used for legitimate scientific purposes. All materials used in the research were provided by Bartin University Scientific Research Projects Unit (Project No: 2021-FEN-A-016).

Data analysis

Data were analysed using IBM SPSS 25 (Armonk, NY, USA). The skewness and kurtosis coefficients of the scores were assessed, revealing that these coefficients fell within the ±2 range. This indicates that the distribution of the scores can be considered approximately normal, as values within this range suggest a relatively symmetrical distribution with moderate peakiness. Based on these findings, descriptive statistical analysis was conducted for the demographic data, and repeated measures ANOVA was used to analyze the repeated measurements, provided the data met the normal distribution criteria. The chi-square test was also employed to compare categorical data. A post hoc power analysis was performed using the G*Power 3.1 program after the research.

Table 1. Demographic and clinical characteristics of the participants (n=326)[a]

	Experimental group (n=163)		Control group (n=163)		t	p
	Mean±SD	Min–Max	Mean±SD	Min–Max		
Age	75.71±9.29	61–93	75.66±9.32	60–94	0.048	0.962
Height (cm)	170.67±8.56	150–180	170.59±8.50	150–185	0.084	0.933
Weight (kg)	72.21±10.96	50–95	72.44±11.36	49–110	-0.184	0.855
Blood values						
Hemoglobin (g/dL)	11.69±1.73	7.6–14.1	11.67±1.73	7.6–14.1	0.108	0.994
Platelets ($\times 10^9$/L)	255.85±79.27	80–491	258.87±82.78	82–490	-0.336	0.681
Blood glucose (mg/dL)	154.87±86.86	84–413	154.20±86.30	89–410	0.070	0.921
Urea (mg/dL)	53.80±24.46	23–114	54.20±24.59	23–116	-0.147	0.860
Uric acid (mg/dL)	3.71±1.51	1.49–6.40	3.64±1.47	1.51–6.39	0.400	0.682
INR	1.02±0.05	0.92–1.14	1.02±0.05	0.92–1.14	-0.214	0.803
PO_2 (mmHg)	71.15±17.43	34.2–104.2	70.05±17.89	36.1–100.0	0.559	0.576
PCO_2 (mmHg)	39.66±6.13	32.2–66.5	38.91±5.14	32.2–53.9	1.202	0.230
HCO_3 (mmol/L)	24.19±3.88	18.6–32.3	24.22±3.94	18.2–29.0	-0.071	0.807
pH	7.40±0.04	7.24–7.68	7.39±0.03	7.27–7.57	0.324	0.746
Respiration rate (breaths/min)	19.53±0.90	18–22	19.52±0.85	18–20	0.126	0.900
Peripheral capillary oxygen saturation (%)	93.70±2.39	87–98	93.72±2.36	90–98	-0.093	0.926
Body temperature (°)	36.32±0.39	34.5–36.8	36.41±0.41	34.5–37.0	0.302	0.702
Heart rate (beats/min)	88.95±13.40	57–115	89.21±13.43	61–111	-0.173	0.895
	n	%	n	%	X^2	p
Gender						
Female	116	71.2	106	65	1.412	0.235
Male	47	28.8	57	35		
Smoking						
Yes	16	9.8	9	5.5	3.829	0.147
No	147	90.2	154	94.5		
Steroid use						
Yes	96	58.9	100	61.3	0.205	0.651
No	67	41.1	63	38.7		
Mobilization						
Dependent	6	3.7	7	4.3	0.080	0.777
Independent	157	96.3	156	95.7		
Chronic diseases*						
Hypertension	90	55.2	93	57.1	0.112	0.738
Obesity	19	11.7	17	10.4	0.125	0.724
Allergy	6	3.7	7	4.3	0.080	0.777
Diabetes	20	12.3	19	11.7	0.029	0.864
CRF**	6	3.7	7	4.3	0.080	0.777
Hypercholesterolemia	13	8.0	13	8.0	0.000	1.000
COPD***	19	11.7	20	12.3	0.029	0.864

[a] T – independent sample t test, X^2 – Chi square test, * – multiple response, **CRF – chronic renal failure, ***COPD: – chronic obstructive pulmonary disease

Results

The measurement results of patients in the experimental (n=163) and control (n=163) groups were presented in tables and figures. Each of the total 326 COVID-19 participants received ten days of follow-up care. There were

no material or moral losses incurred by the patients participating in the study. No adverse effects or harm were observed by any of the researchers.

Table 1 shows that both the experimental and control groups were homogeneous in terms of demographic and clinical characteristics, as indicated by p-values greater than 0.05 (Table 1).

The results from the initial observation of patients and Dyspnea-12 scale scores are presented in Table 2. The results indicate that the groups are homogeneous, with no statistically significant difference in the mean Dyspnea-12 scale scores ($p>0.05$). On day 10, both groups experienced a statistically significant decline in their Dyspnea-12 scores, but the decline in the experimental group was more pronounced than in the control group ($p<0.001$). Dyspnea-12 scale score decreased by an average of 15 points in the experimental group, while it decreased by 8 points in the control group (Table 2). A change in ΔD-12 of ≥ 2.8 between Day 1 and Day 10 was considered clinically significant.

Table 2. Comparison of variables according to the measurement times of the experimental and control groups (n=326)[a]

Dispne-12 scale		Experimental (n=163)	Control (n=163)	t	p[1]	
		Mean±SD	Mean±SD			
First day		22.64±7.16	20.44±7.30	2.748	0.412	
5th day		12.84±5.42	16.31±6.81	-5.080	0.004*	
10th day		7.01±4.66	12.99±6.66	-9.388	0.001*	
F		376.987	193.616			
p[2]		0.000*	0.000*			
Bonferonni		1>2 , 2>3	1>2 , 2>3			
Expectoration amounts		n(%)	n (%)	X^2	p[1]	OR (95% CI)
First day	None	125 (50.6)	122 (49.4)	0.338	0.845	
	Less than 2ml	32 (4.2)	33(50.8)			
	2–5 ml	6 (42.9)	8 (57.1)			
5th day	None	143 (52.0)	132 (48.0)	3.440	0.179	
	Less than 2ml	20 (40.0)	30 (60.0)			
	2–5 ml	–	1 (100.0)			
10th day	None	162 (51.8)	151 (48.2)	9.694	0.001*	0.780 (0.010-0.605)
	Less than 2ml	1 (7.7)	12 (92.3)			
	2–5 ml	–	–			

[a] p[1] – independent sample t test significant value, p[2] – F test significant value, F – ANOVA, SD – standard deviation, X^2 – Chi square test, * – p<0.05, OR – odds ratio, CI – confidence interval

The quantity of sputum in patients on the fifth and tenth days is shown in Table 2. The findings indicate that there was no statistically significant difference between the experimental and control groups at admission and on day five ($p>0.05$). However, on the 10th day, sputum production significantly decreased in the experimental group ($p<0.001$, OR=0.780). This suggests that Triflow-assisted coughing exercises and deep breathing significantly reduced sputum production in COVID-19 patients (OR=0.780) (Table 2).

Table 3. Comparison of arterial blood gas and respiratory parameters according to the measurement times of the experimental and control groups[a]

Parameters	Experimental (n=163)	Control (n=163)	t	p[1]
	Mean±SD	Mean±SD		
PO_2 (mmHg)				
First day	71.15±17.43	70.05±17.89	0.559	0.576
5th day	76.21±14.57	71.39±15.85	2.853	0.005*
10th day	80.67±14.54	73.98±15.79	3.981	0.001*
F	64.460	22.110		
p[2]	0.001*	0.001*		
Bonferonni	1<3, 2<3	1<3, 2<3		
PCO_2 (mmHg)				
First day	39.66±6.13	38.91±5.14	1.202	0.230
5th day	39.26±5.20	39.15±4.92	0.211	0.833
10th day	38.44±3.94	38.98±4.01	-1.222	0.233
F	7.079	7.226		
P[2]	0.003*	0.027*		
Bonferonni	2<3	1<2, 3<2		
SPO_2 (%)				
First day	93.70 ±2.39	93.72±2.36	-0.093	0.926
5th day	94.47±2.14	94.15±2.39	1.266	0.206
10th day	96.02±1.80	94.82±2.00	5.690	0.001*
F	144.313	80.433		
P[2]	0.001*	0.001*		
Bonferonni	1<2<3	1<2<3		
Respiratory rate (rate/minute)				
First day	19.53 ±0.90	19.52±0.85	0.126	0.900
5th day	17.31±2.17	19.83±1.14	-13.116	0.001*
10th day	15.06±3.30	18.60±0.13	-12.158	0.001*
F	167.585	66.681		
P[2]	0.001*	0.001*		
Bonferonni	1>2>3	1>3, 2>3		

[a] p[1] – independent sample t test significant value, p[2] – F test significant value, F – ANOVA, SD – standard deviation, *p<0.05

Figure 2B compares arterial PO_2 values for the experimental and control groups at various measurement times. On day 10, PO_2 levels increased in both groups ($p<0.001$), but the increase in the experimental group was statistically significant (Fig. 2B, Table 3). Throughout the study, no statistically significant difference was found between the arterial PCO_2 levels of the experimental and control groups ($p>0.05$). However, arterial PCO_2 levels decreased continuously in the experimental group ($p=0.003$), while in the control group, they increased on day 5 but decreased again on day 10 ($p=0.027$) (Fig. 2A, Table 3). Post hoc analysis revealed that the significant change observed in the experimental group occurred between days 5 and 10 ($p=0.003$) (Fig. 2A, Table 3).

A statistically significant difference in SpO_2 levels was found between the groups on day 10 ($p<0.001$) (Ta-

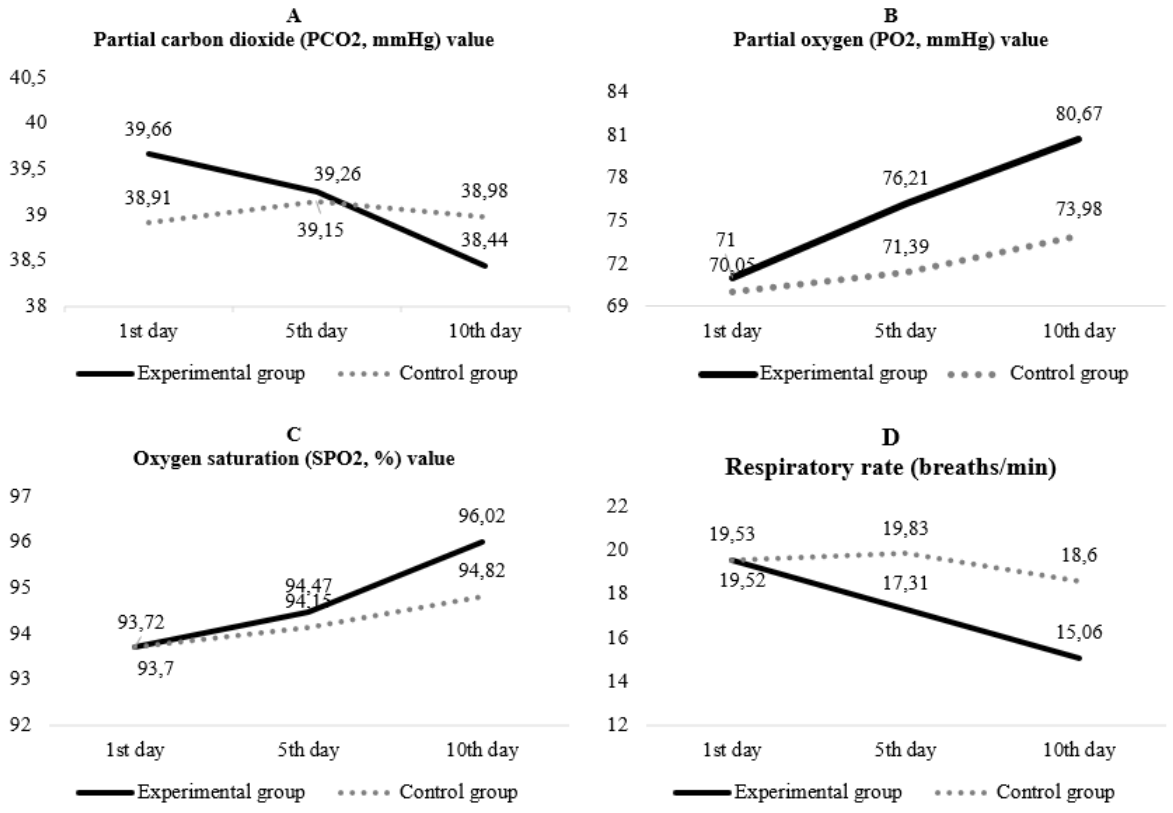

Fig. 2. Comparison of arterial blood gases and respiratory rate values according to measurement time and groups, A: Change in PCO_2 (mmHg) value over time, B: Change in PO_2 (mmHg) value over time; C: Change in SpO_2 (%) over time, D: Change in respiratory rate (breaths/min) over time

ble 3). SpO_2 levels increased on day 10 in both groups compared to the duration of hospital stay ($p<0.001$) (Fig. 2C, Table 3).

Figure 2D shows a statistically significant change in respiratory rates across various measurement periods in both the experimental and control groups ($p<0.001$) (Table 3). Furthermore, changes in respiratory rates were significantly different between the two groups. Patients in the experimental group had lower respiratory rates compared to those in the control group at measurements on days 5 and 10, but these rates remained within clinically acceptable ranges ($p<0.001$) (Fig. 2D, Table 3).

Discussion

The definitive treatment for COVID-19 has not yet been fully established, and the effects of deep breathing exercises as part of care and treatment strategies have not been fully clarified. In the literature, there is a limited number of randomized controlled clinical trials that assess the effectiveness of deep breathing exercises in COVID-19 patients.[17,18]

COVID-19 directly affects respiratory function, often causing dyspnea of varying severity.[19] In this study, dyspnea severity was measured using the Dyspnea-12 scale. The experimental group showed a significantly faster decrease in dyspnea scores on days 5 and 10 compared to baseline ($p<0.05$), suggesting that deep breathing and coughing exercises with Triflow effectively reduce dyspnea in COVID-19 patients. Although overall differences between experimental and control groups were not always statistically significant, the exercises demonstrated symptom relief. Similarly, Öner Cengiz et al. observed beneficial effects of deep breathing exercises on dyspnea severity, though differences between groups were not significant.[18] Zha et al. reported that respiratory rehabilitation, including deep breathing exercises, can effectively manage dyspnea in COVID-19 patients,[19] supporting the overall benefit of these interventions.[20] Abdullahi also reported in a critical review that breathing exercises could be used to reduce dyspnea in COVID-19 patients.[21]

In addition to typical COVID-19 symptoms, about 40% of patients show increased sputum, and autopsies have revealed severe mucoid tracheitis in roughly one-third of non-survivors.[22,23] This highlights the role of respiratory inflammation and mucus in disease severity and outcomes. Effective management of mucus is therefore critical. In our study, only one patient in the experimental group performing Triflow deep breathing exercises produced sputum on day 10, compared to 12

patients in the control group ($p<0.05$; OR=0.780), suggesting that Triflow exercises may reduce sputum production. Similarly, Mollerup applied positive expiratory pressure (PEP-flute) therapy in 378 COVID-19 patients, with 255 reporting sputum symptoms.[24] These findings support the literature, indicating that respiratory exercises can help manage sputum in COVID-19 patients. However, studies on this specific effect remain limited, and further research is needed to confirm these results.

In our study, respiratory rate decreased in both groups, but the reduction was faster in the experimental group performing deep breathing and cough exercises with Triflow. SpO_2 levels also improved more rapidly in this group, suggesting that these exercises enhanced lung capacity and airway clearance, facilitating oxygenation. The respiration rate of COVID-19 patients was found to be 20 breaths per minute in the study by Li et al.[25,26] In another study, it was determined that the respiratory rate in COVID-19 patients exceeded 24 breaths per minute 25. According to research conducted by Cengiz et al., the respiratory rate in the deep breathing exercise group significantly decreased compared to the control group.[18] These findings indicate that deep breathing exercises can effectively improve respiratory parameters in COVID-19 patients, likely by supporting relaxation and accelerating recovery in conjunction with standard treatment. Similarly, in quasi-experimental studies by Kader et al., it was reported that the respiratory rate decreased significantly in the deep breathing exercise group and returned to normal faster than in the control group.[17] In this study, we believe that the decrease in respiratory rate observed in both groups is attributable to reduced virulence and symptom relief due to the treatment process. Additionally, we think that breathing exercises contribute effectively to patient relaxation, as evidenced by the respiratory rate in the experimental group returning to normal limits more quickly than in the control group.

In our study, the baseline SpO_2 levels of patients in both groups were an average 93%. This current study involved a larger sample (n=326) of COVID-19 patients compared to previous studies. The literature reports that the SARS-CoV-2 virus induces inflammatory responses and widespread alveolar damage in the human body. Consequently, changes in O_2, CO_2, SpO_2, and blood pH levels occur.[27] In a study, the SpO_2 levels of patients hospitalized due to COVID-19 were found to be ≤89%.[28] The study by Öner Cengiz et al. examined the effect of breathing exercises on respiratory parameters in 44 COVID-19 patients. They found that SpO_2 levels increased following deep breathing exercises in these patients.[18] In the quasi-experimental study by Kader et al., it was reported that SpO_2 levels in the deep breathing exercise group were significantly higher.[17] These findings are consistent with the existing literature, indicating that our research aligns with previous studies.

Alveolar ventilation and $PaCO_2$ are interconnected. $PaCO_2$ reflects the balance between CO_2 production and its removal. Elevated $PaCO_2$ levels indicate increased pulmonary dead space and a reduced ability of the lungs to expel CO_2.[29] On the 10th day of the trial, it was discovered that the experimental group's PCO_2 levels were noticeably lower than those of the control group. This indicates that the experimental group's arterial PCO_2 levels decreased as a result of engaging in deep breathing exercises. In contrast, the control group exhibited an increase in arterial PCO_2 levels.

It's worth noting that previous studies did not specifically investigate blood gas parameters in relation to deep breathing exercises. Therefore, the findings from your research offer valuable insights into the effect of deep breathing exercises on these blood gas parameters in COVID-19 patients.[17,18] Close monitoring of blood gases is crucial for COVID-19 patients as it guides healthcare professionals in planning treatment and care. The use of Triflow enhances pulmonary function by actively engaging the diaphragm and other inspiratory muscles during breathing exercises. Additionally, these positive findings suggest that patients adapted well to the breathing and cough exercises with Triflow.

Study limitations

The study was conducted exclusively with COVID-19 patients in pandemic clinics, which means its findings may not be generalizable to all COVID-19 patients. However, the results provide a valuable reference for future research on COVID-19 patients with severe pneumonia or those requiring intensive care. The observed impact of deep breathing exercises on respiratory parameters, such as PCO_2 levels, in the experimental group suggests that incorporating these exercises into therapy and care protocols for critically ill COVID-19 patients could be beneficial. Further research is needed to explore the effects of deep breathing exercises on specific subgroups, particularly those with severe pneumonia or in intensive care settings. Such studies could offer targeted insights into how these exercises can improve respiratory function, reduce complications, and enhance overall patient outcomes. This research could ultimately contribute to the development of evidence-based guidelines and interventions to optimize the care of critically ill COVID-19 patients. All patients reported 100% compliance with the exercise program. This should be considered as a potential source of bias since it is based on patient self-reporting.

In this study, all measurements and recordings were carried out by the same researcher, who worked as a clinic nurse. This reduced the risk of interobserver variability and can be considered a strength of the study. However, conducting all assessments by a single observer does not fully eliminate the potential for observer bias. Therefore, future studies could benefit from valida-

tion of the measurements by multiple independent observers. Although patient adherence to the intervention was monitored by the researchers, individual differences in adherence and motivation may have influenced the outcomes. Therefore, variability in treatment adherence should be considered as a potential limitation.

Conclusion

This study demonstrates that deep breathing and coughing exercises with Triflow reduce the severity of dyspnea, improve respiratory parameters, and decrease sputum production in COVID-19 patients. These findings support the idea that such respiratory exercises can help optimize pulmonary function in patients and that incorporating them into routine treatment and care protocols in hospital settings may be beneficial. Furthermore, the study can raise awareness among healthcare professionals and patients about the importance of breathing and coughing exercises and contribute to the development of proactive nursing care strategies aimed at alleviating respiratory distress in COVID-19 patients. In the future, more comprehensive studies with multidisciplinary approaches involving professionals from different disciplines such as physiotherapists and pulmonologists as well as nurses are recommended.

Declarations

Funding

This study was funded by a grant from the Bartin University Scientific Research Projects Unit (Grant No: 2021-FEN-A-016).

Author contributions

Conceptualization, Ö.U. and S.Ç.; Methodology, Ö.U.; Validation, Ö.U., S.Ç.. and S.U.; Formal Analysis, Ö.U., S.Ç., and E.K.; Investigation, Ö.U., S.U., and S.A.; Resources, Ö.U. and S.Ç.; Data Curation, Ö.U..; Writing – Original Draft Preparation, Ö.U., S.U., and S.A.; Writing – Review & Editing, Ö.U., S.Ç., and E.K.; Visualization, Ö.U.; Supervision, S.Ç.; Project Administration, S.Ç.; Funding Acquisition, S.Ç.

Conflicts of interest

The authors declare no competing interests.

Data availability

The datasets generated during and/or analyzed during the current study are available from the corresponding author on reasonable request.

Ethics approval

The study was conducted in accordance with the Declaration of Helsinki, and the protocol was approved by the Ethics Committee of Bartın University Ethical Committee (2021-SBB-0329).

References

1. Special Expert Group for Control of the Epidemic of Novel Coronavirus Pneumonia of the Chinese Preventive Medicine Association. An update on the epidemiological characteristics of novel coronavirus pneumonia (COVID-19). *Zhonghua Liu Xing Bing Xue Za Zhi*. 2020;41(2):139-144. doi:10.3760/cma.j.issn.0254-6450.2020.02.002
2. Li Q, Guan X, Wu P, et al. Early transmission dynamics in Wuhan, China, of novel coronavirus-infected pneumonia. *N Engl J Med*. 2020;382(13):1199-1207. doi:10.1056/NEJMoa2001316
3. Huang C, Wang Y, Li X, et al. Clinical features of patients infected with 2019 novel coronavirus in Wuhan, China. *Lancet*. 2020;395(10223):497-506. doi:10.1016/S0140-6736(20)30183-5
4. Wang D, Hu B, Hu C, et al. Clinical characteristics of 138 hospitalized patients with 2019 novel coronavirus-infected pneumonia in Wuhan, China. *JAMA*. 2020;323(11):1061-1069. doi:10.1001/jama.2020.1585
5. Prabawa IMY, Silakarma D, Manuaba IBAP, Widnyana M, Jeviana A. Chest therapy and breathing exercise in COVID-19 patient: A case report. *Bali Medical Journal*. 2021;10(2):495-498. doi:10.15562/bmj.v10i2.2403
6. Guan WJ, Ni ZY, Hu Y, et al. Clinical characteristics of 2019 novel coronavirus infection in China. *medRxiv*. 2020;1-30. doi:10.1101/2020.02.06.20020974
7. Gonzalez-Gerez JJ, Bernal-Utrera C, Anarte-Lazo E, Garcia-Vidal JA, Botella-Rico JM, Rodriguez-Blanco C. Therapeutic pulmonary telerehabilitation protocol for patients affected by COVID-19, confined to their homes: study protocol for a randomized controlled trial. *Trials*. 2020;21(1). doi:10.1186/s13063-020-04494-w
8. Lewis LK, Williams MT, Olds TS. The active cycle of breathing technique: A systematic review and meta-analysis. *Respir Med*. 2012;106(2):155-172. doi:10.1016/J.RMED.2011.10.014
9. Felten-Barentsz KM, van Oorsouw R, Klooster E, et al. Recommendations for hospital-based physical therapists managing patients with COVID-19. *Phys Ther*. 2020;100(9):1444-1457. doi:10.1093/ptj/pzaa114
10. Polastri M. Physiotherapy in hospitalised patients with COVID-19 Disease: what we know so far. *Int J Ther Rehabil*. 2020;27(3). doi:10.12968/ijtr.2020.0035
11. Sheikh S, Rostami A, Shahbazi A, et al. Clinical effectiveness of guided breathing exercises in reducing anxiety, stress, and depression in COVID-19 patients. *Sci Rep*. 2024;14(1):1-10. doi:10.1038/s41598-024-78162-3
12. Frutos-Reoyo EJ, Cantalapiedra-Puentes E, González-Rebollo AM. Rehabilitación domiciliaria en el paciente con COVID-19. *Rehabilitacion*. 2020;55(2):83. doi:10.1016/J.RH.2020.10.004
13. Sümbüloğlu K, Sümbüloğlu V. *Biostatistics.* 17th ed. Edited by Hatipoğlu T. Ankara: Hatiboğlu Yayınevi; 2016.
14. Yorke J, Moosavi SH, Shuldham C, Jones PW. Quantification of dyspnoea using descriptors: development and

initial testing of the dyspnoea-12. *Thorax*. 2010;65(1):21. doi:10.1136/THX.2009.118521

15. Gök Metin Z, Helvacı A. Dispne-12 ölçeğinin Türkçe geçerlik ve güvenirlik çalışması. *Hacettepe Univ Hemşirelik Fakültesi Derg*. 2018;5(2):102-115. doi:10.31125/hunhemsire.454354
16. T.C. Ministry of Health. COVID-19 Adult treatment algorithm. Accessed May 6, 2025. https://covid19.saglik.gov.tr/TR-66328/eriskin-tedavi-algoritmasi.html.
17. Kader M, Hossain MA, Reddy V, Perera NKP, Rashid M. Effects of short-term breathing exercises on respiratory recovery in patients with COVID-19: A quasi-experimental study. *BMC Sports Sci Med Rehabil*. 2022;14(1):1-10. doi:10.1186/s13102-022-00451-z
18. Öner Cengiz H, Ayhan M, Güner R. Effect of deep breathing exercise with Triflo on dyspnoea, anxiety and quality of life in patients receiving COVID-19 treatment: A randomized controlled trial. *J Clin Nurs*. 2021;31(23):3439-3453. doi:10.1111/jocn.16171
19. Allali G, Marti C, Grosgurin O, Morélot-Panzini C, Similowski T, Adler D. Dyspnea: the vanished warning symptom of COVID-19 pneumonia. *J Med Virol*. 2020;92(11):2272-2273. doi:10.1002/jmv.26172
20. Zha L, Xu X, Wang D, Qiao G, Zhuang W, Huang S. Modified rehabilitation exercises for mild cases of COVID-19. *Ann Cardiothorac Surg*. 2020;9(5):3100-3106. doi:10.21037/apm-20-753
21. Abdullahi A. Safety and efficacy of chest physiotherapy in patients with COVID-19: A critical review. *Front Med*. 2020;7:1-6. doi:10.3389/fmed.2020.00454
22. Khan MA, Khan ZA, Charles M, et al. Cytokine storm and mucus hypersecretion in COVID-19: review of mechanisms. *J Inflamm Res*. 2021;14:175-189. doi:10.2147/JIR.S271292
23. Kumar SS, Binu A, Devan Aswathy R, Nath Lekshmi R. Mucus targeting as a plausible approach to improve lung function in COVID-19 patients. *Med Hypotheses*. 2021;156(110680):1-9. doi:10.1016/j.mehy.2021.110680
24. Mollerup A, Henriksen M, Larsen SC, et al. Effect of PEP flute self-care versus usual care in early COVID-19: non-drug, open-label, randomised controlled trial in a Danish community setting. *BMJ*. 2021;375:e066952. doi:10.1136/bmj-2021-066952
25. Li K, Wu J, Wu F, et al. The clinical and chest CT features associated with severe and critical COVID-19 pneumonia. *Invest Radiol*. 2020;55(6):327-331. doi: 10.1097/RLI.0000000000000672
26. Li X, Ma X. Acute respiratory failure in COVID-19: Is tt "Typical" ARDS? *Crit Care*. 2020;24(1):1-5. doi:10.1186/s13054-020-02911-9
27. Nouri-Vaskeh M, Sharifi A, Khalili N, Zand R, Sharifi A. Dyspneic and non-dyspneic (silent) hypoxemia in COVID-19: possible neurological mechanism. *Clin Neurol Neurosurg*. 2020;198:106217. doi:10.1016/j.clineuro.2020.106217
28. Pan F, Yang L, Li Y, et al. Factors associated with death outcome in patients with severe coronavirus disease-19 (COVID-19): A case-control study. *Int J Med Sci*. 2020;17(9):1281-1292. doi:10.7150/ijms.46614
29. Zheng QN, Xu MY, Zheng Y Le, Wang XY, Zhao H. Prediction of the rehabilitation duration and risk management for mild-moderate COVID-19. *Disaster Med Public Health Prep*. 2020;14(5):652-657. doi:10.1017/DMP.2020.214

Rzeszów University Press 2025
ISSN 2544-1361 (online)
doi: 10.15584/ejcem.2026.1.13

http://www.ejcem.ur.edu.pl
European Journal of Clinical and Experimental Medicine
Eur J Clin Exp Med 2026; 24(1): 56–64

ORIGINAL PAPER

A comparative study of C-reactive protein levels in patients with major depressive disorder with and without suicidal attempts

Arun Seetharaman, Keerthana Suresh, Ramkumar Thirumal, Sriramadesigan Radhakrishnan

Department of Psychiatry, Sri Lakshmi Narayana Institute of Medical Sciences, Pondicherry, India

ABSTRACT

Introduction and aim. Major depressive disorder (MDD) is closely linked to suicidal behavior, and systemic inflammation – particularly elevated C-reactive protein (CRP) – has been proposed as a contributing factor. However, evidence comparing CRP patterns separately in suicide attempters and non-attempters remains limited, especially in underrepresented populations. The aim of this study was to compare serum CRP levels in patients with MDD with and without a history of suicide attempts.

Material and methods. This cross-sectional analytical study included 60 adults diagnosed with MDD according to ICD-10 criteria. Participants were divided into two groups: those with a history of suicide attempts (n=30) and those without such a history (n=30). Depression severity was assessed using the Hamilton Depression Rating Scale (HAM-D). Serum CRP levels were measured using a turbidimetric method. Statistical analyses included Student's t-test, Mann-Whitney U-test, and Pearson's correlation.

Results. CRP levels were significantly higher among suicide attempters compared with non-attempters (4.47±3.53 mg/L vs 2.50±3.59 mg/L; p=0.03). A significant positive correlation between HAM-D scores and CRP levels was observed in the suicide-attempt group (R=0.52; p=0.003), whereas no such correlation was found in non-attempters (R=0.12; p=0.52). Severe depression was more common among suicide attempters (30/44 cases).

Conclusion. This study provides novel evidence that the association between inflammation and depressive symptom severity is present only in patients with a history of suicidal behavior. Elevated CRP may therefore represent a potential marker for identifying MDD patients at increased risk of suicide.

Keywords. C-reactive protein, depressive patients, major depressive disorder, pro-inflammatory marker, suicidal behavior

Introduction

Major depressive disorder (MDD) is one of the leading causes of disability worldwide, ranking second globally in 2020, with 53.2 million anxiety cases and 76.2 million MDD cases.[1,2] Suicidal behavior is a co-morbidity of several neuropsychiatric disorders, including schizophrenia, bipolar disorder, and borderline personality disorder. Among people with mental illnesses, MDD is one of the main preventable causes of death.[3] MDD is a common psychiatric condition with a global point prevalence of 4.7% that causes severe physical health and mental well-being.[4]

Recent studies have demonstrated a clear association between elevated CRP levels and both suicidal behavior and MDD severity. Moslemi et al. studied that increased CRP levels are significantly linked to suicidal behavior in individuals with depression.[5] For instance, elevated CRP levels have been linked to depression and

Corresponding author: Keerthana Suresh, e-mail: drkeesuresh@gmail.com

Received: 28.11.2024 / Revised: 11.02.2025 / Accepted: 19.10.2025 / Published: 30.03.2026

Seetharaman A, Suresh K, Thirumal R, Radhakrishnan S. A comparative study of C-reactive protein levels in patients with major depressive disorder with and without suicidal attempts. *Eur J Clin Exp Med.* 2026;24(1):56–64. doi: 10.15584/ejcem.2026.1.13.

poor antidepressant responses, including treatment resistance. Systemic inflammation raises CRP, a non-specific acute-phase protein. These data imply that CRP may be a distinct predictor for antidepressant therapy response and that anti-inflammatory drugs may help people with high CRP.[6]

Activated immune-inflammatory pathways, including CRP elevation, have been linked to mood disorders like MDD, bipolar disorder (BD), schizophrenia, and suicidal behavior (SB), but studies on CRP's role in SBs have yielded conflicting results. After recent and faraway suicide attempts, pro-inflammatory cytokines and CRP have increased in several studies.[6]

The MDD and CRP are correlated based on the idea that inflammation is a significant factor in MDD pathophysiology. Given that CRP is an inflammatory biomarker, it is increased in patients suffering from MDD, indicating systemic inflammation. This inflammation might disrupt neurotransmitter pathways, particularly those in which serotonin and dopamine are components of mood regulatory circuits. In addition, more severe suicidal ideation and depression have been associated with higher levels of CRP. It may suggest that inflammatory conditions are the ones that exacerbate symptoms in patients with MDD, particularly among those who are suicidal via the triggering of pathways involving processes of both stress and immunity.

The hypothesis that newly diagnosed "drug-naive patients with non-affective psychosis would have higher serum CRP levels than healthy controls and have more severe psychopathology, suicide risk, and alexithymia" was tested by De Beradis et al.[7] Thirty adult CRP levels were measured. Compared to healthy controls and patients at lower risk, those at higher risk for suicide had higher CRP levels. Regardless of psychopathology or depressive symptoms, the current study shows a correlation between CRP, suicide risk and alexithymia, in newly diagnosed, drug-naive patients with non-affective psychosis. Loas et al. examined the relationship between mood or anxiety disorders, alexithymia, anhedonia, recent suicide attempts, suicidal thoughts, impulsivity, CRP, and cholesterol.[8]

As the CRP level spiked, patients were more likely to be in the suicide attempt group compared to the odds of being in the inpatient psychiatric control and/or suicide ideation groups [CI=(1.29, 3.38), OR=2.09 and CI=(1.15, 2.66), OR=1.75 respectively]. Furthermore, compared to people without depression or with mania, those with depression had a considerably higher probability of attempting suicide [CI=(1.97, 54.70), OR=10.38]. Based on CRP levels, there appears to be a gradient in inflammation between mental controls, suicidal ideators, and recent suicide attempters.[9] Miola et al. found suicidal ideation [SI]/behavior factors that could help us understand suicide's pathophysiology and prevent it.[10] Suicidality and CRP levels were shown to be significantly correlated (95% CI 0.476–0.9, SMD 0.688, $p<0.001$). As a result, CRP is a positive inflammatory protein that is produced by the liver's Kupffer cells in reaction to an acute inflammatory event and is readily detectable in plasma by extremely sensitive assays.[11]

Fernández-Sevillano et al. investigated the role of cytokines in suicide attempts as well as how they relate to the psychological components of this intricate, multifaceted occurrence.[12] Participants included 33 MDD patients who have attempted suicide at some point in their lives, 23 non-attempter MDD patients, 20 individuals with an MDD diagnosis and a history of suicide attempts, and 20 healthy controls. Depressive symptoms, aggressive behavior, global functioning, presence of abuse, and attention performance were evaluated in 96 participants. Every participant also had blood extracted for measurement of TNF-α plasma levels, IL2-R, IL-2, IL-6, and IL-4.

Depression can lead to suicidal thoughts, particularly if there are causes for the person to feel pessimistic about the future. Suicidal thoughts is more prevalent in patients with MDD. Suicidal ideation is a significant risk factor for completed suicide in persons with MDD and seems to be a prerequisite for suicide attempts. The prevalence of suicide ideation has been rising in recent years. The 12-month prevalence has varied from 2.3% to 58%, depending on the specific study environment. A number of risk factors for suicidal ideation have also been suggested by earlier research. Suicidal thoughts are linked to low social support, substance use disorder, past suicide attempts, depression and sleep issues, and increased inflammation. Suicidal ideation in MDD patients has also been examined in the studies we mentioned above. In recent years, the relationship between MDD and suicide conduct has gained significant attention. There is currently very few research on the prevalence of suicidal ideation and the factors that are linked to it in MDD patients in Ethiopia.[13,14] Suicidal thoughts that are specific, present, and ongoing are referred to as active suicidal ideation. When someone has a conscious intention to damage himself and some degree of desire – above zero – for death to follow, that person is said to have active SI.[15] According to contemporary views, complex interplay between cultural, environmental, biological and psychological factors can lead to suicidal thoughts and actions.[16]

Orsolini et al. used PubMed to conduct a systematic review on 'CRP' and 'depression.' This evaluation included 56 identified studies.[17] Depression was linked to inflammatory system dysfunction. This study adds to the evidence that CRP and blood levels may be linked to depression. These findings may help develop new treatments and determine if CRP is a depression biomarker. Savita et al. examined the levels of hs-CRP in depressive individuals with and without suicidal thoughts in 2023.[18] The Hamilton Depression Rating Scale (HDRS17), SBQ-R, and BSSI were used to assess

depression and suicidality. Hs-CRP levels are positively correlated with BSSI, HAM-D and SBQ-R scores in depressed and suicidal patients. Similar to this, Grudet et al.[19] calculated the five suicide-related items listed above were part of the suicide composite score. The median of the suicide composite score (6 points) was then used to identify high-grade suicidal ideation (n=100, hg-SI>6 points) and low-grade suicidal ideation (n=99, lg-SI≤6 points). Additionally, recent research has shown a correlation between the lethality of suicide attempts among psychiatric inpatients and the platelet-to-lymphocyte ratio.[20] The association between elevated CRP levels and a higher chance of suicide reattempts highlights the part inflammatory indicators play in suicidal behavior.[21]

Some meta-analyses focused primarily on depressed people and aggregated CRP and suicidality data.[5,22-26] Studies looking at the relationship between CRP and MDD have found a strong link between high CRP levels and both an increased likelihood of suicidal thoughts and actions and the intensity of depressed symptoms.[27] The CRP is associated with suicidality in non-depressed people, as well as suicide thoughts and SB remains unclear. To the best of our knowledge, this is one of the few studies from South India directly comparing CRP levels and depression severity between suicide attempters and non-attempters using standardized ICD-10 and HAM-D assessments. Unlike previous studies, our analysis evaluates the relationship between CRP and depressive symptom severity separately in both groups

Aim

This cross-sectional study aimed to (1) compare serum CRP levels between patients with MDD with and without previous suicide attempts, and (2) evaluate the association between CRP levels and depression severity assessed with the Hamilton Depression Rating Scale (HAM-D).

Material and methods

Assessing CRP levels in depressed patients with and without a history of suicidal thoughts is the goal of this cross-sectional analytical investigation. The potential link between depression, CRP, and suicidal behavior is investigated in this study. The research was carried out at Pondicherry's Sri Lakshmi Narayanan Institute of Medical Science and Hospital (SLIMS) including both outpatient (OP) and inpatient (IP) settings within the Psychiatry Department.

The study population consisted of adult individuals (above the age of 18 years) from the IP and OP services of SLIMS, who were diagnosed with depressive disorder and either had or did not have a history of suicidal attempts during the period under study from July 2022 to January 2024. The source of data included patients diagnosed with depression, categorized into two groups:

- Group A: Patients diagnosed with depression who had a history of suicidal attempts, as per ICD-10 criteria.
- Group B: Patients diagnosed with depression without any history of suicidal attempts, were also diagnosed based on ICD-10 criteria. The study period extended from August 2022 to January 2024.

Sampling method

A convenient sampling method was used to select the participants. According to the sample size calculation, 60 participants in total (30 in each group) would be required to achieve the study's objectives.

Inclusion criteria

- Patients are willing to cooperate in the study.
- Patients with a diagnosis of depression based on the ICD-10 criteria.
- Adults (age >18 years) of both genders.
- Individuals having a history of attempted suicide.

Exclusion criteria

- Patients with co-morbid conditions such as autoimmune diseases, diabetes mellitus, renal insufficiency, pregnancy, tuberculosis, or other disorders known to cause elevated CRP levels.
- Patients presenting with any acute infection (bacterial, viral, or fungal).
- Patients currently taking medications known to affect CRP levels, including anti-inflammatory drugs and oral contraceptives.
- Patients diagnosed with any psychiatric illness other than depression.
- Patients with substance use disorders.
- Patients who did not provide informed consent.

Sample size calculation

The following formula was used to determine the sample size:

$$N = \frac{PQ}{Z\left(1 - \frac{\propto}{2}\right)}$$

where $Z(1 - \alpha/2) = 1.96$ at P = Prevalence = 12%, 95% confidence interval, $Q = 100 - P = 88\%$, d = precision = 3%, with an additional 5% accounted for potential dropout. The calculated sample size indicated that 30 participants were needed in each group, totaling 60 participants for the study.

Method of data collection

This research was clarified to respondents and informed written consent was acquired before their inclusion. Data were collected through direct interviews conducted in person with a standardized questionnaire that

gathered socio-demographic details and assessed depression severity. CRP levels were measured using blood samples analyzed in the laboratory.

CRP analysis

Acute-phase protein CRP is found in normal serum but rises drastically in response to infections, inflammation, and tissue damage. Under such circumstances, the CRP levels can increase to 300 mg/L in 12–24 hours. The anti-CRP-coated latex particles used in the CRP analysis procedure agglutinate when they come into contact with CRP-containing samples. This agglutination is proportional to the CRP concentration and can be measured by turbidimetry.

Analytical procedure

- Preheat the photometer (cuvette holder) and working reagent to 37°C.
- Zero the instrument at 540 nm using distilled water.
- Prepare the cuvette by blending 5.0 µL of the calibrator or sample with 1.0 mL of the working reagent.
- Immediately after adding the sample (A1) and two minutes later (A2), mix thoroughly and record the absorbance.

Methodology

The SLIMS Institutional Ethics Committee gave its clearance for the study to be carried out (IEC/C-P/13/2022). The researcher performed comprehensive mental health assessments, collected detailed histories of depressive disorders, and discussed each case with departmental teaching staff. Prior to starting any medication, baseline CRP levels were measured. Depression diagnosis followed ICD-10 guidelines, and HAM-D was used to measure depression severity. Two independent specialists verified the diagnosis for accuracy.

Statistical methods

SPSS version 21 was used to evaluate the data after it was imported into Microsoft Excel (IBM, Armonk, NY, USA). The data were coded and entered into Epidata software before analysis. Comparisons of qualitative data (frequencies and proportions) were carried out utilizing the Mann-Whitney U-test. Quantitative data were reported as mean and SD, with statistical significance being assessed using t-tests. Odds ratios with 95% confidence intervals were calculated to ascertain the degree of association between variables. A p-value of ≤0.05 was considered statistically significant.

Expected outcomes

The expected outcomes of our proposed study are

- CRP levels may serve as a biomarker to identify depressive patients at risk of suicidal attempts.

Establishing correlations between CRP levels, depression severity, and suicidality could inform early identification and intervention strategies.

Experimental results

Numerous studies have indeed linked inflammation, including elevated levels of CRP, to depression and treatment resistance. Inflammation is believed to play a role in the progression and development of depressive symptoms. Increased levels of CRP, an inflammatory marker, have been linked to an increased risk of depression and poorer response to traditional antidepressant medications.

The following results exhibited the CRP levels in depression patients who have attempted suicide and those who have not can provide valuable insights into this aspect. By examining these associations, we can gain a better understanding of the potential role of inflammation in suicidal behavior and develop targeted interventions to address this complex issue. These findings highlight the importance of monitoring CRP levels in depressive patients, particularly those undergoing suicidal attempts. Hence, the present study created groups among the study cases. Groups include:

- Group A – suicidal attempts
- Group B – no suicidal attempts

Age and gender were sociodemographic profiles in this investigation. In our study, there was a female predominance with 19 cases of suicide attempts and 18 cases of No-suicide attempts. Approximately 11 cases of males were seen in suicide attempts and 12 cases in No-suicide attempts.

Table 1 depicts the 30 attempted suicide instances, patients aged <18–20 (33.3%) were the most prevalent, followed by those aged 31–40 (30%). Over 51–60 had 3% of cases, 41–50 had 7%, and 61–70 had the lowest number (3%). The group with 30 non-suicide cases had the most 41–50 (30%) and 51–60 (26.6%) patients. About 20% were 31–40. Cases were lowest in the age groups <18–20 (10%) and 61–70 (10%).

Table 1. Distribution of age in years

Age categories	Suicide attempt		No suicide attempt	
	Frequency	Percentage	Frequency	Percentage
<18–20	10	33.33%	3	10%
21–30	7	23.3%	1	3.3%
31–40	9	30%	6	20%
41–50	2	6.6%	9	30%
51–60	1	3.3%	8	26.6%
61–70	1	3.3%	3	10%

Comparison between HAM-D scores among study groups

The present study compared the HAM-D scores between suicide attempts and non-suicide attempts using

a student's t-test. The mean/SD range of HAM-D scores among group A was 23.8/2.41, and for group B was 22.36/7.16. The calculated t-score was noted as 1.0440, and the p-value showed 0.3008 (Table 2). This implies that the comparison between HAM D and study groups was statistically insignificant (Fig. 2).

Table 2. Mean and SD distribution of HAM D scores among study groups

Group	Mean	SD	T score	p
Suicide attempt	23.8	2.41	1.0440	0.3008
No suicide attempt	22.36	7.16		

Association between HAMD versus CRP among study groups

The present study found the relation between HAMD versus CRP in suicide attempts and No-suicide attempts using the Karl Pearson correlation. The R^2 among group A was 0.2732. The calculated R value was noted as 0.5227 and the p-value showed 0.003. This implies that the association between HAMD versus CRP among suicidal attempt groups was statistically significant. The R^2 among group B was 0.0149. The calculated R-value was noted as 0.1222, and the p-value showed 0.52 (Table 3). Figures 1 and 2 show the positive and negative correlation between HAMD versus CRP among group A and group B. This implies that the association between HAMD versus CRP among No-suicidal attempt groups was statistically not significant.

Table 3. Karl Pearson's correlation between HAMD versus CRP among study groups

Group	R^2	R	p
Suicide attempt	0.2732	0.5227	0.003
No suicide attempt	0.0149	0.1221	0.52

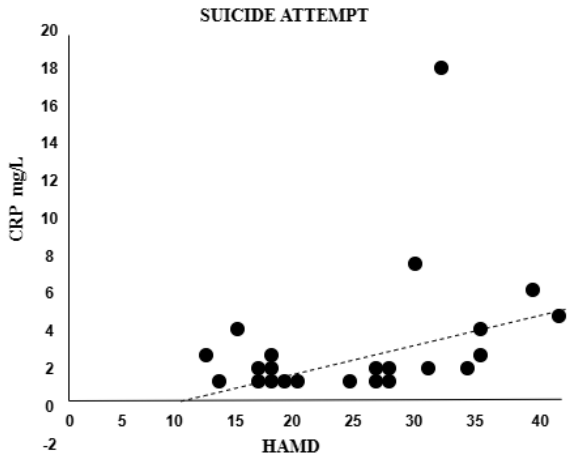

Fig. 1. Positive correlation between HAMD versus CRP among group A

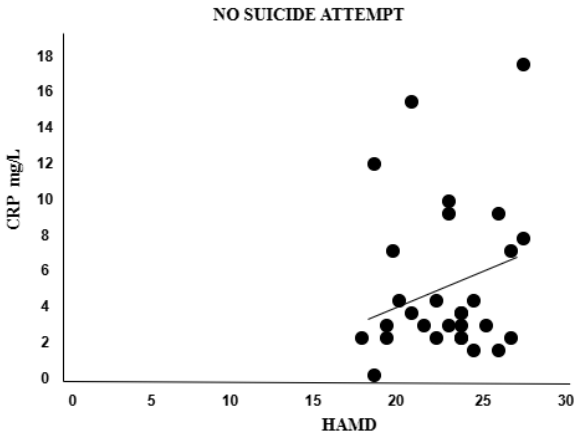

Fig. 2. Negative correlation between HAMD versus CRP among group B

Diagnosis

According to the present study results, Table 4 shows a total of 16 research participants with moderate depression, and no suicidal attempts were seen among all 16 cases. Of the 44 participants with severe depression, about 30 cases were seen with suicidal attempts, and 14 cases were seen with no-suicidal attempts.

Table 4. Distribution of depression diagnosis among total cases and study groups

Diagnosis	Total research participants	Suicide attempt	To suicide attempt
Moderate depression	16	0	16
Severe depression	44	30	14

Mann-Whitney U-test

According to the information provided during statistical analysis, the present study compared the CRP values between moderate depression and severe depression patients using the Mann-Whitney U test. The calculated Z score was noted as 4.45, and the p showed 0.0001 (Table 5). This implies that the comparison between CRP and depression severity in the study population was statistically significant.

Table 5. Comparison between CRP levels and depression severity

Group	CRP	
	Z score	p
Moderate depression	4.45	<0.0001
Severe depression		

Student t-test

According to the information provided, the present study compared CRP between suicide attempts and No-suicide attempts using a student's t-test. The mean/SD range of CRP among group A was 4.47/3.53. The

mean/SD range of CRP among group B was 2.5/3.59. The calculated T-score was noted as 2.14 and the p showed 0.03 (Table 6). This implies that the comparison between CRP and study groups was statistically significant.

Table 6. Variable comparison between CRP and study groups

Group	Mean	SD	T score	p
Suicide attempt	4.47	3.53	2.14	0.03
No suicide attempt	2.5	3.59		

Correlation between CRP and study groups

Based on the Karl Pearson correlation, the R-value of CRP was found to be 0.867. Hence, this implies that the correlation between CRP and study groups was statistically significant with a p<0.05 (Table 7). The positive association of CRP between study groups is depicted in Figure 3. This indicates that there was a strong relationship between CRP levels and the studied variables.

Table 7. Association between CRP and between study groups

Group	CRP	
	R	p
Suicide attempt	0.867	<0.05
No suicide attempt		

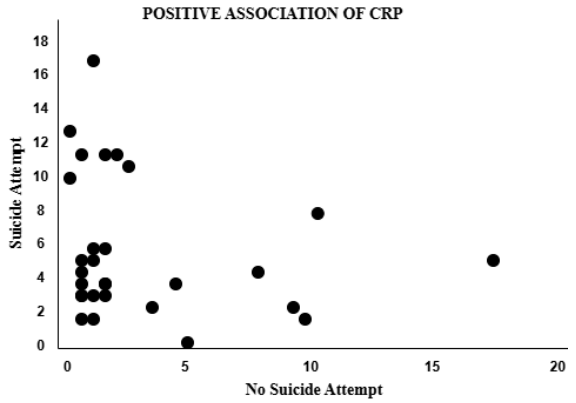

Fig. 3. Positive association of CRP between study groups

There is a high positive connection between the study groups and CRP levels, as indicated by the Pearson correlation coefficient of 0.867. This correlation is statistically significant if the p-value is less than 0.05. Thus, it can be determined that the study groups and CRP levels have a strong and significant correlation.

Discussion

The present study investigates the association between CRP (C-reactive protein) levels and depressive patients with and without a history of suicide attempts, aiming to understand the role of inflammation in suicidal behavior. These results add to the increasing amount of data demonstrating the connection between depression, inflammation, and suicidality, potentially leading to targeted interventions.

Acute-phase inflammatory marker CRP is postulated to be involved in the neuroinflammatory processes, possibly leading to the alterations of neurotransmitter systems, neuroplasticity, and dysregulation of the HPA axis. These mechanisms might explain why an elevated level of CRP correlates with suicidal behavior. Enhanced inflammation could contribute to serotonergic dysfunction, thus potentially leading to increased aggression, impulsivity, and dysregulated emotional processing – factors that are directly related to suicidal attempts and ideation.

Toffol et al. showed considerably higher CRP levels in recent suicide attempters than age- and sex-matched healthy adults.[28] CRP levels in attempted suicide cases were unrelated to background, metabolic, psychopathological, or suicide techniques. Group A had 22.8/3.41 mean/SD HAM-D scores, while group B had 23.36/6.16. The estimated t-score was 3.589 and p-value 0.005. This indicates a substantial comparison between HAM-D and research groups. The two groups' HAM-D symptom mean and SD were calculated. Two groups were compared using the t-test. No significant difference was found between attempters and non-attempters on HAM-D variables.[29] The present study found a significant connection between CRP levels and HAM-D scores in the suicidal attempt group, with an R=0.5227 and a p=0.003. The association between depressive symptoms and inflammation in suicide attempters is statistically significant. However, the no-suicidal attempt group had no significant association between HAM-D scores and CRP levels, with an R=0.1222 and a p=0.52. In non-suicide attempters, depressive symptoms and inflammation were not associated. The US study also found that avoidant-type coping behavior was positively connected with depression ratings for men, women, or both.[30]

In suicide attempters, Malone et al. found greater CRP levels, suicidal ideation, anger, hostility, and impulsivity. The study discovered a strong link between elevated CRP and suicide attempts. Botswick found a positive connection between CRP and suicidal thoughts.[31] These findings imply that elevated CRP levels may increase the risk of suicide in depressed people. Sachs-Ericsson et al. and Dumais et al. observed a substantial correlation between depression severity and suicidal behavior in patients attempting suicide.[32,33] In this research, the Karl Pearson correlation R of CRP is 0.867. Therefore, the connection between CRP and study groups is substantial (p<0.05). This suggests a high correlation between CRP levels and the factors. Another

potential mechanism relates to the central nervous system and its activation through systemic inflammation leading to microglia activation and a potential increase in the production of pro-inflammatory cytokines that would adversely affect mood regulation and cognitive functioning, which is compromised among people with major depressive disorder as well as among suicide attempters.

A Pearson correlation coefficient of 0.867 shows a high positive association between CRP levels and study groups. A p below 0.05 indicates that this link is statistically significant. The correlation is not random. Thus, CRP levels and study groups are strongly correlated. However, Calati et al. observed no significant difference in CRP levels between individuals who attempted suicide more or less than a week before plasma collection or between high and low suicidal ideation.[34] Barzilay et al. found a correlation between CRP levels and suicidal ideation in schizophrenia patients, categorized by CRP levels at admission (CRP > 1 vs. <1 mg/dl).[35] Kim et al. validate that anxiety, CRP, and suicidal attempts are linked.[36] They compared suicide attempters' anxiety and CRP to non-attempters. This study adds to the evidence that inflammation, anxiety, and suicide may be interrelated.

These studies imply that inflammation, as evidenced by higher CRP levels, may increase the risk or severity of suicidal behaviors or thoughts and psychiatric illnesses such as schizophrenia, depression, and anxiety. Understanding these relationships can help identify, prevent, and treat suicide risk. A student's t-test was used to compare HAM-D scores between suicide attempters and non-suicide attempters. Group A had 22.8/3.41 mean/SD HAM-D scores, while group B had 23.36/6.16. The estimated t-score was 3.589 and p-value 0.005. This indicates a substantial HAM-D-study group comparison.

Karl Pearson correlation was used to compare HAM-D and CRP in non-suicide and suicide attempt patients. The computed R-value was 0.5227, 0.003 p-value and R^2 for group A was 0.2732. It was statistically significant to compare HAM-D and CRP in suicidal attempt groups. Similarly, the computed R was 0.1222, p-value 0.52 and R^2 for group B was 0.0149. This means that CRP and HAM-D were not significantly associated with patients without suicide attempts. The Karl Pearson correlation R-value of CRP is 0.867. Therefore, the connection between CRP and study groups is substantial ($p<0.05$). This suggests a high correlation between CRP levels and the factors. A Pearson correlation coefficient of 0.867 shows a high positive association between CRP levels and study groups. This correlation is statistically significant if the p-value is less than 0.05. Thus, CRP levels and study groups are strongly correlated. This would thus mean that considering inflammation as an etiopathogenic factor of suicidal behavior is crucial and would inform targeted therapeutic interventions. Systemic inflammation intensifies depressive symptoms and contributes to the severity of suicidal behavior. These findings agree with the hypothesis that inflammation is pivotal in mental health and its interplay with suicidal behavior.

The novelty of this study lies in demonstrating a significant correlation between CRP levels and depression severity exclusively in suicide attempters, but not in non-attempters. This differential pattern has been rarely reported and may indicate that inflammation plays a more prominent role specifically in the subgroup of MDD patients with suicidal behavior.

Study limitations

The positive association between CRP, depression, and suicidal behavior, though supported by the mentioned studies, is subject to several limitations. First, the predominantly cross-sectional design of these studies, including the one by Kim et al.[24], restricts the inference and highlights the need for longitudinal research to elucidate temporal dynamics and pathways. Elevated CRP levels in suicidal attempters could be due to chemical poisoning, which may mask the interpretation. Third, the sample size is small, limiting the findings' generalizability. Moreover, variations in the technique of measuring CRP, cutoff values, and depression assessment tools among studies contribute to methodological differences that limit the comparability of results. Finally, although CRP is a very common inflammatory marker, it gives a very limited view of inflammation; other markers, such as interleukins or tumor necrosis factor-alpha could be integrated to give a deeper vision into the mechanisms of inflammation that underlie depression and suicidal behavior.

Conclusion

This study demonstrated a strong positive association between the inflammatory marker CRP and depression exclusively among suicide attempters, while no such association was observed in non-attempters. This differential pattern represents a novel finding, suggesting that inflammation may play a more prominent role specifically in the subgroup of MDD patients with suicidal behavior. The results indicated that higher CRP levels were associated with increased depressive symptoms in suicide attempters, supporting the hypothesis that inflammatory activation contributes to the severity of depression and elevates suicide risk.

Understanding this interaction is essential for identifying high-risk individuals, guiding targeted interventions, and improving clinical prevention strategies. These findings highlight the potential utility of CRP as a supplementary clinical marker in assessing suicide risk. Further research is warranted to elucidate the biolog-

ical mechanisms underlying this selective association and to explore whether anti-inflammatory approaches may benefit depressive patients with heightened suicidal vulnerability.

Acknowledgments

The authors are showing their gratitude to the Sri Lakshmi Narayana Institute of Medical Sciences, for the spontaneous support regarding this entire research study.

Declarations

Funding

The authors have clearly stated that they do not have any commercial interest or financial interest. The research costs were easily covered by the researchers.

Author contributions

Conceptualization, A.S. and K.S.; Methodology, K.S.; Software, K.S.; Validation, A.S., K.S. and R.T.; Formal Analysis, K.S.; Investigation, A.S.; Resources, R.T. and S.R.; Data Curation, K.S.; Writing – Original Draft Preparation, K.S.; Writing – Review & Editing, K.S.; Visualization, A.S.; Supervision, A.S.

Conflicts of interest

All authors clearly stated that they do not have any conflicts of interest.

Data availability

Usually, the sets of data are created during and/or analyzed throughout the entire study and are available from the corresponding author upon reasonable request.

Ethics approval

The ethical approval was acquired from the institutional ethical committee of Sri Lakshmi Narayana Institute of Medical Sciences IEC/C-P/13/2022.

References

1. World Health Organization. Depression: A global crisis. 2023. In: WHO Fact Sheet. Geneva: World Health Organization. https://www.who.int/news-room/fact-sheets/detail/depression. Accessed September 20, 2024.
2. Global Burden of Disease Study. 2021. In: Global Burden of Disease. Seattle: Institute for Health Metrics and Evaluation. https://www.healthdata.org/gbd. Accessed September 20, 2024.
3. Naragon-Gainey K, Watson D. The anxiety disorders and suicidal ideation: accounting for co-morbidity via underlying personality traits. *Psychol Med.* 2011;41(7):1437-1447. doi:10.1017/S0033291710002096
4. Al-Hamzawi AO, Bruffaerts R, Bromet EJ, AlKhafaji AM, Kessler RC. The epidemiology of major depressive episode in the Iraqi general population. *PLoS One.* 2015;10(7):e0131937. doi:10.1371/journal.pone.0131937
5. Moslemi H, Fatemian H, Hosseini Y, Moshfeghinia R. C-reactive protein (CRP) level in depressed patients with suicidal behavior: a systematic review and meta-analysis. *J Affect Disord.* 2024:366:423-433. doi:10.1016/j.jad.2024. 08.135
6. Ceciliani F, Giordano A, Spagnolo V. The systemic reaction during inflammation: the acute-phase proteins. *Protein Pept Lett.* 2002;9(3):211-223. doi:10.2174/0929866023408779
7. De Berardis D, Conti CM, Marini S, et al. C-reactive protein level and its relationship with suicide risk and alexithymia among newly diagnosed, drug-naïve patients with non-affective psychosis. *Eur J Inflamm.* 2013;11(1):215-221. doi:10.1177/1721727X1301100120
8. Loas G, Dalleau E, Lecointe H, Yon V. Relationships between anhedonia, alexithymia, impulsivity, suicidal ideation, recent suicide attempt, C-reactive protein, and serum lipid levels among 122 inpatients with mood or anxious disorders. *Psychiatry Res.* 2016;246:296-302. doi:10.1016/j.psychres.2016.09.056
9. Gibbs HM, Davis L, Han X, Clothier J, Eads LA, Cáceda R. Association between C-reactive protein and suicidal behavior in an adult inpatient population. *J Psychiatr Res.* 2016;79:28-33. doi:10.1016/j.jpsychires.2016.04.002
10. Miola A, Dal Porto V, Tadmor T, et al. Increased C-reactive protein concentration and suicidal behavior in people with psychiatric disorders: a systematic review and meta-analysis. *Acta Psychiatr Scand.* 2021;144(6):537-552. doi:10.1111/acps.13351
11. Aguglia A, Natale A, Fusar-Poli L, et al. C-reactive protein as a potential peripheral biomarker for high-lethality suicide attempts. *Life (Basel).* 2022;12(10):1557. doi:10.3390/life12101557
12. Fernández-Sevillano J, González-Ortega I, MacDowell K, et al. Inflammation biomarkers in suicide attempts and their relation to abuse, global functioning, and cognition. *World J Biol Psychiatry.* 2022;23(4):307-317. doi:10.1080/15622975.2021.1988703
13. Klonsky ED, May AM, Saffer BY. Suicide, suicide attempts, and suicidal ideation. *Annu Rev Clin Psychol.* 2016;12:307-330. doi:10.1146/annurev-clinpsy-021815-093204
14. Campisi SC, Carducci B, Akseer N, Zasowski C, Szatmari P, Bhutta ZA. Suicidal behaviours among adolescents from 90 countries: a pooled analysis of the global school-based student health survey. *BMC Public Health.* 2020;20(1):1-11. doi:10.1186/s12889-020-09209-z
15. Liu RT, Bettis AH, Burke TA. Characterizing the phenomenology of passive suicidal ideation: a systematic review and meta-analysis of its prevalence, psychiatric comorbidity, correlates, and comparisons with active suicidal ideation. *Psychol Med.* 2020;50(3):367-383. doi:10.1017/S003329171900391X
16. McKay T, Berzofsky M, Landwehr J, Hsieh P, Smith A. Suicide etiology in youth: differences and similarities by sexual and gender minority status. *Child Youth Serv Rev.* 2019;102:79-90. doi:10.1016/j.childyouth.2019.03.039

17. Orsolini L, Pompili S, Tempia Valenta S, Salvi V, Volpe U. C-reactive protein as a biomarker for major depressive disorder? *Int J Mol Sci.* 2022;23(3):1616. doi:10.3390/ijms23031616
18. Savita V, Pal VS, Bagul K, Mudgal V. A comparative study of picolinic acid levels in patients of severe depression with and without suicidality. *Arch Med Health Sci.* 2023;11(2):198-202. doi:10.4103/amhs.amhs_79_23
19. Grudet C, Lindqvist D, Malm J, Westrin Å, Ventorp F. 25(OH)D levels are decreased in patients with difficult-to-treat depression. *Compr Psychoneuroendocrinol.* 2022;10:100126. doi:10.1016/j.cpnec.2022.100126
20. Aguglia A, Amerio A, Asaro P, et al. High lethality of suicide attempts associated with platelet-to-lymphocyte ratio and mean platelet volume in psychiatric inpatient setting. *World J Biol Psychiatry.* 2021;22(2):119-127. doi:10.1080/15622975.2020.1761033
21. Aguglia A, Solano P, Parisi VM, et al. Predictors of relapse in high lethality suicide attempters: a six-month prospective study. *J Affect Disord.* 2020;271:328-335. doi:10.1016/j.jad.2020.04.006
22. Su YA, Ye C, Xin Q, Si T. Major depressive disorder with suicidal ideation or behavior in Chinese population: a scoping review of current evidence on disease assessment, burden, treatment, and risk factors. *J Affect Disord.* 2023;340:732-742. doi:10.1016/j.jad.2023.08.106
23. Kumar U. *Handbook of Suicidal Behaviour.* Singapore: Springer Singapore; 2017.
24. Ansar W, Ghosh S. CRP: historical perspective, structure, evolution, synthesis, clinical and biological functions. In: *Biology of C Reactive Protein in Health and Disease.* Singapore: Springer; 2016:33-43. doi:10.1007/978-81-322-2680-2_2
25. Gasparini A, Callegari C, Lucca G, Bellini A, Caselli I, Ielmini M. Inflammatory biomarker and response to antidepressant in major depressive disorder: a systematic review and meta-analysis. *Psychopharmacol Bull.* 2022;52(1):36.
26. Osimo EF, Baxter LJ, Lewis G, Jones PB, Khandaker GM. Prevalence of low-grade inflammation in depression: a systematic review and meta-analysis of CRP levels. *Psychol Med.* 2019;49(12):1958-1970. doi:10.1017/S0033291719001454
27. Aguglia A, Solano P, Giacomini G, et al. The association between dyslipidemia and lethality of suicide attempts: a case-control study. *Front Psychiatry.* 2019;10:70. doi:10.3389/fpsyt.2019.00070
28. Toffol E, Miola A, Magnolfi G, Trevisan G, Scocco P. High hs-CRP levels after an attempted suicide: a matched case-control study. *J Affect Disord Rep.* 2022;10:100381. doi:10.1016/j.jadr.2022.100381
29. Srivastava S, Sharma B, Avasthi RK, Kotru M. Comparison between inflammatory biomarkers (high-sensitivity C-reactive protein and neutrophil-lymphocyte ratio) and psychological morbidity in suicide attempt survivors brought to medicine emergency. *Cureus.* 2021;13(8):e17459. doi:10.7759/cureus.17459
30. Baumert J, Lukaschek K, Kruse J, et al. No evidence for an association of posttraumatic stress disorder with circulating levels of CRP and IL-18 in a population-based study. *Cytokine.* 2013;63(2):201-208. doi:10.1016/j.cyto.2013.04.033
31. Pethő-Botswick Á, Kovács MÁ, Simon D, et al. Investigation of peripheral inflammatory biomarkers in association with suicide risk in major depressive disorder. *Front Psychiatry.* 2024;15:1321354. doi:10.3389/fpsyt.2024.1321354
32. Sachs-Ericsson N, Hames JL, Joiner TE, et al. Differences between suicide attempters and nonattempters in depressed older patients: depression severity, white-matter lesions, and cognitive functioning. *Am J Geriatr Psychiatry.* 2014;22(1):75-85. doi:10.1016/j.jagp.2013.01.063
33. Dumais A, Lesage AD, Alda M, et al. Risk factors for suicide completion in major depression: a case-control study of impulsive and aggressive behaviors in men. *Am J Psychiatry.* 2005;162(11):2116-2124. doi:10.1176/appi.ajp.162.11.2116
34. Calati R, Bakhiyi CL, Artero S, Ilgen M, Courtet P. The impact of physical pain on suicidal thoughts and behaviors: meta-analyses. *J Psychiatr Res.* 2015;71:16-32. doi:10.1016/j.jpsychires.2015.09.004
35. Barzilay R, Lobel T, Krivoy A, Shlosberg D, Weizman A, Katz N. Elevated C-reactive protein levels in schizophrenia inpatients is associated with aggressive behavior. *Eur Psychiatry.* 2016;31:8-12. doi:10.1016/j.eurpsy.2015.09.461
36. Kim SY, Jeon SW, Lim WJ, et al. Vitamin D deficiency and suicidal ideation: a cross-sectional study of 157,211 healthy adults. *J Psychosom Res.* 2020;134:110125. doi:10.1016/j.jpsychores.2020.110125

Rzeszów University Press 2026
ISSN 2544-1361 (online)
doi: 10.15584/ejcem.2026.1.14

http://www.ejcem.ur.edu.pl
European Journal of Clinical and Experimental Medicine
Eur J Clin Exp Med 2026; 24 (1): 65–72

ORIGINAL PAPER

Association of the *GPX1* rs1050450 single nucleotide variant and identification of the novel variant rs771425412 in patients with primary osteoporosis from Baghdad, Iraq

Saleen Salam Abdulhadi , Rana Kadhim Mohammed

Department of Biotechnology, College of Science, University of Baghdad, Iraq

ABSTRACT

Introduction and aim. Osteoporosis is a multifactorial bone disorder driven by genetic and environmental factors, with oxidative stress implicated in its pathogenesis. Glutathione peroxidase 1 (GPX1), a key antioxidant enzyme, modulates bone homeostasis by regulating reactive oxygen species. To our knowledge, this is the first study to report the rs771425412 variant of the GPX1 gene in association with primary osteoporosis. This study investigated the association between the single nucleotide variant (rs1050450 C>T and rs771425412 C>A) and the risk of primary osteoporosis in Iraqi patients.

Material and methods. A case-control study was conducted involving 105 patients with primary osteoporosis and 105 age-/sex-matched healthy controls recruited from Baghdad Hospital. Peripheral blood genomic DNA was genotyped by PCR and direct sequencing.

Results. The rs1050450-T allele was significantly more frequent in patients than in controls (25.7% vs. 10.95%; OR=2.68, 95% CI: 1.58–4.55, p<0.001), with the CT genotype increasing the risk (dominant model: OR=3.77, 95% CI: 2.08–6.86). Similarly, the rs771425412-A allele was enriched in patients compared to controls (17.1% vs. 2.9%; OR=7.03, 95% CI: 2.93–16.92, p<0.001), and the CA genotype increased risk (OR=8.61, 95% CI: 3.47–21.3). Haplotype analysis revealed a protective C-C haplotype (OR=0.31, 95% CI: 0.19–0.51), while the T-A (OR=23.2, 95% CI: 3.09–174.3) and C-A (OR=3.15, 95% CI=1.12–8.8) haplotypes were associated with increased susceptibility.

Conclusion. The CT genotype of rs1050450 and the CA genotype of rs771425412 in the *GPX1* gene are significantly associated with an increased susceptibility to primary osteoporosis in the Iraqi population, likely through mechanisms involving impaired oxidative stress regulation.

Keywords. GPX1, osteoporosis, oxidative stress, rs1050450, rs771425412, SNV

Introduction

Osteoporosis is a bone disorder characterized by weakened bone structure that increases the risk of fractures. This condition arises from various factors, including age, genetics, sex, environmental influences, and lifestyle choices.[1] Primary osteoporosis, the most common form of the disease, develops because of age-related changes or hormonal deficiencies, particularly estrogen decline during menopause.[2] This condition differs from secondary osteoporosis, which results from underlying medical conditions or medications.[3] The pathophysiology of primary osteoporosis involves complex interactions between genetic factors, environmental influences, hormonal changes, and lifestyle choices, with genetic components contributing approximately 70% of bone mineral density variation.[4,5]

Corresponding author: Saleen Salam Abdulhadi, e-mail: saleen.s@sc.uobaghdad.edu.iq

Received: 28.06.2025 / Revised: 6.10.2025 / Accepted: 19.10.2025 / Published: 30.03.2026

Abdulhadi SS, Mohammed RK. Association of the *GPX1* rs1050450 single nucleotide variant and identification of the novel variant rs771425412 in patients with primary osteoporosis from Baghdad, Iraq. *Eur J Clin Exp Med.* 2026;24(1):65–72. doi: 10.15584/ejcem.2026.1.14.

Oxidative stress plays a crucial role in bone homeostasis by disrupting the balance between bone formation and resorption.[6] The accumulation of reactive oxygen species (ROS) leads to increased osteoclast activity and enhanced bone resorption while simultaneously inducing apoptosis in osteoblasts and osteocytes, resulting in net bone loss.[7] This oxidative imbalance significantly contributes to the pathogenesis of osteoporosis by altering key signaling pathways, including the upregulation of RANKL and downregulation of osteoprotegerin (OPG), which favors osteoclast differentiation and bone resorption.[8,9]

Glutathione peroxidase 1 (GPX1) stands as a principal contributor to the cellular antioxidant system. Functioning as a selenium-dependent enzyme, its primary role involves the catalytic reduction of harmful hydroperoxides, including hydrogen peroxide, into inert products like water and alcohols.[10] The gene encoding GPX1 is situated on chromosome 3p21.31, spans 1,183 base pairs, and features a two-exon structure interrupted by one intron.[11,12] *GPX1* is the most copious isoform of its kind in human cells, with widespread expression and a predominantly cytoplasmic distribution.[13] A critical aspect of its function is the presence of selenocysteine at the active site. This unique amino acid is encoded by a UGA codon, which typically terminates translation but is co-opted for selenocysteine insertion when guided by SECIS elements in the 3' UTR.[14] Among these variants, a single nucleotide variant (SNV) with a missense mutation, considered the most studied polymorphism in the *GPX1* gene, is rs1050450, which is correlated with various diseases.[15,16]

SNV rs1050450, located in exon 2 of the *GPX1* gene at position 198, is a single substitution from cytosine to thymine, which alters the function of the synthesized protein by changing the amino acid from proline to leucine.[17] The role of *GPX1* and its variants in osteoporosis may vary across different populations owing to genetic diversity, environmental factors, and lifestyle choices.[18] Population-specific studies are essential for understanding how SNVs such as rs1050450 (Pro198Leu) affect *GPX1* activity and its association with bone health. For example, the frequency of the T allele of rs1050450 may differ between populations, potentially influencing the prevalence of osteoporosis in these groups.[15,19] In contrast to the well-characterized rs1050450 variant, rs771425412 appears to be a less commonly studied polymorphism in GPX1. This C>A transversion results in a missense mutation, changing the codon from CCA to CAA, which leads to an amino acid substitution of proline to glutamine at codon 198 (p.Pro198Gln). This non-conservative change, replacing a rigid proline with a polar glutamine, could potentially alter the local protein structure and stability of the GPX1 enzyme, thereby impacting its antioxidant function. The limited literature specifically addressing this variant suggests that it may represent a rarer genetic variation with potentially different functional implications compared to the more prevalent Pro198Leu polymorphism.[20] Crucially, the variant rs771425412 remains poorly characterized in osteoporosis, with no population-specific data from Iraq or similar regions. This study aimed to investigate the association between two GPX1 variants (rs1050450 and rs771425412) and primary osteoporosis in Iraqi patients, introducing rs771425412 as a newly identified variant in this context.

Material and methods

Ethical Approval

The study protocol received ethical sanction from the Ethics Committee of the Department of Biotechnology, College of Science, University of Baghdad (Reference: CSEC/1023/0069 on October 30, 2023). All procedures conformed to the ethical standards of the Declaration of Helsinki. Prior to any study procedures, written informed consent was secured from every participant. From November 2023 to August 2024, a total of 210 subjects within the age range of 32–75 years were recruited. The study population consisted of 105 patients diagnosed with primary osteoporosis (75 females, 30 males) and 105 healthy controls matched for age and sex. Patients were recruited from those attending the Baghdad Teaching Hospital and Al-Wasit Hospital in Baghdad Province.

Dual energy X-ray absorptiometry (DEXA) scan

Each participant was examined by a physician, and bone mineral density (BMD) was measured via a DEXA scan of the hip and spine. Participants were classified as healthy controls (T-score ≥ -1.0 SD) or osteoporosis patients (T-score ≤ -2.5 SD), according to the World Health Organization (WHO) criteria.[1]

Including and exclusion criteria for blood samples

Patients aged 32–75 years were confirmed to have primary osteoporosis. Individuals with medical conditions known to affect bone metabolism, such as chronic diseases or other systemic and metabolic bone disorders, were excluded. None of the participants had recently taken medications that could influence bone metabolism. All participants completed a questionnaire to provide clinical data, including BMI, comorbidities, lifestyle factors (alcohol consumption, smoking, physical activity), and medication history.

Blood samples collection

Approximately 5 mL of venous blood was collected from each participant. Of this, 2 mL was transferred to an EDTA-containing tube for the analysis of GPX1 variants using polymerase chain reaction (PCR) and direct DNA sequencing.

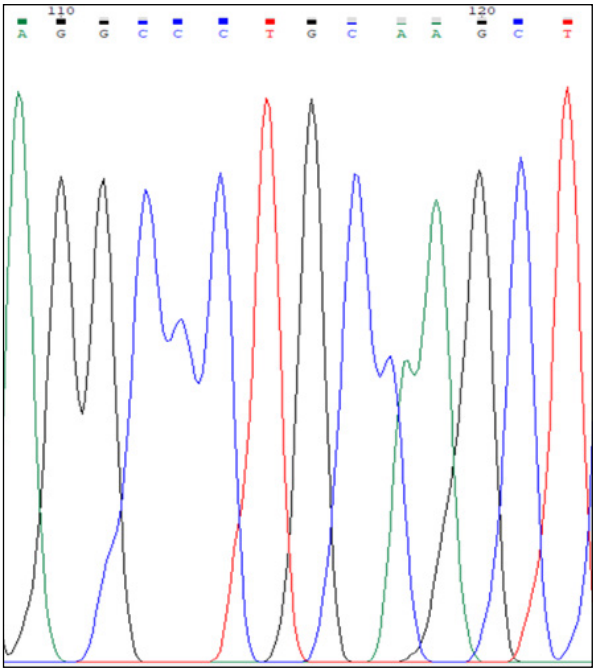

(rs771425412 C>A)

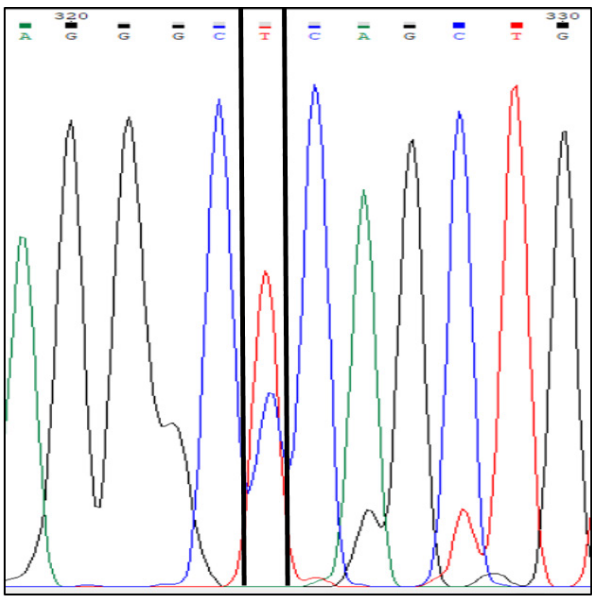

(rs1050450 C>T)

Fig. 1. DNA sequence chromatograms of *GPX1* gene single nucleotide polymorphisms (rs1050450 and rs rs771425412). ChromasPro software was used to generate the chromatogram

Genetic analysis of GPX1

Genomic DNA was extracted from blood samples using the EasyPure® Blood Genomic DNA Kit (TransGen Biotech, Cat. No. EE121-01), and its purity and concentration were assessed using a NanoDrop spectrophotometer (Thermo Fisher Scientific, USA). A 665 bp region of exon 2 of the GPX1 gene, containing the SNV rs1050450, was amplified using newly designed primers (Forward: 5′-CGCCAAGAACGAAGAGATTC-3′; Reverse: 5′-CCTGGGCAATAGAGCAAAAA-3′) from Alpha DNA Ltd. (Montreal, QC, Canada). PCR was performed in a 25 µL reaction volume containing 12.5 µL of 2xEasyTaq® PCR SuperMix, 1 µL of each primer, 6 µL of gDNA, and 4.5 µL of nuclease-free water. The thermal cycling conditions were as follows: initial denaturation at 94°C for 5 minutes; 35 cycles of 94°C for 30 seconds, 56°C for 30 seconds, and 72°C for 30 seconds; and a final extension at 72°C for 5 minutes.

Sequencing and aata analysis

Genotyping of the GPX1 exon 2 SNVs was performed by Sanger sequencing (Macrogen Corporation, Seoul, South Korea). The resulting sequences were analyzed with ChromasPro software and aligned to the GPX1 reference sequence using the Basic Local Alignment Search Tool (BLAST).

The sequence chromatograms of the GPX1 SNVs rs1050450 and rs771425412 were analyzed, as shown in Figure 1. Primers were designed to amplify a region within exon 2 of GPX1 gene, specifically targeting the known SNV rs1050450 (Pro198Leu). However, upon sequencing and alignment of the amplified products using the NCBI reference sequence, an additional SNV, rs771425412 was consistently detected within the same amplified region. This variant was observed in multiple samples with a high frequency in premenopausal women. The NCBI GenBank accession numbers (PV656547, PQ793280, and PQ768535).

Statistical analysis

Statistical analyses were performed using SPSS Statistics for Windows, Version 26.0 (IBM Corp., Armonk, NY, USA). Sample size power was calculated using G*Power, Version 3.1.9.7.[21] Allele and genotype frequencies were calculated and assessed for Hardy-Weinberg equilibrium (HWE). Associations between genotypes and disease risk were estimated using odds ratios (ORs) with 95% confidence intervals (CIs) computed via multinomial logistic regression. The significance of categorical data was assessed using Fisher's exact test (two-sided), with the Bonferroni correction applied for multiple testing. Linkage disequilibrium (LD) and haplotype frequencies were analyzed using the SHEsis web platform.[22]

Results

This case-control study included 105 primary osteoporotic patients and 105 age-/sex-matched healthy controls. A post hoc power analysis confirmed the statistical validity of the sample size (power=0.95). The proportion of women with primary osteoporosis was significantly higher than that of men ($p<0.0001$). Among patients with osteoporosis, 30 men (28.6%) and 75 women (71.4%) were affected, reflecting the same proportions observed in the healthy control (HC) group. According to menopausal status for women, 30 women (28.6%)

were premenopausal, while 45 women (42.9%) were postmenopausal.

The quality of the extracted DNA was confirmed using gel electrophoresis, as shown in Figure 2. Gel electrophoresis results show the PCR products. The bands had a molecular size of approximately 700 bp. As shown in Figure 3.

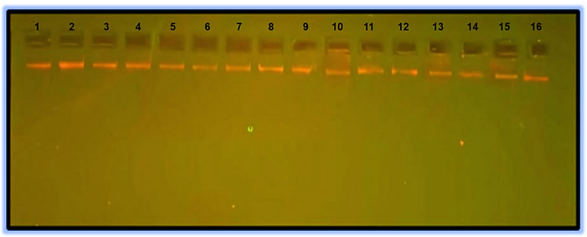

Fig. 2. Genomic DNA electrophoresis; chromosomal DNA bands extracted from human blood samples were visualized under the short wave UV light after staining with the ethidium bromide (EtBr) on (1%) of agarose gel at (70 volts for 30 min), lanes (1-8): healthy controls, lanes (9-16): osteoporosis patients

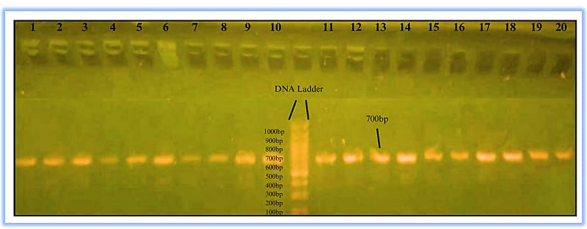

Fig. 3. Agarose gel electrophoresis of PCR products amplified from exon 2 of the *GPX1* gene. Clear bands around 700 bp were observed in both control and patient samples, the gel was run on 1.5% agarose stained with ethidium bromide, lane (1-10): exon2 products for healthy controls, DNA ladder (1000 bp), lanes (11-20): exon2 products for primary osteoporosis patients

Genotype frequencies were notably assessed for HWE, and the genotype distributions of rs1050450 significantly deviated from HWE in the osteoporosis group (p=0.0004), whereas controls showed equilibrium (p=0.2076). Conversely, rs771425412 also deviated slightly in patients (p=0.034) but was in equilibrium among controls (p=0.763), this is presented in Table 1. For rs1050450, the T allele showed a significantly higher frequency in patients (25.7%) than in controls (10.95%), and was associated with an increased risk of osteoporosis (OR=2.68; 95% CI: 1.58–4.55; p<0.001). The dominant model (CT+TT vs. CC) further supported this association (OR=3.77; 95% CI: 2.08–6.86). Similarly, the overdominant and codominant models yielded statistically significant results.

For rs771425412, the A allele was significantly enriched in patients (17.1%) compared with controls (2.9%), corresponding to an increased risk of osteoporosis (OR=7.03; 95% CI: 2.93–16.92; p<0.001). In the dominant model (CA + AA vs. CC), the risk remained substantial (OR=8.61; 95% CI: 3.47–21.3).

Table 1. Multinomial logistic regression analysis combined with HWE analysis of SNVs ((rs1050450-rs771425412) of the *GPX1* gene in primary osteoporosis patients (controls were the reference group))*

SNV/ genetic model	Allele/ genotype/	Pt, n=105		HC, n=105		OR (95% CI)	p
		n	%	n	%		
rs1050450 C/T							
Allele	C	156	74.3	178	89.1	Reference; 1.0	
	T	54	25.7	23	10.95	2.68 (1.58–4.55)	p<0.001
Recessive	CC+CT	105	100.0	105	100.0	Reference; 1.0	
	TT	ND	ND	ND	ND	7.39 (0.15–372.3)	p>0.999
Dominant	CC	51	48.6	82	78.1	Reference; 1.0	
	CT+TT	54	51.4	23	21.9	3.77 (2.08–6.86)	p<0.001
Over-dominant	CC+TT	51	48.6	82	78.1	Reference; 1.0	
	CT	54	51.4	23	21.9	3.77 (2.08–6.86)	p<0.001
Co-dominant	CC	51	48.6	82	78.1	Reference; 1.0	
	CT	54	51.4	23	21.9	3.77 (2.08–6.86)	p<0.001
	TT	ND	ND	ND	ND	4.16 (0.06-301.3)	p>0.999
HWE p		0.0004		0.2076			
rs771425412 C/A							
Allele	C	174	82.9	204	97.1	Reference; 1.0	
	A	36	17.1	6	2.9	7.03 (2.93–16.92)	p<0.001
Recessive	CC+CA	105	100.0	105	100.0	Reference; 1.0	
	AA	ND	ND	ND	ND	7.39 (0.15–372.4)	p>0.999
Dominant	CC	69	65.7	99	94.3	Reference; 1.0	
	CA+AA	36	34.3	6	5.7	8.61 (3.47–21.3)	p<0.001
Over-dominant	CC+AA	69	65.7	99	94.3	Reference; 1.0	
	CA	36	34.3	6	5.7	8.61 (3.47–21.3)	p<0.001
Co-dominant	CC	69	65.7	99	94.3	Reference; 1.0	
	CA	36	34.3	6	5.7	8.61 (3.47–21.3)	p<0.001
	AA	ND	ND	ND	ND	0.06 (0.01-0.52)	p = 0.049
HWE p		0.034		0.763			

* SNV – single nucleotide variant, HWE – Hardy-Weinberg equilibrium, Pt – patients, HC – healthy controls, OR – odds ratio, CI – confidence interval, p – two-tailed probability; pc – Bonferroni correction probability, ND – not detected

Haplotype analysis (in the order rs1050450-rs771425412) identified four haplotypes (C-C, T-C, T-A, C-A) with frequencies of 67.1, 15.7, 1.0%, and 7.1%, respectively, in osteoporosis patients. Compared with the control, the expression of the C-C haplotype (OR=0.31; 95% CI: 0.19–0.5; p=2.06). The T-A haplotype was expressed (OR=23.2; 95% CI: 3.09–174.3; p=1.19). The expression of the C-A haplotype was significantly different (OR=3.15, 95% CI=1.12-8.8; p=0.2). The results are illustrated in Table 2.

Analysis of linkage disequilibrium (LD) revealed that *GPX1* rs1050450 and rs771425412 SNVs: D' (D-prime) measures the degree of LD (non-random association) between the two SNVs Figure 4. A value of 0.41 indicates

moderate LD, meaning that the SNVs are not completely independent, but do not always segregate. Additionally, R^2 (RS) quantifies the correlation between allele frequencies of the two SNVs. A low R^2 (0.08).

Table 2. Haplotype analysis for SNVs (rs1050450-rs771425412) located in the second exon of *GPX1* gene*

Haplotype (rs1050450-rs771425412)						
	Pt, n=105		HC, n=105		OR (95% CI)	p
	n	%	n	%		
C-C	141	67.1	182	86.6	0.31 (0.19-0.51)	p=2.06
T-C	33	15.7	22	10.4	1.59 (0.89-2.84)	p=0.11
T-A	21	1.0	1	0.4	23.2 (3.09-174.3)	p=1.19
C-A	15	7.1	5	2.3	3.15 (1.12-8.8)	p=0.02

* SNV – single nucleotide variant, Pt – patients, HC – healthy controls, OR – odds ratio, CI – confidence interval, p – two-tailed probability

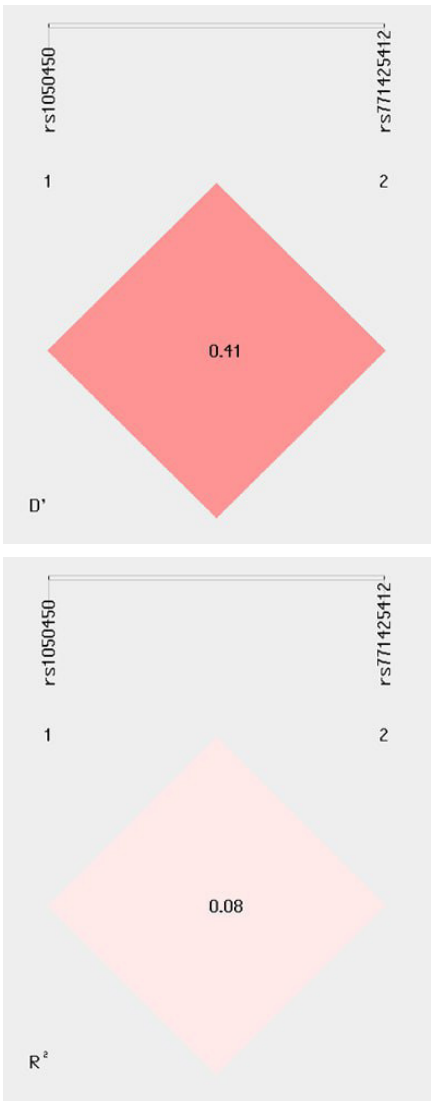

Fig. 4. Pairwise analysis depicting linkage disequilibrium plot coefficient (D') and RS between two SNVs (rs1050450 and rs771425412) for the gene showing the LD coefficient (D'; 0.41) and RS (R2; 0.08)

Discussion

A key finding was a discrepancy in the rs771425412 variant. While dbSNP annotates it as a Pro→Leu substitution, our sequencing identified a Pro→Gln change (CCA→CAA) in the Iraqi cohort. This suggests we may have detected a rare, previously unannotated sub-variant or a novel SNV at the same position, primarily observed in premenopausal women, which would currently be classified as a variant of uncertain significance (VUS). VUS variants are mostly missense; therefore, they are difficult to classify as either pathogenic or benign based on the guidelines set by the American College of Medical Genetics and Genomics and the Association for Molecular Pathology.[23] VUS are especially prevalent in the context of rare variants because they lack sufficient population frequency or functional data to be confidently classified as pathogenic or benign.[23,24] Despite ongoing advancements in genomics and data sharing, some rare variants, particularly those in underrepresented populations or with limited functional evidence, will likely remain uncertain by 2030.[25] Continued innovation and global collaboration are essential to reduce this uncertainty in rare disease diagnostics. The importance of global data sharing underscores the resolution of VUS classifications in the future.[25]

HWE analysis revealed that both rs1050450 and rs771425412 significantly deviated from equilibrium in patients but not in controls. This observed deviation in patients indicates a potential pathogenic role of these variants in susceptibility to osteoporosis. The deviations are characterized primarily by an increase in heterozygotes along with significant associations observed in dominant and over dominant genetic models.[26] These findings may suggest that heterozygosity at this locus disrupts the normal balance of antioxidant defense, thereby contributing to increased oxidative stress that induces bone loss.[19] Importantly, the presence of HWE in the control group supports the reliability of the genotyping process that reflects true biological differences associated with disease status.[26]

Haplotype analysis revealed significant differences in haplotype distribution between patients and controls. Among the identified haplotypes, the C-C haplotype was significantly more frequent in controls and conferred a protective effect (OR=0.31; p=2.06). This finding may be explained by its potential to maintain normal GPX1 activity, thereby enhancing antioxidant defenses and reducing bone loss. Conversely, the T-A and C-A haplotypes were more frequent in patients and showed strong and moderate associations with disease risk, respectively. These results indicate that the combination of alleles may be utilized to obtain more effective results not captured by single SNV analysis.

Regarding rs1050450, this SNV has been previously associated with various diseases, such as cancer and

bone diseases, such as arthritis, osteopenia, and osteoporosis.[27–29] *GPX1* activity is negatively influenced by substituting the amino acid Lue with the T variant instead of the amino acid Pro with the C variant.[30] The CT genotype was significantly more prevalent in the patient group. This suggests that this polymorphism may contribute to disease susceptibility by impairing antioxidant defense mechanisms in bone tissue. Conversely, individuals with the CC genotype exhibited protective effects against the disease. This protective effect may be attributed to the higher enzymatic activity of *GPX1*, which encodes glutathione peroxidase 1. Previous studies have demonstrated that individuals carrying the CC genotype tend to have more efficient oxidative stress responses than those carrying the CT or TT genotypes.[31,32] The functional variant SNV rs1050450 may alter the activity of glutathione peroxidase 1, an enzyme critical in detoxifying reactive oxygen species. The present results are consistent with prior reports of sex-specific metabolic dysfunction linked to the Leu allele and found that in men, the T (Leu) allele was linked to metabolic syndrome, elevated insulin levels, and hypertension. At the same time, in women, it correlates with morbid obesity, hyperinsulinemia, and insulin resistance.[33–35] These findings suggest that the Leu allele may impair metabolic function in a sex-dependent manner, possibly due to hormonal influences on oxidative stress pathways.[33–35] However, the stronger association in women could reflect the synergistic effects of estrogen decline, especially in post-menopausal women, and reduce *GPX1* activity, further amplifying oxidative damage.[29,35] *GPX1* polymorphic variants may influence disease susceptibility through mechanisms involving oxidative stress regulation, potentially due to linkage disequilibrium effects within specific ethnic groups. A recent study provided valuable evidence that the *GPX1* rs1050450 polymorphism influences oxidative stress markers, supporting the biological plausibility of these findings.[36] However, contrasting results were reported in studies that found no significant association between the *GPX1* Pro198Leu (rs1050450) variant and T2D.[37,38] The functional impact of the T allele on *GPX1* may be more pronounced in conditions such as osteoporosis, in which oxidative stress directly affects tissue integrity (such as bone) rather than peripheral nerves. While the CT genotype association aligns with *GPX1* reduced antioxidant capacity, the tissue-specific selenoprotein regulation demonstrated by Ogino et al. suggests that osteoporosis risk in Leu carriers may be modifiable by selenium status environment interaction, warranting further study.[39]

The identification of rs771425412 within exon 2 of *GPX1* raises the possibility that it may affect protein structure and function, potentially influencing redox regulation. Individuals carrying the heterozygous CA genotype were found to be at higher risk, suggesting this variant may impair the *GPX1* enzyme's function through an amino acid change, independently of the known rs1050450 polymorphism. While direct evidence for this specific variant is limited, its location in an exon indicates a potential mechanism affecting redox regulation, underscoring the need for further functional studies to confirm its role. Schembri et al. highlighted the importance of investigating rare variants, which are essential for uncovering the full spectrum of genetic contributions to complex diseases such as osteoporosis.[40] These findings highlight the potential of exon variants such as rs771425412 to compromise *GPX1* antioxidant function.[30] The findings indicated that *GPX1* polymorphisms may similarly influence the susceptibility to primary osteoporosis, supporting the value of population genetic specific investigations. The results of the current study are in line with several studies that linked *GPX1* variants to oxidative stress with osteoporosis.[19,40] To our knowledge, this is the first study to demonstrate an association between the *GPX1* rs771425412 SNV and patients with osteoporosis. The lack of literature on this SNV across bone-related and systemic diseases highlights it as a potentially overlooked locus in *GPX1* and oxidative stress.

The modest sample size may have limited the ability to confidently detect rare genotypes. This study did not assess the correlation between genotype and densitometry-based osteoporosis severity, which represents an important direction for future research, thereby enabling more reliable and clinically relevant conclusions. Future research should combine the incorporation of environmental and lifestyle factors, such as dietary selenium, vitamin D intake, and smoking, which are known to influence oxidative stress and bone metabolism.

Conclusion

This study established a significant association between specific genotypes of the *GPX1* gene and susceptibility to primary osteoporosis in an Iraqi population. The findings indicate that individuals carrying the CT genotype of the rs1050450 variant and the CA genotype of the rs771425412 variant are at a significantly higher risk of developing primary osteoporosis. Conversely, the CC genotype for both variants appears to confer a protective effect. Haplotype analysis further reinforced these findings, revealing that the combination of alleles constituting the C-C haplotype was protective, while the T-A and C-A haplotypes were associated with significantly increased risk. Collectively, these results suggest that specific genetic constitutions, particularly the heterozygous genotypes CT and CA of GPX1, contribute to osteoporosis pathogenesis likely by disrupting the enzyme's ability to regulate oxidative stress, thereby tipping the balance towards bone resorption.

Acknowledgements

We sincerely acknowledge the kind support and cooperation of the medical staff at Baghdad Teaching Hospital and Alwasity Hospital in Baghdad Province.

Declarations

Funding

This study was conducted without financial or external funding.

Author contributions

Conceptualization, S.S.A. and R.K.M.; Methodology, S.S.A.; Software, S.S.A.; Validation, S.S.A. and R.K.M.; Formal Analysis, S.S.A.; Investigation, S.S.A.; Resources, S.S.A.; Data Curation, S.S.A.; Writing – original draft preparation, S.S.A.; writing – Review & Editing, S.S.A.; Visualization, R.K.M.; Supervision, R.K.M.; Project Administration, S.S.A.; Funding Acquisition, R.K.M..

Conflicts of interest

The authors declare that there are no conflicts of interest related to this study.

Data availability

The datasets used and analyzed during the current study are available from the corresponding author upon reasonable request.

Ethics approval

This case-control study was approved by the Ethics Committee of the Department of Biotechnology, College of Science, University of Baghdad, Baghdad, Iraq [Ref. CSEC/1023/0069) on October 30, 2023].

References

1. Aibar-Almazán A, Voltes-Martínez A, Castellote-Caballero Y, Afanador-Restrepo DF, Carcelén-Fraile MDC, López-Ruiz E. Current Status of the Diagnosis and Management of Osteoporosis. *Int J Mol Sci*. 2022;23(16):9465. doi:10.3390/ijms23169465
2. Amarnath SS, Kumar V, Das SL. Classification of Osteoporosis. *Indian J Orthop*. 2023;57(1):49-54. doi:10.1007/s43465-023-01058-3
3. Ebeling PR, Nguyen HH, Aleksova J, Vincent AJ, Wong P, Milat F. Secondary osteoporosis. *Endocr Rev*. 2022;43(2):240-313. doi:10.1210/endrev/bnab028.
4. Sobh MM, Abdalbary M, Elnagar S, et al. Secondary osteoporosis and metabolic bone diseases. *J Clin Med*. 2022;11(9):2382. doi:10.3390/jcm11092382.
5. Al Anouti F, Taha Z, Shamim S, Khalaf K, Al Kaabi L, Alsafar H. An insight into the paradigms of osteoporosis: From genetics to biomechanics. *Bone Rep*. 2019;11:100216. doi:10.1016/j.bonr.2019.100216.
6. Kimball JS, Johnson JP, Carlson DA. Oxidative stress and osteoporosis. *JBJS*. 2021;103(15):1451-1461. doi:10.2106/JBJS.20.00989.
7. Domazetovic V, Marcucci G, Iantomasi T, Brandi ML, Vincenzini MT. Oxidative stress in bone remodeling: role of antioxidants. *Clin Cases Miner Bone Metab*. 2017;14(2):209. doi:10.11138/ccmbm/2017.14.1.209.
8. Alshaikhli RJ, Alkazaz AA, Aljanabi AA. Association of PARP1 Gene Single Nucleotide Polymorphisms with Papillary Thyroid Carcinoma in The Iraqi population. *Iraqi J Sci*. 2024:108-118. doi.org/10.24996/ijs.2024.64.1.10.
9. Zhu C, Shen S, Zhang S, Huang M, Zhang L, Chen X. Autophagy in Bone Remodeling: A Regulator of Oxidative Stress. *Front Endocrinol (Lausanne)*. 2022;13:898634. doi:10.3389/fendo.2022.898634
10. Zhao Q, Tang Y, Zhang L, Sun N, Liu Q, Zhang R. Biological functions of selenoprotein glutathione peroxidases (Gpxs) and their expression in osteoarthritis. *J Inflamm Res*. 2023:183-196. doi:10.2147/JIR.S388934.
11. Zhao Y, Wang H, Zhou J, Shao Q. Glutathione peroxidase GPX1 and its dichotomous roles in cancer. *Cancers (Basel)*. 2022;14(10):2560. doi:10.3390/cancers14102560.
12. Laribi A, Aouf S, Gabbouj S, Bouaouinaa N, Zakhama A, Harizi H. Human glutathione peroxidase codon 198 variant increases nasopharyngeal carcinoma risk and progression. *Eur Arch Oto-Rhino-Laryngology*. 2021;278(10):1-8. doi:10.1007/s00405-021-06628-5.
13. Dawood HH, Mohammed RK. The Association between Single Nucleotide Polymorphisms rs1042522 and rs1642785 in the TP53 gene and Acute Myeloid leukemia in a sample of the Baghdad/Iraq population. *Baghdad Sci J*. 2024;21(3):909. doi:10.21123/bsj.2023.8207.
14. Handy DE, Loscalzo J. The role of glutathione peroxidase-1 in health and disease. *Free Radic Biol Med*. 2022;188:146-161. doi:10.1016/j.freeradbiomed.2022.06.004.
15. Buraczynska M, Buraczynska K, Dragan M, Ksiazek A. Pro198Leu polymorphism in the glutathione peroxidase 1 gene contributes to diabetic peripheral neuropathy in type 2 diabetes patients. *Neuromolecular Med*. 2017;19:147-153. doi:10.1007/s12017-016-8438-2.
16. Ściskalska M, Milnerowicz H. Association of genetic variants in the GPX1 and GPX4 genes with the activities of glutathione-dependent enzymes, their interaction with smoking and the risk of acute pancreatitis. *Biomed Pharmacother*. 2022;146:112591. doi:10.1016/j.biopha.2021.112591.
17. Wang C, Zhang R, Chen N, et al. Association between glutathione peroxidase-1 (GPX1) Rs1050450 polymorphisms and cancer risk. *Int J Clin Exp Pathol*. 2017;10(9):9527.
18. Bani-Wais DFN, Ad'hiah AH. The 5'untranslated region variant rs3811050 C/T of the interleukin-38 encoding gene is associated with susceptibility to rheumatoid arthritis in Iraqi women. *Mol Biol Rep*. 2024;51(1):589. doi:10.1007/s11033-024-09529-y.
19. Jiménez-Ortega RF, Aparicio-Bautista DI, Becerra-Cervera A, et al. Association Study between Antioxidant Nutrient Intake and Low Bone Mineral Density with Oxidative Stress-Single Nucleotide Variants: GPX1 (rs1050450 and rs17650792), SOD2 (rs4880) and CAT (rs769217)

in Mexican Women. *Antioxidants*. 2023;12(12):2089. doi:10.3390/antiox12122089.
20. Barbosa P, Abo El-Magd NF, Hesketh J, Bermano G. The role of rs713041 glutathione peroxidase 4 (GPX4) single nucleotide polymorphism on disease susceptibility in humans: a systematic review and meta-analysis. *Int J Mol Sci*. 2022;23(24):15762. doi:10.3390/ijms232415762.
21. Bashi MA, Ad'hiah AH. Susceptibility to acute myeloid leukemia: Influence of genetic variants of interleukins 37 and 38. *Clin Chim Acta*. 2025;576:120386. doi:10.1016/j.cca.2025.120386
22. Yong Y, He L. SHEsis, a powerful software platform for analyses of linkage disequilibrium, haplotype construction, and genetic association at polymorphism loci. *Cell Res*. 2005;15(2):97. doi:10.1038/sj.cr.7290272.
23. Fayer S, Horton C, Dines JN, et al. Closing the gap: Systematic integration of multiplexed functional data resolves variants of uncertain significance in BRCA1, TP53, and PTEN. *Am J Hum Genet*. 2021;108(12):2248-2258. doi:10.1016/j.ajhg.2021.11.001
24. Tabet D, Parikh V, Mali P, Roth FP, Claussnitzer M. Scalable Functional Assays for the Interpretation of Human Genetic Variation. *Annu Rev Genet*. 2022;56:441-465. doi:10.1146/annurev-genet-072920-032107
25. Fowler DM, Rehm HL. Will variants of uncertain significance still exist in 2030? *Am J Hum Genet*. 2024;111(1):5-10. doi:10.1016/j.ajhg.2023.11.005
26. Chen B, Cole JW, Grond-Ginsbach C. Departure from Hardy Weinberg Equilibrium and Genotyping Error. *Front Genet*. 2017;8:167. doi:10.3389/fgene.2017.00167
27. Ferreira RR, Carvalho RV, Coelho LL, et al. Current understanding of human polymorphism in selenoprotein genes: a review of its significance as a risk biomarker. *Int J Mol Sci*. 2024;25(3):1402. doi:10.3390/ijms25031402
28. Iantomasi T, Romagnoli C, Palmini G, et al. Oxidative stress and inflammation in osteoporosis: molecular mechanisms involved and the relationship with microRNAs. *Int J Mol Sci*. 2023;24(4):3772. doi:10.3390/ijms24043772
29. Janowska M, Potocka N, Paszek S, et al. An assessment of GPX1 (rs1050450), DIO2 (rs225014) and SEPP1 (rs7579) gene polymorphisms in women with endometrial cancer. *Genes (Basel)*. 2022;13(2):188. doi:10.3390/genes13020188
30. Iqbal MW, Shahab M, Zheng G, et al. Analysis of damaging non-synonymous SNPs in GPx1 gene associated with the progression of diverse cancers through a comprehensive in silico approach. *Sci Rep*. 2024;14(1):28690. doi:10.1038/s41598-024-78232-6
31. Irfan S, Rani A, Sameem M, Nawaz SK, Liaqat I, Arshad M. Association of rs1800668 polymorphism in glutathione peroxidase-1 gene and risk of rheumatoid arthritis in Pakistani population. *Pakistan J Med Sci*. 2016;32(5):1204. doi:10.12669/pjms.325.10325
32. Goričar K, Debevec T, Dolžan V, et al. Antioxidant and neurodevelopmental gene polymorphisms in prematurely born individuals influence hypoxia-related oxidative stress. *Sci Rep*. 2024;14(1):14956. doi:0.1038/s41598-024-65647-4
33. Hernández Guerrero CÁ, Hernández Chávez P, Martínez Castro N, Parra Carriedo A, García del Río SL, Pérez Lizaur AB. Glutathione peroxidase-1 Pro200Leu polymorphism (rs1050450) is associated with morbid obesity independently of the presence of prediabetes or diabetes in women from Central Mexico. 2015;32(4):1516-1525. doi:10.3305/nh.2015.32.4.9500
34. Donadio JLS, Guerra-Shinohara EM, Rogero MM, Cozzolino SMF. Influence of gender and SNPs in GPX1 gene on biomarkers of selenium status in healthy Brazilians. *Nutrients*. 2016;8(5):81. doi:10.3390/nu8050081
35. Tarhonska K, Raimondi S, Specchia C, et al. Association of allelic combinations in selenoprotein and redox related genes with markers of lipid metabolism and oxidative stress–multimarkers analysis in a cross-sectional study. *J Trace Elem Med Biol*. 2022;69:126873. doi:10.1016/j.jtemb.2021.126873
36. Mansoor MA, Stea TH, Slettan A, et al. Impact of single nucleotide polymorphisms (SNPs) in antioxidant-enzyme genes on the concentrations of folate, homocysteine and glutathione in plasma from healthy subjects after folic acid supplementation–a randomized controlled crossover trial. *Genes Nutr*. 2025;20(1):1. doi:10.1186/s12263-024-00761-6
37. Kasznicki J, Sliwinska A, Kosmalski M, Merecz A, Majsterek I, Drzewoski J. Genetic polymorphisms (Pro197Leu of Gpx1,+ 35A/C of SOD1,– 262C/T of CAT), the level of antioxidant proteins (GPx1, SOD1, CAT) and the risk of distal symmetric polyneuropathy in Polish patients with type 2 diabetes mellitus. *Adv Med Sci*. 2016;61(1):123-129. doi:10.1016/j.advms.2015.10.006
38. Buraczynska M, Buraczynska K, Dragan M, Ksiazek A. Pro198Leu polymorphism in the glutathione peroxidase 1 gene contributes to diabetic peripheral neuropathy in type 2 diabetes patients. *Neuromolecular Med*. 2017;19:147-153. doi:10.1007/s12017-016-8438-2
39. Ogino H, Murano K, Okuno T, Ueno H. Relationship between Serum Concentrations and Muscular Expressions of Selenoproteins on Selenium-Supplemented Insulin Resistance Mouse Model. *Biol Pharm Bull*. 2024;47(5):1000-1007. doi:10.1248/bpb.b23-00662
40. Schembri M, Formosa MM. Identification of osteoporosis genes using family studies. *Front Endocrinol (Lausanne)*. 2024;15:1455689. doi:10.3389/fendo.2024.1455689

Rzeszów University Press 2025
ISSN 2544-1361 (online)
doi: 10.15584/ejcem.2026.1.15

http://www.ejcem.ur.edu.pl
European Journal of Clinical and Experimental Medicine
Eur J Clin Exp Med 2026; 24 (1): 73–82

ORIGINAL PAPER

Toward a non-invasive diagnostic tool for *Helicobacter pylori* – insights from ELISA-based biomarker profiling

Hameed Majeed Radhi [1], Mohsin Abbas Sahip [2], Redha Dawud Abdalredha [3]

[1] Department of Animal Production, College of Agriculture, University of Misan, Maysan, Iraq
[2] Department of Pathological Analysis, College of Science, University of Wasit, Kut, Wasit Governorate, Iraq
[3] Al-Furat Al-Awsat Technical University, Najaf, Najaf Governorate, Iraq

ABSTRACT

Introduction and aim. This study aimed to evaluate the diagnostic performance of a novel ELISA-based panel of virulence-associated antibodies (anti-CagA, anti-UreB, and anti-HpNAP IgG) for early detection of *Helicobacter pylori* infection.

Material and methods. In this cross-sectional study of 40 dyspeptic patients, ELISA results were compared with histopathology and stool antigen testing as reference standards. Diagnostic accuracy was assessed using receiver operating characteristic (ROC) curve analysis, and predictors were evaluated through logistic regression.

Results. Anti-CagA IgG achieved the highest diagnostic performance (AUC=0.95; sensitivity=90.9%; specificity=94.4%), followed by anti-UreB (AUC=0.92) and anti-HpNAP (AUC=0.89). The combined biomarker model reached an AUC of 0.97, demonstrating strong correlation with both infection status and symptom severity. Agreement between stool antigen testing and histopathology was high (κ=0.80).

Conclusion. This study provides the first regional validation of a standardized three-marker ELISA panel that demonstrated high accuracy as a non-invasive diagnostic approach for early *H. pylori* detection, offering a cost-effective tool for use in resource-limited settings.

Keywords. anti-CagA IgG, biomarker panel, ELISA, *Helicobacter pylori*, histopathology, non-invasive diagnosis

Introduction

Helicobacter pylori is a Gram-negative, spiral-shaped bacterium that chronically colonizes the gastric mucosa of nearly half the global population, with prevalence reaching 60–80% in developing regions.[1] While most infected individuals remain asymptomatic, persistent colonization is etiologically linked to peptic ulcer disease, mucosa-associated lymphoid tissue (MALT) lymphoma, and non-cardia gastric adenocarcinoma.[2] Consequently, *H. pylori* has been classified as a Group I carcinogen by the International Agency for Research on Cancer.[3]

The prompt identification and precise assessment of active *H. pylori* infection are imperative to avert the advancement of disease. Traditional diagnostic methodologies encompass invasive procedures such as histopathological examination and rapid urease testing, as well as non-invasive alternatives including the urea breath test (UBT), stool antigen testing (SAT), or serological analysis.[4] Although UBT and SAT provide high sensitivity and specificity, they can be costly, require specialized equipment, or have limited availability in resource-constrained settings.[5] Importantly, validation work from Iraq has compared invasive and non-invasive

Corresponding author: Redha Dawud Abdalredha, e-mail: redha.dawud.chm@atu.edu.iq

Received: 10.08.2025 / Revised: 15.09.2025 / Accepted: 19.10.2025 / Published: 30.03.2026

Radhi HM, Sahip MA, Abdalredha RD. Toward a non-invasive diagnostic tool for *Helicobacter pylori* – insights from ELISA-based biomarker profiling. *Eur J Clin Exp Med.* 2026;24(1):73–82. doi: 10.15584/ejcem.2026.1.15.

approaches head-to-head, underscoring practical trade-offs and supporting context-specific test selection.[6]

Serological assays based on whole cell or general antigen IgG measurement are inexpensive and widely used, but a major limitation is their inability to distinguish between active and past infection, leading to false positives especially in high seroprevalence populations.[7] To improve diagnostic specificity and clinical relevance, researchers have turned to virulence-associated antigens, such as CagA, urease subunit B (UreB), and HP-NAP – which reflect active infection and host immune engagement.[8,9] Moreover, recent studies have highlighted the importance of incorporating molecular insights into diagnostic research, including resistance-related genetic variations such as 23S rRNA point mutations in *H. pylori* clinical isolates.[10]

CagA (cytotoxin-associated gene A) is a key *H. pylori* virulence factor translocated into gastric epithelial cells via a type IV secretion system, where it alters signaling pathways, induces chronic inflammation, and increases neoplastic risk.[11] Serum anti-CagA IgG levels have been shown to correlate strongly with strain virulence and are more predictive of active disease than total IgG, especially in populations with mixed cagA+ and cagA– strain prevalence.[12-14]

Neutrophil-activating protein (HP-NAP) is involved in immune modulation – activating neutrophils via TLR2 and promoting reactive oxygen species production and Th1 cytokine responses thus contributing to gastric inflammation.[15] As a potent antigen, HP-NAP is a candidate diagnostic biomarker and potential therapeutic target in gastric disease.[16]

Urease subunit B (UreB) plays a central role in acid resistance and colonization by catalyzing urea hydrolysis and facilitating bacterial survival in the acidic gastric environment.[17] Urease, composed of the UreA and UreB subunits, is essential for bacterial survival in the acidic gastric environment. Its activation requires accessory proteins (UreE, UreF, UreG, UreH) for nickel incorporation into the active site, and heat-shock proteins for proper folding and stability.[18] The GroES cochaperonin HspA serves as a nickel-binding chaperone aiding urease maturation, while Hsp60 (GroEL) physically interacts with urease to maintain activity under acidic stress.[19] UreB is an immunodominant antigen, and anti-UreB IgG is frequently detected in infected patients and incorporated into serological panel of three ELISAs improved diagnostic accuracy.[20] While direct, consistent correlations between anti-UreB antibody levels and histologic bacterial density remain inconclusive, higher total anti-*H. pylori* IgG titers have been associated with greater mucosal bacterial load and more severe gastritis.[21]

Combining responses to multiple virulence factors in a multiplex enzyme-linked immunosorbent assay (ELISA) can improve diagnostic performance. For example, one study identified that antibody reactivity against cytotoxin-associated gene A (CagA), *H. pylori* chaperone (GroEL), and hook-associated protein 2 homologue (FliD) was significantly associated with the risk of *H. pylori* exposure, with odds ratios indicating a strong correlation. A risk score based on these antibodies achieved an area under the curve of 0.976, effectively differentiating currently infected or eradicated individuals from those without infection.[7] Microfluidic multiplex serology platforms including virulence factors like CagA have achieved sensitivities up to 99% and specificities of 100%.[22]

Given the diagnostic limitations of single-antigen serology and the importance of detecting active infection precision, our study was designed to evaluate a panel of three serological biomarkers that include anti-CagA IgG, Anti-UreB IgG, and Anti-HP-NAP IgG quantified via ELISA. The intended benchmark was not to replace gold-standard tests such as UBT or SAT, which remain reference standards, but rather to provide a cost-effective and accessible adjunct with accuracy approaching these methods. This framing reflects practical needs in resource-limited or primary care settings where breath tests, endoscopy, or molecular assays may be unavailable. We assessed their diagnostic accuracy against stool antigen testing and histopathology as gold standards. Although the urea breath test (UBT) is often regarded as the non-invasive gold standard, it was not included in this study because it is not routinely available in our setting due to cost and equipment constraints. Instead, we employed stool antigen testing (SAT) as a validated, affordable, and widely used non-invasive comparator, and histopathology as the invasive gold standard. We recognize that this choice may limit direct comparability with UBT-based studies, and have highlighted this as a methodological limitation. Additionally, we explored:

1. Which biomarker has the greatest independent predictive power for histopathological infection.
2. Whether symptomatology impacts diagnostic performance.
3. A combined predictive model to enhance non-invasive detection.

Aim

This study introduces a novel, non-invasive serological approach that integrates three virulence-associated *H. pylori* antigens (CagA, UreB, and HP-NAP) into a standardized ELISA panel. Unlike previous multiplex assays using experimental antigens, this combination employs commercially available kits, offering a practical and accessible diagnostic tool for early *H. pylori* detection in resource-limited settings.

Material and methods

Study design and ethical considerations

This cross-sectional observational study was conducted

at Al-Hakim Teaching Hospital – Maysan between October, 2024 and May, 2025 (ethical approval no.: 24548, approval date: 15 October 2024). The study aimed to evaluate the diagnostic performance of serological panel of three ELISAs for early detection of *H. pylori* infection. The study protocol was approved by the Institutional Review Board of Al-Hakim Teaching Hospital – Maysan, and written informed consent was obtained from all participants before enrollment. All procedures complied with the Declaration of Helsinki.

Sample size justification

The target sample size of 40 participants was determined based on an anticipated area under the ROC curve (AUC) of 0.90 for the primary biomarker (Anti-CagA IgG), a null hypothesis value of 0.70, α=0.05, and 80% power, using MedCalc sample size calculation for diagnostic accuracy studies. This calculation indicated that a minimum of 38 subjects (balanced between positive and negative cases) was required, so we enrolled 40 to account for potential exclusions.

Design limitations

As a cross-sectional study, biomarker levels and infection status were assessed at a single time point, precluding evaluation of temporal changes, causality, or post-eradication antibody kinetics.

Study population

Inclusion criteria

Participants were adults aged 18 to 65 years presenting with upper gastrointestinal symptoms including epigastric pain, bloating, heartburn, or nausea. All participants were referred for diagnostic upper gastrointestinal endoscopy.

Exclusion criteria

Patients were excluded if they had received *H. pylori* eradication therapy in the past, or were diagnosed with chronic systemic illnesses or immunosuppressive conditions. Inability to provide informed consent also resulted in exclusion. History of eradication therapy was determined through patient self-report obtained during structured interviews, and whenever possible was cross-verified against hospital or clinic medical records. We acknowledge that reliance on self-report may introduce recall bias.

Demographic and clinical data collection

Demographic and clinical data were obtained using a structured case report form (CRF). The following variables were recorded:

– Age, sex, BMI, residence, smoking status, alcohol consumption, NSAID use, PPI use, family history (gastric cancer or peptic ulcer), ulcer history.

Symptom evaluation

Symptom duration

The duration of dyspeptic symptoms was recorded in months, as reported by the patient.

Symptom severity

Symptom severity was assessed using a 5-point Likert scale based on the participant's self-assessment of their most bothersome symptom. The scale was defined as follows:

1. (Very mild): occasional discomfort with no impact on daily life.
2. (Mild): manageable symptoms without medication.
3. (Moderate): symptoms present with occasional use of medication.
4. (Severe): symptoms interfere with daily activities.
5. (Very severe): symptoms significantly impair function and require medical attention.

Sample collection

Blood samples

Venous blood (5 mL) was collected into plain tubes. Samples were allowed to clot and centrifuged at 3000 rpm for 10 minutes to separate serum, which was then aliquoted and stored at –20°C until ELISA analysis.

Stool samples

Fresh stool specimens were collected in sterile containers. Samples were stored at 2–8°C if analyzed within 24 hours or frozen at –20°C for delayed testing. Stool antigen detection was performed using a commercial *H. pylori* stool antigen ELISA kit.

Gastric biopsy

During upper gastrointestinal endoscopy, two mucosal biopsy specimens were obtained from the antrum and corpus. One sample was fixed in 10% formalin for histopathological examination using hematoxylin and eosin (H&E) and Giemsa stains.

Serological biomarker analysis

Serum IgG antibodies against *H. pylori* neutrophil-activating protein (HP-NAP), urease subunit B (UreB), and cytotoxin-associated gene A (CagA) were quantified using commercially available indirect ELISAs and the manufacturers' instructions: HP-NAP (MyBioSource, MBS2514577; detection range 3.12–200 ng/mL), UreB (Cloud-Clone, SEA970Hu; 1.56–100 ng/mL), and CagA (Abcam, ab108736; 1–300 U/mL). Serum was initially diluted 1:100, 100 µL was added to antigen-coated wells, and plates were processed per kit protocols; absorbance was read at 450 nm and concentrations were interpolated from the standard curve. Specimens with absorbance above the top calibrator at the initial dilution were re-assayed at higher dilutions (typically 1:200–1:800) so that readings fell within the validated standard-curve range,

and final results were obtained by back-calculating with the applied dilution factor. In our dataset, 18/40 (45%) anti-UreB results exceeded 100 ng/mL at the sample level and were quantified after re-dilution (maximum 251.7 ng/mL). All anti-HP-NAP values fell within 3.12–200 ng/mL (maximum 166.9 ng/mL). One anti-CagA specimen exceeded 300 U/mL and was similarly resolved by additional dilution (maximum 373.4 U/mL). No values were extrapolated beyond the standard curve for final reporting. Anti-HP-NAP and anti-UreB are reported in ng/mL, and anti-CagA in U/mL.

Reference standard for H. pylori infection

H. pylori-positive status was defined as a positive result from histopathology testing. Patients with c negative results were considered *H. pylori*-negative. Participants with discordant results were excluded from diagnostic performance analysis. We acknowledge that histopathology alone is an imperfect gold standard, and that international guidelines generally recommend at least two concordant tests (e.g., histology, culture, RUT, SAT/UBT). Our approach reflects pragmatic constraints in our setting, but may introduce selection bias and limit comparability with dual-reference studies.

Statistical analysis

All data were analyzed using IBM SPSS Statistics version 26.0 (IBM Corp., Armonk, NY, USA) and GraphPad Prism version 9.0 (GraphPad Software, San Diego, CA, USA). Continuous variables were assessed for normality using the Shapiro–Wilk test. Normally distributed variables are presented as mean±standard deviation (SD), while non-normally distributed data are reported as median and interquartile range (IQR). Categorical variables are expressed as frequencies and percentages.

Between-group comparisons were performed using the independent samples t-test for normally distributed variables or the Mann-Whitney U test for non-parametric data. The chi-square (χ^2) test or Fisher's exact test was used for categorical comparisons as appropriate.

Receiver operating characteristic (ROC) curve analysis was used to evaluate the diagnostic accuracy of each biomarker, and the area under the curve (AUC) with 95% confidence intervals (CI) was reported. The optimal cut-off values were determined using Youden's Index. Multivariate logistic regression was conducted to identify independent predictors of *H. pylori* infection, with odds ratios (OR) and 95% CIs reported. A p-value<0.05 was considered statistically significant. Multiple comparisons: No formal correction (e.g., Bonferroni) was applied, given the exploratory nature of the biomarker analyses and the relatively small number of primary comparisons. This increases the potential for type I error, and findings should therefore be interpreted with caution and validated in larger datasets.

Results

No statistically significant differences were observed between *H. pylori*-positive and -negative groups regarding age, sex, BMI, ulcer history, PPI use, or recent antibiotic exposure (p>0.05 for all). However, participants with *H. pylori* infection reported significantly higher symptom severity scores (3.6±1.7) compared to uninfected individuals (2.6±1.5; p=0.04) as shown in Table 1.

Table 1. Baseline characteristics of study participants*

Characteristic		Overall (n=40)	*H. pylori* negative (n=18)	*H. pylori* positive (n=22)	p
Age (years), mean±SD		41.0±13.5	37.2±13.9	44.0±12.5	0.10
Sex, n (%)	Male	13 (32.5%)	4 (22.2%)	9 (40.9%)	0.34
	Female	27 (67.5%)	14 (77.8%)	13 (59.1%)	
BMI, mean±SD		24.4±3.5	24.1±3.8	24.6±3.3	0.47
Symptom severity (Likert), mean±SD		3.1±1.7	2.6±1.5	3.6±1.7	0.04
Ulcer history, n (%)		5 (12.5%)	3 (16.7%)	2 (9.1%)	0.49
PPI use, n (%)		7 (17.5%)	2 (11.1%)	5 (22.7%)	0.24
Recent antibiotics, n (%)		7 (17.5%)	2 (11.1%)	5 (22.7%)	0.24

* tests – t-test (continuous), χ^2 – Fisher's (categorical)

All three serological biomarkers – anti-HpNAP IgG, anti-UreB IgG, and anti-CagA IgG – were significantly elevated in the *H. pylori* stool antigen-positive group compared to the negative group. Anti-HpNAP IgG levels were markedly higher in the positive group (112.1±32.1 ng/mL) than in the negative group (69.9±23.9 ng/mL; p<0.0001). Similarly, anti-UreB IgG and anti-CagA IgG showed significant differences, with values of 153.9±50.1 ng/mL vs. 102.0±40.8 ng/mL (p=0.0003), and 198.3±62.2 U/mL vs. 93.1±60.4 U/mL (p<0.0001), respectively as shown in Table 2.

Table 2. Stool antigen result

Parameters	Negative group (n=18) Mean±SD	Positive group (n=22) Mean±SD	p
Anti HpNAP IgG (ng/mL)	69.9±23.9	112.1±32.1	<0.0001
Anti UreB IgG (ng/mL)	102±40.8	153.9±50.1	0.0003
Anti CagA IgG (U/mL)	93.1±60.4	198.3±62.2	<0.0001

Significant elevations in all three serological biomarkers were observed among participants with histopathologically confirmed *H. pylori* infection compared to those without. Anti-HpNAP IgG levels were significantly higher in the infected group (112.4±33.8 ng/mL) versus the non-infected group (68.0±22.7 ng/mL; p<0.001). Likewise, anti-UreB IgG concentrations were elevated in the positive group (165.0±49.4 ng/mL) compared to negatives (87.7±29.0 ng/mL; p<0.001). The most notable difference was found in anti-CagA IgG, with mean values of 204.8±66.7 U/mL in positives versus 78.2±35.8 U/mL in negatives (p<0.001) as shown in Table 3.

There was strong concordance between the stool antigen test and histopathology results. Among the 40 participants, the tests agreed in 36 cases (90%) as shown in Table 4. Specifically, 19 patients tested positive on both stool antigen and histopathology, while 17 were negative on both. The Cohen's kappa coefficient (κ) was 0.80 (95% CI: 0.61–0.99), indicating substantial agreement between the two diagnostic modalities.

Table 3. Biomarker levels by *H. pylori* status*

Biomarker	H. pylori negative (n=18)	H. pylori positive (n=22)	p
Anti-HpNAP IgG (ng/mL)	68.0±22.7	112.4±33.8	<0.001
Anti-UreB IgG (ng/mL)	87.7±29.0	165.0±49.4	<0.001
Anti-CagA IgG (U/mL)	78.2±35.8	204.8±66.7	<0.001

* data – mean±SD, test – Independent t-test/Mann-Whitney U

Table 4. Strong agreement (κ=0.80) between stool antigen and histopathology*

Stool antigen vs. histopathology	Histopathology+	Histopathology-	Total
Stool antigen+	19	1	20
Stool antigen-	3	17	20
Total	22	18	40

* agreement: 90% (36/40), Cohen's κ=0.80 (95% CI: 0.61–0.99)

As presented in Table 5 and Figures 1, 2, and 3, the three ELISA-based biomarkers demonstrated excellent diagnostic performance compared to histopathological confirmation of H. pylori infection. Anti-CagA IgG, at a cutoff value of ≥120 U/mL, achieved the highest diagnostic accuracy with a sensitivity of 90.9% (95% CI: 70.8–98.9), specificity of 94.4% (95% CI: 72.7–99.9), and an AUC of 0.95 (95% CI: 0.89–1.00). Anti-UreB IgG also showed strong diagnostic power (AUC=0.92), with sensitivity of 86.4% and specificity of 88.9% at a cutoff of ≥110 ng/mL. Anti-HpNAP IgG demonstrated slightly lower values but still performed well, with an AUC of 0.89, sensitivity of 81.8%, and specificity of 83.3%.

Table 5. Diagnostic accuracy of biomarkers*

Biomarker (Cut-off)	Sensitivity (95% CI)	Specificity (95% CI)	AUC (95% CI)
Anti-HpNAP IgG (≥85 ng/mL)	81.8% (59.7–94.8%)	83.3% (58.6–96.4%)	0.89 (0.79–0.99)
Anti-UreB IgG (≥110 ng/mL)	86.4% (65.1–97.1%)	88.9% (65.3–98.6%)	0.92 (0.84–1.00)
Anti-CagA IgG (≥120 U/mL)	90.9% (70.8–98.9%)	94.4% (72.7–99.9%)	0.95 (0.89–1.00)

*AUC – area under ROC curve, cut-offs optimized via Youden's index

Subgroup analysis revealed notable variation in the diagnostic performance of Anti-CagA IgG across different symptom profiles, when histopathology was used as the reference standard as shown in Table 6. The highest diagnostic accuracy was observed in patients presenting with bloating, with an AUC of 0.97 (95% CI: 0.91–1.00) and sensitivity of 91.7% at 90% specificity using a cutoff of ≥115 U/mL. This was followed by the epigastric pain group (AUC=0.94), nausea/mixed symptoms (AUC=0.92), and heartburn (AUC=0.89). While high accuracy was retained across all symptom subgroups, the optimal diagnostic threshold varied slightly, ranging from ≥115 to ≥122 U/mL. Given the small subgroup sizes, these variations likely reflect sample-specific effects and should be regarded as exploratory rather than definitive. For consistency and to minimize overfitting, the primary diagnostic cutoff for anti-CagA IgG in this study is the single Youden's Index–derived threshold of ≥120 U/mL from the overall cohort.

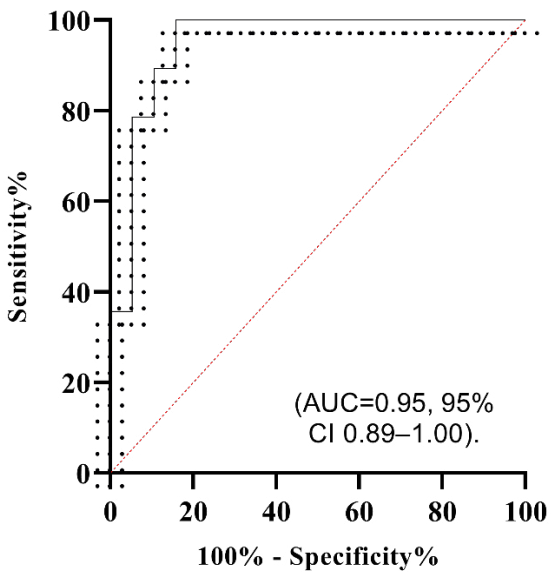

Fig. 1. ROC curve of anti-CagA IgG for *H. pylori* diagnosis (AUC=0.95, 95% CI 0.89–1.00)

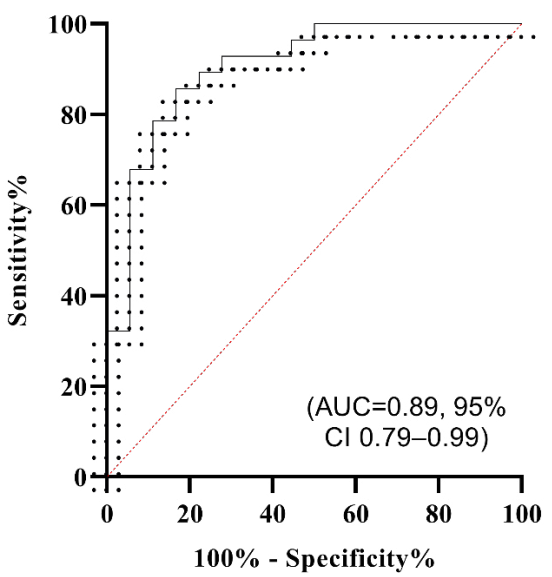

Fig. 2. ROC curve of anti-HpNAP IgG for *H. pylori* diagnosis (AUC=0.89, 95% CI 0.79–0.99)

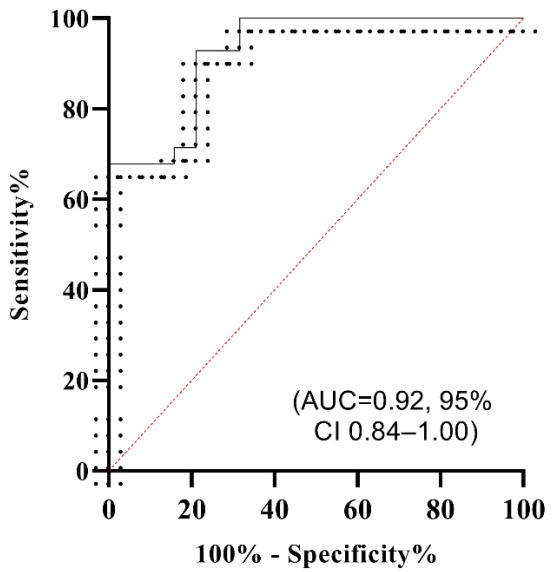

Fig. 3. ROC curve of anti-UreB IgG for *H. pylori* diagnosis (AUC=0.92, 95% CI 0.84–1.00)

Table 6. Biomarker performance in symptomatic subgroups*

Symptom subgroup	Anti-CagA IgG AUC (95% CI)	Sensitivity at 90% specificity	Optimal cut-off (U/mL)
Epigastric pain	0.94 (0.83–1.00)	88.9%	≥118
Heartburn	0.89 (0.71–1.00)	83.3%	≥122
Bloating	0.97 (0.91–1.00)	91.7%	≥115
Nausea/Mixed	0.92 (0.80–1.00)	85.7%	≥120

* reveals symptom-specific variations in Anti-CagA IgG diagnostic accuracy

Multivariate logistic regression analysis identified anti-CagA IgG as the strongest independent predictor of histopathologically confirmed *H. pylori* infection as shown in Table 7. For every 50 U/mL increase in anti-CagA IgG, the odds of infection increased by over threefold (adjusted OR=3.21; 95% CI: 1.75–5.89; p<0.001). Anti-UreB IgG also remained a significant predictor (OR=1.87; 95% CI: 1.12–3.12; p=0.02). Although age >50 years and symptom severity ≥3 showed trends toward association (ORs=1.95 and 2.41, respectively), they did not reach statistical significance (p=0.13 and p=0.06). The overall model demonstrated excellent diagnostic discrimination, with an AUC of 0.97 (95% CI: 0.93–1.00).

Table 7. Combined biomarker diagnostic model*

Predictor	Adjusted OR	95% CI	p
Anti-CagA IgG (per 50 U/mL)	3.21	1.75–5.89	<0.001
Anti-UreB IgG (per 50 ng/mL)	1.87	1.12–3.12	0.02
Age >50 years	1.95	0.82–4.64	0.13
Symptom severity ≥3	2.41	0.97–6.01	0.06

* model AUC=0.97 (0.93–1.00), anti-CagA is the strongest independent predictor

Stratification by risk factor profile revealed that anti-CagA IgG levels were significantly higher among *H. pylori*-positive patients with high-risk features, defined as concurrent smoking and a family history of gastric cancer. Given the very small number of participants in these strata (e.g., *H. pylori*+ high-risk, n=4; *H. pylori*– high-risk, n=2), these results should be interpreted as exploratory and descriptive rather than definitive. The median anti-CagA IgG concentration in the high-risk *H. pylori*-positive group was 286.4 U/mL [IQR: 222.3–293.3], markedly higher than the low-risk *H. pylori*-positive group (204.1 U/mL [171.5–229.4]; p<0.001) as shown in Table 8. In *H. pylori*-negative individuals, a similar pattern was observed, with slightly elevated values in high-risk participants.

Table 8. Biomarker levels by risk factor profiles*

Group	n	Anti-CagA IgG (U/mL) (*Median* [IQR])	p
***H. pylori*– low risk**	16	81.5 [67.3–102.8]	<0.001
***H. pylori*– high risk**	2	114.2 [107.0–121.4]	
***H. pylori*+ low risk**	18	204.1 [171.5–229.4]	
***H. pylori*+ high risk**	4	286.4 [222.3–293.3]	

* high-risk *H. pylori*+ patients show markedly elevated anti-CagA levels (median 286 vs 204 U/mL)

Discussion

The present study demonstrates exceptional diagnostic performance for *H. pylori* serum biomarkers, with anti-CagA IgG achieving the highest accuracy (AUC=0.95) among the three evaluated antibodies. These findings align with and extend previous research while revealing important insights into the clinical utility of combined biomarker approaches for *H. pylori* diagnosis. While the antigens evaluated here have each been studied in prior serological panels, our work contributes by validating a pragmatic three-marker combination (anti-CagA, anti-UreB, anti-HpNAP) in a Middle Eastern clinical cohort using standardized, commercially available ELISA kits. This combination leverages biological complementarity, demonstrates strong additive diagnostic performance in multivariate models, and offers feasibility in resource-limited contexts where UBT or PCR may not be readily available.

Our results showing anti-CagA IgG sensitivity of 90.9% and specificity of 94.4% with an optimal cutoff of ≥120 U/mL represent a significant advancement over many previous studies. The comprehensive evaluation by Duquesne, et al.[23] in Cuba's primary care setting reported Hp-IgG ELISA sensitivity of 97.8% but specificity of only 71.1%, highlighting the superior specificity achieved by our anti-CagA approach. Their study, which included adult dyspeptic patients and used multiple reference standards, demonstrated that while serology maintains high sensitivity, specificity often remains a limiting factor. Our anti-CagA results address this lim-

itation, achieving both high sensitivity and specificity, which is crucial for clinical decision-making where false positives can lead to unnecessary treatment.

The superior performance of anti-CagA antibodies in our study is consistent with the mechanistic understanding provided by Seo, et al.[24] in their Korean pediatric population study. Their research demonstrated that CagA presence was the major factor driving high anti-*H. pylori* IgG and IgA levels regardless of age, with antibody levels correlating significantly with chronic gastritis degree and *H. pylori* infiltration ($p<0.001$). The authors found that CagA-positive strains induced stronger antibody responses even in children under 5 years, supporting our observation that Anti-CagA antibodies provide robust diagnostic discrimination. Their finding that 94% of Korean *H. pylori* strains were CagA-positive aligns with our population's high anti-CagA responsiveness, suggesting geographic and strain-related factors influence biomarker performance.

The large-scale Beijing population study by Yu, et al.[25] provides important context for interpreting our results in broader clinical applications. Their evaluation of 1,678 participants revealed *H. pylori* IgG sensitivity of 74.24% and specificity of 90.45% compared to 13C-UBT, with a Cohen's kappa of 0.64. While their overall sensitivity was lower than our anti-CagA results, their high specificity (90.45%) supports the clinical utility of *H. pylori* serology in population screening. Notably, their finding of 73.5% antibody positivity in allergic disease patients versus 29.3% in non-allergic populations ($p<0.001$) suggests that immune status may influence antibody responses, potentially explaining some of the variability observed across different studies and populations.

The comprehensive biomarkers review by Shiota and Yamaoka[26] provides crucial perspective on the variability we observe across studies. Their analysis of 29 commercial kits revealed accuracy ranging from 73.9% to 97.8% for ELISA tests, with sensitivity spanning 57.8% to 100% and specificity from 57.4% to 97.9%. Only four ELISA tests achieved >90% performance across all five criteria (sensitivity, specificity, PPV, NPV, accuracy), emphasizing the importance of careful test selection and validation. Their observation that *H. pylori* antibody titers vary greatly depending on test kit used underscores the significance of our standardized approach and the superior performance we achieved with anti-CagA antibodies.

The protein array technology study by Han, et al.[27] offers valuable comparison for our multi-biomarker approach. Their evaluation of 180 clinical samples demonstrated anti-UreB IgG sensitivity of 93.4% and specificity of 94.8%, closely matching our anti-UreB results (86.4% sensitivity, 88.9% specificity). However, their anti-CagA performance (95.4% sensitivity, 94.4% specificity) was remarkably similar to our findings, validating the reproducibility of anti-CagA as a superior diagnostic marker. The rapid 30-minute turnaround time achieved by their protein array system supports the clinical feasibility of multi-biomarker testing, which our combined model (AUC=0.97) demonstrates can provide near-perfect diagnostic accuracy.

Our combined biomarker model, achieving AUC=0.97 with anti-CagA as the strongest independent predictor (OR=3.21, $p<0.001$) and anti-UreB providing significant additive value (OR=1.87, $p=0.02$), represents a novel advancement in *H. pylori* diagnostics. This approach addresses the limitations identified in previous single-biomarker studies while capitalizing on the complementary diagnostic information provided by different *H. pylori* antigens. The model's exceptional performance suggests that the biological diversity of immune responses to different *H. pylori* components can be leveraged to achieve diagnostic accuracy approaching that of invasive methods.

The risk stratification analysis revealing markedly elevated anti-CagA levels in high-risk H. pylori-positive patients (286.4 vs 204.1 U/mL, representing a 40.2% increase) extends previous findings linking CagA seropositivity to gastric cancer risk. This observation is consistent with regional findings showing that smoking and alcohol consumption are significantly associated with increased risk of H. pylori infection in Iraqi patients.[28] However, given the small subgroup sizes, these estimates are unstable and should be regarded as exploratory signals that require confirmation in larger cohorts.

The landmark study by Parsonnet, et al.[29], established that CagA-positive H. pylori infection confers considerably higher gastric cancer risk than CagA-negative strains. Our dose-response relationship between risk factors and anti-CagA levels provides quantitative support for this association, suggesting that antibody levels may serve as surrogate markers for disease severity and cancer risk. The Japanese American population study by Nomura, et al.[30] further validated CagA seropositivity as a gastric cancer biomarker, demonstrating that specific antibody responses correlate with cancer risk in population-based studies.

Our symptom-specific analysis revealing differential anti-CagA performance across clinical presentations (AUC ranging from 0.89 for heartburn to 0.97 for bloating) provides novel insights not extensively explored in previous literature. The consistently high performance across all symptom subgroups (AUC>0.89) suggests that anti-CagA antibodies maintain diagnostic utility regardless of clinical presentation, addressing a key limitation of symptom-based diagnostic approaches. The variation in optimal cutoffs (115–122 U/mL) across symptom groups indicates potential symptom-specific influences on antibody response. However, these find-

ings should be considered exploratory due to the small strata sizes, and our study emphasizes the single Youden's Index – derived cutoff (≥120 U/mL) as the primary diagnostic threshold. Future research with larger cohorts may determine whether subgroup-specific thresholds provide additional clinical value.

The excellent agreement between stool antigen testing and histopathology (κ=0.80, 90% overall agreement) in our study validates both reference standards and supports the reliability of our biomarker evaluations. This level of concordance exceeds many previous studies and provides confidence in our diagnostic performance estimates. The minimal discordance (only 4 cases, 10%) with predominantly false negatives rather than false positives suggests that our biomarker approach may detect cases missed by conventional methods, potentially improving overall diagnostic sensitivity in clinical practice.

The exceptional diagnostic performance of anti-CagA antibodies observed in our study reflects the unique biological properties of the CagA protein and its central role in *H. pylori* pathogenesis.

The observed performance hierarchy is consistent with the biology of these antigens: CagA's type-IV-secretion–mediated translocation and downstream signaling[31,32], its conserved immunodominant epitopes and exposure during bacterial attachment[33,34]; UreB's essential role in acid resistance and additional immunomodulatory interactions[35-37]; and HpNAP's neutrophil/innate activation profile.[16,38] These mechanisms provide plausibility for robust Anti-CagA and complementary anti-UreB responses in active infection.

CagA and UreB sequence variation can influence antigenicity and may contribute to site-to-site performance differences.[39,40] This, together with kit-to-kit variability[24], supports our emphasis on local calibration of cut-offs.

Our findings carry important clinical implications. First, anti-CagA IgG alone or in combination with anti-UreB IgG may serve as a non-invasive serological panel with accuracy comparable to invasive methods for diagnosing *H. pylori* infection. Second, in settings where endoscopy or breath testing is unavailable or contraindicated, this panel could guide diagnostic decisions and prioritize patients for further evaluation. Third, anti-HpNAP IgG, while slightly less accurate, offers additional inflammatory insight and may have prognostic value in future longitudinal studies.

We also observed that symptom severity was elevated in infected individuals, although not an independent predictor suggesting that while clinical presentation may hint at infection, biomarkers provide more objective and specific diagnostic value.

Strengths of this study include the use of histopathology and stool antigen testing as reference standards, rigorous ROC and multivariate analyses, and the combined evaluation of three biologically distinct biomarkers. The demonstration of high AUC values and robust odds ratios confirms both accuracy and relevance.

Limitations include the modest sample size (n=40), which may limit generalizability; the cross-sectional design – precluding temporal assessment of seroconversion or response to eradication; and limited evaluation of demographic modifiers (e.g., rural vs. urban). In addition, inclusion was restricted to symptomatic patients undergoing endoscopy, which introduces spectrum bias and may limit extrapolation of our findings to asymptomatic carriers or population-based screening contexts. In addition, while our ELISA-based assays show high performance, variations between kit manufacturers and local strain prevalence may affect external validity. Furthermore, prior eradication history was primarily based on self-report, with only partial confirmation from medical records, raising the possibility of recall bias. In addition, defining infection status by histopathology alone (with discordant cases excluded) diverges from guideline recommendations that require two concordant reference tests. While this approach minimized misclassification in our dataset, it may have introduced selection bias and reduced comparability with other validation studies. Finally. the results should be regarded as hypothesis-generating, providing a rationale for larger multicenter studies that can assess generalizability, validate cutoffs, and explore integration with newer diagnostic strategies.

Future research should involve larger, multicenter validation cohorts, ideally with follow-up after eradication therapy to assess antibody decline and treatment response. Combining serological panels with molecular detection (e.g., PCR or breath tests) could enhance both sensitivity and specificity, especially in areas with high seroprevalence.[41] Further, understanding variations in biomarker levels by CagA genotype and bacterial strain diversity would refine cutoff values across populations.

Mechanistic studies evaluating HP-NAP immunomodulatory pathways and their potential as vaccine candidates or therapeutic adjuvants (e.g. in allergy/cancer immunotherapy) may offer translational applications beyond diagnostics.[16] Additionally, evaluating these biomarkers among pediatric or high-risk subgroups, or in patients with dysplasia or early gastric malignancy, would extend clinical relevance.

Conclusion

All three ELISA-based markers – anti-HpNAP IgG, anti-UreB IgG, and anti-CagA IgG –demonstrated strong diagnostic potential, with anti-CagA showing the highest accuracy. The combined use of anti-CagA and anti-UreB in a standardized, non-invasive ELISA panel represents a novel and practical diagnostic approach for early Helicobacter pylori detection, particularly relevant for resource-limited settings.

Although based on a single-center cohort, these results provide the first regional validation of this three-marker panel and support further multicenter studies to confirm its clinical utility and integration with molecular or breath-based diagnostics.

Acknowledgments

The authors express their gratitude to the staff of the endoscopy unit and pathology laboratory at the Al-Hakim Teaching Hospital – Maysan, as well as to all participants who contributed to this research.

Declarations

Funding

No external funding was received for this study.

Author contributions

Conceptualization, H.M.R. and M.A.S.; Methodology, H.M.R.; Software, H.M.R.; Validation, H.M.R., M.A.S. and R.D.A.; Formal Analysis, H.M.R.; Investigation, H.M.R.; Resources, H.M.R.; Data Curation, H.M.R.; Writing – Original Draft Preparation, H.M.R.; Writing – Review & Editing, H.M.R., M.A.S. and R.D.A.; Visualization, H.M.R.; Supervision, M.A.S.; Project Administration, H.M.R.; Funding Acquisition, M.A.S.

Conflicts of interest

The authors declare that they have no conflicts of interest.

Data availability

Data supporting the findings of this study are available from the corresponding author upon reasonable request.

Ethics approval

The study protocol was approved by the Institutional Review Board of Al-Hakim Teaching Hospital – Maysan (ethical approval no.: 24548, approval date: 15 October 2024).

References

1. Shirani M, Pakzad R, Haddadi MH, et al. The global prevalence of gastric cancer in *Helicobacter pylori*-infected individuals: a systematic review and meta-analysis. *BMC Infect Dis.* 2023;23(1):543. doi:10.1186/s12879-023-08504-5
2. Kumar N. Status of *Helicobacter pylori* in gut microbiome and precision medicine. In: *Precision Medicine and Human Health*. Bentham Science Publishers; 2024:153-176. doi:10.2174/9789815223583124010 1
3. Chivu RF, Bobirca F, Melesteu I, Patrascu T. The role of *Helicobacter pylori* infection in the development of gastric cancer: review of the literature. *Chirurgia (Bucur).* 2024;119(eCollection):1-10. doi:10.21614/chirurgia.119.eC.2971
4. Jeon HJ, Choi HS. Various diagnostic methods for *Helicobacter pylori* infection. *Korean J Med.* 2024;99(2):104-110. doi:10.3904/kjm.2024.99.2.104
5. Lestari HM, Gustinanda J, Tejaputri NA, et al. Stool antigen examination as a diagnostic tool for dyspeptic patients caused by *Helicobacter pylori* infection: a case-based literature review. *Open Access Maced J Med Sci.* 2021;9(F):305-309. doi:10.3889/oamjms.2021.5568
6. Hussein RA, Al-Ouqaili MT, Majeed YH. Detection of *Helicobacter pylori* infection by invasive and non-invasive techniques in patients with gastrointestinal diseases from Iraq: a validation study. *PLoS One.* 2021;16(8):e0256393. doi:10.1371/journal.pone.0256393
7. Li Z-X, Bronny K, Formichella L, et al. A multiserological line assay to discriminate current from past *Helicobacter pylori* infection. *Clin Microbiol Infect.* 2024;30(1):114-121. doi:10.1016/j.cmi.2023.10.006
8. Fu H-W. *Helicobacter pylori* neutrophil-activating protein: from molecular pathogenesis to clinical applications. *World J Gastroenterol.* 2014;20(18):5294-5301. doi:10.3748/wjg.v20.i18.5294
9. Mahmoodzadeh AS, Moazamian E, Shamsedin SA, Kaydani GA. Prevalence of virulence genes and antigen pattern in *Helicobacter pylori*-infected patients and inflammatory cytokine levels compared with non-infected individuals. *Jundishapur J Microbiol.* 2022;15(2):e121144. doi:10.5812/jjm-121144
10. Hussein RA, Al-Ouqaili MT, Majeed YH. Detection of clarithromycin resistance and 23S rRNA point mutations in *Helicobacter pylori*: phenotypic and molecular methods. *Saudi J Biol Sci.* 2022;29(1):513-520. doi:10.1016/j.sjbs.2021.09.024
11. Ansari S, Yamaoka Y. *Helicobacter pylori* virulence factor CagA-mediated gastric pathogenicity. *Int J Mol Sci.* 2020;21(19):7430. doi:10.3390/ijms21197430
12. Atherton J. CagA, the cag pathogenicity island and *Helicobacter pylori* virulence. *Gut.* 1999;44(3):307-308. doi:10.1136/gut.44.3.307
13. Ilie M, Dascălu L, Chifiriuc C, et al. Correlation of anti-*Helicobacter pylori* CagA IgG with resistance to first-line treatment, bleeding gastroduodenal ulcers and gastric cancer. *Roum Arch Microbiol Immunol.* 2011;70(3):101-104.
14. Loffeld RJ, Werdmuller BF, Kusters JG, Kuipers EJ. IgG antibody titer against *Helicobacter pylori* correlates with CagA-positive strains. *FEMS Immunol Med Microbiol.* 2000;28(2):139-141. doi:10.1111/j.1574-695X.2000.tb01468.x
15. Codolo G, Coletta S, D'Elios MM, de Bernard M. HP-NAP of *Helicobacter pylori*: the power of immunomodulation. *Front Immunol.* 2022;13:944139. doi:10.3389/fimmu.2022.944139
16. Fu H-W, Lai Y-C. The role of *Helicobacter pylori* neutrophil-activating protein in pathogenesis and therapeutic development. *Int J Mol Sci.* 2022;24(1):91. doi:10.3390/ijms24010091

17. Wen Y, Feng J, Scott DR, Marcus EA, Sachs G. A cis-encoded antisense RNA controls expression of ureB in *Helicobacter pylori*. *J Bacteriol.* 2011;193(1):40-51. doi:10.1128/JB.00800-10
18. Ge R-G, Wang D-X, Hao M-C, Sun X-S. Nickel trafficking system responsible for urease maturation in *Helicobacter pylori*. *World J Gastroenterol.* 2013;19(45):8211-8217. doi:10.3748/wjg.v19.i45.8211
19. Schauer K, Muller C, Carriere M, et al. The *Helicobacter pylori* GroES cochaperonin HspA functions as a specialized nickel chaperone. *J Bacteriol.* 2010;192(5):1231-1237. doi:10.1128/JB.01216-09
20. Huifang G, Wenhong Z, Dongqing W, et al. Rapid screening of dominant B-cell epitopes of UreB by fluorescence polarization assay. *Chin J Biochem Mol Biol.* 2006;33(1):83-86. doi:10.1186/1556-276x-8-118
21. Peng J, Xie J, Liu D, et al. Impact of *Helicobacter pylori* colonization density and depth on gastritis severity. *Ann Clin Microbiol Antimicrob.* 2024;23(1):4. doi:10.1186/s12941-024-00666-7
22. Filomena A, Guenther A, Planatscher H, et al. Performance of a multiplex serological *Helicobacter pylori* assay on a microfluidic platform. *Proteomes.* 2017;5(4):24. doi:10.3390/proteomes5040024
23. Duquesne A, Falcón R, Galindo B, et al. Diagnostic accuracy for *Helicobacter pylori* infection among dyspeptic adults in Cuban primary care. *Microorganisms.* 2023;11(4):997. doi:10.3390/microorganisms11040997
24. Seo J-H, Lim CW, Park JS, et al. Correlations between CagA antigen and serum anti-*Helicobacter pylori* IgG and IgA in children. *J Korean Med Sci.* 2016;31(3):417-423. doi:10.3346/jkms.2016.31.3.417
25. Yu J-H, Zhao Y, Wang X-F, Xu Y-C. Evaluation of anti-*Helicobacter pylori* IgG for detection of infection in different populations. *Diagnostics.* 2022;12(5):1214. doi:10.3390/diagnostics12051214
26. Shiota S, Yamaoka Y. Biomarkers for *Helicobacter pylori* infection and gastroduodenal disease. *Biomark Med.* 2014;8(9):1127-1137. doi:10.2217/bmm.14.72
27. Han F-C, Li X-J, Jiang H, et al. Detection of *Helicobacter pylori* antibody profile in serum by protein array. *World J Gastroenterol.* 2006;12(25):4044-4049. doi:10.3748/wjg.v12.i25.4044
28. Hussein RA, Al-Ouqaili MT, Majeed YH. Association between alcohol, smoking, and *Helicobacter pylori* infection in Iraqi patients. *J Emerg Med Trauma Acute Care.* 2022;2022(6):12. doi:10.5339/jemtac.2022.aimco.12
29. Parsonnet J, Friedman G, Orentreich N, Vogelman H. Risk for gastric cancer in CagA-positive vs CagA-negative *Helicobacter pylori* infection. *Gut.* 1997;40(3):297-301. doi:10.1136/gut.40.3.297
30. Nomura AM, Lee J, Stemmermann GN, Nomura RY, Perez-Perez GI, Blaser MJ. *Helicobacter pylori* CagA seropositivity and gastric carcinoma risk in Japanese Americans. *J Infect Dis.* 2002;186(8):1138-1144. doi:10.1086/343808
31. Dudek I, Forma A, Hamerska J, et al. CagA virulence and epithelial–mesenchymal transition in gastric cancer. *J Educ Health Sport.* 2022;12(4):62-75. doi:10.12775/JEHS.2022.12.04.005
32. Wang H, Zhao M, Shi F, et al. Signaling pathways induced by *Helicobacter pylori* CagA. *Front Cell Infect Microbiol.* 2023;13:1062803. doi:10.3389/fcimb.2023.1062803
33. Covacci A, Censini S, Bugnoli M, et al. Molecular characterization of the 128-kDa immunodominant antigen of *Helicobacter pylori*. *Proc Natl Acad Sci U S A.* 1993;90(12):5791-5795. doi:10.1073/pnas.90.12.5791
34. Marzhoseyni Z, Mousavi MJ, Ghotloo S. *Helicobacter pylori* antigens as immunomodulators. *Helicobacter.* 2024;29(1):e13058. doi:10.1111/hel.13058
35. Carosella N, Brock KP, Zambelli B, et al. Functional contacts for urease activation in *Helicobacter pylori*. *Front Chem Biol.* 2023;2:1243564. doi:10.3389/fchbi.2023.1243564
36. Beswick EJ, Pinchuk IV, Minch K, et al. Urease B subunit binds CD74 and induces NF-κB and IL-8 in gastric epithelial cells. *Infect Immun.* 2006;74(2):1148-1155. doi:10.1128/IAI.74.2.1148-1155.2006
37. Kolopaking MS. Urease, gastric bacteria and gastritis. *Acta Med Indones.* 2022;54(1):1-1.
38. Wen S-H, Hong Z-W, Chen C-C, Chang H-W, Fu H-W. HP-NAP activates TLR2 inducing IL-8 secretion. *Int J Mol Sci.* 2021;22(21):11560. doi:10.3390/ijms222111560
39. Ji X, Sun Z, Wu H, et al. Stronger dysregulation by East Asian-type CagA on intracellular signaling. *BMC Microbiol.* 2024;24(1):467. doi:10.1186/s12866-024-03619-4
40. Clayton C, Kleanthous H, Coates P, Morgan D, Tabaqchali S. Sensitive detection of *Helicobacter pylori* by PCR. *J Clin Microbiol.* 1992;30(1):192-200. doi:10.1128/jcm.30.1.192-200.1992
41. Shallal ZS. Comparison between serological and molecular detection of *Helicobacter pylori*. *Acad Int J Med Update.* 2025;3(1):1-10. doi:10.59675/U311

Rzeszów University Press 2026
ISSN 2544-1361 (online)
doi: 10.15584/ejcem.2026.1.16

http://www.ejcem.ur.edu.pl
European Journal of Clinical and Experimental Medicine
Eur J Clin Exp Med 2026; 24 (1): 83–95

ORIGINAL PAPER

Identification of hepatotoxicity of untreated and UV-irradiated $GdYVO_4:Eu^{3+}$ nanoparticles

Oksana Nakonechna [1], Galina Gubina-Vakulick [2], Valeriy Miasoiedov [3], Tatyana Gorbach [1], Svitlana Denysenko [1], Svitlana Yefimova [4], Vladimir Klochkov [4], Svitlana Stetsenko [1], Irina Vasylyeva [1], Daria Yankovska [5]

[1] Department of Biochemistry, Kharkiv National Medical University, Kharkiv, Ukraine
[2] Department of Pathological Anatomy, Kharkiv National Medical University, Kharkiv, Ukraine
[3] Department of Medical Biology, Kharkiv National Medical University, Kharkiv, Ukraine
[4] Institute of Scintillation Materials, NAS of Ukraine, Kharkiv, Ukraine
[5] Research Institute of Experimental and Clinical Medicine, Kharkiv National Medical University, Kharkiv, Ukraine

ABSTRACT

Introduction and aim. Gadolinium–yttrium orthovanadate $GdYVO_4:Eu^{3+}$ nanoparticles (NPs) display dual redox activity, acting as pro-oxidants or antioxidants depending on the surrounding environment, concentration, and pretreatment conditions, a property that can be harnessed for potential oncological therapies. This study aims to evaluate the effect of untreated and UV-irradiated NPs administered orally on blood biochemical parameters, liver tissue, and histological condition of liver tissue in an experiment on laboratory rats.

Material and methods. Male rats of the WAG population received oral colloidal NPs solutions (in untreated and UV-irradiated forms) at different doses: (50, 100, 200) μg/kg of body weight for 14 days. The content of medium-weight molecules, alanine aminotransferase activity, direct and indirect bilirubin content, and von Willebrand factor content were determined in blood serum. The content of reduced glutathione, superoxide dismutase, diene conjugates, and TBK-active products was determined in liver homogenates. Liver tissue samples were examined using morphological and morphometric methods.

Results. The formation of oxidative stress, intoxication, damage to endothelial cells, impaired membrane permeability, destruction of hepatocytes, and destruction of sinusoidal endothelial cells were detected.

Conclusion. It has been established that the introduction of GdYVO4: Eu^{3+} NP, both in untreated and UV-irradiated forms, induces dose-dependent effects, including oxidative stress, endothelial dysfunction, intoxication, damage to hepatocyte membranes, functional and histological damage to the liver, with more pronounced effects observed for UV-irradiated NPs.

Keywords. gadolinium-yttrium orthovanadate nanoparticles, hepatotoxicity, oxidative stress, UV-irradiation

Introduction

Scientific progress in chemistry and physics has opened new avenues in the field of nanobiotechnology, enabling the synthesis of specific nanoparticles (NP) and their widespread use in medical applications for the therapy and diagnosis of various serious diseases, particularly cancer.[1] The utilization of nanomaterials holds promise for targeted drug delivery to specific organs, early

Corresponding author: Svitlana Denysenko, e-mail: sa.denysenko@knmu.edu.ua

Received: 12.06.2025 / Revised: 9.10.2025 / Accepted: 26.10.2025 / Published: 30.03.2026

Nakonechna O, Gubina-Vakulick G, Miasoiedov V, Gorbach T, Denysenko S, Yefimova S et al. Identification of hepatotoxicity of untreated and UV-irradiated $GdYVO_4:Eu^{3+}$ nanoparticles. *J Clin Exp Med.* 2026;24(1):83–95. doi: 10.15584/ejcem.2026.1.16.

diagnosis, and treatment of oncologic diseases, as well as coating of surgical instruments and implants with nanoparticles, and the development of new antimicrobial agents, vaccines, and drugs.[2]

Despite the advancements, the impact of synthesized NPs on living organisms remains insufficiently studied. In recent years, there has been growing scientific interest in inorganic nanomaterials based on rare-earth metals.[3-4] The colloidal solutions of these materials exhibit luminescence, offering an expanded capability to monitor biochemical processes.[5] Currently, stable gadolinium compounds are commonly used as magnetic resonance contrast agents, serving as radiosensitizers in radiation therapy of oncological diseases.[6] NPs with rare-earth (RE) ions have unique optical properties and biocompatibility,[7] high photostability, absence of flicker effect, narrow emission lines, and prolonged luminescence.[8] This makes it possible to use such NPs for DNA detection, protein detection of proteins and study of their interactions, imaging in vivo and in vitro.[7] It has been shown that NPs can be used to increase the efficiency of chemotherapy.[9] Complexes based on rare-earth metals are used in gene therapy.[10-12] It was found that many complexes of rare earth metals based on inorganic compounds have antiproliferative,[13] antibacterial[14] anti-inflammatory[15] properties. Tkachenko and his coauthors showed that GdYVO4: Eu^{3+} NP prevent the development of carrageenan-induced intestinal inflammation.[16] $REVO_4$:Eu^{3+} (RE=Gd,Y,La) nanoparticles were found to have antioxidant properties.[16-17] At the same time, there are works showing that REVO4: Eu^{3+} NP exhibit pro-oxidant properties and inhibit enzymes of the antioxidant system (AOS).[18-20] It was found that gadolinium-based nanocomplexes can accumulate in tumor tissues and increase their sensitivity to radiation therapy.[21] At the same time, a number of authors note the presence of negative consequences of the use of gadolinium NP as contrast materials. The authors pay special attention to pathological consequences in brain, kidney, skin, and bone tissues, and to the development of general hypersensitivity reactions.[22] Taking into account the promising application of nanoparticles with RE ions, it should be taken into account that colloidal solutions of nanoparticles themselves can exhibit biological activity. They have unique physical and chemical properties and are characterized by a wide spectrum of biological action.[23] Their effect on living organisms, including toxic effects, is due, as a rule, to the high chemical and catalytic activity of the specific surface area of NPs, which is insignificant in particles of the same nature but of larger size in most cases.[24] Due to their small size, NPs are able to penetrate through the skin, digestive and respiratory systems and accumulate in cells of organs and tissues. The interaction of NPs with proteins is considered; the resulting complex can induce conformational changes in protein molecules.[25-26] $GdYVO_4$:Eu^{3+} NPs are characterized by unique redox flexibility: depending on external conditions, they can promote or suppress the formation of reactive oxygen species (ROS). UV pretreatment was shown to shift their activity from antioxidant to pro-oxidant, highlighting its potential for redox-modulating biomedical applications.[27-28] This property of $GdYVO_4$:Eu^{3+} that provides the prospect of their application in medicine, in particular oncology. In *in vitro* experiments, activated GdYVO4: Eu^{3+} NP was shown to induce the development of oxidative stress in leukocytes, leading to increased generation of ROS and activation of apoptosis.[28] This feature of action may be key in the treatment of cancer, but in other diseases may cause the development of fibrosis.[29] The probability of the development of pathologic conditions caused by the use of nanomaterials is quite real, so the elucidation of the causes of the toxic action of NPs is now becoming the subject of a new direction in experimental medicine.[30] In many world studies, the analysis of developing toxic damage was carried out taking into account normal or decompensated kidney function in patients (or experimental animals), since the excretion of these substances from the body is carried out mainly through the kidneys. In cases of problematic excretion of gadolinium-containing contrast agent through the kidneys, gadolinium accumulated in tissues. The name of such a pathological condition Gadolinium deposition disease was suggested.[20] Current sources of scientific literature do not contain enough information; at the same time, such studies are necessary, since the accumulation of NP in the liver after their administration into the blood is significant.

Aim

The aim of this work is to evaluate the possibility of its hepatotoxic effect on the biochemical parameters of blood, liver homogenates, and the liver histological state in laboratory rats based on in vivo study of the cumulative effect of untreated and UV-irradiated $GdYVO_4$:Eu^{3+} nanoparticles in different concentrations.

Material and methods

The GdYVO4: Eu^{3+} (GdYVO) nanoparticles were supplied by the Institute of Scintillation Materials of the National Academy of Sciences of Ukraine under a cooperation agreement with Kharkiv National Medical University (No. 173/09-19n). GdYVO NPs were synthesized by a previously described method[31] and provided as colloidal aqueous solutions containing 1 g/L of solid phase, consisting of nearly spherical particles with an average diameter of ~2 nm. To minimize possible toxic effects, the substance was administered in small doses of 50, 100, and 200 μg/kg body weight for 14 days. Nonirradiated and UV irradiated GdYVO NPs were administered (immediately before administration to rats, GdYVO NP was activated by training for 20 min with

UV light, in a quartz cuvette at a distance of 20 cm from the irradiation source, using a UV irradiation source of "Quartz-125" type, (λ=210-400 nm) according to the method described previously.[27-28] The substance was administered orally using automatic dosing.

Animal groups

The experiments were carried out in male WAG rats weighing between 180 and 200 g, housed in standard vivarium conditions with natural light and provided with a balanced diet. The rats were randomly assigned to seven groups, each consisting of six individuals.

1. Control group (Gr. C1):
Orally received 0.18-0.20 ml of drinking water.
2. Experimental group 2 (EG-50):
Received a solution of GdYVO NP at a dose of 50 μg/kg body weight.
3. Experimental group 3 (EG-100):
Received a GdYVO NP solution at a dose of 100 μg/kg body weight.
4. Experimental group 4 (EG-200):
Received a GdYVO NP solution at a dose of 200 μg/kg body weight.
5. Experimental group 5 (EGA-50):
Received a solution of UV-activated GdYVO NPs at a dose of 50 μg/kg body weight.
6. Experimental group 6 (EGA-100):
Received a solution of UV-activated GdYVO NPs at a dose of 100 μg/kg body weight.
7. Experimental group 7 (EGA-200):
Received a solution of UV-activated GdYVO NPs at a dose of 200 μg/kg body weight.

This ensures clarity about the nature of the GdYVO NPs in each group, indicating whether it were untreated or UV-activated.

Material collection

At the end of the administration of GdYVO NP solution administration on the next day, rats were removed from the experiment by decapitation using a guillotine, blood was collected, and the liver was isolated at autopsy. The liver suspension (approximately 300 mg) was ground with scissors in a mortar on ice, then saline was added (at the rate of 10 ml of saline per 1g of tissue), homogenized in a Potter homogenizer (on ice) until a homogeneous mass was obtained. The homogenate was centrifuged at 600 g for 10 minutes (centrifuge Universal 320R). The supernatant was used for biochemical studies. Serum was obtained from blood (coagulation followed by centrifugation) and used for biochemical studies.

Another piece of liver tissue was fixed in 10% neutral formalin for morphologic studies.

When working with experimental animals, we were guided by the provisions of the European Convention for the Protection of Vertebrate Animals (Strasbourg, 18.03.1986, revised and amended in 2006), the Law of Ukraine Nos. 3447 - IV, Articles 26, 31 "On the Protection of Animals against Cruelty", "General ethical principles of experiments on animals", adopted by the Fifth National Congress on Bioethics (Kiev, 2013).

The following biochemical techniques were used: - to assess the level of intoxication, the content of medium mass molecules (MMM) in blood serum was determined by the express method[32] to assess the activity of lipid peroxidation (LPO), the content of diene conjugates (DC) and TBA-active products in liver homogenates. The DC content was determined according to the method described in reference 33. The DC content in the sample was expressed in mM/g protein. The concentration of TBA-active products in liver homogenates was determined using the test with 2-thiobarbituric acid according to the method of Botsoglow et al.[34] The content of TBA-active products was expressed in μM/g protein; – the amount of protein in tissues was determined by the spectrophotometric method;[35] – the state of the antioxidant system was evaluated by the content of reduced glutathione and the content of superoxide dismutase (SOD) in liver homogenates. SOD content was determined by an immunoenzymatic method using SOD ELISA Kit, Elabscience (USA), expressed in pkg/mL. Measurements were performed on a semiautomatic analyzer Stat Fax (USA). The determination of reduced glutathione was performed according to the method of Teidze[36] and Tupper.[37] The content of reduced glutathione was expressed in mM/g tissue. Measurements were performed on a Scolar PV-128 spectrophotometer; To evaluate the integrity of hepatocyte membranes, the activity of alanine aminotransferase (AlAT) in serum was determined using reagent kits from "Filisit Diagnostics" (Dnipro City, UA); – to assess liver function the content of direct (DB) and indirect (IB) bilirubin in blood serum was determined. The determination was carried out using a set of reagents from the company "Filisit Diagnostics" (Dnepr city, UA); – to assess the state of the blood vessel endothelium in experimental rats, we determined the content of Willibrandt factor (vWF) in the blood serum of rats. The determination was carried out by immunoenzymatic method using the Elabscience VWF ELISA KIT reagent kit from Elabscience Biottchnology (USA). Measurements were made on a Stat Fax semiautomatic immunoenzyme analyzer (USA). Statistical processing of the data obtained in the studies was carried out using the Graph Pad Prizm 5 program (Grath Pad Soflware, USA) using the non-parametric Mann-Whitney U criterion (comparison between two independent groups of variables). Results were presented as Median (Me) and interquartile interval Me [25%, 75%]. Differences at $p<0.05$ were considered statistically significant. To determine the effect of NPs on the functional state of the liver, we performed morphological

and morphometric studies. After fixation, liver pieces were subjected to paraffin embedding and 4-5 μm thick slices were stained with chromic hematoxylin-eosin and gallocyanin alum by Einarson for nucleic acids. Microscopic examination of liver micro preparations was performed using a microscope with a digital camera. Using Photoshop 13, the optical density of the cytoplasm of hepatocytes in the second zone of the acinus was determined on Einarson stained liver micrographs, which allows one to judge the content of RNA in the cytoplasm and, therefore, the level of protein synthetic function.[38]

Results

Biochemical research

For science and practice, it is important to determine the concentrations of colloidal solution of GdYVO NPs, at which they will be safe for the body and, at the same time, capable of having a therapeutic effect. On the basis of this, we used in experiments various concentrations of colloidal solution of GdYVO NPs for oral administration, as well as their native and activated forms. The study of the content of medium molecules (MM) (a universal indicator of intoxication) showed that its level in the blood in rats of the EG-50 group, compared with the animals of the control group, does not differ statistically. The most significant difference in MM content of MM was observed at doses of 100 and 200 μg/kg. An increase in the dose of orally administered GdYVO NPs leads to a proportional increase in the content of MM, that is, an increase in the level of intoxication. The same dependence is characteristic for activated NPs (Fig. 1).

It should be noted that the MM content in rat serum at all applied concentrations of untreated and UV-irradiated NPs is significantly higher than in the control group. Significant differences in MM content between the indices when using inactivated and activated NPs were revealed only at the dose of 200 μg/kg body weight. Consequently, oral administration of untreated and UV-irradiated GdYVO NPs to rats is accompanied by the development of intoxication, the degree of which increases with increasing dose. A higher toxicity of UV-irradiated GdYVO NP, compared to untreated ones, was revealed only at a dose of 200 μg/kg body weight.

To assess the integrity of hepatocyte membranes under intoxication we have we studied the activity of alanine aminotransferase in blood serum of rats (Table 1).

Table 1. AlAT activity (μM/hour/mL) in blood serum during oral administration of colloidal solution of GdYVO4: Eu3 + NP, [Me (25,75)] to rats*

Indicator	Gr.Cl	Gr. EG-50	Gr. EGA-50	Gr. EG-100	Gr. EGA-100	Gr. EG-200	Gr. EGA-200
AlAT	0.135 [0.119;0.153]	0.109 [0.087;0.115] p_1=0,0057	0.150 [0.137; 0.168] p_1=0.0305 p_2=0.0067	0.223 [0.188; 0.220] p_1=0.0022	0.275 [0.258; 0.293] p_1=0.0022 p_2=0.0043	0.315 [0.298; 0.335] p_1=0.0022	0.355 [0.378; 0.550] p_1=0.0022 p_1=0.0034

*AlAT – alanine aminotransferase, p1 – probability of differences between control and experimental groups, p2 – probability of differences between native and activated groups within one dose

As can be seen from the data given in Table 1, at oral administration of colloidal solution of untreated GdYVO NPs at a dose of 50 μg/kg, the activity of AlAT is even lower than in the control group. ItIn case of administration of UV-irradiated GdYVO NPs, AlAT activity is, slightly higher, and there is an insignificant change in membrane permeability. When rats received a dose of 100 μg/kg, there was a significant increase in serum ALAT activity in serum both in the case of untreated and UV-irradiated GdYVO NP, and in the case of UV-irradiated NP to a greater extent. Changes of the same nature, but more pronounced, occur with oral administration of GdYVO NP at a dose of 200 μg/kg. Consequently, at doses of 100 and 200 μg/kg there is a significant dose-dependent change in permeability of the hepatocyte membrane. The study of the concentration of lipid peroxidation (LPO) products in the liver homogenates of experimental rats showed that in the EG-50 and EG-100 the content of DC increased significantly and in the corresponding groups EGA-50 and EGA-100 the degree of increase is even greater (Table 2). As can be seen from the data given in the table, the

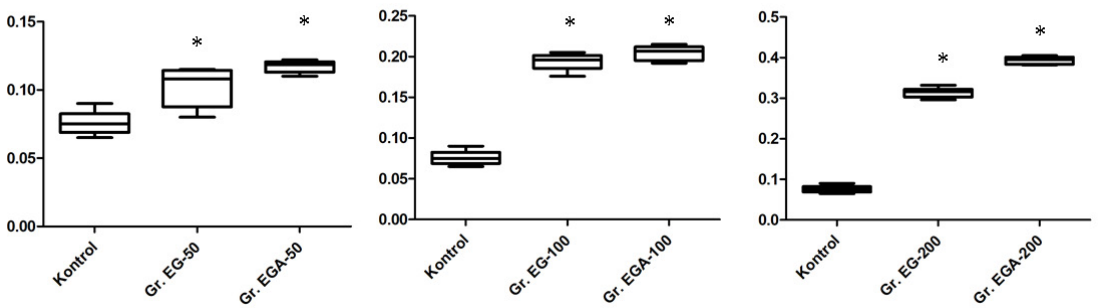

Fig. 1. Content of middle molecules (standard units) in the blood serum of rats after administration of the GdYVO4: Eu^{3+} NP solution (in untreated and UV-irradiated forms), each group compared to the control group, * p <0.05

higher the administered dose of GdYVO NPs, the greater the index value.

Table 2. Content of DC and TBA active products in liver tissue homogenates in rats during oral administration of a colloidal solution of GdYVO4: Eu^{3+} NP (in untreated and UV-irradiated forms), [Me (25, 75)]*

Groups/Indicators	DC, mM/g protein	TBA-active products, μM/g protein
Gr. Cl	58.71 [58.54; 60.88]	26.63 [24.32;27.22]
Gr. EG-50	62.01 [60.39; 62.85]	27.35 [26.78; 28.12]
	p_1=0.0260	p_1=0.0047
Gr. EGA-50	65.93 [64.97; 66.91]	28.34 [27.39; 28.75]
	$p_{1=}$0.0022	$p_{1=}$0.0032
	$p_{2=}$0.0024	p_2=0.0028
Gr. EG-100	74.43 [72.00; 75.46]	31.12 [29.88; 32.25]
	$p_{1=}$0.0023	p_1=0.0035
Gr. EGA-100	79.02 [76.38; 80,50]	32.36 [32.07; 32.86]
	p_1=0.0022	p_1=0.0029
	p_2=0.0043	p_2=0.0021
Gr. EG-200	90.85 [89.17; 91.70]	36.45 [36.12; 37.03]
	p_1=0.0022	p_1=0.0024
Gr. EGA-200	98.15 [96.35; 99.79]	38.42 [37.94; 38.66]
	p_1=0.0022	p_1=0.0039
	p_2=0.0022	p_2=0.0121

* DC – diene conjugates, p_1 – probability of differences between control and experimental groups, p2 – probability of differences between native and activated groups within one dose

Table 3. Content of SOD and glutathione in liver tissue homogenates in rats during oral administration of colloidal solution of GdYVO4: Eu^{3+} NP (in untreated and UV-irradiated form) [Me (25, 75)]*

Groups/Indicators	SOD, pkg/mL	Glutathione, mM/g tissue
Gr. Cl	2.11 [1.97; 2.21]	25.73 [25.53; 25.97]
Gr. EG-50	3.75 [3.71; 3.86]	27,00 [26.92; 27.25]
	p_1=0.0056	p_1=0.0038
Gr. EGA-50	3.82 [3.77; 3.89]	26.48 [26.34; 26.75]
	p_1=0.0031	p_1=0.0056
	p_2=0.0502	p_2=0.0347
Gr. EG-100	1.95 [1.90; 2.06]	23.42 [23.27; 23.56]
	p_1=0.0067	p_1=0.0022
Gr. EGA-100	2.03 [1.98; 2.09]	20.34 [20.19; 20.58]
	p_1=0.0058	p_1=0.0022
	p_2=0.0487	p_2=0.0039
Gr. EG-200	0.87 [0.85; 0.91]	19.22 [19.13; 19.46]
	p_1=0.0018	p_1=0.0019
Gr. EGA-200	0.69 [0.64; 0.73]	16.34 [16.19; 16.57]
	p_1=0.0019	p_1=0.0019
	p_2=0.0022	p_2=0.0019

* SOD – superoxide dismutase, p_1 – probability of differences between control and experimental groups, p2 – probability of differences between the untreated and UV-irradiated groups within one dose

As can be seen from the data in Table 2, the rats of EG-200 and EGA-200 groups have the highest content of DC in liver homogenates among all groups. We also can say that the level of increase in DC concentration in general is higher with introduction UV-irradiated GdYVO NPs, even among lower administered concentrations. Analysis of the the content of end products of the active products of lipid peroxidation TBA showed that their concentration in liver homogenates changes significantly (but reliably) changes in rats of the EG-50 and increases EGA-50 groups, and significantly increases in the EG-100 and EGA-100 groups and to the greatest extent in rats of the EG-200 and EGA-200 groups (Table 2).

As can be seen from the data obtained by us, at the introduction of UV-irradiated GdYVO NPs the degree of increase in the concentration of end products of LPO is higher than that at the introduction of untreated NPs, which indicates higher pro-oxidant properties of UV-irradiated GdYVO NPs. One of the main indicators of the the state of antioxidant system is the following superoxide dismutase (SOD) (Table 3).

As can be seen from the data we received when introducing the SOD content SOD significantly increased equally in the EG-50 and EGA-50 groups of rats, compared to the C1 group. In rats in the EG-100 and EGA-100 groups, the SOD content decreases, and in the case of the introduction of untreated GdYVO NPs, the degree of decrease in the enzyme content is significantly higher. In rats in the EG-200 and EGA-200 groups, an even more pronounced and significant decrease in SOD content is observed compared to the control group, and in the EGA-200 group, the decrease in the enzyme content is more pronounced than in the EG-200 group. Equally important for characterizing the state of the antioxidant system in the liver is the study of the content of reduced glutathione, reflecting the state of the glutathione system. The results of the study of the reduced glutathione in liver homogenates from experimental rats are presented in Table 3. As can be seen from the data we obtained, in the group of rats EG-50 and EGA-50, the reduced glutathione is significantly higher than in the control group. In the rat groups, the content of SH-glutathione EG-100 and EGA-100 is lower than in the control, and in EG-100 is significantly lower than in gr. EGA-100. The same dependence is typical for the EG-200 and EGA-200 groups. Consequently, UV-irradiated and untreated NPs (to a greater extent), administered at a low dose (50 μg/kg), have restorative properties, increasing the adaptive potential. At higher doses, untreated GdYVO NPs do not exhibit reducing properties, while UV-irradiated NPs exhibit pro-oxidant properties. To assess possible damage to the endothelium in the presence of intoxication, the concentration of vWF was studied (Table 4).

At the application of only UV-irradiated NP at a dose of 50 μg/kg, there is a significant increase in the content of FVB compared to the animals of the control group. At doses of 100 μg/kg and 200 μg/kg, significant dose-dependent differences in vWF content between the control and experimental groups of rats, as well as between the untreated and UV-irradiated groups with-

in the same dose-dependent differences. The data obtained by us indicate that endothelial dysfunction is significantly expressed in rats when NPs are administered both UV-irradiated and untreated at doses of 100 and 200 μg/kg, to a greater extent when using UV-irradiated GdYVO NPs. At a dose of 50 μg/kg endothelial dysfunction develops only when UV-irradiated NPs are used.

Table 4. Content of Willibrandt factor (vWF), indirect (IB), and direct (DB) bilirubin in rat blood serum during oral administration of colloidal solution of GdYVO4: Eu^{3+} NP (in untreated and UV-irradiated form), [Me (25, 75)]*

Groups/Indicators	vWF , ng/ml	IB, μM/l	DB, μM/l
Gr. Cl	4.79 [4.62; 4.94]	9.85 [9.35; 10.23]	2.79 [2.63; 2.86]
Gr. EG-50	5.04 [4.89; 5.35]	9.92 [9.67; 10.19]	2.03 [1.97; 2.08]
	p_1=0.0931	p_1=0.270	p_1=0.0058
Gr. EGA-50	6.05 [5.84; 6.19]	11.15 [11.03; 11.27]	1.82 [1.78; 1.97]
	p_1=0.0022	p_1=0.0055	p_1=0.0035
	p_2=0.0022	p_2=0.0034	p_2=0.0045
Gr. EG-100	13.97 [13.72; 14.06]	13.05 [12.96; 13.17]	1.88 [1.79; 1.94]
	p_1=0.0022	p_1=0.0025	p_1=0.0032
Gr. EGA-100	17.16 [17.13; 17.46]	14.55 [14.12; 14.67]	1.72 [1.68; 1.81]
	p_1=0.0022	p_1=0.0022	p_1=0.0022
	p_2=0.0022	p_2=0.0034	p_2=0.0022
Gr. EG-200	34.50 [34.41; 34.72]	15.98 [15.47; 16.22]	1.52 [1.44; 1.59]
	p_1=0.0022	p_1=0.0022	p_1=0.0019
Gr. EGA-200	49.08 [48.97; 49.31]	16.59 [16.22; 17.08]	1.43 [1.39; 1.48]
	p_1=0.0022	p_1=0.0019	p_1=0.0018
	p_2=0.0022	p_2=0.0043	p_2=0.0035

* p1 – probability of differences between control and experimental groups, p2 – probability of differences between untreated and UV irradiated groups within one dose

It is known that one of the most important functions of the liver is the conversion of toxic indirect bilirubin (IB) into nontoxic, water-soluble bilirubin diglucuronide (direct bilirubin, DB). In this regard, in order to evaluate the detoxifying function of rat liver during administration of untreated and UV-irradiated GdYVO NP, we studied the content of DB and IB in the blood serum of experimental rats. The IB content in the blood of the group of rats (EG-50) practically does not differ from the level of the control group, and in the EGA-50 group it was significantly higher than in the control group. In the EG-100 and EGA-100 groups IB concentration is significantly higher than in the control group, and in the EGA-100 group of rats it is significantly higher than in the EG-100 group. The same character of changes, but more pronounced, is observed in groups EG-200 and EGA-200. The DB content in rats of groups EG-100 and EGA-100 groups is significantly lower than in the control group, and in rats of the EGA-100 gr. rats it is significantly lower than in rats of the EG100 gr. are established between the DB content in the control group of rats and in the groups of rats EG-200 and EGA-200. As can be seen from a data obtained by us, the dose-dependent increase in the IB content with a decrease in the DB content is observed during the introduction of GdYVO NPs, especially in the case of UV-activated NPs. The data obtained indicate that the introduction of NPs (particularly UV-irradiated) leads to a decrease in the conjugation process, which is obviously associated with a decrease in the activity (or content) of the conjugation enzyme UGT-glucuroniltransferase and indicates a decrease in the detoxification function of the liver and impaired hepatocyte integrity. Thus, the biochemical assays used in this study showed dose-dependent intoxication of the body, the development of oxidative stress in the liver, and the activity of the GdYVO NPs was enhanced by preliminary activation (UV-irradiation). The circulation of NPs in the bloodstream leads to a dose-dependent death of the vascular endothelium. Furthermore, the entry of NPs from the intestine through the portal system× to the liver led to an increase in the content of NPs against the background of a decrease in the content of DB in the blood serum.

Morphological studies

The morphological study of liver tissue allowed to confirm pathological metabolic changes. In intact animals (C1 gr.) the lobular structure of the liver, with well visible beams of hepatocytes well-visible beams of hepatocytes, with correct, id est not altered placement of triads and central veins. The space around the triads (periportal space) has no leukocytic infiltrates. Central veins do not have a collagen layer in the wall. At the same time in the central vein and surrounding sinusoids there is a varying degree of marked hemorrhage, probably due to extinction of the cardiac function during slaughter and the development of general venous hemorrhage. The nuclei of the hepatocytes are light-colored, with small clumps of chromatin, and the cytoplasm in the periportal zone darker than in the area around the central vein (Fig. 2). In microdissections stained with gallocyanin-chromic alum according to Einarson (histochemical staining for nucleic acids), cytophotometry was performed. Cytophotometric determination of the optical density of hepatocyte cytoplasm in the intermediate zone of the liver lobe: Dk=0.226±0.018 CU of optical density, which can be considered as an indicator of the level of RNA present in the cytoplasm. Sinusoids are lined by endothelium with dark, flat nuclei, the presence of Kupffer cells is moderate.

In animals, which received a course of GdYVO NP at the minimum dose (EG-50 gr.), the histological picture of the appearance of signs of minimal damage to liver tissue, which is accompanied by regeneration and increase in its morpho-functional activity. Namely: in the intermediate (2nd) zone of liver acinuses, there are found areas with absence or decrease in the number of endotheliocytes and Kupffer cells in the lining of sinusoids (Fig. 2). In these areas, hepatocytes have a dark

pycnotic nucleus. In other parts of this zone, there is an increase in the number of endotheliocytes and Kupffer cells in the lining of the sinusoids, and hepatocytes, respectively, with a larger nucleus and a higher RNA content in the cytoplasm.

When staining micropreparations with gallocyanin-chromium alum according to Einarson, the average optical density of the hepatocyte cytoplasm in this zone of the liver lobules is less than in C1 gr. (Fig.4). It was possible to detect a section of the sinusoid where an endothelial "kidney" was formed as a result of endotheliocyte proliferation to replenish the dead endothelial lining of the sinusoid (Fig. 2). The periportal space is somewhat expanded with the appearance of minimal leukocyte infiltration. The central veins and adjacent sinusoids are full-blooded to a greater extent than in C1 gr., in some places the endothelial cover of the central veins is desquamated.

In EGA-50 gr. the damage to the endothelium of sinusoids and hepatocytes in the intermediate zone of the liver lobes is noticeably more pronounced, small areas of hepatocyte death appear similar to the area occupied by 3-5 nearby hepatocytes. At complete lysis, these hepatocytes forms a very small pseudocyst, with a few leukocytes. On micro drugs stained with gallocyanin-chromic alum, the focal decrease in RNA content in the cytoplasm of hepatocytes in the intermediate zone and the focal increase, obviously, in young regenerated hepatocytes. When micro-drugs are staining with gallocyanin-chromic alum by Einarson, the average value of

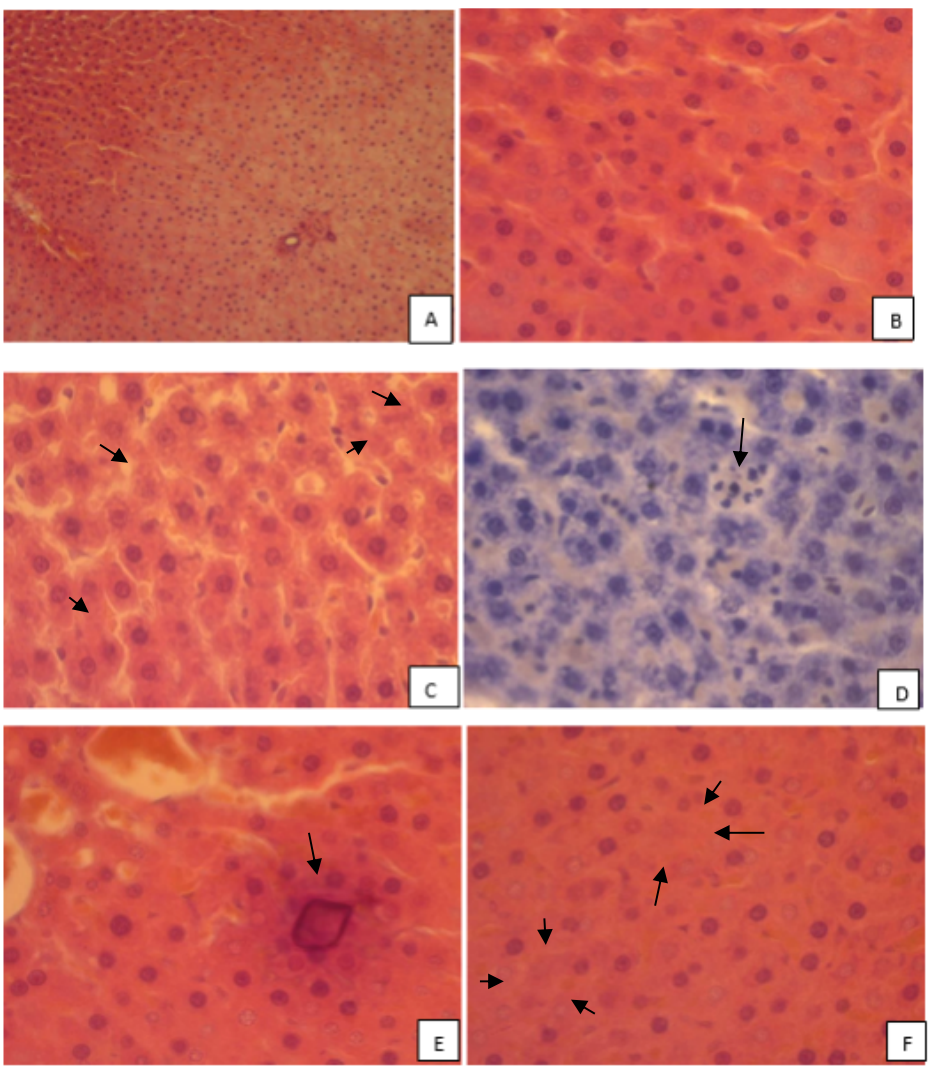

Fig. 2. Microslides of the liver routinely stained with hematoxylin and eosin (A, B, C, E, F), Einarson's gallocyanin stain (D). A: Control group – well-preserved liver histostructure; periportal infiltrate is absent (×100); B: Control group – In the 2nd zone nuclei of hepatocytes are light colored, euchromic and moderately heterochromic, the cytoplasm is eosinophilic, non-vacuolated (×400); C: Gr. EG-50 – In the 2nd zone of acinus many small focuses with full karyolysis of hepatocytes, functioning hepatocytes have larger and lighter nuclei, the cytoplasm is non-uniformly eosinophilic, lower number of sinusoids endotheliocytes of sinusoids (×400); D: Gr. EGA50 – a small focus of necrosis with neutrophil infiltrate of neutrophils (×400); E: Gr. EG-100 – small petrification in the necrosis zone (×400); F: Gr. EG-100 – Hepatocytes in the 2nd zone with a significant decrease in the number of sinusoid endotheliocytes and collapse of sinusoids

optical density of hepatocyte cytoplasm in this zone of the hepatic lobules is unreliably lower than in gr. C1 and unreliably differs from the value of this index in experimental groups of this index in EG-50 (Fig. 4). A small leukocytic infiltrate is observed in the periportal spaces. Additionally, there is more pronounced chromatin margination in the nuclei of hepatocytes located in the zone around the central vein, which is a sign of apoptosis vein, which is a sign of apoptosis.

When animals receive a daily dose of GdYVO NPs 100μg/kg (EG-100) liver damage increases compared to EG-50 gr.: in the 2nd zone the areas dominate, where sinusoids collapsed due to the absence of endothelium and Kupffer cells and therefore such areas look like continuous complexes of hepatocytes without bar structure (Fig. 3). The nuclei of these hepatocytes are dark and hyperchromic, and the cytoplasm has a reduced RNA content. When staining micro-preparations with gallo-

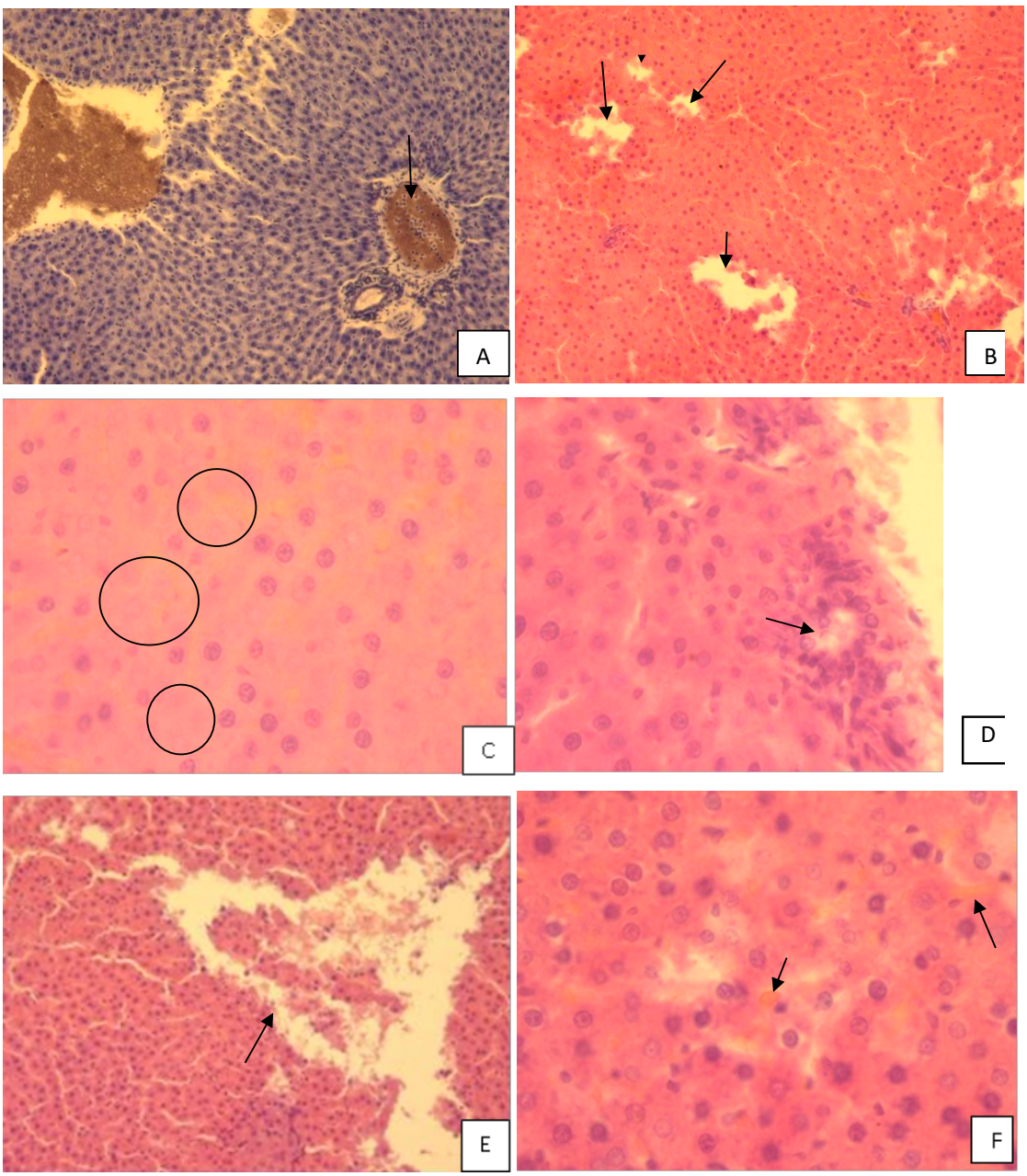

Fig. 3. Microslides of the liver routinely stained with hematoxylin and eosin (B, C, D, E, F), Einarson's gallocyanin stain (A), A: Gr. EG-100 – reduction in trabeculae, large number of leukocytes in blood in a branch of v. portae (×100); B: Gr. EGA-100 – presence of several small pseudocysts in the second zone sites (×100); C: Gr. EG-200 – mosaic picture of the death of small groups of hepatocytes with signs of karyolysis (×400); D: Gr. EGA-200 – inflammation of a biliary duct in the triad, partial destruction of its wall by an infiltrate (×400); E: Gr. EGA-200 – a large pseudocyst with dead hepatocytes not yet lysed in the lumen (×100); F: Gr. EGA-200 – parallel to hepatocyte destruction, dilatation of biliary capillary dilation with cholestasis is observed (×400)

cyanin-chromium alum according to Einarson, the average optical density of the cytoplasm of hepatocytes in this zone of the liver lobules is significantly less than in 1 gr. There is a small infiltration in the periportal spaces, and fullness is present not only in the central veins, but also in the branches of the portal vein, where venous blood contains a large amount of leukocytes.

In EGA-100 gr., the damage to the sinusoid lining and hepatocytes is stimulated so much compared to gr. stimulated, as compared to EG-100 gr, that numerous small pseudocysts are formed in the liver tissue in the same location, numerous small pseudocysts are formed in the hepatic tissue in the same localization, resulting from the death of groups of hepatocytes. The absence of leukocytes around the perimeter of these pseudocysts is noteworthy, indicating that the foci of hepatocyte death are likely to be formed by apoptosis rather than necrosis. Small periportal leukocytic infiltrates are combined with bile duct hyperplasia (3-4).

Obviously, hepatocyte death is so intensive that the reparative potential of young hepatocytes in the periportal zone is insufficient, and figures of hepatocyte mitosis are found in the central parts of the space between the central vein and the triad. When staining microdissections Einarson Gallocyanin-Chrome Alum average value of the optical density of cytoplasm of hepatocytes in this hepatic lobule zone was higher than in C1 gr. and in EG100 gr. (Fig. 4), probably caused by the general decrease in the number of hepatocytes in the second zone and compensatory activation of the morphofunctional state of working hepatocytes.

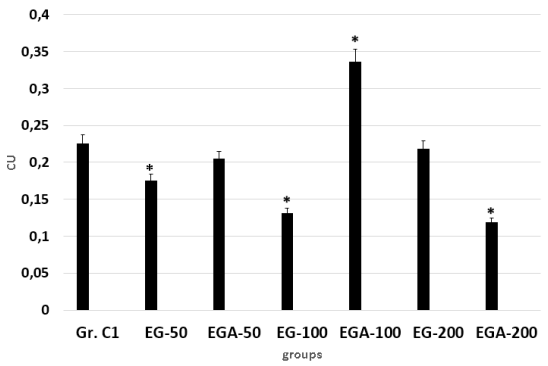

Fig. 4. Optical density of hepatocyte cytoplasm (conditional units, CU) during oral administration of colloidal solution of GdYVO4: Eu^{3+} NP (in untreated and UV-irradiated forms), each group compared to the control group, * – p <0.05

In animals that received the maximum daily dose (EG-200 gr), hepatocytes die even more intensely than in EG-100. Frequent areas of liver tissue, mainly in the intermediate zone, where the trabecular structure is absent, which means that sinusoids have "lost" endothelial lining and collapsed, and hepatocytes in the form of groups of different sizes are in a state of karyolysis (Fig. 3). The optical density of the cytoplasm of functioning hepatocytes in micro-drug staining according to Einarson, in comparison with EG-100 gr. compared to EG-100 gr, is reliably higher, which can also be conditioned by the higher morphofunctional activity of such hepatocytes, which, obviously, has a compensatory significance. The consequence of the focal death of hepatocytes without adequate regeneration is the convergence of triads and central veins. Periportal space with leukocytic infiltrate, increased number of bile ducts. In EGA-200 gr. pseudocysts are more numerous and larger. In the preserved sinusoids there are many lymphocytes and macrophages. Hepatocytes have cytoplasm with a very low RNA content: the optical density of the cytoplasm at Einarson staining is 0.119±0.021 CU of optical density, that is, in these conditions there is a decompensation of the ability of functioning hepatocytes to synthesize RNA. The periportal space has even more pronounced leukocytic infiltration. The wall of the bile duct in the portal tract can be segmentally infiltrated and practically destroyed by leukocytes. In this way, the morphological analysis also confirmed a dose-dependent hepatic tissue lesion induced by $GdYVO_4:Eu^{3+}$ NPs, with the damage further enhanced by UV-activated NPs.

Discussion

Recently, nanomaterials with controllable pro and antioxidant properties have attracted considerable attention as a novel therapeutic approach for various diseases, including cancer.[39] Among them, GdYVO4: Eu3 + nanoparticles (GdYVO NPs) with tunable redox activity appear particularly promising for anticancer applications due to their ability to modulate toxicity.[17-19,27,28] At the microscopic level, the enhanced toxicity of UV-irradiated GdYVO NPs can be attributed to their photocatalytic properties. Specifically, UV exposure induces the generation of electron–hole pairs.[27,28] In nanoparticles with a high density of structural defects, these defects act as traps for photoinduced charge carriers, allowing them to accumulate. Over time, trapped carriers migrate to the surface of the nanoparticle, where they interact with oxygen and water molecules, producing ROS such as $O_2^{\bullet-}$ and ×OH, a phenomenon referred to as "dark ROS generation".[27,28] Furthermore, it has been shown that UV pre-treatment of GdYVO NPs leads to partial reduction of Eu^{3+} to Eu2 +.18 Electrons stored in Eu^{2+} can subsequently drive ROS production even in the absence of light.[18] Furthermore, the ultrasmall size of GdYVO NPs (~ 2 нм) may further influence their cellular internalization and subcellular interactions, thus contributing to their cytotoxic effects.[23,40]

The objective of our study was to assess the risk of toxic liver damage with oral administration of a colloidal solution of NPs depending on the dose and UV ir-

radiation. Our investigation of MM in the blood serum of experimental rats revealed a significant increase in content, particularly in groups subjected to doses of 100 and 200 μg/kg (EG-100, EGA-100, EG-200 and EGA-200). In particular, this increase was more pronounced in groups where NPs were irradiated with UV light at these doses. Surprisingly, even in the EG-50 and EGA-50 groups, a substantial increase in MM content was observed. These findings suggest a dose-dependent intoxication in rats. It is plausible that toxicity is associated not directly associated with NPs themselves, but rather with their complexation with proteins.[25-26] Investigation of AlAT activity in blood has revealed that the introduction of NPs $GdYVO_4:Eu^{3+}$ into the organism induces a dose-dependent increase in hepatocyte membrane permeability. Specifically, within the EG-50 and EGA-50 groups of rats, no discernible disturbance in permeability was observed. On the contrary, within the EG-100 and EGA-100 groups, a notable increase in permeability was detected. The most substantial increase, surpassing the values observed in the control group, was observed in the EG-200 and EGA-200 rat groups. More pronounced disorders are observed in rats injected with activated NPs, which may be the cause of structural and metabolic disorders in the liver. Microscopic examination of hepatic tissue revealed toxic damage to hepatocytes, primarily concentrated in the intermediate zone of the liver lobule-where venous blood from the gastrointestinal tract enters the sinusoids through the v. portae system. The intensity of hepatocyte damage is significantly with the dose of NPs administered to the animals. In the EG-50 group, this damage is characterized by areas with pyknotic nuclei and weak histochemical staining of the cytoplasm for RNA. In contrast, in the EG-200 group, the damage is more severe, manifesting itself as large pseudocysts formed during the course of the experiment. These pseudocysts likely result from the utilization of the cytoplasm, indicating the death of hepatocytes. Preliminary UV activation of NPs at all doses administered led to more pronounced damage to hepatocytes. The degree of destruction in liver tissue across all main groups, including the EGA groups, aligns with the concurrent increase in the content of MMM and AlAT activity in serum. As described above, HP intake of HPs into the organism does not exclude the possibility of activation of the peroxidation process.[19] The data obtained by us indicate that in oral administration of colloidal solution of $GdYVO_4:Eu^{3+}$ in groups of rats EG-100, EGA100, EG-200 and EGA-200 showed a dose-dependent increase in the content of LPO products against the background of decreased content of SOD and glutathione (the main components of the antioxidant system) which indicates the development of oxidative stress. The development of oxidative stress is more pronounced when NPs is administered at a dose of 200 μg/kg. Among the EG-50 and EGA-50 groups, the development of oxidative stress, apparently, is prevented by increasing AOS activity. It should be noted that we revealed an interesting fact: only when nanoparticles are administered at a dose of 50 μg/kg, UV-irradiated and, to a greater extent, untreated NPs have pronounced antioxidant properties. According to data of other researchers, obtained by the introduction of similar NPs but do not have in their yttrium composition, pronounced antioxidant properties are observed even in oral administration in doses of 200-300 μg/kg for 20 days.[41] Apparently, the composition of NPs significantly affects both their adhesive properties and the redox potential of the system.[42]

Morphologically, we have also confirmed the "unfolding" of both intracellular and cellular regeneration of hepatocytes in response to their destruction. In the EG-50 group, many hepatocytes emerge around foci containing dying hepatocytes, characterized by larger and lighter-colored nuclei. A comparative analysis of the cytophotometrically determined RNA content in the hepatocyte cytoplasm (Ill.2) prompts us to explore the unexpectedly high level of RNA in the EGA-100 group, surpassing that of the EG-100 group. Examination of liver micropreparations in the intermediate zone of the lobe reveals that in the EGA-100 group, there are relatively few hepatocytes in a wild-type state compared to the EG-100 group. However, pseudocysts are larger and more frequent. Consequently, it can be argued that preirradiation of NPs administered in a high dose enhances the process of hepatocyte death and dystrophy. The remaining 'healthy' hepatocytes work more intensively, leading to a higher RNA content in the cytoplasm. At the maximum dose of nanoparticles in the EGA-200 group, dystrophic hepatocytes dominate among the remaining cells. Therefore, the RNA content in these hepatocytes is lower than in the EG-200 group. It is known that intoxication, the presence of oxidative stress, and direct contact of NPs with endotheliocytes are risk factors for endothelial damage.[43-45] As described above, a dose-dependent increase in the vWF content in the blood was revealed in all rats' groups (except for EG-50 gr.), more pronounced in rats in the EGA groups. Consequently, endothelial damage endsothelium damage occurs in rats of all groups except EGA. The maximum damage is in the rats EGA-200 group. Morphological examination revealed that in all major groups, the endothelium of the sinusoids and the arteries of the portal tract was severely damaged and desquamated. Only in EG-50 gr. there is an active proliferation of endotheliocytes in parallel, which corresponds to the data of the biochemical study on the content of vWF in blood serum. The analysis of bilirubin fractions revealed a dose-dependent increase in the content of IB against the background of DB decrease, to a greater extent at the introduction of activated NPs, which indicates a decrease in the activity or amount of UDP-glucanosyl-

transferase, integrity of hepatocyte membranes. The violation of bile production was revealed morphologically: At the application of doses of 100 and 200 μg/kg there is observed proliferation of bile ducts is observed in "triads", which is a compensatory mechanism in the compensatory mechanism in biliary hepatitis and biliary cirrhosis of the liver. The presence of oxidative stress, intoxication, endotheliocyte damage, membrane permeability disorders, hepatocyte destruction, decreased DB production and destruction of sinusoidal endotheliocytes allows us to assume that in the liver dose-dependent structural and metabolic disorders develop in the liver (EG-50 EG-100 g.EG-200). At the minimal dose of 50 μg/kg, the structural and metabolic disorders are fully compensated. UVa NPs lead to increase of the level of structural-metabolic disorders in liver tissue (EGA50≤EGA-100≤EGA-200), which is also shown biochemically and morphologically.

Conclusion

The colloidal solution of $GdYVO_4:Eu^{3+}$ NPs, UV irradiated to a greater extent, has a pronounced dose-dependent toxicity when administered to rats at the doses studied for 14 days.

The administration of colloidal $GdYVO_4:Eu^{3+}$ NPs to rats at doses of 100 and 200 μg/kg body weight is accompanied by the development of oxidative stress, which is most pronounced for UV-irradiated NPs.

Intoxication, the development of oxidative stress, and direct contact of the nanoparticles with the endothelium contribute to the development of dose-dependent endothelial dysfunction, especially for UV-irradiated NPs, as evidenced by the increase in the concentration of vWF, maximally expressed at a dose of 200 μg/kg.

The increase in the activity of the indicator enzyme AlAT in blood serum and decrease in the DB level on the background of increased IB (most pronounced at administration of untreated and UV-irradiated NPs at a dose of 200 μg/kg of weight) testify about functional disorders (detoxification function) in the liver.

The data obtained by us allow us to conclude that colloidal solution of GdYVO4: Eu^{3+} NP at oral administration to rats in doses of 100 and 200 μg/kg of weight for 14 days can induce cell apoptosis mediated by the development of oxidative stress and significant damage to endothelium vessels. The possible therapeutic effect in cancer treatment will be accompanied by significant morphologic and functional liver damage, which requires the use of hepatoprotectors.

When administering colloidal solution of GdYVO4: Eu^{3+} NP at a dose of 50 mcg / kg weight, no significant changes in the parameters were not revealed.

Acknowledgments

The authors thank KhNMU (Kharkiv National Medical University) for support.

Declarations

Funding

The study was supported by the Ukrainian Ministry of Health using the funds provided by the state budget as a fragment of a research entitled 'Research of Efficiency, Mechanisms of Action and Safety of Use of Orthovanadate Nanoparticles of Rare Earth Elements for Optimization of Radiation Therapy in the Conditions of Oncopathology" (state registration number 0121U110920).

Author contributions

Conceptualization, O.N., and G.G-V.; Methodology, T.G. and S.S.; Software, I.V.; Validation, V.M. and O.N.; Formal Analysis, D.Y.; Investigation, I.V. and D.Y.; Resources, O.N.; Data Curation, S.D.; Writing – Original Draft Preparation, T.G., S.D; Writing – Review & Editing, O.N., S.Y., V.K. and G.G-V.; Visualization, S.D.; Supervision, S.D. and G. G-V; Project Administration, V.M.; Funding Acquisition, O.N.

Conflicts of interest

The authors declare no competing interests.

Data availability

The data supporting the findings of this study are available from the corresponding author upon reasonable request.

Ethics approval

The study protocol was approved by the Ethics Committee of Kharkiv National Medical University (protocol No. 5; 09.17.2019).

References

1. Raj S, Khurana S, Choudhari R, et al. Specific targeting cancer cells with nanoparticles and drug delivery in cancer therapy. *Semin Cancer Biol*. 2021;69:166-177. doi:10.1016/j.semcancer.2019.11.002
2. Yetisgin AA, Cetinel S, Zuvin M, Kosar A, Kutlu O. Therapeutic Nanoparticles and Their Targeted Delivery Applications. *Molecules*. 2020;25(9):2193. doi:10.3390/molecules25092193
3. Thakur N, Thakur S, Chatterjee S, Das J, Sil PC. Nanoparticles as Smart Carriers for Enhanced Cancer Immunotherapy. *Front Chem*. 2020;8:597806. doi:10.3389/fchem.2020.597806
4. Pavelić K, Kraljević Pavelić S, Bulog A, et al. Nanoparticles in Medicine: Current Status in Cancer Treatment. *Int J Mol Sci*. 2023;24(16):12827. doi:10.3390/ijms241612827
5. Abdesselem M, Schoeffel M, Maurin I, et al. Multifunctional rare-earth vanadate nanoparticles: luminescent labels, oxidant sensors, and MRI contrast agents. *ACS Nano.* 2017;8(11):11126-11137. doi:10.1021/nn504170x
6. Howard D, Sebastian S, Le QV-C, Thierry B, Kempson I. Chemical Mechanisms of Nanoparticle Radiosensitization

and Radioprotection: A Review of Structure-Function Relationships Influencing Reactive Oxygen Species. *Int J Mol Sci*. 2020;21(2):579. doi:10.3390/ijms21020579

7. Liu Y, Zhang P, Li F, et al. Metal-based NanoEnhancers for Future Radiotherapy: Radiosensitizing and Synergistic Effects on Tumor Cells. *Theranostics*. 2018;8(7):1824-1849. doi:10.7150/thno.22172
8. Jackson N, Cecchi D, Beckham W, Chithrani DB. Application of High-Z Nanoparticles to Enhance Current Radiotherapy Treatment. *Molecules*. 2024;29(11):2438. doi:10.3390/molecules29112438
9. Ge H, Wang D, Pan Y, et al. Sequence-Dependent DNA Functionalization of Upconversion Nanoparticles and Their Programmable Assemblies. *Angew Chem Int Ed Engl*. 2020;59(21):8133-8137. doi:10.1002/anie.202000831
10. Shi J, Yang X, Li Y, et al. MicroRNA-responsive release of Cas9/sgRNA from DNA nanoflower for cytosolic protein delivery and enhanced genome editing. *Biomaterials*. 2020;256:120221. doi:10.1016/j.biomaterials.2020.120221
11. Bakshi S, Zakharchenko A, Minko S, Kolpashchikov DM, Katz E. Towards Nanomaterials for Cancer Theranostics: A System of DNA-Modified Magnetic Nanoparticles for Detection and Suppression of RNA Marker in Cancer Cells. Magnetochemistry. 2019;5(2):24. doi:10.3390/magnetochemistry5020024
12. Ahmadzada T, Reid G, McKenzie DR. Fundamentals of siRNA and miRNA therapeutics and a review of targeted nanoparticle delivery systems in breast cancer. *Biophys Rev*. 2018;10(1):69-86. doi:10.1007/s12551-017-0392-1
13. Wang L, Hu C, Shao L. The antimicrobial activity of nanoparticles: present situation and prospects for the future. *Int J Nanomedicine*. 2017;12:1227-1249. doi:10.2147/IJN.S121956
14. Agarwal H, Nakara A, Shanmugam VK. Anti-inflammatory mechanism of various metal and metal oxide nanoparticles synthesized using plant extracts: A review. *Biomed Pharmacother*. 2019;109:2561-2572. doi:10.1016/j.biopha.2018.11.116
15. Tkachenko A, Pogozhykh D, Onishchenko A, et al. Gadolinium Orthovanadate $GdVO_4$:Eu^{3+} Nanoparticles Ameliorate Carragttnan-indused intestinal Inflammation *Journal of Farmacy and Nutrition Sciences*, 2021;11:40-48. doi: https;//doi.org/ 10.29169/ 1927-5951.2021.11.06
16. Yefimova SL, Maksimchuk PO, Seminko VV, et al. Janus-faced redox activity of $LnVO_4$:Eu^{3+} (Ln= Gd, Y, and La) nanoparticles. *J Phys Chem C*. 2019;123(24):15323-15329. doi.org/10.1021/acs.jpcc.9b03040
17. Maksimchuk PO, Hubenko KO, Grygorova GV, Klochkov VK, Sorokin AV, Yefimova SL. Impact of Eu^{3+} ions on prooxidant activity of ReVO4 : Eu3= nanoparticals. *J Phys Chem C*. 2021;125(2):1564-1569. doi.org/10. 1021/ acs.jpcc.Oc10028
18. Maksimchuk PO, Yefimova SL, Omielaieva VV, et al. X-ray Induced Hydroxyl Radical Generation by $GdYVO_4$:Eu^{3+} Nanoparticles in Aqueous Solution: Main Mechanisms. *Crystals*. 2020;10(5):370. https://doi.org/10.3390/cryst10050370
19. Anselmo AC, Mitragotri S. Nanoparticles in the clinic: An update. *Bioeng Transl Med*. 2019;4(3):e10143. doi:10.1002/btm2.10143
20. Kasi PB, Mallela VR, Ambrozkiewicz F, Trailin A, Liška V, Hemminki K. Theranostics Nanomedicine Applications for Colorectal Cancer and Metastasis: Recent Advances. *Int J Mol Sci*. 2023;24(9):7922. doi:10.3390/ijms24097922
21. Davies J, Siebenhandl-Wolff P, Tranquart F, Jones P, Evans P. Gadolinium: pharmacokinetics and toxicity in humans and laboratory animals following contrast agent administration. *Arch Toxicol*. 2022;96(2):403-429. doi:10.1007/s00204-021-03189-8
22. Radulescu DM, Surdu VA, Ficai A, Ficai D, Grumezescu AM, Andronescu E. Green Synthesis of Metal and Metal Oxide Nanoparticles: A Review of the Principles and Biomedical Applications. *Int J Mol Sci*. 2023;24(20):15397. doi:10.3390/ijms242015397
23. Khan I, Saeed K, Nanoparticles properties? Applications and toxicitts. *Arabian Journal of Chemistry* 2019;12(7);908-931 doi:10. 1016/ i Arabic. 2017.05.0
24. Sun H, Jiang C, Wu L, Bai X, Zhai S. Cytotoxicity-Related Bioeffects Induced by Nanoparticles: The Role of Surface Chemistry. *Front Bioeng Biotechnol*. 2019;7:414. doi:10.3389/fbioe.2019.00414
25. Önal Acet B, Gül D, Stauber RH, Odabaşı M, Acet Ö. A Review for Uncovering the "Protein-Nanoparticle Alliance": Implications of the Protein Corona for Biomedical Applications. *Nanomaterials (Basel)*. 2024;14(10):823. doi:10.3390/nano14100823
26. Maksimchuk P, Yefimova S, Hubenko K, et al. Dark reactive oxygen species generation in ReVO:Eu^{3+}(Re=Gd, Y) nanoparticles in aqueous solutions. *J Phys Chem C*. 2020;124(6):3843-3850. doi:10.1021/acs.jpcc.9b10143
27. Yefimova SL, Maksimchuk PO, Hubenko KO, et al. Light-triggered redox activity of $GdYVO_4$:Eu^{3+} nanoparticles. *Spectrochim Acta A Mol Biomol Spectrosc*. 2020;242:118741. doi:10.1016/j.saa.2020.118741
28. Onishchenko A, Myasoedov V, Yefimova S, et al. UV Light-Activated $GdYVO_4$:Eu^{3+} Nanoparticles Induce Reactive Oxygen Species Generation in Leukocytes Without Affecting Erythrocytes In Vitro. *Biol Trace Elem Res*. 2022;200(6):2777-2792. doi:10.1007/s12011-021-02867-z
29. Weng TI, Chen HJ, Lu CW, et al. Exposure of Macrophages to Low-Dose Gadolinium-Based Contrast Medium: Impact on Oxidative Stress and Cytokines Production. *Contrast Media Mol Imaging*. 2018;2018:3535769. doi:10.1155/2018/3535769
30. Klochkov VK, Malyshenko AL, Sedyh OO, Malyukin YuV. Wet-chemical syntesis and characterization of luminescent colloidal nanoparticles $ReVO_4$: Eu^{3+} (Re=La, Gd, Y) with rod- like and spindle-like shape. *Fanctional materials*. 2011;1:111-115.
31. Dzyubanovsky II, Vervega BM, Pidruchna SR, Melnyk NA. Syndrome of endogenous intoxication at experimen-

tal peritonitis against the background of diabetes. *Bulletin of Scientific Research*. 2019;1:135-139. doi:10.11603/2415-8798.2019.1.10004.

32. Stoscheck CM. Quantitation of protein. *Methods Enzymol*. 1990;182:50-68. doi:10.1016/0076-6879(90)82008-p
33. Botsoglou NA, Fletouris DJ, Papageorgiou G, et al. Rapid, sensitive, and specific thiobarbituric acid method for measuring lipid peroxidation in animal tissue, food, and feedstuff samples. *Journal of Agricultural and Food Chemistry*. 1994;42(9):1931-1937. doi:10.1021/JF00045A019
34. Cammansky I, Cruener V. Spectrofotometric methods for measuring diene conjugation. *Clin Chem Acta*. 1997;259:177-179
35. Tietze F. Enzymic method for quantitative determination of nanogram amounts of total and oxidized glutathione: applications to mammalian blood and other tissues. *Anal Biochem*. 1969;27(3):502-522. doi:10.1016/0003-2697(69)90064-5
36. Tupper J, Tozer GM, Dachs GU. Use of horseradish peroxidase for gene-directed enzyme prodrug therapy with paracetamol. *Br J Cancer*. 2004;90(9):1858-1862. doi:10.1038/sj.bjc.6601780
37. Zelditch ML, Swiderski DL, Sheets HD, Fink WL. Geometric Morphometrics for Biologists: A Primer. 3rd ed. Elsevier Academic Press; 2012:488 p. ISBN 978-0-12-386903-6
38. Yang B, Chen Y, Shi J. Reactive Oxygen Species (ROS)-Based Nanomedicine. *Chem Rev*. 2019;119:4881-4985. https://doi.org/10.1021/acs.chemrev.8b00626
39. Mosquera J, García I, Liz-Marzán LM. Cellular Uptake of Nanoparticles versus Small Molecules: A Matter of Size. *Acc Chem Res*. 2018;51(9):2305-2313. doi:10.1021/acs.accounts.8b00292
40. Nikitchenko YV, Klochkov VK, Kavok NS, et al. Age-Related Effects of Orthovanadate Nanoparticles Involve Activation of GSH-Dependent Antioxidant System in Liver Mitochondria. *Biol Trace Elem Res*. 2021;199(2):649-659. doi:10.1007/s12011-020-02196-7
41. Mundekkad D, Cho WC. Nanoparticles in Clinical Translation for Cancer Therapy. *Int J Mol Sci*. 2022;23(3):1685. doi:10.3390/ijms23031685
42. Xuan L, Ju Z, Skonieczna M, Zhou PK, Huang R. Nanoparticles-induced potential toxicity on human health: Applications, toxicity mechanisms, and evaluation models. *MedComm (2020)*. 2023;4(4):e327. doi:10.1002/mco2.327
43. Min Y, Suminda GGD, Heo Y, Kim M, Ghosh M, Son YO. Metal-Based Nanoparticles and Their Relevant Consequences on Cytotoxicity Cascade and Induced Oxidative Stress. *Antioxidants (Basel)*. 2023;12(3):703. doi:10.3390/antiox12030703
44. Huang C, Liu X, Wu Q, et al. Cardiovascular toxic effects of nanoparticles and corresponding molecular mechanisms. *Environ Pollut*. 2024;356:124360. doi:10.1016/j.envpol.2024.124360
45. Xi WS, Tang H, Liu YY, et al. Cytotoxicity of vanadium oxide nanoparticles and titanium dioxide-coated vanadium oxide nanoparticles to human lung cells. *J Appl Toxicol*. 2020;40(5):567-577. doi:10.1002/jat.3926

Rzeszów University Press 2026
ISSN 2544-1361 (online)
doi: 10.15584/ejcem.2026.1.17

http://www.ejcem.ur.edu.pl
European Journal of Clinical and Experimental Medicine
Eur J Clin Exp Med 2026; 24 (1): 96–103

ORIGINAL PAPER

Evaluation of autonomic imbalance in irritable bowel syndrome and functional dyspepsia

Leroy D'Souza [1], Prakash Banahalli Chikkaiah [1], Prashanth K. S. [2], Maanini Singhvi [1]

[1] Department of Medicine, Bangalore Medical College and Research Institute, Kalasipalya, Bengaluru, Karnataka, India
[2] Department of Physiology, Bangalore Medical College and Research Institute, Kalasipalya, Bengaluru, Karnataka, India

ABSTRACT

Introduction and aim. Irritable bowel syndrome (IBS) and functional dyspepsia (FD) are functional gastrointestinal disorders that may involve autonomic imbalance. This study assessed autonomic nervous system activity using short-term heart rate variability (HRV). To our knowledge, this is the first study in an Indian population to directly compare autonomic modulation across IBS subtypes and FD using a unified HRV protocol, demonstrating subtype-specific alterations – particularly reduced LF/HF in IBS-diarrhea (IBS-D).

Material and methods. Thirty IBS patients and thirty FD patients diagnosed using the Rome IV criteria, along with thirty healthy controls, were enrolled. Short-term HRV analysis was performed following ECG acquisition using the LABCHART platform.

Results. Mean low-frequency/high-frequency (LF/HF) ratio was 1.26±0.83 in IBS, 1.40±1.171 in FD, and 1.60±1.196 in controls. High-frequency (HF) power values (ms^2) were 733.9±1661.16 (IBS), 534.18±778.28 (FD), and 674.87±1187.16 (controls), with no significant differences among the three groups ($p>0.05$). Subgroup analysis revealed significantly lower LF/HF values in IBS-D compared to controls (0.98±0.69 vs. 1.60±1.196; $p=0.038$), while HF values did not differ ($p>0.05$). No significant differences were found between IBS-constipation (IBS-C) patients and controls.

Conclusion. IBS-D patients exhibited decreased LF/HF and increased HF values, indicating enhanced parasympathetic modulation, which may contribute to diarrhea-predominant symptoms. IBS-C patients showed a trend toward higher LF/HF and lower HF values, compatible with increased sympathetic modulation, although results were not statistically significant. FD patients showed no autonomic differences relative to controls. These findings highlight subtype-specific autonomic patterns in IBS and provide novel HRV-based insights from an Indian cohort.

Keywords. autonomic imbalance, autonomic nervous system, constipation, dyspepsia, gastrointestinal diseases, irritable bowel syndrome

Introduction

Functional gastrointestinal disorders (FGIDs) arise as a result of the interaction between the gut and the brain. It is a group of disorders characterized by motility disturbance, visceral hypersensitivity, altered gut microbiota, and altered central nervous system processing.[1] Two major functional GI disorders affecting the population are – irritable bowel syndrome (IBS) and functional dyspepsia (FD). IBS is a chronic gastrointestinal disease characterized largely by abdominal pain and changes in stool consistency and frequency. Global prevalence of IBS was found to be 11.2%.[2] Its prevalence in India varies from 4.2 to 14%.[3] Functional dyspepsia is characterized by epigastric pain, discomfort, early satiety, and

Corresponding author: Maanini Singhvi, e-mail: maanini.singhvi2002@gmail.com

Received: 3.08.2025 / Revised: 7.10.2025 / Accepted: 28.10.2025 / Published: 30.03.2026

D'Souza L, Chikkaiah PB, Prashanth KS, Singhvi M. Evaluation of autonomic imbalance in irritable bowel syndrome and functional dyspepsia. *Eur J Clin Exp Med.* 2026;24(1):96–103. doi: 10.15584/ejcem.2026.1.17.

burning. Global prevalence of FD has been demonstrated to be varying between 11–29.2%.[4]

The pathophysiology of IBS and FD is yet to be clearly worked out. Various mechanisms have been proposed for IBS ranging from alteration in the gut microbiome (dysbiosis) and neurotransmitter imbalance[5] to dysregulation of the hypothalamus-pituitary-adrenal (HPA) axis.[6] Loss of vagal tone and receptive relaxation of the stomach to food has been implicated to contribute to the pathogenesis of FD.[7] Abnormal gastric emptying has also been implicated in FD pathogenesis.[8] Psychological stress and presence of other psychiatric co-morbidities has been shown to affect the etiopathogenesis of both IBS and FD.[9,10]

Recently, working out the mechanisms producing underlying differences between the IBS subtypes i.e., IBS-Diarrhea predominant (IBS-D) and IBS-Constipation predominant (IBS-C) together with understanding the role of the vagus nerve in IBS is being encouraged as a research priority.[11] HRV (Heart-rate variability) analysis is a well-validated method that can be used to non-invasively assess autonomic functioning. It is based on the principle of beat-to-beat variation i.e., changes in the RR intervals (time between successive R waves of an ECG) between heart beats.[12,13] As discussed above, IBS and FD significantly overlap in pathophysiology. However, there is a lack of studies investigating HRV patterns in IBS and FD in the same setting. Additionally, previous studies comparing the HRV patterns of IBS subtypes are few and utilize the older ROME III criteria for diagnosis.[14] Further, there exists a gap in autonomic research in the Indian population. The Indian population has shown several variations in comparison to other Asian populations such as a higher prevalence of the IBS-Diarrhea subtype, higher prevalence in older age groups etc.[15]

As already discussed, functional GI disorders are disorders of interaction between the gut and brain whose effects manifest as abnormalities in gastric emptying time, abnormal receptive relaxation of the stomach, and altered intestinal motility and secretions. Gastrointestinal motility and secretions are mainly controlled by the intrinsic enteric nervous system whose functions are modulated externally by the autonomic system via the vagus and sympathetic nerves, which are in turn, are controlled by the brain. Thus, it can be hypothesized that autonomic dysfunction might be the cause of disease in these patients.

In the current study, we aim to use the short-term 5-minute HRV recording to assess the autonomic functioning in two functional GI disorders - IBD and FD in the Indian population. We also aim to investigate if there is a difference in HRV patterns in IBS subtypes- IBS-D and IBS-C. We will be employing the ROME IV criteria for the diagnosis of our patients.

Aim

This study aims to determine whether patients with IBS, its clinical subtypes, and FD exhibit autonomic dysfunction, and to characterize their sympathetic and parasympathetic modulation using short-term HRV analysis. Importantly, this work provides one of the first comparative assessments of autonomic activity across IBS subtypes and FD within a single standardized HRV protocol, highlighting potential subtype-specific autonomic patterns – particularly in IBS-diarrhea.

Material and methods

Study design and setting

This is a cross-sectional study set in a tertiary health center in urban India. The sample size was determined using an appropriate formula-

Using reference article[16],

$$n=\frac{2(z\alpha + z1-\beta)^2\sigma^2}{d^2}$$

Where, $z\alpha$=Standard table value for 95 percent Confidence Interval=1.96

$z1-\beta$=Standard table value for 80 percent power=0.9

σ=Standard deviation=14.1

d=10.6=effect size

$$n=2(1.96+0.9)^2(14.1)^2$$
$$(10.6)^2$$
$$n=28.9$$

Hence, 30 IBS, 30 FD and 30 controls were chosen as the sample size. Due clearance from the Institutional ethics committee was received before initiating the study.

Materials used and participants

PowerLab 26T (4 channel, 16-bit resolution polygraph) *(AD Instruments, Colorado Springs, USA)*, LABCHART 8 (*AD Instruments, Colorado Springs, USA)*, HRV 2.0 module *(AD Instruments, Colorado Springs, USA)*, and 3M™ Red Dot™ monitoring electrodes (*3M, Maplewood, USA*) were used in our study.

Consecutive patients belonging to the age group of 18-80 years who presented to the outpatient gastroenterology clinic were included. Subjects were recruited between August 2023 and July 2024. IBS or FD was diagnosed based on the ROME IV criteria by an experienced gastroenterologist.[17] Controls were volunteers recruited on the basis of age and socioeconomic matching. Each patient and control underwent abdominal ultrasound, routine blood tests, as well as thyroid function tests. FD patients underwent upper GI endoscopy to rule out structural disease. IBS patients were classified based on Bristol stool scale and ROME IV criteria for various IBS subtypes. IBS patients were divided into two subsets - IBS-D and IBS-C.[18]

Patients with IBS-M (Mixed) and those diagnosed with both IBS and FD were excluded. Patients or con-

trols with other gastrointestinal diseases, psychiatric illness, thyroid disease, diabetes mellitus, cardiac arrhythmias and those on medications such as NSAIDs, prokinetic drugs, antidiarrheal, laxatives, antispasmodic agents, tricyclic antidepressants, and SSRIs were excluded. Participants who had a history of caffeine intake or smoking within the last 24 hours were also excluded.

HRV recording

Readings were taken in the autonomic function test (AFT) lab. The readings were taken at the same time (11 AM –1 PM) every day to minimize error caused by diurnal variation of HRV.

Patients were given 15 minutes of rest to stabilize their respiratory and heart rates. Blood pressure, heart rate and respiratory rates were noted. ECG was recorded in the lead I configuration (negative electrode – right wrist, positive electrode – left wrist, and ground electrode – right ankle). ECG wires were connected to a bio amp which was connected to the PowerLab 26T machine. Patients were instructed to breathe according to the metronome set at 12 breaths/minute.

Real-time ECG signals appearing on the screen were refined to acquire clean signals. A high pass filter of 0.5 Hz and a low pass filter of 50 Hz was applied and a range of 5 mV was set. Data was acquired continuously for 5 minutes in supine posture at a rate of 500 Hz. The R wave peaks were automatically detected by the software. Ectopic beats (<5), noise, spikes and artifacts were automatically excluded from analysis by using Labchart's beat classifier view and also by manual screening of the recording. Any recording which had more than 5 ectopic beats or more than 5 seconds of aberrant ECG signal was completely repeated. Eleven recordings were repeated due to the above reasons.

HRV analysis

In the frequency-domain analysis of HRV, the spectral analysis was applied in our study, which decomposes the R-R interval time series into its fundamental oscillatory components. Very low frequency (VLF) oscillations were set between 0-0.04 Hz. High frequency (HF) was set between 0.15–0.40 Hz; low frequency variations (LF) were between 0.04-0.15 Hz. LF/HF ratio (LF/HF) was calculated to derive the sympatho-vagal balance.[19,20]

The time domain parameters of HRV consist of SDNN (Standard Deviation of Normal-to-Normal Intervals), RMSSD (Root Mean Square of Successive Differences) and pNN50 (Percentage of NN50), where, normal to normal interval (NN), is the time period between two consecutive heartbeats originating from the sinus node. SDNN (standard deviation of all NN intervals) offers a global measure of overall HRV, while pNN50 and RMSSD are specific markers of parasympathetic (vagal) activity.[19,20] These parameters are relevant for the long-term heart rate variability and were not considered in the current analysis.

The HRV recording from our subjects was analyzed automatically by Labchart's HRV 2.0 module. The frequency domain outcome parameters (HF, LF/HF) were obtained. The report of each patient was saved in a database.

Statistical analysis

Analysis was done by exporting the data to SPSS software version 25.0 (*IBM, Armonk, NY, USA*). Mean age and standard deviation were calculated. Normality assessment was done using visual assessment of the histogram. One-way ANOVA was used to compare the age differences of the three groups. Chi-square test was used to compare the gender profile between the three groups. Non-parametric tests were used for HF and LF/HF analysis as the data was non-normally distributed. Statistical significance for HF and LF/HF was analyzed using the Kruskal Wallis test. Analysis between the IBS subtypes was done using Mann Whitney U test. Rank biserial correlation was used as a measure of effect size. P values <0.05 were taken to be statistically significant.

Results

The study involved a total of 90 participants broken down into three groups namely, 30 controls, 30 IBS patients and 30 FD patients. Sub-groups within the IBS cohort included 19 participants with IBS-D and 11 with IBS-C. The mean age of the participants did not vary significantly between the groups (39.07±15.935 for controls, 41.57±15.476 for IBS and 41.17±11.341 for FD patients) (Table 1). There was no significant statistical difference in the gender profile between controls and FD patients although the IBS group had a greater proportion of males (Table 1).

Table 1. Age profile of the three groups

Group	Control	IBS	FD	p
Sample size	30	30	30	–
Mean age in years (SD)	39.07 (15.935)	41.57 (15.476)	41.17 (11.341)	0.771
Gender (Male/Female)	17/13	24/6	18/12	0.121

Heart rate of IBS patients was higher (78.78±16.44) and that of FD patients was lower (76.14±12.03) in comparison to controls (77.96±13.62) but the heart rate did not vary significantly between IBS, FD and controls. (Table 2).

The mean LF/HF value for IBS patients was 1.26±0.839 for IBS, 1.4±1.171 for FD and 1.6±1.196 for controls. HF values (in ms^2) were 733.9±1661.16 for IBS, 534.18±778.28 for FD and 674.87±1187.16 for controls. A comparison of HF and LF/HF values between the three groups using statistical tools showed no statistically significant difference (p=0.36) (Table 2).

Table 2. Heart rate and spectral domain measures of HRV*

Group	HR	HF (ms²)	LF/HF
IBS	78.79	733.9±1661	1.26±0.839
IBS-D subgroup	77.10	934.63±2043	0.98±0.69*
IBS-C subgroup	80.50	387.18±524.9	1.75±0.88
FD	76.14	534.18±778	1.4±1.171
Healthy controls	77.96	674.87±1187	1.6±1.196

* p=0.038 compared to controls, all other values – p>0.05 compared to controls

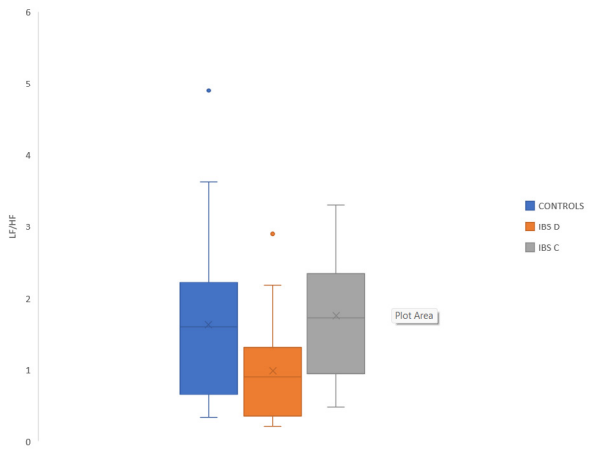

Fig. 1. Box-and-whisker plot showing distribution, outliers, and mean of the LF/HF values of IBS subtypes and controls

Figures 2 and 3 show representative HRV power spectrum plots and Poincaré plots of a healthy control and an IBS-D patient.

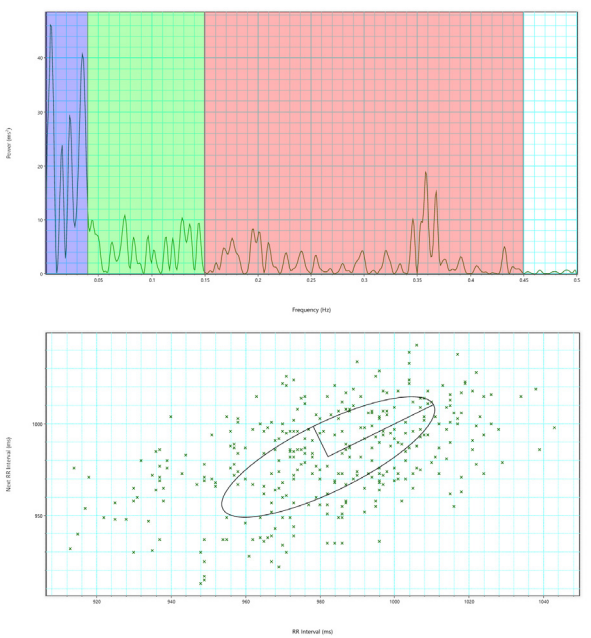

Fig. 2. HRV power spectrum plot of a healthy control with LF/HF of 0.7, corresponding Poincaré plot is shown

Subgroup analysis in the IBS group showed that the mean of the LF/HF values of the IBS-D group was the least (0.98±0.69), followed by controls (1.6±1.19), and IBS-C (1.75±0.88). The HF values (in ms²), on the other hand, were found to be least in the IBS-C (387.18±524.9) followed by controls (674.87±1187.16), and IBS-D (934.63±2043.71). A statistically significant difference was found (p=0.038) in the LF/HF values between IBS-D patients and healthy controls, with a moderate effect (rank-biserial correlation=0.353, 95% CI [0.035, 0.608]). On the other hand, there was no difference in the HF values between the 2 groups (p>0.05). IBS-C showed no difference in either parameter compared to controls (p>0.05) (Fig. 1 and Table 2).

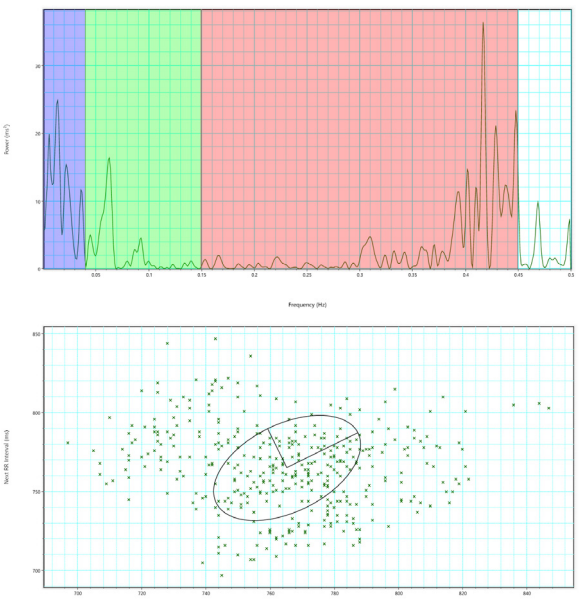

Fig. 3. HRV power spectrum of a patient with IBS-D with LF/HF of 0.26 showing high HF component and parasympathetic dominance (top), the corresponding Poincaré plot shows increased short-term variability with greater scattering of points

Discussion

Various studies have employed a wide array of tools, designs and parameters to assess autonomic function in patients. A lack of standardization exists, with studies using different methods for collecting data, taking varied lengths of readings, applying different software for analysis of HRV, and considering various outcome measures for physiological interpretation of results. In the current study, we have used short-term recording of HRV with ECG for recording. Short-term, 5-minute recording was chosen as it is convenient to replicate in clinical practice in the future and represents the dynamic relationship between the sympathetic and parasympathetic branches of the autonomic nervous system. The vagus nerve is inhibited on inspiration, and consequently, the heart rate increases. On expiration, the heart rate decreases due to relatively higher vagal tone. This con-

stant fluctuation results in respiratory sinus arrhythmia, which along with the baroreceptor reflex, contributes to short term HRV. [19] Only the frequency domain parameters were considered for analysis as they are deemed to be a better metric in the short-term recording.[19] Hence, we cannot compare time-domain parameters of other studies with our results.

HRV analysis showed no statistical difference between the parameters selected for analysis, namely, LF/HF and HF between each group - IBS, FD, and controls. Studies comparing IBS and controls have shown results similar to our study, where the HRV patterns did not differ significantly from controls.[16,21] These insignificant results in the IBS subgroup may have arisen as we combined patients of IBS-C and IBS-D under the same group. The opposing pathophysiological mechanisms in IBS-D and IBS-C may have contributed to the results being insignificant. Previous studies on IBS have emphasized on categorizing patients separately based on bowel patterns – evaluating IBS-D and IBS-C separately.[22] Another possible explanation for the insignificant results may be that changes in the autonomic nervous system (ANS) only in certain IBS patients, such as those who have suffered childhood trauma or life stressors. IBS is considered a heterogeneous disorder with different pathophysiological mechanisms leading to similar symptoms. Other studies demonstrated results divergent from our study and showed increased sympathetic dominance.[23-25]

In patients with FD, our results differed from previous research. Previous studies have hypothesized that delayed gastric emptying is due to reduced antral tone, which is affected by the vagus.[26] Studies have found a decreased vagal tone and sympathetic dominance in FD patients, indicated by increased LF/HF and decreased HF.[27, 28] It must be noted that these studies made use of the long-term method of HRV recording. Other studies showed a decreased vagal response after a meal only in patients with delayed gastric emptying.[29] Hence, our results, which showed no difference between FD and controls could be due to the accentuation of ANS abnormalities during meals in these patients.

Subgroup analysis of IBS showed that the LF/HF in IBS-D was significantly lower compared to controls. LF/HF values in IBS-C were higher compared to healthy controls but the difference was not found to be significant. As we already know, the parasympathetic nervous system increases colonic transit time and the sympathetic nervous system decreases gut motility. As LF/HF signifies sympatho-vagal balance, our results showing higher LF/HF in IBS-C and lower LF/HF in IBS-D compared to controls shows that there is a relative sympathetic dominance in IBS-C patients and a relative parasympathetic dominance in IBS-D patients. This could also possibly explain the diarrhea-predominant symptoms seen in IBS-D. This conclusion remains speculative considering the low sample size and cross-sectional design of our study. However, similar conclusions were drawn by a study assessing autonomic function using postural adjustment ratio and colon transit time in IBS subtypes by Aggarwal et al.[30] However, the authors did not include HRV analysis in their study. Jarrett et al.[31] on the other hand concluded that IBS-C patients diagnosed using ROME III had lower HF and significantly higher LF/HF than in controls. However, unlike our results, the IBS-D patients did not differ with controls. The authors used long-term HRV recordings for their analysis and this might have caused the conflicting results. Similar results were also obtained in a study confined to IBS-C patients diagnosed using the ROME III criteria where the authors found that LF/HF was higher and HF was lower in the IBS-C group in comparison to controls.[14] Hence, our study is the was able to find a difference in frequency-domain HRV parameters between IBS-D and controls. It is also important to note that the majority of the studies discussed above either used the long-term recording of HRV or used ROME III to diagnose patients. Our study differed from these studies by using the ROME IV criteria for diagnosis and the 5-minute recording of HRV. Additionally, our study provides one of the first IBS subtype-specific HRV comparisons within the Indian population.

Our study also showed that the HF band was higher in the IBS-D subtype and lower in the IBS-C subtype in comparison to controls, thus indicating higher vagal modulation in IBS-D and lower vagal activity in IBS-C. These results comply with the interpretation of our results for the LF/HF parameter in our study. This further suggests a higher parasympathetic modulation in IBS-D and higher sympathetic modulation in IBS-C. These results also suggest that sympathetic dominance in IBS-C could be due to vagal withdrawal instead of relative sympathetic dominance. Further, the parasympathetic dominance in IBS-D could be from vagal hyperactivity rather than sympathetic withdrawal.

Stress is thought to play a major role in initiating functional GI disease and patients also report a flare up of symptoms during periods of stress.[32, 33] Centers of the brain influencing stress might have an influence on the ANS. A review of case report forms of patients involved in our study showed presence of symptoms such as palpitations, fibromyalgia, and increased perspiration in many patients. These symptoms could further suggest the presence of autonomic imbalance in patients with functional GI disease.

Our findings have two significant clinical implications. Firstly, our findings show that patients with IBS-D and IBS-C differ in their autonomic profile using the short-term recording of HRV. This paves the way for the potential use of short-term HRV as a biomarker in IBS.

Secondly, our findings support the premise of augmenting the ANS for potential therapeutic benefit in IBS and FD. In fact, studies which have attempted to do so have already shown promising results. A study exploring the effect of taVNS (Transcutaneous Auricular Vagal Nerve Stimulation) in FD showed patients reported reduced symptoms of dyspepsia, decreased the scores of anxiety, depression, and improved gastric accommodation.[34] Another study on the therapeutic effect of auricular acupressure in IBS showed that participants had a lower frequency of diarrhea, abdominal pain and discomfort at the end of the trial.[35] Additionally, CBT and hypnosis are also being used as complementary treatment options for IBS and FD and likely work by increasing vagal tone.[36] Further studies are required on ANS abnormalities in FGIDs which would add to the understanding of the disease process and to the development of effective treatment strategies.

Study limitations

Our study has a few limitations. The major limitation of our study is the small sample size of the main (IBS, FD, HC) and subtype disease groups (IBS-D, IBS-C). It may have affected the strength and reliability of our results. The sample size may not have been sufficient to detect subtle differences in autonomic function in our patients. Additionally, the study's cross-sectional design limits the possibility to comment on causality and pathophysiological associations. This could have caused an error in HRV recordings by causing a bias in the HF values. We did not perform any autonomic testing additional to HRV to assess our subjects. Furthermore, we did not assess any changes prior to and following food intake. HRV analysis brings its own set of possibilities for errors. Gender could not be matched across the groups and might have changed our findings. Depression and anxiety levels/subclinical disease are also known to affect HRV results,[37] and were not taken into account, although patients with a known diagnosis of either of the two were excluded.

Conclusion

In conclusion, this study identified distinct autonomic patterns among IBS subtypes using short-term HRV analysis. Patients with IBS-diarrhea demonstrated significantly reduced LF/HF ratios, consistent with enhanced parasympathetic modulation, whereas IBS-constipation patients showed a trend toward higher LF/HF and lower HF values, suggesting relative sympathetic predominance. However, these differences were not statistically significant. No autonomic abnormalities were observed in patients with functional dyspepsia compared with healthy controls. Additionally, this study provides one of the first subtype-specific HRV comparisons within an Indian cohort using a standardized protocol, highlighting autonomic heterogeneity within IBS. Given the small sample size, particularly in the IBS-C subgroup, and the cross-sectional design, these findings should be interpreted cautiously. Larger, longitudinal studies are warranted to confirm these observations and to further explore whether autonomic modulation contributes to symptom expression or could serve as a therapeutic target in functional gastrointestinal disorders.

Declarations

Funding

No funding was received to conduct this study. The authors have no financial interests to disclose.

Author contributions

Conceptualization, L.D.; Methodology, L.D; Software, L.D.; Validation, L.D., P.K.S. and P.C.B.; Formal Analysis, L.D.; Investigation, L.D.; Resources, L.D.; Data Curation, L.D.; Writing – Original Draft Preparation, L.D. and P.K.S.; Writing – Review & Editing, L.D. and M.S.; Visualization, L.D. and M.S.; Supervision, P.C.B.; Project Administration, P.K.S. and P.C.B.

Conflicts of interests

The authors declare no competing interests.

Data availability

The datasets generated during and/or analysed during the current study are available from the corresponding author on reasonable request.

Ethics approval

The study was conducted in accordance with the Declaration of Helsinki, and the protocol was approved on 16/6/2023 by the BMCRI Institutional Ethics Committee, Bangalore Medical College and Research Institute, Bangalore (No: BMCRI/PS/85/2022-23).

References

1. Mearin F, Lacy BE, Chang L, et al. Bowel Disorders. *Gastroenterology*. 2016:S0016-5085(16)00222-5. doi:10.1053/j.gastro.2016.02.031
2. Lovell RM, Ford AC. Global prevalence of and risk factors for irritable bowel syndrome: a meta-analysis. *Clin Gastroenterol Hepatol*. 2012;10(7):712-721.e4. doi:10.1016/j.cgh.2012.02.029
3. Makharia GK, Verma AK, Amarchand R, et al. Prevalence of irritable bowel syndrome: a community-based study from northern India. *Neurogastroenterol Motil*. 2011;17(1):82-87. doi:10.5056/jnm.2011.17.1.82
4. Mahadeva S, Goh KL. Epidemiology of functional dyspepsia: a global perspective. *World J Gastroenterol.* 2006;12(17):2661-2666. doi:10.3748/wjg.v12.i17.2661
5. Mishima Y, Ishihara S. Enteric microbiota-mediated serotonergic signaling in pathogenesis of irritable bowel

syndrome. *Int J Mol Sci*. 2021;22(19):10235. doi:10.3390/ijms221910235
6. Chang L, Sundaresh S, Elliott J, et al. Dysregulation of the hypothalamic-pituitary-adrenal (HPA) axis in irritable bowel syndrome. *Neurogastroenterol Motil*. 2009;21(2):149-159. doi:10.1111/j.1365-2982.2008.01268.x
7. Kindt S, Tack J. Impaired gastric accommodation and its role in dyspepsia. *Gut*. 2006;55(12):1685-1691. doi:10.1136/gut.2006.098275
8. Park SY, Acosta A, Camilleri M, et al. Gastric motor dysfunction in patients with functional gastroduodenal symptoms. *Am J Gastroenterol*. 2017;112(11):1689-1699. doi:10.1038/ajg.2017.144
9. Qin HY, Cheng CW, Tang XD, Bian ZX. Impact of psychological stress on irritable bowel syndrome. *World J Gastroenterol.* 2014;20(39):14126-14131. doi:10.3748/wjg.v20.i39.14126
10. Van Oudenhove L, Aziz Q. The role of psychosocial factors and psychiatric disorders in functional dyspepsia. *Nat Rev Gastroenterol Hepatol*. 2013;10(3):158-167. doi:10.1038/nrgastro.2013.2
11. Black CJ, Ford AC. Global burden of irritable bowel syndrome: trends, predictions and risk factors. *Nat Rev Gastroenterol Hepatol*. 2020;17(8):473-486. doi:10.1038/s41575-020-0290-3
12. Vanderlei LC, Pastre CM, Hoshi RA, Carvalho TD, Godoy MF. Basic notions of heart rate variability and its clinical applicability. *Rev Bras Cir Cardiovasc*. 2009;24(2):205-217. doi:10.1590/s0102-76382009000200013
13. Sessa F, Anna V, Messina G, et al. Heart rate variability as predictive factor for sudden cardiac death. *Aging (Albany NY).* 2018;10(2):166-177. doi:10.18632/aging.101369
14. Mazur M, Furgała A, Jabłoński K, Mach T, Thor P. Autonomic nervous system activity in constipation--predominant irritable bowel syndrome patients. *Med Sci Monit*. 2012;18(8):CR493-CR499. doi:10.12659/MSM.883525
15. Chua AS. Prevalence of irritable bowel syndrome in northern India. *Neurogastroenterol Motil*. 2011;17(1):6-8. doi:10.5056/jnm.2011.17.1.6
16. Manabe N, Tanaka T, Hata J, Kusunoki H, Haruma K. Pathophysiology underlying irritable bowel syndrome—from the viewpoint of dysfunction of autonomic nervous system activity. *J Smooth Muscle Res.* 2009;45(1):15-23. doi:10.1540/jsmr.45.15
17. The Rome Foundation. Rome IV criteria. Available at: https://theromefoundation.org/rome-iv/rome-iv-criteria/. Accessed August 15, 2023.
18. O'Donnell LJ, Virjee J, Heaton KW. Detection of pseudodiarrhea by simple clinical assessment of intestinal transit rate. *BMJ*. 1990;300(6722):439-440. doi:10.1136/bmj.300.6722.439
19. Shaffer F, Ginsberg JP. An overview of heart rate variability metrics and norms. Front Public Health. 2017;5:258. doi:10.3389/fpubh.2017.00258
20. Shaffer F, McCraty R, Zerr CL. A healthy heart is not a metronome: an integrative review of the heart's anatomy and heart rate variability. *Front Psychol*. 2014;5:1040. doi:10.3389/fpsyg.2014.01040
21. Cheng P, Shih W, Alberto M, et al. Autonomic response to a visceral stressor is dysregulated in irritable bowel syndrome and correlates with duration of disease. *Neurogastroenterol Motil.* 2013;25(10):e650-e659. doi:10.1111/nmo.12177
22. Park HJ. Heart rate variability as a measure of disease state in irritable bowel syndrome. Asian Nurs Res (Korean Soc Nurs Sci). 2008;2(1):5-16. doi:10.1016/S1976-1317(08)60024-0
23. Mazur M, Furgała A, Jabłoński K, et al. Dysfunction of the autonomic nervous system activity is responsible for gastric myoelectric disturbances in irritable bowel syndrome patients. *J Physiol Pharmacol*. 2007;58(3):131-139.
24. Karling P, Nyhlin H, Wiklund U, et al. Spectral analysis of heart rate variability in patients with irritable bowel syndrome. *Scand J Gastroenterol.* 1998;33(6):572-576. doi:10.1080/00365529850171800
25. Pellissier S, Dantzer C, Canini F, et al. Psychological adjustment and autonomic disturbances in inflammatory bowel diseases and irritable bowel syndrome. *Psychoneuroendocrinology.* 2010;35(5):653-662. doi:10.1016/j.psyneuen.2009.10.004
26. Hausken T, Svebak S, Wilhelmsen I, et al. Low vagal tone and antral dysmotility in patients with functional dyspepsia. *Psychosom Med.* 1993;55(1):12-22. doi:10.1097/00006842-199301000-00003
27. Tominaga K, Fujikawa Y, Tsumoto C, et al. Disorder of autonomic nervous system and its vulnerability to external stimulation in functional dyspepsia. *J Clin Biochem Nutr.* 2016;58(2):161-165. doi:10.3164/jcbn.15-140
28. Lorena SL, Figueiredo MJ, Almeida JR, Mesquita MA. Autonomic function in patients with functional dyspepsia assessed by 24-hour heart rate variability. *Dig Dis Sci*. 2002;47(1):27-31. doi:10.1023/A:1013246900041
29. Guo WJ, Yao SK, Zhang YL, et al. Impaired vagal activity to meal in patients with functional dyspepsia and delayed gastric emptying. *J Int Med Res.* 2018;46(2):792-801. doi:10.1177/0305735617734958
30. Aggarwal A, Cutts TF, Abell TL, et al. Predominant symptoms in irritable bowel syndrome correlate with specific autonomic nervous system abnormalities. *Gastroenterology.* 1994;106(4):945-950. doi:10.1016/0016-5085(94)90850-0
31. Jarrett ME, Han CJ, Cain KC, et al. Relationships of abdominal pain, reports to visceral and temperature pain sensitivity, conditioned pain modulation, and heart rate variability in irritable bowel syndrome. *Neurogastroenterol Motil.* 2016;28(7):1094-1103. doi:10.1111/nmo.12812
32. Chey WY, Jin HO, Lee MH, et al. Colonic motility abnormality in patients with irritable bowel syndrome exhibiting abdominal pain and diarrhea. *Am J Ga-*

stroenterol. 2001;96(5):1499-1506. doi:10.1111/j.1572--0241.2001.03715.x

33. Mustafa Y. When the gut speaks: the hidden toll of irritable bowel syndrome on body and mind. *Gastroenterology & Endoscopy*. 2025;3:135-151. doi:10.1016/j.gande.2025.05.002
34. Zhu Y, Xu F, Lu D, et al. Transcutaneous auricular vagal nerve stimulation improves functional dyspepsia by enhancing vagal efferent activity. *Am J Physiol Gastrointest Liver Physiol*. 2021;320(5):G700-G711. doi:10.1152/ajpgi.00238.2020
35. Go GY, Park H. Effects of auricular acupressure on women with irritable bowel syndrome. *Gastroenterol Nurs.* 2020;43(2):E24-E34. doi:10.1097/SGA.0000000000000397
36. Lucini D, Malacarne M, Solaro N, et al. Complementary medicine for the management of chronic stress: superiority of active versus passive techniques. *J Hypertens*. 2009;27(12):2421-2428. doi:10.1097/HJH.0b013e328331fa80
37. Hamilton JL, Alloy LB. Atypical reactivity of heart rate variability to stress and depression across development: systematic review of the literature and directions for future research. *Clin Psychol Rev*. 2016;50:67-79. doi:10.1016/j.cpr.2016.09.003

Rzeszów University Press 2026
ISSN 2544-1361 (online)
doi: 10.15584/ejcem.2026.1.18

http://www.ejcem.ur.edu.pl
European Journal of Clinical and Experimental Medicine
Eur J Clin Exp Med 2026; 24 (1): 104–111

ORIGINAL PAPER

Histochemical evaluation of ethanol extracts of *Senecio biafrae* leaves in mercury chloride-induced hepatic injury in adult male Wistar rats

Anthony Oluwasesan Ibitoye [1,2], David Olawale Adeyemi [1]

[1] Department of Anatomy and Cell Biology, Faculty of Basic Medical Sciences, Obafemi Awolowo University, Ile-Ife, Nigeria
[2] Department of Nursing Science, Kings University, Ode Omu, Osun State, Nigeria

ABSTRACT

Introduction and aim. Mercury chloride is a potent hepatotoxin that disrupts liver architecture, glucose metabolism, and nuclear integrity. To our knowledge, no previous study has evaluated the histochemical effects of the ethanol extract of *Senecio biafrae* leaves (EESBL) on mercury chloride-induced hepatic injury. This study presents new evidence for the glycogen stabilizing and genoprotective properties of its compounds.

Material and methods. Forty-nine adult Wistar rats were randomly assigned to seven groups (n=7 per group). Except for the control, all received 4 mg/kg mercury chloride orally for 21 days. Group II rats were sacrificed immediately after exposure, while group III underwent a 21-day recovery. Group IV received 2 mg/kg silymarin, and also Groups V–VII received 200, 400, and 600 mg/kg EESBL, respectively, for 21 days. Liver tissues were harvested for histochemical evaluation using periodic acid-Schiff (PAS) and Feulgen staining.

Results. Mercury chloride significantly depleted liver glycogen stores (PAS-positive area: control 75.00±0.56% vs toxic 20.00±1.09%). EESBL restored glycogen storage in a dose-dependent manner (200 mg/kg: 52.02±0.56%; 400 mg/kg: 60.00±0.57%; 600 mg/kg: 72.06±0.57%), approaching silymarin (68.00±0.57%). Nuclear DNA integrity was markedly affected by $HgCl_2$ (Feulgen-positive area: control 16.20±0.19% vs toxic 9.00±0.33%). EESBL improved nuclear morphology and DNA intensity (200 mg/kg: 11.11±0.12%; 400 mg/kg: 13.20±0.44%; 600 mg/kg: 14.06±0.33%), comparable to silymarin (14.00±0.25%) (all $p<0.001$).

Conclusion. EESBL demonstrated protective effects against mercury chloride-induced hepatotoxicity by stabilizing hepatic glycogen metabolism and nuclear structure, underscoring its therapeutic potential in mitigating heavy metal-induced liver injury.

Keywords. DNA integrity, Feulgen staining, glycogen storage, hepatic injury, mercury chloride, PAS reaction

Introduction

Mercury chloride ($HgCl_2$), a highly toxic inorganic compound, is commonly encountered through environmental and occupational sources such as mining, industrial effluents, battery manufacturing and pharmaceutical waste disposal.[1,2] Exposure in humans and animals occurs primarily through the consumption of tainted food or water, breathing in airborne contaminants, or contact with the skin. Once absorbed, mercury ions bind to sulfhydryl groups in proteins and also accumulate in vital organs, particularly the liver and kidneys.[3,4] In the liver, mercury disrupts key cellu-

Corresponding author: Anthony Oluwasesan Ibitoye, e-mail: ao.ibitoye@kingsuniversity.edu.ng

Received: 29.06.2025 / Revised: 30.09.2025 / Accepted: 28.10.2025 / Published: 30.03.2026

Ibitoye AO, Adeyemi DO. Histochemical evaluation of ethanol extracts of *Senecio biafrae* leaves in mercury chloride-induced hepatic injury in adult male Wistar rats. *Eur J Clin Exp Med.* 2026;24(1):104–111. doi: 10.15584/ejcem.2026.1.18.

lar processes, including glucose metabolism and DNA stability.[5,6] The liver is essential for metabolic control, encompassing glycogen storage, detoxification, and maintenance of genomic integrity.[7,8] Its highly organized architecture rich in hepatocytes and a structured extracellular matrix (ECM) supports these vital physiological functions. As the primary site for glycogen synthesis and storage, the liver maintains the systemic energy balance.[7-9] Furthermore, the nucleus safeguards genetic material, making DNA integrity essential for liver regeneration and function.[10]

Mercury chloride doses in rodent models are typically classified as low, moderate, or high based on toxicological and experimental data. Low doses (1 mg/kg/day) mimic chronic environmental exposure and generally result in mild biochemical or histological changes without overt tissue damage.[11] Moderate doses (2–7 mg/kg) are associated with oxidative stress, DNA damage, and mild to moderate liver or renal lesions.[12] High doses (7 mg / kg) induce acute toxicity, characterized by hepatocellular necrosis, nuclear condensation, and widespread tissue degeneration.[13] These dose classifications are critical to modeling human exposure and evaluating the efficacy of therapeutic interventions.

To evaluate alterations in liver tissue, histochemical staining techniques offer a precise visualization of intracellular biochemical changes at the microscopic level.[14] The periodic acid-Schiff reaction (PAS) detects glycogen deposits, while the Feulgen reaction identifies nuclear DNA, providing sensitive markers of cytoplasmic and nuclear integrity, respectively. Together, these staining methods enable a comprehensive histochemical assessment of hepatocyte injury and recovery in experimental models of hepatotoxicity.[15]

In the search for safe and effective interventions, the therapeutic value of medicinal plants has drawn interest in mitigating toxicant-induced tissue damage.[16,17] *Senecio biafrae*, a leafy vegetable widely consumed in West Africa (including Nigeria, Benin and Ghana), is traditionally valued for its nutritional and therapeutic properties.[18] Phytochemical studies have identified flavonoids, phenolics, alkaloids, saponins, tannins, and vitamins as key bioactive constituents of *S. biafrae*.[19] These substances are recognized for their anti-inflammatory, antioxidant, and also cytoprotective activities. However, the specific effects of these constituents on liver histoarchitecture after mercury chloride-induced hepatotoxicity remain largely underexplored.

Aim

This study aims to investigate the histochemical effects of the ethanol extract of *S. biafrae* leaves (EESBL) on mercury-chloride-induced hepatic injury, specifically its ability to restore glycogen reserves and maintain nuclear DNA integrity. To our knowledge, this is the first study to provide histochemical evidence of the protective effects of *S. biafrae* on mercury-induced alterations in hepatic metabolism and nuclear architecture.

Material and methods

Chemicals and drugs

Mercury chloride (white crystalline form; British Drug Houses Ltd., Poole, England) was used as a hepatotoxic agent. Silymarin tablets (Silybon-70® 70 mg; Micro Labs Ltd., India) served as the reference hepatoprotective agent. Diethyl ether (≥ 99.8%; British Drug Houses Ltd., Poole, England) was utilized for anesthesia.

Gathering and authentication of plant materials

For this investigation, green *Senecio biafrae* leaves were collected and authenticated at Obafemi Awolowo University's Department of Botany in Ile-Ife. For future use, a sample from the voucher (IFE/18215) was placed in the departmental herbarium.

The preparation of ethanol extract of Senecio biafrae leaf

The collected leaves were air dried, pulverized, and extracted three times with 80% ethanol at standard temperature under continuous magnetic stirring every 24 hours. The combined extracts were filtered using Whatman No. 1 filter paper, condensed in a low pressure rotary evaporator and then lyophilized. Before being used, the drained extract was kept in a drying device.[20]

Experimental animals

The Animal Holding, College of Health Sciences, Obafemi Awolowo University, Ile-Ife, provided 49 adult male Wistar rats weighing between 180 and 200 grams. The animals were kept in conventional laboratory settings (12 hours light/dark cycle, temperature, and relative humidity) with unlimited access to clean water and standard rat food (Ace Feeds, Osogbo, Nigeria). The Institute of Public Health, Obafemi Awolowo University, Ile-Ife's Health Research and Ethics Committee (HREC) granted ethical approval (IPH/OAU/12/2543). In accordance with the National Institutes of Health's Guide for the Care and Use of Laboratory Animals, the rats were treated humanely.[21]

Experimental design

Animals were randomly assigned to seven groups (n=7 per group)

- Group I (Control): Distilled water (2 mL/kg, through oral) for 42 days.
- Group II (Toxic control): Mercury chloride (4 mg/kg/day, orally) for 21 days; sacrificed 24 h after the last dose.
- Group III (Recovery): Mercury chloride (4 mg/kg/day, orally) for 21 days; observed without treatment for another 21 days.

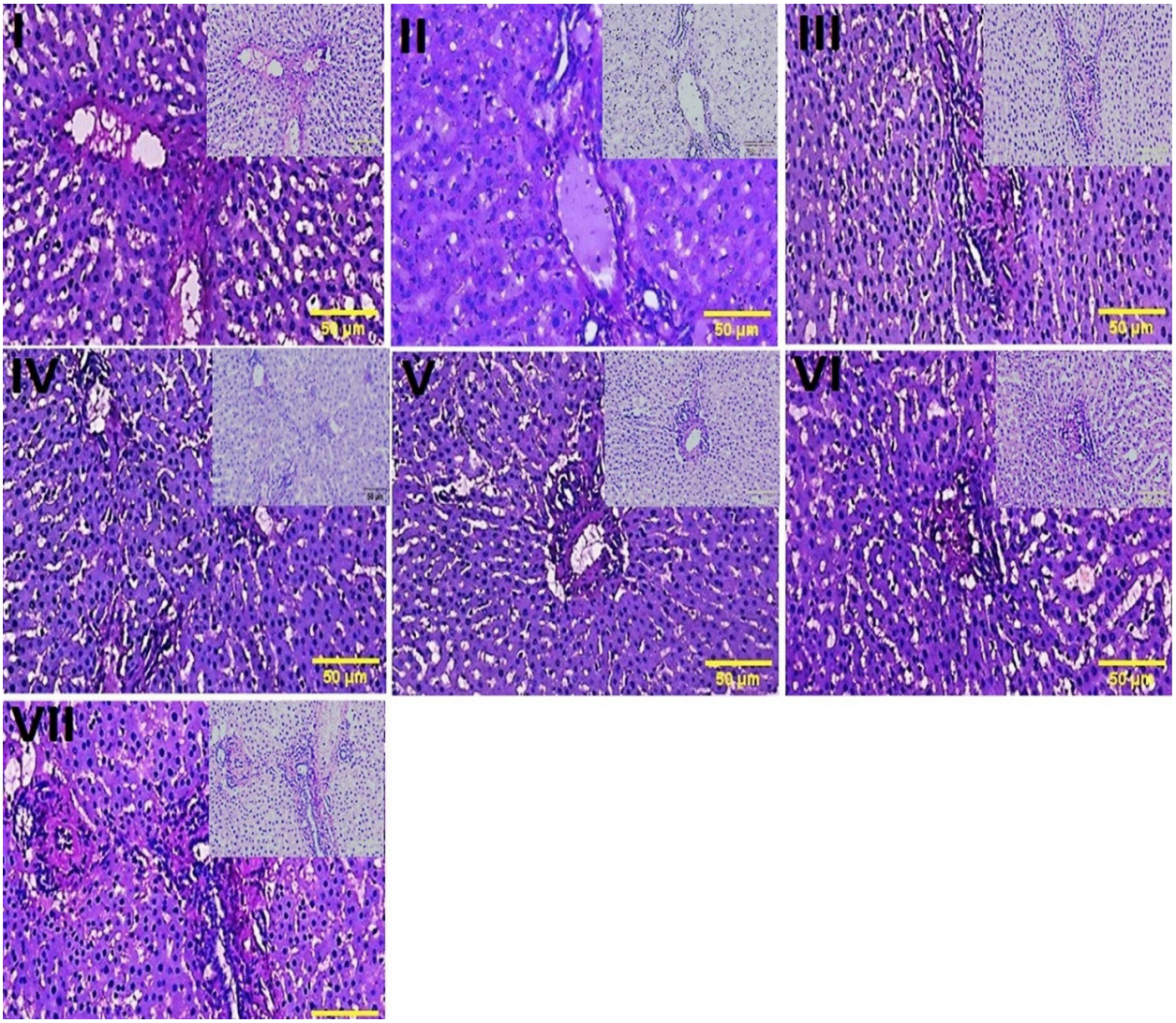

Fig. 1. Representative microscopy images of PAS-stained liver sections, I: Diffuse, severe PAS signal staining with uniform distribution throughout the lobule (normal glycogen storage), II: Markedly reduced PAS positivity with an irregular staining pattern, III, V: Partial restoration of PAS reactivity with improved, yet nonuniform staining, IV, VI, VII: Moderate PAS positivity indicates restored glycogen accumulation in hepatocytes. Insets: Diastase-digested sections serving as negative control (scale bar=50 µm)

- Group IV (Standard treatment): Mercury chloride (4 mg/kg/day, orally) for 21 days; followed by silymarin (2 mg/kg, orally 12-hourly) for 21 days.
- Group V-VII (Test treatment): Mercury chloride (4 mg/kg/day, orally) for 21 days; followed by ethanol extract of EESBL at 200, 400, and 600 mg/kg/day, respectively, for 21 days.

Tissue collection and processing

All rats were sacrificed under diethyl ether anesthesia twenty-four hours after the last treatment. The entire liver was excised and weighed and the median lobe was harvested uniformly from all animals to eliminate lobe-specific variability in response to toxic insult.[22]

Histochemical procedure

10% neutral buffered formalin (NBF) was used to fix liver samples by total immersion for 48 hours for the histochemical demonstration of glycogen and DNA. The Drury and Wallington paraffin wax embedding technique was used to process tissues for light microscopic examination.[23]

Process for periodic acid-Schiff (PAS) Staining

The PAS reaction was used for the demonstration of (carbohydrate) glycogen deposition. Deparaffinized tissue sections were rehydrated through descending alcohol concentrations and then treated with a 1% aqueous periodic acid solution for 10 minutes; This oxidation step creates aldehyde groups from tissue carbohydrates, which then react with Schiff reagent for 30 minutes,

turning the tissue sections a light pink color. After being washed in lukewarm water, the sections darken to vibrant pink. In contrast, the tissue was counterstained with Harris hematoxylin, turning the nuclei blue. The glycogen and other carbohydrates are stained with magenta, allowing their identification in the tissue. In PAS with diastase digestion (PAS-D), tissue sections were pretreated with amylase enzyme to digest glycogen, leaving only other carbohydrate deposits visible, helping to identify glycogen content.[23, 24]

Feulgen staining procedure

The Feulgen reaction was used to demonstrate the contents of deoxyribonucleic acid (DNA) contents. The procedure was carried out as described by Feulgen and Rossenbeck (1924).[23] This method relies on the acid hydrolysis of DNA to expose aldehydes on deoxyribose sugar, which are then detected by Schiff's reagent. Deparaffinized tissues were rehydrated in descending concentrations of alcohol for 2 minutes each, followed by mild hydrolysis in prewarmed 1N hydrochloric acid at 60°C for 8 minutes. After rinsing, Schiff's reagent was applied for 1.5 hours, which binds to exposed aldehydes, resulting in a magenta color. The sections are then treated with sulfurous acid and washed with running water before being counterstained with light green for contrast. DNA is stained magenta, while the cytoplasm is stained green. At the same time, as the test sections were hydrolyzed, the control sections were also left in distilled water for the same time for hydrolysis. Both the test and control sections go through the same procedure and process. The control section was negative, showing no trace of magenta coloration, confirming the specificity of the reaction.[23,25]

Photomicrography and image analysis

Permanent pictures of stained sections were captured using a LEICA research microscope (DM750) attached to a digital photography device (LEICA ICC50). On every micrograph, the scale bars were combined. Using a computer that runs image analysis software (ImageJ® NIH, US) according to the manufacturer's instructions, PAS and Feulgen stained micrographs were measured for staining intensity and nuclear damage using the approach described by Amber.[26] To analyze particular regions of the micrographs, ImageJ® region of interest (ROI) management tool was used. After obtaining average gray values for each of the three ROI, the means were calculated and examined.

Statistical analysis

GraphPad Prism (version 9.3, GraphPad Software, San Diego, CA, USA) was used to analyze the data, and the results were presented as mean±standard error of the mean (SEM). One-way analysis of variance (ANOVA) with the Tukey post hoc test was used to evaluate whether there were significant differences between the means of the group. A 0.05 alpha threshold was considered significant.

Results

Effect of ethanol extract of S. biafrae leaves on hepatic glycogen

As depicted in Figure 1, a photomicrograph of liver sections subjected to PAS staining revealed that group I rats showed normal glycogen storage within the cytoplasm of their hepatocytes, evident by the intense and diffuse PAS staining, while in group II rats, mercury chloride caused abnormal glycogen storage, exhibited by a marked reduction in PAS positivity, reflecting glycogen depletion. However, EESBL-treated groups (V-VII) showed dose-dependent restoration of PAS staining, demonstrated by the consistent glycogen storage, with the 600 mg/kg dose showing near-normal glycogen distribution. This was comparable to the silymarin-administered rats, which had considerable glycogen reserves. The digested region of the glycogen store was disclosed by diastase control among the set (Insets, Fig. 1).

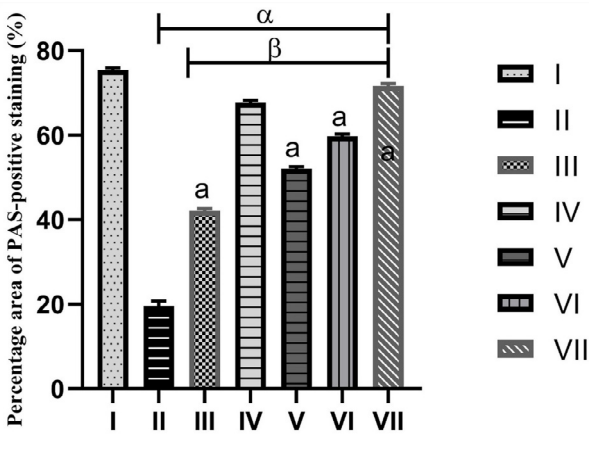

Fig. 2. Percentage area of PAS-positive staining for glycogen granules of the liver of adult Wistar rats exposed to $HgCl_2$ toxicity. Each bar represents Mean±SEM. The bars with superscript (α) are significantly different from I; the groups with alphabet (a) are significantly different from IV, however, the bars with superscript (β) are significantly different from II, using one-way ANOVA, Tukey test at $p<0.05$

Glycogen store morphometry

As shown in Figure 2, the percentage area of PAS-positive staining within the Region of Interest (ROI) in the seven experimental groups. Group I rats showed high PAS positivity (75.00±0.56), which indicates abundant glycogen stores compared with group II rats with very low PAS positivity (20.00±1.09) due to glycogen depletion caused by mercury chloride. There is a partial resto-

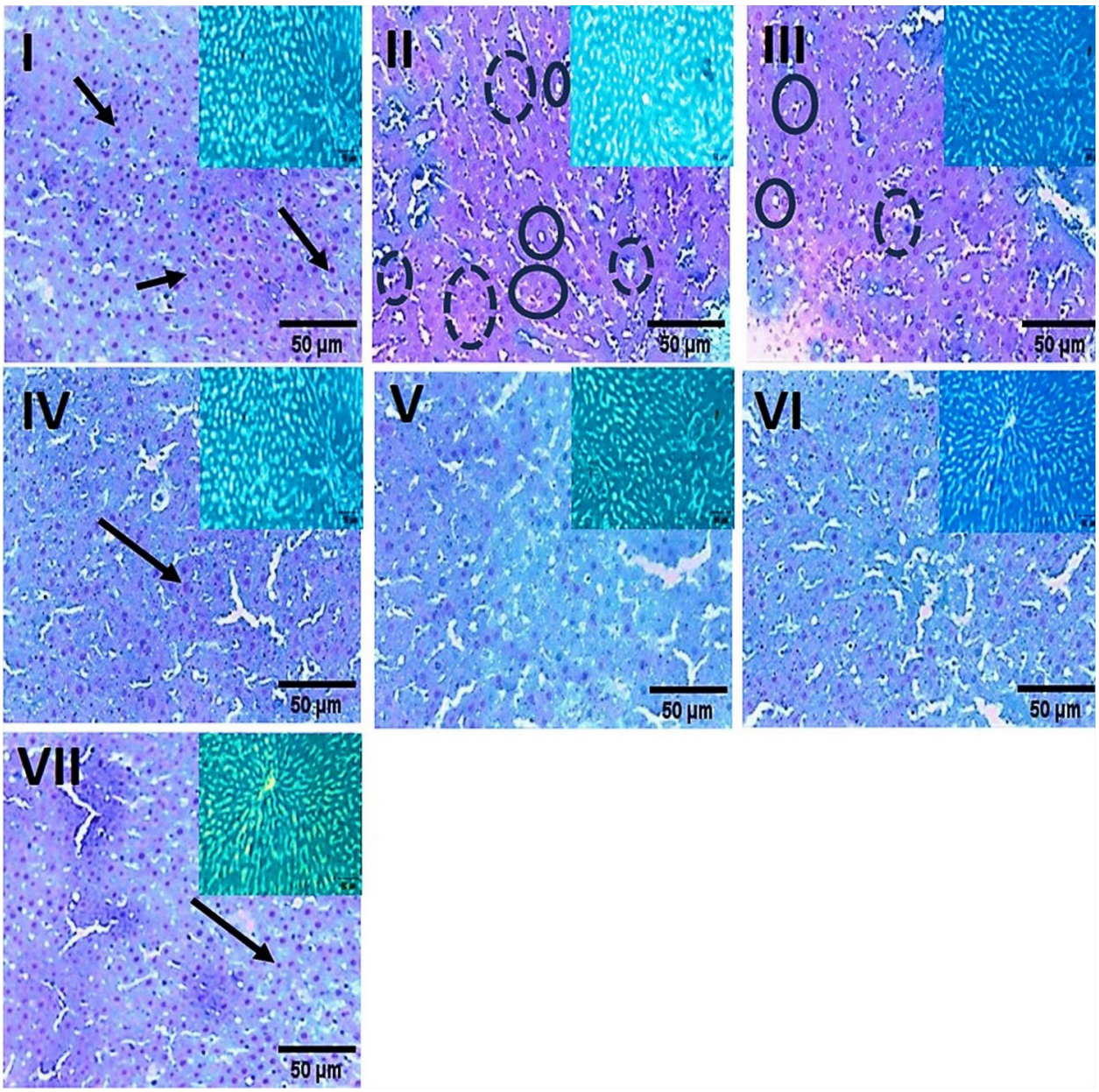

Fig. 3. Representative photomicrographs of liver sections stained with the Feulgen reaction for DNA, I: uniform magenta staining of nuclei, with regular nuclear size, shape, and even chromatin distribution (normal), II: Irregular nuclear morphology, chromatin fading (rounded circles), and fragmentation (dotted circles); prominent pyknosis, III, V: Reduced chromatin condensation, fewer pyknotic nuclei, and improved nuclear morphology, IV, VI, VII: Moderately restored nuclear features with reduced chromatin condensation. Insets: Unhydrolyzed sections showing the absence of DNA-specific staining (scale bar=50 µm)

ration of glycogen stores in group III rats (42.10±0.57), in contrast to the control group and the treatment groups. Silymarin-treated group IV rats displayed near-normal glycogen stores (68.00±0.57) in contrast to EESBL-treated rats and group I rats. EESBL-treated rats (groups V-VII) dose-dependently restored glycogen stores (52.02±0.56, 60.00±0.57, 72.06±0.57, respectively) compared with group II rats (20.00±1.09). 200 and 400 mg/kg EESBL showed moderate recovery of glycogen stores, in contrast to the control group, although 600 mg/kg EESBL almost matched the control group ($F=833.00$; $p<0.001$).

Effect of the ethanol extract of S. biafrae leaves on hepatic nuclear DNA

Photomicrograph Representative sections of liver exposed to Feulgen staining, as shown in Figure 3, revealed the following observations: group I rats exhibited well-defined Hepatocyte nucleoplasm has euchromatic nuclei with unique nuclear DNA, while mercury chloride caused DNA fragmentation and lightly stained nuclei, chromatin condensation, and pleomorphism, indicating DNA degradation as observed in group II rats. Groups III and V rats showed reduced chromatin condensation, improved nuclear morphology, and few-

er pyknotic nuclei. However, EESBL treatment markedly restored nuclear DNA staining, especially in the 400 600 mg/kg groups, preserving nuclear morphology similar to that of the silymarin-treated group IV rats. Unhydrolyzed sections (control) showed no specific nuclear staining (Insets, Fig. 3).

Nuclear DNA morphometry

As shown in Figure 4, the percentage area of Feulgen stained nuclear DNA in the seven experimental groups revealed that mercury chloride significantly distorts nuclear morphology, indicating nuclear damage and DNA loss in group II rats (9.00±0.33) when compared to group I rats (16.20±0.19), which revealed intact nuclear DNA and normal nuclear morphology. There is a slight improvement in group III rats (11.00±0.31) when compared to group II rats, which suggests partial spontaneous recovery, but is still insufficient to restore DNA integrity. However, EESBL demonstrated a dose-dependent improvement in the restoration of nuclear DNA integrity, evident by a significant increase ($p < 0.001$) in the nuclear DNA in rats given EESBL (11.11±0.12, 13.20±0.44, 14.06±0.33, respectively) compared with group II rats (9.00±0.33). Silymarin-treated group IV rats had a substantial rise in area covered by nuclear DNA (14.00±0.25) when contrasted with the toxic group (9.00±0.33); this is comparable to 600 mg/kg EESBL (group VII), suggesting that there is an increased restorative effect at a higher dose of EESBL comparable to the control group ($F=55.36$; $p<0.001$).

Discussion

Mercury-induced hepatotoxicity remains a major toxicological concern due to its deleterious effects on hepatic nuclear integrity and metabolic regulation. The liver, as a vital organ in detoxification and glucose homeostasis, is highly susceptible to $HgCl_2$ toxicity. In this study, $HgCl_2$ exposure resulted in marked hepatic glycogen depletion and nuclear damage, evidenced by reduced PAS and Feulgen staining. These findings align with the established role in inducing oxidative stress, altering glycogen metabolism, and promoting DNA strand breaks.[2,3] Under normal physiology, the liver stores glycogen postprandially and mobilizes it during fasting via glycogenesis and glycogenolysis.[27,28] Mercury disrupts this balance by inhibiting key enzymes such as glycogen synthase, glucose-6-phosphatase, and phosphoenolpyruvate carboxykinase (PEPCK), leading to hypoglycemia and energy deficits.[29,30] Cytologically, this manifests as reduced PAS positive hepatocytes and cytoarchitectural disarray. This finding aligns with a study of Mohamed et al.[31] who observed weakened PAS reactions in rats treated with $HgCl_2$, confirming the toxic impact of mercury on liver glycogen stores. In particular, the administration of the EESBL ethanol extract at 400 and 600 mg/kg preserved glycogen stores, restored PAS reactivity, and maintained hepatocyte structure, comparable to silymarin treatment. This cytoprotective effect is likely due to the antioxidative and enzyme-stabilizing properties of EESBL.

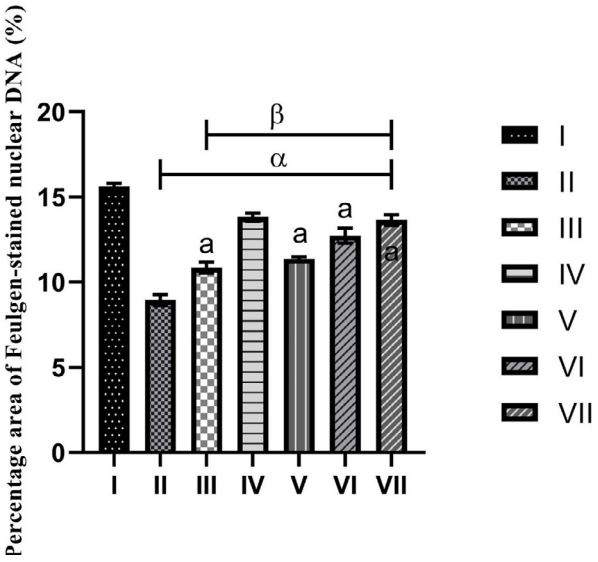

Fig. 4. Percentage area of Feulgen stained by nuclear DNA of adult Wistar rats exposed to $HgCl_2$ toxicity. Every line shows the mean±SEM the bars with superscript (α) are noticeably distinct from I; the groups with alphabet (a) are substantially different from IV, however, the bars with By one-way ANOVA and the Tukey test at $p<0.05$, superscripts (β) are substantially distinct from II

Similarly, mercury-induced genotoxicity, marked by chromatin condensation, pyknotic nuclei, nuclear fragmentation, and nucleolar disruption, was improved in EESBL-treated groups, which showed improved Feulgen staining and fewer nuclear abnormalities. Mercury chloride-induced oxidative stress is known to trigger DNA fragmentation and suppress DNA repair pathways,[32] including base and nucleotide excision repair.[33,34] Beyond direct DNA damage, mercury chloride impairs the cellular capacity for DNA repair.[34] Its exposure has been shown to downregulate the expression of critical repair base excision enzymes are among the DNA healing enzymes, and also nucleotide excision repair pathways.[35,36] The observed nuclear restoration suggests EESBL mitigates genomic instability and promotes hepatocellular regeneration in a dose-dependent manner comparable to the Silymarin-treated group. By eliminating free radicals, chelating mercury ions, and boosting antioxidant enzymes, phytochemicals in EESBL, especially flavonoids, may prevent mercury toxicity and maintain nuclear integrity and the breakdown of glycogen.

This research shows, for the first time, the histochemical evidence of *S. biafrae's* cytoprotective, hepato-

protective, and genoprotective effects in $HgCl_2$-induced toxicity, reinforcing its therapeutic potential beyond traditional antioxidant models.

Conclusion

Histochemical analyzes using PAS and Feulgen staining, in this study, have provided compelling evidence of the metabolic and nuclear disturbances caused by mercury chloride in the liver. These findings highlight the potential effect of the ethanol extract of *S. biafrae* leaves on stabilizing hepatic metabolic and nuclear architecture, reinforcing its relevance in mitigating mercury chloride-induced disruptions in liver structure and function.

Further studies should investigate the molecular pathways through which EESBL exerts its effect, particularly its influence on Nrf2/ARE signaling, mitochondrial biogenesis, apoptosis regulation (eg, Bcl-2, Bax, Caspase-3), and DNA repair gene expression, to elucidate its mechanisms at transcriptional and proteomic levels.

Acknowledgements

The authors thank Mr. M.S. Ige of Obafemi Awolowo University, Department of Anatomy and Cell Biology, for his technical help in preparing the histochemical slides.

Declarations

Funding

No particular grant from governmental, private, or charity funding organizations was obtained for this study.

Author contributions

Conceptualization, A.O.I. and D.O.A.; Methodology, A.O.I. and D.O.A.; Software, A.O.I.; Validation, D.O.A.; Investigation, A.O.I.; Writing – Original Draft Preparation, A.O.I.; Writing – Review & Editing, A.O.I. and D.O.A.; Visualization, D.O.A.; Supervision, D.O.A.

Conflicts of interest

No competing goals are disclosed by the writers.

Data availability

The appropriate author can provide the datasets created and examined for this study upon adequate request.

Ethics approval

The Health Research and Ethics Committee of the Institute of Public Health at Obafemi Awolowo University in Ile-Ife granted ethical approval (IPH/OAU/12/2543). The National Institutes of Health's Guide for the Care and Use of Laboratory Animals was followed in providing rats with proper care.

References

1. Agency for Toxic Substances and Diseases Registry (ATSDR). Toxicological Profile for Mercury. *Atlanta, GA: U.S. Department of Health and Human Services*; 2022. https://www.atsdr.cdc.gov/toxprofiles/tp46.pdf.
2. Ruggieri F, Majorani C, Domanico F, Alimonti A. Mercury in children: current state on exposure through human biomonitoring studies. *Int J Environ Res Public Health*. 2017;14(5):519. doi:10.3390/ijerph14050519
3. Clarkson TW, Magos L. The toxicology of mercury and its chemical compounds. *Crit Rev Toxicol.* 2006;36(8):609-662. doi:10.1080/10408440600845619
4. Balali-Mood M, Naseri K, Tahergorabi Z, Khazdair MR, Sadeghi M. Toxic mechanisms of five heavy metals: mercury, lead, chromium, cadmium, and arsenic. *Front Pharmacol*. 2021;12:643972. doi: 10.3389/fphar.2021.643972
5. Crespo-López ME, Macêdo GL, Pereira SI, et al. Mercury and human genotoxicity: critical considerations and possible molecular mechanisms. *Pharmacol Res*. 2009;60(4):212-220. doi:10.1016/j.phrs.2009.02.011
6. Maqbool F, Bahadar H, Hassani S, et al. Biochemical evidence on the potential role of methyl mercury in hepatic glucose metabolism through inflammatory signaling and free radical pathways. *J Cell Biochem*. 2019;120(9):16195-16205. doi:10.1002/jcb.28899
7. Liu X, Wang H, Liang X, Roberts MS. Hepatic metabolism in liver health and disease. In: *Liver Pathophysiology*. Academic Press; 2017:391-400. doi:10.1016/B978-0-12-804274-8.00030-8
8. Kanungo S, Wells K, Tribett T, El-Gharbawy A. Glycogen metabolism and glycogen storage disorders. *Ann Transl Med*. 2018;6(24):474. doi:10.21037/atm.2018.10.59
9. Adeva-Andany MM, González-Lucán M, Donapetry-García C, Fernández-Fernández C, Ameneiros-Rodríguez E. Glycogen metabolism in humans. *BBA Clin*. 2016;5:85-100. doi:10.1016/j.bbacli.2016.02.001
10. Schulze RJ, Schott MB, Casey CA, Tuma PL, McNiven MA. The cell biology of the hepatocyte: a membrane trafficking machine. *J Cell Biol.* 2019;218(7):2096-2112. doi:10.1083/jcb.201903090
11. Obun FE, Aliu TB, Popoola DA, Raji RO. Toxicological implications and therapeutic approaches in heavy metal exposure: focus on lead and mercury. *AROC Nat Prod Res*. 2025;5:1-10. doi:10.53858/arocnpr05010110
12. Kasmi S, Bkhairia I, Harrabi B, et al. Modulatory effects of quercetin on liver histopathological, biochemical, hematological, oxidative stress, and DNA alterations in rats exposed to graded doses of SCORE 250. *Toxicol Mech Methods.* 2018;28(1):12-22. doi:10.1080/15376516.2017.1351507
13. Basu N, Goodrich JM, Head J. Ecotoxicology of mercury in fish and wildlife: recent advances. *Ecotoxicol.* 2016;25(5): 1093-1100. doi:10.1038/jes.2015.52
14. Iezzoni JC. Diagnostic histochemistry in hepatic pathology. *Semin Diagn Pathol.* 2018;35(6):381-389. doi:10.1016/j.hpr.2022.300651

15. Kilic KD, Gokhan A, Sozmen EY, Uysal A. Liver histology and biochemistry of exposed newborn and infant rats with experimental aflatoxicosis. *Pakistan Veterinary Journal.* 2022;42(4). doi:10.29261/pakvetj/2022.066
16. Saad B, Zaid H, Shanak S, et al. Introduction to medicinal plant safety and efficacy. In: Anti-Diabetes and Anti-Obesity Medicinal Plants and Phytochemicals: Safety, Efficacy, and Action Mechanisms. 2017:21-55. doi:10.1007/978-3-319-54102-0
17. Balkrishna A, Sharma N, Srivastava D, et al. Exploring the safety, efficacy, and bioactivity of herbal medicines: bridging traditional wisdom and modern science in healthcare. *Future Integr Med.* 2024;3(1):35-49. doi:10.14218/FIM.2023.00086
18. Michael OA, Banji OM, Olufunso AB, et al. Determination of nutrients, antinutrients, and antioxidants concentrations in some edible forest vegetables in Ondo and Oyo State, South Western Nigeria. *Niger J Nutr Sci.* 2023;44(2). doi:10.36349/easjnfs.2024.v06i06.005
19. Borokini FB, Olaleye MT, Lajide L. Nutritional and chemical compositions of two underutilized vegetables in Nigeria. *Bangladesh J Sci Ind Res.* 2017;52(3):201-208. doi:10.3329/bjsir.v52i3.34156.
20. Ayoola GA, Johnson OO, Adeyemi DK, Lapite OM, Doherty CO. Antioxidant and hypoglycaemic activities of the ethanol extract of *Senecio biafrae* leaves. *J Chem Soc Nigeria.* 2017;42(2):59-62.
21. National Research Council (NRC), Institute of Laboratory Animal Research (ILAR). *Guide for the Care and Use of Laboratory Animals*. 8th ed. Washington, DC: National Academy Press; 2011:246. doi:10.1007/978-981-16-0987-9
22. Matsubara T, Touchi A, Masuda Y, Takeuchi Y. Carbon tetrachloride-induced hepatotoxicity in rats: evidence for different susceptibilities of rat liver lobes. *Jpn J Pharmacol.* 1983;33(2):435-445. doi:10.3390/toxics11070625
23. Bancroft JD, Gamble M. *Theory and Practice of Histological Techniques*. Elsevier Health Sciences; 2008.
24. Kilcoyne M, Gerlach JQ, Farrell MP, Bhavanandan VP, Joshi L. Periodic acid-Schiff's reagent assay for carbohydrates in a microtiter plate format. *Anal Biochem*. 2011;416(1):18-26. doi:10.1016/j.ab.2011.05.006
25. Mello MLS, de Campos Vidal B. The Feulgen reaction: a brief review and new perspectives. *Acta Histochem*. 2017;119(6):603-609. doi:10.1016/j.acthis.2017.07.002
26. Amber WS, Musa SA, Sambo SJ, Agbon AN. Nephroprotective effect of Citrus sinensis L. on mercury-exposed Wistar rats. *Ann Trop Pathol.* 2020;11(2):157-165.
27. Qaid MM, Abdelrahman MM. Role of insulin and other related hormones in energy metabolism: a review. *Cogent Food Agric.* 2016;2(1):1267691. doi:10.1080/23311932.2016.1267691
28. Lema-Pérez L. Main organs involved in glucose. In: *Sugar Intake: Risks and Benefits and the Global Diabetes Epidemic.* 2021:121.
29. Mandl J. Glycogen–endoplasmic reticulum connection in the liver. *Int J Mol Sci.* 2023;24(2):1074. doi:10.3390/ijms24021074
30. Hantzidiamantis PJ, Awosika AO, Lappin SL. Physiology, glucose. In: *StatPearls Publishing;* 2024.
31. Mohamed MEB, El-Meligy M, Bushra RR, Mohamed EK. Effect of mercuric chloride exposure during pregnancy and lactation on the postnatal development of the liver in the albino rat. *Egypt J Anat.* 2019;42(1):10-27. doi:10.21608/ejana.2019.251310
32. Lindström MS, Bartek J, Maya-Mendoza A. p53 at the crossroad of DNA replication and ribosome biogenesis stress pathways. *Cell Death Differ.* 2022;29(5):972-982. doi:10.1038/s41418-022-00999-w
33. Cannan WJ, Pederson DS. Mechanisms and consequences of double-strand DNA break formation in chromatin. *J Cell Physiol*. 2016;231(1):3-14. doi:10.1002/jcp.25048
34. Caldecott KW. Causes and consequences of DNA single--strand breaks. *Trends Biochem Sci.* 2024;49(1):68-78. doi:10.1016/j.tibs.2023.11.001
35. Singh P, Mitra P, Goyal T. Evaluation of DNA damage and expressions of DNA repair gene in occupationally lead--exposed workers (Jodhpur, India). *Biol Trace Elem Res.* 2021;199:1707-1714. doi:10.1007/s12011-020-02298-2
36. Hemmaphan S, Bordeerat NK. Genotoxic effects of lead and their impact on the expression of DNA repair genes. *Int J Environ Res Public Health*. 2022;19(7):4307. doi:10.3390/ijerph19074307

Rzeszów University Press 2025
ISSN 2544-1361 (online)
doi: 10.15584/ejcem.2026.1.20

http://www.ejcem.ur.edu.pl
European Journal of Clinical and Experimental Medicine
Eur J Clin Exp Med 2026; 24 (1): 112–121

ORIGINAL PAPER

Serial high-sensitivity troponin I monitoring as a prognostic marker in acute ischemic stroke

Nirmala Devi Chandrasekaran [1,2,3], Abinaya P.V. [2], Mohammed Suhail Tazeem [2], Parameswaran K. [2], Dev Sudersan Venkatesan [4], Dhivakar Ramalingam [4], Velure Raja Rao Mohan Rao [3]

[1] Department of Internal Medicine, Shri Sathya Sai Medical College and Research Institute, Sri Balaji Vidyapeeth Deemed University, Puducherry, India
[2] Department of Internal Medicine, SRM Medical College Hospital and Research Center, Faculty of Medicine and Health Sciences, SRM Institute of Science and Technology, Kattankulathur, Chengalpattu District, Tamil Nadu, India
[3] Department of Internal Medicine, Chettinad Hospital and Research Institute, Chettinad Academy of Research and Education, Kelambakkam, Chengalpattu District, Tamil Nadu, India
[4] Department of Pharmacy Practice, SRM Medical College Hospital and Research Center, Faculty of Medicine and Health Sciences, SRM Institute of Science and Technology, Kattankulathur, Chengalpattu District, Tamil Nadu, India

ABSTRACT

Introduction and aim. Acute ischemic stroke (AIS) is a complex disease with multifactorial etiologies, often masking underlying cardiovascular morbidities that contribute to clinical outcomes. This study explored the role of serial high-sensitivity troponin I (hs-TnI) monitoring in AIS patients as a prognostic marker of cardiovascular morbidity and mortality. The results offer substantial information on the relationship between hs-TnI elevations and clinical, electrocardiographic (ECG), echocardiographic (ECHO), and angiographic parameters in patients with AIS.

Material and methods. A prospective observational study was conducted on 60 patients with AIS in a tertiary care center, Tamil Nadu. Hs-TnI levels were measured at the time of admission and after 48 h together with ECG, ECHO. Angiographic evaluations were done in patients with elevated hs-TnI at 48 h after admission.

Results. Among the study population, hs-TnI levels increased significantly from 11.7% at admission to 20% after 48 h (p=0.02). Logistic regression showed hs-TnI at 48 h predicted mortality (odds ratio [OR]=28.5, 95% confidence interval [CI]: 5.9–137.1, p<0.001) and coronary artery disease (CAD) (OR=48.2, 95% CI: 9.8–236.5, p<0.001).

Conclusion. Serial monitoring of hs-TnI in AIS patients revealed its potential role in the identification of culprit lesions on coronary angiogram, which is correlated with the presence of CAD and mortality.

Keywords. acute ischemic stroke, cardiac mortality, high-sensitivity troponin I

Introduction

Acute ischemic stroke (AIS) is among the leading causes of mortality and disability contributing to the economic burden of the disease worldwide. AIS is often accompanied by cardiovascular complications that may remain undiagnosed, exacerbating patient outcomes.[1]

Corresponding author: Nirmala Devi Chandrasekaran, e-mail: nirmaladevi@sssmcri.ac.in

Received: 23.04.2025 / Revised: 3.11.2025 / Accepted: 9.11.2025 / Published: 30.03.2026

Chandrasekaran ND, Abinaya PV, Tazeem MS, Parameswaran K, Venkatesan DS, Ramalingam D, Rao VRRM. Serial high-sensitivity troponin I monitoring as a prognostic marker in acute ischemic stroke. *Eur J Clin Exp Med.* 2026;24(1):112–121. doi: 10.15584/ejcem.2026.1.20.

Key predictors of outcomes in AIS include the following clinical determinants, such as age, location of the injury, stroke severity, and presence of comorbidities. Cardiac manifestations such as myocardial infarction, arrhythmias, and left ventricular dysfunction are frequently observed in AIS patients.[2] The prognostic relevance of such abnormalities remains underexplored. Identifying patients at risk for underlying cardiovascular disease (CVD) early in the course of stroke management is crucial for optimizing clinical interventions thereby reducing morbidity and mortality.[3]

Troponin and CK-MB are cardiac biomarkers that identify and quantify myocardial injury and prognosis in stroke patients, but the outcomes have been conflicting and uncertain.[4] High-sensitivity troponin I (hs-TnI) is one such established biomarker that is also identified in conditions such as sepsis, heart failure, chronic kidney disease, cardiomyopathy etc.[5] Increasing evidence suggests that the cardiac dysfunction, arrhythmia, results from stroke induced disruption of the central autonomic pathways leading to neural-cardiac dysregulation. This is referred to as Stroke-Heart syndrome that typically occurs between 72 h and 30 days of AIS.[6,7] The Fourth Universal definition of myocardial infarction, states that myocardial injury is indicated by the elevation of cardiac troponin above the 99th percentile upper reference limit (URL).[8] Troponin peaks after 12–48 h and remains elevated for 4–10 days.[9]

The recent systematic review and meta-analysis by Gulia A et al. concluded that elevated cTn levels were associated with mortality during hospital stay and follow-up periods in patients with AIS underscoring its clinical importance.[10] Current guidelines recommend routine baseline assessment of cardiac troponin in patients with AIS yet its association with the need of invasive diagnostic and therapeutic modalities, long term consequences of troponin elevation and the timeframe for serial testing remain poorly elucidated.[11] We hypothesize that dynamic changes in hs-TnI levels over the first 48 h post-admission may provide valuable insights into the presence of undiagnosed cardiac pathology.[12,13] Furthermore, by identifying patients with an increased cardiovascular risk profile, serial hs-TnI monitoring may facilitate early therapeutic interventions, improving overall patient outcomes.[14]

Justification of the study

Contemporary studies involving patients with AIS have shown that hs-TnI is elevated in 30–60% of the patients.[15] While guidelines do not mandate a specific 48 h troponin check, this timeframe window was chosen for detection of delayed or evolving cardiac injury as evidenced by stroke heart syndrome. Persistently elevated levels may also be linked to ongoing cardiac strain and measuring at 48 h may allow for clinical stabilization, risk benefit assessment and mitigate confounders from non-coronary causes of troponin elevation.

Aim

The aim of this study was to evaluate the clinical utility of serial hs-TnI monitoring in AIS patients over the first 48 h of admission through its correlation with electrocardiographic (ECG) echocardiographic (ECHO) and angiographic abnormalities in terms of the presence of significant coronary artery occlusion and to determine its prognostic value in predicting cardiovascular mortality and morbidity.

Material and methods

Study design and setting

A prospective observational study was undertaken at a tertiary care academic medical center in South India between September 2023 and April 2024. The study was carried out at the Department of General Medicine at a tertiary care academic center equipped with facilities for neuroimaging, cardiac investigations and coronary angiography (CAG). The study sought to evaluate elevation of hs-TnI at baseline and at 48 h in AIS patients, correlate the same with ECG ECHO and angiographic observations and to investigate the prognostic significance of serial hs-TnI measurements in AIS patients while adjusting for potential confounding variables.

Sample size

Assuming an odds ratio of 3.0, α=0.05, and 80% power, the required sample size was calculated to be 52, using G power. A sample size of 60 was chosen to adjust for potential dropouts and missing data.

Inclusion and exclusion criteria

A total of 60 patients diagnosed with new-onset AIS based on Magnetic Resonance Imaging (MRI) findings, and aged more than 18 years were enrolled. Patients with hemorrhagic stroke, recurrent CVA, CKD, COPD and known coronary artery disease (CAD) were excluded to limit non-coronary causes for hs-TnI elevation. Patients who died within 48 h of admission or left against medical advice or those who developed stroke in-hospital admission were also excluded.

Data collection

Each patient underwent a comprehensive clinical evaluation that included a detailed medical history, vital signs, and relevant laboratory investigations. Demographic details such as age, gender, smoking status, and alcohol consumption were recorded. The presence of comorbidities, including systemic hypertension type 2 diabetes mellitus (T2DM) and dyslipidemia, preexisting coronary artery disease (CAD) along with their treatments was documented. Key variables included hs-

TnI levels at baseline and at 48 h, Electrocardiogram, transthoracic echocardiography, coronary angiography (CAG) and in-hospital cardiovascular morbidity and mortality. Potential confounders such as prior cardiac disease, age, medication use and renal function were documented and adjusted for in the analysis.

Stroke classification

Stroke types were categorized based on MRI findings into anterior cerebral artery (ACA) middle cerebral artery (MCA) infarct, lacunar stroke, multi-infarct stroke, posterior cerebral artery (PCA) infarct, pontine infarct, and thalamic stroke.

Hospital stay and outcome measures

The duration of hospitalization was recorded for each patient, with categories ranging from 2–8 days to more than 14 days. Clinical outcomes including mortality, presence of coronary artery occlusions, were also assessed.

Laboratory investigations

Routine laboratory tests, including fasting lipid profile, fasting blood sugar (FBS), postprandial blood sugar (PPBS), glycated haemoglobin (HbA1C), urea, and creatinine, were performed. These biomarkers were analysed in relation to troponin I levels and cardiovascular risk stratification.

Cardiac assessment

Serial hs-TnI levels were measured at two time points: upon admission and 48 h post-admission. Patients were classified based on reference values from an Asian study where the 99th percentile upper reference limit (URL) for hs-TnI was established at 33.9 ng/L, with gender-specific values of 38.41 ng/L for males and 15.73 ng/L for females.[16] The myocardial injury was considered acute if there was dynamic rising and/or falling (20%) pattern of cTn values.[15] All participants in this study underwent a standard 12 lead ECG at the time of admission and repeated if indicated clinically. ECGs were obtained at a paper speed of 25 mm/s with an amplitude calibration of 10 mm/mV and were interpreted by qualified physicians. ECG changes such as sinus tachycardia T-wave inversions, ST-segment abnormalities (elevation and depression), left bundle branch block (LBBB), right bundle branch block (RBBB) were recorded. ECHO parameters, including regional wall motion abnormalities (RWMAs), left ventricular ejection fraction (LVEF), left ventricular hypertrophy (LVH), were recorded. Left ventricular ejection fraction (LVEF) is classified according to the American College of Cardiology (ACC).[17] The regional wall motion abnormalities (RWMA) were assessed by the Wall Motion Score Index (WMSI).[18] All the cardiac interpretations were reviewed and confirmed by a cardiologist blinded to the patient's troponin values.

Angiographic findings

CAG was performed in patients of AIS with elevated hs-TnI at 48 h, to identify the presence of CAD, its location and severity. CAD is defined as obstructive if the diameter stenosis >50% and non-obstructive will be used to indicate CAD <50% stenosis. Culprit lesion is defined as the coronary artery lesion that demonstrates plaque rupture, erosion or intraluminal thrombi.[19] Angiographic findings were interpreted by cardiologists blinded to the troponin levels. The outcomes measured were changes in hs-TnI levels at 48 h, presence of coronary lesions in angiography. Number of patients who died during the in hospital follow up was recorded.

Statistical analysis

The participants baseline characteristics were summarized using descriptive statistical methods. Chi-square and Fisher's exact tests were applied to compare categorical variables, while continuous variables were assessed using independent t-tests or Mann-Whitney U tests based on normality. Spearman's correlation was used for exploratory analysis of associations involving ordinal or non-normally distributed data, including CAD and mortality. Logistic regression was employed for binary outcome modeling (e.g., presence of CAD, mortality) to estimate adjusted odds ratios. The predictors of mortality were identified by univariate and multivariate logistic regression models. Variables included in the multivariate logistic regression were age, gender, T2DM Systemic hypertension , dyslipidemia, stroke type, and hs-TnI at 48 h. Multicollinearity was assessed using the Variance Inflation Factor (VIF), and all included variables had VIF values below 2.0, indicating no significant collinearity. The odds ratios (ORs) with 95% confidence intervals (CIs) were calculated and statistical significance was set at $p<0.05$. Analyses were performed using SPSS (IBM, Armonk, NY, USA).

Ethical considerations

The study was approved by the Institutional Ethics Committee (IEC) of Chettinad Hospital and Research Centre, Tamil Nadu, India (074/IHEC/2020). Written informed consent was obtained from all the patients. The Institutional Human Ethics Committee approved our proposal (Proposal Number 074/IHEC/July2020). This prospective observational study was conducted in India where registration with Clinical Trials Registry India is not mandatory for such studies. Retrospective registration is considered and future studies will comply with the same.

Results

Demographic and clinical characteristics

The study included 60 patients diagnosed with AIS, with a male predominance (60%) and a majority aged above

60 years (56.7%). Patients aged between 40 and 60 years constituted 40%, whereas only 3.3% were between 20 and 40 years. Comorbid conditions were highly prevalent, with T2DM in 53.3%, Systemic hypertension in 46.7%, and dyslipidemia in 26.7%. Lifestyle risk factors included smoking (63.3%) and alcohol consumption (46.7%) (Table 1).

The clinical parameters of the study population were monitored from admission to 48 h thereafter, revealing significant changes to emphasize the need for serial prognostic monitoring.

Laboratory findings and correlations

Various biochemical parameters have been assessed (Table 1). Biochemical analysis showed a mean FBS of 170±80 mg/dL and postprandial blood sugar (PPBS) of 253±96 mg/dL. HbA1C had a mean of 7.2±1.6%, indicating poor glycaemic control. Total cholesterol (TC) levels averaged 232±7.6 mg/dL, indicating hypercholesterolemia in the cohort. Triglycerides (TG) levels were at a mean of 145±7 mg/dL. High-density lipoprotein (HDL) cholesterol averaged 39.5±6.1 mg/dL, which is below the recommended level, suggesting a risk factor for CVD. Low-density lipoprotein (LDL) levels were elevated (mean 182±33 mg/dL), indicating a high risk for atherosclerosis contributing to cardiovascular risk.

Pearson correlation analysis revealed strong positive associations between hs-TnI (admission vs. 48 h) (r=0.86), FBS and PPBS (r=0.83), and HbA1C and PPBS (r=0.81). Moderate correlations were found between hs-TnI (48 h) and HbA1C (r=0.29)

hs-TnI trends and significance

hs-TnI levels exhibited dynamic changes over 48 h (Table 2). At admission, 61.6% of patients had normal hs-TnI levels, which declined to 55.0% at 48 h (p=0.042). Conversely, the proportion of patients with high levels increased from 38.3% to 45.0% over the same period (p=0.038), indicating a statistically significant upward trend.

ECG and ECHO findings

ECG and ECHO findings have been listed in Table 2. ECG abnormalities were observed in 55% of patients at admission and increased to 60% at 48 h. Notable changes included an increase in T-wave inversions in inferior leads from 25% to 36.7% (p=0.03). ST depression in the anterior (ANT) leads was consistent at 18.3%, and in the lateral leads at 5%. T-wave inversions in the anterior leads were initially observed in 1.7% but were not noted at 48 h. Severe LVEF impairment rose significantly from 5% to 13.3% (p=0.02), severe hypokinesia increased from 8.3% to 10% (p=0.01). RWMAs slightly decreased from 36.7% to 33.3% (p=0.01).

Table 1. Patient demographics, clinical characteristics, and laboratory findings (n=60)*

Category	Details	Frequency n (%) or mean±SD
Demographics		
Age (years)	20–40	2 (3.3)
	40–60	24 (40.0)
	>60	34 (56.7)
Gender	Male	36 (60.0)
	Female	24 (40.0)
Comorbidities		
	T2DM	32 (53.3)
	Systemic hypertension	28 (46.7)
	Dyslipidemia	16 (26.7)
Lifestyle	Smoker	38 (63.3)
	Alcohol consumer	28 (46.7)
Clinical data		
Stroke subtype (MRI)	MCA	22 (36.7)
	Multi-infarct	9 (15.0)
	Lacunar stroke	8 (13.3)
	PCA	5 (8.3)
	Cerebellar/pontine infarct	7 (11.7)
	Other	9 (15.0)
Hospital stay (days)	2–8	41 (68.3)
	9–14	16 (26.7)
	>14	3 (5.0)
Laboratory findings		
	FBS	170±80 mg/dL
	PPBS	253±96 mg/dL
	HbA1c	7.2±1.6 %
	TC	232±7.6 mg/dL
	LDL	182±33 mg/dL
	HDL	39.5±6.1 mg/dL
	TG)	145±7 mg/dL

* percentages are calculated based on the total study population (n=60), stroke subtypes were categorized based on MRI findings, comorbidities were documented based on clinical history and prior diagnosis, MCA – middle cerebral artery, MRI – magnetic resonance imaging, PCA – posterior cerebral artery, laboratory values are presented as mean±standard deviation (SD), reference ranges (for general adult population): TC<200 mg/dL, TG<150 mg/dL, HDL>40 mg/dL (men)/>50 mg/dL (women), LDL<100 mg/dL, FBS 70–99 mg/dL, PPBS<140 mg/dL, HbA1c 4.0–5.6%, urea 8–20 mg/dL, creatinine Female: 0.50–1.10 mg/dL; male: 0.70–1.30 mg/dL[20]

Correlation analysis

Chi-square tests revealed that hypertension, T2DM, dyslipidemia, and stroke type significantly influenced patient outcomes (p<0.0001). Pearson's correlation analysis demonstrated a strong positive correlation between troponin I levels at admission and 48 h (r=0.86), as well as between FBS and PPBS (r=0.83) .

Multiple regression analysis demonstrated that the predictive model for troponin I (R^2=0.158, adjusted

R^2=0.062) had weak explanatory power. These findings suggest that additional clinical variables, such as stroke severity and inflammatory markers, should be integrated into future predictive models for better prognostic accuracy.

Table 2. Temporal trends in cardiac parameters (n=60)*

Parameter	Admission, n (%)	At 48 hours, n (%)	Change	p	95% CI for change
hs-Troponin I Level					
Normal	37 (61.6)	33 (55.0)	↓	0.042*	
High	23 (38.3)	27 (45.0)	↑	0.038*	(0.51-1.00)
ECG findings					
T-wave inversions (inferior)	15 (25.0)	22 (36.7)	↑	0.03*	(0.65-1.00)
ST depression (anterior)	11 (18.3)	11 (18.3)	No change	-	
Left bundle branch block (LBBB)	9 (15.0)	7 (11.7)	↓	0.42	
Echocardiographic findings					
Mild LVEF impairment	11 (18.3)	7 (11.7)	↓		
Moderate LVEF impairment	5 (8.3)	6 (10)	↑		
Severe LVEF impairment	3 (5.0)	8 (13.3)	↑	(0.57 – 1.00)	0.02*
Regional wall motion abnormalities	22 (36.7)	20 (33.3)	↓	(0.00–0.66)	0.01*
Mild hypokinesia	18 (30)	16 (26.7)	↓		
Moderate hypokinesia	1 (1.7)	0 (0)	↓		
Severe hypokinesia	5 (8.3)	6 (10)	↑	(0.21–1.00)	0.01*
LVH (left ventricular hypertrophy)	28 (46.7)	20 (33.3)	↓	(0.00–0.32)	0.01*

* a significant proportion of patients showed dynamic changes in hs-TnI levels between admission and 48 h, CI – confidence interval, hs-TnI – high-sensitivity troponin I, ECG – electrocardiogram, ECHO – echocardiography, LVEF – left ventricular ejection fraction, LVH – left ventricular hypertrophy

Mortality and length of hospital stay

The spearman's correlation analysis further confirmed that troponin I is a key biomarker for both CAD and mortality risk. Two weeks post-stroke, 11 patients with high hs-TnI levels succumbed (p<0.001) indicating a significant positive relationship with mortality (ρ=0.75), reinforcing its role as an indicator of mortality Additionally there was a positive correlation between hs-TnI and presence of CAD (ρ=0.87) (Table 3). A moderate correlation between CAD and death (ρ=0.60) indicates that individuals diagnosed with CAD in AIS patients face a higher risk of dying in the present study population. With all correlations showing high statistical significance (p<0.001), these findings emphasize the importance of serial monitoring of hs-TnI levels in clinical practice to predict both CAD and death risk. While hs-TnI elevation showed a minor trend toward prolonged hospitalization, no statistically significant association was found between troponin I and hospital stay duration.

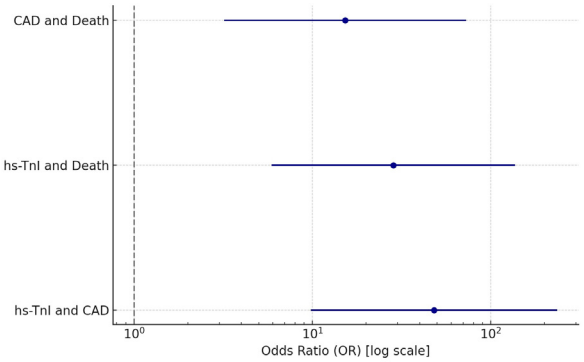

Fig. 1. Forest plot depicting associations of hs-TnI with mortality and CAD

Forest plot showing odds ratios (OR) with 95% CI for associations between hs-TnI, coronary artery disease (CAD), and mortality in AIS patients. Elevated hs-TnI was significantly associated with both CAD (OR =48.2, 95%CI: 9.8–236.5) and mortality (OR=28.5, 95%CI: 5.9–137.1). Presence of CAD also increased the odds of death (OR=15.3, 95% CI: 3.2–72.8). None of the CIs cross the null value (OR=1), indicating statistically significant associations across all pairs.

Angiographic findings

A total of 25 patients with AIS underwent CAG as part of the study. The CAG findings summarized in Table 3 revealed that 8 patients (32%) had obstructive CAD, while 7 patients (28%) had non-obstructive CAD. Notably, 10 patients (40%) demonstrated normal coronary arteries on angiography.

Analysis of vessel involvement showed that the left anterior descending artery (LAD) was the most frequently affected vessel, involved in 10 cases (40%), followed closely by the right coronary artery (RCA) in 9 cases (36%). The left circumflex artery (LCX) was involved in 5 cases (20%).

Assessment of the extent of coronary artery involvement revealed that single-vessel disease (SVD) was present in 9 patients (36%), while double-vessel disease (DVD) and triple-vessel disease (TVD) were each found in 3 patients (12%), respectively .

Regarding the nature of coronary lesions, calcified plaques were identified in 10 patients (40%), while non-calcified lesions were present in 8 patients (32%). Additionally, culprit lesions – those potentially responsible for significant ischemic events – were observed in 6 patients (24%).

Table 3. Correlations and angiographic findings

Category	Details	Results
Correlation analysis		
Correlation pair	Spearman's ρ (p)	OR and (95% CI)
hs-TnI and CAD	0.87 (<0.001)	48.2 (9.8–236.5)
hs-TnI and Death	0.75 (<0.001)	28.5 (5.9–137.1)
CAD and Death	0.60 (<0.001)	15.3 (3.2–72.8)
Coronary angiography (n=25)	Finding	Number of cases (%)
Overall result	Obstructive CAD	8 (32.0)
	Non-obstructive CAD	7 (28.0)
	Normal coronaries	10 (40.0)
Vessel involvement	Left anterior descending (LAD)	10 (40.0)
	Right coronary artery (RCA)	9 (36.0)
	Left circumflex (LCX)	5 (20.0)
Extent of disease	Single-vessel disease	9 (36.0)
	Double-/Triple-vessel disease	6 (24.0)
Lesion type	Calcified lesion	10 (40.0)
	Non-calcified lesion	8 (32.0)
	Culprit lesion	6 (24.0)

* percentages are calculated based on the total number of patients (n=25), the data on extent of disease were available for 15 patients, remaining 10 patients had normal coronaries, lesion types are not mutually exclusive, some patients had multiple lesion types

Discussion

AIS is a multifaceted condition with various underlying causes, frequently revealing cardiovascular comorbidities that influence patient outcomes. This study investigated the potential of serial hs-TnI measurements in AIS patients as a prognostic marker for cardiovascular morbidity and mortality. The recognition of cardiac involvement in acute stroke dates back to the late 1970s, when Norris et al. studied the rise of cardiac biomarkers in AIS patients, identifying myocardial dysfunction as a consequence rather than a cause of the stroke.[21] Serial measurements allow differentiation between acute and chronic myocardial injury. Studies have demonstrated that dynamic troponin patterns (defined by fluctuations of more than 20%) are associated with evolving myocardial injury whereas stable levels suggest chronic cardiac pathology.[22] In parallel, findings from our study revealed a significant increase in the proportion of AIS patients with elevated hs-TnI at 48 h (from 38.3% to 45%; p=0.038). while the number of patients with normal hs-TnI levels showed a decline (from 61.6% to 55%), thus revealing dynamic changes. The consistency between the above observed changes and Rosso et al. paradigm further highlights the importance of serial troponin measurements as opposed to single point values.[22] Serial hs-TnI assay revealed dynamic elevation at 48 h signifying evolving myocardial injury that might otherwise remain undetected and can unmask hidden or subclinical cardiac dysfunction.

The evolving nature of the cardiac biomarker demonstrates the interplay between neurological insult and cardiac dysfunction-central to the concept of Stroke-Heart Syndrome. It encompasses the clinical spectrum that includes acute myocardial injury, type 1 and 2 myocardial infarction–ischemic and non-ischemic manifestations like left ventricular dysfunction, cardiac arrhythmias, ECG changes, Takotsubo syndrome and contraction band necrosis.[6,7] Prediction of acute coronary syndrome in AIS by Nolte et al. concluded type 1 MI was common mechanism of myocardial injury in stroke and a higher baseline hs-cTn values, whereas our study aligned with the concept of evolving myocardial stress in AIS supporting the need for comprehensive cardiac evaluation in management of AIS patients.[23]

In this study ECG abnormalities were observed in 55% of patients at admission an increased to 60% at 48 h, with significant increase in T-wave inversions in the inferior leads (p=0.03) with no significant changes in ST depression or bundle branch blocks. The study by Fure et al. on ECG abnormalities in the early stage of ischemic stroke identified the following: prolonged QTc, ST-segment depression, atrial fibrillation, and T wave inversion. ST depression and Q waves were associated with an increase in TnT levels.[24] Severe LVEF impairment increased from 5% to 13.3% (p=0.02), in those patients with hs-TnI elevations after 48 h however mild LVEF impairment got resolved after 48 h. ECHO abnormalities like RWMA s in the septum and inferior wall with variable grades of severity was observed in patients with acute stroke with elevated troponin levels and was consistent after the 48 h interval with a statistical significance. These findings are in accordance with the results by a study done by Amir Darke et al., in which 67% of patients with elevated troponin had new RWMA.[19] These findings highlight the evolving nature of cardiac dysfunction in AIS patients, underscoring the importance of serial cardiac monitoring. Given the significant correlations between Troponin I and ECG/ECHO abnormalities, angiographic screening may be warranted in AIS patients with unexplained dynamic hs-TnI elevations to identify underlying CAD.

This study highlights a significant prevalence of CAD among patients with AIS. Of the 25 patients who underwent CAG, obstructive CAD was found in 32%, non-obstructive CAD in 28%, and normal coronaries in 40%. These findings suggest that a substantial proportion of stroke patients have coexisting but variable degrees of coronary involvement. The LAD was the most commonly involved vessel, followed by the RCA and LCX. SVD was more frequent than multi-vessel involvement, suggesting a different pathophysiological mechanism compared to patients

with acute coronary syndrome. Lesion analysis revealed calcified plaques in 40%, non-calcified plaques in 32%, and culprit lesions in 24% of patients. This suggests both chronic and potentially unstable coronary pathology among stroke patients. These findings are in accordance with TRELAS study which concluded prevalence of SVD was higher than multivessel involvement and significantly lesser prevalence of culprit lesion compared with NSTE-ACS patients (7 out of 29 vs. 23 of 29).[25] As discussed earlier both ischemic and non-ischemic causes leads to the elevation of hs-TnI in patients with AIS. The differentiation between true CAD versus neurogenic myocardial injury lies in the fact that the former would typically present with dynamic change of cTn>20%, new ischemic ECG changes, imaging evidence of RWMAs whereas the latter has predominantly insular involvement, QT prolongation, global LV dysfunction.[26] Coronary Angiography is considered gold standard in aiding the differentiation between the two.[8] The presence of culprit lesion indicated significant CAD, which aligns with 24% occurrence of culprit lesions in our study.[25] Mortality are also observed even after exclusion of patients with known CAD. 40% of patients with elevated hs-TnI had normal coronaries. Thus it is concluded that not all troponin elevation in stroke indicates true CAD and integration of cardiac and neurological diagnostic modalities would be vital.

MRI findings revealed that MCA infarcts were the most prevalent stroke type (36.7%), followed by multi-infarct strokes (15%) and lacunar strokes (13.3%). Stroke type significantly influenced outcomes (p=0.001), with larger infarcts associated with higher troponin I elevations and increased cardiovascular complications. Von Rennenberg et al. concluded that a strong correlation between elevated cardiac biomarkers in patients with acute stroke were significantly linked to abnormal cardiac MRI findings such as focal fibrosis, LVH, decreased LVEF and left atrial dilatation.[27] These findings emphasize the need for thorough cardiac assessment and timely integration of cardiology in stroke care. Stroke was significantly more common in the right cerebral hemisphere in patients with increased troponin I without any ischemic changes on the ECG. In patients with elevated troponin, the functional status based on Modified Rankin Scale showed a significant worsening in 30 days post-stroke.[28] The major risk factors for cardiovascular morbidity includes diabetes mellitus, hypertension, dyslipidemia. In this study the mean FBS of 170±80 mg/dL and PPBS of 253±96 mg/dL with a mean HbA1C of 7.2±1.6%, indicated poorer glycemic control in patients with elevated troponin levels. A lower recommended level of HDL cholesterol of 39.5±6.1 mg/dL along with raised LDL levels with a mean of 182±33 mg/dL, suggests a high risk for atherosclerosis thus contributing to cardiovascular risk. The meta-analysis by YuFan et al. demonstrated an association between cardiac troponin elevation and all-cause mortality (RR: 2.53) in patients with AIS.[29] The analysis of PROCIS-B cohort by Scheitz et al., highlighted that elevated hs cTnT Was linked to increased risk of recurrent vascular events and mortality in individuals experiencing their first ever mild to moderate ischemic stroke.[30]

Baseline levels of cTnI were associated with a higher risk of mortality both in hospital and at 6 months follow-up with an increased likelihood of non-fatal cardiac events.[31] In this study 11 patients with high levels succumbed during the hospital stay thereby revealing the nexus between troponin and cardiovascular mortality in the study cohort. The cause of death during the first week of ischemic stroke includes cerebral edema and hemorrhagic transformation whereas heart failure, acute myocardial infarction, ventricular fibrillation, ventricular tachycardia, are the predominant causes of death within first 3 months of stroke attributed to autonomic dysfunction in lesions of insular cortex.[32] Overall, patients with dynamic changes were more likely to show ischemic changes in ECG, reduced LVEF, RWMAs and higher prevalence of angiographically confirmed CAD suggesting serial hs Troponin measurements more effectively indicate the likelihood of in-hospital mortality and cardiovascular outcomes as evidenced by strong positive correlations between Troponin I levels and both CAD (ρ=0.87, p<0.001) and mortality (ρ=0.75, p<0.001).

Evidence of damaged myocardial fibers were present in patients with intracranial lesions.

Myocardial alterations following stroke resembles those that of Takotsubo Cardiomyopathy characterized by autonomic imbalance with increased catecholamine release.[33] Evidence from recent research suggested that cardiac biomarkers were associated with vascular cognitive impairment and dementia.[34]

Damage to the right dorsal anterior insular cortex in stroke disrupts autonomic regulation, leading to heightened sympathetic activity and increased risk of myocardial injury.[35] The concentration of troponin rises over several days which can be detected by serial measurements after stroke onset. Several studies showed elevated troponin at admission is a prognostic marker and an individual predictor of mortality at 30 days, 6 months and a mean follow-up at 19 months of ischemic stroke.[36] The underlying cause of elevated troponin levels is associated with both increased case fatality and higher degree of disability. In summary, guidelines support baseline hs-TnI testing in all ischemic stroke patients for early cardiac risk detection.

Clinical and research implications

The findings of this study emphasize the need for routine serial hs-TnI monitoring in AIS patients, as dynamic changes in the levels may provide early indicators of cardiac stress. Given the significant correlations between hs-TnI and ECG/ECHO abnormalities, and coronary angiogram findings, stroke management protocols should integrate cardiac assessments to optimize risk stratification. Furthermore, angiographic screening may be warranted in AIS patients with unexplained hs-TnI elevations to identify underlying CAD.

Study limitations

The present study had a small sample size from a single centre and most of the patients were from critical care. Further studies involving larger sample size would provide more insights. Excluding patients who died or were discharged early may have led to selection bias, which could possibly restrict the generalizability of the results. Exploring the role of inflammation, autonomic dysfunction, and neuro-cardiac interactions in AIS patients with elevated hs-TnI would provide a better understanding of the correlation. Another limitation of the study was lack of long term follow-up of patients and no stroke severity score like NIHSS were adjusted in analysis. Additionally, larger multicenter studies with longer follow-up periods could help establish the prognostic utility of troponin I in predicting long-term cardiovascular outcomes in stroke patients.

Conclusion

In conclusion, serial hs-TnI elevations in acute ischaemic stroke patients are associated with evolving cardiovascular complications, particularly in those with preexisting metabolic disorders and silent coronary artery disease. The dynamic changes of hs-TnI correlate with abnormalities in ECG, ECHO, and angiographic findings, emphasizing its role in cardiovascular risk assessment. The integration of serial troponin I monitoring in AIS protocols may enhance early detection of cardiac complications, ultimately improving clinical outcomes in stroke patients. Hs-TnI is an independent predictor of cardiovascular mortality. Hence it serves as a marker with prognostic significance .Further studies are needed to refine predictive models and explore targeted interventions for AIS patients with elevated troponin I levels.

Acknowledgments

The authors would like to thank SRM Medical College Hospital and Research Centre, SRM Institute of Science and Technology, Kattankulathur and Chettinad Hospital and Research Institute, Kelambakkam for providing technical resources and support.

Declarations

Funding

No funding received for this study.

Author contributions

Conceptualization, N.D.C. and P.V.A.; Methodology, N.D.C. and P.V.A.; Software, N.D.C., M.S.T.; Validation, N.D.C. and P.V.A.; Formal Analysis, D.S.V., P.V.A. and D.R.; Investigation, P.V.A., P.K. and D.S.V.; Resources, N.D.C. and P.V.A.; Data Curation, N.D.C.; Writing – Original Draft Preparation, N.D.C. and P.V.A.; Writing – Review & Editing, N.D.C., P.V.A., and D.S.V.; Visualization, N.D.C. and P.V.A.; Supervision, N.D.C. and P.V.A., V.M.R.; Project Administration, N.D.C.

Conflicts of interest

The authors declare that they have no conflicts of interest.

Data availability

All data generated or analyzed during this study are included in this published article. Additional data are available from the corresponding author upon reasonable request.

Ethics approval

The study adhered to the guidelines set forth in the Declaration of Helsinki, and the protocol was approved by the Ethics Committee of the Institutional Ethics Committee of Chettinad Hospital and Research Institute, Tamil Nadu, India (074/IHEC/2020).

References

1. Huang X, Lu Z, Li T, et al. Comorbidity patterns in patients with first-ever acute ischemic stroke and their associations with functional outcomes. *Neuroepidemiology.* 2025;59(1):1-13. doi:10.1159/000544170
2. König IR, Ziegler A, Bluhmki E, et al. Predicting long-term outcome after acute ischemic stroke: a simple index works in patients from controlled clinical trials. *Stroke.* 2008;39(6):1821-1826. doi:10.1161/STROKEAHA.107.505867
3. Lip GYH, Lane DA, Lenarczyk R, et al. Integrated care for optimizing the management of stroke and associated heart disease: a position paper of the European Society of Cardiology Council on Stroke. *Eur Heart J.* 2022;43(26):2442-2460. doi:10.1093/eurheartj/ehac245
4. Ion A, Stafie C, Mitu O, et al. Biomarkers utility: at the borderline between cardiology and neurology. *J Cardiovasc Dev Dis.* 2021;8(11):141. doi:10.3390/jcdd8110139
5. Raber I, McCarthy CP, Januzzi JL Jr. A test in context: interpretation of high-sensitivity cardiac troponin assays in different clinical settings. *J Am Coll Cardiol.* 2021;77(10):1357-1367. doi:10.1016/j.jacc.2021.01.011
6. Scheitz JF, Sposato LA, Schulz-Menger J, Nolte CH, Backs J, Endres M. Stroke–heart syndrome: recent advances

and challenges. *J Am Heart Assoc.* 2022;11(17):e026528. doi:10.1161/JAHA.122.026528
7. Scheitz JF, Nolte CH, Doehner W, Hachinski V, Endres M. Stroke–heart syndrome: clinical presentation and underlying mechanisms. *Lancet Neurol.* 2018;17(12):1109-1120. doi:10.1016/S1474-4422(18)30336-3
8. Thygesen K, Alpert JS, Jaffe AS, et al. Fourth universal definition of myocardial infarction (2018). *J Am Coll Cardiol.* 2018;72(18):2231-2264. doi:10.1016/j.jacc.2018.08.1038
9. Lazar DR, Lazar FL, Homorodean C, et al. High-sensitivity troponin: a review on characteristics, assessment, and clinical implications. *Dis Markers.* 2022;2022:9713326. doi:10.1155/2022/9713326
10. Gulia A, Srivastava M, Kumar P. Elevated troponin levels as a predictor of mortality in patients with acute stroke: a systematic review and meta-analysis. *Front Neurol.* 2024;15:1351925. doi:10.3389/fneur.2024.1351925
11. Powers WJ, Rabinstein AA, Ackerson T, et al. 2018 guidelines for the early management of patients with acute ischemic stroke: a guideline for healthcare professionals from the American Heart Association/American Stroke Association. *Stroke.* 2018;49(3):e46-e99. doi:10.1161/STR.0000000000000158
12. Vilela E, Bastos J, Rodrigues R, Nunes JP. High-sensitivity troponin after running: a systematic review. *Neth J Med.* 2014;72(1):5-9.
13. Jensen JK, Atar D, Mickley H. Mechanism of troponin elevations in patients with acute ischemic stroke. *Am J Cardiol.* 2007;99(6):867-870. doi:0.1016/j.amjcard.2006.10.052
14. Leite L, Matos P, Leon-Justel A, et al. High-sensitivity troponins: potential biomarkers of cardiovascular risk for primary prevention. *Front Cardiovasc Med.* 2022;9:1054959. doi:10.3389/fcvm.2022.1054959
15. Scheitz JF, Stengl H, Nolte CH, Landmesser U, Endres M. Neurological update: use of cardiac troponin in patients with stroke. *J Neurol.* 2021;268(6):2284-2292. doi:10.1007/s00415-020-10349-w
16. Bahadur K, Ijaz A, Salahuddin M, Alam A. Determination of high-sensitive cardiac troponin I 99th percentile upper reference limits in a healthy Pakistani population. *Pak J Med Sci.* 2020;36(6):1303-1307. doi:10.12669/pjms.36.6.2328
17. Kosaraju A, Goyal A, Grigorova Y, Makaryus AN. Left Ventricular Ejection Fraction. *StatPearls.* Treasure Island, FL: StatPearls Publishing; 2025.
18. Armstrong WF, Ryan T. *Feigenbaum's Echocardiography.* 7th ed. Philadelphia, PA: Lippincott Williams & Wilkins; 2012:1-1676.
19. Writing Committee Members, Gulati M, Levy PD, et al. 2021 AHA/ACC/ASE/CHEST/SAEM/SCCT/SCMR guideline for the evaluation and diagnosis of chest pain: a report of the American College of Cardiology/American Heart Association Joint Committee on Clinical Practice Guidelines. *J Am Coll Cardiol.* 2021;78(22):e187-e285. doi:10.1016/j.jacc.2021.07.053
20. ABIM Laboratory Test Reference Ranges - January 2022. Study notes Radioimmunoassay. Docsity. https://www.docsity.com/en/docs/abim-laboratory-test-reference-ranges-january-2022/8916253/. Accessed October 28, 2025.
21. Norris JW, Hachinski VC, Myers MG, Callow J, Wong T, Moore RW. Serum cardiac enzymes in stroke. *Stroke.* 1979;10(5):548-553. doi:10.1161/01.STR.10.5.548
22. Rosso M, Ramaswamy S, Mulatu Y, et al. Rising cardiac troponin: a prognostic biomarker for mortality after acute ischemic stroke. *J Am Heart Assoc.* 2024;13(4):e032922. doi:10.1161/JAHA.123.032922
23. Nolte CH, von Rennenberg R, Litmeier S, et al. Type 1 myocardial infarction in patients with acute ischemic stroke. *JAMA Neurol.* 2024;81(7):703-711. doi:10.1001/jamaneurol.2024.1552
24. Fure B, Bruun Wyller T, Thommessen B. Electrocardiographic and troponin T changes in acute ischemic stroke. *J Intern Med.* 2006;259(6):592-597. doi:10.1111/j.1365-2796.2006.01639.x
25. Mochmann HC, Scheitz JF, Petzold GC, et al. Coronary angiographic findings in acute ischemic stroke patients with elevated cardiac troponin: the troponin elevation in acute ischemic stroke (TRELAS) study. *Circulation.* 2016;133(13):1264-1271. doi:10.1161/CIRCULATIONAHA.115.018547
26. Wang L, Ma L, Ren C, et al. Stroke–heart syndrome: current progress and future outlook. *J Neurol.* 2024;271(8):4813-4825. doi:10.1007/s00415-024-12480-4
27. von Rennenberg R, Herm J, Krause T, et al. Elevation of cardiac biomarkers in stroke is associated with pathological findings on cardiac MRI: results of the Heart and Brain Interfaces in Acute Stroke study. *Int J Stroke.* 2023;18(2):180-186. doi:10.1177/17474930221095698
28. Lasek-Bal A, Kowalewska-Twardela T, Gąsior Z, et al. The significance of troponin elevation for the clinical course and outcome of first-ever ischemic stroke. *Cerebrovasc Dis.* 2014;38(3):212-218. doi:10.1159/000365839
29. Fan Y, Jiang M, Gong D, Man C, Chen Y. Cardiac troponin for predicting all-cause mortality in patients with acute ischemic stroke: a meta-analysis. *Biosci Rep.* 2018;38(2):BSR20171676. doi:10.1042/BSR20171178
30. Scheitz JF, Lim J, Broersen LH, et al. High-sensitivity cardiac troponin T and recurrent vascular events after first ischemic stroke. *J Am Heart Assoc.* 2021;10(10):e018326. doi:10.1161/JAHA.120.018326
31. Di Angelantonio E, Fiorelli M, Toni D, et al. Prognostic significance of admission levels of troponin I in patients with acute ischemic stroke. *J Neurol Neurosurg Psychiatry.* 2005;76(1):76-81.
32. Sörös P, Hachinski V. Cardiovascular and neurological causes of sudden death after ischemic stroke. *Lancet Neurol.* 2012;11(2):179-188. doi:0.1016/S1474-4422(11)70291-5
33. Kolin A, Norris JW. Myocardial damage from acute cerebral lesions. *Stroke.* 1984;15(6):990-993. doi:10.1161/01.STR.15.6.990

34. Johansen MC, von Rennenberg R, Nolte CH, et al. Role of cardiac biomarkers in stroke and cognitive impairment. *Stroke.* 2024;55(9):2376-2384. doi:10.1161/STROKEAHA.123.044143
35. Krause T, Werner K, Fiebach JB, et al. Stroke in right dorsal anterior insular cortex is related to myocardial injury. *Ann Neurol.* 2017;81(4):502-511. doi:10.1002/ana.24906
36. Iltumur K, Yavavli A, Apak I, Ariturk Z, Toprak N. Elevated plasma N-terminal pro-brain natriuretic peptide levels in acute ischemic stroke. *Am Heart J.* 2006;151(5):1115-1122. doi:10.1016/j.ahj.2005.05.022

Rzeszów University Press 2025
ISSN 2544-1361 (online)
doi: 10.15584/ejcem.2026.1.21

http://www.ejcem.ur.edu.pl
European Journal of Clinical and Experimental Medicine
Eur J Clin Exp Med 2026;24(1): 122–128

ORIGINAL PAPER

Association of the DeRitis ratio with insulin resistance in non-obese adults – a cross-sectional study from South India

Sachin Kumar , Vignessh Raveekumaran , Sethuraj Selvaraj , K.S. Chenthil

Department of General Medicine, Mahatma Gandhi Medical College and Research Institute, Sri Balaji Vidyapeeth (Deemed to be University), Pondicherry, India

ABSTRACT

Introduction and aim. Beyond overt obesity, insulin resistance (IR) is increasingly recognized in non-obese individuals, particularly South Asians. Liver enzymes, especially aspartate aminotransferase (AST) and alanine aminotransferase (ALT), and their ratio (DeRitis) have emerged as potential surrogate markers of metabolic dysfunction. To the best of our knowledge, this is the first study to evaluate the DeRitis ratio as a surrogate marker of IR specifically in non-obese South Indian adults, addressing an important evidence gap. With this background, the aim was to estimate the IR prevalence in non-obese adults by homeostasis model assessment of IR (HOMA-IR) and to assess the correlation and diagnostic performance of the DeRitis ratio.

Material and methods. This cross-sectional study included 100 non-obese adults (body mass index (BMI) <25kg/m^2) selected using a convenience sampling technique attending a tertiary care hospital in Pondicherry, India. Data collected by structured proforma and biochemical assays of fasting plasma glucose, fasting insulin, and liver enzymes. HOMA-IR ≥2.5 as confirmed IR. The correlation and diagnostic accuracy of the DeRitis ratio for predicting IR was analyzed using SPSS software (V_25.0); $p<0.05$ considered statistically significant.

Results. IR (HOMA-IR 2.5) was present in 13% of participants. Overweight individuals showed significantly higher fasting insulin levels and HOMA-IR values compared to adults with normal BMI. The DeRitis ratio was positively correlated with HOMA-IR ($r=0.516$, $p<0.001$). Using the cut-off AST/ALT >1.0, the ratio demonstrated good discriminatory ability for IR (AUC=0.778), with 82.5% sensitivity and 83.3% specificity.

Conclusion. The DeRitis ratio shows moderate discrimination for IR and may aid in screening where insulin assays are limited. Validation in larger, multicenter cohorts is warranted.

Keywords. alanine transaminase, aspartate aminotransferase, body weight, India, insulin resistance

Introduction

Obesity is a multifactorial disease that has escalated globally, now affecting roughly one in eight people and surpassing one billion individuals, with adult obesity more than doubling since 1990 and adolescent obesity quadrupling, underscoring a substantial cardiometabolic burden.[1,2] Elevated hepatic enzymes, particularly alanine aminotransferase (ALT), aspartate aminotransferase (AST), and γ-glutamyl transferase (GGT), track closely with adiposity and metabolic dysfunction, reflecting steatosis, inflammation, and hepatocellular injury that accompany obesity.[3,4] Several population-based studies have consistently demonstrated that even modest elevations in liver enzymes are associated with IR, metabolic syndrome, and future diabetes risk across diverse ethnic groups, reinforcing the liver's centrality in

Corresponding author: Vignessh Raveekumaran, e-mail: vignesshr@mgmcri.ac.in

Received: 16.09.2025 / Revised: 16.11.2025 / Accepted: 22.11.2025 / Published: 30.03.2026

Kumar S, Raveekumaran V, Selvaraj S, Chenthil KS. Association of the DeRitis ratio with insulin resistance in non-obese adults – a cross-sectional study from South India. *Eur J Clin Exp Med.* 2026;24(1):122–128. doi: 10.15584/ejcem.2026.1.21.

obesity-related risk stratification.[3,5,6] These findings support the growth recognition of hepatic biomarkers as early indicators of metabolic dysfunction.

IR is a hallmark of obesity, driven by adipose-tissue inflammation, lipotoxicity, ectopic fat deposition, and endocrine-immune cross-talk that impair insulin-receptor signalling across liver, skeletal muscle, and adipose tissue.[7–9] These processes include cytokine-mediated serine phosphorylation of insulin-signalling intermediates, mitochondrial stress, and altered adipokine profiles, collectively propagating systemic IR and its sequelae, including type-2 diabetes mellitus (T2DM), dyslipidaemia, and non-alcoholic fatty liver disease (NAFLD).[6,7,9]

Uncertainty surrounds the possible mechanism linking obesity to serum levels of liver enzymes. However, some studies have shown that obesity is found to be associated with an increase in DNA methylation in liver tissues, thereby increasing oxidative stress in the tissue, and this ultimately leads to liver destruction.[10] The DeRitis ratio (AST/ALT), originally proposed by Fernando DeRitis in 1957, is widely used as a biochemical index of hepatocellular injury and a versatile prognostic marker across liver and systemic illnesses, reflecting shifts in mitochondrial versus cytosolic enzyme release, necro-inflammatory activity, and extrahepatic sources of AST.[11,12]

Recent studies have shown that the DeRitis ratio is one of the independent markers of mortality.[12,13] Beyond its classical use in liver disease, emerging research highlights its potential role as a metabolic biomarker. Multiple population datasets indicate that transaminase-based indices related to metabolic risk, like in non-obese Japanese adults, the ALT/AST (inverse of De-Ritis) ratio, were the best surrogate of IR (Homeostasis Model Assessment of insulin resistance (HOMA-IR)),[14] while a large Korean cohort analysis showed DeRitis outperforming single-enzyme measures for predicting dysglycemia and IR.[15] These reports collectively indicate that liver enzyme ratios may capture early hepatic-metabolic interactions even before overt disease manifestations. Earlier work also linked elevated ALT with future T2DM and declining hepatic insulin sensitivity, reinforcing the liver-IR nexus.[16] However, these findings have been predominantly documented in East Asian population,[17,18] and there remains limited evidence from South Asian settings, where metabolic risk occurs at lower BMI thresholds and hepatic fat accumulation is common even among non-obese individuals.

Despite growing evidence that transaminase-based ratios reflect metabolic risk, Indian data in non-obese adults remain limited and none have specifically evaluated the DeRitis ratio as a potential surrogate marker of IR in non-obese adults. Given India's high and heterogenous obesity/overweight burden and the constrained availability of insulin assays in peripheral settings, a simple, inexpensive biochemical marker is clinically valuable.[19] Hence, this study was undertaken as a prospective, single center observational study in Pondicherry to examine the association between the DeRitis ratio and IR in non-obese adults and evaluate the ability of the DeRitis ratio to discriminate IR defined by HOMA-IR.

Aim

The primary objective of this study was to investigate the association between the DeRitis ratio and IR (HOMA-IR ≥2.5) in non-obese South Indian adults, addressing an existing evidence gap in this population. The secondary objectives were to assess the diagnostic performance of the DeRitis ratio in identifying IR and to evaluate its correlation with HOMA-IR.

Material and methods

Study design and setting

This hospital-based cross-sectional observational study was conducted in the Department of General Medicine at a tertiary care center in Pondicherry, India for a period of 12 months after obtaining Institutional Human Ethics Committee approval (MGMCRI/Res/01/2023/115/IHEC/106). All procedures performed in this study were in accordance with the ethical standards of the institutional and national research committee(s) and with the Helsinki Declaration (as revised in 2013). From all the participants, written informed consent was obtained during the data collection.

Study population

Adults aged 18–60 years attending the outpatient clinic with non-obese body mass index (BMI) (BMI<25.0kg/m^2) according to Asian cut-off were eligible.[20] BMI was categorized using Asian BMI cut-offs as normal BMI is 18.5–22.9 kg/m^2; overweight: BMI 23.0–24.9 kg/m^2; and obese: ≥25.0 kg/m^2.[20]

The exclusion criteria were patients with known liver diseases, significant alcohol intake, viral hepatitis or hepatotoxic drug use, known DM, hypertension, or other endocrine disorders, with acute illness or infection at the time of evaluation, and pregnant/lactating women.

Sample size and sampling technique

The sample size was calculated based on the 6.2% prevalence of IR reported in a study by Kawamoto et al. (2012) performed in Japan,[14] among non-obese individuals. Using the formula, $n=(Z^2pq)/d^2$ with p (prevalence) as 6.2%, 5% alpha error, 20% beta error and allowable error of 5% (d), (substituting as $n=(1.96)^{2*}0.062^*(1-0.062)/(0.05)^2=90$) the sample size calculated was 90 (Open Epi (v3.0)). Allowing 10% for attrition rate, the required sample size was 100 participants. By convenience sampling techniques, patients were selected for the study until the desired sample size was achieved.

Outcomes

Primary – the prevalence of IR (HOMA-IR ≥2.5); secondary – (i) correlation between DeRitis ratio and HOMA-IR, (ii) diagnostic performance of AST/ALT for IR.

Study procedures

Data collection included demographic details, anthropometric measurements, and clinical history, which were recorded using a structured proforma. Then the patients were subjected to various biochemical analyses. Fasting venous blood samples were collected after an overnight fast of 8-10 hours. The following parameters were measured:

- Fasting plasma glucose (FPG) by the glucose oxidase-peroxidase method
- Fasting insulin by chemiluminescent (E-CLIA) immunoassay (Manufacturer – Cobas E411; Assay type ROCHE ELECSYS 2010; quality control at Biorad (Level 3))
- The AST and ALT were prepared using standard enzymatic methods (Manufacturer – Cobas C311; Assay type International federation of clinical chemistry (IFCC) method; quality control at Biorad (Level 3))

The DeRitis ratio[12] was calculated DeRitis ratio = AST/ALT and used to evaluate the liver function and disease severity. An elevated ratio (>1) suggests liver damage, and ≤1 was considered normal.[12]

The HOMA-IR[21] was computed using the formula

$$\text{HOMA} - \text{IR} = \frac{\text{Fasting insulin}\left(\frac{\mu U}{mL}\right) \times \text{Fasting glucose}\left(\frac{mg}{dL}\right)}{405}$$

IR was defined as HOMA-IR ≥2.5 (based on validated Asian cut-off).

Statistical analysis

The data was entered into Microsoft Excel and analyzed using SPSS version 25.0 (IBM, Armonk, NY, USA). Continuous variables were expressed as mean±standard deviation (SD) or median (interquartile range (IQR)) depending on normality (assessed by the Shapiro-Wilk normality test and Q-Q plot). Categorical variables were presented as proportions. An independent t-test or Mann-Whitney U-test was used to compare the continuous variables, and the homogeneity of variances were performed using the Levene's test, if violated Welch's test was used. Chi-square test or Fisher's exact test was applied for categorical variables. Pearson's correlation coefficient assessed the relationship between the DeRitis ratio and HOMA-IR after confirming its linearity and absence of extreme outliers. The diagnostic performance of the DeRitis ratio for IR was evaluated using Receiver Operating Characteristics (ROC) curve. The primary diagnostic threshold was pre-specified as DeRitis ratio >1.0, reflecting a conventional clinical cut-off used to indicate the elevation of the ratio in liver disease. At this priori cut-off, sensitivity, specificity, predictive values, and overall diagnostic accuracy, were calculated with area under the curve (AUC) at 95% CI. Youden's index was additionally computed to summarize the balance between the sensitivity and specificity. A p-value <0.05 was considered statistically significant.

Results

Participant flow and baseline characteristics are presented in Table 1, and associations with BMI is presented in Table 2.

Table 1. Socio-demographic characteristics and risk factors of the study participants (n=100)*

Variables		Results n (%)
Age (in years)	18–30	14 (14.0)
	31–40	20 (20.0)
	41–50	26 (26.0)
	51–60	32 (32.0)
	>60	8 (8.0)
Gender	Male	43 (43.0)
	Female	57 (57.0)
SES	Class I	12 (12.0)
	Class II	16 (16.0)
	Class III	16 (16.0)
	Class IV	24 (24.0)
	Class V	32 (32.0)
Locality	Rural	50 (50.0)
	Urban	50 (50.0)
Smoking	Present	41 (41.0)
	Absent	59 (59.0)
Alcohol consumption	Present	40 (40.0)
	Absent	60 (60.0)
Diet pattern	Vegetarian	49 (49.0)
	Non-vegetarian	51 (51.0)
BMI (kg/m^2)	Overweight (23.1 – 24.9)	39 (39.0)
	Normal (<23)	61 (61.0)

* SES – socio-economic status as per the B.G. Prasad scale

Overall, 13% of participants were identified with IR (HOMA-IR ≥2.5). Using the DeRitis ratio (>1), approximately 43% of patients were identified as having insulin resistance (IR), with a significantly higher prevalence in the overweight group (33 out of 39; 84.6%) compared to the normal BMI group (10 out of 61; 16.4%), which was statistically significant (p<0.001, Table 3).

Similarly, the mean DeRitis ratio among patients with normal BMI was 1.084±0.060, compared to 0.920±0.035 for overweight patients, and the difference between the two groups was statistically significant (p<0.05). The rest of the biochemical parameters and their association with BMI are presented in Table 3.

Table 2. Association of sociodemographic and risk factors in relation to the BMI (Pearson's chi-square test)

Variables	BMI (kg/m²)		p
	Normal (< 23) (n=61) n (%)	Overweight (23.1–24.9) (n=39) n (%)	
Age (in years)			
18-30	10 (16.4)	4 (10.3)	0.035
31-40	15 (24.6)	5 (12.8)	
41-50	18 (29.5)	8 (20.5)	
51-60	12 (19.7)	20 (51.3)	
>60	6 (9.8)	2 (5.1)	
Gender			
Male	35 (57.4)	8 (20.5)	0.001
Female	26 (42.6)	31 (79.5)	
Socio-economic status (according to the B.G. Prasad scale)			
Class I	10 (16.4)	2 (5.1)	0.021
Class II	12 (19.7)	4 (10.2)	
Class III	10 (16.4)	6 (15.4)	
Class IV	16 (26.2)	8 (20.5)	
Class V	13 (19.7)	19 (48.7)	
Locality			
Rural	40 (65.6)	10 (25.6)	0.001
Urban	21 (34.4)	29 (74.4)	
Smoking status			
Present	10 (16.4)	31 (79.5)	<0.001
Absent	51 (83.6)	8 (20.5)	
Alcohol consumption			
Present	15 (24.6)	25 (64.1)	0.001
Absent	46 (75.4)	14 (35.6)	
Dietary pattern			
Vegetarian	35 (57.4)	14 (35.9)	0.022
Non-vegetarian	26 (42.6)	25 (64.1)	

Table 3. Association of biochemical parameters in relation to the BMI*

Variables	BMI (kg/m²)		p
	Normal (n=61) (< 23)	Overweight (n=39) (23.1–24.9)	
ALT	16.28 ± 1.25	23.05 ± 1.61	<0.001
AST	17.61 ± 1.41	21.23 ± 1.61	<0.001
DeRitis ratio	1.08 ± 0.06	0.92 ± 0.03	<0.001
FBS	87.59 ± 3.11	94.92 ± 4.69	<0.001
Fasting insulin	5.34 ± 2.04	8.35 ± 1.90	<0.001
HOMA-IR	1.16 ± 0.53	1.97 ± 0.50	<0.001
HOMA-IR ranges			
<1.6	51 (83.6)	7 (17.9)	<0.001
1.6–2.5	7 (11.5)	22 (56.4)	
≥2.5	3 (4.9)	10 (25.6)	
DeRitis ratio and IR diagnosis			
>1	10 (16.4)	33 (84.6)	<0.001
≤1	51 (83.6)	6 (15.4)	

* data were presented in the form of frequency (percentage) or mean ± standard deviation, based on the type of variables, Student's t-test

A significant positive correlation was observed between the DeRitis ratio and HOMA-IR (Pearson's r=0.516; p<0.001), indicating that higher IR was associated with an altered transaminase ratio. The ROC curve demonstrated an AUC of 0.778 (95% CI: 0.675–0.865), confirming the discriminatory ability of the DeRitis ratio in detecting IR. The overall diagnostic accuracy was 83% (95% CI: 74.3–90.1%), and Youden's index was 66%, suggesting that the DeRitis ratio demonstrated moderate discrimination for identifying IR among non-obese patients and is presented in Table 4 and Figure 1.

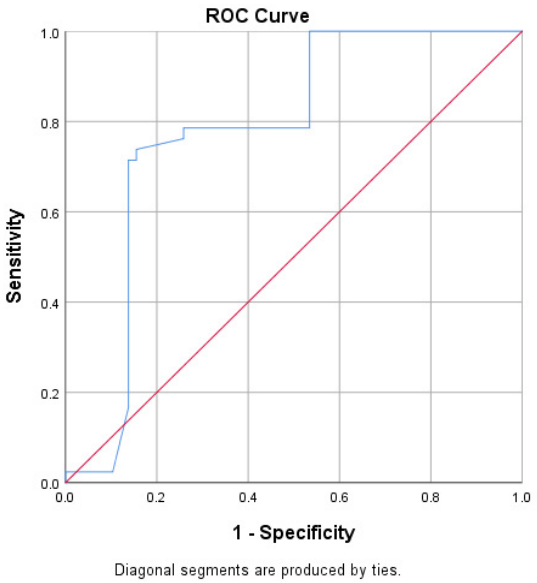

Fig. 1. ROC curve of the DeRitis ratio for the diagnosis of insulin resistance

Table 4. Diagnostic accuracy of DeRitis ratio for insulin resistance diagnosis*

Variables	Result	95% CI
Sensitivity (%)	82.50	57.3–96.2
Specificity (%)	83.33	73.4–90.9
Positive predictive value (%)	76.74	50.1–93.2
Negative predictive value (%)	87.72	78.5–94.0
Accuracy	83	74.3–90.1
Area under the curve*	0.778	0.675–0.865
Youden's index (J) (%)	66	

* the 95% confidence interval (CI) was calculated using DeLong's estimate, with a standard error (SE) of approximately 0.048; diagnostic accuracy was assessed at the pre-specified threshold of a DeRitis ratio greater than 1.0, CI – confidence interval

Discussion

This present cross-sectional study of 100 non-obese adults in Pondicherry demonstrated that 43% had IR, with prevalence markedly higher among overweight individuals (84.6%) compared to participants with normal BMI (16.4%). The research identified a substantial correlation between the DeRitis ratio and HOMA-IR (r=0.516; p<0.001), with ROC analysis producing an

AUC of 0.778 and a diagnostic accuracy of 83%. These findings suggest that the DeRitis ratio can serve as a simple, inexpensive biochemical marker for identifying IR in non-obese adults, complementing or substituting for insulin-based assays in resource-limited settings.

Obesity and overweight are now established as major public health problems. The WHO estimated that obesity affects over a billion people globally, with prevalence doubling since 1990.[2,5] In the present study, the prevalence of overweight was 39%. In India, recent estimates place obesity prevalence between 11.8% and 40.3%, varying by region and gender.[19,22] In this study population, while restricted to non-obese individuals, it highlights that IR is not limited to overt obesity, reinforcing prior evidence that metabolic dysfunction can occur even at lower BMI thresholds in Asian population warranting re-evaluation of risk stratification paradigms for this population.[23,24]

When comparing the ALT and AST levels between the groups, the mean ALT among overweight people is 23.05±1.614 IU/L vs 6.28±1.255 IU/L in normal BMI patients and is statistically significant, and the mean AST among overweight and normal patients (21.23±1.613 IU/L vs 17.61±1.41 IU/L) is statistically significant. Similar to our results, a study done by Jalili et al.,[4] showed that ALT and AST levels were found to be higher among the obese than the non-obese individuals. This finding was further supported by Momo et al.[25] and Song et al.[26], where liver enzymes such as ALT and AST were found to be higher among obese individuals. Although the mechanism is not understood, it is found that increased accumulation of fat in liver cells and disruption of hepatocytes results in elevated liver enzymes.[3,6,10]

The DeRitis ratio, introduced by DeRitis in 1957,[12,27] has long served as a biomarker of hepatic injury, mitochondrial compromise, and systemic inflammatory load. Recently, its prognostic value has expanded to cover NAFLD, cardiovascular outcomes, and malignancies.[11,28] The present study extends its utility, demonstrating that even within non-obese cohorts, shifts in transaminase balance mirror metabolic risk and correlate with IR.[14,15] Mechanistically, IR in obesity arises from ectopic lipid accumulation, inflammatory cytokine cascades, and mitochondrial dysfunction, culminating in hepatic lipotoxicity and altered enzyme release.[7,8] A reduced AST/ALT ratio reflects relative ALT elevation due to hepatocellular steatosis and mitochondrial injury. In the non-obese population, this pattern hints at subclinical NAFLD. The present study results, revealing lower DeRitis ratios in individuals with IR, align with observed biochemical shifts in early metabolic derangement.

In the present study, the DeRitis ratio between the participants in the overweight (0.920±0.035) and normal groups (1.084±0.060) was compared and found to be statistically significant and higher among the overweight participants. A study by Ndrepepa et al.,[12] found that the DeRitis ratio was >1.0 among obese participants, and >2 was noted among participants with alcoholic fatty liver disease. The DeRitis ratio was also found to be associated with the increased risk of mortality among participants with obesity.[11,13,28]

The HOMA-IR is used to assess IR in individuals; in our study, the mean HOMA-IR among the overweight and normal BMI participants was 1.97±0.51 vs 1.17±0.53. Our finding of a moderate positive correlation between the DeRitis ratio and HOMA-IR (r=0.516) is consistent with earlier surveys demonstrating that ALT/AST or AST/ALT ratios are valid surrogates of IR. The study by Lee et al.,[29] showed that the obese individuals were found to have higher levels of HOMA-IR values than the non-obese individuals. Similarly, a study by Raj et al.,[30] also showed a positive correlation between the HOMA-IR and the BMI. A study by Kawamoto et al.,[14] found that ALT/AST is the best IR surrogate in non-obese Japanese adults, and Han et al.,[15] confirmed this in a large Korean cohort. Vozarova et al., further reported that elevated ALT predicts future T2DM.[16] We are adding to this corpus by validating that the DeRitis ratio performs comparably in predicting IR among the non-obese Indian adults, thus reinforcing its prospective clinical relevance in screening and risk stratification.

Given the low cost and widespread availability of transaminases, the AST/ALT ratio may complement risk screening in situations where insulin assays are unavailable; however, its performance is insufficient for diagnosis and requires external validation. To align claims with the evidence, we intentionally avoid diagnostic language and frame the DeRitis ratio as a screening adjunct rather than a standalone test.

This study is among the few from South India that specifically investigates the association between the DeRitis Ratio and IR in non-obese adults, an often-overlooked subgroup in metabolic research at lower BMI compared with Japanese and Korean cohorts.[14,15,26] By demonstrating a significant association between the DeRitis ratio and IR in this ethnic group, the study fills an important geographic and metabolic evidence gap and extends the applicability of transaminase-based markers to a high-risk South Asian population. Moreover, the use of standardised biochemical methods improved the internal validity of the findings. The inclusion of both normal and overweight participants within the non-obese BMI range allowed meaningful subgroup comparisons. The diagnostic evaluation of the DeRitis Ratio adds quantitative rigour and translational clinical value.

Nonetheless, this study has limited novelty relative to prior enzyme-based markers; the sample size is small, from a single tertiary center, which limits precision and generalizability. The cross-sectional design precludes causal inference and may introduce spectrum bias. More-

over, the assessment of HOMA-IR has inherent methodological constraints and is considered a surrogate and not a gold-standard clamp. The HOMA-IR index is influenced by pancreatic β-cell function and showed variability with age, sex, and pubertal stages, which might affect its accuracy across different physiological states. Because HOMA-IR provides only a static estimate derived from fasting glucose and insulin, it does not capture dynamic glucose-insulin interactions over a 24-hour period. Additionally, its reproducibility has been reported as moderate and lower for indices such as the Quantitative Insulin Sensitivity Check Index (QUICKI).[31] Recent evidence suggests that the triglyceride-glucose (TyG) index demonstrates superior diagnostic performance for IR[32] and could be explored in future studies for comparison. Although the present study demonstrates a significant association between the DeRitis ratio and IR, it is important to acknowledge the role of potential confounders that might influence the study findings. Factors such as hepatic steatosis by imaging, alcohol intake quantification, diet, physical activity, medications, raising residual confounding and spectrum bias.

Future multicenter studies with larger, more diverse cohorts are recommended to validate the association between the DeRitis ratio and IR in non-obese adults. Comparative analyses using alternative IR indices such as the TyG index, QUICKI, and clamp-based methods could provide more robust evidence and determine which index most accurately reflects metabolic risk in the South Asian population. Incorporating validated dietary assessment, objective alcohol consumption measures, and liver imaging along with longitudinal follow-up could help establish temporal relationships between hepatic enzyme alterations and metabolic dysfunction and yield more precise estimates of the independent relationship between DeRitis ratio and IR. Exploring sex- and age-specific cut-offs for both HOMA-IR and the DeRitis ratio would also improve diagnostic precision in clinical screening.

Conclusion

Given the rising burden of metabolic disorders in India, even among individuals with normal or near-normal BMI, the DeRitis ratio offers a simple, inexpensive, and readily available biochemical marker for early identification of at-risk individuals. The present study demonstrated that the DeRitis ratio is associated with IR and shows moderate discrimination. Findings should be viewed as hypothesis-generating and require confirmation in larger, multicenter cohorts with a comprehensive confounder assessment.

Acknowledgements

We thank all the laboratory technicians, medical interns and nurses for their generous assistance and support. I also extend my gratitude to the patients for their willingness and consistent support.

Declarations

Funding

This research did not receive any specific funding from any public, commercial, or no-for-profit-sector agencies.

Author contributions

Conceptualization, K.S.C., S.S. and V.R.; Methodology, V.R.; Software, S.K.; Validation, K.S.C., and S.S.; Formal Analysis, S.K. and V.R.; Investigation, S.K.; Resources, S.K. and V.R.; Data Curation, V.R; Writing – Original Draft Preparation, S.K. and V.R..; Writing – Review & Editing, K.S.C. and S.S.; Visualization, V.R..; Supervision, K.S.C.; Project Administration, V.R.; Funding Acquisition, S.K.

Conflicts of interest

With respect to the research, authorship, and publication of this article, the authors declared no potential conflicts of interest.

Data availability

This published article includes all the data generated or analyzed during the study.

Ethics approval

This study was approved by the Institutional Ethical Committee (MGMCRI/Res/01/2023/115/IHEC/106).

References

1. NCD Risk Factor Collaboration (NCD-RisC). Worldwide trends in underweight and obesity from 1990 to 2022: a pooled analysis of 3663 population-representative studies with 222 million children, adolescents, and adults. *Lancet*. 2024;403(10431):1027-1050. doi:10.1016/S0140-6736(23)02750-2
2. James WPT. WHO recognition of the global obesity epidemic. *Int J Obes*. 2008;32(suppl 7):S120-S126. doi:10.1038/ijo.2008.247
3. El-Eshmawy MM. Impact of obesity on liver function tests: Is nonalcoholic fatty liver disease the only player? A review article. *Porto Biomed J*. 2023;8(5):e228. doi:10.1097/j.pbj.0000000000000228
4. Jalili V, Poorahmadi Z, Hasanpour Ardekanizadeh N, et al. The association between obesity with serum levels of liver enzymes, alanine aminotransferase, aspartate aminotransferase, alkaline phosphatase and gamma-glutamyl transferase in adult women. *Endocrinol Diabetes Metab*. 2022;5(6):e367. doi:10.1002/edm2.367
5. World Health Organization. One in eight people are now living with obesity. WHO News. https://www.who.int/news/item/01-03-2024-one-in-eight-people-are-now-living-with-obesity. Accessed September 3, 2025.

6. Ghotbi S, Joukar F, Orang Goorabzarmakhi M, et al. Evaluation of elevated serum liver enzymes and metabolic syndrome in the PERSIAN Guilan cohort study population. *Heliyon*. 2024;10(11):e32449. doi:10.1016/j.heliyon.2024.e32449
7. Arneth B. Mechanisms of Insulin Resistance in Patients with Obesity. *Endocrines*. 2024;5(2):153-165. doi:10.3390/endocrines5020011
8. Zhao X, An X, Yang C, Sun W, Ji H, Lian F. The crucial role and mechanism of insulin resistance in metabolic disease. *Front Endocrinol*. 2023;14:1149239. doi:10.3389/fendo.2023.1149239
9. Jin X, Qiu T, Li L, et al. Pathophysiology of obesity and its associated diseases. *Acta Pharm Sin B*. 2023;13(6):2403-2424. doi:10.1016/j.apsb.2023.01.012
10. Geißler C, Krause C, Neumann AM, et al. Dietary induction of obesity and insulin resistance is associated with changes in Fgf21 DNA methylation in liver of mice. *J Nutr Biochem*. 2022;100:108907. doi:10.1016/j.jnutbio.2021.108907
11. Shaikh SM, Varma A, Kumar S, Acharya S, Patil R. Navigating disease management: a comprehensive review of the De Ritis ratio in clinical medicine. *Cureus*. 2024;16(7):e64447. doi:10.7759/cureus.64447
12. Ndrepepa G, Holdenrieder S, Kastrati A. Prognostic value of DeRitis ratio with aspartate aminotransferase and alanine aminotransferase within the reference range. *Clin Chim Acta*. 2023;538:46-52. doi:10.1016/j.cca.2022.11.005
13. Li Q, Lan W. Association between DeRitis ratio (AST/ALT) and mortality in patients with chronic kidney disease: a retrospective cohort study. *Sci Rep*. 2025;15:9649. doi:10.1038/s41598-025-93184-1
14. Kawamoto R, Kohara K, Kusunoki T, Tabara Y, Abe M, Miki T. Alanine aminotransferase/aspartate aminotransferase ratio is the best surrogate marker for insulin resistance in non-obese Japanese adults. *Cardiovasc Diabetol*. 2012;11(1):117. doi:10.1186/1475-2840-11-117
15. Han SK, Seo MJ, Lee T, Kim MY. Effectiveness of the ALT/AST ratio for predicting insulin resistance in a Korean population: A large-scale, cross-sectional cohort study. *PLOS ONE*. 2024;19(5):e0303333. doi:10.1371/journal.pone.0303333
16. Vozarova B, Stefan N, Lindsay RS, et al. High alanine aminotransferase is associated with decreased hepatic insulin sensitivity and predicts the development of type 2 diabetes. *Diabetes*. 2002;51(6):1889-1895. doi:10.2337/diabetes.51.6.1889
17. Narayan KMV, Kanaya AM. Why are South Asians prone to type 2 diabetes? A hypothesis based on underexplored pathways. *Diabetologia*. 2020;63(6):1103-1109. doi:10.1007/s00125-020-05132-5
18. Misra A, Soares MJ, Mohan V, et al. Body fat, metabolic syndrome and hyperglycemia in South Asians. *J Diabetes Complications*. 2018;32(11):1068-1075. doi:10.1016/j.jdiacomp.2018.08.001
19. Venkatrao M, Nagarathna R, Majumdar V, Patil SS, Rathi S, Nagendra H. Prevalence of obesity in India and its neurological implications: a multifactor analysis of a nationwide cross-sectional study. *Ann Neurosci*. 2020;27(3-4):153-161. doi:10.1177/0972753120987465
20. Mahajan K, Batra A. Obesity in adult asian indians- the ideal BMI cut-off. *Indian Heart J*. 2018;70(1):195. doi:10.1016/j.ihj.2017.11.020
21. Minh HV, Tien HA, Sinh CT, et al. Assessment of preferred methods to measure insulin resistance in Asian patients with hypertension. *J Clin Hypertens*. 2021;23(3):529-537. doi:10.1111/jch.14155
22. Ahirwar R, Mondal PR. Prevalence of obesity in India: A systematic review. *Diabetes Metab Syndr Clin Res Rev*. 2019;13(1):318-321. doi:10.1016/j.dsx.2018.08.032
23. Misra A, Khurana L. Obesity and the metabolic syndrome in developing countries. *J Clin Endocrinol Metab*. 2008;93(11 Suppl 1):S9-30. doi:10.1210/jc.2008-1595
24. Chan K, De Souza LR, Kobayashi K, Fuller-Thomson E. Diabetes and diabetes care among non-obese South Asian Americans: Findings from a population-based study. *Diabetes Metab Syndr*. 2019;13(1):96-102. doi:10.1016/j.dsx.2018.08.025
25. Momo FR, Hoque MR, Sarkar S, Faysal MR, Mitu SA, Suchi SS. Comparison of serum alanine aminotransferase and aspartate aminotransferase among obese and non-obese adults. *Mymensingh Med J MMJ*. 2024;33(4):955-961.
26. Song HR, Yun KE, Park HS. Relation between alanine aminotransferase concentrations and visceral fat accumulation among nondiabetic overweight Korean women. *Am J Clin Nutr*. 2008;88(1):16-21. doi:10.1093/ajcn/88.1.16
27. DeRitis F, Coltorti M, Giusti G. An enzymic test for the diagnosis of viral hepatitis: The transaminase serum activities. *Clin Chim Acta*. 2006;369(2):148-152. doi:10.1016/j.cca.2006.05.001
28. Botros M, Sikaris KA. The De Ritis ratio: the test of time. *Clin Biochem Rev*. 2013;34(3):117-130.
29. Lee S, Lacy ME, Jankowich M, Correa A, Wu WC. Association between obesity phenotypes of insulin resistance and risk of type 2 diabetes in African Americans: The Jackson Heart Study. *J Clin Transl Endocrinol*. 2020;19:100210. doi:10.1016/j.jcte.2019.100210
30. Raj A, Vijayakumar V. Correlation of HOMA IR with BMI. *Asian J Med Res*. 2021;10(3):5-8.
31. Mirzaalian Y, Nourian M, Gholamalizadeh M, et al. The association of quantitative insulin sensitivity indices (HOMA-IR and QUICKI) with anthropometric and cardiometabolic indicators in adolescents. *Arch Med Sci Atheroscler Dis*. 2019;4:e32-e37. doi:10.5114/amsad.2019.84411
32. Park MS. Triglyceride-glucose index predicts future metabolic syndrome in an adult population, Korea: a prospective cohort study. *Ann Clin Nutr Metab*. 2024;16(3):168-172. doi:10.15747/ACNM.2024.16.3.168

Rzeszów University Press 2026
ISSN 2544-1361 (online)
doi: 10.15584/ejcem.2026.1.22

http://www.ejcem.ur.edu.pl
European Journal of Clinical and Experimental Medicine
Eur J Clin Exp Med 2026; 24 (1): 129–137

ORIGINAL PAPER

Correlation of thyroid hormones with levels of iron and selenium in women with hypothyroidism in Basrah, Iraq

Maha Abood Hasani [1,2], Rana Dawood Salman [2], Falah Hassan Shari [3]

[1] Basrah Health Directory, Basrah, Iraq
[2] Department of Clinical Laboratory Sciences, College of Pharmacy, University of Basrah, Basrah, Iraq
[3] Department of Clinical Laboratory Sciences, College of Pharmacy, Almaaqal University, Basrah, Iraq

ABSTRACT

Introduction and aim. Trace elements play a critical role in thyroid hormone synthesis and metabolism; however, data on their combined alterations in hypothyroid women from the Middle East remain limited. This study aimed to evaluate the relationship between serum selenium (Se) and iron (Fe) levels and thyroid function in women with overt and subclinical hypothyroidism compared with euthyroid controls.

Material and methods. In this case-control study, 312 women were enrolled, including 194 patients with hypothyroidism and 118 age- and body mass index-matched euthyroid controls recruited in Basra, Iraq. Serum thyroid-stimulating hormone (TSH), free thyroxine (FT4), iron (Fe), and Se were measured using standardized automated assays.

Results. Hypothyroid women had significantly higher median thyroid-stimulating hormone levels than controls (4.51 [1.9–7.5] vs. 1.45 [0.98–2.1] mU/L; p<0.0001) and lower median free thyroxine concentrations (12.48 [9.0–16.47] vs. 16.73 [14.16–20.59] pmol/L; p<0.0001). Serum iron levels were significantly reduced in hypothyroid patients (11.52 [7.79–15.83] vs. 15.90 [10.47–19.42] µmol/L; p<0.0001), as were selenium levels (0.81 [0.55–1.12] vs. 1.45 [1.18–1.92] µmol/L; p<0.0001). Age correlated positively with thyroid-stimulating hormone (Spearman's ρ=0.449, p<0.001) and negatively with free thyroxine (ρ=-0.301, p=0.007), while no significant correlations were observed for iron or selenium.

Conclusion. Women with hypothyroidism exhibited combined selenium and iron deficiencies alongside marked hormonal disturbances. To our knowledge, this is one of the first large case-control studies in women from southern Iraq to simultaneously assess selenium and iron status in relation to thyroid function. These findings support the potential clinical relevance of routine micronutrient assessment in hypothyroid patients, particularly in regions with known dietary deficiencies.

Keywords. hypothyroidism, iron, selenium, trace elements, women

Introduction

Hypothyroidism is an endocrine disorder characterized by a severe reduction in circulating thyroid hormones. Common etiologic factors include autoimmune thyroid disease, thyroidectomy, or therapeutic iodine radiotherapy. Even in iodine-replete regions, prevalence may reach 11.7%.[1,2] Epidemiological data on thyroid disorders in the Middle East are limited and largely anecdotal; however, Basra is considered a highly endemic area, with local findings indicating a particularly high prevalence of hypothyroidism among women[3] Thyroid hormones are essential for numerous physiological processes, including thermoregulation, carbohydrate, protein and lipid metabolism, electrolyte balance, and mineral homeostasis.[4]

Corresponding author: Maha Abood Hasani, e-mail: mahaalmammory1000@gmail.com

Received: 21.10.2025 / Revised: 22.11.2025 / Accepted: 23.11.2025 / Published: 30.03.2026

Hasani MA, Salman RD, Shari FH. Correlation of thyroid hormones with levels of iron and selenium in women with hypothyroidism in Basrah, Iraq. *Eur J Clin Exp Med.* 2026;24(1):129–137. doi: 10.15584/ejcem.2026.1.22.

Among the micronutrients implicated in thyroid function, selenium (Se) and iron (Fe) are indispensable for thyroid hormone synthesis and metabolism.[5]

Although the total selenium content of the human body is relatively small (10–20 mg), the thyroid gland contains one of the highest concentrations per gram of tissue, reflecting its strong dependence on selenoproteins (SePs) for normal function.[6,7] During thyroid hormone synthesis, hydrogen peroxide (H_2O_2) is required as an oxidizing agent for iodination. However, excessive H_2O_2 – particularly in the context of iodine deficiency and elevated TSH – can lead to oxidative injury of thyrocytes. Selenium-dependent enzymes, including glutathione peroxidases (GPxs) and thioredoxin reductases (TRs), function as key thiol-redox systems that neutralize H_2O_2 and lipid hydroperoxides, thereby maintaining cellular membrane integrity and limiting oxidative damage.[8]

The GPx family consists of several isoenzymes (GPx1–GPx6). GPx1 is abundant in the cytosol and reduces H_2O_2 and free hydroperoxides, while GPx3 and GPx4 are particularly relevant within the thyroid gland. GPx3 acts extracellularly, whereas GPx4 (phospholipid hydroperoxidase) regulates phospholipid and cholesterol hydroperoxide reduction, contributing to membrane stability and apoptotic control.[9] Through these mechanisms, selenium plays a central role in antioxidative and inflammation-protective defense. Insufficient selenium intake decreases GPx activity, weakens antioxidative capacity, and increases the risk of thyrocyte injury and apoptosis. Additionally, selenium is required as a cofactor for iodothyronine deiodinases, which convert thyroxine (T_4) to the biologically active triiodothyronine (T_3), supporting normal thyroid hormone metabolism and protecting the gland from oxidative stress.[10,11] According to the World Health Organization, the recommended daily selenium intake for adults is 55 μg.[12]

Selenium availability varies considerably worldwide. Selenium-rich soils are found in regions such as Australia, Ireland, and North America, whereas large areas of Europe, New Zealand, and China are selenium-poor. Importantly, several Middle Eastern countries, including Iraq, have been reported to exhibit low-to-moderate selenium intake due to poor soil selenium content, potentially predisposing their populations to marginal selenium deficiency and altered thyroid hormone metabolism.[13]

Iron is also essential for normal thyroid function. It acts as a cofactor for thyroid peroxidase (TPO), the heme-containing enzyme that catalyzes iodination and coupling reactions during thyroid hormone synthesis. Iron deficiency reduces TPO activity, thereby impairing the production of thyroid hormones. Furthermore, as a key component of hemoglobin, iron supports oxygen delivery to tissues and participates in multiple enzymatic pathways essential for cellular metabolism. Iron deficiency may also diminish erythropoiesis and decrease erythropoietin secretion, further contributing to impaired thyroid hormone synthesis.[14] Despite the established role of selenium and iron in thyroid hormone metabolism, data on their simultaneous alterations in women with hypothyroidism from the Middle East remain scarce. To our knowledge, this is one of the first studies in southern Iraq to jointly evaluate selenium and iron status in relation to thyroid function in a large female case–control cohort.

Aim

The aim of this study was to assess the relationship between serum selenium and iron levels and thyroid function in women with overt and subclinical hypothyroidism compared with euthyroid controls, addressing the lack of data from the Middle Eastern population.

Material and methods

Study design and subjects

The present retrospective case-control study was organized at the Faiha Specialized Diabetes, Endocrine, and Metabolism Center (FDEMC) laboratories in Basra, Southern Iraq, from November 2024 to May 2025.

Ethical approval

The study was approved by the Institutional Review Board of the College of Pharmacy, University of Basrah (Approval No. EC 81, dated 10/11/2024). Written informed consent was obtained from all participants prior to study enrollment.

Participants and eligibility criteria

Enrollment included women clinically diagnosed with primary and subclinical hypothyroidism, as established through clinical evaluation and laboratory tests for thyroid function, particularly serum FT4 levels and TSH concentrations. A control group of euthyroid women has been established to enable comparative analyses. The participants were selected based on predefined eligibility criteria as follows:

Inclusion criteria

- Women aged 18–78 years, covering both the reproductive period and the menopausal transition, which may influence thyroid function and mineral metabolism.
- Clinically diagnosed primary (overt) hypothyroidism, defined as:
  - TSH>4.2 mU/L
  - FT4<12 pmol/L
- Clinically diagnosed subclinical hypothyroidism, defined as:
  - TSH>4.2 mU/L
  - FT4 within the normal reference range (12.0–21.9 pmol/L)

- Reference ranges (manufacturer instructions):
  - TSH: 0.27–4.2 mU/L
  - FT4: 12.0–21.9 pmol/L

Exclusion criteria

Participants were excluded if they had any of the following:

- other thyroid diseases (e.g., autoimmune thyroid disorders such as Hashimoto's thyroiditis), excluded based on review of available medical records
- major systemic conditions (e.g., diabetes mellitus, chronic kidney disease),
- use of hormonal contraceptives or any nutritional supplements (e.g., selenium, iron, multivitamins),
- smoking,
- malabsorption syndromes,
- pregnancy,
- other endocrine disorders,
- lack of consent to participate.

Levothyroxine treatment status was recorded descriptively and was not used as an exclusion criterion.

A summary of the selection process is presented in Figure 1.

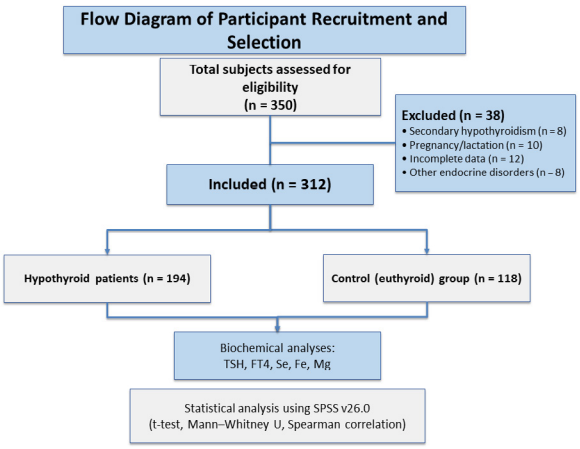

Fig. 1. Flow diagram of participant recruitment and selection process

Dietary and lifestyle considerations

To minimize dietary and lifestyle confounding, women taking any nutritional supplements (selenium, iron, or multivitamins) were excluded, and all participants were recruited from the same geographical and socioeconomic background. Dietary intake and lifestyle behaviors were not quantitatively assessed and are acknowledged as a methodological limitation; however, the shared environmental and cultural dietary patterns of the study population help reduce major variability in selenium and iron intake.

Sample size calculation

Sample size was calculated based on expected differences in serum selenium and iron levels between hypothyroid and euthyroid women, assuming an effect size of d=0.35–0.40, α=0.05, and power=0.90.[15]

A structured questionnaire was administered to collect demographic information, including questions on nutritional habits, socioeconomic status, medication use, and family history.

Blood collection and biochemical measurements

Following a 12-hour period of overnight fasting, a venous blood sample of approximately 5 mL was taken from all patients and controls under strict aseptic conditions and transferred to a sterile yellow top gel tube. Blood samples were allowed to clot and centrifuged at 5000 rpm for 5 minutes to obtain serum. Serum was isolated and preserved at -20°C till examination.

Thyroid hormone measurements

Serum thyroid hormones (FT4 and TSH) were computed via electrochemiluminescence immunoassay using a cobas e411analyzer (Roche Diagnostics, Germany).[16]

Trace-element measurements

Serum iron was quantified in vitro on the Roche/Hitachi Cobas C311 system (Roche Diagnostics, Germany) through a Ferrozine colorimetric endpoint by using IronGen.2 reagents, where the absorbance at 570 nm is directly related to iron concentration.[17,18]

Serum selenium was determined using a colorimetric assay (Elabscience®, Cat. No. E-BC-K776-M, China) according to the manufacturer's protocol. Selenium Assay Validation and Performance – The assay was performed on a microplate reader at 420 nm (range 415–425 nm). Intra- and inter-assay precision coefficients of variation (CV) were 0.3–0.4% and 0.5–0.7%, respectively, and mean recovery was 103.7%.

A colorimetric method was selected due to its validated analytical performance—adequate sensitivity for physiological selenium levels, excellent precision (CV <1%), and high recovery—while being fully compatible with our laboratory workflow and high-throughput processing. Selenium concentrations were reported in SI units (μmol/L) and were consistent with the Results section.

Statistical analysis

Data were processed with SPSS, version 26.0 (IBM, Armonk, NY, USA). Normality was tested by Kolmogorov-Smirnov test. Quantitative variables were presented as mean±SD for normally distributed ones or median (Q1–Q3) for those not following a normal distribution. Baseline differences of means were examined using an independent-samples t-test or Mann-Whitney U test as appropriate, and for categorical variables, the Chi-square (χ^2) test was used. Associations were tested using Spearman's rank-correlation coefficient (ρ). Statistical

significance was set at a two-tailed p<0.05. Graphs were made on GraphPad Prism, version 8 (USA).

Results

Demographic, reproductive, and anthropometric characteristics of the study population

A total of 312 women, including 118 controls and 194 hypothyroid patients, were included in a retrospective analysis. Baseline characteristics are shown in Table 1.

Table 1. Demographic and clinical characteristics of the study participants*

Variable	Control (n=118)	Hypothyroid (n=194)	p
Sociodemographic data			
Age (years), median (range)	41 (26–55)	43.5 (30–58)	0.446
Residence, n (%)	Urban 73 (61.86 %) Rural 45 (38.14 %)	Urban 139 (71.6 %) Rural 55 (28.3 %)	0.08
Income status, n (%)	Low 20 (16.94 %) Medium 76 (64.4 %) High 22 (18.64 %)	Low 82 (42.2 %) Medium 98 (50.5 %) High 14 (7.2 %)	<0.0001
Marital status, n (%)	Single 12 (10.16%) Married 96 (81.35%) Divorced 0 (0%) Widow 10 (8.47%)	Single 31 (15.9%) Married 133 (68.5%) Divorced 4 (2%) Widow 26 (13.4%)	0.614
Reproductive characteristics			
Cycle status, n (%)	Regular 59 (50 %) Irregular 21 (17.79 %) Menopause 38 (32.2 %) Amenorrhea 0 (0 %)	Regular 18 (9.3 %) Irregular 75 (38.6 %) Menopause 78 (40.2 %) Amenorrhea 23 (11.8 %)	<0.0001
Childbearing, n (%)	Yes 115 (97.46 %) No 3 (2.54 %)	Yes 165 (85 %) No 29 (14.9 %)	0.0004
Anthropometric data			
Height (m), median (range)	159 (1.54–1.64)	1.59 (1.55–1.63)	0.489
Weight (kg), mean±SD	75.3±18.1	79.5±18.4	0.051
BMI (kg/m^2), mean±SD	29.75 ± 5.3	31.54 ± 6.7	0.117
Disease-related data			
Duration of disease (years), median (range)	–	5.0 (2.0–8.0)	–
Family history of disease, n (%)	No 118 (100 %)	Yes 96 (49.4 %) No 98 (50.5 %)	<0.0001
Levothyroxine therapy, n (%)			
50 µg 1×1	–	119 (61.3 %)	–
50 µg 1×2	–	8 (4.1 %)	–
100 µg 1×1	–	63 (32.4 %)	–
Discontinued	–	4 (2.0 %)	–

* Data were tested for normality using the Kolmogorov–Smirnov test; normally distributed data are presented as mean±SD and non-normal data as median [interquartile range, IQR], comparisons were performed using the t-test, Mann–Whitney U, Chi-square, or Fisher's exact test, as appropriate

The two populations did not differ for a common age; the median ages were 41 and 43.5 years respectively (p=0.446), confirming that the groups were age-matched. With respect to residence distribution, for hypothyroid women, more lived in city areas (71.6%) than controls (61.8%); however, the difference was not significant (p=0.08).

Income status differed markedly between groups (p<0.0001): low-income individuals were more frequent among hypothyroid cases (42.2%) than among controls (16.9%), while high-income participants were fewer (7.2% vs. 18.6%, respectively).

Marital status did not vary significantly (p=0.614); most participants in both groups were married, and the proportions of single, divorced, and widowed women were comparable. Irregular and menopausal cycles were markedly more frequent in the hypothyroid group, and amenorrhea occurred exclusively among hypothyroid patients (11.9%). Childbearing history also differed significantly (p=0.0004), as nearly all controls had given birth (97.5%) compared with 85% of hypothyroid women.

Anthropometric data were largely comparable between groups. Median height was 1.59 m in both (p=0.489). The mean body weight tended to be higher in hypothyroid patients (79.5±18.4 kg) than controls (75.3±18.1 kg), though the difference narrowly missed statistical significance (p=0.051). Similarly, BMI values were slightly higher among hypothyroid women (31.5±6.7 kg/m^2) than controls (29.8±5.3 kg/m^2, p=0.117).

Among hypothyroid patients, the median disease duration was 5 years (range: 2–8 years). Approximately half (49.5%) reported a family history of thyroid disease, a rate significantly higher than in controls (0%; p<0.0001), suggesting a potential familial or genetic predisposition. Regarding levothyroxine therapy, most patients (61.3%) were receiving 50 µg daily, 32.5% were on 100 µg daily, 4.1% were taking 50 µg twice daily, and 2.1% had discontinued treatment.

Comparison of biochemical and clinical parameters between control and patient groups

Descriptive and comparative analyses were conducted for serum TSH, FT4, Fe, and Se across the control and hypothyroid groups. As the data were not normally distributed, intergroup comparisons were performed using the Mann-Whitney U test, and differences were considered statistically significant at p<0.05.

Hypothyroid patients showed a significant increase in TSH levels compared to the control group (p<0.0001), which was associated with a large effect size (r=0.50, CI: 2.1–3.4). In contrast, the concentration of FT4 was significantly lower in the hypothyroid group (p<0.0001), with a large effect (r=–0.7, 95% CI: -7 to -2.8). In addition, serum levels of iron and selenium were significantly decreased in hypothyroid patients compared with controls (p<0.0001). Reduction in Fe showed a moderate effect size (r=0.36, 95% CI: -4.8 to -1.8), while that of Se was high (r=0.64, 95% CI: -0.78 to -0.56).

A comprehensive summary of these findings is presented in Table 2.

Table 2. Comparison of TSH, FT4, iron, and selenium levels between control and patient groups*

Parameter	Control (Median [IQR])	Patient (Median [IQR])	p	Effect size (r)	95% CI of difference
TSH (mU/L)	1.45 (0.98–2.1)	4.51 (1.9–7.5)	<0.0001	0.5	2.10 to 3.40
FT4 (pmol/L)	16.73 (14.16–20.59)	12.48 (9.0–16.47)	<0.0001	0.7	-7.00 to -2.80
Fe (µmol/L)	15.90 (10.47–19.42)	11.52 (7.79–15.83)	<0.0001	0.36	-4.80 to -1.80
Se (µmol/L)	1.45 (1.18–1.92)	0.81 (0.55–1.12)	<0.0001	0.64	-0.78 to -0.56

* Values are expressed as median [interquartile range, IQR], statistical significance between groups was assessed using the Mann–Whitney U test, effect sizes (r) were interpreted as small (0.10–0.29), moderate (0.30–0.49), or large (≥ 0.50)

The pattern of the results is also represented by comparison in Figure 2, showing trends toward hormonal and biochemical changes between study groups. The graph presents an evident negative relationship between thyroid function and trace-element status. Error bars represent the interquartile range, reflecting variability within each group, particularly the wider dispersion of TSH levels among hypothyroid patients, consistent with differences in disease severity and treatment status.

Statistical correlation results between age and each biochemical parameter in the hypothyroid group

The correlation between age and various categories of biochemical parameters in hypothyroid patients was calculated by Spearman's rank correlation coefficient (ρ). As reported in Table 3, there was a statistically significant moderate positive correlation between age and serum TSH (ρ=+0.449, p<0.001), showing that also TSH increases with aging. This indicates that the severity of thyroid failure or the extent of pituitary input becomes more severe with increasing age.

Inversely, serum FT4 negatively correlated with age (ρ=-0.301, p=0.007), showing the decrease of T4 concentration in the bloodstream with aging.

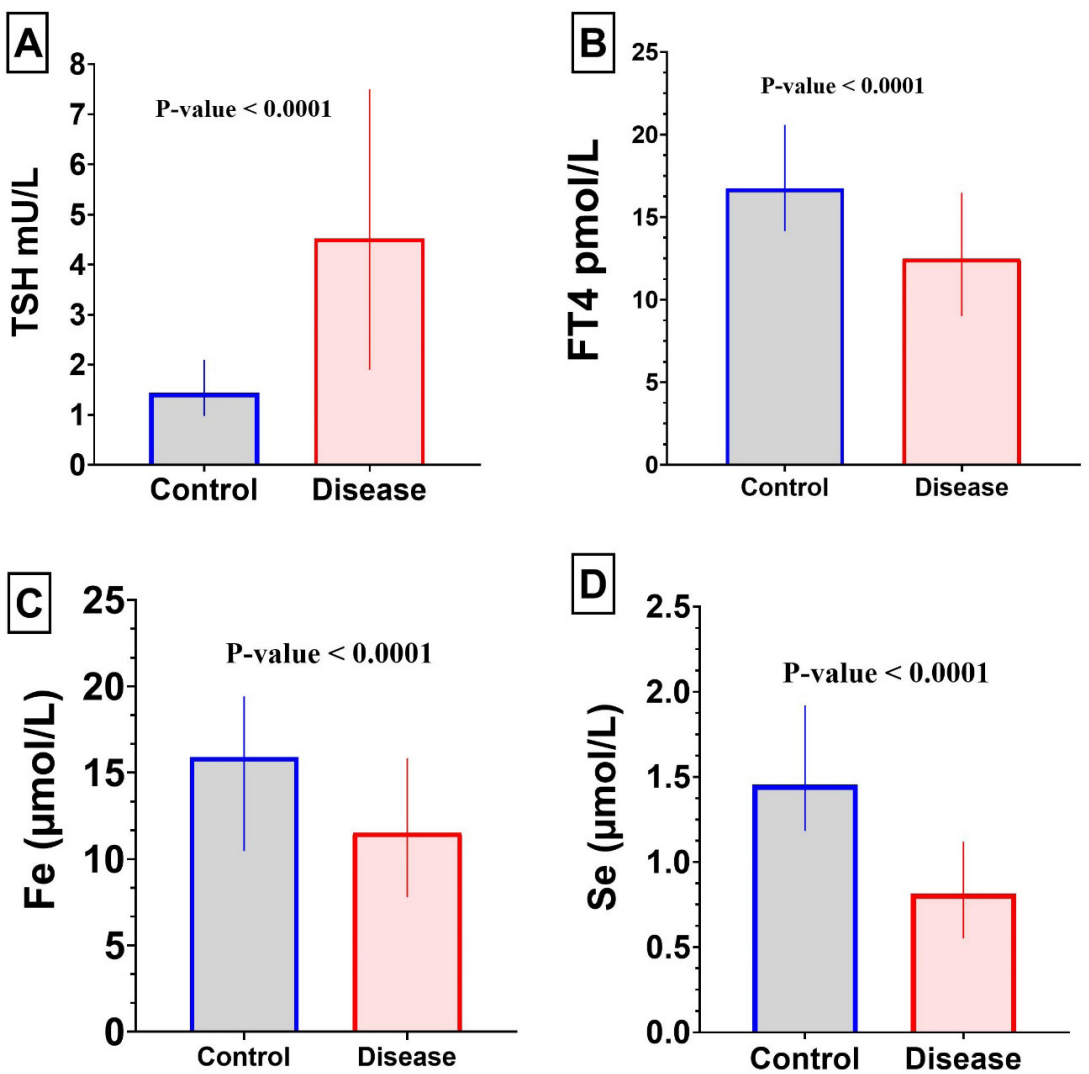

Fig. 2. Comparative visualization of (A) TSH, (B) FT4, (C) iron, and (D) selenium levels in hypothyroid patients and control subjects, values are expressed as median (interquartile range, IQR), and group comparisons were analyzed using the Mann-Whitney U test

Age was not associated with serum iron (ρ=-0.068, p=0.559) or selenium (ρ=–0.152, p=0.187). These results show that the trace-element status of hypothyroid patients is age-independent. The lack of correlation between serum levels of Fe and Se could indicate that changes are less influenced by age than by nutritional or pathological causes.

Table 3. Spearman's correlation between age and biochemical parameters in patients with hypothyroidism

Parameter	Spearman's ρ (Correlation coefficient)	p	Interpretation
TSH (mU/L)	+0.45 ↑	>0.0001	significant moderate positive correlation – TSH levels tend to increase with age
FT4 (pmol/L)	–0.30 ↓	0.007	significant negative correlation – FT4 levels decrease slightly as age increases
Fe (µmol/L)	–0.06 ↓	0.559	no significant correlation – serum iron is independent of age
Se (µmol/L)	–0.15 ↓	0.187	weak and non-significant negative trend – selenium levels slightly decrease with age, but not significantly

Discussion

The present study investigated the relationship between thyroid hormones and two essential trace elements – selenium and iron – in women diagnosed with hypothyroidism in Basra, Iraq. Although the hypothyroid and euthyroid groups were comparable in age and BMI, they differed significantly in income, menstrual regularity, parity, and family history – factors frequently associated with thyroid dysfunction and hormonal imbalance. The clear elevation in TSH and reduction in FT4, selenium, and iron among hypothyroid participants support the hypothesis that altered trace-element status may contribute to impaired thyroid hormone production, disturbed metabolism, and diminished antioxidative defense within the thyroid gland.[19]

Hypothyroid women exhibited a markedly lower median serum selenium concentration (0.81 µmol/L) compared with the control group (1.45 µmol/L), consistent with findings reported from Iran and other selenium-deficient regions.[20] Reduced selenium status – together with elevated TSH and lower T3/T4 ratios – may reflect impaired deiodination and weakening of the thyroid's antioxidative capacity, thereby reducing its functional reserve. DIO1 and DIO2, the key enzymes responsible for converting T4 into biologically active T3, are selenoproteins containing selenocysteine at their catalytic centers; their activity depends directly on adequate selenium availability. Experimental studies show that selenium-deficient animals exhibit significantly reduced DIO1 and DIO2 activity across tissues including liver, kidney, and brain.[21]

A recent review by Köhrle emphasized that the thyroid gland retains high selenium levels and expresses multiple selenoproteins, including deiodinases, and that selenium deficiency impairs both thyroid hormone production and metabolism through decreased selenoprotein expression.[22] In women with primary or subclinical hypothyroidism, low selenium may therefore reduce peripheral T4-to-T3 conversion, potentially causing relative T3 deficiency or increased rT3 formation, thereby diminishing thyroid hormone action in peripheral tissues. This provides a physiological rationale for the associations observed in the present cohort.

The absence of a strong association between selenium and FT4 in our results may reflect the multifactorial nature of thyroid regulation, where oxidative stress, genetic variation, and other micronutrient deficiencies influence hormone kinetics. In some individuals, normal T4-to-T3 conversion may be maintained despite low selenium through compensatory mechanisms such as hierarchical selenium distribution to essential selenoproteins and adaptive upregulation of DIO2 activity in peripheral tissues.

Nonetheless, the inverse relationship between selenium and TSH suggests that reduced selenium status may compromise negative-feedback regulation along the hypothalamic-pituitary-thyroid (HPT) axis. Given that the thyroid is one of the organs richest in selenium, adequate selenium intake is critical for maintaining redox homeostasis and protecting thyrocytes from H_2O_2-induced oxidative injury during hormone biosynthesis.[23,24] Epidemiological evidence supports these findings: Wu et al. reported a 3.6-fold higher prevalence of hypothyroidism among individuals with low selenium status, and serum selenium showed an inverse association with autoimmune thyroiditis, subclinical hypothyroidism, and goiter (odds ratio: 0.47–0.75). Experimental studies likewise demonstrate that selenium deficiency negatively affects T3 production and degradation, consistent with reduced DIO1 activity.[25]

In addition to selenium deficiency, hypothyroid women in this study had significantly lower serum iron concentrations. This aligns with previous research showing that iron deficiency impairs thyroid function.[26,27] Iron is indispensable for thyroid hormone synthesis because TPO – the enzyme responsible for iodide oxidation and coupling – is heme-dependent. Iron deficiency reduces TPO activity, thereby impeding thyroid hormone biosynthesis. Beyond TPO, iron deficiency may also disrupt peripheral thyroid hormone activation. A 2023 review by Garofalo et al. reported that iron deficiency interferes with thyroxine deiodinase activity and reduces T4-to-T3 conversion.[14]

Although the exact molecular pathways remain incompletely defined, experimental and clinical evidence strongly supports an effect of iron status on thyroid hormone metabolism. Beard et al. demonstrated that iron-deficient anemic rats have markedly reduced he-

patic 5′-deiodinase activity and lower plasma T3 turnover, indicating impaired peripheral conversion of T4 to T3.[28] More recent data by Monko et al. showed that cellular iron deficiency disrupts thyroid-hormone–regulated gene expression in developing hippocampal neurons, underscoring the importance of iron for downstream T3-dependent transcription.[29] In Chinese women during early pregnancy, Li et al. reported that low iron status was associated with alterations in thyroid hormone markers, including lower FT4.[30] A 2021 systematic review and meta-analysis by Luo et al. further concluded that iron deficiency is a significant risk factor for thyroid dysfunction, partly through impaired deiodinase activity and reduced T4-to-T3 conversion.[31]

In the present cohort, low serum iron may therefore impair peripheral deiodination and exacerbate hormonal imbalance, compounding the deficit associated with primary thyroid failure. It is also possible that low selenium and iron reflect consequences of hypothyroidism rather than primary causes, as thyroid hormone deficiency is known to reduce gastric absorption, impair intestinal motility, and alter iron mobilization.[32] Additionally, iron deficiency reduces TPO activity, further impairing thyroid hormone synthesis.[33] This bidirectional interaction underscores the importance of screening for micronutrient deficiencies in hypothyroid patients, particularly in regions where dietary deficits are common. Improving selenium and iron intake may offer meaningful benefits for thyroid function and clinical outcomes.[34,35] Previous studies investigating trace and toxic metals in hypothyroid and goitrous populations also support the concept that disturbances in essential elements such as selenium and iron occur alongside alterations in other biologically relevant metals, reinforcing the importance of comprehensive micronutrient assessment in thyroid disorders.[36–39]

Correlation analysis showed a moderate positive relationship between TSH and age, and a weak negative relationship between FT4 and age, suggesting that older hypothyroid patients tend to exhibit higher TSH and lower FT4 levels.[40] In contrast, age showed no significant association with selenium or iron, indicating that their levels may be shaped more by nutritional, metabolic, or disease-related factors than by chronological aging.[41] These findings are consistent with evidence that aging alters the HPT axis through impaired TSH metabolism, altered pituitary sensitivity, and diminished negative feedback.

The inverse association between age and FT4 observed in this study suggests that aging may exacerbate declining thyroid hormone production or reduce peripheral T4-to-T3 conversion. Although healthy older adults often maintain normal FT4 through compensatory TSH increases, such compensatory mechanisms may be insufficient in individuals with hypothyroidism. The lack of age-related variation in selenium or iron supports the notion that trace-element status reflects external nutritional and physiological determinants rather than aging alone.[40,42]

Clinical implications

These findings underscore the potential clinical value of assessing selenium and iron status in women with hypothyroidism, particularly in regions with known micronutrient deficiencies such as Basra. Optimizing dietary intake or considering targeted supplementation may support thyroid hormone metabolism and improve clinical outcomes; however, therapeutic recommendations should await confirmation from controlled interventional studies.

Study limitations

This study has several limitations. Dietary intake of selenium and iron was not evaluated, and other relevant factors – including vitamin D status, inflammatory markers, and autoimmune thyroid antibodies – were not assessed, all of which may influence thyroid function or trace-element metabolism. The cross-sectional design limits causal inference, and unmeasured confounders may persist despite group matching.

Future directions

Future research should incorporate longitudinal and interventional study designs to clarify the directionality of the observed associations and to determine whether correcting selenium and iron deficiencies can improve thyroid hormone profiles, deiodinase activity, or patient-reported outcomes. Randomized controlled trials are particularly needed to establish causality and to identify subgroups of hypothyroid women who may benefit most from micronutrient optimization.

Conclusion

In conclusion, women with hypothyroidism exhibited significantly lower selenium and iron levels together with marked disturbances in thyroid hormone parameters. These findings support a close association between trace-element status and thyroid dysfunction. The observed age-related changes in thyroid-stimulating hormone and free thyroxine further emphasize the complexity of thyroid regulation in hypothyroid women. Future interventional studies are needed to determine whether correcting selenium and iron deficiencies may improve thyroid function and clinical outcomes.

Acknowledgments

This study originates from a Master's thesis submitted to the Department of Clinical Laboratory Sciences at the College of Pharmacy, University of Basrah. The authors gratefully acknowledge the college's continuous support and valuable assistance during this research.

Declarations

Funding
Not applicable

Author contributions
Conceptualization, R.S. and F.H.; Methodology, M.H.; Software, R.S.; Validation, R.S. and F.H.; Formal Analysis, M.H.; Investigation, M.H.; Resources, R.S.; Data Curation, F.H.; Writing – Original Draft Preparation, M.H.; Writing – Review & Editing, R.S.; Visualization, F.H.; Supervision, R.S. and F.H.; Project Administration, M.H.

Conflicts of interest
The authors declare no competing interests.

Data availability
The corresponding author can be contacted to request access to the data, which will be made available upon reasonable request.

Ethics approval
The study was approved by the Research Ethics Committee of the University of Basrah, College of Pharmacy (Approval No. EC 81, dated 10/11/2024), and conducted in accordance with CIOMS/WHO ethical guidelines and the Belmont Report.

References

1. Wyne KL, Nair L, Schneiderman CP, et al. Hypothyroidism prevalence in the United States: a retrospective study combining National Health and Nutrition Examination Survey and claims data, 2009–2019. *J Endocr Soc*. 2022;7(1):1-11. doi:10.1210/jendso/bvac172
2. Al-Abdulaziz BA, Khalaf QH, Thuwaini MM. Correlation of zinc serum level with hypo- and hyperthyroidism. *Rev Latinoam Hipertens*. 2022;17(5):332-337. doi:10.5281/zenodo.7369239
3. Mansour AA, Ali Alhamza AH, Abdullah Almomin AMS, et al. Patterns of thyroid disease in Basrah, Iraq: a retrospective study. *J Endocr Soc*. 2020;4(suppl 1):SUN-418. doi:10.1210/jendso/bvaa046.772
4. Shahid MA, Ashraf MA, Sharma S. Physiology, thyroid hormone. In: *StatPearls*. Treasure Island, FL: StatPearls Publishing; 2025.
5. Zhou Q, Xue S, Zhang L, Chen G. Trace elements and the thyroid. *Front Endocrinol (Lausanne)*. 2022;13:904889. doi:10.3389/fendo.2022.904889
6. Zhao Y, Jia M, Chen W, Liu Z. The neuroprotective effects of intermittent fasting on brain aging and neurodegenerative diseases via regulating mitochondrial function. *Free Radic Biol Med*. 2022;182:206-218. doi:10.1016/j.freeradbiomed.2022.02.021
7. Tinggi U. Selenium: its role as antioxidant in human health. *Environ Health Prev Med*. 2008;13(2):102-108. doi:10.1007/s12199-007-0019-4
8. Kieliszek M, Bano I. Selenium as an important factor in various disease states: a review. *EXCLI J*. 2022;21:948-966. doi:10.17179/excli2022-5137
9. de Souza LSL, Campos R de O, Braga Filho J de S, et al. Selenium nutritional status and thyroid dysfunction. *Arch Endocrinol Metab*. 2025;69:1-13. doi:10.20945/2359-4292-2023-0348
10. Wang F, Li C, Li S, Cui L, Zhao J, Liao L. Selenium and thyroid diseases. *Front Endocrinol (Lausanne)*. 2023;14:1133000. doi:10.3389/fendo.2023.1133000
11. Bano I, Hassan MF, Kieliszek M. A comprehensive review of selenium as a key regulator in thyroid health. *Biol Trace Elem Res*. Published online May 13, 2025. doi:10.1007/s12011-025-04653-7
12. Kieliszek M, Serrano Sandoval SN. The importance of selenium in food enrichment processes: a comprehensive review. *J Trace Elem Med Biol*. 2023;79:127260. doi:10.1016/j.jtemb.2023.127260
13. Kieliszek M, Bano I, Zare H. A comprehensive review on selenium and its effects on human health and distribution in Middle Eastern countries. *Biol Trace Elem Res*. 2022;200(3):971-987. doi:10.1007/s12011-021-02716-z
14. Garofalo V, Condorelli RA, Cannarella R, Aversa A, Calogero AE, La Vignera S. Relationship between Iron Deficiency and Thyroid Function: A Systematic Review and Meta-Analysis. *Nutrients*. 2023;15(22):4790. doi:10.3390/nu15224790
15. Talebi S, Ghaedi E, Sadeghi E, et al. Trace element status and hypothyroidism: a systematic review and meta-analysis. *Biol Trace Elem Res*. 2020;197(1):1-14. doi:10.1007/s12011-019-01963-5
16. Pathan A, Yasin J, Sharma C, Alkaabi J, Agha A. Assessing thyroid peroxidase antibodies in Emirati medical students: a cross-sectional pilot study. *Front Endocrinol (Lausanne)*. 2025;16:1582933. doi:10.3389/fendo.2025.1582933
17. Lukovac T, Hil OA, Popović M, et al. Serum biomarker analysis in pediatric ADHD: implications of homocysteine, vitamin B12, vitamin D, ferritin, and iron levels. *Children*. 2024;11(4):497. doi:10.3390/children11040497
18. Chittineedi P, Pandrangi SL, Bellala RS, et al. Analyzing the drivers of cancer relapse: hypocalcemia and iron absorption in hormone-dependent female cancers. *Am J Transl Res*. 2022;14(9):6563-6573.
19. Rostami R, Nourooz-Zadeh S, Mohammadi A, Khalkhali HR, Ferns G, Nourooz-Zadeh J. Serum selenium status and its interrelationship with serum biomarkers of thyroid function and antioxidant defense in Hashimoto's thyroiditis. *Antioxidants (Basel)*. 2020;9(11):1070. doi:10.3390/antiox9111070
20. Heidari Z, Sheikhi V. Serum selenium status in Graves' disease and Hashimoto's thyroiditis in an iodine-sufficient area. *Journal of Research in Medical Sciences*. 2022;27(1):87. doi:10.4103/jrms.jrms_57_21
21. Arthur J, Nicol F, Beckett G. Selenium deficiency, thyroid hormone metabolism, and thyroid hormone deiodinases.

Am J Clin Nutr. 1993;57(2):236S-239S. doi:10.1093/ajcn/57.2.236S

22. Köhrle J. Selenium, iodine and iron—essential trace elements for thyroid hormone synthesis and metabolism. *Int J Mol Sci*. 2023;24(4):3393. doi:10.3390/ijms24043393
23. Adeleye OO, Ogunleye OO, Sodipo OO, Ale AO, Akinola IJ. Thyroid disorders and serum selenium levels in a Southwestern Nigerian population. *Int J Endocrinol*. 2025;2025(1):6915227. doi:10.1155/ije/6915227
24. Durmała K, Pyc G, Bęben D, et al. Correlation between selenium levels and thyroid cancer: a literature review. *J Pre Clin Clin Res*. 2024;18(4):345-352. doi:10.26444/jpccr/195942
25. Rostami R, Beiranvand A, Nourooz-Zadeh S, Rostami M, Mohammadi A, Nourooz-Zadeh J. Association between essential trace elements and thyroid antibodies in the blood of women with newly diagnosed Hashimoto's thyroiditis. *Int J Endocrinol Metab*. 2024;22(2):e145599. doi:10.5812/ijem-145599
26. Swapnika TG, Sabitha Rani SS, Dipankar S, Itagi ABH, Vamshidhar IS. A comparative study of iron status in subclinical hypothyroid and euthyroid subjects in a tertiary care hospital. *Cureus.* 2024;16(1):1-7. doi:10.7759/cureus.52007
27. Koç Ş, Güngör K, Dokuzeylül Güngör N, Uzunlulu M. Iron deficiency in women with thyroid-specific autoantibodies: a case control study. *J Exp Clin Med*. 2022;39(1):194-198. doi:10.52142/omujecm.39.1.38
28. Beard J, Tobin B, Green W. Evidence for thyroid hormone deficiency in iron-deficient anemic rats. *J Nutr*. 1989;119(5):772-778. doi:10.1093/jn/119.5.772
29. Monko TR, Tripp EH, Burr SE, et al. Cellular iron deficiency disrupts thyroid hormone regulated gene expression in developing hippocampal neurons. *J Nutr*. 2023;154(1):49. doi:10.1016/j.tjnut.2023.11.007
30. Li S, Gao X, Wei Y, Zhu G, Yang C. The relationship between iron deficiency and thyroid function in Chinese women during early pregnancy. *J Nutr Sci Vitaminol (Tokyo)*. 2016;62(6):397-401. doi:10.3177/jnsv.62.397
31. Luo J, Wang X, Yuan L, Guo L. Iron deficiency, a risk factor of thyroid disorders in reproductive-age and pregnant women: a systematic review and meta-analysis. *Front Endocrinol (Lausanne)*. 2021;12:629831. doi:10.3389/fendo.2021.629831
32. Abdulmawjood SA, Altamer ZA. The relationship of hypothyroidism to iron deficiency in the body: Review Article. *NTU Journal of Pure Sciences*. 2024;3(1):32-35. doi:10.56286/NTUJPS.V3I1.516
33. Zhang HY, Teng XC, Shan ZY, et al. Association between iron deficiency and prevalence of thyroid autoimmunity in pregnant and non-pregnant women of childbearing age: A cross-sectional study. *Chin Med J (Engl)*. 2019;132(18):2143-2149. doi:10.1097/CM9.0000000000000409
34. Gierach M, Rudewicz M, Junik R. Iron and ferritin deficiency in women with hypothyroidism and chronic lymphocytic thyroiditis: a systematic review. *Endokrynol Pol.* 2024;75(3):253-261. doi:10.5603/ep.97860
35. Shulhai AM, Rotondo R, Petraroli M, et al. The role of nutrition on thyroid function. *Nutrients*. 2024;16(15):2496. doi:10.3390/nu16152496
36. Kandhro GA, Kazi TG, Afridi HI, et al. Evaluation of iron in serum and urine and their relation with thyroid function in female goitrous patients. *Biol Trace Elem Res*. 2008;125(3):203-212. doi:10.1007/s12011-008-8174-z
37. Kazi TG, Kandhro GA, Sirajuddin, et al. Evaluation of iodine, iron, and selenium in biological samples of thyroid mother and their newly born babies. *Early Hum Dev.* 2010;86(10):649-655. doi:10.1016/j.earlhumdev.2010.07.010
38. Afridi HI, Kazi TG, Ghulam NK, et al. Interactions between cadmium and zinc in the biological samples of Pakistani smokers and nonsmokers cardiovascular disease patients. *Biol Trace Elem Res*. 2011;139(3):257-268. doi:10.1007/S12011-009-8607-3
39. Kandhro GA, Kazi T, Sirajuddin, et al. Effects of selenium supplementation on iodine and thyroid hormone status in a selected population with goitre in Pakistan. *Clin Lab*. Published online 2011.
40. Taylor PN, Lansdown A, Witczak J, et al. Age-related variation in thyroid function – a narrative review highlighting important implications for research and clinical practice. *Thyroid Res*. 2023;16(1):1-12. doi:10.1186/s13044-023-00149-5
41. Bai YZ, Gao YX, Zhang SQ. Identification of factors on blood selenium levels in US adults: a cross-sectional study. *Nutrients*. 2024;16(11):1734. doi:10.3390/nu16111734
42. Baudry J, Kopp JF, Boeing H, Kipp AP, Schwerdtle T, Schulze MB. Changes of trace element status during aging: results of the EPIC-Potsdam cohort study. *Eur J Nutr*. 2020;59(7):3045-3058. doi:10.1007/s00394-019-02143-w

Rzeszów University Press 2026
ISSN 2544-1361 (online)
doi: 10.15584/ejcem.2026.1.23

http://www.ejcem.ur.edu.pl
European Journal of Clinical and Experimental Medicine
Eur J Clin Exp Med 2026; 24 (1): 138–149

ORIGINAL PAPER

Pulmonoprotective effect of carnosol on LPS-induced cytokine storm model in mice

Ahmed F. Abed Mansoor [1], Ahmed Rahmah Abu-Raghif [2], Hayder Ridha-Salman [3], Furqan Mohammed Al-Asady [4,5], Maytham Razaq Shleghm [1], Muataz Naeem Hussein [2]

[1] Department of Pharmacology and Toxicology, College of Pharmacy- National University of Science and Technology, An Nasiriyah, Dhi Qar, Iraq
[2] Al-Nahrain University, College of Medicine, Department of Pharmacology, Baghdad, Iraq
[3] Al-Mustaqbal University, College of Pharmacy, Hilla, Babylon, Iraq
[4] University of Hilla, College of Pharmacy, Babylon, Iraq
[5] University of Babylon, Hammurabi College of Medicine, Hillah, Iraq

ABSTRACT

Introduction and aim. The cytokine storm represents a severe hyperinflammatory response that can lead to acute lung injury and organ failure. Carnosol, a phenolic diterpene derived from *Rosmarinus officinalis*, exhibits documented antioxidant and anti-inflammatory properties. The aim was to evaluate the effects of carnosol, alone and in combination with methylprednisolone acetate (MPA), in a lipopolysaccharide (LPS)-induced cytokine storm model in mice.

Material and methods. Sixty male mice were randomly assigned to six groups: control, lipopolysaccharide (LPS), vehicle, carnosol (120 mg/kg), methylprednisolone acetate (50 mg/kg), and combined carnosol plus methylprednisolone acetate (half doses). Treatments were administered for seven days following LPS induction. Pulmonary concentrations of interleukin-1 beta (IL-1β), interleukin-6 (IL-6), and tumor necrosis factor alpha (TNF-α) were quantified using enzyme-linked immunosorbent assay, and lung histopathology was evaluated.

Results. Lipopolysaccharide administration significantly increased pulmonary cytokine levels compared with controls (IL-1β: 85.8±13.5 vs. 11.5±3.8 pg/g; IL-6: 93.0±8.5 vs.16.6±4.8 pg/g; TNF-α: 144.4±10.1 vs.18.6±0.01 pg/g; all $p<0.05$). Treatment with carnosol significantly reduced IL-1β, IL-6, and TNF-α levels compared with the LPS group ($p<0.05$). The combined carnosol and methylprednisolone acetate therapy produced the greatest cytokine attenuation (e.g. IL-6: 24.6±1.8 pg/g vs. LPS; $p<0.05$) and was associated with the most pronounced improvement in lung histopathological scores ($p<0.05$).

Conclusion. Carnosol attenuates lipopolysaccharide-induced pulmonary inflammation and cytokine overproduction in a murine model. Its combination with methylprednisolone acetate may enhance anti-inflammatory efficacy and allow for glucocorticoid dose reduction. These findings provide preclinical evidence supporting further mechanistic and translational studies.

Keywords. ARDS, carnosol, COVID-19, mouse model, phenolic diterpenes

Corresponding author: Hayder Ridha-Salman, e-mail: hayder80.ridha@gmail.com; haider.redha@uomus.edu.iq

Received: 5.09.2025 / Revised: 20.11.2025 / Accepted: 10.12.2025 / Published: 30.03.2026

Mansoor AFA, Abu-Raghif AR, Ridha-Salman H, Al-Asady FM, Shleghm MR, Hussein MN. Pulmonoprotective effect of carnosol on LPS-induced cytokine storm model in mice. *Eur J Clin Exp Med.* 2026;24(1):138–149. doi: 10.15584/ejcem.2026.1.23.

Introduction

Cytokine storm syndrome is a pathophysiological state of systemic hyper-inflammation caused by uncontrolled release of pro-inflammatory cytokines, which results in tissue damage, organ failure, and high mortality.[1,2] It is initiated by infectious (bacterial endotoxins, viral infections) and non-infectious stimuli (malignancy, autoimmunity).[3-5] In the context of severe inflammation, an uncontrolled release of cytokines is associated with complications, including acute respiratory distress syndrome (ARDS), multiple organ failure, and death.[6-8] Increased concentrations of key mediators such as interleukin (IL)-1β, IL-6, and tumor necrosis factor (TNF)-α are constantly correlated with disease severity and bad prognosis.[9-11]

Lipopolysaccharide (LPS) – abundant in the Gram-negative bacterial membrane – is a popular tool for modeling cytokine storms, as it efficiently stimulates innate immunity and induces a strong production of an excessive amount of cytokines.[12-14] LPS-mediated inflammation is transmitted by well-defined signaling pathways culminating in transcriptional induction of pro-inflammatory cytokines with consequent systemic inflammatory damage. While these pathways have been well-characterized in the literature, their prolonged activation is a central mechanism underlying cytokine storm pathology.[15]

Glucocorticoids have represented a mainstay to treat severe inflammatory diseases because of their powerful immunosuppressive and anti-inflammatory activities.[16,17] Synthetic glucocorticoids, including methylprednisolone acetate (MPA), can efficiently inhibit the production of cytokines and immune cell invasion. These are, however, associated with immunosuppression and an increased risk of infection as well as decreased tissue repair and metabolic derangement.[18,19] Unfortunately, long-term or high-dose glucocorticoid therapy is also connected with severe side effects. These shortcomings highlight the demand for alternative or adjuvant anti-inflammatory remedies able to effectively suppress cytokine storms with less systemic toxicity.

Natural products can be considered as an important reservoir of bioactive compounds possessing versatile pharmacological activities.[20,21] Carnosol, a natural phenolic diterpene found in rosemary (*Rosmarinus officinalis*), sage, and other herbs, possesses robust antioxidant, anti-inflammatory, anti-proliferative, and immune-modulating activities.[22] Multiple preclinical investigations have revealed carnosol anti-inflammatory efficacy in a variety of animal models, confirming its capacity to inhibit inflammatory mediators, modify immune cell function, and ameliorate oxidative stress.[23] Although these outcomes corroborate its anti-inflammatory capacity, previous studies have primarily been based on experimental disease or endpoints that may not allow for direct comparison with established anti-inflammatory therapies.

However, to the best of our knowledge, there have been no in vivo studies that systematically compare the anti-inflammatory activity of carnosol with typical glucocorticoid compounds as well as attempt to evaluate their combined effects under LPS-induced cytokine storm conditions. This gap needs to be addressed to provide critical insight into whether carnosol can be utilized as a complementary or alternative treatment for controlling exaggerated hyperinflammatory responses.

Aim

Therefore, the aim of this study was to assess the anti-inflammatory effects of carnosol alone and in combination with methylprednisolone acetate by using the LPS-driven cytokine storm model in vivo. Direct comparison of these interventions aims to clarify the therapeutic potential and translational importance from preclinical studies for carnosol as a molecule dampening in a setting of exacerbated systemic inflammation. This research fills in these gaps by clarifying the core hypothesis that carnosol mitigates the LPS-driven cytokine storm in mice and prevents lung damage, with the added likelihood that its combined action with MPA could permit glucocorticoid dosage reductions while offering safer anti-inflammatory therapy. The investigation's primary endpoint was to evaluate pulmonary tissue concentrations of IL-1β, IL-6, and TNF-α 24 hours after LPS injections. The secondary endpoints are lung histopathology scores.

Material and methods

Carnosol, MPA, and LPS were obtained from Sigma Aldrich Chemical Company (St. Louis, MO, USA). Dimethyl sulfoxide (DMSO) was acquired from Chem-Lab NV (Zedelgem, Belgium). Formaldehyde was supplied from Sinopharm Chemical Reagent Co., Ltd. Commercial enzyme-linked immunosorbent assay (ELISA) kits for mouse TNF-α, IL-1β, and IL-6 were purchased from Sunlong Biotech Co., Ltd. Hematoxylin and eosin (H&E) staining reagents were procured from BDH Chemicals (Poole, UK).

Reagents and kits are reported as per the standardized company name, city, and country.

Experimental animals and ethical consideration

A total of 60 male Swiss albino mice (pathogen-free, aged 7–8 weeks, weighing 25–30 g) were used in this study. All animals were housed under controlled laboratory conditions, including a 12-hour light/dark cycle and an ambient temperature maintained at 18–22°C. Standard rodent chow and water were provided ad libitum. A 14-day acclimatization period was allowed prior to the commencement of the experiments. No animals satisfied the

humane endpoint criteria; hence, no exclusions were imposed. All experimental procedures were approved by the Animal Ethics Committee of Al-Nahrain University, College of Medicine (approval date: November 21, 2021; Approval No. 20215951), and adhered to the guidelines for the care and use of laboratory animals.

Sample size calculation, randomization, and blinding

The sample size was determined for the primary endpoint of expected differences in pulmonary TNF-α levels with a statistical power of 80% at a significance level of α=0.05. The minimum number needed was 8 animals for each study group; we used 10 mice per group to allow for biological variability and probable losses.

Mice were arbitrarily assigned into 6 groups (n = 10 per group) employing a software-generated randomization sequence. Staff performing the biochemical analyses (ELISA assays and quantitation) were blinded to group assignment throughout sample processing, assay execution, and data analysis. Histopathological analysis and scoring were performed in a blinded manner by an experienced histopathologist during slide reading and scoring.

Experimental design

For induction of a cytokine storm, mice were challenged with a single intraperitoneal (i.p.) injection of LPS (5 mg/kg). Therapeutic interventions started 1 h after LPS and proceeded once per day for 7 days as follows:

– Control group (Healthy): received no treatment.

LPS group (Induction): injected with LPS alone (5 mg/kg, i.p.).[24]

DMSO (Vehicle) group: received LPS then 1% DMSO (0.3 mL, i.p.).[25]

Methylprednisolone group (MPA): were given LPS and then treated with MPA (50 mg/kg, i.p.).[26]

Carnosol group: challenged with LPS and then treated with carnosol (120 mg/kg, i.p.).[27]

– Carnosol + Methylprednisolone combination group (Carnosol+MPA): injected with LPS, and after 1 h obtained carnosol (60 mg/kg) and MPA (25 mg/kg), independently, via i.p. administration.

The carnosol dose (120 mg/kg) and MPA (50 mg/kg) were selected based on previously published experimental studies demonstrating therapeutic efficacy without evident toxicity in rodent models.[28]

These established doses were adopted to ensure comparability with existing literature and to minimize the risk of dose-related adverse effects. Figure 1 displays a simplified representation of the research methodology and treatment schedule.

Formulation of tested agents

Carnosol was dissolved in a 1% DMSO and diluted with sterilized saline to achieve an ultimate working concentration of 10 mg/mL Dosing volumes were estimated according to body weight for delivering 120 mg/kg (0.36 mL) of carnosol. MPA was mixed in 1% DMSO and subsequently diluted with sterilized saline to provide a 5 mg/mL working solution and was delivered intraperitoneally at 50 mg/kg using individually calculated volumes (0.3 mL). Carnosol and MPA were regularly injected intraperitoneally spanning a period of 7 days to assure continuous systemic exposure and guarantee predictable therapeutic actions throughout the LPS-driven inflammatory stages. In the combination treatment group, carnosol and MPA were given separately through the i.p. route with no premixed preparation.

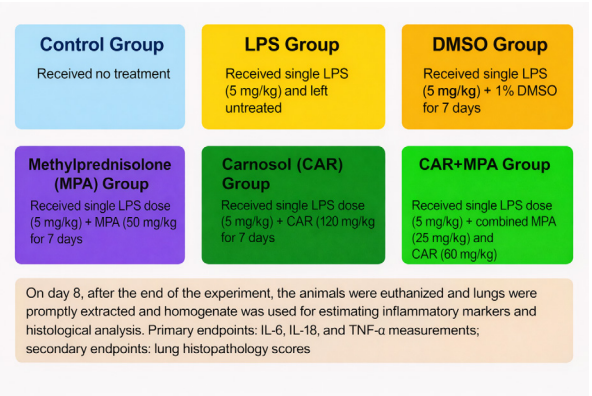

Fig. 1. Schematic diagram illustrating the experimental design and treatment timeline

Cytokine storm model (induction protocol)

LPS stock solution was prepared freshly according to the manufacturer's protocol by dissolving LPS powder in sterile normal saline solution and then mixing by vortex before use.[29] A cytokine storm was elicited by a single i.p. injection of LPS (5 mg/kg).[21,30]

Animal euthanasia and lung tissue homogenization

On day 8, after the last dosage of medications was administered, the animals were euthanized with an intraperitoneal injection of ketamine (80 mg/kg) and xylazine (8 mg/kg) for ensuring the complete suppression of pain reflexes before sacrificing. The chest cavity was cautiously opened, and the lungs were promptly evacuated. After that, the lung tissues were split into two parts. One part was fixed in 10% neutral-buffered formalin for the histopathological study, and the other part was softly cleansed with ice-cold sterilized saline, wiped dry with a paper towel, and homogenized in phosphate-buffered saline at a 10% w/v mixture via a tissue homogenizing device. The pulmonary homogenates were spun out at 10,000×g for 15 minutes at 4°C, and the resultant supernatants were gathered for ELISA analyses.

Cytokine measurement methodology

The concentrations of TNF-α, IL-1β, and IL-6 in the lung tissue samples were measured by ELISA with commercially

available kits according to the manufacturer's instructions. All measurements were carried out in a double-blind system.[31,32] The optical density was read at 450 nm, and cytokine concentrations were determined from standard curves and expressed as pg per mg of tissue.[33,34]

Histopathological examination

Lung tissues were fixed in 10% neutral-buffered formalin for at least 24 hours to preserve morphology, then processed through graded ethanol concentrations, cleared with xylene, and embedded in paraffin wax.[35,36] Paraffin blocks were sectioned at 4–5 µm using a rotary microtome. Sections were floated in a warm water bath to remove folds, mounted onto clean slides, and air-dried at 37°C. Standard H&E staining was used to assess tissue architecture. Slides were deparaffinized, rehydrated, stained with hematoxylin, differentiated in acid alcohol, blued, and counterstained with eosin.[31,37] After dehydration and clearing, sections were mounted with coverslips. Histopathological evaluations and scoring systems were conducted by a single experienced histopathologist who was blinded to group assignments. All the specimens were examined microscopically at various magnifications (10×, 40×).

Scoring of histopathological changes

A partially quantitative evaluation procedure with an array of 0 to 4 was adopted to assess histopathology abnormalities dependent on alveolar morphology, interstitial inflammation, edema, and hemorrhaging at 10× and 40× amplification. Grade 0 (0% negative) meant that there was no visible injury, and the lung structure was normal. Grade 1 (1–33% mild positive) illustrated mild alveolar wall thickenings and minimal involvement of inflammatory cells. Grade 2 displayed modest swelling, inflammatory invasion, and noticeable alveolar septal thickenings (33–66% moderate positive). Severe septal thickenings, intense inflammatory migration, and substantial edema or hemorrhage were indicative of grade 3. Grade 4 (66–100% severely positive) revealed extensive bleeding, significant inflammatory cell infiltration, alveolar collapse, and diffuse alveolar damage. Scale bars were used to illustrate typical features in representative photos for each grade. Multiple non-overlapping microscopy regions from each tissue segment were examined and averaged for calculating sample-level grade. All portions were evaluated separately by a specialist histopathologist who was totally unaware of the treatment assignment. Recorded lesion outcomes were also matched to a recognized acute lung damage grading tool for comparison with prior research.[38]

Analytical statistics

Data were statistically analyzed through SPSS software (IBM Corp., Armonk, NY, USA) and described as mean ± standard deviation (SD). Data were tested for normality of distribution by the Shapiro–Wilk test before statistical examination. One-way analysis of variance (ANOVA) was used with normality and homogeneity of variances checked, and Tukey's post-hoc test for comparison between multiple groups. Values of $p<0.05$ were considered significant.[39]

Results

Preventive effect of tested agents on IL-1β, IL-6, and TNF-α levels

LPS treatment markedly elevated the levels of IL-1β, IL-6, and TNF-α in lung tissues when compared with the healthy control group ($p<0.05$). Such elevations were also evident in the DMSO group ($p<0.05$). In contrast, mice treated with MPA, carnosol, or their combined treatment revealed a remarkable decrement in the pulmonary levels of IL-1β, IL-6, and TNF-α cytokines in comparison to mice treated with LPS or DMSO ($p<0.05$), as detailed in Figures 2–4.

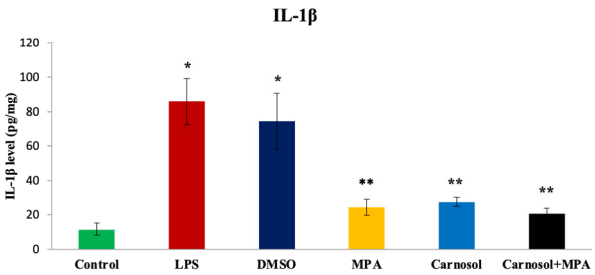

Fig. 2. Impact of the tested agents on IL-1β levels in mouse lung tissue, data are reflected as mean±SD, * – indicates a remarkable difference vs. the control group ($p<0.05$), ** – indicates a remarkable difference vs. the LPS and DMSO groups ($p<0.05$), and # – indicates a remarkable difference vs. the carnosol and/or MPA group ($p<0.05$)

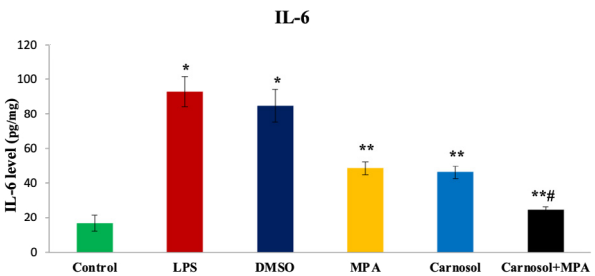

Fig. 3. Impact of the tested agents on IL-6 levels in mouse lung tissue, data are reflected as mean±SD, * – indicates a remarkable difference vs. the control group ($p<0.05$), ** – indicates a remarkable difference vs. the LPS and DMSO groups ($p<0.05$), and # – indicates a remarkable difference vs. the carnosol and/or MPA group ($p<0.05$)

Notably, the carnosol+MPA combination group produced the best results, demonstrating a substantially greater reduction in IL-6 and TNF-α concentra-

tions than the groups individually treated with MPA or carnosol ($p<0.05$), while IL-1β decline was comparable across all treatment groups (Figures 2–4).

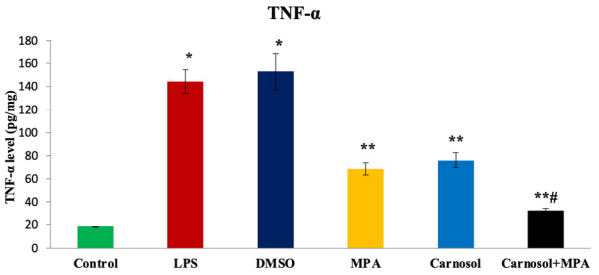

Fig. 4. Impact of the tested agents on TNF-α levels in mouse lung tissue, data are reflected as mean±SD, * – indicates a remarkable difference vs. the control group ($p<0.05$), ** – indicates a remarkable difference vs. the LPS and DMSO groups ($p<0.05$), and # –indicates a remarkable difference vs. the carnosol and/or MPA group ($p<0.05$)

Preventive effect of tested agents on lung histopathological scores

The histopathologic scores of the lungs were significantly higher in the LPS and DMSO groups than those of the healthy control group ($p<0.05$). Treatment with MPA, carnosol, or their combined administration significantly decreased histological scores compared to the LPS and DMSO groups ($p<0.05$) (Figure 5).

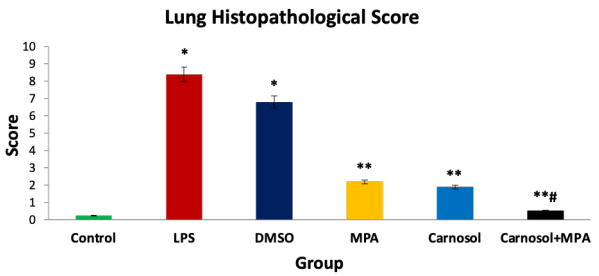

Fig. 5. Impact of the tested agents on lung histological scoring, data are reflected as mean±SD, * – indicates a remarkable difference vs. the control group ($p<0.05$), ** – indicates a remarkable difference vs. the LPS and DMSO groups ($p<0.05$), and # – indicates a remarkable difference vs. the carnosol and/or MPA group ($p<0.05$)

Preventive effect of tested agents on lung histopathological changes

In the healthy control group, lung histology demonstrated a well-maintained pulmonary architecture, characterized by intact alveolar structures and preserved capillary endothelium. Only minimal, nonspecific inflammatory changes were evident (Figure 6A). Conversely, the LPS-induced group showed extensive pathological damage, including intense acute inflammation, prominent vascular congestion, disruption of capillary integrity, thickening of alveolar septa, reduction of airspace volume, and hyaline membranes formation (Figure 6B).

In the DMSO group, lung histology demonstrated an acute inflammatory process of moderate to severe degree, with mild congestion of blood vessels, diffuse alveolar wall thickening, and areas of capillary breakdown with hyaline membrane deposition, as clarified in Figure 7A. Tissue samples from the MPA group enjoyed minimal inflammatory involvement, featuring localized blood vessel engorgement, irregular enlargement of the alveolar septa, disruption of capillary structures, and occasional accumulation of hyaline membranes, accompanied by a slight narrowing of the airspaces as explained in Figure 7B.

Lung histology from the carnosol group indicated intact alveolar walls and capillaries, lacking any vascular congestion or inflammation as seen in Figure 8A. Likewise, tissues from the Carnosol+MPA group displayed normal lung structure, including clear alveoli and no evidence of inflammation, congestion, or hyaline membranes as described in Figure 8B.

Discussion

Cytokine storm induction

Hypercytokinemia is an uncontrolled systemic inflammatory response typically driven by bacterial or viral infections and is accompanied by overproduction of inflammatory cytokines. In our study, intraperitoneal LPS challenge caused severe pulmonary inflammation with a marked increase in IL-1β, IL-6, and TNF-α levels. This experimental model is widely accepted to mimic critical biochemical and histopathological criteria of acute lung inflammatory injury, and it has served as a consistent tool for the testing of anti-inflammatory agents.[40] Although cytokine storm has been associated with severe pathologies such as sepsis and ARDS, the present results must be viewed within a meticulously managed preclinical animal model.

Preventive effects of tested agents on IL-1 β IL-6, and TNF-α level in LPS-induced cytokine storm in mice

The findings of this investigation indicated LPS provoked an extensive pulmonary inflammatory response characterized by the highest levels of IL-1β, IL-6, and TNF-α. These cytokines are critical intermediaries for the cytokine storm and have important functions in propagating inflammatory cascades and leukocyte recruitment as well as tissue injury in experimental models of acute lung inflammation.[41] Treatment with either carnosol, MPA, or their combination substantially suppressed the increments of LPS-induced cytokines. The demonstrated IL-1β inhibition is of particular interest because this cytokine is produced after TLR4 stimulation and inflammasome-dependent processing, participating in the enhancement of subsequent cytokine release.[42,43] Down-

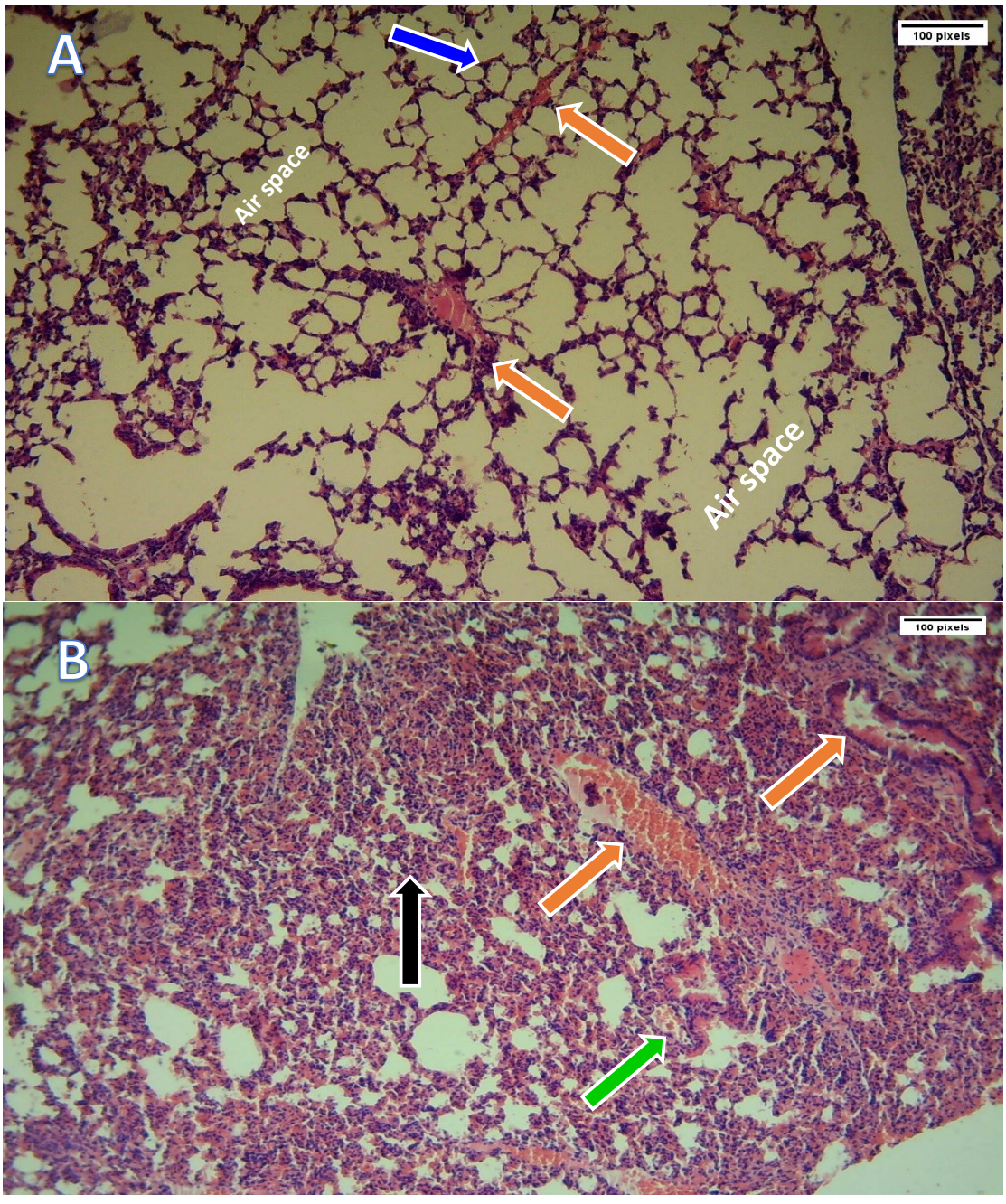

Fig. 6. Representative lung histology of control and LPS-treated mice, A: The control group showing intact alveolar architecture (blue arrow), B: LPS group demonstrating severe inflammatory infiltration (black arrow), vascular congestion (red arrow), septal thickening, and hyaline membranes (green arrow), photomicrographs captured at 10× magnification (H&E stain, scale bar=100 µm)

regulation of IL-1β after carnosol exposure is also in line with findings reporting that carnosol inhibits synthesis of pro-inflammatory cytokines such as IL-1β, IL-6, and TNF-α from activated immune cells.[44,45]

IL-6, a key biomarker in the pathogenesis of cytokine storm and systemic inflammation, exhibited a notable increase after the LPS challenge. Similar results in experimental models have shown that IL-6 is a principal modulator of cytokine cascade activation involving the hyperinflammatory state.[40,46] However, a prominent decrease in IL-6 was apparent following the treatment protocol with carnosol, MPA, or their combination. Of note, the combined administration of carnosol with MPA was more effective in the downregulation of IL-6 than either agent alone. The carnosol-mediated attenuation of IL-6 levels is supported by earlier data showing that this phytochemical exerts wide anti-inflammatory actions, owing to its capacity to dampen macrophage activation during cytokine storms and to block major inflammatory response regulators like IL-6, TNF-α, and IL-1β.[47] Although we did not explore the intracellular signaling pathways in the current study, it has been

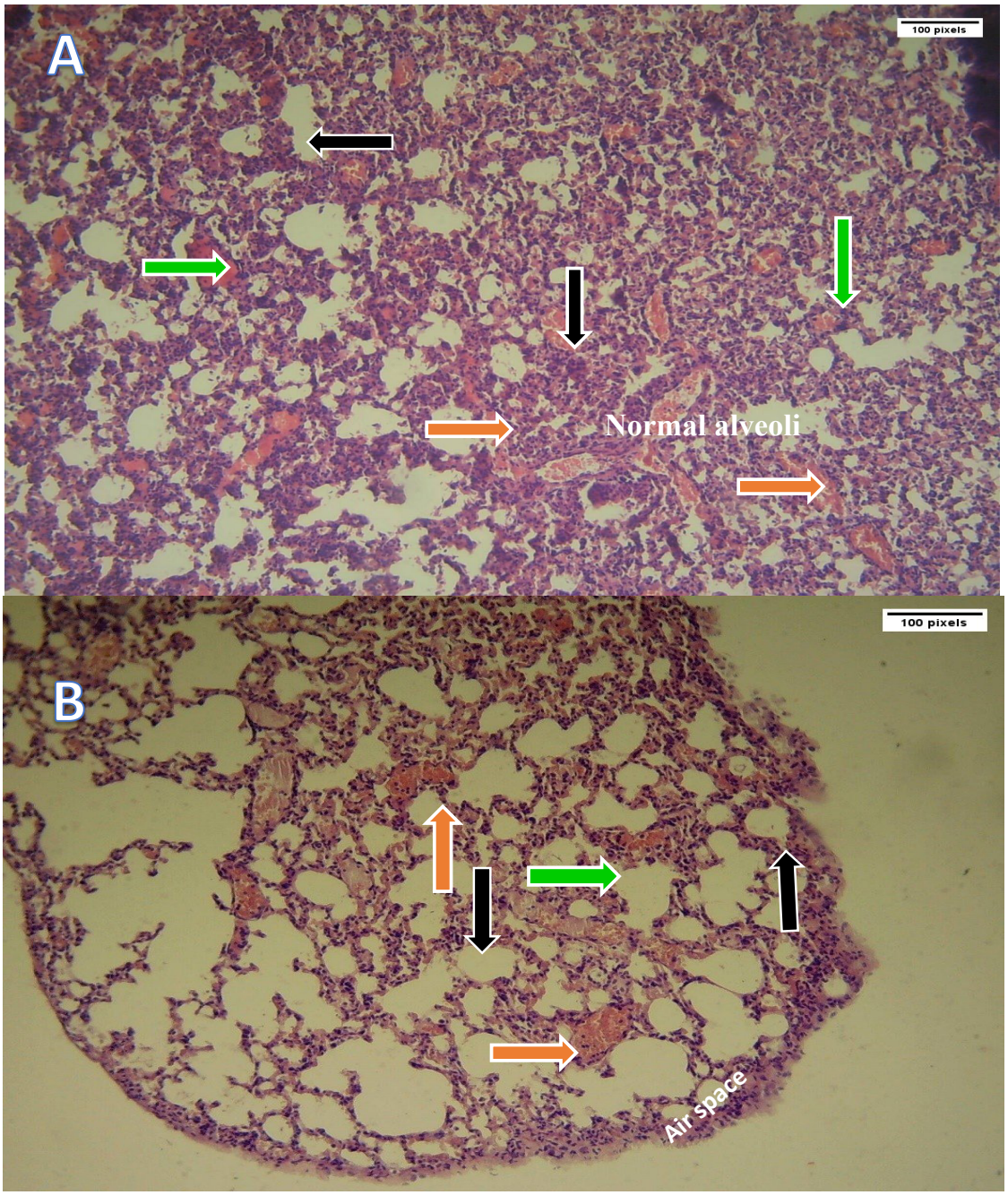

Fig. 7. Histological analysis of lung tissue in DMSO and MPA groups, A: The DMSO group showing moderate-to-severe inflammation (black arrow), mild congestion (red arrow), septal thickening, and hyaline membranes (green arrow), B: MPA-treated group exhibiting mild inflammatory changes (black arrow), scattered vascular congestion (red arrow), focal alveolar thickening, and partial hyaline deposition (green arrow), photomicrographs captured at 10× magnification (H&E stain, scale bar=100 µm)

demonstrated in other works that carnosol effects on IL-6 are related to NF-κB and MAPK antagonism or through stimulating PPAR-γ–dependent anti-inflammatory axis.[48,49] Such mechanisms are well described in inflammatory models and could give a justification for the noticed diminution in cytokines.

Likewise, TNF-α expression dramatically rose after LPS exposure and diminished with carnosol and MPA interventions. TNF-α is a proximal mediator of cytokine storms and significantly contributes to endothelial dysfunction and tissue damage.[50-52] Former experimental observations revealed that carnosol and related polyphenolic constituents hinder generation of TNF-α, IL-1β, and IL-6 through interfering with transactivation of pro-inflammatory genes and modulating activated macrophages.[53,54] Although these pathways were not assayed in our experiment, the differences among treatment groups would suggest that carnosol exerts an anti-inflammatory effect detected by other authors using different preclinical models.[55,56]

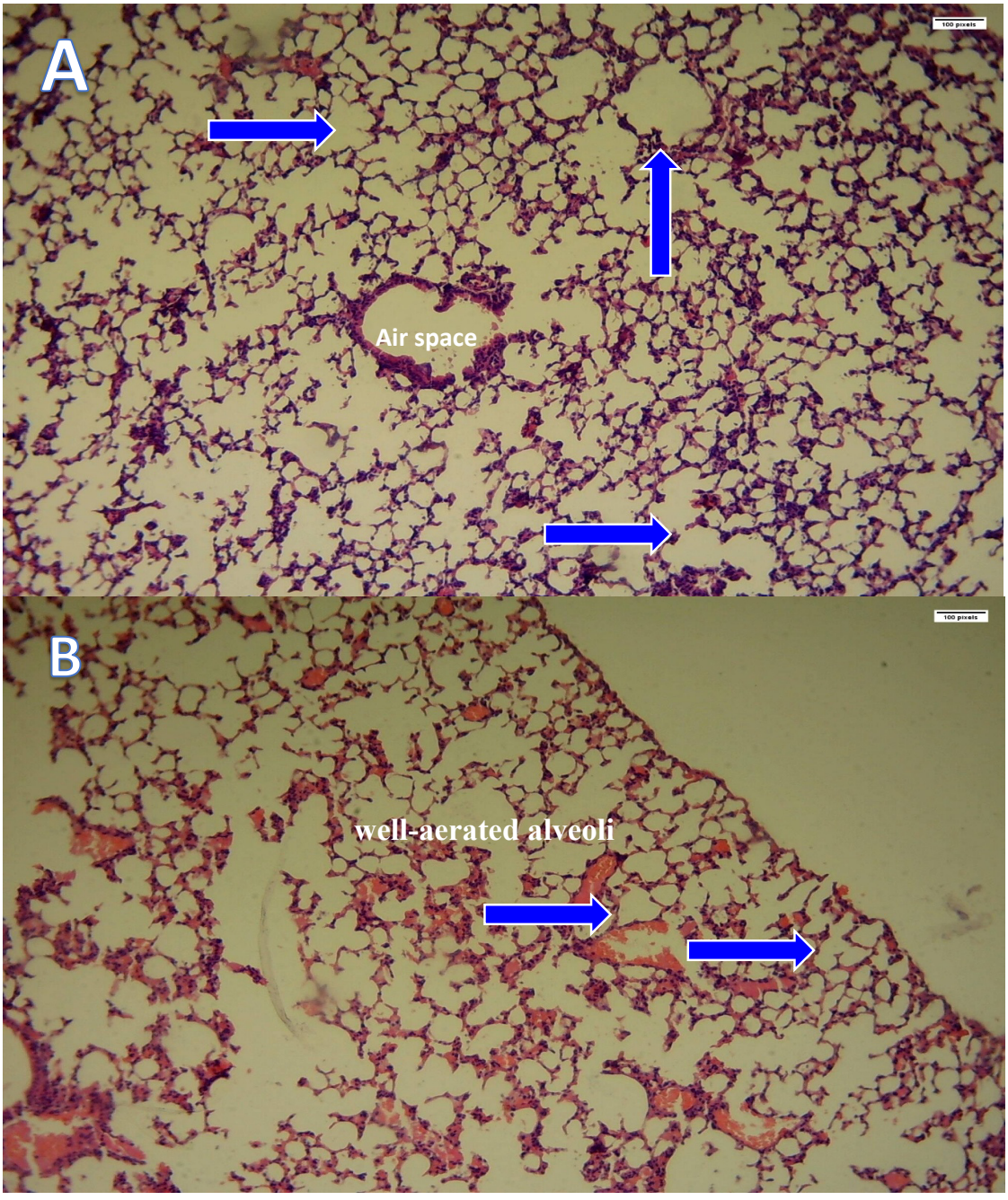

Fig. 8. Lung tissue morphology in CAR- and CAR+MPA-treated mice, A: CAR group displaying preserved alveolar structure (blue arrow), intact capillaries, and absence of inflammation or congestion, B: CAR+MPA group showing well-aerated alveoli, normal septal thickness, and no pathological alterations, photomicrographs captured at 10× magnification (H&E stain, scale bar=100 μm)

Remarkably, combined carnosol plus MPA led to higher mitigation of IL-6 and TNF-α values at individual dosages of both agents, hinting at a putative synergistic anti-inflammatory activity under this experimental setting. This finding is preliminary and is valid only for the current animal model since there was no pharmacodynamic or dose-saving study carried out.

Taken together, these results demonstrate the effective alleviation of LPS-evoked cytokine storm by carnosol through downregulation of pivotal proinflammatory mediators. When used in combination with MPA, carnosol can even potentiate cytokine suppression without evidence of additional toxicity, indicating that it could be a supplemental anti-inflammatory agent in experimental models of cytokine storm.

Effects of tested compounds on histopathological analysis

Following the LPS challenge, severe lung histopathological changes were observed, such as inflammatory cell infiltrates, vascular congestion, thickening of alveolar

septal walls, and hyaline membrane formation, which are typical features of acute lung injury described in earlier investigations.[57,58] These histological aberrations are a reflection of downstream tissue effects secondary to the overproduction of cytokines.

Carnosol, MPA, and Carnosol+MPA-treated animals revealed noteworthy diminution in lung injury scores and maintenance of alveolar architecture. These results are in line with previous efforts describing the pulmonoprotective activities of carnosol against experimental lung injury.[59,60]

According to related literature, the proposed histological amelioration might be attributed to reduced generation of inflammatory mediators and oxidative stress, events that were not directly proved in our current work.[61,62]

Use of a standardized histopathological scoring system, blinded evaluation, and assessment of multiple tissue regions supports the robustness of these findings and allows comparison with existing grading systems for acute lung injury.

Comparative effects of carnosol and MPA

While both carnosol and MPA share the pharmacological ability to ameliorate LPS-induced cytokine storms, their working mechanisms are fundamentally distinct. MPA is a synthetic glucocorticoid that exerts its effects mainly by means of glucocorticoid receptor-mediated transcriptional repression, resulting in wide-range inhibition of immune cell activation and cytokine secretion.[16,24] Although efficient in combating inflammation, this phenomenon is accompanied by systemic immunosuppression and potential complications such as increased risk of infection and metabolic abnormalities.[63,64] Conversely, carnosol, a nature-derived polyphenolic diterpene, displays anti-inflammatory properties due to its exclusive ability to target some critical intracellular signaling pathways, such as activation of PPAR-γ, reduction in MAPK phosphorylation, and suppression of NF-κB-dependent activity, accompanied by a reduction in the transcription of pro-inflammatory cytokines (TNF-α, IL-6, and IL-1β), as well as strengthening antioxidant defenses with lipid peroxidation inhibition.[65,66] Such focused management might explain how carnosol is able to suppress exaggerated inflammatory reactions without the generalized systemic immunosuppression typically observed with corticosteroids, thus offering a potentially safer therapeutic profile.[23,48]

Study limitations

This study has several limitations. First, it was conducted using an LPS-evoked cytokine storm model in mice, which may not fully replicate the complexity of human hyper-inflammatory conditions, including COVID-19-related cytokine storms. Second, treatments were administered for only 7 days, so long-term outcomes and potential delayed effects of carnosol and combination therapy were not assessed. Third, the study focused primarily on lung tissue, and systemic effects on other organs commonly affected by cytokine storm, such as the liver, kidneys, and heart, were not evaluated. Importantly, while our biochemical and histological analyses provide indirect evidence of anti-inflammatory activity, the absence of mechanistic assays targeting key pathways such as NF-κB, MAPK, and PPAR-γ, together with the lack of pharmacokinetic and dosage–response studies and a formal toxicity evaluation, constrains the depth of interpretation. Future studies are warranted to address these aspects and to further elucidate the molecular mechanisms underlying carnosol therapeutic potential. Finally, only a single dose of carnosol and MPA and one combination regimen were tested, highlighting the need for further studies to optimize dosing strategies and assess potential toxicity at varying concentrations. The subsequent evaluation may also include distribution-sensitive representations that offer more insights into the flow of data and deep patterns.

Conclusion

In this murine model of LPS-evoked cytokine storm, carnosol remarkably decreased the levels of pulmonary pro-inflammatory cytokines (IL-1B, IL-6, and TNF-α) and mitigated lung histopathological alterations. The co-administration of carnosol and MPA resulted in a more profound amelioration of the tested inflammatory biomarkers compared to either treatment alone under these experimental settings. These observations offer preclinical evidence that carnosol demonstrates anti-inflammatory and pneumoprotective properties in acute inflammation of the lung. Interpretation of the observed effects of combined therapy should be cautious and restricted to the current animal model, consistent with no clinical or dose-sparing advantage. Still, additional investigations are warranted to clarify the mechanisms, dose–response correlations, and translational potential of carnosol alone or combined with corticosteroids in various experimental contexts.

Acknowledgements

The results of this study constitute a fundamental part of a PhD thesis submitted to the Department of Pharmacology, College of Medicine, Al-Nahrain University.

Declarations

Funding

The research did not receive any external or commercial funding.

Author contributions

Conceptualization, A.F.A.M., A.R.A.R., and H.R.-S.; Methodology, A.F.A.M.; Software, H.R.-S., M.R.S., and

M.N.H.; Validation, A.R.A.R., H.R.-S., and F.M.A.; Formal Analysis, A.F.A.M. and M.N.H.; Investigation, F.M.A. and M.N.H.; Resources, A.F.A.M. and M.R.S.; Data Curation, F.M.A. and M.R.S.; Writing – Original Draft Preparation, A.F.A.M..; Writing – Review & Editing, A.R.A.R. and H.R.-S.; Visualization, A.R.A.R. and H.R.-S.; Supervision, A.R.A.R.; Project Administration, F.M.A., M.R.S., and M.N.H.; Funding Acquisition, A.F.A.M.

Conflicts of interest

The authors declare no conflicts of interest related to this research.

Data availability

The data supporting the findings of this study are available from the corresponding author upon reasonable request.

Ethics approval

The Institutional Review Board (IRB) of Al-Nahrain University, College of Medicine, approved this study on November 21, 2021, with Approval No. 20215951. All animal procedures adhered to the 3Rs (Replacement, Reduction, and Refinement) ethical rules to lessen animal use and suffering. Humane endpoints were defined, and analgesia was deployed to relieve pain or discomfort as needed.

References

1. Feuillet V, Canard B, Trautmann A. Combining antivirals and immunomodulators to fight COVID-19. *Trends Immunol.* 2021;42(1):31-44. doi:10.1016/j.it.2020.11.003
2. Al-Saray D, Al-Asady FM, Tuhair T. Role of antibodies against SARS-CoV-2 in the detection of coronavirus, its transmissibility and immunological status determination among different populations in Babylon Province. *Open Access Maced J Med Sci.* 2022;10(A):644-649. doi:10.3889/oamjms.2022.9372
3. Picchianti Diamanti A, Rosado MM, Pioli C, Sesti G, Laganà B. Cytokine release syndrome in COVID-19 patients: a new scenario for an old concern. *Int J Mol Sci.* 2020;21(9):3330. doi:10.3390/ijms21093330
4. Omran T, Al-Asady FM, Sajit EJ, Al-Saadi H. Assessment of D-dimer level and C-reactive protein in correlation with CT findings in positive PCR–COVID-19 patients. *Malays J Microbiol.* 2025;21(1):135-142. doi:10.21161/mjm.230200
5. Al-Taie SF, Fedwi MM, Merza M, et al. Evaluation of different sedation scales in the ICU management of COVID-19 patients. *Sci Rep.* 2025;15(1):28782. doi:10.1038/s41598-025-14421-1
6. Kozlov EM, Ivanova E, Grechko AV, et al. Involvement of oxidative stress and the innate immune system in SARS-CoV-2 infection. *Diseases.* 2021;9(1):17. doi:10.3390/diseases9010017
7. Al-Asady FM, Omran TZ, Abood FM. Humoral immunity role in diagnosis of COVID-19 among people visited a tertiary care hospital in Hilla City. *Med J Babylon.* 2023;20(3):497-502. doi:10.4103/MJBL.MJBL_124_23
8. Ayad ZM, Al-Ameedi AI, Hajwal SK, et al. Relationship between paediatric antibiotic misuse and recurrent acute respiratory tract infection. *Pharmakeftiki.* 2025;37(2 suppl):193-197. doi:10.60988/p.v37i2S.188
9. Luty RS, Abbas SF, Haji SA, Ridha-Salman H. Hepatoprotective effect of catechin on acetaminophen-induced liver injury in rats. *Comp Clin Pathol.* 2025;34(4):705-718. doi:10.1007/s00580-025-03682-x
10. Yahiya YI, Hadi NR, Abu Raghif A, et al. Protective effect of IAXO-102 on renal ischemia-reperfusion injury in rats. *J Med Life.* 2023;16(4):623-630. doi:10.25122/jml-2022-0280
11. Raheem AK, Abu-Raghif AR, Abbas AH, et al. Quercetin mitigates sepsis-induced renal injury via inhibiting inflammatory and oxidative pathways in mice. *J Mol Histol.* 2025;56(3):184. doi:10.1007/s10735-025-10442-2
12. Raheem AKK, Abu-Raghif AR, Zigam QA. Cilostazol protects against sepsis-induced kidney impairment in a mice model. *J Med Chem Sci.* 2023;6(5):1193-1203. doi:10.26655/jmchemsci.2023.5.25
13. Aal-Aaboda M, Abu Raghif AR, Hadi NR. Effect of lipopolysaccharide from Rhodobacter sphaeroides on inflammatory pathway and oxidative stress in renal ischemia/reperfusion injury in male rats. *Arch Razi Inst.* 2021;76(4):1013-1024. doi:10.22092/ari.2021.356003.1761
14. Shareef SM, Kathem SH, Ridha-Salman H. L-carvone alleviates lipopolysaccharide-induced acute kidney injury via modulation of MyD88-dependent and independent signaling pathways in mice. *Mol Biol Rep.* 2025;53(1):39. doi:10.1007/s11033-025-11213-8
15. Montazersaheb S, Hosseiniyan Khatibi SM, Hejazi MS, et al. COVID-19 infection: an overview on cytokine storm and related interventions. *Virol J.* 2022;19(1):92. doi:10.1186/s12985-022-01814-1
16. Coutinho AE, Chapman KE. The anti-inflammatory and immunosuppressive effects of glucocorticoids, recent developments and mechanistic insights. *Mol Cell Endocrinol.* 2011;335(1):2-13. doi:10.1016/j.mce.2010.04.005
17. Farooq Ali B, Abu-Raghif AR, Ridha-Salman H. Protective effect of cinnarizine on imiquimod-induced mouse model of psoriasis. *J Res Pharm.* 2025;29(4):1783-1791. doi:10.12991/jrespharm.1734970
18. Obaid SH, Gatea FK. Effect of kaempferol, amygdalin, and methylprednisolone alone and in combination in induced cytokine storm in mice. *Acta Pharm Sci.* 2024;62(4):735-747. doi:10.23893/1307-2080.APS6248
19. Al-Jabr KH, Alhumaidan LS, Alghamdi AA, et al. Awareness of side effects of corticosteroids among users and non-users in Saudi Arabia. *J Pharm Bioallied Sci.* 2024;16(suppl 2):S1612-S1618. doi:10.4103/jpbs.jpbs_925_23
20. Wang L, Waltenberger B, Pferschy-Wenzig EM, et al. Natural product agonists of peroxisome proliferator-activated receptor gamma (PPARγ): a review. *Biochem Pharmacol.* 2014;92(1):73-89. doi:10.1016/j.bcp.2014.07.018

21. Al-Rajhi SH, Shihab EM, Ridha-Salman H, et al. Protective effect of a combined glutathione and prednisolone administration on mice subjected to a lipopolysaccharide-induced cytokine storm. *Pharmakeftiki.* 2025;37(2 suppl):122-126. doi:10.60988/p.v37i2S.157
22. Poeckel D, Greiner C, Verhoff M, et al. Carnosic acid and carnosol inhibit human 5-lipoxygenase and suppress pro-inflammatory responses. *Biochem Pharmacol.* 2008;76(1):91-97. doi:10.1016/j.bcp.2008.04.013
23. Maione F, Cantone V, Pace S, et al. Anti-inflammatory and analgesic activity of carnosol and carnosic acid in vivo and in vitro and in silico analysis of their target interactions. *Br J Pharmacol.* 2017;174(11):1497-1508. doi:10.1111/bph.13545
24. Tariq ZT, Abu-Raghif AR, Raheem AK, et al. Huperzine A versus epicatechin: a comparative study of their potential protective effect on lipopolysaccharide-induced lung injury in mice. *Pharmakeftiki.* 2025;37(2 suppl). doi:10.60988/p.v37i2S.244
25. Aal-Aaboda M, Raghif ARA, Almudhafer RH, Hadi NR. Lipopolysaccharide from Rhodobacter spheroids modulate toll-like receptors expression and tissue damage in an animal model of bilateral renal ischemic reperfusion injury. *J Med Life.* 2022;15(5):685. doi:10.25122/jml-2021-0255
26. Abed-Mansoor A, Abu-Raghif AR. Attenuated effects of rivastigmine in induced cytokine storm in mice. *J Emerg Med Trauma Acute Care.* 2022;2022(3):12. doi:10.5339/jemtac.2022.ismc.12
27. Shi W, Xu G, Zhan X, et al. Carnosol inhibits inflammasome activation by directly targeting HSP90 to treat inflammasome-mediated diseases. *Cell Death Dis.* 2020;11(4):252. doi:10.1038/s41419-020-2460-x
28. Al-Naimi MS, Abu-Raghif AR, Fawzi HA. Novel therapeutic effects of rifaximin in combination with methylprednisolone for LPS-induced oxidative stress and inflammation in mice: An in vivo study. *Toxicol Rep.* 2024;13:101808. doi:10.1016/j.toxrep.2024.101808
29. Sadiq A, Zalzala M. The possible protective effect of safranal on the lipopolysaccharide-induced acute lung injury in mice. *Int J Drug Deliv Technol.* 2021;11:771-776. doi:10.25258/ijddt.11.3.19
30. Shao C, Lin S, Liu S, et al. HIF1 α-induced glycolysis in macrophage is essential for the protective effect of ouabain during endotoxemia. *Oxid Med Cell Longev.* 2019;2019:7136585. doi:10.1155/2019/7136585
31. AlBairmani RJH, Shihab EM, Ridha-Salman H, et al. D-limonene attenuates D-galactose-induced skin aging mouse model. *J Mol Histol.* 2025;56(6):364. doi:10.1007/s10735-025-10654-6
32. Sharif SJ, Kadhim HM, Ahmed BS, et al. Gastroprotective and therapeutic effects of emodin on rat model of diclofenac-induced gastric ulceration. *Naunyn Schmiedebergs Arch Pharmacol.* 2025. doi:10.1007/s00210-025-04701-y
33. Tofiq SH, Idan HM. Hematological assessments of children with oral aphthous ulcer in Diyala Governorate, Iraq. *J Appl Hematol.* 2024;15(2):111-115. doi:10.4103/joah.joah_23_24
34. Idan HM, Hasani RA-M, Othman IQ. Effect of anemia on oral cavity and hematological assessments. *Diyala J Med.* 2024;26(1):153-162. doi:10.26505/djm.v26i1.1087
35. Hassan SF, Abu Raghif AR, Kadhim EJ, et al. Phytochemical composition, antioxidant, antihyperlipidemic, and hepatoprotective effects of phenolic components of Iraqi sumac (Rhus coriaria). *Eur J Clin Exp Med.* 2025;23(3):1-24. doi:10.15584/ejcem.2025.3.29
36. Abbod MS, Al-Jawad FH, Anoze AA, et al. Antiatherosclerotic effect of L-thyroxine and verapamil combination on thoracic aorta of hyperlipidemic rabbits. *Int J Pharm Sci Rev Res.* 2014;27(1):254-260.
37. Hussein MN, Abu-Raghif AR, Ridha-Salman H, et al. Flavonoids from Conyza Canadensis mitigates CDNB-induced mouse model of atopic dermatitis. *Comp Clin Pathol.* 2025;34(5):987-1010. doi:10.1007/s00580-025-03709-3
38. Hulse EJ, Smith SH, Wallace WA, et al. Development of a histopathology scoring system for the pulmonary complications of organophosphorus insecticide poisoning in a pig model. *PLoS One.* 2020;15(10):e0240563. doi:10.1371/journal.pone.0240563
39. Daniel WW, Cross CL. Biostatistics: a foundation for analysis in the health sciences. Hoboken, NJ: John Wiley & Sons; 2018.
40. Tang Y, Liu J, Zhang D, et al. Cytokine storm in COVID-19: evidence and treatment strategies. *Front Immunol.* 2020;11:1708. doi:10.3389/fimmu.2020.01708
41. Al-Ani B, ShamsEldeen AM, Kamar SS, et al. Lipopolysaccharide induces acute lung injury and alveolar haemorrhage in association with the cytokine storm, coagulopathy and AT1R/JAK/STAT augmentation in a rat model that mimics moderate and severe Covid-19 pathology. *Clin Exp Pharmacol Physiol.* 2022;49(4):483-491. doi:10.1111/1440-1681.13620
42. Dinarello CA. A clinical perspective of IL-1β as the gatekeeper of inflammation. *Eur J Immunol.* 2011;41(5):1203-1217. doi:10.1002/eji.201141550
43. Schroder K, Tschopp J. The inflammasomes. *Cell.* 2010;140(6):821-832. doi:10.1016/j.cell.2010.01.040
44. Chen J, Sun N, Li F, et al. Carnosol alleviates collagen-induced arthritis by inhibiting Th17-mediated immunity and favoring suppressive activity of regulatory T cells. *Biomed Res Int.* 2023;2023:1179973. doi:10.1155/2023/1179973
45. Lee JE, Im DS. Suppressive effect of carnosol on ovalbumin-induced allergic asthma. *Biomol Ther.* 2021;29(1):58-63. doi:10.4062/biomolther.2020.050
46. Ishijima T, Nakajima K. Inflammatory cytokines TNFα, IL-1β, and IL-6 are induced in endotoxin-stimulated microglia through different signaling cascades. *Sci Prog.* 2021;104(4):00368504211054985. doi:10.1177/00368504211054985

47. Sapra L, Bhardwaj A, Azam Z, et al. Phytotherapy for treatment of cytokine storm in COVID-19. *Front Biosci (Landmark Ed)*. 2021;26(5):51-75. doi:10.52586/4924
48. Gazzillo E, Saviano A, Raucci F, et al. Carnosol modulates mPGES-1/PPAR-γ biological axis: from in silico to in vivo clinical imaging and investigations. *Biomed Pharmacother.* 2025;191:118407.
49. Li L, Pan Z, Ning D, et al. Rosmanol and carnosol synergistically alleviate rheumatoid arthritis through inhibiting TLR4/NF-κB/MAPK pathway. *Molecules*. 2021;27(1):78. doi:10.3390/molecules27010078
50. Kadhim HM, Al-Mosawi AM. Effects of Emodin and Salvianolic Acid on Carbon Tetrachloride (CCl4)-induced Lung Fibrosis in Mice Model. *Int J Drug Deliv Technol*. 2021;11(4):1269-1274. doi:10.25258/ijddt.11.4.25
51. Zein L, Grossmann J, Swoboda H, et al. Haptoglobin buffers lipopolysaccharides to delay activation of NFκB. *Front Immunol*. 2024;15:1401527.
52. Shareef SM, Kathem SH, Ridha-Salman H. Nephroprotective Effect of L-Carvone on a Mouse Model of LPS-Induced Sepsis-Associated Renal Injury via Regulation of TLR4/NF-κB/AP-1/IRF-3 and Nrf2/iNOS Molecular Signaling Cascades. *J Taibah Univ Med Sci*. 2026;21(1):49-66. doi:10.1016/j.jtumed.2025.12.008
53. Habtemariam S. Anti-inflammatory therapeutic mechanisms of natural products: insight from rosemary diterpenes, carnosic acid and carnosol. *Biomedicines*. 2023;11(2):545. doi:10.3390/biomedicines11020545
54. Schwager J, Hoeller U, Wolfram S, et al. Carnosol and Related Substances Modulate Chemokine and Cytokine Production in Macrophages and Chondrocytes. *Molecules*. 2016;21(4):465. doi:10.3390/molecules21040465
55. Chen CC, Chen HL, Hsieh CW, et al. Upregulation of NF-E2-related factor-2-dependent glutathione by carnosol provokes a cytoprotective response and enhances cell survival. *Acta Pharmacol Sin*. 2011;32(1):62-69. doi:10.1038/aps.2010.181
56. Lee DY, Hwang CJ, Choi JY, et al. Inhibitory effect of carnosol on phthalic anhydride-induced atopic dermatitis via inhibition of STAT3. *Biomol Ther*. 2017;25(5):535-544. doi:10.4062/biomolther.2017.006
57. Bhargava R, Janssen W, Altmann C, et al. Intratracheal IL-6 protects against lung inflammation in direct, but not indirect, causes of acute lung injury in mice. *PLoS One*. 2013;8(5):e61405. doi:10.1371/journal.pone.0061405
58. Fan H, Cook JA. Molecular mechanisms of endotoxin tolerance. *J Endotoxin Res*. 2004;10(2):71-84. doi:10.1179/096805104225003997
59. Ciavarella C, Motta I, Valente S, et al. Pharmacological (or Synthetic) and Nutritional Agonists of PPAR-γ as Candidates for Cytokine Storm Modulation in COVID-19 Disease. *Molecules*. 2020;25(9):2076. doi:10.3390/molecules25092076
60. Zhang YA, Li FW, Dong YX, et al. PPAR-γ regulates the polarization of M2 macrophages to improve the microenvironment for autologous fat grafting. *FASEB J*. 2024;38(8):e23613.
61. Li Q, Liu L, Sun H, et al. Carnosic acid protects against lipopolysaccharide-induced acute lung injury in mice. *Exp Ther Med*. 2019;18(5):3707-3714. doi:10.3892/etm.2019.8042
62. Tian XF, Yao JH, Zhang XS, et al. Protective effect of carnosol on lung injury induced by intestinal ischemia/reperfusion. *Surg Today*. 2010;40(9):858-865. doi:10.1007/s00595-009-4170-y
63. Fernandes RM, Wingert A, Vandermeer B, et al. Safety of corticosteroids in the treatment of acute respiratory disease in children: a systematic review and meta-analysis. *BMJ Open*. 2019;9(8):e028511. doi:10.1136/bmjopen-2018-028511
64. Abbas AH, Hassan ZM, Albarki MA, et al. Mitigative effects of a topically-applied combination of cimifugin and vinpocetine on a murine psoriasis-like model. *Pharmakeftiki*. 2025;37(2S). doi:10.60988/p.v37i2S.134
65. Kashyap D, Kumar G, Sharma A, et al. Mechanistic insight into carnosol-mediated pharmacological effects: Recent trends and advancements. *Life Sci*. 2017;169:27-36. doi:10.1016/j.lfs.2016.11.013
66. Singh D, Mittal N, Siddiqui M. A review on pharmacological potentials of phenolic diterpenes carnosic acid and carnosol obtained from Rosmarinus officinalis L. and modern extraction methods implicated in their recovery. *Trends Phytochem Res*. 2023;7(3):156-169. doi:10.30495/tpr.2023.1990761.1365

Rzeszów University Press 2026
ISSN 2544-1361 (online)
doi: 10.15584/ejcem.2026.1.26

http://www.ejcem.ur.edu.pl
European Journal of Clinical and Experimental Medicine
Eur J Clin Exp Med 2026; 24 (1): 150–163

ORIGINAL PAPER

Effect of retatrutide on body weight, lipid profile, liver function, oxidative stress, and inflammation in experimental obesity in male rats

Zinah Meteab Rahi AL-shibil [1], Zahraa J. Kadhim [2]

[1] Al-Najaf Health Directorate, Ministry of Health, Najaf, Iraq
[2] Department of Pharmacology and Toxicology, Faculty of Pharmacy, University of Kufa, Najaf, Iraq

ABSTRACT

Introduction and aim. Obesity is a global health concern associated with an increased risk of diabetes, cardiovascular disease, hypertension, and non-alcoholic fatty liver disease, often driven by chronic low-grade inflammation. Recent evidence suggests that retatrutide, a novel GIPR/GLP-1R/GCGR tri-agonist, possesses anti-inflammatory properties in addition to its known effects on glucose metabolism, lipid profiles, and weight reduction. However, comprehensive preclinical data on retatrutide's direct impact on hepatic inflammation, oxidative stress, and FGF21 regulation in diet-induced obesity models remain limited. This study aims to investigate the potential protective effect of retatrutide on inflammatory and oxidative stress status in diet-induced obesity in male rats, thereby providing mechanistic insight into its hepatoprotective actions.

Material and methods. Twenty-eight adult male Sprague-Dawley rats were randomly assigned to four groups: normal controls (standard chow for 12 weeks), obese controls (HF/sucrose diet for 12 weeks), vehicle-treated (HF/sucrose for 8 weeks, then normal saline S.C. for 4 weeks with HF/sucrose), and retatrutide-treated (HF/sucrose for 8 weeks, then retatrutide 25 nmol/kg S.C. for 4 weeks with HF/sucrose). Serum insulin, lipid profile, liver enzymes, blood glucose, and FGF21 were measured from blood samples. Crucially, tumor necrosis factor- α (TNF-α), malondialdehyde (MDA), and glutathione (GSH) levels were measured in liver tissue samples.

Results. Modeling obesity using HF/sucrose diet significantly increased insulin levels, blood glucose, liver enzymes, lipid profile, serum FGF21, and body weight. It also considerably elevated hepatic MDA and TNF-α while reducing GSH levels. Retatrutide treatment resulted in significant improvements across most parameters compared to both the obesity and vehicle-treated groups ($p<0.0001$). Specifically, retatrutide-treated rats showed significant reductions in body weight (e.g., approximately 25% reduction compared to obese controls), blood glucose (e.g., from 107±5.944 mg/dL to 85.714±4.785 mg/dL), and liver enzymes AST (e.g., from 89.843±4.533 U/L to 48.959±4.816U/L) and ALP (e.g., from 168.451±28.384 U/L to 97.526±13.446 U/L). Lipid profile parameters, including cholesterol (e.g., from 232.325±23.058mg/dL to 105.881±26.225 mg/dL), triglycerides (e.g., from 112.140±11.450 mg/dL to 30.355±9.479 mg/dL), and LDL (e.g., from 171.557±17.678 mg/dL to 51.341±21.858 mg/dL), were significantly improved, while HDL (e.g., from 38.339±9.670 mg/dL to 65.759±13.828 mg/dL) was significantly increased. Hepatic inflammatory (TNF-α, e.g., from 115.621±5.682 pg/mL to 92.715±5.647 pg/mL) and oxidative stress markers (MDA, e.g., from 5.409±1.078 nmol/ml to 3.120±0.401 nmol/mL) were significantly reduced, and hepatic GSH levels (e.g., from 1.220±0.545 ng/mL to 2.895±0.475 ng/mL) were significantly increased, serum FGF21 (e.g. from 115.367±6.921 pg/mL to 87.445±4.279 pg/mL). These parameters were largely restored to near-control levels in the retatrutide-treated group.

Corresponding author: Zinah M. Rahi AL-shibil, e-mail: zinahm.alshibil@student.uokufa.edu.iq

Received: 25.10.2025 / Revised: 12.12.2025 / Accepted: 28.12.2025 / Published: 30.03.2026

AL-shibil ZMR, Kadhim ZJ. Effect of retatrutide on body weight, lipid profile, liver function, oxidative stress, and inflammation in experimental obesity in male rats. *Eur J Clin Exp Med.* 2026;24(1):150–163. doi: 10.15584/ejcem.2026.1.26.

Conclusion. This study assessed the hepatoprotective effect of retatrutide in a diet-induced obesity model. While the metabolic benefits of incretin-based therapies are well documented, data on retatrutide's direct impact on liver-specific inflammatory and oxidative stress pathways remain limited. This study is among the first to simultaneously evaluate hepatic TNF-α, oxidative stress markers (MDA and GSH), and circulating FGF21 following retatrutide treatment in obese rats, thereby providing mechanistic insight into its hepatoprotective actions beyond weight loss and glycemic control.

Keywords. inflammation, liver, obesity, retatrutide, weight loss

Introduction

Metabolic dysregulation associated with obesity arises when caloric intake consistently exceeds caloric expenditure. Adipose tissue depots expand when surplus energy is converted into triglycerides, resulting in increased body fat and weight gain.[1]

Since 1980, the proportion of individuals classified as overweight or obese has increased fourfold. According to the World Health Organization (WHO) 2024 Global Obesity Report, the prevalence of obesity has continued to escalate dramatically. As of 2023, approximately 43% of adults globally are classified as overweight or obese, representing a significant increase from previous decades. The WHO projects that by 2025, obesity will affect over 1.2 billion people worldwide.[2] In the Middle East and North Africa region, obesity prevalence has reached 28-35%, representing one of the highest rates globally.[3] This escalating epidemic is associated with increased incidence of non-communicable diseases, including type 2 diabetes mellitus, cardiovascular disease, and non-alcoholic fatty liver disease (NAFLD).[4]

Metabolic dysregulation resulting from obesity is correlated with increased concentrations of inflammatory cytokines in the bloodstream relative to individuals with lower body weight. It is proposed that these cytokines play a role in the onset of insulin resistance. In obesity, the principal source of pro-inflammatory cytokines is adipose tissue, predominantly produced by infiltrating macrophages, but adipocytes also play a role in this process. Weight loss results in a decrease in blood levels of these cytokines.[5] The gut microbiota is associated with the pathogenesis of obesity and related metabolic disorders through various potential mechanisms. This encompasses (a) a significant prevalence of carbohydrate-fermenting bacteria, which enhances the biosynthesis of short-chain fatty acids, providing the host with an alternative energy source ultimately stored as lipids or glucose; (b) heightened intestinal permeability to bacterial lipopolysaccharides (LPS), resulting in elevated systemic LPS levels that exacerbate low-grade inflammation and insulin resistance; and (c) augmented activity of the gut endocannabinoid system.[6] The prevalent consequences of metabolic dysregulation in obesity include diabetes, cardiovascular disease, and respiratory issues.[7] Recent research suggests that the prevalence of wheeze and bronchial hyper-responsiveness, commonly associated with asthma, is elevated in overweight and obese persons. Furthermore, certain research indicates that health issues related to obesity may increase the risk of developing deep vein thrombosis, pulmonary embolism, and complications of breathing, including pulmonary hypertension and pneumonia. Weight reduction has demonstrated effectiveness in alleviating the symptoms and severity of several respiratory disorders, including obstructive sleep apnea and asthma.[8]

Moreover, obesity is a contributing factor to the onset of gallbladder disease, non-alcoholic fatty liver disease (NAFLD),[9] pancreatitis, and male fertility issues, including reduced sperm count and heightened incidence of erectile dysfunction.[10] Furthermore, in females, it leads to diminished fertility, poorer outcomes following fertility treatment, and a heightened frequency of pregnancy loss, neurological disorders, immune system dysfunction,[11] musculoskeletal issues, renal illness, and psychosocial complications.[12] Dietary modifications, lifestyle alterations, physical exercise, therapeutic interventions, and surgical procedures can diminish the prevalence of health issues associated with obesity.[13]

Retatrutide (LY3437943) is an experimental medication that represents a novel class of metabolic pharmaceuticals created by Eli Lilly. Retatrutide is a novel tri-agonist peptide targeting the glucagon receptor (GCGR), glucose-dependent insulinotropic polypeptide receptor (GIPR), and glucagon-like peptide-1 receptor (GLP-1R), exhibiting 2.9-fold and 2.5-fold reduced potency at GCGR and GLP-1R, respectively, and 8.9-fold enhanced potency at the human GIP receptor. The mechanisms of action of retatrutide target the GIP, GLP-1, and glucagon receptors, resulting in enhanced glucose regulation, weight reduction, and metabolic wellness.[14] Retatrutide demonstrates decreased pro-inflammatory cytokine expression. Preclinical investigations indicate that retatrutide reduces the expression of pro-inflammatory cytokines, including TNF-α.[15] The clinical indications include obesity management,[16] type 2 diabetes,[17] non-alcoholic fatty liver disease,[18] and potentially other conditions linked to metabolic dysregulation, cardiovascular risk,[19] and cancer progression.[20]

The integrated approach – via concurrent modulation of multiple incretin receptors – offers the potential for improved weight loss outcomes, superior glycemic control, beneficial impacts on hepatic fat accumulation relative to conventional treatments, and enhancements in essential metabolic indicators, such as lipid profiles, blood pressure, and HbA1c levels. The drug's versatility positions it as a strong candidate for obesity

management and the treatment of several metabolic disorders, potentially serving as a foundational element in multi-indication therapeutic strategies.[21]

Although GLP-1 receptor agonists (e.g., liraglutide, semaglutide) and GIP/GLP-1 dual agonists (e.g., tirzepatide) reliably reduce body weight and improve metabolic outcomes in both humans and rodents, including better glucose control and improved lipid profiles. However, comprehensive preclinical data on the triple-agonist retatrutide in diet-induced obesity models are still limited.[22]

Importantly, retatrutide's effects on key liver-related mechanisms have not been well defined, including hepatic oxidative stress (malondialdehyde (MDA) and glutathione (GSH) measured together), hepatic inflammation (TNF-α), and the metabolic regulator FGF21, and the optimal rodent dosing schedule remains unclear. This study addresses these gaps by measuring MDA, GSH, hepatic TNF-α, and serum FGF21 in a diet-induced obesity model while applying a concise daily dosing regimen designed to improve peptide stability,[23] thereby clarifying retatrutide's hepatoprotective mechanisms and supporting translational relevance.

Aim

The purpose of this study is to examine the impact of retatrutide on body weight, level of inflammation, and oxidative stress in hepatic tissue by estimating the levels of MDA, GSH, TNF-α, and FGF21, and measuring serum biochemical parameters including liver function enzymes, lipid profiles, and insulin resistance levels.

Material and methods

Animal preparation

A total of 28 mature male Sprague-Dawley rats, aged 8–10 weeks and weighing between 200 and 230 grams, were sourced from the Faculty of Science, University of Kufa. They were kept in the animal department of the Faculty of Science at the University of Kufa under standard conditions. The average daily temperature was maintained at 24±2°C with 60–65% humidity, and the rats had unrestricted access to food and tap water. The animals were housed in cages with 3-4 rats per cage, with a 12-hour light/dark cycle. All experimental techniques and animal handling were conducted after clearance from the Institutional Animal Care and Use Committee (IACUC) at Kufa University, following the submission of the requisite documentation (NO. 2121) on January 23, 2025.

Compliance with ethical standards

All experimental procedures were conducted in accordance with:

- The Guide for the Care and Use of Laboratory Animals (NIH)
- ARRIVE 2.0 guidelines for reporting animal research
- Institutional policies and regulations

Study design

After a 7-day acclimatization period, a computer-generated sequence was used to randomly assign twenty-eight Sprague-Dawley rats into four experimental groups, seven rats per each group. Investigators were blinded to treatment allocation during outcome assessment. However, due to the nature of the intervention, blinding during treatment administration was not feasible.

Sample size calculation

The sample size was determined to ensure adequate statistical power while maintaining the error degrees of freedom (DFw) within the range of 10 to 20. Based on the formula Min (n) = 10/(k+2) and Max (n) = 20/(k+1), where k represents the number of groups, a minimum of 7 animals and a maximum of 11 animals per group were indicated. Consequently, 7 animals per group were selected for this study.[24,25]

Experimental groups

- Control group: The rats in this group received standard chow for 12 weeks.
- Obesity group: The rats in this group received a high-fat/sucrose diet (HF/sucrose diet) for 12 weeks.
- Vehicle-treated group: The rats in this group were fed HF/sucrose diet for eight weeks, then received subcutaneous injections of normal saline every morning for four weeks along with the HF/sucrose diet.
- Retatrutide-treated group: After eight weeks of HF/sucrose diet, the rats in this group received 25 nmol (0.118 mg/kg) of retatrutide S.C. every morning for four weeks along with the HF/sucrose diet.

Table 1. Nutritional composition of standard chow and high-fat/sucrose diet

Nutrient	Standard chow (LabDiet 5008)	HF/sucrose diet
Protein	~20%	~15-18%
Carbohydrate	~60%	~25-30% + 30% sucrose solution
Fat	5%	30%
Fiber	~5%	~3-4%
Ash	~8%	~6-7%
Metabolizable energy (kcal/g)	~3.5	~4.8

Experimental diet

The 30% sucrose solution for the HF/sucrose diet group was formulated by dissolving 300 g of refined sucrose in 1000 ml of water. The fluid was filtered and administered to the rats in glass containers. This 30% sucrose concentration was chosen to effectively induce metabolic dysregulation and obesity in rodent models, consistent with established protocols.[26] To create high-fat chow, standard chow pellets containing 5% fat (LabDiet 5008, LabDiet, St. Louis, MO) were triturated, and 750

g of this powder was combined with 250 g of Beef fat to achieve a final fat content of 30%. Water was incorporated into the mixture to achieve a uniform dough; thereafter, pellets were manually formed, allowed to dry, and provided to the HF/sucrose diet group. The nutritional composition of the standard chow and high-fat/sucrose diet is detailed in Table 1.[27]

Dose calculation

Retatrutide (cat. No. Z-peptide-24080802, China) powder with 98.89% purity was used in this study. The human clinical dose is 8 mg/week, which corresponds to 0.019 mg/kg/day for a 60 kg individual.[16] Translating dosages from humans to animals is an essential phase in preclinical research; however, it is crucial to understand the process and its constraints. The predominant and recommended approach employs Body surface area (BSA), which has a superior correlation with metabolic rate and physiological processes compared to body weight alone.[28]

Using BSA conversion based on the formula:

Animal dose (mg/kg) =human dose (mg/kg) × (human Km factor/animal Km factor)

Where Km=body weight (kg)/body surface area (m^2)

Step-by-step calculation

1. Identify the known values:
– Human dose: 0.019 mg/kg
– Human Km factor: For a 60 kg human, the Km factor is 37
– Rat Km factor: For a 150-200g rat, the Km factor is 6
2. Apply the formula:
– Rat dose (mg/kg) =0.019 mg/kg × (37 / 6)
– Rat dose (mg/kg) =0.019 mg/kg × 6.17
– Rat dose≈0.118 mg/kg
3. Convert to Molar Units:
– Molecular weight for retatrutide=4731.33 g/mol
– 0.118 mg=0.118×10^{-3} g=1.18×10^{-4} g
– mol/kg=$1.18\times10^{-4}/4731.33=2.494\times10^{-8}$ mol/kg
– 2.494×10^{-8} mol/kg×10^9=24.94 nmol/kg≈25 nmol/kg

Rationale for daily vs. weekly administration

Retatrutide was administered daily rather than weekly (as used clinically) for the following reasons:

1. Peptide stability: Peptides undergo rapid enzymatic degradation with short plasma half-lives. Daily dosing of GLP-1 agonists is required to achieve weight loss in rats due to species-specific pharmacokinetic and metabolic differences. Rats have higher basal metabolic rates and faster drug clearance than humans, necessitating more frequent dosing based on allometric scaling. Pharmacokinetic studies have shown that daily administration of long-acting GLP-1 agonists is necessary in rats to maintain therapeutic drug levels and achieve steady-state exposure comparable to weekly dosing in humans. (typically 2-4 hours for GLP-1 analogs).[23]
2. Bioavailability: Weekly dosing would result in suboptimal and fluctuating drug concentrations, with periods of inadequate therapeutic levels.[29]
3. Sustained effect: Daily subcutaneous administration ensures stable peptide concentrations and sustained biological effects throughout the treatment period.

Important limitation – lack of PK/PD data: However, we acknowledge that no pharmacokinetic (PK) or pharmacodynamic (PD) data specifically validating this daily dosing schedule in rats are available in the literature. This represents an empirical choice based on general peptide pharmacology principles, and actual retatrutide PK/PD in rats may differ from other GLP-1 analogs.[22] This limitation is further discussed in the study limitations section.

Blood sample collection

Male rats were anesthetized using intraperitoneal injections of ketamine hydrochloride (100 mg/kg) (Sigma-Aldrich, USA, Cat. No. K2753) combined with xylazine hydrochloride (10 mg/kg) (Sigma-Aldrich, USA, Cat. No. X1251).[30] The level of anesthesia was monitored throughout the procedure by assessing pedal withdrawal response, corneal reflex, and breathing rate. Body temperature was maintained between 36.8°C and 37.3°C using a feedback-controlled heating pad. Blood samples were collected via direct cardiac puncture using a 5 mL syringe into a gel tube (Medic-Home, China). The serum was separated by centrifugation at 3000 rpm for 15 minutes using a centrifuge (Hettich, Germany). Serum samples were then separated into Eppendorf tubes for subsequent measurement of blood glucose, serum insulin, liver enzymes, and lipid profile using a spectrophotometer (Emclab, Germany), and for identification of FGF21 using a rat-specific enzyme-linked immunosorbent assay (ELISA) kit. Investigators were blinded to treatment allocation during sample analysis. For liver enzymes aspartate transaminase (AST, Bioresearch, Jordan, Cat. No. CZ005), alanine aminotransferase (ALT, Bioresearch, Jordan, Cat. No. CZ003), alkaline phosphatase (ALP, Bioresearch, Jordan, Cat. No. CZ001) the three kits with spectrophotometric wavelength 340).

Tissue sample preparation

A midline abdominal incision was performed to access the liver in every animal. The rat was then immediately euthanized under ethical guidelines. Afterward, clots and red blood cells were removed with ice-cold PBS (phosphate-buffered saline). The tissue was finely chopped and mixed with a volume of cold PBS buffer (w:v=1:9; 100 mg of tissue sample was mixed with 900

μL of PBS buffer) using a glass homogenizer on ice at -80°C. Next, the mixtures were centrifuged at 10,000×g for 5 minutes to obtain the supernatant. ELISA assays were employed to determine the concentration of GSH, TNF-α, and MDA. Investigators were blinded to treatment allocation during sample analysis.

Biochemical parameter measurement

Blood glucose levels were measured using the ACCU-CHEK Active glucometer (Roche, Germany). Animal body weights were obtained using an electronic balance. Serum insulin levels were measured using a Rat Insulin ELISA Kit (Ideal Medical Technology, Shanghai, Cat. No. ADL-EL-RT00483, detection range: 0, 6.25, 12.5, 25, 50, 100 μIU/ml) to assess pancreatic β-cell function and insulin secretion in response to the obesity model and retatrutide treatment. Tumor necrosis factor-alpha (TNF-α) was quantified using a Rat TNF-α ELISA Kit (Ideal Medical Technology, Shanghai, Cat. No. ADL-EL-RT00160, detection range: 0, 20, 40, 80, 160, 320 pg/ml), serving as a key marker of hepatic inflammation in obesity-related liver disease. Fibroblast growth factor 21 (FGF21), a metabolic regulator, was measured using a Rat FGF21 ELISA Kit (Ideal Medical Technology, Shanghai, Cat. No. ADL-EL-RT01162, detection range: 0, 15, 30, 60, 120, 240 pg/ml) to assess metabolic stress. Reduced glutathione (GSH), the primary intracellular antioxidant, was determined using a Rat GSH ELISA Kit (Ideal Medical Technology, Shanghai, Cat. No. ADL-EL-RT00896, detection range: 0, 0.5, 1, 2, 4, 8 ng/ml) as a marker of hepatic antioxidant defense capacity. Malondialdehyde (MDA), a marker of lipid peroxidation and oxidative stress, was quantified using a Rat MDA ELISA Kit (Ideal Medical Technology, Shanghai, Cat. No. ADL-EL-RT01047, detection range: 0, 0.3, 0.6, 1.2, 2.4, 4.8 nmol/ml). Tissue MDA and GSH levels were quantified from homogenates and normalized to total protein content using the Bradford assay method.

For liver enzymes, AST (Bioresearch, Jordan, Cat. No. CZ005), ALT (Bioresearch, Jordan, Cat. No. CZ003), and ALP (Bioresearch, Jordan, Cat. No. CZ001) were measured spectrophotometrically at a wavelength of 340 nm. The kinetic/IFCC method was applied for AST and ALT, while the kinetic/DGKC method was used for ALP.

HOMA-IR calculation

HOMA-IR was calculated using the formula (Matthews et al., 1985):

HOMA-IR= [Fasting Insulin (μU/mL) ×fasting glucose (mg/dL)]/405

This formula is a validated index of insulin resistance in rodent models and provides a non-invasive assessment of hepatic insulin sensitivity.[31]

Lipid profile analysis

A spectrophotometer (Emclab, Germany) was used to measure liver enzymes and lipid profiles. Serum total cholesterol, triglycerides, and high-density lipoprotein cholesterol (HDL-C) were determined enzymatically using commercial assay kits. Low-density lipoprotein cholesterol (LDL-C) and very-low-density lipoprotein cholesterol (VLDL-C) were calculated using the Friedewald formula (Friedewald et al., 1972):

LDL-C=total cholesterol−HDL-C−(triglycerides/5)

This formula was originally developed for human plasma samples and assumes a fixed relationship between triglycerides and VLDL cholesterol. Therefore, its application to rat serum should be used with caution,[32] but is still widely used in rodent studies for consistency with existing literature.

Food intake monitoring

Food intake was not quantitatively measured in this study. Therefore, any statements regarding food consumption in the Discussion section are based on observational assessments rather than systematic quantitative measurements.

Statistical analysis

Statistical analyses were conducted using GraphPad Prism version 10.6 (GraphPad Software, San Diego, CA, USA). Data are expressed as mean ± standard deviation (SD). Outcomes measured at a single time point were analyzed using one-way ANOVA followed by Tukey's post hoc test for multiple comparisons. Repeated measures data collected over weeks 0–4 were analyzed using mixed-model ANOVA, with treatment group, time, and their interaction as fixed effects and individual animals as a random effect. Assumptions of normality and homogeneity of variance were assessed and met. Statistical significance was set at $p < 0.05$, and results are reported with F-statistics, degrees of freedom, and exact p-values.

Results

Effect of HF/sucrose diet on body weight and fasting glucose before treatment

At baseline (Week 8, before treatment initiation), after eight weeks of diet feeding, the body weight of all groups fed HF/sucrose diet was significantly higher than that of the control diet group ($p<0.0001$ for all comparisons). However, there were no significant differences in body weight between the groups designated for vehicle treatment and retatrutide treatment ($p=0.1466–0.4953$), indicating successful randomization and comparable baseline weights for assessing treatment effects. Fasting blood glucose levels were not significantly different among all groups ($p=0.93–0.99$), indicating that glucose dysregulation had not yet developed at this early stage of obesity induction.as shown in (Table 2).

Table 2. Body weight and fasting blood glucose before treatment (week 8) [a]

Groups	Control diet	HF/sucrose diet (obesity)	HF/sucrose diet (before vehicle)	HF/sucrose diet (before treatment)
Body weight (g)	254.857 ±16.847	345.571 ±19.251****	338.571 ±33.645****	368.000 ±27.214****
Fasting blood glucose (mg/dL)	105.143 ±6.229	107.714 ±6.601	106.571 ±6.779	107.000 ±5.944

[a] data are presented as mean±SD of seven rats in each group, **** – p<0.0001 (all HF/sucrose diet groups vs. control group), fasting blood glucose was not significantly different among all groups (p=0.93-0.99), (mixed-model ANOVA, Tukey's test)

Effect of HF/sucrose diet and retatrutide on weight change

As mentioned earlier, at baseline, the body weight of groups fed HF/sucrose diet was higher than that of the control diet group. After week 1 of treatment with retatrutide medication, the obesity, vehicle, and retatrutide groups were significantly higher than the control diet group (p=0.0001, p=0.0001, p=0.0001, respectively). The obesity and vehicle groups were not significantly different (p=0.0902), and the vehicle and retatrutide groups were not significantly different (p=0.0619).

In week 2 of treatment, the obesity and vehicle groups were significantly higher than the control diet group (p=0.0001, p=0.0001, respectively). The obesity and vehicle groups were not significantly different (p=0.0936), the control and retatrutide groups were not significantly different (p=0.7685), and retatrutide was significantly lower than obesity (p=0.0001).

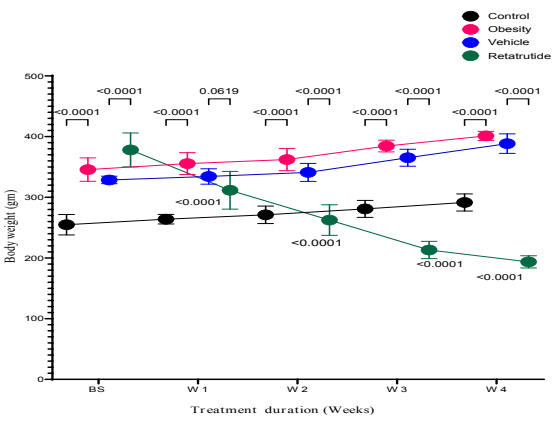

Fig. 1. Effect of retatrutide on body weight during the 4-week treatment period**,** rats fed HF/sucrose diet were treated with retatrutide 25 nmol/kg daily for 4 weeks, in the vehicle group, rats were administered vehicle (normal saline), BS – baseline, data are presented as mean±SD of seven rats in each group, p<0.0001 retatrutide significantly decreased compared to the obesity group, p<0.0001 obesity significantly increased compared to the control group (mixed-model, Tukey's test)

In week 3 of treatment, the obesity and vehicle groups were significantly higher than the control diet group (p=0.0001, p=0.0001, respectively). The obesity and vehicle groups were not significantly different (p=0.1466), and retatrutide was significantly lower than obesity (p=0.0001).

In week 4 of treatment, the obesity and vehicle groups were significantly higher than the control diet group (p=0.0001, p=0.0001, respectively). The obesity and vehicle groups were not significantly different (p=0.4953), and retatrutide was significantly lower than obesity (p=0.0001), F (12, 120) =55.54 as shown in Figure 1.

Effect of HF/sucrose diet and retatrutide on fasting blood glucose

At baseline, the fasting blood glucose levels of the groups fed HF/sucrose diet and the control diet were not significantly different among all groups, as shown in Table 2.

After week 1 of treatment with retatrutide medication, the obesity and vehicle groups were significantly different than the control diet group (p=0.0073, p=0.0240, respectively). The obesity and vehicle groups were not significantly different (p=0.6033), and retatrutide was significantly lower than obesity (p=0.0004).

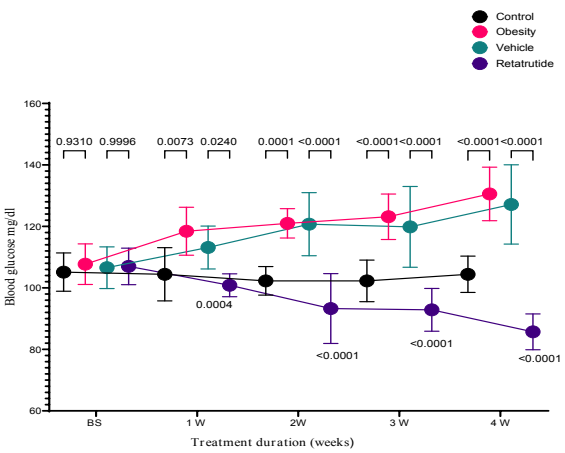

Fig. 2. Effect of retatrutide on fasting blood glucose during the 4-week treatment period**,** rats fed HF/sucrose diet were treated with retatrutide 25 nmol/kg daily for four weeks, in the vehicle group, rats were administered vehicle (normal saline), BS – baseline, data are presented as mean±SD of seven rats in each group, p<0.0001 retatrutide significantly decreased compared to the obesity group, p<0.0001 obesity significantly increased compared to the control group (mixed-model, Tukey's test).

In week 2 of treatment, the obesity and vehicle groups were significantly higher than the control diet group (p=0.001, p=0.001, respectively). The obesity and vehicle groups were not significantly different (p=0.9999), and retatrutide was significantly lower than obesity (p=0.0001).

In week 3 of treatment, the obesity and vehicle groups were significantly higher than the control diet group (p=0.0001, p=0.0001, respectively). The obesity and vehicle groups were not significantly different (p=0.8677), and retatrutide was significantly lower than obesity (p=0.0001).

In week 4 of treatment, the obesity and vehicle groups were significantly higher than the control diet group (p=0.0001, p=0.0001, respectively). The obesity and vehicle groups were not significantly different (p=0.8525), and retatrutide was significantly lower than obesity (p=0.0001), F (12, 120)=6.782 as shown in Figure 2.

Effect of retatrutide on insulin resistance

The HOMA-IR levels in the obesity group were significantly increased (p=0.0001) compared to the control diet group. Conversely, the retatrutide group exhibited a significant decrease (p=0.0001) in HOMA-IR levels compared to the obesity group. There was no statistically significant difference (p=0.9057) in HOMA-IR between the vehicle and obesity groups, or between the retatrutide and control diet groups (p=0.2008), F (3, 24) = 51.81.as shown in Table 3.

Table 3. Effect of retatrutide on HOMA-IR[a]

Groups	HOMA-IR
Control diet	2.14±0.32
HF/sucrose diet (obesity)	6.78±0.85****
Vehicle+HF/sucrose diet	6.52±0.91
Retatrutide+HF/sucrose diet	2.35±0.48††††

[a] data are presented as mean±SD of seven rats in each group, **** – p<0.0001 HF/sucrose diet (obesity) significantly increased compared to control group, †††† – p<0.0001 retatrutide+HF/sucrose diet significantly decreased compared to obesity (one-way ANOVA, Tukey's test)

Effect of HF/sucrose diet and retatrutide on serum liver enzymes

ALT levels were significantly increased in the obesity and vehicle groups compared to the control group (p=0.0366, p=0.0494, respectively). The retatrutide group showed no significant difference compared to the obesity group (p=0.1635) or the control group (p=0.8785). The obesity and vehicle groups were not significantly different (p=0.9990), F (3, 24) =4.232.

AST levels were significantly increased in the obesity and vehicle groups compared to the control group (p=0.0001, p=0.0001, respectively). The retatrutide group showed a significant decrease compared to the obesity group (p=0.0001) and no significant difference compared to the control group (p=0.4019). The obesity and vehicle groups were not significantly different (p=0.9504), F (3, 24) =92.74.

ALP levels were significantly increased in the obesity and vehicle groups compared to the control group (p=0.0001, p=0.0001, respectively). The retatrutide group showed a significant decrease compared to the obesity group (p=0.0001) and no significant difference compared to the control group (p=0.4392). The obesity and vehicle groups were not significantly different (p=0.9999), F (3, 24)=50.00.as shown in Table 4.

Table 4. Effect of retatrutide on serum liver enzymes[a]

Biochemical parameter (U/L)	Control diet	HF/sucrose diet (obesity)	Vehicle+HF/ sucrose diet	Retatrutide+HF/ sucrose diet
ALT	28.43±4.52	38.71±6.89*	36.85±7.23	32.14±5.67
AST	45.29±5.34	98.57±8.91****	97.14±9.45	52.43±6.78††††
ALP	52.86±6.23	112.43±10.56****	111.71±11.34	58.29±7.45††††

[a] data are presented as mean±SD of seven rats in each group, * – p<0.05 (ALT in obesity vs. control), **** – p<0.0001 (AST and ALP in HF/sucrose diet (obesity) vs. control), †††† – p<0.0001 (AST and ALP in retatrutide+HF/ sucrose diet vs. HF/sucrose (obesity)), ALT was not significantly different between retatrutide and obesity groups (p=0.1635), (one-way ANOVA, Tukey's test)

The lack of statistical significance in ALT levels between the retatrutide-treated and obesity groups, while AST and ALP showed significant reductions, may be attributed to the differential sensitivity and specificity of these liver enzymes as markers of hepatocellular injury. ALT is the most sensitive marker of hepatocyte damage but can be influenced by multiple factors and may require longer treatment periods for complete normalization. The 4-week treatment duration was sufficient to significantly reduce the more robust markers (AST and ALP), but may have been insufficient for complete ALT normalization. This pattern is consistent with previous studies of GLP-1/GIP receptor agonists, where longer treatment periods (12–24 weeks) are typically required for complete normalization of all liver enzyme markers.

Effect of HF/sucrose diet and retatrutide on serum lipid profile

Cholesterol levels were significantly increased in the obesity and vehicle groups compared to the control group (p=0.0001, p=0.0001, respectively). The retatrutide group showed a significant decrease compared to both the obesity group (p=0.0001) and the control group (p=0.0001). The obesity and vehicle groups were not significantly different (p=0.6919).

Triglyceride (TG) levels were significantly increased in the obesity and vehicle groups compared to the control group (p=0.0001, p=0.0001, respectively). The retatrutide group showed a significant decrease compared to the obesity group (p=0.0001) but no significant difference compared to the control group (p=0.9986). The obesity and vehicle groups were not significantly different (p=0.2385).

High-density lipoprotein (HDL) levels were significantly decreased in the obesity and vehicle groups compared to the control group (p=0.0001, p=0.0001, re-

spectively). The retatrutide group showed a significant increase compared to the obesity group (p=0.0045) but no significant difference compared to the control group (p=0.4073). The obesity and vehicle groups were not significantly different (p=0.9117).

Low-density lipoprotein (LDL) levels were significantly increased in the obesity and vehicle groups compared to the control group (p=0.0001, p=0.0001, respectively). The retatrutide group showed a significant decrease compared to the obesity group (p=0.0001) but no significant difference compared to the control group (p=0.3247). The obesity and vehicle groups were not significantly different (p=0.9999).

Very-low-density lipoprotein (VLDL) levels were significantly increased in the obesity and vehicle groups compared to the control group (p=0.0488, p=0.0285, respectively). The retatrutide group showed a significant decrease compared to the obesity group (p=0.0448) but no significant difference compared to the control group (p=0.9999). The obesity and vehicle groups were not significantly different (p=0.9970), F (12, 120)=48.32 as shown in Table 5.

Table 5. Effect of retatrutide on serum lipid profile[a]

Biochemical parameter (mg/dL)	Control diet	HF/sucrose diet (obesity)	Vehicle+HF/ sucrose diet	Retatrutide+HF/ sucrose diet	p (vehicle vs. retatrutide)
Cholesterol	164.463 ±15.391	241.085 ±22.002****	232.325 ±23.058	105.881 ±26.225****†	<0.0001
TG	47.905 ±10.740	140.937 ±10.931****	112.140 ±11.450	30.356 ±9.479****†	<0.0001
HDL	78.185 ±10.125	33.069 ±13.949****	38.339 ±9.670	65.759 ±13.828**†	0.0045
LDL	76.696 ±19.774	179.827 ±21.412****	171.557 ±17.678	51.341 ±21.858****†	<0.0001
VLDL	9.581 ±2.148	28.187 ±2.186*	22.428 ±2.290	9.193 ±5.551*†	0.0448

[a] data are presented as mean±SD of seven rats in each group, **** – p<0.0001 (cholesterol, TG, LDL); * – p<0.05 (VLDL) in HF/sucrose diet (obesity) significantly increased compared to control group, except HDL, **** – p<0.0001 HF/sucrose diet (obesity) is significantly decreased compared to control group, **** p<0.0001 (cholesterol, TG, LDL), * p<0.05 (VLDL) in retatrutide+HF/sucrose diet significantly decrease compared to HF/sucrose diet (obesity) except** p<0.01 (HDL) significant increase compared to HF/sucrose diet (obesity), † – indicates significant difference from HF/sucrose diet (obesity) group. comparisons between vehicle+HF/sucrose diet vs. retatrutide+HF/sucrose diet show highly significant differences for all parameters (p shown in final column) (one-way ANOVA, Tukey's test)

Effect of HF/sucrose diet and retatrutide on tumor necrosis factor-α (TNF-α)

There was a significant increase (p=0.0066) in TNF-α levels in the obesity group compared to the control group. The retatrutide group showed a significant decrease (p=0.0049) compared to the obesity group and no significant difference with the control group (p=0.9993). There was no significant difference between the obesity and vehicle groups (p=0.9998), F (3, 24)=8. 964 as shown in Figure 3.

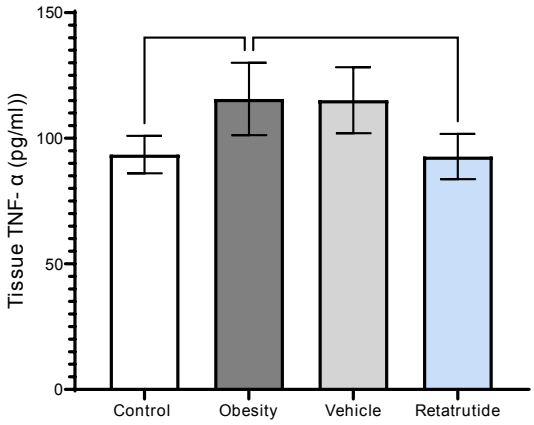

Fig. 3. Effect of retatrutide on hepatic TNF-α levels, rats fed HF/sucrose diet were treated with retatrutide 25 nmol/kg daily for four weeks. In the vehicle group, rats were administered vehicle (normal saline), data are presented as mean±SD of seven rats in each group, obesity group significantly increased compared to control group (p=0.0066), retatrutide group significantly decreased compared to obesity group (p=0.0049) (one-way ANOVA, Tukey's test)

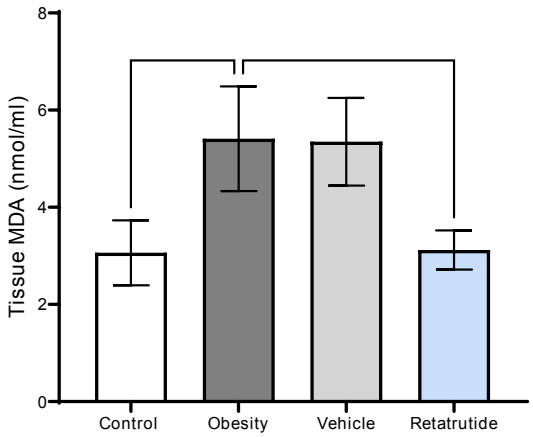

Fig. 4. Effect of retatrutide on hepatic MDA levels (lipid peroxidation marker): rats fed HF/sucrose diet were treated with retatrutide 25 nmol/kg daily for four weeks. In the vehicle group, rats were administered vehicle (normal saline), data are presented as mean±SD of seven rats in each group. p<0.0001 obesity group significantly increased compared to control group. p<0.0001 retatrutide group significantly decreased compared to obesity group. (one-way ANOVA, Tukey's test)

Effect of HF/sucrose diet and retatrutide on MDA

The findings demonstrated a significant elevation in MDA levels (p=0.0001) in the obesity group compared to the control group. The retatrutide-treated group showed a significant reduction (p<0.0001) compared to the obesity group. There was no significant difference between the obesity and vehicle groups (p=0.9990) or between the control and retatrutide groups (p=0.9991), F (3, 24)=18.90 as shown in Figure 4.

Effect of HF/sucrose diet and retatrutide on GSH

Conversely, the antioxidant GSH demonstrated a significant reduction (p=0.0001) in the obesity group compared to the control group. The retatrutide-treated group showed a significant elevation (p=0.0001) compared to the obesity group. There was no significant difference between the obesity and vehicle groups (p=0.9971) or between the control and retatrutide groups (p=0.9998), F (3, 24)=28.18 as shown in Figure 5.

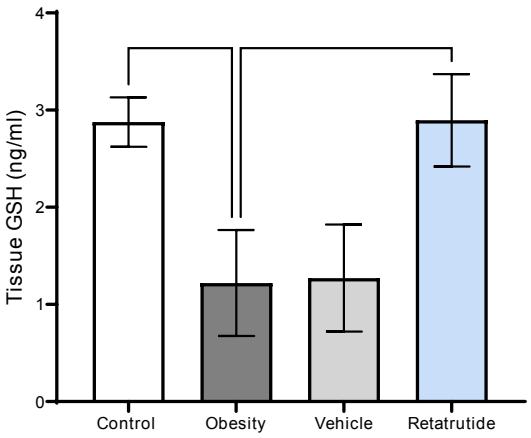

Fig. 5. Effect of retatrutide on hepatic GSH levels (antioxidant marker), rats fed HF/sucrose diet were treated with retatrutide 25 nmol/kg daily for four weeks. In the vehicle group, rats were administered vehicle (normal saline), data are presented as mean±SD of seven rats in each group, p<0.0001 obesity group significantly decreased compared to control group, p<0.0001 retatrutide group significantly increased compared to obesity group (one-way ANOVA, Tukey's test)

Effect of HF/sucrose diet and retatrutide on FGF21

There was a significant increase (p=0.0015) in FGF21 levels in the obesity group compared to the control group. After treatment with retatrutide medication, there was a significant decrease (p=0.0063) compared to the obesity group and no significant difference with the control group (p=0.9361). There was no significant difference between the obese and vehicle groups (p=0.9999), F(3, 24)=10.53 as shown in Figure 6.

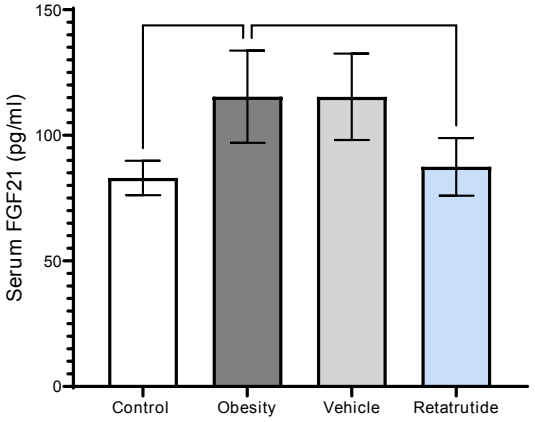

Fig. 6. Effect of retatrutide on serum FGF21 levels, rats fed HF/sucrose diet were treated with retatrutide 25 nmol/kg daily for four weeks, in the vehicle group, rats were administered vehicle (normal saline), data are presented as mean±SD of seven rats in each group, p=0.0015 obesity group significantly increased compared to control group, p=0.0063 retatrutide group showed significant decrease compared to obesity group, (one-way ANOVA, Tukey's test)

Discussion

Metabolic dysregulation linked to obesity and overweight, stemming from excessive food intake, is now acknowledged as a distinct chronic illness that significantly contributes to the global epidemic of chronic, non-communicable diseases.[33] Palatable foods, particularly those rich in sugar and fat, enhance appetite and inhibit satiety signals. The rats induced with obesity were verified as obese after exhibiting significantly higher body weight compared to the negative control rats, following their respective diets. Both animals and humans experience obesity due to a diet rich in fats. Previous studies have demonstrated a positive link between body weight or weight gain and the fat and sugar content of the diet, as evidenced in Table 2 showing a high increase in weight after 8 weeks of feeding HF/sucrose.[34]

In our experience, we used pure peptide powder that was reconstituted in sterile water and administered daily instead of weekly to ensure constant bioactivity. Peptides undergo rapid enzymatic breakdown and possess brief plasma half-lives, resulting in diminished effectiveness over time.[23] For GLP-1 agonists to achieve weight loss in rats a daily dosing is required. This can be justified firstly by allometric scaling of rat metabolic rates to human as rats have much higher basal metabolic rates and faster renal clearance. Secondly, according to the pharmacokinetic studies, to achieve a therapeutic level of a drug, the frequency of dosing must be changed according to the drug half-life in certain species. In a previous pharmacokinetic study, it was found that daily dosing of long-acting GLP-1 agonist is necessary in rat studies. Another pharmacological study demonstrated that to mimic the human weekly dosing of GLP1 agonist

in rats, a daily administration of the drug is required to obtain a steady-state concentration. Daily administration guarantees consistent peptide concentration and biological effects,[29]

though daily dosing was empirical and not validated in the literature. The findings indicated that after 12 weeks of weekly glucometer assessments, the control group exhibited significantly lower blood glucose levels compared to the obesity and obesity plus vehicle groups. Subsequent to the introduction of obesity, an elevation in glucose levels is noted. Animals subjected to a high-fat/sucrose diet exhibited elevated blood glucose levels; through many mechanisms, sustained exposure to high-fat conditions enhances fatty acid oxidation while diminishing glucose oxidation.[35] Obese rats and obese rats administered vehicle had significantly higher insulin resistance (HOMA-IR) levels than rats on a control diet. Blood glucose levels and insulin resistance were considerably reduced when retatrutide was administered subcutaneously for four weeks, because it acts on triple hormone receptors (GLP-1, GIP, and glucagon). These receptors are highly distributed, especially in the small intestine and brain, which delays gastric emptying and increases satiety, suppresses appetite, slows digestion, increases fat metabolism, and increases insulin sensitivity, leading to weight loss and glycemic control.[17] Consequently, being overweight is a major contributor to the onset and progression of insulin resistance.[36] With regards to weight after twelve weeks of HF/sucrose diet and measuring weekly, animals exhibited significantly elevated weight compared to control diet. There was a significant reduction in weight in the retatrutide group that was administered S.C. for four weeks, compared to the obesity and obesity plus vehicle groups. Retatrutide facilitated weight reduction by diminishing food consumption, as we observed in our experiment where male rats reduced HF/sucrose diet intake.[21]

The study found that obesity significantly increased AST, ALP, and ALT levels compared to the control diet group. When using retatrutide medication, there was a significant decrease in hepatic ALP and AST compared to the obesity group, while ALT was not significant; this is somewhat consistent with what was found in some studies, taking into account the short research period of only 12 weeks.[18] The results may be different if the study duration were longer.[16] The results showed a highly significant increase in cholesterol, triglycerides, LDL, and VLDL levels in the obesity group compared to the control group, while HDL showed a significant decrease.[37] When using retatrutide, there was a significant decrease in cholesterol, LDL, triglycerides, and VLDL levels, and a significant increase in HDL compared to the obesity group. The safety profile aligns with GLP-1 receptor agonists and GIP with GLP-1 receptor agonists.[16] It is worth mentioning that we used the Friedewald formula to calculate LDL; this formula was originally developed for human plasma samples and assumes a fixed relationship between triglycerides and VLDL cholesterol. Therefore, its application to rat serum should be used with caution, but it is still widely used in rodent studies.[38]

The group treated with retatrutide showed a significant decrease in the hepatic inflammatory marker TNF-α compared to the obesity group that did not receive treatment. These results support earlier studies in this field.[39,40] Retatrutide also reduces inflammation. Indeed, substantial data indicate that retatrutide can potentially modify or decrease inflammatory processes.[15] Our understanding suggests it is not exactly clear by which mechanism, but may be explained by two main mechanisms via which retatrutide reduces inflammation: altering immune system activation and decreasing levels of inflammatory cytokines.[41] Retatrutide induces immune reprogramming systemically.[20]

The significant reduction in hepatic TNF-α following retatrutide treatment ($p=0.0049$) supports a direct anti-inflammatory action of this triple-agonist. Mechanistically, this effect may involve GLP-1 receptor signaling, as GLP-1 activation can suppress NF-κB activity in hepatocytes and macrophages,[15] thereby lowering pro-inflammatory cytokine production. In addition, the marked weight loss observed with retatrutide likely contributes indirectly by reducing adipose tissue mass and adipose inflammation, a major systemic source of TNF-α driven by macrophage infiltration. Retatrutide may also act directly on hepatic immune cells (e.g., Kupffer cells/macrophages), attenuating cytokine output independent of weight reduction.

Consistent with this interpretation, hepatic TNF-α (inflammation) and MDA (oxidative stress) showed a positive correlation with the atherogenic index,[42] indicating that greater inflammatory and oxidative burden aligns with a more atherogenic lipid pattern. This relationship is biologically plausible because high-fat, high-cholesterol dietary exposure promotes weight gain and worsens circulating lipid and cholesterol levels, which can amplify both oxidative stress and inflammatory signaling and thereby increase cardiovascular risk profiles.[37]

The study's data suggested that obesity resulted in heightened lipid peroxidation, as evidenced by increased MDA levels and decreased GSH levels. Mitochondrial glutathione depletion leads to heightened mitochondrial reactive oxygen species exposure, which disrupts bioenergetics and facilitates the opening of the mitochondrial permeability transition pore, a crucial event in cell death.[43]

Retatrutide appears to mitigate hepatic oxidative stress by improving both sides of the redox balance – reducing oxidative damage while restoring antioxidant capacity.[44] In this study, hepatic MDA, a lipid peroxidation marker, was markedly reduced versus the obese group

($p<0.0001$), indicating less membrane lipid damage and overall oxidative injury in hepatocytes. In parallel, GSH, a key intracellular antioxidant, was significantly depleted in the obese and obese+vehicle groups, but retatrutide substantially increased hepatic GSH compared with obesity ($p<0.0001$). The combined pattern – lower MDA alongside higher GSH – strongly suggests that retatrutide restores hepatic antioxidant defenses rather than merely masking oxidative injury.[45]

Mechanistically, GSH restoration may occur through several complementary routes: (1) reduced reactive oxygen species (ROS) generation due to dampened inflammatory signaling and improved mitochondrial function, (2) enhanced GSH synthesis supported by better cellular energetics and substrate availability, and (3) reduced GSH consumption because the oxidative burden is lower. Prior work with GLP-1–based therapies report similar antioxidant shifts (decreased MDA[46] and increased GSH[47]) in liver and adipose tissue, supporting the plausibility of these pathways; importantly, retatrutide's triple-agonist profile may further amplify mitochondrial and metabolic recovery via additional glucagon receptor signaling, potentially strengthening antioxidant outcomes beyond GLP-1/GIP agonism alone.[14]

Elevated levels of FGF21 have been correlated with many metabolic disorders, including obesity and type 2 diabetes mellitus (T2DM).[48] Serum FGF21 concentrations are typically elevated in cases of obesity and fatty liver disease (non-alcoholic fatty liver disease or NAFLD).[49] This elevation is frequently regarded as a compensatory mechanism to metabolic stress and insulin resistance, although it may also signify a state of FGF21 resistance. The study found that obesity significantly increased FGF21 in both the obese and obese+vehicle groups. Serum FGF21 circulation decreased in the retatrutide group, indicating improved FGF21 receptor sensitivity.[50]

The observed reduction in FGF21 after retatrutide treatment likely reflects relief of the metabolic strain imposed by diet-induced obesity and a shift toward more normalized metabolic regulation. In obesity, FGF21 is often elevated as a compensatory "stress hormone" response to insulin resistance, dyslipidemia, and hepatic lipid overload. By promoting weight loss and improving glycemic control, retatrutide may lower this systemic and hepatic metabolic stress, thereby reducing the need for compensatory FGF21 upregulation.[51]

In addition, declining circulating FGF21 may indicate improved responsiveness of the FGF21 pathway (i.e., reduced "FGF21 resistance") and restoration of downstream receptor signaling, consistent with improved metabolic homeostasis. This is clinically meaningful because effective FGF21 signaling supports lipid handling, glucose regulation, mitochondrial function, and hepatic metabolic recovery; thus, the reduction in FGF21 with retatrutide aligns with a broader normalization of cardiometabolic and liver-related physiology rather than a loss of a protective factor.[52]

Study limitations

This study has several limitations. Liver histopathology was not performed, limiting direct assessment of steatosis, inflammation, and fibrosis. The 4-week treatment duration may have been insufficient to capture maximal hepatic improvement, and inclusion of only male rats restricts generalizability across sexes. The dosing regimen was empirical and not supported by rat-specific PK/PD data, and only a single dose was evaluated without comprehensive safety assessment. Methodological constraints include the use of the Friedewald formula for lipid calculations, lack of quantitative food-intake monitoring, and limited existing rodent data on retatrutide. Future studies should incorporate histological analyses, extended treatment duration, both sexes, PK/PD-guided dosing, dose–response evaluation, and broader toxicity assessments.

Conclusion

This study provided evidence that retatrutide effectively improves weight loss, decreases blood glucose, improves lipid profile, and protects hepatic tissues through decreased inflammation and oxidative stress marker levels.

Acknowledgements

We would like to thank all those who contributed to the completion of this study, including the animal care staff at the Faculty of Science, University of Kufa, for their assistance with animal husbandry and care.

Declarations

Funding

No specific funding from a public, private, or nonprofit institution was provided for this investigation.

Author contributions

Conceptualization: Z.M.R.A. and Z.J.K.; Methodology: Z.M.R.A.; Software: Z.M.R.A.; Validation: Z.M.R.A. and Z.J.K.; Formal Analysis: Z.J.K.; Investigation: Z.M.R.A.; Resources: Z.J.K.; Data Curation: Z.M.R.A.; Writing – Original Draft Preparation: Z.M.R.A.; Writing – Review & Editing: Z.J.K.; Visualization: Z.M.R.A.; Supervision: Z.J.K.; Project Administration: Z.M.R.A.

Conflicts of interest

The authors declare that they have no conflicts of interest.

Data availability

All clinical and statistical data and materials are available upon reasonable request from the corresponding author.

Ethics approval

The study followed the ARRIVE 2.0 guidelines for reporting animal experiments and complied with ethical standards. Approval was obtained from the Institutional Animal Care and Use Committee (IACUC) at the University of Kufa, Iraq, following the submission of the required documentation (NO. 2121) on January 23, 2025.

References

1. Swinburn BA, Sacks G, Hall KD, et al. The global obesity pandemic: shaped by global drivers and local environments. *Lancet*. 2011;378(9793):804-814. doi:10.1016/S0140-6736(11)60813-1
2. Pillai G, Varghis J, Binu S, James R. Assessing the rising tide: a comprehensive analysis of overweight and obesity prevalence among adults. *Int J Multidiscip Res*. 2025;7(2):IJFMR250242715. doi:10.36948/ijfmr.2025.v07i02.42715
3. Farrag NS, Cheskin LJ, Farag MK. A systematic review of childhood obesity in the Middle East and North Africa (MENA) region: prevalence and risk factors meta-analysis. *Adv Pediatr Res*. 2017;4:8. doi:10.12715/apr.2017.4.8
4. Hildebrand S, Pfeifer A. The obesity pandemic and its impact on non-communicable disease burden. *Pflugers Arch*. 2025;477(5):657-668. doi:10.1007/s00424-025-03066-8
5. Gregor MF, Hotamisligil GS. Inflammatory mechanisms in obesity. *Annu Rev Immunol*. 2011;29(1):415-445. doi:10.1146/annurev-immunol-031210-101322
6. Muscogiuri G, Cantone E, Cassarano S, et al. Gut microbiota: a new path to treat obesity. *Int J Obes Suppl*. 2019;9(1):10-19. doi:10.1038/s41367-019-0011-7
7. Blüher M. An overview of obesity-related complications: The epidemiological evidence linking body weight and other markers of obesity to adverse health outcomes. *Diabetes Obes Metab*. 2025;27(S2):3-19. doi:10.1111/dom.16263
8. Shah NM, Kaltsakas G. Respiratory complications of obesity: from early changes to respiratory failure. *Breathe*. 2023;19(1):220263. doi:10.1183/20734735.0263-2022
9. Fabbrini E, Sullivan S, Klein S. Obesity and nonalcoholic fatty liver disease: biochemical, metabolic, and clinical implications. *Hepatology*. 2010;51(2):679-89. doi:10.1002/hep.23280
10. Feng R, Cheng D, Zhang W, Zhang J, Chen S, Xia Y. Immune microenvironment dysregulation: a contributing factor to obesity-associated male infertility. *Biomedicines*. 2025;13(6):1314. doi:10.3390/biomedicines13061314
11. Carolan E, Hogan AE, Corrigan M, et al. The impact of childhood obesity on inflammation, innate immune cell frequency, and metabolic microRNA expression. *J Clin Endocrinol Metab*. 2014;99(3):E474-8. doi:10.1210/jc.2013-3529
12. Chu DT, Minh Nguyet NT, Nga VT, et al. An update on obesity: Mental consequences and psychological interventions. *Diabetes Metab Syndr*. 2019;13(1):155-160. doi:10.1016/j.dsx.2018.07.015
13. Wadden TA, Tronieri JS, Butryn ML. Lifestyle modification approaches for the treatment of obesity in adults. *American Psychologist*. 2020;75(2):235-251. doi:10.1037/amp0000517
14. Coskun T, Urva S, Roell WC, et al. LY3437943, a novel triple glucagon, GIP, and GLP-1 receptor agonist for glycemic control and weight loss: From discovery to clinical proof of concept. *Cell Metab*. 2022;34(9):1234-1247.e9. doi:10.1016/j.cmet.2022.07.013
15. Ma J, Hu X, Zhang W, Tao M, Wang M, Lu W. Comparison of the effects of liraglutide, tirzepatide, and retatrutide on diabetic kidney disease in db/db mice. *Endocrine*. 2024;87(1):159-69. doi:10.1007/s12020-024-03998-8
16. Jastreboff AM, Kaplan LM, Frías JP, et al. Triple-hormone-receptor agonist retatrutide for obesity: a phase 2 trial. *N Engl J Med*. 2023;389(6):514-26. doi:10.1056/NEJMoa2301972
17. Rosenstock J, Frias J, Jastreboff AM, et al. Retatrutide, a GIP, GLP-1 and glucagon receptor agonist, for people with type 2 diabetes: a randomised, double-blind, placebo and active-controlled, parallel-group, phase 2 trial conducted in the USA. *Lancet*. 2023;402(10401):529-544. doi:10.1016/S0140-6736(23)01053-X
18. Sanyal AJ, Kaplan LM, Frias JP, et al. Triple hormone receptor agonist retatrutide for metabolic dysfunction-associated steatotic liver disease: a randomized phase 2a trial. *Nat Med*. 2024;30(7):2037-2048. doi:10.1038/s41591-024-03018-2
19. Neumann J, Ahlrep U, Hofmann B, Gergs U. Inotropic effects of retatrutide in isolated human atrial preparations. *Naunyn Schmiedebergs Arch Pharmacol*. 2025. doi:10.1007/s00210-025-04421-3
20. Marathe SJ, Grey EW, Bohm MS, et al. Incretin triple agonist retatrutide (LY3437943) alleviates obesity-associated cancer progression. *NPJ Metab Health Dis*. 2025;3(1):10. doi:10.1038/s44324-025-00054-5
21. Katsi V, Koutsopoulos G, Fragoulis C, Dimitriadis K, Tsioufis K. Retatrutide—a game changer in obesity pharmacotherapy. *Biomolecules*. 2025;15(6):796. doi:10.3390/biom15060796
22. Winkler G, Kis JT, Arapovicsné Kiss K, Schandl L. From GLP1 receptor agonists to triple hormone receptor activation supplemented with glucagon receptor agonism. *Orv Hetil*. 2023;164(42):1656-1664. doi:10.1556/650.2023.32894
23. Knop FK, Urva S, Rettiganti M, et al. A long-acting glucose-dependent insulinotropic polypeptide receptor agonist improves the gastrointestinal tolerability of glucagon-like peptide-1 receptor agonist therapy. *Diabetes Obes Metab*. 2024;26(11):5474-5478. doi:10.1111/dom.15875
24. Pakgohar A, Mehrannia H. Sample size calculation in clinical trial and animal studies. *Iran J Diabetes Obes*. 2024. doi:10.18502/ijdo.v16i1.15241

25. Abebe HT. Determination of sample size and errors. In: Promoting Statistical Practice and Collaboration in Developing Countries. Chapman and Hall/CRC; 2022:321-38. doi:10.1201/9781003261148-27
26. Cruz Hernández JH, Rosado Lomán WN, Gómez-Crisóstomo NP, et al. High sugar but not high fat diet consumption induces hepatic metabolic disruption and up-regulation of mitochondrial fission-associated protein Drp1 in a model of moderate obesity. *Arch Physiol Biochem*. 2023;129(1):233-240. doi:10.1080/13813455.2020.1812666
27. Almeida-Suhett CP, Scott JM, Graham A, Chen Y, Deuster PA. Control diet in a high-fat diet study in mice: Regular chow and purified low-fat diet have similar effects on phenotypic, metabolic, and behavioral outcomes. *Nutr Neurosci*. 2019;22(1):19-28. doi:10.1080/1028415X.2017.1349359
28. Nair A, Jacob S. A simple practice guide for dose conversion between animals and human. *J Basic Clin Pharm*. 2016;7(2):27. doi:10.4103/0976-0105.177703
29. Kohler A, Jülke EM, Stichel J, Beck-Sickinger AG. Comparison of protocols to test peptide stability in blood plasma and cell culture supernatants. *ACS Pharmacol Transl Sci*. 2024;7(11):3618-25. doi:10.1021/acsptsci.4c00503
30. Alaasam ER, Janabi AM, Al-Buthabhak KM, et al. Nephroprotective role of resveratrol in renal ischemia-reperfusion injury: a preclinical study in Sprague-Dawley rats. *BMC Pharmacol Toxicol*. 2024;25(1):82. doi:10.1186/s40360-024-00809-8
31. Majid H, Masood Q, Khan AH. Homeostatic model assessment for insulin resistance (HOMA-IR): a better marker for evaluating insulin resistance than fasting insulin in women with polycystic ovarian syndrome. *J Coll Physicians Surg Pak*. 2017;27(3):123-6.
32. Nair SS, Kiran R, Jisna KK, Prathima MB, Sushith P, D'sa J. Comparison of ten formulae for calculating low-density lipoprotein cholesterol with direct low-density lipoprotein cholesterol measurement. *Curr Med Res Pract*. 2024;14(5):192-199. doi:10.4103/cmrp.cmrp_98_24
33. Rubino F, Puhl RM, Cummings DE, et al. Joint international consensus statement for ending stigma of obesity. *Nat Med*. 2020;26(4):485-497. doi:10.1038/s41591-020-0803-x
34. Kurita Y, Ohki T, Soejima E, et al. A high-fat/high-sucrose diet induces WNT4 expression in mouse pancreatic β-cells. *Kurume Med J*. 2018;65(2):55-62. doi:10.2739/kurumemedj.MS652008
35. Chen NG, Reaven GM. Fatty acid inhibition of glucose-stimulated insulin secretion is enhanced in pancreatic islets from insulin-resistant rats. *Metabolism*. 1999;48(10):1314-1317. doi:10.1016/S0026-0495(99)90273-1
36. Hocking S, Samocha-Bonet D, Milner KL, Greenfield JR, Chisholm DJ. Adiposity and insulin resistance in humans: the role of the different tissue and cellular lipid depots. *Endocr Rev*. 2013;34(4):463-500. doi:10.1210/er.2012-1041
37. Han Q, Yeung SC, Ip MSM, Mak JCW. Dysregulation of cardiac lipid parameters in high-fat high-cholesterol diet-induced rat model. *Lipids Health Dis*. 2018;17(1):255. doi:10.1186/s12944-018-0905-3
38. Chen Y, Zhang X, Pan B, et al. A modified formula for calculating low-density lipoprotein cholesterol values. *Lipids Health Dis*. 2010;9(1):52. doi:10.1186/1476-511X-9-52
39. Sourris KC, Ding Y, Maxwell SS, et al. Glucagon-like peptide-1 receptor signaling modifies the extent of diabetic kidney disease through dampening the receptor for advanced glycation end products–induced inflammation. *Kidney Int*. 2024;105(1):132-149. doi:10.1016/j.kint.2023.09.029
40. Alathary A, Al-Isawi Z. Tirzepatide therapy counters inflammatory and apoptotic responses induced by high-fat diet in rat liver. *Wiad Lek*. 2025;(4):797-805. doi:10.36740/WLek/202970
41. Al Khafaji AM, Bairam AF. Synergistic antitumor and apoptotic activity of sitagliptin or linagliptin plus cisplatin against A549 lung cancer cells (an in vitro study). *J Contemp Med Sci*. 2024;10(3). doi:10.22317/jcms.v10i3.1555
42. Yang RL, Shi YH, Hao G, Li W, Le GW. Increasing oxidative stress with progressive hyperlipidemia in human: relation between malondialdehyde and atherogenic index. *J Clin Biochem Nutr*. 2008;43(3):154-8. doi:10.3164/jcbn.2008044
43. Lenaz G, Nesci S, eds. Impaired mitochondrial bioenergetics under pathological conditions. MDPI; 2022. doi:10.3390/books978-3-0365-4647-6
44. Heerspink HJL, Lu Z, Du Y, et al. The effect of retatrutide on kidney parameters in participants with type 2 diabetes mellitus and/or obesity. *Kidney Int Rep*. 2025;10(6):1980-92. doi:10.1016/j.ekir.2025.03.049
45. Labarrere CA, Kassab GS. Glutathione: A Samsonian life-sustaining small molecule that protects against oxidative stress, ageing and damaging inflammation. *Front Nutr*. 2022;9. doi:10.3389/fnut.2022.1007816
46. Alzubaidy DHM, Al-Isawi ZJK. Investigating the impact of semaglutide on hepatic oxidative stress in obese male rats induced by high-fat diet. *Maaen J Med Sci*. 2024;3(3). doi:10.55810/2789-9136.1050
47. Alkhafaji GA, Janabi AM. GIP/GLP-1 dual agonist tirzepatide ameliorates renal ischemia/reperfusion damage in rats. *Int J Appl Pharm*. 2025:165-73. doi:10.22159/ijap.2025v17i2.53156
48. Mraz M, Bartlova M, Lacinova Z, et al. Serum concentrations and tissue expression of a novel endocrine regulator fibroblast growth factor-21 in patients with type 2 diabetes and obesity. *Clin Endocrinol (Oxf)*. 2009;71(3):369-375. doi:10.1111/j.1365-2265.2008.03502.x
49. Filimidou I, Orfanidou M, Goulas A, Giouleme O, Polyzos SA. Circulating fibroblast growth factor-21 in patients with nonalcoholic fatty liver disease: a systematic review and meta-analysis. *Curr Obes Rep*. 2025;14(1):51. doi:10.1007/s13679-025-00643-x

50. Negroiu CE, Tudorașcu RI, Beznă MC, Ungureanu AI, Honțaru SO, Dănoiu S. The role of FGF21 in the interplay between obesity and non-alcoholic fatty liver disease: a narrative review. *Rom J Morphol Embryol*. 2024;65(2):159-172. doi:10.47162/RJME.65.2.02
51. Szczepańska E, Gietka-Czernel M. FGF21: a novel regulator of glucose and lipid metabolism and whole-body energy balance. Horm Metab Res. 2022;54(04):203-11. doi:10.1055/a-1778-4159
52. Falamarzi K, Malekpour M, Tafti MF, Azarpira N, Behboodi M, Zarei M. The role of FGF21 and its analogs on liver associated diseases. *Front Med (Lausanne)*. 2022;9:967375. doi:10.3389/fmed.2022.967375

Rzeszów University Press 2026
ISSN 2544-1361 (online)
doi: 10.15584/ejcem.2026.1.1

http://www.ejcem.ur.edu.pl
European Journal of Clinical and Experimental Medicine
Eur J Clin Exp Med 2026; 24 (1): 164–172

REVIEW PAPER

Drug-induced nephrotoxicity – a review of therapeutic activity of selenium and zinc in preclinical studies

Dayo Rotimi Omotoso , Favour Chinaemerem Egwuatu

Department of Human Anatomy, Redeemer's University, Ede, Osun State, Nigeria

ABSTRACT

Introduction and aim. Certain drugs cause nephrotoxicity and renal dysfunction through induction of oxidative stress and activation of inflammatory and apoptotic signaling pathways within the renal tissue. To mitigate drug nephrotoxicity, the therapeutic potential of trace elements such as selenium (Se) and zinc (Zn) has been experimentally explored. The current knowledge and mechanisms are hereby summarized in this review.

Literature search. This narrative review was carried out through a critical assessment of relevant articles published in scientific databases like Google Scholar, PubMed, Scopus, and Web of Science.

Analysis of the literature. The antioxidant, antiapoptotic and anti-inflammatory properties of Se and Zn culminate in their therapeutic activity against drugs nephrotoxicity. The nephroprotective effect of Se and Zn has been characterized with suppression of renal oxidative stress (reduced malondialdehyde, protein cabonyl and elevated levels of superoxide dismutase, glutathione, glutathione peroxidase, catalase, total antioxidant capacity levels); upregulation of anti-apoptotic and anti-inflammatory markers (Bcl-2, heme oxygenase-1, factor related to nuclear factor erythroid 2; downregulation of pro-apoptotic and pro-inflammatory like inducible nitric oxide synthase, nitric oxide, tumor necrosis factor-α, interleukin-6, nuclear factor kappa light chain enhancer of activated B cells NF-κB, and Bax, leading to reparation of renal histomorphology and improved renal function (indicated by reduced serum creatinine, urea, BUN levels).

Conclusion. The therapeutic activity of Se and Zn against drugs nephrotoxicity underscores their potential role in the management of nephrotoxicity due to pharmacotherapy.

Keywords. drugs nephrotoxicity, selenium nephroprotection, zinc nephroprotection

Introduction

The kidney is a vital organ that performs several essential functions in the body, particularly related to maintaining body homeostasis.[1,2] In essence, it plays crucial role in maintaining the overall body health by removing toxic wastes and metabolites, regulating body fluid balance and osmolality, maintaining acid-base equilibrium, secreting hormones, and controlling the arterial pressure.[1,3,4] Due to its essential functions, the kidney is often exposed to and could bioaccumulate potential toxins (regarded as nephrotoxicants or nephrotoxins) which would in turn cause nephrotoxicity.[3,5] Nephrotoxicity thereby involves the degeneration of renal morphological components and loss of their functionality due to the toxic effects of nephrotoxins including chemotherapeutic agents.[2,6] Hence, the critical role of the kidney tissue in the removal of xenobiotics (including chemotherapeutic agents) from the body makes it prone to their toxic effects.

Drug-induced kidney toxicity has been characterized with renal histopathological changes such as ep-

Corresponding author: Dayo Rotimi Omotoso, e-mail: omotosod@run.edu.ng

Received: 5.06.2025 / Revised: 29.06.2025 / Accepted: 18.07.2025 / Published: 30.03.2026

Omotoso DR, Egwuatu FC. Drug-induced nephrotoxicity – a review of therapeutic activity of selenium and zinc in preclinical studies. *Eur J Clin Exp Med.* 2026;24(1):164–172. doi: 10.15584/ejcem.2026.1.1.

ithelial necrosis, glomerular congestion, interstitial edema and inflammation, tubular dilatation, which often lead to renal functional impairments and kidney failure.[7-9] The associated impairment of renal function has been further characterized by significant alteration of markers of renal function such as glomerular filtration rate, urine output, serum levels of electrolytes, and waste products of protein and muscle metabolism.[9,10] Essentially, nephrotoxicity is characterized with glomerular damage, inflammation, crystal nephropathy, renal tubular cell toxicity, rhabdomyolysis, and thrombotic microangiopathy.[11,12] As a risk factor of acute kidney injury and chronic kidney disease, nephrotoxicity poses great public health concern that requires effective therapeutic intervention.

Trace elements are essential elements that are required (in very low concentrations) to play an essential role in many physiological and metabolic processes of the body.[13] They have been shown to exhibit antioxidant, anti-inflammatory and anti-apoptotic effects which thereby underscore their therapeutic potential against various tissue pathologies.[14] Accordingly, the therapeutic potential of trace elements has been explored in preclinical studies to mitigate or ameliorate drug-induced nephrotoxicity.

Aim

In this review, the aim was to elaborate on the therapeutic activity of trace elements, including selenium and zinc, against drug nephrotoxicity in preclinical studies. Furthermore, the associated mechanisms of therapeutic activity of the selected trace elements were highlighted.

Literature search

Published articles were sought in multiple scientific databases including Google Scholar, PubMed, Scopus, and Web of Science and assessed to select those that are relevant to the objective of the review. The search keywords included: 'drug nephrotoxicity', 'trace element nephroprotection', 'trace elements mitigate drug nephrotoxicity', 'antioxidants effect of trace elements'. The literature search was conducted between 1 April and 30 April 2025, and articles selected from preliminary search results were further critically evaluated to identify those that contain relevant findings on the therapeutic role of selenium and zinc against drug-induced nephrotoxicity in preclinical studies. The inclusion criteria included only articles that provided relevant findings, articles published in English and in peer-reviewed journals. Other non-compliant articles were excluded from the review.

Analysis of the literature

Induction of oxidative stress and activation of inflammatory and apoptotic signaling pathways within kidney tissue, following exposure to nephrotoxicants (including drugs), have been demonstrated as pivotal cellular mechanisms of the resulting nephrotoxicity.[18] Hence, the antioxidant, anti-inflammatory, and anti-apoptotic properties of selected trace elements (selenium and zinc) underscored the rationale for their therapeutic application to mitigate drug-induced nephrotoxicity in preclinical studies as presented in this review.

Drug-induced nephrotoxicity in preclinical studies

Nephrotoxicity due to drug administration occurs as an adverse effect of pharmacotherapy and commonly presents in the form of acute kidney injury, renal tubular disorders, glomerular damage, and nephrolithiasis and could lead to renal failure.[19] Although, the selected drugs under review have different structural conformation (Fig. 1), preclinical studies have demonstrated their relatively similar nephrotoxic mechanisms (Table 1).

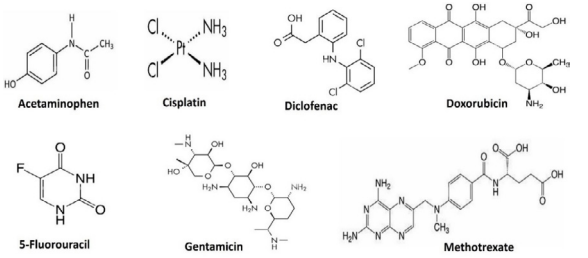

Fig. 1. Molecular structures of selected drugs that cause nephrotoxicity

Acetaminophen (or paracetamol) is a common analgesic and antipyretic agent that has been demonstrated to exhibit nephrotoxicity through the induction of endoplasmic reticulum (ER) stress and apoptosis within kidney tissue.[20] Acetaminophen-induced nephrotoxicity has been characterized by distortion of renal histomorphology, elevated levels of kidney injury molecule-1 (KIM-1), interleukin-18 (IL-18), serum blood urea nitrogen (BUN) and creatinine.[20,21] Acetaminophen exposure further caused upregulation of inducible nitric oxide synthase (iNOS), PERK, activating transcription factor 6 (ATF6), nuclear factor kappa-light chain-enhancer of activated B cells (NF-κB), p53, caspases 3 and downregulation of Bcl-2 and Bcl-xL expressions.[20] Acetaminophen-induced nephrotoxicity also caused decline of tissue antioxidant levels, including superoxide dismutase (SOD), catalase (CAT), glutathione peroxidase (GPx), elevated levels of inflammatory markers (tumor necrosis factor-α (TNF-α), IL-1β, IL-33) and apoptotic marker (caspase-3).[21,22] Moreover, acetaminophen exposure caused increase in total oxidant status (TOS), and inhibition of nuclear factor erythroid-related factor 2 (Nrf2) signaling pathway.[22,23]

Furthermore, cisplatin is a common and effective anticancer drug which has been indicated to cause nephrotoxicity by induction of oxidative stress, in-

flammatory response and apoptosis of renal tubular cells.[24] Cellular mechanisms of cisplatin-induced nephrotoxicity included induction of oxidative stress, ER stress, mitochondrial dysfunction, DNA damage and stress responses such as inflammation, autophagy, cell cycle arrest, senescence, and apoptosis.[25] Additionally, exposure to cisplatin caused elevated levels of plasma renal markers including creatinine, urea uric acid and BUN, reduced levels of SOD, CAT, GPx and glutathione (GSH), renal histopathological changes including renal tubular cell death, vacuolization, vascular congestion.[26] Cisplatin-induced nephrotoxicity has been further characterized with increased levels of oxidative stress, inflammatory and apoptotic markers (MDA, NO, iNOS, TNF-α, NF-κB, IL-1β, caspase-3 and Bax).[27,28]

Diclofenac is a non-steroidal anti-inflammatory drug (NSAID), commonly applied as analgesic or anti-inflammatory agent, and has been indicated to cause organ toxicity (like kidney) via increased generation of reactive oxygen species (ROS).[29] Diclofenac-mediated nephrotoxicity has been characterized with elevated levels of protein carbonyl (PC), urea, creatinine, uric acid, MDA, hydrogen peroxide, decreased antioxidant enzyme activities (SOD, CAT, GPx) and reduced antioxidant (GSH). 30, 31, Exposure to Diclofenac exposure further resulted in renal histopathological changes, reduced glomerular filtration rate, up-regulation of inflammatory and apoptotic factors including KIM-1, TNF-α, IL-6, IL-18, NF-κB, STAT3, Bax, p53, HIF-1α, caspase-3, and cyclooxygenase-2 (COX-2) while heme oxygenase-1 (HO-1), Nrf2, adenosine 5'-monophosphate-activated protein kinase (AMPK), and sirtuin-1 (SIRT-1) expressions were downregulated.[32-34]

Doxorubicin is an anthracycline anticancer drug which has been reported to cause a toxic effect on body tissue such as the kidney through ROS production, oxidative stress, apoptosis, inflammation and dysregulated autophagic flow, thereby limiting its clinical application.[35,36] Doxorubicin-induced nephrotoxicity was characterized by a marked decline of activities of antioxidant enzymes (SOD, CAT, GSH), elevated plasma levels of creatinine, urea, uric acid and renal MDA, cholesterol, calcium and sodium concentrations.[37] Moreover, doxorubicin exposure caused renal histopathological changes (including glomerular atrophy, tubular congestion and degeneration, inflammatory cell infiltrations), increased levels of BUN, NO, hydrogen peroxide (H_2O_2), upregulation of NF-κB, IL-1β, IL-6, caspase-3 and elevated apoptotic index.[38,39] Other mechanisms of doxorubicin-induced nephrotoxicity included decline in renal glutathione reductase (GR) activity and elevated levels of TNF- α and plasma neutrophil gelatinase-associated lipocalin (NGAL).[40]

Furthermore, the application of 5-fluorouracil as an anticancer drug has resulted into serious adverse effects, including hepatotoxicity and nephrotoxicity through induction of oxidative stress, inflammation and apoptosis.[41,42] 5-fluorouracil-induced nephrotoxicity has been characterized by renal histopathological changes (including tubular congestion, degeneration and atrophic glomeruli), marked increase in serum levels of uric acid, creatinine, urea, NO and MDA, decreased activity of antioxidant enzymes (CAT, SOD, GPx) and GSH level.[42,43] Other mechanisms of 5-fluorouracil-induced nephrotoxicity included up-regulation of lipocalin-2, KIM-1, increased levels of TNF-α, NF-κB and IL-6 linked with up-regulated expressions of ERK1 / 2 and VCAM-1, down-regulation of IL-10, Nrf2, HO-1, and FXR factors.[44,45] In addition, 5-fluorouracil administration further resulted in an increased Bax/Bcl-2 ratio, overexpression of iNOS and upregulation of caspase-3 within renal tissue.[46]

Gentamicin, an aminoglycoside antibiotic widely applied as antibiotic to treat Gram-negative bacterial infections, has been reported to exhibit nephrotoxicity due to induction of oxidative stress and activation of apoptotic and inflammatory signaling pathways.[47] Exposure to gentamicin in preclinical studies resulted in renal histopathology (such as tubular necrosis and tubulointerstitial inflammation), decreased renal antioxidant enzymes (SOD, GSH, CAT), elevated TOS, oxidative stress index (OSI) MDA, iNOS, NO, TNF-α levels.[47-49] Other mechanisms of gentamicin-induced nephrotoxicity included up-regulation of NF-κB p65, IL-1β, IL-6, IL-18, p38-MAPK, NGAL, KIM-1, caspase-9, caspase-3 and Bax while Bcl-2, HO-1 and Nrf2 were downregulated within kidney tissue.[47,50,51]

Methotrexate is an effective anticancer and immunosuppressive drug that exhibits characteristic adverse effect including nephrotoxicity due to associated oxidative damage and inflammatory responses in renal tissue.[52] Methotrexate-induced nephrotoxicity has been characterized by marked distortion of renal histoarchitecture, elevated serum creatinine, BUN, reduced renal CAT, glutathione-S-transferase (GST), GSH, and increased levels of NO, IL-1β, TNF-α.[53,54] In preclinical studies, exposure to methotrexate exposure further resulted in impaired mitochondrial biogenesis, reduced SOD and increased MDA levels, upregulation of TLR-4, TNF-α, NF-κB. IL-6, caspase-3, Bax, beclin-1, LC-3, and down-regulation of Bcl-2, Nrf2, HO-1.[52,55,56]

Some other chemotherapeutic agents that exhibit nephrotoxicity essentially through the aforementioned mechanisms include cyclophosphamide (an alkylating anticancer drug), vancomycin (a glycopeptide antibiotic drug), tenofovir/lamivudine/efavirenz (a combination antiretroviral drug) and cyclosporine A (an immunosuppressive agent).[57-60]

Table 1. General profile of selected drugs and mechanisms of nephrotoxicity in preclinical studies

Selected drugs (Applications)	Molecular formula/weight	Experimental model	Dosage/ Route of administration	Mechanisms of nephrotoxicity	References
Acetaminophen (Analgesic, antipyretic agent)	$C_8H_9NO_2$/ 151.16 g/mol	Experimental rats (Wistar, Sprague Dawley)	- 2 g/kg single dose/ oral - 500 mg/kg single dose, intraperitoneal (ip)	renal histopathological changes - elevated levels of markers of oxidative stress, pro-inflammatory and apoptotic factors. - decreased renal function - reduced renal antioxidant levels - downregulation of anti-apoptotic factors	Coban et al.[20] Aktas et al.[21] Ozatik et al.[22] Shi et al.[23]
Cisplatin (Anticancer agent)	$Pt(NH_3)_2Cl_2$/ 300.10 g/mol	Experimental rats (Wistar, Sprague Dawley)	- 7 mg/kg single dose/ ip - 5 mg/kg single dose / ip	- decline of renal function; - reduced activities of renal antioxidants - distortion of renal histomorphology - increased levels of oxidative stress markers - increased expressions of pro-inflammatory and apoptotic factors	Tang et al.[25] El-Rhman et al.[26] Shinde et al.[27] Qi et al.[28]
Diclofenac (Analgesic, antipyretic agent)	$C_{14}H_{11}Cl_2NO_2$/ 296.15 g/mol	Experimental rats (Wistar, Sprague Dawley)	- 50 mg/kg daily for 7 days / ip. - 150 mg/kg daily for 6 days / ip	- decreased renal function - increased levels of oxidative stress markers - decreased activities of renal antioxidants - increased levels of pro-inflammatory markers - upregulation of pro-apoptotic factors - downregulation of anti-inflammatory factors	Moradi et al.[30] Karimi-Matloub et al.[31] Alorabi et al.[32] Comez et al.[33] Mansoure et al.[34]
Doxorubicin (Anticancer agent)	$C_{27}H_{29}NO_{11}$/ 543.52 g/mol	Experimental rats (Wistar, Sprague Dawley)	- 15 mg/kg single dose/ i.p. - 20 mg/kg single dose/ i.p. - 3 mg/kg daily for 6 weeks / ip.	- decrease in levels of renal antioxidants and reduced renal function - increased levels of oxidative stress markers - prominent renal histopathological changes - upregulation of pro-inflammatory and apoptotic signaling	Ikewuchi et al.[36] Afsar et al.[37] Altinkaynak et al.[38] Hekmat et al.[39] Al Suleimani et al.[40]
5-Fluorouracil (Anticancer agent)	$C_4H_3FN_2O_2$/ 130.08 g/mol	Experimental rats (Wistar, Sprague Dawley)	- 150 mg/kg single dose (day 8) / ip.	- renal histopathological changes - decreased renal function and activity of renal antioxidants - up-regulation of pro-inflammatory and apoptotic factors - downregulation of anti-inflammatory factors	Famurewa et al.[41] Mansoori et al.[42] El-Gendy et al.[43] Althagafy et al.[44] Albadrani et al.[45] Al-Ghamdi et al.[46]
Gentamicin (Antibiotic agent)	$C_{21}H_{43}N_5O_7$/ 477.60 g/mol	Experimental rats (Wistar, Sprague Dawley)	- 100 mg/kg daily for 8 days / ip - 100 mg/kg daily from day 8-14 of the 15-day study / ip	- renal histopathological changes - decreased activities of renal antioxidants - elevated levels of oxidative stress markers - up-regulation of inflammoapoptotic factors - down-regulation of anti-apoptotic signaling	Akila et al.[47] Abukhalil et al.[48] Saeedavi et al.[49] Dik et al.[50] Nadeem et al.[51]
Methotrexate (Anticancer or antirheumatic agent)	$C_{20}H_{22}N_8O_5$/ 454.44 g/mol	Experimental rats (Wistar, Sprague Dawley)	- 20 mg/kg single dose/ i.p.	- distortion of renal histoarchitecture - elevated serum creatinine, BUN levels - reduced levels of renal antioxidants - upregulation of inflammatory and apoptotic factors - down-regulation of anti-apoptotic expressions	Mishriki et al.[53] Morsy et al.[54] Wasfey et al.[55] Kandemir et al.[56]

Therapeutic activity of selenium against drug-induced nephrotoxicity

Selenium (Se) is a trace element vital to human health in trace amounts but could exhibit an adverse effect at high concentration.[61,62] Deficiency of Se has been associated with increased susceptibility of the body to various pathologies.[63] Its important role in body antioxidant defense system, metabolic homeostasis, and immune functions underscores its therapeutic potential, which has been widely harnessed to mitigate tissues' toxicity, including the kidney. In a previous study, intraperitoneal (ip) exposure of Se (0.5 or 1 mg/kg) mitigated cyclophosphamide-induced nephrotoxicity and reversed associated mechanisms via increased total antioxidant capacity (TAC), reduced TOS, OSI, serum creatinine and reparation of renal histomorphology.[57] The oral administration of Se (0.1 mg/kg for 90 days) further caused a protective effect against tenofovir/lamivudine/efavirenz-induced nephrotoxicity, characterized with elevation of renal antioxidant levels (GSH, SOD, GPx, CAT) levels, reduction of the level of MDA, improved renal function (marked by reduced serum creatinine, uric acid, urea) and amelioration of renal histopathological changes.[58]

Furthermore, exposure to Se nanoparticles (0.5, 1 and 2 mg/kg) demonstrated a protective effect against vancomycin nephrotoxicity through a significant decrease in the levels of MDA, iNOS, NO, TNF-α, and KIM-1, increased Bcl-2 and reduced Bax, caspase-3, caspase-9.59 Furthermore, daily ip administration of Se (1 mg/kg for 8 days) mitigated gentamicin-induced nephrotoxicity, indicated by reduced serum levels of renal function markers (urea, creatinine), reduced levels of MDA and PC levels, and amelioration of renal histopathological changes.[64] Furthermore, administration of Se (1.5 mg/kg/day for 5 days, ip) demonstrated protective effect (in combination exposure with vitamin E) against cisplatin nephrotoxicity, characterized with decrease of plasma levels of MDA, urea, creatinine, elevated levels of GSH, GPx, CAT and reparation of renal histopathological changes (Fig. 2).[65]

Therapeutic activity of zinc against drug-induced nephrotoxicity

Zinc (Zn) is an important trace element that participates in several physiological and biochemical processes of the body.[66] It further participates in the body's antioxidant system, promotes vitamin D, down-regulates prostaglandin synthesis, and enhance immune responses of the body.[67,68] Essentially, the antioxidant and anti-inflammatory effects of Zn have been explored to mitigate drug-induced nephrotoxicity. In a previous study, the mitigation of cisplatin-induced nephrotoxicity was demonstrated by Zn administration (6 mg/kg, ip) and further characterized by reduced serum urea, creatinine, MDA, TNF-α levels, down-regulation of renal Bax and heat shock proteins.[69] The protective effect of Zn administration (25 and 50 mg/kg) has been further demonstrated against gentamicin-induced nephrotoxicity and characterized with restoration of renal function indicated by decreased serum urea, creatinine.[70]

Furthermore, the therapeutic activity of Zn supplementation (10 mg/kg/day for 10 days), based on its antioxidant potential, has been demonstrated against cyclosporine A-induced nephrotoxicity in the experimental model and indicated by reduced serum levels of creatinine, BUN and kidney tissue damage score.[71] Furthermore, Zinc oxide nanoparticles (ZnONPs) have demonstrated a therapeutic effect against doxorubicin-induced nephrotoxicity indicated by elevated levels of renal antioxidants (SOD, GPx, CAT), decline in MDA levels, downregulation of inflammatory markers (IL-6, NF-κB), improved renal function and improved renal histomorphology.[72] Additionally, pretreatment with ZnONPs (5 mg/kg ip) exhibited protective effect against cisplatin nephrotoxicity as demonstrated by reduced serum levels of renal function markers (creatinine, BUN), elevated levels of renal antioxidants (SOD, CAT, GR), reduction of renal MDA level, upregulation of anti-inflammatory markers (HO-1 and Nrf2), downregulation of apoptotic factor (Bax) within the kidney tissue.[73]

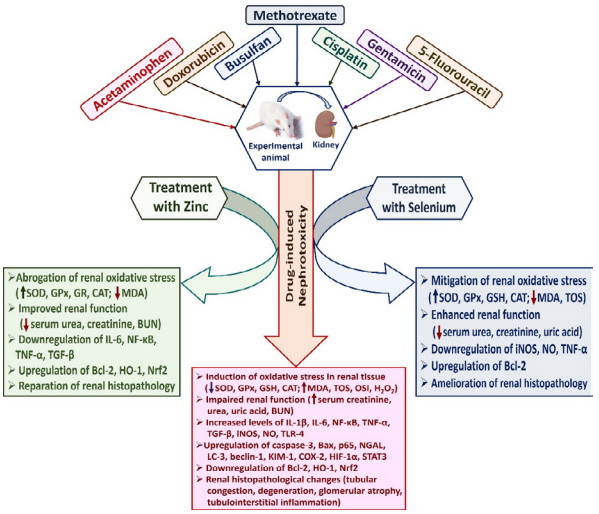

Fig. 2. Schematic summary of mechanisms of drug-induced nephrotoxicity and therapeutic activity of selenium and zinc

Safety concerns and dose-response considerations

Recent studies have reported some concerns regarding selenium exposure at high dosage levels that include adverse metabolic effects of selenoproteins and their potential to stimulate tumor formation.[74] Similarly, reports have associated excess zinc exposure with clinical symptoms such as anemia, neutropenia, while the deficiency also poses significant health risks.[75] Therefore, the dosage and duration of exposure to these trace elements require strict regulation both in health and disease.

Conclusion

Exposure to certain drugs mainly results into nephrotoxicity through induction of oxidative stress and activation of inflammatory and apoptotic signaling pathways within the renal tissue. On the other hand, trace elements such as Selenium and zinc have demonstrated therapeutic activity against drug nephrotoxicity in preclinical studies based on their antioxidant, antiapoptotic, and anti-inflammato-

Table 3. General Profile and therapeutic mechanisms of selected trace elements against drugs nephrotoxicity in preclinical studies

Trace element (symbol/atomic number/mass)	Sources	Biological functions	Experimental model	Treatment regimen	Therapeutic mechanisms against drug-induced nephrotoxicity	References
Selenium (Se/34/76.96 u)	Garlic, nuts, cabbage, rice, potatoes, oats, fishes, eggs, meats, lentils	- Formation of key enzymes, proteins (selenoproteins) - Antioxidant, anti-cancer, anti-inflammatory effect - Immune booster	Experimental rats (Wistar, Sprague Dawley)	- 0.1 mg/kg for 90 days/oral - 1.5 mg/kg/ daily for 5 days/ip	- elevated renal GSH, SOD, GPx, and CAT levels - reduced serum levels of urea, creatinine, and uric acid - decreased levels of TOS, OSI, MDA, PC, - Down-regulation of iNOS, NO, TNF-α and up-regulation of Bcl-2 expressions - amelioration of renal histopathology	Gunes et al.[57] Adikwu et al.[58] Mehanna et al.[59] Bai et al.[61] Genchi et al.[62] Randjelovic et al.[64] Aksoy et al.[65]
Zinc (Zn/30/65.41 u)	Oysters, pork, fish, liver, meat, wheat, mollusks, dairy products, oats, dried peas, nuts, cheese	- Gene regulation - Enzyme cofactor - Wound repair, hair growth - Development of muscle, bone, and cartilage	Experimental rats (Wistar, Sprague Dawley)	- 10 mg/kg/daily for 10 days/oral - 5 mg/kg single dose /ip - 6 mg/kg single dose/ip	- increased renal SOD, GPx, GR, CAT levels - decrease in serum levels of urea, creatinine, BUN - decreased MDA levels - downregulation of IL-6, NF-κB, TNF-α, TGF-β and upregulation of Bcl-2, HO-1, Nrf2 expressions - amelioration of renal histopathology	Al-Fartusie et al.[66] Lahhoba et al.[68] Kone et al.[70] Choopani et al.[71] Elgohary et al.[72] Barakat et al.[73]

ry properties. The efficacy of Selenium and Zinc as mitigants of drug nephrotoxicity thereby underscores their potential role in the management of nephrotoxicity that occurs during pharmacotherapy.

Declarations

Funding
The research has received no funding.

Author contributions
Conceptualization, D.R.O. and F.C.E.; Methodology, D.R.O.; Software, F.C.E.; Validation, D.R.O. and F.C.E.; Formal Analysis, D.R.O.; Investigation, F.C.E.; Resources, D.R.O.; Data Curation, D.R.O.; Writing – Original Draft Preparation, F.C.E.; Writing – Review & Editing, D.R.O; Supervision, D.R.O.

Conflicts of interest
The authors declare that they have no competing interests.

Data availability
The data supporting the findings of this review study have been included in the article.

Ethics approval
Not applicable.

References

1. Sembulingam K, Sembulingam P. *Essentials of Medical Physiology.* 5th ed. Jaypee Brothers Medical Publishers Ltd; 2010:288.
2. Al-Naimi MS, Rasheed HA, Hussien NR, Al-Kuraishy HM, Al-Gareeb AI. Nephrotoxicity: role and significance of renal biomarkers in the early detection of acute renal injury. *J Adv Pharm Technol Res.* 2019;10(3):95-99. doi:10.4103/japtr.JAPTR_336_18
3. Omotoso DR, Lawal OS, Olatomide OD, Okojie IG. Nephroprotective effect of *Cissampelos owariensis* extract on renal histomorphology of Wistar rats during exposure to carbon tetrachloride-induced nephropathy. *Asia J Biol.* 2019;8(4):1-10. doi:10.9734/AJOB/2019/v8i430071
4. Molaei E, Molaei A, Abedi F, Hayes WA, Karimi G. Nephroprotective activity of natural products against chemical toxicants: the role of Nrf2/ARE signaling pathway. *Food Sci Nutr.* 2021;9(6):3362-3384. doi:10.1002/fsn3.2320
5. Okwuonu UC, Omotoso DR, Bienonwu EO, Adagbonyin O, Dappa J. Histomorphological profile of liver and kidney tissues of albino Wistar rats following exposure to cadmium-induced damage and ascorbic acid supplementation. Acad Anat Int. 2020;6(1):15-19. doi:10.21276/aanat.2020.6.1.5
6. Yadav R, Kumar D, Singh J, Jangra A. Environmental toxicants and nephrotoxicity: implications on mechanisms and therapeutic strategies. *Toxicol.* 2024;504:153784. doi:10.1016/j.tox.2024.153784
7. Omotoso DR, Olajumoke JM. Ameliorative effects of ascorbic acid and *Allium sativum* (garlic) ethanol extract on renal parenchyma of gentamicin-induced nephropathic rats. *J Complement Alt Med Res.* 2020;9(4):1-8. doi:10.9734/JOCAMR/2020/V9I430146
8. Omotoso DR, Owonikoko WM, Ehiemere WP. Comparative amelioration of renal histomorphology by ascorbic acid and *Camellia sinensis* extract in Wistar rats exposed to lead-induced nephropathy. *Ann Med Res.* 2020;27(8):2161-2165. doi:10.5455/annalsmedres.2020.02.105
9. Xu M, Xu S, Yi X. A comparative analysis of drug-induced kidney injury adverse reactions between cyclosporine and tacrolimus based on the FAERS database. *BMC Immunol.* 2025;26:35. doi:10.1186/s12865-025-00714-7
10. Pazhayattil GS, Shirali AC. Drug-induced impairment of renal function. *Int J Nephrol Renovasc Dis.* 2014;7:457-468. doi:10.2147/IJNRD.S39747
11. Kim SY, Moon A. Drug-induced nephrotoxicity and its biomarkers. Biomol Ther (Seoul). 2012;20(3):268-272. doi:10.4062/biomolther.2012.20.3.268
12. Al-Naimi MS, Rasheed HA, Hussien NR, Al-Kuraishy HM, Al-Gareeb AI. Nephrotoxicity: Role and significance of renal biomarkers in the early detection of acute renal injury. J Adv Pharm Technol Res. 2019;10(3):95-99. doi:10.4103/japtr.JAPTR_336_18
13. Islam MR, Akash S, Jony MH, et al. Exploring the potential function of trace elements in human health: a therapeutic perspective. *Mol Cell Biochem.* 2023;478:2141-2171. doi:10.1007/s11010-022-04638-3
14. Jahankhani K, Taghipour N, Mashhadi Rafiee M, Nikoonezhad M, Mehdizadeh M, Mosaffa N. Therapeutic effect of trace elements on multiple myeloma and mechanisms of cancer process. *Food Chem Toxicol.* 2023;179:113983. doi:10.1016/j.fct.2023.113983
15. Barker T. Vitamins and human health: systematic reviews and original research. *Nutrients.* 2023;15(13):2888. doi:10.3390/nu15132888
16. Zhang FF, Barr SI, McNulty H, Li D, Blumberg JB. Health effects of vitamin and mineral supplements. *BMJ.* 2020;369:m2511. doi:10.1136/bmj.m2511
17. Rai SN, Singh P, Steinbusch HWM, Vamanu E, Ashraf G, Singh MP. The role of vitamins in neurodegenerative disease: an update. *Biomed.* 2021;9(10):1284. doi:10.3390/biomedicines9101284
18. Barnett LMA, Cummings BS. Cellular and molecular mechanisms of kidney toxicity. *Semin Nephrol.* 2019;39(2):141-151. doi:10.1093/toxsci/kfy159
19. Reis AMM. Drug-induced nephrotoxicity. In: Braund R, ed. *Renal Medicine and Clinical Pharmacy*. Vol 1. Cham, Switzerland: Springer; 2020. doi:10.1007/978-3-030-37655-0_6
20. Çoban FK, İnce S, Demirel HH, İslam İ, Aytuğ H. Acetaminophen-induced nephrotoxicity: suppression of apoptosis and endoplasmic reticulum stress using boric acid. *Biol Trace Elem Res.* 2023;201(1):242-249. doi:10.1007/s12011-022-03114-9

21. Aktas Senocak E, Utlu N, Kurt S, Kucukler S, Mehmet F. Sodium pentaborate prevents acetaminophen-induced hepatorenal injury by suppressing oxidative stress, lipid peroxidation, apoptosis, and inflammatory cytokines in rats. *Biol Trace Elem Res.* 2024;202:1164-1173. doi:10.1007/s12011-023-03755-4
22. Ozatik FY, Teksen Y, Kadioglu E, Ozatik O, Bayat Z. Effects of hydrogen sulfide on acetaminophen-induced acute renal toxicity in rats. *Int Urol Nephrol.* 2019;51(4):745-754. doi:10.1007/s11255-018-2053-0
23. Shi J, Peng X, Huang J, Zhang M, Wang Y. Dihydromyricetin alleviated acetaminophen-induced acute kidney injury via nrf2-dependent anti-oxidative and anti-inflammatory effects. *Int J Mol Sci.* 2025;26(5):2365. doi:10.3390/ijms26052365
24. Volarevic V, Djokovic B, Jankovic MG, et al. Molecular mechanisms of cisplatin-induced nephrotoxicity: a balance on the knife edge between renoprotection and tumor toxicity. *J Biomed Sci.* 2019;26:25. doi:10.1186/s12929-019-0518-9
25. Tang C, Livingston MJ, Safirstein R, Dong Z. Cisplatin nephrotoxicity: new insights and therapeutic implications. *Nat Rev Nephrol.* 2023;19:53-72. doi:10.1038/s41581-022-00631-7
26. El-Rhman RH, El-Naga RN, Gad AM, Tadros MG, Hassaneen SK. Dibenzazepine attenuates against cisplatin--induced nephrotoxicity in rats: involvement of NOTCH pathway. *Front Pharmacol.* 2020;11:567852. doi:10.3389/fphar.2020.567852
27. Shinde SD, Jain PG, Cheke RS, Surana SJ, Gunjegaonkar SM. Abrogation of cisplatin-induced nephrotoxicity in rats and HEK-293 cell lines by formononetin: in vivo and in vitro study. *Comp Clin Pathol.* 2021;30:617-625. doi:10.1007/s00580-021-03252-x
28. Qi J, Gao L. Linarin protects against cisplatin-induced nephrotoxicity via subsiding proinflammatory and oxidative stress biomarkers in male Wistar rats. *Pharmacognosy Mag.* 2024;0(0). doi:10.1177/09731296241297432
29. Famurewa AC, Akunna GG, Nwafor J, Chukwu OC, Ekeleme-Egedigwe CA, Oluniran JN. Nephroprotective activity of virgin coconut oil on diclofenac-induced oxidative nephrotoxicity is associated with antioxidant and anti-inflammatory effects in rats. *Avicenna J Phytomed.* 2020;10(3):316-324
30. Moradi A, Abolfathi M, Javadian M, et al. Gallic Acid Exerts Nephroprotective, Anti-Oxidative Stress, and Anti--Inflammatory Effects Against Diclofenac-Induced Renal Injury in Male rats. *Arch Med Res.* 2021;52(4):380-388. doi:10.1016/j.arcmed.2020.12.005
31. Karimi-Matloub S, Namavari R, Hatefi-Hesari F, et al. The nephroprotective effect of ellagic acid against diclofenac--induced renal injury in male rats: role of Nrf2/HO-1 and NF-κB/TNF-α pathways. *Biologia* 2022;77:3633-3643. doi:10.1007/s11756-022-01217-1
32. Alorabi M, Cavalu S, Al-Kuraishy HM, et al. Pentoxifylline and berberine mitigate diclofenac-induced acute nephrotoxicity in male rats via modulation of inflammation and oxidative stress. *Biomed Pharmacother.* 2022;152:113225. doi:10.1016/j.biopha.2022.113225
33. Comez M, Cellat M, Kuzu M, et al. The effect of tyrosol on diclofenac sodium-induced acute nephrotoxicity in rats. *J Biochem Mol Toxicol.* 2024;38(1):e23582. doi:10.1002/jbt.23582
34. Mansoure AN, Elshal M, Helal MG. Inhibitory effect of diacerein on diclofenac-induced acute nephrotoxicity in rats *via* modulating SIRT1/HIF-1α/NF-κB and SIRT1/p53 regulatory axes. *Int Immunopharmacol.* 2024;131:111776. doi:10.1016/j.intimp.2024.111776
35. Lu C, Wei J, Gao C, et al. Molecular signaling pathways in doxorubicin-induced nephrotoxicity and potential therapeutic agents. *Int Immunopharmacol.* 2025;144:113373. doi:10.1016/j.intimp.2024.113373
36. Ikewuchi CC, Ifeanacho MO, Ikewuchi JC. Moderation of doxorubicin-induced nephrotoxicity in Wistar rats by aqueous leaf-extracts of *Chromolaena odorata* and *Tridax procumbens*. *Porto Biomed J.* 2021;6(1):e129. doi:10.1097/j.pbj.0000000000000129
37. Afsar T, Razak S, Almajwal A, Al-Disi D. Doxorubicin-induced alterations in kidney functioning, oxidative stress, DNA damage, and renal tissue morphology; improvement by *Acacia hydaspica* tannin-rich ethyl acetate fraction. *Saudi J Biol Sci.* 2020;27(9):2251-2260. doi:10.1016/j.sjbs.2020.07.011
38. Altinkaynak Y, Kural B, Akcan BA, et al. Protective effects of L-theanine against doxorubicin-induced nephrotoxicity in rats. *Biomed Pharmacother.* 2018;108:1524-1534. doi:10.1016/j.biopha.2018.09.171
39. Hekmat AS, Chenari A, Alipanah H. et al. Protective effect of alamandine on doxorubicin-induced nephrotoxicity in rats. *BMC Pharmacol Toxicol.* 2021;22:31 doi:10.1186/s40360-021-00494-x
40. Al Suleimani Y, Al Maskari R, Ali BH, et al. Nephroprotective effects of diminazene on doxorubicin-induced acute kidney injury in rats. *Toxicol Rep.* 2023;11:460-468. doi:10.1016/j.toxrep.2023.11.005
41. Famurewa AC, Aja PM, Balogun ME, et al. Prophylactic administration of naringin prevents anticancer drug 5-fluorouracil-induced hepatorenal toxicity via suppressing lipid peroxidation and oxidative stress in rats. *Pharmacol Res Nat Prod.* 2025;6:100137. doi:10.1016/j.prenap.2024.100137
42. Mansoori R, Kazemi S, Almasi D, et al. Therapeutic benefit of melatonin in 5-fluorouracil-induced renal and hepatic injury. *Basic Clin Pharmacol Toxicol.* 2023;134(3):397-411. doi:10.1111/bcpt.13976
43. El-Gendy HF, El-Bahrawy MM, Mansour DA, et al. Unraveling the potential of *Saccharum officinarum* and *Chlorella vulgaris* towards 5-fluorouracil-induced nephrotoxicity in rats. *Pharmaceutics.* 2024;17(7):885. doi:10.3390/ph17070885
44. Althagafy HS, Hassanein EHM. Morin Mitigates 5-Fluorouracil-Induced Nephrotoxicity by Activating Nrf2/

HO-1 and FXR, and Suppressing ERK/VCAM-1 and NF-κB Pathways. *Int Immunopharmacol.* 2025;148:114092. doi:10.1016/j.intimp.2025.114092

45. Albadrani GM, Altyar AE, Kensara OA, et al. Lycopene alleviates 5-fluorouracil-induced nephrotoxicity by modulating PPAR-γ, Nrf2/HO-1, and NF-κB/TNF-α/IL-6 signals. *Renal Failure.* 2024;46(2). doi:10.1080/0886022X.2024.2423843
46. Al-Ghamdi AH, Mohamed MZ, Elbadry RM, Fouad AA. Kidney protective effect of sitagliptin in 5-fluorouracil--challenged rats. *Pharmacia.* 2024;71:1-5. doi:10.3897/pharmacia.71.e114441
47. Akila AA, Gad RA, Ewees MGED, Abdul-Hamid M, Abdel-Reheim ES. Clopidogrel protects against gentamicin-induced nephrotoxicity through targeting oxidative stress, apoptosis, and coagulation pathways. *Naunyn Schmiedebergs Arch Pharmacol.* 2025;398:2609-2625. doi:10.1007/s00210-024-03380-5
48. Abukhalil MH, Al-Alami Z, Altaie HAA, et al. Galangin prevents gentamicin-induced nephrotoxicity by modulating oxidative damage, inflammation, and apoptosis in rats. *Naunyn Schmiedebergs Arch Pharmacol.* 2025;398:3717-3729. doi:10.1007/s00210-024-03449-1
49. Saeedavi M, Goudarzi M, Fatemi I, et al. Gentisic acid mitigates gentamicin-induced nephrotoxicity in rats. *Tissue Cell.* 2023;84:102191. doi:10.1016/j.tice.2023.102191
50. Dik B, Hatipoglu D, Ates MB. Potential effects of Resatorvid and alpha lipoic acid on gentamicin-induced nephrotoxicity in rats. *Pharmacol Res Persp.*2024;12(4):e1222. doi:10.1002/prp2.1222
51. Nadeem RI, Aboutaleb AS, Younis NS, Ahmed HI. Diosmin mitigates gentamicin-induced nephrotoxicity in rats: insights on miR-21 and -155 expression, Nrf2/HO-1 and p38-MAPK/NF-κB pathways. Toxics. 2023;11(1):48. doi:10.3390/toxics11010048
52. Rafique Z, Aabid M, Nadeem H, et al. Nephroprotective Potential of 1,3,4-Oxadiazole Derivative Against Methotrexate-Induced Nephrotoxicity in Rats by Upregulating Nrf2 and Downregulating NF-κB and TNF-α Signaling Pathways. *J Biochem Mol Toxicol.* 2024;38(12):e70084. doi:10.1002/jbt.70084
53. Mishriki AA, Khalifa AK, Ibrahim DA, et al. Empagliflozin mitigates methotrexate-induced nephrotoxicity in male albino rats: insights on the crosstalk of AMPK/Nrf2 signaling pathway. *Futur J Pharm Sci.* 2024;10:95. doi:10.1186/s43094-024-00669-3
54. Morsy MA, El-Sheikh AAK, Abdel-Hafez SMN, Kandeel M, Abdel-Gaber SA. Paeonol Protects Against Methotrexate-Induced Nephrotoxicity *via* Upregulation of P-gp Expression and Inhibition of TLR4/NF-κB Pathway. *Front Pharmacol.* 2022;13: 774387. doi:10.3389/fphar.2022.774387
55. Wasfey EF, Shaaban M, Essam M, et al. Infliximab Ameliorates Methotrexate-Induced Nephrotoxicity in Experimental Rat Model: Impact on Oxidative Stress, Mitochondrial Biogenesis, Apoptotic and Autophagic Machineries. *Cell Biochem Biophys.* 2023;81(4):717-726. doi:10.1007/s12013-023-01168-7
56. Kandemir FM, Kucukler S, Caglayan C, Gur C, Batil AA, Gülçin I. Therapeutic effects of silymarin and naringin on methotrexate-induced nephrotoxicity in rats: Biochemical evaluation of anti-inflammatory, antiapoptotic, and antiautophagic properties. *J Food Biochem.* 2017;41(5):e12398. doi:10.1111/jfbc.12398
57. Gunes S, Sahinturk V, Uslu S, Ayhanci A, Kacar S, Uyar R. Protective effects of selenium on cyclophosphamide-induced oxidative stress and kidney injury. Biol Trace Elem Res. 2018;185(1):116-123. doi:10.1007/s12011-017-1231-8
58. Adikwu E, Ezerioha CE, Biradee I. Selenium Protects against Tenofovir/Lamivudine/Efavirenz-Induced Nephrotoxicity in Rats. *J Nat Sci Med.* 5(2):157-162. doi:10.4103/jnsm.jnsm_153_20
59. Mehanna ET, Khalaf SS, Mesbah NM, Abo-Elmatty DM, Hafez MM. Anti-oxidant, anti-apoptotic, and mitochondrial regulatory effects of selenium nanoparticles against vancomycin induced nephrotoxicity in experimental rats. *Life Sci.* 2022;288:120098. doi:10.1016/j.lfs.2021.120098
60. Wu Q, Wang X, Nepovimova E, Wang Y, Yang H, Kuca K. Mechanism of cyclosporine A nephrotoxicity: Oxidative stress, autophagy, and signalings. *Food Chem Toxicol.* 2018;118:889-907. doi:10.1016/j.fct.2018.06.054
61. Bai S, Zhang M, Tang S, et al. Effects and impact of selenium on human health, A review. *Molecules.* 2024;30(1):50. doi:10.3390/molecules30010050
62. Genchi G, Lauria G, Catalano A, Sinicropi MS, Carocci A. biological activity of selenium and its impact on human health. *Int J Mol Sci.* 2023;24(3):2633. doi:10.3390/ijms24032633
63. Bjørklund G, Shanaida M, Lysiuk R, et al. Selenium: an antioxidant with a critical role in anti-aging. Molecules. 2022;27(19):6613. doi:10.3390/molecules27196613
64. Randjelovic P, Veljkovic S, Stojiljkovic N, et al. Protective effect of selenium on gentamicin-induced oxidative stress and nephrotoxicity in rats. *Drug Chem Toxicol.* 2011;35(2):141-148. doi:10.3109/01480545.2011.589446
65. Aksoy A, Karaoglu A, Akpolat N, Naziroglu M, Ozturk T, Karagoz ZK. Protective role of selenium and high dose vitamin E against cisplatin - induced nephrotoxicty in rats. *Asian Pac J Cancer Prev.* 2015;16(16):6877-6882. doi:10.7314/apjcp.2015
66. Al-Fartusie FS, Mohssan SN. Essential trace elements and their vital roles in human body. *Ind J Adv Chem Sci.* 2017;5(3):127-136. doi:10.22607/IJACS.2017.503003
67. Kloubert V, Rink L. Zinc as a micronutrient and its preventive role of oxidative damage in cells. *Food Func.* 2015;6:3195-3204. doi:10.1039/c5fo00630a
68. Lahhoba QR, Al-sanafd AE, Mohammede NY, et al. Mineral and trace elements, dietary sources, biological effects, deficiency, and toxicity: A review. *Eurasian Chem Commun.* 2023;5:536-555. doi:10.22034/ecc.2023.381964.1594

69. Tuzcu M, Sahin N, Dogukan A, et al. Protective role of zinc picolinate on cisplatin-induced nephrotoxicity in rats. *J Ren Nutr.* 2010;20(6):398-407. doi:10.1053/j.jrn.2010.04.002
70. Kone SD, Gnahoue G, Yapi FH. Evaluation of preventive effects of zinc, vitamin D and their combination against nephrotoxicity induced by gentamicin in rats. Eur J Biotechnol Biosci. 2019;7(2):23-29.
71. Choopani S, Kasaei S, Talebi A, et al. Cyclosporine-A induced nephrotoxicity in male and female rats: Is zinc a suitable protective supplement? *Biomed Res Ther*. 5(12): 2888-2897. doi:10.15419/bmrat.v5i12.507
72. Elgohary A, Metwalli F, Mostafa NY, Reffat M, El-Khawaga OY. Zinc oxide nanoparticles regulate NF-kB expression and restrict inflammation response in doxorubicin-induced kidney injury in rats. *Toxicol Environ Health Sci.* 2023;15:437-448. doi:10.1007/s13530-023-00194-5
73. Barakat LAA, Barakat N, Zakaria MM, Khirallah SM. Protective role of zinc oxide nanoparticles in kidney injury induced by cisplatin in rats. *Life Sci*. 2020;262:118503. doi:10.1016/j.lfs.2020.118503
74. Vinceti M, Filippini T, Jablonska E, Saito Y, Wise LA. Safety of selenium exposure and limitations of selenoprotein maximization: Molecular and epidemiologic perspectives. *Environ Res.* 2022;211:113092. doi:10.1016/j.envres.2022.113092
75. Schoofs H, Schmit J, Rink L. Zinc toxicity: understanding the limits. Molecules. 2024;29(13):3130. doi:10.3390/molecules29133130.

Rzeszów University Press 2026
ISSN 2544-1361 (online)
doi: 10.15584/ejcem.2026.1.5

http://www.ejcem.ur.edu.pl
European Journal of Clinical and Experimental Medicine
Eur J Clin Exp Med 2026; 24 (1): 173–180

REVIEW PAPER

Mapping the use of virtual reality in health promotion and weight management among overweight and obese individuals – a scoping review

Reema Joshi , Mansi Bhatt

Dr. D. Y. Patil College of Physiotherapy, Dr. D. Y. Patil Vidyapeeth, Pimpri, Pune, Maharashtra, India

ABSTRACT

Introduction and aim. Obesity and overweight, defined by excess body fat, are major global public health challenges. Virtual reality (VR) is emerging as a novel tool for health promotion and weight management. This scoping review aimed to map existing research on VR applications in overweight and obese populations.

Material and methods. Following PRISMA-ScR guidelines, systematic searches were conducted in PubMed, SCOPUS, EBSCO, Pedro, Embase, Web of Science, and Google Scholar up to March 2025. Keywords included 'obese', 'overweight' and "virtual reality." Eligible studies were cross-sectional, experimental or randomized controlled trials involving overweight or obese individuals exposed to VR-based interventions targeting physical health, behavior change, or weight control. Two reviewers independently screened and extracted the data.

Results. Ten studies published between 2012 and 2025 were included. Most involved adolescents and women, with limited representation of men and older adults. VR interventions varied in immersion, platform, and focus, targeting physical activity, behavioral change, and nutrition. Outcomes commonly included body composition, physical activity, emotional well-being, and diet. Heterogeneity prevented meta-analysis.

Conclusion. VR holds promise as a multidimensional tool for the management of obesity. However, more inclusive, culturally adapted, and long-term studies are needed to validate its effectiveness and applicability in diverse populations.

Keywords. adiposity, obesity, overweight, virtual reality, weight loss

Introduction

Obesity is defined as 'abnormal or excessive fat accumulation that presents a health risk'.[1] Overweight refers to a condition in which an individual carries excess body fat that can affect health, whereas obesity indicates a more severe degree of fat accumulation with a greater risk of adverse health outcomes. Both conditions arise from an imbalance between energy intake (diet) and energy expenditure (physical activity), leading to fat deposition at subcutaneous and ectopic sites. Although recent data suggest a plateau in the prevalence of overweight and obesity among children and adults in several countries, these conditions remain significant public health concerns.[2] They are strongly associated with chronic diseases such as hypertension, coronary heart disease, type 2 diabetes, stroke, gallbladder disease, certain cancers, osteoarthritis, and sleep apnea.[3] In light of the rising global burden, there is an urgent need for advanced treatment strategies that enable early intervention and prevent obesity-related complications. Early identification of overweight individuals within the community and the provision of timely targeted interventions are

Corresponding author: Mansi Bhatt, e-mail: mjbhatt2210@gmail.com

Received: 31.05.2025 / Revised: 12.08.2025 / Accepted: 24.08.2025 / Published: 30.03.2026

Joshi R, Bhatt M. Mapping the use of virtual reality in health promotion and weight management among overweight and obese individuals – a scoping review. *Eur J Clin Exp Med.* 2026;24(1):173–180. doi: 10.15584/ejcem.2026.1.5.

essential steps toward mitigating the long-term health risks associated with excess weight.

VR is an emerging transformative technology with significant potential in the medical field. By creating a controlled artificial environment, virtual reality bypasses the complexities of physical settings, thereby accommodating a wide range of therapeutic needs. Its applications include the treatment of neurological and psychiatric disorders, such as pain, anxiety, and depression, as well as the rehabilitation of neurodegenerative conditions such as Parkinson's disease and stroke. A key advantage of VR lies in its ability to generate a convincing illusion of reality, providing users with a heightened sense of presence and immersion.[3] Furthermore, VR has been shown to improve cognitive function and concentration, while its interactive nature encourages greater user participation.[4] Unlike traditional forms of physical activity, VR-based exercise has been found to elevate mood, increase enjoyment, and reduce the risk of burnout.[5,7] The recreational aspects of VR support deep immersion, boost motivation, and enhance learning outcomes.[5] By offering simulated experiential learning, VR holds promise in addressing the limitations of existing online weight management programs.[8] When combined with physical activity, immersive virtual reality (IVR) has been shown to increase physiological and metabolic demands without raising, and sometimes even reducing, perceived exertion.[9]

This scoping review maps and synthesizes the existing literature on VR-based interventions for overweight and obesity. Instead of evaluating the clinical effectiveness of these interventions, the review focuses on exploring the breadth, scope, and characteristics of current research. The key themes explored include aspects such as user engagement, adherence, psychological and behavioral outcomes, and the integration of VR into long-term health practices.

Aim

In contrast to previous systematic reviews and meta-analyses that emphasize quantifiable outcomes such as weight loss or reduction in body mass index (BMI), this review provides a broader descriptive overview of how VR is currently being utilized in weight management contexts. It also examines the use of VR in both community and clinical settings, highlighting reported aspects of feasibility, usability, and cost. By identifying knowledge gaps and summarizing the existing landscape, this review aims to inform future research, technological development, and policy in the field of VR-based obesity interventions.

Material and methods

Study design

This scoping review was conducted with the primary objective of mapping and synthesizing the existing literature on the application of VR interventions for the management of overweight and obesity. The methodological approach was guided by the extension of preferred reporting items for systematic reviews and Meta-Analyses extension for scoping reviews (PRISMA-ScR), which provided a structured and transparent framework to ensure methodological rigor and reproducibility throughout the review process. This study constitutes a scoping review and was not registered in PROSPERO, as PROSPERO does not accept scoping review protocols. The protocol was drafted a priori to guide the methodological approach, in accordance with the PRISMA-ScR recommendations.

Search strategy

A systematic search of the literature was performed on six major electronic databases: PubMed, SCOPUS, EBSCO, PEDro, Embase, Web of Science, and Google Scholar during April and May 2024. The search was restricted to full-text articles published in English between January 2012 and April 2025. To enhance the completeness of the search, a combination of relevant keywords and Boolean operators was used, such as: ("virtual reality" OR "VR") AND ("obesity" OR "obesity" OR "overweight") AND ("intervention" OR "treatment" OR "therapy"). In addition to database searches, reference lists of all eligible studies were manually screened to identify any relevant articles that may not have been retrieved by electronic searches. Although the agreement was not formally quantified using statistical measures such as Cohen's kappa, the review process maintained a high level of consistency and transparency.

Eligibility criteria

Studies were considered eligible for inclusion if they involved overweight or obese individuals, regardless of age or gender, and employed a VR-based intervention aimed at improving physical health, facilitating behavior change or promoting weight reduction. Only empirical studies adopting randomized controlled trials or quasi-experimental designs were included to ensure the reliability and applicability of the findings. Studies were excluded if they involved participants with serious comorbid conditions unrelated to obesity, lacked an interactive VR component, or were non-empirical in nature such as reviews, editorials, protocols, or conference abstracts.

Study selection process

The initial database search yielded a total of 1,172 records. After the removal of 653 duplicates and 21 records excluded by automated filtering tools, 498 unique articles remained for title and abstract screening. Based on relevance to the research objectives, 36 articles were retrieved for full-text evaluation. Following a thorough

review using the predefined inclusion and exclusion criteria, 10 studies were deemed eligible and included in the final synthesis. The entire selection and selection process was independently by two reviewers. Disagreements at any stage were resolved by discussion and consensus. A third reviewer was available for arbitration, but was not required, as consensus was consistently achieved. The study identification and selection process are visually presented in the updated PRISMA-ScR flow diagram (Fig. 1).

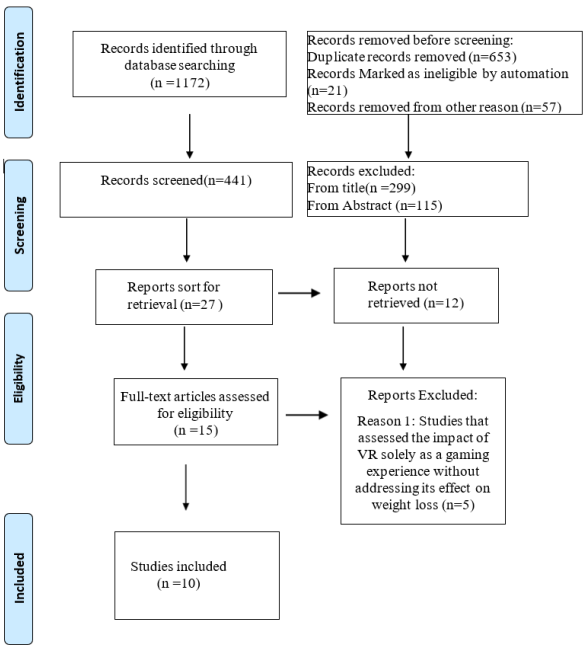

Fig. 1. PRISMA-ScR flow diagram

Data extraction and verification

A structured data chart form was developed and used to extract key information from each included study. Extracted variables included the author and year of publication, geographic location, study design, sample size and demographic characteristics, nature and duration of the VR intervention, outcome measures and principal findings. All data were independently verified by a second reviewer to ensure accuracy, completeness, and consistency between sources.

Quality appraisal

Although a formal risk of bias assessment is not a mandatory component of scoping reviews, a basic methodological assessment was conducted to provide contextual insights into the strength of the evidence. The Cochrane Risk of Bias tool was descriptively applied to the randomized controlled trials included in the review. This evaluation did not influence study selection or synthesis, but served to offer an additional layer of interpretive context regarding study quality.

Data synthesis

Given the variability in study designs, intervention protocols, and reported results, a meta-analysis was deemed inappropriate. Instead, a qualitative narrative and thematic synthesis was undertaken. The extracted data was thematically analyzed to identify recurring patterns and conceptual domains. An open coding approach was used to manually code relevant findings from each study, and similar codes were grouped into descriptive themes. The coding was performed iteratively and reviewed by the research team to ensure consistency and alignment with the study objectives. The synthesis focused on key themes such as physical health outcomes associated with VR interventions, psychological impacts on participants, levels of user engagement and adherence, feasibility of implementation in various settings, and the sustainability of the intervention effects over time.

Results

This scoping review included ten full-text articles, encompassing a cumulative sample of 960 participants. The findings were thematically organized according to the stated objectives, which focused on physiological outcomes, emotional responses, compliance, and sustainability. A tabulated summary of the studies is presented in Table 1, providing a structured overview of the literature on VR interventions in overweight and obese populations.

Physical health outcomes

Several studies reported improvements in physiological parameters following VR interventions. In particular, a Korean study demonstrated significant reductions in body mass index (BMI) among overweight middle-aged women, attributed to VR-facilitated physical activity.[10] Navarro et al. similarly reported reductions in BMI and body weight through the use of VR-enhanced exercise protocols. Most studies employed standard anthropometric tools such as calibrated stadiometers and digital weighing scales, although detailed measures of body composition (eg, fat mass or lean body mass) were rarely reported.[11] Furthermore, the brevity of intervention periods in many studies presents limitations in assessing long-term physiological efficacy. The study by Mologne et al. further demonstrated improvements in cardiometabolic parameters using an immersive VR exergame in a 12-week trial.[12]

Psychological outcomes

VR interventions were consistently associated with positive emotional changes. Several studies documented reductions in depressive symptoms and anxiety levels, as well as improvements in the affective states.[10,11] Na-

Table 1. Characteristics of key references

Sr no	Location	Author	Study design	Duration	subjects	Outcome assessed	Results	Limitations
1	Korea	Eun-young Seon (2023)	Randomized controlled trial	8 weeks	75 overweight middle-aged women (45-65year old)	BMI (extensometer, weight scale); Depression (PHQ-9); Exercise enjoyment (NRS); Immersion (Sports immersion scale)	In middle-aged overweight women, virtual reality had a positive impact on BMI, depression scores, enjoyment of exercise, and immersion in exercise	Repeated studies are required for verification of the effect of VR as an intervention in middle aged women
2	China	Qian Wu (2023)	Randomized controlled trial	8 weeks	220 overweight adolescents	Primary outcome: bioelectrical impedance, secondary outcome: physical and brain related parameters	Virtual reality improved quality of life and encouraged overweight adolescents to participate in sports	Blinding not possible due to the nature of intervention
3	USA	Suzanne Phelan (2021)	Randomized controlled trial	4 weeks	15 overweight/obese adults	Demographic data, calibrated standard digital weigh scale and Harpenden stadiometer	While both the treatment and control groups experienced weight loss, the virtual reality approach was more liked by the participants than the conventional approach	Future research is required to test the feasibility of the VR approach in other weight control skills in a larger sample size and a longer evaluation period to determine behavioral weight loss using different outcomes
4	USA	John Graham Thomas (2020)	Randomized controlled trial	6 months	146 Overweight/Obese adults	Weight (digital BWB-800 scale); Weight Control Strategies Scale	All groups lost weight; experienced Weight Watchers had better results	More research is needed to improve the outcomes of experience success by identifying the behavioral mechanisms
5	Spain	Jessica Navarro (2020)	Randomized controlled trial	2 weeks	42 overweight and obese women	Anthropometric and sociodemographic data. Questionnaires: Body shape questionnaire, International Physical activity, PACES, PASAS, Behavioral regulation in exercise questionnaire, Avatar identification modified questionnaire	Online VR intervention improved PA and self-efficacy; ideal avatar reduced anxiety	No follow-up; more outcomes are needed for long-term effects
6	United Kingdom	Leighton Jones (2019)	Experimental design	Single session of exercise	21 Overweight adults	Questionnaire: Attention scale, Feeling scale, PACES, Immersive experience questionnaire, PRETIE-Q Near infrared device to calculate hemoglobin difference	BMI decreased considerably in both groups. The waist-hip ratio did not differ between the pre- and post-test findings. The results imply that VR improved the emotional experience during exercise	Further studies are required to see the long-term sustainability of VR on Affective experience. Studies are required on the obese population and an equal distribution of genders
7	Spain	Rosa M. Banos (2016)	Counterbalanced design	Single session was taken	A total of 109 students among them 33 were overweight	Anthropometric Data: Height-calibrated stadiometer, weight-standard beam balance scale, BMI calculated Heart rate: NUUBO TIPS Attentional strategies tool, Feeling scale, Eston-Parfitt scale, Enjoyment and preference scale	The findings showed that overweight children experienced a higher level of attention distraction when using virtual reality	Future studies are needed to intrinsically motivate overweight and obese children to be more physically active using VR.
8	USA	D.K. Sullivan (2016)	Randomized controlled trial	18 months	202 overweight and obese individuals	Primary outcome: weight maintenance, levels of physical activity, energy intake, macronutrient composition, consumption of fruits and diet, problem solving skills and experiential lessons	The VR group had better weight maintenance; Face-to-face clinic achieved greater weight loss	Barriers to long-term weight loss maintenance need study
9	USA	Elizabeth Behm-Morwitz (2016)	Randomized controlled trial	4-week program	92 overweight adults	Body measurements and surveys were taken	VR group showed increased motivation and achieved weight loss goals	Long-term sustainability needs evaluation in broader populations
10	USA	Jeanne D. Jhonston (2012)	Randomized control trial	12-Week program	38 overweight adults	Demographic data, BMI, Physical activity scale, Weight efficacy lifestyle questionnaire	Both groups lost weight; VR group showed better questionnaire outcomes	Larger studies with web-based VR needed

varro et al. noted increased self-efficacy and emotional engagement with exercise, suggesting that VR may foster psychological readiness for physical activity.[11] A UK-based study observed increased emotional variability during VR exercise, suggesting that immersive environments, while engaging, can also trigger unpredictable emotional responses in some individuals.[13] Another study involving overweight children used VR as a distraction during exercise, leading to more positive affective experiences.[14]

Compliance and motivation

Motivational factors and adherence to exercise protocols were frequently enhanced through VR interventions. Studies indicated that the immersive and interactive nature of VR increased the enthusiasm of participants, which translated into improved compliance. Behm-Morawitz et al. observed that participants showed a greater willingness to engage in novel physical activities when guided by VR platforms.[15] Similarly, Wu et al. found that VR-based interventions encouraged consistent participation among overweight adolescents, largely driven by enhanced engagement and interest.[16] Thomas et al. showed that VR-based interventions helped participants develop behavioral skills related to physical activity, contributing to increased motivation.[17]

Sustainability

Although the short-term results were promising, evidence on the long-term sustainability of VR interventions remains insufficient. Most studies had limited follow-up durations, preventing conclusive assessments of weight maintenance or sustained behavior change. Sullivan et al. emphasized the practicality of web-based VR systems, which offer flexibility and accessibility, potentially supporting long-term adherence.[18] Phelan et al. demonstrated the feasibility of integrating VR into behavioral weight management programs, although their study was limited in scope.[19] The current evidence base is constrained by population homogeneity, primarily involving women and adolescent participants, and by geographic concentration in European and North American regions. Only a few studies originated in Asian settings, indicating a need for a larger demographic representation in future research.[16]

Discussion

This scoping review aims to comprehensively map the existing literature on virtual VR interventions for weight management in overweight individuals. By consolidating diverse evidence, it identifies key themes, highlights research gaps, and informs future investigative priorities, rather than evaluating the effectiveness of the intervention. The findings suggest that VR serves as a promising adjunct to conventional therapies, supporting weight loss, promoting physical activity, and improving emotional well-being across varied populations. Despite heterogeneity in study designs, participant profiles, and outcome measures, all included studies reported at least one positive health outcome, underscoring VR's multifaceted therapeutic potential.

Therapeutic potential and mechanisms

VR interventions improve outcomes by combining behavioral and cognitive strategies within immersive environments. These platforms support self-monitoring of dietary intake, exercise adherence, and weight control, often complementing traditional programs. They foster self-efficacy, body image satisfaction, and motivation, facilitating long-term habit formation and healthier lifestyle choices.[20,21] Real-time feedback and multisensory stimulation can promote neural plasticity associated with behavioral change and emotional regulation.

Additionally, VR enables customized exposure therapy that reduces anxiety surrounding eating and exercise by disrupting maladaptive memory patterns through simulated scenarios.[23] This controlled exposure aids emotional regulation, reduces avoidance behavior, and supports healthier routines. Avatar-based self-representation has also been linked to increased motivation and adherence, allowing users to embody healthier versions of themselves, thereby strengthening their commitment to weight-related goals.[20,21]

In addition, VR can simulate diverse real-world settings, overcoming environmental barriers such as poor weather or unsafe exercise conditions. This flexibility improves access and consistency in physical activity, particularly for people with limited resources or mobility. By embedding cognitive behavioral techniques into engaging, interactive experiences, VR addresses both physiological and psychological dimensions of overweight management, often beyond the scope of traditional interventions.[20]

Engagement and accessibility

One of the key advantages lies in enhancing user engagement and enjoyment during physical activity, which supports the adherence to the intervention and long-term success. Interactive features, including personalized avatars, have been shown to increase motivation, although not all studies report statistically significant differences in outcomes compared to standard methods.[22] Notably, men remain underrepresented in VR-based weight loss research, reflecting broader trends in male participation in obesity trials and warranting targeted recruitment strategies.[23,24] Commercially available VR programs offer scalable, cost-effective alternatives to conventional behavioral interventions. However, their inconsistent incorporation of evidence-based components requires careful evaluation of design and efficacy.

Diversity of VR interventions

The VR interventions in the included studies demonstrated substantial heterogeneity in type, level of immersion, and therapeutic intent. For example, Seo et al. employed a fully immersive VR cycling system, while Sullivan et al. used a non-immersive, avatar-based platform within Second Life. Others, such as Navarro et al., integrated VR with cognitive behavioral strategies targeting self-efficacy and body image.[10,18,11] This variability, ranging from game-based to therapeutic VR, poses challenges in comparing results and synthesizing findings. Additionally, inconsistent reporting of VR components limits cross-study comparability. Future research should classify VR modalities more clearly and analyze outcomes accordingly to enable more precise interpretation and application in obesity management.

Population gaps and representation

A consistent shortcoming in studies is the underrepresentation of specific subgroups, particularly men, older adults, and individuals from low and middle-income countries. The predominance of female and adolescent participants mirrors broader patterns in obesity and digital health research but limits the generalizability of the findings.[25] Tailored recruitment strategies are essential to ensure gender balance and age diversity in future trials. Furthermore, most of the studies were conducted in western settings and published in English, which could overlook the sociocultural factors influencing the acceptability and effectiveness of VR interventions in non-Western populations. Context-specific adaptation is critical, especially in regions with unique nutritional, behavioral, or infrastructure challenges.

Limitations and research gaps

Several methodological limitations constrain the current evidence base. Variations in intervention duration, sample sizes, and study quality limit generalizability and comparability. The predominance of short-term follow-up restricts insights into long-term efficacy. The exclusive inclusion of English-language studies and underrepresentation of research in Asian populations further narrow geographic and cultural applicability. Older adults, despite facing a growing burden of overweight-related health concerns, remain significantly underrepresented. The heterogeneity of VR interventions and inconsistent reporting between studies limited the comparability of findings and hindered the ability to assess overall efficacy of the intervention. The technical challenges inherent to VR technology also warrant consideration. High costs, variable accessibility, potential usability issues, and adverse effects such as cyber sickness can limit widespread adoption. Furthermore, effective implementation requires user training and ongoing support, aspects often underexplored in existing research.

Future directions

Future research should prioritize large, well-powered randomized controlled trials with standardized protocols, extended follow-up, and blinding of the evaluator to enhance methodological rigor. Regionally adapted VR interventions that account for sociocultural, demographic, and environmental factors are essential, particularly in densely populated or low-resource settings. Inclusion of underrepresented groups, especially males and older adults, will improve generalizability and offer insights throughout life. Given the involvement of minors in several studies, future investigations must also address ethical considerations such as cognitive safety, content appropriateness, and long-term exposure effects. The establishment of standardized guidelines for the safe and effective use of VR in pediatric populations is critical. Multidisciplinary collaboration among healthcare professionals, behavioral scientists, and technologists will further ensure the development of relevant, usable, and sustainable interventions.

Clinical implications

VR offers a safe, practical, and user-friendly tool to support weight loss and improve psychological and physiological outcomes. It holds promise as a cost-effective alternative or complement to traditional care, particularly in settings with limited access to in-person services. Although the initial findings are encouraging, their long-term impact in diverse populations requires further validation through rigorous and inclusive research.

Review limitations

This review is limited by the restriction to English-language publications and may have missed relevant studies in other languages or unpublished data. Database selection and search strategies, while comprehensive, could have introduced selection bias. These factors should be taken into account when interpreting the mapped evidence.

Conclusion

This scoping review maps the evolving landscape of VR interventions for overweight management, highlighting therapeutic promise alongside critical research gaps. Addressing methodological weaknesses, diversifying study populations, and overcoming technical challenges are essential for translating VR potential into effective, equitable clinical practice.

Declarations

Funding

This research did not receive external funding.

Author contributions

Conceptualization, M.B. and R.J.; Methodology, M.B.; Software, M.B.; Validation, R.J. and M.B.; Formal Analysis, R.J.; Investigation, M.B.; Resources, M.B.; Data Curation, R.J.; Writing – Original Draft Preparation, M.B.; Writing – Review & Editing, M.B.; Visualization, R.J.; Supervision, R.J.; Project Administration, R.J.

Conflicts of interest

The authors declare that they have no competing interests.

Data availability

In this study, no new data was generated or analyzed in this study.

Ethics approval

This study did not require ethical approval, as it is a scoping review of previously published literature.

Reference

1. World Health Organization. Obesity and overweight. Published May 7, 2025. Accessed May 30, 2025. https://www.who.int/news-room/fact-sheets/detail/obesity-and-overweight
2. Ng M, Fleming T, Robinson M, et al. Global, regional, and national prevalence of overweight and obesity in children and adults during 1980-2013: a systematic analysis for the Global Burden of Disease Study 2013. *Lancet*. 2014;384(9945):766-781. doi:10.1016/S0140-6736(14)60460-8
3. Marques A, Peralta M, Naia A, Loureiro N, de Matos MG. Prevalence of adult overweight and obesity in 20 European countries, 2014. *Eur J Public Health*. 2018;28(2):295-300. doi:10.1093/eurpub/ckx143
4. Hubbard VS. Defining overweight and obesity: what are the issues? *Am J Clin Nutr.* 2000;72(5):1067-1068. doi:10.1093/ajcn/72.5.1067
5. Sanchez-Vives MV, Slater M. From presence to consciousness through virtual reality. *Nat Rev Neurosci.* 2005;6(4):332-339. doi:10.1038/nrn1651
6. Sveistrup H, Thornton M, Bryanton C, et al. Outcomes of intervention programs using flatscreen virtual reality. *Conf Proc IEEE Eng Med Biol Soc*. 2004;2004:4856-4858. doi:10.1109/IEMBS.2004.1404343
7. Warburton DE, Bredin SS, Horita LT, et al. The health benefits of interactive video game exercise. *Appl Physiol Nutr Metab.* 2007;32(4):655-663. doi:10.1139/H07-038
8. Ferrer-Garcia M, Gutiérrez-Maldonado J, Riva G. Virtual reality based treatments in eating disorders and obesity: a review. *J Contemp Psychother.* 2013;43:207-221. doi:10.1007/s10879-013-9240-1
9. Cho H, Sohng KY. The effect of a virtual reality exercise program on physical fitness, body composition, and fatigue in hemodialysis patients. *J Phys Ther Sci*. 2014;26(10):1661-1665. doi:10.1589/jpts.26.1661
10. Seo EY, Kim YS, Lee YJ, Hur MH. Virtual reality exercise program effects on body mass index, depression, exercise fun and exercise immersion in overweight middle-aged women: a randomized controlled trial. *Int J Environ Res Public Health*. 2023;20(2):900. doi:10.3390/ijerph20020900
11. Navarro J, Cebolla A, Llorens R, Borrego A, Baños RM. Manipulating self-avatar body dimensions in virtual worlds to complement an internet-delivered intervention to increase physical activity in overweight women. *Int J Environ Res Public Health*. 2020;17(11):4045. doi:10.3390/ijerph17114045
12. Jones L, Ekkekakis P. Affect and prefrontal hemodynamics during exercise under immersive audiovisual stimulation: improving the experience of exercise for overweight adults. *J Sport Health Sci*. 2019;8(4):325-338. doi:10.1016/j.jshs.2018.06.008
13. Mologne MS, Hu J, Carrillo E, et al. The efficacy of an immersive virtual reality exergame incorporating an adaptive cable resistance system on fitness and cardiometabolic measures: a 12-week randomized controlled trial. *Int J Environ Res Public Health.* 2022;20(1):210. doi:10.3390/ijerph20010210
14. Baños RM, Escobar P, Cebolla A, et al. Using virtual reality to distract overweight children from bodily sensations during exercise. *Cyberpsychol Behav Soc Netw*. 2016;19(2):115-119. doi:10.1089/cyber.2015.0340
15. Behm-Morawitz E, Lewallen J, Choi G. A second chance at health: how a 3D virtual world can improve health self-efficacy for weight loss management among adults. *Cyberpsychol Behav Soc Netw*. 2016;19(2):74-79. doi:10.1089/cyber.2015.0366
16. Wu Q, Han R, Li Z, et al. Effect of virtual reality-based exercise and physical exercise on adolescents with overweight and obesity: study protocol for a randomized controlled trial. *BMJ Open*. 2023;13(10):e075332. doi:10.1136/bmjopen-2023-075332
17. Thomas J, Goldstein C, Bond D, Hadley W, Tuerk P. Web-based virtual reality to enhance behavioural skills training and weight loss in a commercial online weight management programme: the Experience Success randomized trial. *Obes Sci Pract*. 2020;6:e451. doi:10.1002/osp4.451
18. Sullivan DK, Goetz JR, Gibson CA, et al. A virtual reality intervention (Second Life) to improve weight maintenance: rationale and design for an 18-month randomized trial. *Contemp Clin Trials.* 2016;46:77-84. doi:10.1016/j.cct.2015.12.010
19. Phelan S, Peruvemba S, Levinson D, et al. Feasibility of a virtual reality based approach to improve behavioral weight management outcomes. *Pilot Feasibility Stud*. 2021;7(1):129. doi:10.1186/s40814-021-00865-5
20. Castelnuovo G, Pietrabissa G, Manzoni GM, et al. Cognitive behavioral therapy to aid weight loss in obese patients: current perspectives. *Psychol Res Behav Manag*. 2017;10:165-173. doi:10.2147/PRBM.S113092

21. Manzoni GM, Cattivelli R, Molinari E, Castelnuovo G. Virtual reality-based behavioral therapy for obesity and binge-eating disorder: a systematic review. *J Clin Med*. 2019;8(5):738. doi:10.3390/jcm8050738
22. Dascal J, Reid M, IsHak WW, et al. Virtual reality and medical inpatients: a systematic review of randomized, controlled trials. *Innov Clin Neurosci*. 2017;14(1-2):14-25.
23. De Carvalho MR, Dias TR, Duchesne M, Nardi AE, Appolinario JC. Virtual reality as a promising strategy in the assessment and treatment of bulimia nervosa and binge eating disorder: a systematic review. *Behav Sci (Basel)*. 2017;7(3):43. doi:10.3390/bs7030043
24. Young KS, Rennalls SJ, Leppanen J, et al. Exposure to food in anorexia nervosa and brain correlates of food-related anxiety: findings from a pilot study. *J Affect Disord*. 2020;274:1068-1077. doi:10.1016/j.jad.2020.05.001
25. Robertson C, Archibald D, Avenell A, et al. Systematic reviews of and integrated report on the quantitative, qualitative and economic evidence base for the management of obesity in men. *Health Technol Assess*. 2014;18(35):v-424. doi:10.3310/hta18350

Rzeszów University Press 2026
ISSN 2544-1361 (online)
doi: 10.15584/ejcem.2026.1.10

http://www.ejcem.ur.edu.pl
European Journal of Clinical and Experimental Medicine
Eur J Clin Exp Med 2026; 24 (1): 181–191

REVIEW PAPER

Humanized NSG mice – a modern approach to modelling systemic lupus erythematosus in preclinical modeling

Jyotirupa Mochahari , Rikngam Gibo , Phiwansiewdor Syiem , Purbajit Chetia

Department of Pharmacology, NETES Institute of Pharmaceutical Science, NEMCARE Group of Institutions, Guwahati, Assam, India

ABSTRACT

Introduction and aim. Systemic lupus erythematosus (SLE) is a complex autoimmune illness characterized by widespread immune dysregulation and involvement of several organ systems. Conventional mouse models, although crucial for understanding basic immunopathogenic pathways, inadequately mimic human-specific immunological responses, hence constraining translational relevance. This review offers a comprehensive understanding of humanized NSG mice in systemic lupus erythematosus research, outlining techniques for engraftment, model-specific immune reconstitution characteristics, and their respective applications in simulating acute and chronic disease phenotypes.

Literature search. A comprehensive analysis of studies published between 2017 to 2025 was conducted in PubMed, Scopus, Web of Science and Google Scholar database. After removing the duplicates, a total of 87 articles were employed to finalize this study.

Analysis of literature. Humanized NSG mice successfully recapitulate major immunopathological features of systemic lupus erythematosus. Among numerous approaches, $CD34^+$ hematopoietic stem cell models best mimic chronic phenotype, while PBMC and pristane-based systems mimic acute and environmentally triggered forms. Recent advances include cytokine knock-in and HLA transgenic derivatives improving immune reconstitution and translational dependability.

Conclusion. This review provides the first integrative synthesis of humanized NSG mouse models applied to SLE, highlighting their translational potential and methodological advancements from 2017–2025. Collectively, these innovations establish humanized NSG mice as essential preclinical tools bridging experimental immunology with precision medicine in lupus research and therapy development.

Keywords. hematopoietic stem cell, humanized mouse model, immunopathogenesis, NSG mice, SLE

Introduction

Systemic lupus erythematosus (SLE), is a chronic autoimmune illness that is characterized by the dysregulation of the immune system and the development of pathogenic autoantibodies.[1] These autoantibodies target nuclear and cytoplasmic antigens resulting in inflammation and multi-organ damage.[2,3] At the clinical level, SLE is characterized by a wide variety of symptoms, including but not limited to fatigue, joint pain, malar rash, photosensitivity, and more serious consequences such as lupus nephritis, neuropsychiatric lupus, and hematological abnormalities.[4] Multiple factors contribute to the development of SLE, which is characterized by a complex interaction between genetic predisposition, epigenetic alterations, environmental stressors, and hormonal variables.[5,6] Numerous susceptibility loci related

Corresponding author: Purbajit Chetia, e-mail: purbajit.chetia@gmail.com, purbajit@ngiguwahati.in

Received: 17.06.2025 / Revised: 2.09.2025 / Accepted: 5.10.2025 / Published: 30.03.2026

Mochahari J, Gibo R, Syiem P, Chetia P. Humanized NSG mice – a modern approach to modelling systemic lupus erythematosus in preclinical research. *Eur J Clin Exp Med.* 2026;24(1):181–191. doi: 10.15584/ejcem.2026.1.10.

with immune regulation have been found through the use of genome-wide association studies (GWAS). These loci include genes that are involved in the type I interferon pathway, the HLA complex, and the clearance of apoptotic cells within the body.[7] Certain environmental triggers, such as ultraviolet radiation, infections (especially the Epstein-Barr virus), and certain medications, have the potential to initiate or aggravate illness flares in SLE, while the higher prevalence in females highlights the potential role of estrogen.[8,9] SLE is marked by a loss of immunological self-tolerance, leading to the activation of autoreactive T and B cells and interferon-alpha (IFN-α), responsible for producing immunological complexes, causing tissue deposition, and activating the complement cascade, resulting in chronic inflammation and organ dysfunction.[10,11] Preclinical models are indispensable for the investigation of disease mechanisms and the development of therapeutics. The replication of key features such as lymphoproliferation, autoantibody production (e.g., anti-dsDNA, anti-Sm), and lupus-like kidney pathology has substantially advanced our understanding of SLE in classical murine models such as MRL/lpr, NZB/W F1, and BXSB.[12,13] Despite their significant contributions, classical rodent models are severely constrained by the fundamental differences between the immune systems of mice and humans, as well as the cytokine signaling and gene expression profiles.[14,15] In light of these constraints, a paradigm shift has transpired towards the utilization of humanized mouse models, particularly the NOD-scid IL2Rγ^null (NSG) strain, which, owing to its severely compromised adaptive and innate immunity, has become the benchmark for facilitating the engraftment of the human immune system.[16,17] Humanized NSG mice are progressively utilized to emulate human-specific characteristics of SLE, including autoreactive immune responses, cytokine synthesis, and tissue injury. They provide a significant platform for investigating disease mechanisms, discovering novel therapeutic targets, and evaluating therapy efficacy and safety.[18] In spite of availability of numerous murine model of SLE, no previous review has yet systematically explored the recent advancements in humanized NSG mice and their role in elucidating SLE immunopathogenesis and therapeutic modelling.

Aim

This review aims to provide a thorough understanding of humanized NSG mice in SLE research, detailing the techniques for engraftment, model-specific immune reconstitution characteristics, and their applications in simulating acute and chronic disease phenotypes. Additionally, comparative insights into limitation, challenges recent improvements, and future views are also included.

Literature search

A comprehensive literature study was conducted to identify peer-reviewed studies published between January 2017 and May 2025. This evaluation includes electronic journal articles obtained from esteemed databases such as PubMed, Google Scholar, Web of Science, and Scopus. The search methodology incorporated Medical Subject Headings (MeSH) alongside relevant free-text terms, including "systemic lupus erythematosus" or "SLE," "Humanized NSG mice," "SLE animal model," and "immunological biomarkers," as well as other specialized search expressions (Fig.1). Articles not in English, together with conference abstracts, editorials, and opinion pieces, were excluded. Following the screening and elimination of duplicates, a total of 87 pertinent publications were chosen to inform this comprehensive review.

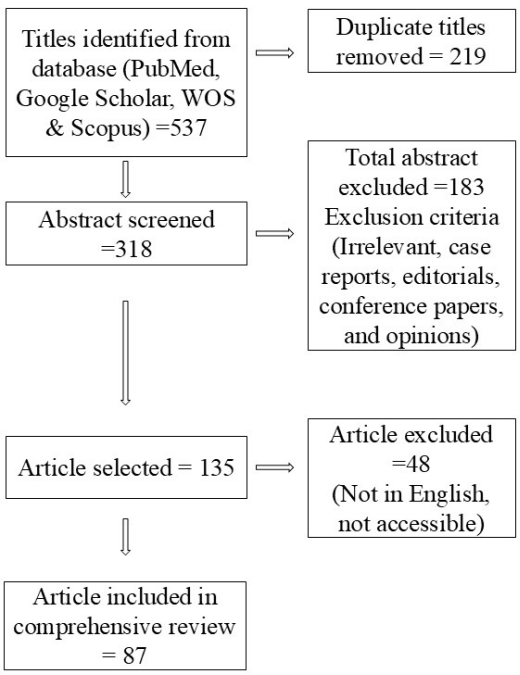

Fig. 1. Schematic representation of the literature search and selection process used in this comprehensive review

Analysis of the literature

Background of NSG mice

The NSG mouse strain is a triple-immunodeficient model that serves as a crucial platform in translational biomedical research, especially for the reconstitution of the human immune system. This model contains compound mutations in the Prkdc gene, which is responsible for the severe combined immunodeficiency (scid) phenotype.[19] The Prkdc mutation leads to a malfunctioning V(D)J recombination system, resulting in the cessation of mature T and B cell maturation, therefore compromising the mouse adaptive immune system.[20] The precise deletion of the interleukin-2 receptor common gamma chain (Il2rg) gene, referred to as IL-2Rγ^null, disrupts signaling through essential interleu-

kins (e.g., IL-2, IL-4, IL-7, IL-9, IL-15, and IL-21) that are vital for lymphoid lineage development and homeostasis, especially regarding the maturation and cytolytic function of natural killer (NK) cells.[21] The combined impact of these mutations results in a significant immunological deficiency, marked by both adaptive and innate immune failure, which incapacitates the host from initiating alloimmune or xenogeneic immune responses. This immunological niche establishes a xenotolerant milieu that facilitates the effective and durable engraftment of human hematopoietic stem and progenitor cells (HSPCs) or peripheral blood mononuclear cells (PBMCs).[22] Post-transplantation, human cells differentiate into several immune cell types, facilitating the development of a human-like immune system in mice, so allowing researchers to examine human-specific immunological responses.[23] Furthermore, the absence of murine major histocompatibility complex (MHC) reduces graft-versus-host and host-versus-graft immunological reactions, facilitating prolonged engraftment, enduring hematopoietic production, and effective immunological responses.[24] Thus, NSG mice function as a biologically pertinent surrogate model for assessing human hematopoiesis, immunopathology, tumor immunoediting, infectious disease dynamics, and immunotherapeutic strategies in physiologically relevant contexts.[25]

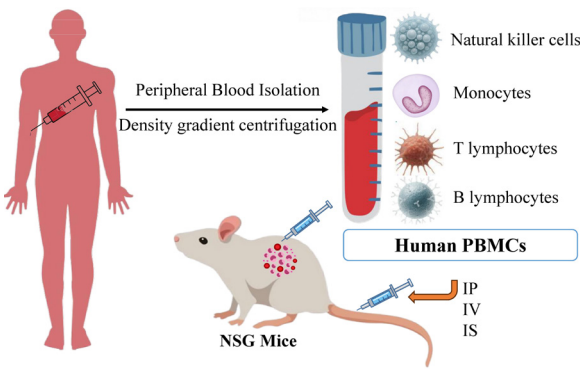

Fig. 2. Schematic representation of human PBMC isolation and engraftment in NSG mice

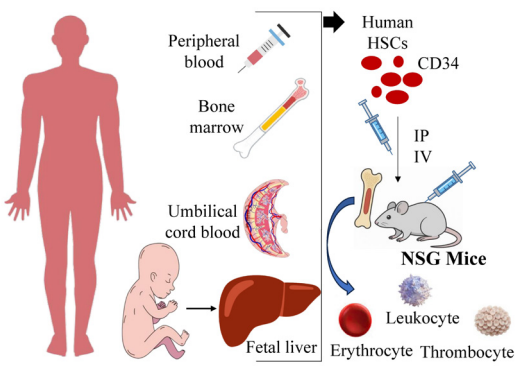

Fig. 3. Schematic representation of human CD34⁺ HSC isolation and engraftment in NSG mice

Types of humanizations

PBMC engraftment

PBMC engraftment is a humanization technique involving the intravenous injection of isolated human immune cells predominantly lymphocytes (T cells, B cells), monocytes, and natural killer (NK) cells into immunodeficient mice, such as NSG mice.[26] Peripheral blood mononuclear cells (PBMCs) are often extracted from the peripheral blood of healthy donors or patients using density gradient centrifugation (Fig. 2) and are subsequently delivered intravenously, commonly via the lateral tail vein of the mice.[27] The significant immunodeficiency of NSG mice allows engrafted human cells to survive, multiply, and partially reconstitute elements of the human immune system within the mouse host. Post-xenotransplantation, human immune cells invade peripheral lymphoid organs, with functional human T cells identifiable within 1–2 weeks.[28] The PBMC model is ideally suited for brief immuno-oncology or infectious disease research that use fast T-cell kinetics without necessitating extended immune monitoring.[29]

CD34⁺ hematopoietic stem cell engraftment

Hematopoietic stem cells (HSCs) are multipotent, immature cells that possess the ability for self-renewal and differentiation into all blood cell lineages, encompassing erythrocytes, leukocytes, and thrombocytes.[30] The expression of the surface glycoprotein CD34 is a defining property of early HSCs and progenitor cells, serving as a crucial marker for their identification and isolation. CD34 facilitates the selective enrichment of these cells from sources including bone marrow, umbilical cord blood, or mobilized peripheral blood (Fig. 3), hence aiding their application in transplantation, regenerative medicine, and the generation of humanized mice models.[31] During the engraftment of CD34⁺ hematopoietic stem cells (HSC), human CD34-positive stem and progenitor cells are transplanted into a recipient, typically an immunodeficient host such as NSG mice. These cells migrate to the bone marrow, establish residence within hematopoietic niches, and differentiate into all principal blood and immune cell lineages.[32] In the context of mobilized peripheral blood, donors undergo pre-treatment with granulocyte colony-stimulating factor (G-CSF), a cytokine that promotes the release of hematopoietic stem cells (HSCs) from the bone marrow into peripheral circulation, thereby enabling their collection via apheresis.[33] Among these sources, umbilical cord blood is preferred for its accessibility, significant proliferative capacity, and reduced occurrence of graft-versus-host disease. Fetal liver-derived HSCs, however less prevalent due to ethical and logistical issues, have high engraftment efficiency and robust hematopoietic reconstitution.[34] This model recapitulates key aspects of human hematopoiesis and adaptive immunity, provid-

ing a strong foundation for exploring immunological development, autoimmune disease mechanisms, immunotherapy effectiveness, and host-pathogen interactions in settings that closely resemble physiology.[35]

Development of humanized NSG mice for SLE

PBMC engraftment protocols: acute SLE modelling via mature immune cell transfer

Peripheral blood mononuclear cells (PBMCs), comprising a diverse array of immunocompetent cells such as T lymphocytes, B lymphocytes, monocytes, and natural killer (NK) cells, are extracted from lupus patients experiencing active disease flares via Ficoll-Hypaque density gradient centrifugation.[36] This xenotransplantation model facilitates rapid immune cell reconstitution, generally occurring within 7 to 14 days following injection. Flow cytometric assessment of human leukocyte antigens (CD45+, CD3+, CD19+, HLA-DR+) in peripheral circulation and lymphoid tissues is utilized to confirm engraftment kinetics and lineage-specific reconstitution.[37] This model resembles acute lupus and facilitates the examination of early immunological irregularities, including skewed TCR repertoires, hyperactive CD4+ T cells, and atypical B cell activation.[38] Furthermore, human-specific proinflammatory cytokines (e.g., IFN-α, IL-6, TNF-α) and immunoglobulins (IgG, IgM, including anti-dsDNA autoantibodies) are identifiable in recipient serum, acting as surrogate biomarkers for disease progression.[39] This substantial T-cell proliferation is often accompanied by the emergence of xenogeneic Graft-versus-Host Disease (xeno-GVHD), a notable confounder in longitudinal investigations. Xeno-GVHD results from the alloreactive T-cell identification of murine major histocompatibility complex (MHC)-deficient tissues within 4-6 weeks, causing multisystem inflammatory disease; this timeframe is ideal for assessing the development of immunological dysregulation associated with SLE before the onset of GVHD.[40]

CD34+ hematopoietic stem cell (HSC) engraftment: chronic SLE and immune ontogeny

The transplantation of human $CD34^+$ hematopoietic stem and progenitor cells (HSPCs) into immunodeficient NSG mice has become an effective method for reconstituting a functional human immune system. This model provides a distinctive platform to investigate the chronic immunopathology of SLE and the development of human immune responses in vivo.[41] As previously mentioned, the pretreatment of donors with granulocyte colony-stimulating factor (G-CSF) is crucial for mobilizing hematopoietic stem cells (HSCs) into the peripheral circulation for effective collection.[42] Before HSC transplantation, recipient NSG mice undergo myeloablative conditioning usually through sublethal total body irradiation (100–250 cGy) or chemotherapeutic agents like busulfan to eliminate endogenous hematopoietic cells and create vacant niches in the bone marrow microenvironment, thus promoting successful engraftment of human stem cells.[43] Following engraftment, $CD34^+$ progenitors migrate to the mouse bone marrow and gradually develop into all principal hematopoietic lineages, encompassing lymphoid (T, B, NK cells) and myeloid (monocytes, dendritic cells, granulocytes) compartments.[44] This framework promotes the advancement of efficient hematopoiesis, immunoglobulin class switching, and the generation of antigen-specific immune responses. Unlike the PBMC-based paradigm, the engraftment kinetics are markedly prolonged, with complete immune reconstitution often requiring 8 to 12 weeks.[45] The danger of xeno-GVHD is significantly reduced due to the naivety of the newly produced immune cells and the lack of pre-primed alloreactive T-cell subsets.[46] This method is especially beneficial for modelling the chronic nature and systemic signs of SLE.[47] It facilitates longitudinal investigations of immunological development, encompassing B cell tolerance checkpoints, somatic hypermutation, class-switch recombination, and the manufacture of high-affinity autoreactive antibodies.[48] When hematopoietic stem cells (HSCs) are obtained from lupus patients or individuals with established predisposing genotypes (e.g., IRF5, STAT4, PTPN22 variants), the resulting human immune system (HIS) mice display patient-specific immune signatures, including modified interferon signaling pathways, plasma blast hyperplasia, and deficiencies in regulatory T cells (Tregs).[49,50] The lack of GVHD facilitates the long-term observation of autoimmune development, therapeutic intervention, and relapse.[51]

Pristane-induced lupus in humanized NSG mice: a dual-hit model of autoimmunity

Pristane (2,6,10,14-tetramethylpentadecane), an environmentally significant hydrocarbon oil, serves as a strong lupus-inducing drug in mouse models by eliciting type I interferon responses through the activation of plasmacytoid dendritic cells (pDCs) and Toll-like receptor 7 (TLR7) signaling.[52] When injected intraperitoneally to humanized NSG mice, namely those reconstituted with CD34+ HSCs, pristane functions as an immunological adjuvant that enhances the autoimmune phenotype by provoking abnormal activation of human immune elements.[53] This combinatorial system simulates gene-environment interactions crucial to SLE pathogenesis, offering a precise platform to assess environmental triggers of illness onset and exacerbation. It amplifies the histological and serological characteristics of lupus, encompassing glomerulonephritis, vasculitis, and circulating immune complexes enriched with anti-RNP and anti-Sm antibodies.[54] Moreover, the pristane model highlights the synthesis of human IFN-α

and BAFF (B-cell activating factor), thereby enhancing B cell viability and autoantibody production.[55] Through the integration of genetic humanization and an environmental stimulus, the pristane-induced model provides a more authentic approach to examining the intricate etiology of lupus.[56] Table 1 presents a comparative analysis of various humanized mouse models employed in SLE research. Each row delineates a specific model type, encompassing the origin of human cells, techniques of engraftment, dynamics of immune reconstitution, and principal scientific applications.

Table 1. A comparison of humanized mouse models in SLE research

Parameter	PBMC engraftment model	CD34⁺ HSC engraftment model	Pristane-induced humanized model
Source of human cells	Peripheral blood from healthy donors or SLE patients	Cord blood, fetal liver, bone marrow, or mobilized peripheral blood	CD34⁺ HSCs or PBMCs
Engraftment site and route	Intravenous (tail vein)	Neonatal intrahepatic or adult intravenous	Intravenous (IV) + Intraperitoneal (Pristane)
Cell types introduced	Mature immune cells (T cells, B cells, NK cells, monocytes)	Hematopoietic stem/progenitor cells (CD34⁺)	Same as PBMC or CD34⁺, plus environmental modulation
Engraftment onset/time to reconstitution	Rapid (1–2 weeks post-injection)	Delayed (8–12 weeks post-conditioning)	Variable (depends on cell source)
Immune components reconstituted	Partial (T cells dominate)	Multilineage (T, B, NK, myeloid)	Multilineage + environmental trigger-induced activation
Immune reconstitution	Primarily T-cell reconstitution	Comprehensive immune system development	Immune response shaped by both human cells and pristane-induced inflammation
Lymphoid organ development	Limited (no thymopoiesis or germinal centers)	Robust (thymic T-cell development, splenic architecture)	Variable; may enhance inflammatory signaling pathways
GVHD risk	High (xeno-GVHD within 3–5 weeks)	Low to negligible	Moderate
Conditioning requirement	None	Required (irradiation or busulfan)	Required (same as PBMC/CD34⁺) + pristane injection
Duration of usefulness	Short-term (typically ≤6 weeks)	Long-term (months to over a year)	Intermediate to long-term
Suitability for autoimmunity models	Limited (T-cell biased, artificial)	High (endogenous repertoire, physiological development)	High (accelerated autoimmunity, gene-environment interactions)
Timeframe for study use	4–6 weeks	≥6 months	Variable depending on design
Best/key applications	T-cell cytotoxicity, early immune activation, xeno-GVHD studies	Vaccine response, chronic lupus phenotypes, personalized immune modeling	Accelerated lupus onset, IFN-I pathway, gene-environment interaction studies

Limitations and challenges of humanized NSG mice for SLE modeling

Incomplete immune system reconstitution and functional disparity

Although CD34⁺ HSC engraftment enables multilineage differentiation, the resulting immune system is still immature in both quantity and function.[57] Central and peripheral tolerance mechanisms are compromised by lymphoid tissue architecture, germinal center development, and thymic selection deficiencies. Human B cells in NSG mice generally have inadequate class-switch recombination and somatic hypermutation, reducing the model's ability to recreate SLE's high-affinity, pathogenic autoantibody profiles.[58] The lack of a completely functional human complement system makes modelling immune complex-mediated end-organ damage like glomerulonephritis more difficult.[59]

Xenogeneic graft-versus-host disease and temporal constraints

Despite its rapidity, PBMC-based humanization is hindered by the premature onset of xenogeneic graft-versus-host disease (xeno-GVHD) occurring within 4–6 weeks post-engraftment. This prevents long-term autoimmune progression and treatment efficacy studies.[60] The alloreactivity of mature human T cells to mice MHC-deficient tissues induces multisystem inflammation that resembles yet obscures lupus pathophysiology. Lupus-specific immune responses and generic xenogeneic reactivity are obscured by this immunological confounder.[61]

Lack of human lymphoid organogenesis and microenvironmental support

NSG mice lack organized secondary lymphoid organs such lymph nodes and functional Peyer's patches. This anatomical gap hinders antigen presentation, T-B cell collaboration, and lymphoid follicle growth. Therefore, autoreactive germinal center reactions and memory responses are greatly reduced.[62] As the murine stromal and cytokine environment is unsuitable for human hematopoiesis and immune cell function, transgenic or cytokine knock-in strains (e.g., NSG-SGM3, MISTRG) are needed to provide complexity and variety.[63]

Limited recapitulation of SLE heterogeneity

Despite better translational platforms than conventional mouse strains, humanized NSG mice still approximate complicated SLE. Gene and epigenetic variability in human SLE is difficult to recreate in single donor cell-engrafted mice.[64] These models cannot reproduce clinical SLE's polygenic vulnerability, stochastic disease flares, and sex-biased prevalence. This restricts research on patient-specific responses and sex hormone–driven immunomodulation, which are critical to SLE pathogenesis.[65]

Technical, ethical, and economic barriers

Humanized NSG mice development is difficult and resource-intensive, requiring quality human biological components, careful pathogen screening, and special-

ized animal facilities. Variations in engraftment, myeloablation, and donor cell survival can dramatically impact immunological outcomes.[66] Ethical problems of using human fetal tissues and regulatory monitoring of human-animal chimaeras further limit these models' acceptability and scalability.[67]

Recent advances in humanized NSG mice models for SLE research

Cytokine knock-in and transgenic NSG derivatives

Transgenic NSG substrains, such as NSG-SGM3, MISTRG, and NSG-IL15, exhibit enhanced hematopoietic production and functional maturity of humanized immune subsets. These strains have human cytokine knock-ins for SCF, GM-CSF, IL-3, M-CSF, and thrombopoietin to establish a xenocompatible cytokine milieu.[68] Myelopoiesis, dendritic cell formation, and monocyte/macrophage activity have improved, which are essential for accurately recreating SLE's myeloid-driven inflammation and interferon-driven immunopathology.[69]

HLA-transgenic NSG mice and autoreactivity modeling

Recent research has focused on developing HLA-restricted NSG mice models that express human MHC molecules (e.g., HLA-DR, HLA-A2). These models enable HLA-restricted positive and negative T cell selection during human hematopoiesis under self-MHC limitations.[70] This breakthrough is crucial for investigating the autoreactive T cell repertoire, antigen-specific tolerance breakdown, and pathogenic T follicular helper (Tfh) cells, a key component of lupus pathogenesis.[71] These platforms provide unmatched insights into autoimmunity's genetic and structural foundation, especially in HLA-associated disease susceptibility regions.[72]

Multi-donor and patient-derived xenografts for precision modeling

Recent studies have used pooled PBMC or $CD34^+$ HSC engraftments from various lupus patients to create a mosaic immune system that accounts for genetic and epigenetic variation.[73] Patient-derived xenograft (PDX) systems have also been modified for lupus modelling, notably using cells from high-risk polymorphism carriers (e.g., IRF5, STAT4, TNFAIP3, TYK2). These methods enable personalized lupus sub phenotype modelling and stratified therapy response evaluation.[74]

Human immune system organoids and hybridized murine platforms

The BLT (bone marrow-liver-thymus) paradigm shows how HSCs can be co-engrafted with human immunological organs such thymic tissue or mesenteric lymph node fragments.[75] These designs improve human immunological ontogeny, T cell education, and mouse tertiary lymphoid structure creation.[76] Hybrid animals with human liver or renal tissues can also examine organ-specific lupus symptoms including lupus nephritis and neuropsychiatric SLE in humanized inflammatory situations. Disease modelling and treatment trials become much more physiologically relevant using these methods.[77]

Human microbiota and environmental triggers in NSG mice models

Recent advances have included human microbiota transplantation (HMT) in NSG mice due to the involvement of microbial dysbiosis and environmental stresses in lupus flares. Mucosal immunity and systemic immune calibration are modulated by this host-compatible microbial ecology.[78] To replicate gene–environment interactions that cause lupus onset and exacerbation, UV radiation, TLR agonists, and pristane are being integrated into humanized systems. These combinatorial systems connect reductionist concepts to real-world autoimmune triggers.[79]

Advanced imaging and intravital immunophenotyping

Modern imaging methods like intravital two-photon microscopy, bioluminescence imaging, and PET are being used on humanized NSG mice models. During lupus development, these methods provide spatiotemporal visualization of immune cell trafficking, tissue infiltration, and microenvironmental interactions.[80,81] Combining high-dimensional flow cytometry and single-cell transcriptomics allows real-time cellular and molecular dynamics analysis at unprecedented granularity.[82] As shown in Fig. 4, a narrative illustration emphasizes recent advances in humanized NSG mouse models for SLE, particularly their role in improving immune system reconstitution and disease modeling.

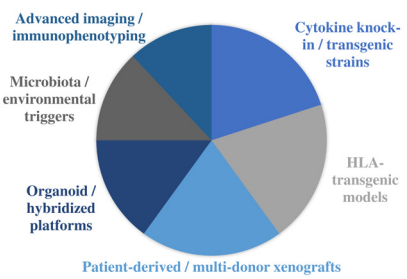

Fig. 4. Narrative illustration emphasizing recent advances in humanized NSG mice models for SLE

Future prospect

Recent advancements in biotechnology may significantly enhance the immunological accuracy and translational applicability of humanized NSG mice utilized in the research of SLE.[19] Engraftment with human thymic tissue can facilitate genuine thymopoiesis and central tolerance, whereas genetically modified strains like NSG-SGM3 and MISTRG, which express human cyto-

kines, are anticipated to enhance hematopoietic reconstitution and the efficacy of antigen-presenting cells.[83] Integrative multi-omics methodologies, encompassing genomes, epigenomics, and spatial transcriptomics, provide robust instruments to elucidate organ-specific immunological anomalies implicated in lupus pathogenesis.[84] Furthermore, the utilization of artificial intelligence and machine learning facilitates data-driven simulations and automated histopathological evaluations, enhancing model refinement and improving therapy predictions.[85] The development of individualized humanization protocols utilizing autologous hematopoietic cells or cells from other ethnic backgrounds facilitates the modelling of individual immunological profiles and genetic vulnerabilities.[86] To translate these innovations into well recognized preclinical platforms effectively, It is imperative to address ethical and regulatory components, Good Laboratory Practice (GLP) adherence, and improve scalability through automation and biofabrication.[87] Fig. 5 provides a narrative-based overview of the emerging applications and future prospects of humanized NSG mouse models in SLE research. These novel methodologies integrate experimental immunology with precision medicine, heralding a new era for lupus research.

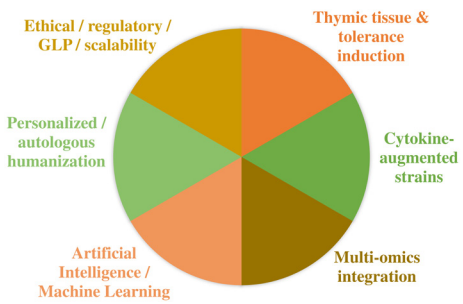

Fig. 5. Narrative illustration highlighting the future prospects of humanized NSG mice models in SLE research

Conclusion

The development of humanized NSG (NOD-scid IL-2Rγ^null) mice has significantly transformed the study environment for SLE, providing an exceptional platform for replicating human-specific immune dynamics with translational significance. These models facilitate the engraftment of patient-derived PBMCs or $CD34^+$ hematopoietic stem cells, offering mechanistic insights into autoimmunity that surpass the constraints of conventional murine systems. Despite significant obstacles, including poor immune development, xeno-GVHD, and inadequate lymphoid architecture, constant advances are enhancing model accuracy. Innovations like human cytokine knock-in strains, co-engraftment of thymic and organoid tissues, HLA-transgenic platforms, and integrative omics technologies synergistically enhance the functional and structural complexity of these models. The integration of AI-driven analytics and personalized engraftment procedures is enhancing precision modelling, facilitating individualized evaluations of pathogenesis and therapy effectiveness. With the progression towards standardization, ethical transparency, and scalable biomanufacturing, humanized NSG mice are set to become essential instruments in connecting laboratory testing with clinical application in lupus research. These advanced platforms clarify the complex foundations of SLE and outline a progressive approach for creating targeted, patient-focused immunotherapies.

Acknowledgments

The authors express their gratitude to the Management, Nemcare Group of Institutions, Guwahati, Assam, for necessary facilities.

Declaration

Funding

No external funding was received for this review.

Author contributions

Conceptualization, P.C. and J.M.; Resources, J.M., R.G., P.S.; Data Curation, R.G. and P.S. Validation: P.C.; Original Draft Preparation, J.M. and R.G.; Writing – Review & Editing, J.M. and P.C.; Supervision, P.C.

Conflicts of interest

The authors assert that they have no conflicts of interest.

Data availability

Not applicable

Ethics approval

Not applicable

Use of AI and AI-assisted technologies in the writing process

AI-assisted tools such as ChatGPT, QuillBot, Turnitin, and Mendeley were used for conceptual guidance, language refinement, plagiarism detection, and reference management. The content was reviewed and verified by the author for accuracy.

Reference

1. Arnaud L, Chasset F, Martin T. Immunopathogenesis of systemic lupus erythematosus: an update. *Autoimmun Rev.* 2024;23(10):103648. doi:10.1016/j.autrev.2024.103648
2. Ahmed AB, Chetia P. Selegiline modulates inflammatory indicators in RAW 264.7 macrophages and LPS-aggravated CFA-induced rheumatoid arthritis in rats. *Eur J Clin Exp Med.* 2024;22(1):6-16. doi:10.15584/ejcem.2024.1.12
3. Su X, Yu H, Lei Q, et al. Systemic lupus erythematosus:pathogenesis and targeted therapy. *Mol Biomed.* 2024;5(1):54. doi:10.1186/s43556-024-00217-8

4. Benseler SM, Silverman ED. Systemic Lupus Erythematosus. *Rheum Dis Clin North Am*. 2007;33(3):471-498. doi: 10.1016/j.rdc.2007.07.008
5. Lin SY, Huang YW, Błochowiak K. Autoimmune diseases and their various manifestations in the oral cavity: a systematic review. *Eur J Clin Exp Med*. 2023;21(3):627-638. doi:10.15584/ejcem.2023.3.16
6. Gaballah H, Abd-Elkhalek R, Hussein O, El-Wahab SA. Association of *TNFAIP3* gene polymorphism (rs5029939) with susceptibility and clinical phenotype of systemic lupus erythematosus. *Arch Rheumatol*. Published online October 16, 2021. doi:10.46497/ArchRheumatol.2022.8769
7. Laurynenka V, Harley JB. The 330 risk loci known for systemic lupus erythematosus (SLE): a review. *Front Lupus*. 2024;2. doi:10.3389/flupu.2024.1398035
8. Crow MK. Pathogenesis of systemic lupus erythematosus: risks, mechanisms and therapeutic targets. *Ann Rheum Dis*. 2023;82(8):999-1014. doi:10.1136/ard-2022-223741
9. Vieira AA, Almada-Correia I, Inácio J, Costa-Reis P, da Rocha ST. Female-bias in systemic lupus erythematosus: How much is the X chromosome to blame? *Biol Sex Differ*. 2024;15(1):76. doi:10.1186/s13293-024-00650-y
10. Dai X, Fan Y, Zhao X. Systemic lupus erythematosus: updated insights on the pathogenesis, diagnosis, prevention and therapeutics. *Signal Transduct Target Ther*. 2025;10(1):102. doi:10.1038/s41392-025-02168-0
11. Londe AC, Fernandez-Ruiz R, Julio PR, Appenzeller S, Niewold TB. Type I Interferons in Autoimmunity: Implications in Clinical Phenotypes and Treatment Response. *J Rheumatol*. 2023;50(9):1103-1113. doi:10.3899/jrheum.2022-0827
12. Katikaneni D, Morel L, Scindia Y. Animal models of lupus nephritis: the past, present and a future outlook. *Autoimmunity*. 2024;57(1). doi:10.1080/08916934.2024.2319203
13. Polis B, Cuda CM, Putterman C. Animal models of neuropsychiatric systemic lupus erythematosus: deciphering the complexity and guiding therapeutic development. *Autoimmunity*. 2024;57(1). doi:10.1080/08916934.2024.2330387
14. Bin Y, Ren J, Zhang H, et al. Against all odds: The road to success in the development of human immune reconstitution mice. *Anim Model Exp Med*. 2024;7(4):460-470. doi:10.1002/ame2.12407
15. Moore E, Reynolds JA, Davidson A, et al. Promise and complexity of lupus mouse models. *Nat Immunol*. 2021;22(6):683-686. doi:10.1038/s41590-021-00914-4
16. Campilan B, Schroeder C, Sagaityte E, et al. Animal model considerations for chordoma research: reproducing the tumor microenvironment in vivo with humanized mice. *Front Oncol*. 2024;14. doi:10.3389/fonc.2024.1330254
17. Chen J, Liao S, Zhou H, et al. Humanized Mouse Models of Systemic Lupus Erythematosus: Opportunities and Challenges. *Front Immunol*. 2022;12. doi:10.3389/fimmu.2021.816956
18. Chen J, Liao S, Xiao Z, et al. The development and improvement of immunodeficient mice and humanized immune system mouse models. *Front Immunol*. 2022;13. doi:10.3389/fimmu.2022.1007579
19. Chupp DP, Rivera CE, Zhou Y, et al. A humanized mouse that mounts mature class-switched, hypermutated and neutralizing antibody responses. *Nat Immunol*. 2024;25(8):1489-1506. doi:10.1038/s41590-024-01880-3
20. Li H, Zhang Y, Zhang B, Chen D. A novel PRKDC mutation caused B lymphocytes V(D)J rearrangement disorder in the SLE-DAH like symptoms patient. *Pediatr Rheumatol*. 2023;21(1):84. doi:10.1186/s12969-023-00840-9
21. Aryee K, Shultz LD, Burzenski LM, Greiner DL, Brehm MA. NOD- scid IL2rγnull mice lacking TLR4 support human immune system development and the study of human-specific innate immunity. *J Leukoc Biol*. 2023;113(5):418-433. doi:10.1093/jleuko/qiac020
22. Shan L, Flavell RA, Herndler-Brandstetter D. Development of humanized mouse models for studying human NK cells in health and disease. In: Herndler-Brandstetter D, Flavell RA, eds. *Human NK Cells: Methods and Protocols*. New York, NY: Springer; 2022:53-66. doi:10.1007/978-1-0716-2160-8_5
23. Long JE, Jankovic M, Maddalo D. Drug discovery oncology in a mouse: concepts, models and limitations. *Futur Sci OA*. 2021;7(8). doi:10.2144/fsoa-2021-0019
24. Karnik I, Her Z, Neo SH, Liu WN, Chen Q. Emerging preclinical applications of humanized mouse models in the discovery and validation of novel immunotherapeutics and their mechanisms of action for improved cancer treatment. *Pharmaceutics*. 2023;15(6):1600. doi:10.3390/pharmaceutics15061600
25. Mihaylova N, Chipinski P, Bradyanova S, et al. Suppression of autoreactive T and B lymphocytes by anti-annexin A1 antibody in a humanized NSG murine model of systemic lupus erythematosus. *Clin Exp Immunol*. 2020;199(3):278-293. doi:10.1111/cei.13399
26. Yu CI, Maser R, Marches F, Banchereau J, Palucka K. Engraftment of adult hematopoietic stem and progenitor cells in a novel model of humanized mice. *iScience*. 2024;27(3):109238. doi:10.1016/j.isci.2024.109238
27. Dinh B, Hoeksema MA, Spann NJ, et al. Isolation and cryopreservation of highly viable human peripheral blood mononuclear cells from whole blood: A guide for beginners. *J Vis Exp*. 2024;(212). doi:10.3791/66794
28. Sykes M, Sachs DH. Progress in xenotransplantation: overcoming immune barriers. *Nat Rev Nephrol*. 2022;18(12):745-761. doi:10.1038/s41581-022-00624-6
29. Wang W, Li Y, Lin K, Wang X, Tu Y, Zhuo Z. Progress in building clinically relevant patient-derived tumor xenograft models for cancer research. *Anim Model Exp Med*. 2023;6(5):381-398. doi:10.1002/ame2.12349
30. Lee JY, Hong SH. Hematopoietic stem cells and their roles in tissue regeneration. *Int J Stem Cells*. 2020;13(1):1-12. doi:10.15283/ijsc19127

31. Zhang Y, Shen B, Guan X, et al. Safety and efficacy of ex vivo expanded CD34+ stem cells in murine and primate models. *Stem Cell Res Ther*. 2019;10(1):173. doi:10.1186/s13287-019-1275-0
32. Brendel C, Rio P, Verhoeyen E. Humanized mice are precious tools for evaluation of hematopoietic gene therapies and preclinical modeling to move towards a clinical trial. *Biochem Pharmacol*. 2020;174:113711. doi:10.1016/j.bcp.2019.113711
33. Miner Xie, Shanshan Zhang, Fang Dong, et al. Granulocyte colony-stimulating factor directly acts on mouse lymphoid-biased but not myeloid-biased hematopoietic stem cells. *Haematologica*. 2020;106(6):1647-1658. doi:10.3324/haematol.2019.239251
34. Sanchez-Petitto G, Rezvani K, Daher M, et al. Umbilical cord blood transplantation: connecting its origin to its future. *Stem Cells Transl Med*. 2023;12(2):55-71. doi:10.1093/stcltm/szac086
35. Sefik E, Xiao T, Chiorazzi M, et al. Engineering mice to study human immunity. *Annu Rev Immunol*. 2025;43(1):451-487. doi:10.1146/annurev-immunol-082523-124415
36. Chen W, Hong SH, Jenks SA, et al. Distinct transcriptomes and autocrine cytokines underpin maturation and survival of antibody-secreting cells in systemic lupus erythematosus. *Nat Commun*. 2024;15(1):1899. doi:10.1038/s41467-024-46053-w
37. Ménoret S, Ouisse LH, Tesson L, et al. In vivo analysis of human immune responses in immunodeficient rats. *Transplantation*. 2020;104(4):715-723. doi:10.1097/TP.0000000000003047
38. Akama-Garren EH, Carroll MC. Lupus susceptibility loci predispose mice to clonal lymphocytic responses and myeloid expansion. *J Immunol*. 2022;208(10):2403-2424. doi:10.4049/jimmunol.2200098
39. Wakiya R, Ueeda K, Nakashima S, et al. Effect of add-on hydroxychloroquine therapy on serum proinflammatory cytokine levels in patients with systemic lupus erythematosus. *Sci Rep*. 2022;12(1):10175. doi:10.1038/s41598-022-14571-6
40. Ktena YP, Koldobskiy MA, Barbato MI, et al. Donor T cell DNMT3a regulates alloreactivity in mouse models of hematopoietic stem cell transplantation. *J Clin Invest*. 2022;132(13). doi:10.1172/JCI158047
41. Morvan MG, Teque F, Ye L, et al. Genetically edited CD34 + cells derived from human iPS cells in vivo but not in vitro engraft and differentiate into HIV-resistant cells. *Proc Natl Acad Sci*. 2021;118(20). doi:10.1073/pnas.2102404118
42. Chuprin J, Buettner H, Seedhom MO, et al. Humanized mouse models for immuno-oncology research. *Nat Rev Clin Oncol*. 2023;20(3):192-206. doi:10.1038/s41571-022-00721-2
43. Garcia-Perez L, van Roon L, Schilham MW, Lankester AC, Pike-Overzet K, Staal FJT. Combining mobilizing agents with busulfan to reduce chemotherapy-based conditioning for hematopoietic stem cell transplantation. *Cells*. 2021;10(5):1077. doi:10.3390/cells10051077
44. Gutierrez-Barbosa H, Medina-Moreno S, Perdomo-Celis F, et al. A Comparison of lymphoid and myeloid cells derived from human hematopoietic stem cells xenografted into NOD-derived mouse strains. *Microorganisms*. 2023;11(6):1548. doi:10.3390/microorganisms11061548
45. Liu Y, Wu W, Cai C, Zhang H, Shen H, Han Y. Patient-derived xenograft models in cancer therapy: technologies and applications. *Signal Transduct Target Ther*. 2023;8(1):160. doi:10.1038/s41392-023-01419-2
46. Khosravi-Maharlooei M, Li HW, Sykes M. T Cell development and responses in human immune system mice. *Annu Rev Immunol*. 2025;43(1):83-112. doi:10.1146/annurev-immunol-082223-041615
47. Gunawan M, Her Z, Liu M, et al. A novel human systemic lupus erythematosus model in humanised mice. *Sci Rep*. 2017;7(1):16642. doi:10.1038/s41598-017-16999-7
48. von Hofsten S, Fenton KA, Pedersen HL. Human and murine toll-like receptor-driven disease in systemic lupus erythematosus. *Int J Mol Sci*. 2024;25(10):5351. doi:10.3390/ijms25105351
49. Zare Moghaddam M, Mousavi MJ, Ghotloo S. Stem cell-based therapy for systemic lupus erythematous. *J Transl Autoimmun*. 2024;8:100241. doi:10.1016/j.jtauto.2024.100241
50. Song Y, Li J, Wu Y. Evolving understanding of autoimmune mechanisms and new therapeutic strategies of autoimmune disorders. *Signal Transduct Target Ther*. 2024;9(1):263. doi:10.1038/s41392-024-01952-8
51. Teshima T, Boelens JJ, Matsuoka KI. Novel insights into GVHD and immune reconstitution after allogeneic hematopoietic cell transplantation. *Blood cell Ther*. 2023;6(2):42-48. doi:10.31547/bct-2022-023
52. Yun Y, Wang X, Xu J, et al. Pristane induced lupus mice as a model for neuropsychiatric lupus (NPSLE). *Behav Brain Funct*. 2023;19(1):3. doi:10.1186/s12993-023-00205-y
53. Pannu N, Bhatnagar A. Oxidative stress and immune complexes: Pathogenic mechanisms in pristane induced murine model of lupus. *Immunobiology*. 2020;225(1):151871. doi:10.1016/j.imbio.2019.11.006
54. Xu D, Reilly CM. HDAC6 knockout alleviates pristane-induced lupus. *J Immunol*. 2022;208(Supplement_1):104.13-104.13. doi:10.4049/jimmunol.208.Supp.104.13
55. Zhou Y, Yang B, Long H, et al. Immune cell alterations in a pristane-induced lupus model in C57BL/6J mice. *Rheumatol Autoimmun*. Published online January 21, 2025. doi:10.1002/rai2.12164
56. Mizui M, Tsokos GC. Animal models: systemic autoimmune diseases. In: *The Autoimmune Diseases*. Elsevier; 2020:533-551. doi:10.1016/B978-0-12-812102-3.00029-4
57. O'Brien LJ, Walpole CM, Leal-Rojas IM, et al. Characterization of human engraftment and hemophagocytic lymphohistiocytosis in NSG-SGM3 neonate mice engrafted with purified CD34+ hematopoietic stem cells. *Exp Hematol*. 2024;130:104134. doi:10.1016/j.exphem.2023.11.008

58. Gavish A, Chain B, Salame TM, et al. From pseudo to real--time dynamics of T cell thymic differentiation. *iScience*. 2023;26(1):105826. doi:10.1016/j.isci.2022.105826
59. Zoshima T, Hara S, Yamagishi M, et al. Possible role of complement factor H in podocytes in clearing glomerular subendothelial immune complex deposits. *Sci Rep*. 2019;9(1):7857. doi:10.1038/s41598-019-44380-3
60. Haque M, Boardman D, Lam A, et al. Modelling graft--versus-host disease in mice using human peripheral blood mononuclear cells. *BIO-PROTOCOL*. 2022;12(23). doi:10.21769/BioProtoc.4566
61. Darguzyte M, Antczak P, Bachurski D, et al. Long-term human immune reconstitution, T-cell development, and immune reactivity in mice lacking the murine major histocompatibility complex: validation with cellular and gene expression profiles. *Cells*. 2024;13(20):1686. doi:10.3390/cells13201686
62. Kitsera M, Brunetti JE, Rodríguez E. Recent developments in NSG and NRG humanized mouse models for their use in viral and immune research. *Viruses*. 2023;15(2):478. doi:10.3390/v15020478
63. Saito Y, Shultz LD, Ishikawa F. Understanding normal and malignant human hematopoiesis using next-generation humanized mice. *Trends Immunol*. 2020;41(8):706-720. doi:10.1016/j.it.2020.06.004
64. Adams DE, Shao WH. Epigenetic alterations in immune cells of systemic lupus erythematosus and therapeutic implications. *Cells*. 2022;11(3):506. doi:10.3390/cells11030506
65. Tsokos GC. The immunology of systemic lupus erythematosus. *Nat Immunol*. 2024;25(8):1332-1343. doi:10.1038/s41590-024-01898-7
66. Walsh NC, Kenney LL, Jangalwe S, et al. Humanized mouse models of clinical disease. *Annu Rev Pathol Mech Dis*. 2017;12(1):187-215. doi: 10.1146/annurev-pathol-052016-100332
67. Kwisda K, White L, Hübner D. Ethical arguments concerning human-animal chimera research: a systematic review. *BMC Med Ethics*. 2020;21(1):24. doi:10.1186/s12910-020-00465-7
68. Du EJ, Muench MO. A Monocytic barrier to the humanization of immunodeficient mice. *Curr Stem Cell Res Ther*. 2024;19(7):959-980. doi:10.2174/011574888X263597231001164351
69. Greene JT, Brian BF, Senevirathne SE, Freedman TS. Regulation of myeloid-cell activation. *Curr Opin Immunol*. 2021;73:34-42. doi:10.1016/j.coi.2021.09.004
70. Alves da Costa T, Lang J, Torres RM, Pelanda R. The development of human immune system mice and their use to study tolerance and autoimmunity. *J Transl Autoimmun*. 2019;2:100021. doi:10.1016/j.jtauto.2019.100021
71. Liu J, Zhang X, Cao X. Dendritic cells in systemic lupus erythematosus: from pathogenesis to therapeutic applications. *J Autoimmun*. 2022;132:102856. doi: 10.1016/j.jaut.2022.102856
72. Luo S, Long H, Lu Q. Recent advances in understanding pathogenesis and therapeutic strategies of systemic lupus erythematosus. *Int Immunopharmacol*. 2020;89:107028. doi:10.1016/j.intimp.2020.107028
73. Araki Y, Mimura T. Epigenetic dysregulation in the pathogenesis of systemic lupus erythematosus. *Int J Mol Sci*. 2024;25(2):1019. doi:10.3390/ijms25021019
74. Qin R, Liang Y, Zhou F. Advances in the application of patient-derived xenograft models in acute leukemia resistance. *Cancer Drug Resist*. Published online May 28, 2025. doi:10.20517/cdr.2025.18
75. Yan H, Semple KM, Gonzaléz CM, Howard KE. Bone marrow-liver-thymus (BLT) immune humanized mice as a model to predict cytokine release syndrome. *Transl Res*. 2019;210:43-56. doi:10.1016/j.trsl.2019.04.007
76. Shah D, Soper B, Shopland L. Cytokine release syndrome and cancer immunotherapies – historical challenges and promising futures. *Front Immunol*. 2023;14. doi:10.3389/fimmu.2023.1190379
77. Justiz-Vaillant AA, Gopaul D, Soodeen S, et al. Neuropsychiatric systemic lupus erythematosus: molecules involved in its imunopathogenesis, clinical features, and treatment. *Molecules*. 2024;29(4):747. doi:10.3390/molecules29040747
78. Toumi E, Mezouar S, Plauzolles A, et al. Gut microbiota in SLE: from animal models to clinical evidence and pharmacological perspectives. *Lupus Sci Med*. 2023;10(1):e000776. doi:10.1136/lupus-2022-000776
79. Liu JL, Woo JMP, Parks CG, Costenbader KH, Jacobsen S, Bernatsky S. Systemic lupus erythematosus risk. *Rheum Dis Clin North Am*. 2022;48(4):827-843. doi:10.1016/j.rdc.2022.06.005
80. Zhang Y, Cui D. Evolving models and tools for microglial studies in the central nervous system. *Neurosci Bull*. 2021;37(8):1218-1233. doi:10.1007/s12264-021-00706-8
81. Bouchalova P, Bouchal P. Current methods for studying metastatic potential of tumor cells. *Cancer Cell Int*. 2022;22(1):394. doi:10.1186/s12935-022-02801-w
82. Zhang X, Song B, Carlino MJ, et al. An immunophenotype-coupled transcriptomic atlas of human hematopoietic progenitors. *Nat Immunol*. 2024;25(4):703-715. doi:10.1038/s41590-024-01782-4
83. Fukuhara T, Ueda Y, Lee SI, et al. Thymocyte development of humanized mice is promoted by interactions with human-derived antigen presenting cells upon immunization. *Int J Mol Sci*. 2023;24(14):11705. doi:10.3390/ijms241411705
84. Lim J, Park C, Kim M, Kim H, Kim J, Lee DS. Advances in single-cell omics and multiomics for high-resolution molecular profiling. *Exp Mol Med*. 2024;56(3):515-526. doi:10.1038/s12276-024-01186-2
85. Asif A, Rajpoot K, Graham S, Snead D, Minhas F, Rajpoot N. Unleashing the potential of AI for pathology: challenges and recommendations. *J Pathol*. 2023;260(5):564-577. doi:10.1002/path.6168

86. Kumari R, Feuer G, Bourré L. Humanized mouse models for immuno-oncology drug discovery. *Curr Protoc*. 2023;3(8):e852. doi:10.1002/cpz1.852

87. Nieto D, Jiménez G, Moroni L, López-Ruiz E, Gálvez-Martín P, Marchal JA. Biofabrication approaches and regulatory framework of metastatic tumor-on-a-chip models for precision oncology. *Med Res Rev*. 2022;42(5):1978-2001. doi:10.1002/med.21914

Rzeszów University Press 2026
ISSN 2544-1361 (online)
doi: 10.15584/ejcem.2026.1.19

http://www.ejcem.ur.edu.pl
European Journal of Clinical and Experimental Medicine
Eur J Clin Exp Med 2026; 24 (1): 192–200

REVIEW PAPER

Ocular and systemic adverse effects of topical non-steroidal anti-inflammatory drugs – a narrative review with quantitative synthesis

Sankhajyoti Saha [1], Moubani Dutta [2]

[1] Department of Optometry and Vision Science, NSHM Knowledge Campus, Kolkata, India
[2] Department of Dietetics and Nutrition, NSHM Knowledge Campus, Kolkata, India

ABSTRACT

Introduction and aim. The impacts of topical ophthalmic non-steroidal anti-inflammatory drugs (NSAIDs) have been studied, with instances of an unprecedented quantitative assessment of adverse drug reaction prevalence among several NSAID classes. This study aimed to systematically observe and synthesize the relevant information on the pharmacodynamic mechanism of adverse drug reactions (ADR) corresponding to topical NSAID administration.

Literature search. A preliminary search on PubMed Central, Google Scholar, and ScienceDirect databases yielded 83 articles.

Analysis of literature. Conditions such as corneal perforation, ulceration, infiltration, keratitis, melt, corneal issues involving epithelial defects, tissue loss, stromal thinning, and delayed wound healing accentuate a comprehensive range of consequences on corneal integrity and physiology. The topical NSAID group also conveys more diversified systemic adverse reactions involving dilated ventricle, tricuspid regurgitation, pulmonary insufficiency, closure of the ductus arteriosus, and prenatal ductal constriction, which constitute a concern for their impact on cardiac activity and developing embryos.

Conclusion. Burning sensation is reported to be the most commonly reported frequency after photophobia. Notably, preferential COX-2 inhibitors had a significantly greater prevalence of ADRs than both nonselective COX inhibitors (mean difference=1.05, p=0.023) and selective COX-2 inhibitors. Longitudinal studies with frequent follow-ups are essential to fully characterize the incidence, severity, and long-term effects of adverse consequences.

Keywords. adverse drug reactions, anti-inflammatory medications, ocular drug delivery, ocular pharmacokinetics, topical ophthalmic non-steroidal anti-inflammatory drugs

Introduction

One of the cornerstones of healthcare is the administration of drugs. Adverse drug reactions are a frequent cause of practitioner-related litigation in ophthalmology. Owing to potentially devastating triggers, drug oversight can be expensive to prosecute, compensate, and/or resolve.[1,2] Regularly recommended drugs may have detrimental impacts on the eyes, about distinct parts of the eyes. Monitoring toxicity, limiting dosage, attempting to alternate therapies, and divulging negative effects are all ways to lessen the risk.[3-5]

Adverse drug reactions (ADR) are deleterious, unintended, but preventable, as briefed by the WHO. Reporting ADR, with qualitative information, eventually improves medication safety across the globe and can impact prompt protocols that promote patients' safety.[6] The majority of the most prevalent sources of adverse medication effects associated with the sequel of ocu-

Corresponding author: Sankhajyoti Saha, e-mail: sankhajyoti.saha39@gmail.com

Received: 1.07.2025 / Revised: 11.10.2025 / Accepted: 9.11.2025 / Published: 30.03.2026

Saha S, Dutta M. Ocular and systemic adverse effects of topical non-steroidal anti-inflammatory drugs – a narrative review with quantitative synthesis. *Eur J Clin Exp Med.* 2026;24(1):192–200. doi: 10.15584/ejcem.2026.1.19.

lar complications are NSAIDs (approximately 25% of all adverse drug events).[7-9] Considerable adverse effects relating to the eyes may result from their application, necessitating close observation in clinical contexts.[10] Eyelids, conjunctiva, and cornea are often impacted by exposure to drugs, which may culminate in inflammation and hypersensitivity responses.[11-14] Patients with crippled corneas as an aftermath of surgical procedure, diabetes, or autoimmune disorders are at increased risk for NSAID-induced corneal melt (NICM), which initially raised concerns but has now been validated. The precise repetition in the form of dose and duration of NSAIDs is yet uncertain, and possibly had a profound effect on the occurrence of adverse effects.[15] The current evidences does not provide a definitive, class-specific comparison of the occurrence of adverse medication reactions associated with NSAIDs. A comprehensive narrative evaluation is required to synthesize fragmented material and elucidate these risk disparities among principal NSAID classes.

Aim

The aim of this narrative review was to synthesize current evidence on ocular and systemic adverse reactions to topical ophthalmic NSAIDs and to provide a quantitative overview of the prevalence of these adverse effects, including comparative analysis across non-selective, selective, and preferential COX-2 inhibitors.

Literature search

We focused our search exclusively on peer-reviewed publications, and employed a strategic construction to uncover information about the adverse effects of NSAIDs on the eyes, concentrated on keywords and Medical Subject Headings (MeSH) corresponding to "Administration, topical", "Anti-inflammatory agents, non-steroidal/adverse effects", "Anti-inflammatory agents, Non-steroidal/therapeutic use", "Cornea/drug effects", "Cyclooxygenase 2", "Cyclooxygenase 2 inhibitors", "Cyclooxygenase inhibitors/pharmacology", "Diclofenac/adverse effects", "Drug Hypersensitivity/diagnosis", "Drug hypersensitivity/etiology", "Drug hypersensitivity/therapy", "Drug-related side effects and adverse reactions", "Eye", "Hypersensitivity/complications", "Ketorolac tromethamine", "Ophthalmic solutions", "Ophthalmic solutions/administration & dosage", "Ophthalmic solutions/therapeutic use". A preliminary search on PubMed Central, Google Scholar, and the ScienceDirect database yielded 347 text articles. Studies with clear outcome data, such as clinical trials, cohort, and case-control studies, that reported adverse reactions to topical NSAID use in human subjects met the inclusion criteria. Animal research, conference papers, and studies with insufficient or imprecise adverse event data were not included. In the initial phase, articles were initially eliminated due to retracted publications, unclear reporting of the specific treatment regimen, incorrect outcome measures, inappropriate interventions, and publications that were not retrieved (Fig. 1).[16] The reporting frequency with which each ADR is documented in the literature is the sole factor used to calculate Reporting frequency (%), whereas frequency of reporting in publications (%) shows the percentage of included studies that documented the particular adverse drug reaction. All interval estimates are now explicitly labeled as "95% CI" for clarity. The ADR ranking, utilizing reporting frequency and publication-based reporting frequency, serves as a preliminary measure for individualized drug-risk assessment and may yield clinically and financially significant insights.

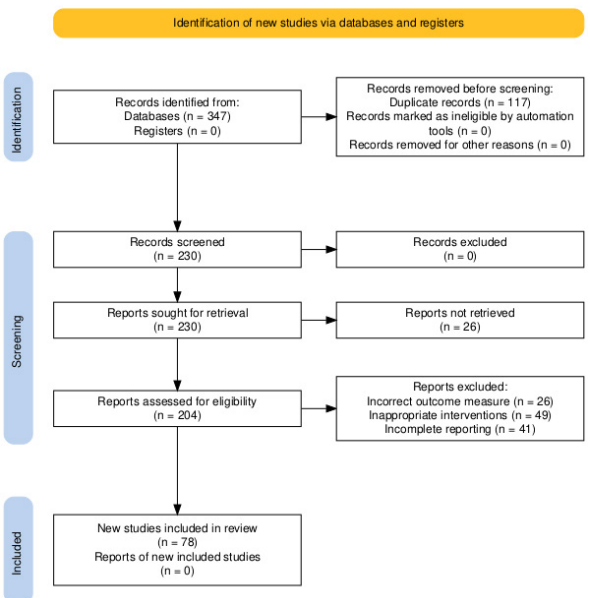

Fig 1. The literature selection processing[16]

All literature that has been identified has been reviewed by two authors who worked separately on data abstraction. Since publications conducted between 2000 and 2025 had precedence in the review, a few convincing fundamental studies before 2000 were solicited to establish the suitability of each identified literature for our analysis.

Analysis of the literature

Comprehensive description of adverse effects

Reported adverse effects

Multiple studies have established an elevated prevalence of various adverse effects corresponding to the use of topical NSAIDs (Table 1).

The cornea seems highly exposed, demonstrating conditions such as corneal perforation, ulceration, infiltration, keratitis, and melt, all indicative of severe damage to the transparent outermost layer of the eye. In addition to the comprehensive adverse ocular effects, Cardiovascular issues are significant, involving dilat-

ed ventricle, tricuspid regurgitation, pulmonary insufficiency, closure of the ductus arteriosus, and prenatal ductal constriction, which constitute a concern for their impact on cardiac activity and developing embryos.

Table 1. The tabulation of reported adverse effects[17-50]

Adverse effects/sign	Reporting frequency (%)	Frequency of reporting in publications (%)
Corneal perforation	16.81	28.12
Corneal ulcer	5.31	6.25
Corneal infiltration	4.42	9.37
Declined corneal sensation	12.39	31.25
Keratitis	4.42	6.25
Tissue loss	4.42	6.25
Epithelial defect	6.19	12.50
Corneal melt	7.08	12.50
Descemetocele	6.19	9.37
Epithelial wound	0.88	3.12
Superficial punctate	0.88	3.12
Delayed corneal wound healing	0.88	3.12
Stromal thinning	0.88	3.12
Reduced corneal responsiveness	2.65	3.12
Lower Schirmer value	1.77	3.12
Scleral melt	1.77	3.12
Hyperemia	3.54	9.37
Conjunctival injection	0.88	3.12
Edematous swelling of the eyelids	0.88	3.12
Periorbital dermatitis	0.88	3.12
Iritis	0.88	3.12
Eye pruritus	1.77	6.25
Posterior capsule opacification	0.88	3.12
Iris prolapse	0.88	3.12
Neurotrophic keratopathy	0.88	3.12
Shrunken eye	0.88	3.12
Low concentration of breast milk	2.65	3.12
Dilated ventricle	0.88	3.12
Tricuspid regurgitation	0.88	3.12
Pulmonary insufficiency	16.81	28.12
Closure of the ductus arteriosus	5.31	6.25
Prenatal ductal constriction	4.42	9.37
Asthma	12.39	31.25

Spearman correlation between frequency of reporting in publications and reporting frequency of adverse effects in included studies

Table 2. Correlations between frequency of reporting in publications and reporting frequency of adverse effects[a]

			Frequency of reporting in publications (%)	Reporting frequency (%)
Spearman's rho	Frequency of reporting in publications (%)	Correlation coefficient	1.00	0.89**
		Sig. (2-tailed)	.	<0.001
		n	33	33
	Reporting frequency (%)	Correlation coefficient	0.89**	1.00
		Sig. (2-tailed)	<0.001	.
		n	33	33

a ** – correlation is significant at the 0.01 level (2-tailed)

The Spearman's correlation analysis demonstrated a strong positive association between study frequency and prevalence, with a correlation value (ρ) of 0.891, as the data were non-normally distributed and ordinal in nature, and that standard tie-handling procedures inherent to the Spearman method. This indicates that the prevalence is likely to increase in accordance with study frequency. At the value of 0.01, the association is statistically significant ($p<0.001$, two-tailed), signifying that this association would not have emerged by default (Table 2).

Ranking

Table 3. Ranks assigned to each data point based on the frequency of reporting in publications and reporting frequency of adverse effects

Adverse effects/sign	Rank of reporting frequency	Rank of the frequency of reporting in publications
Corneal perforation	33.00	32.00
Corneal ulcer	28.00	23.50
Corneal infiltration	26.00	27.00
Declined corneal sensation	32.00	33.00
Keratitis	26.00	23.50
Tissue loss	26.00	23.50
Epithelial defect	29.50	30.00
Corneal melt	31.00	30.00
Descemetocele	29.50	27.00
Epithelial wound	9.00	11.00
Superficial punctate	9.00	11.00
Delayed corneal wound healing	9.000	11.00
Stromal thinning	9.00	11.00
Reduced corneal responsiveness	21.50	11.00
Lower Schirmer value	19.00	11.00
Scleral melt	19.00	11.00
Hyperemia	23.50	27.00
Conjunctival injection	9.00	11.00
Edematous swelling of the eyelids	9.00	11.00
Periorbital dermatitis	9.00	11.00
Iritis	9.00	11.00
Eye pruritus	19.00	23.50
Posterior capsule opacification	9.00	11.00
Iris prolapse	9.00	11.00
Neurotrophic keratopathy	9.00	11.00
Shrunken eye	9.00	11.00
Low concentration of breast milk	21.50	11.00
Dilated ventricle	9.00	11.00
Tricuspid regurgitation	9.00	11.00
Pulmonary insufficiency	9.00	11.00
Closure of the ductus arteriosus	9.00	11.00
Prenatal ductal constriction	9.00	11.00
Asthma	23.50	30.00

In Spearman's correlation, raw numbers are modified into ranks to appraise the magnitude and direction of an exponential equation between two variables. Substantially higher rank (e.g., 33.00, 32.00, 30.00) in-

dicate studies with relatively greater frequencies, while lower rank values (e.g., 11.00) correspond to studies with smaller frequencies. Recurring ranks like 11.00 and 23.50 suggest identical ranks, implying that several studies shared equal frequency (Table 3).

Reported symptoms

Multiple investigations have established an elevated incidence of symptoms corresponding to the use of topical NSAIDs.

Table 4. The tabulation of symptoms reported in publications[17,18,20,22,25,40,41]

Symptoms	Reporting frequency (%)	Frequency of reporting in publications (%)	Rank of reporting frequency	Rank of frequency of reporting in publications
Pain	13.04	9.37	3.50	3.50
Photophobia	21.73	15.60	5.00	5.50
Burning sensation	34.78	15.60	6.00	5.50
Stinging	13.04	9.37	3.50	3.50
Eye irritation	8.69	6.25	1.50	1.50
Partial vision loss	8.69	6.25	1.50	1.50

In reported adverse eye symptoms, burning sensation is implied to be the most prevalent, impacting 34.78% of individuals. Subsequently, photophobia remains a profound concern for 21.73% of those affected. Both pain and stinging are specified by 13.04% of individuals, exhibiting a considerable amount of difficulty (Table 4). Burning sensation and photophobia arise as the most frequent symptoms (ranked 6.0 and 5.0, respectively) and also scored strongly concerning frequency (5.5 for both), indicating that these are the frequently occurring and described symptoms within participants, feasibly expressive of underlying ocular surface disorder or digital eye strain (Table 4).

Correlations

Table 5. Correlations between the frequency of reporting in publications and reporting frequency of reported symptoms[a]

			Frequency of reporting in publications	Reporting frequency
Spearman's rho	Frequency of reporting in publications	Correlation Coefficient	1.00	0.98**
		Sig. (2-tailed)	.	<0.001
		N	6	6
	Reporting frequency	Correlation Coefficient	0.98**	1.00
		Sig. (2-tailed)	<0.001	.
		N	6	6

a ** – correlation is significant at the 0.01 level (2-tailed)

A Spearman's rank correlation analysis portrayed a statistically significant (ρ=0.985, p<0.001) observation, proposing a compatible trend in the literature where reported symptoms also emerge to be more extensive amidst the population exposed to the drug (Table 5).

Pharmacodynamic basis of adverse effects

Post hoc tests

Table 6. Multiple comparisons (Tukey HSD) with the specific NSAID group differencesa

Dependent variable: prevalence						
Tukey HSD						
(I) Drug group	(J) Drug group	Mean difference (I-J)	Std. Error	Sig.	95% Confidence interval	
					Lower bound	Upper bound
Nonselective COX inhibitors	Preferential COX-2 inhibitors	-1.046*	.39	.023	-1.97	-0.12
	Selective COX-2 inhibitors	0.35	0.39	0.64	-0.58	1.28
Preferential COX-2 inhibitors	Nonselective COX inhibitors	1.04*	0.39	0.02	0.12	1.97
	Selective COX-2 inhibitors	1.39*	0.39	0.002	.47	2.32
Selective COX-2 inhibitors	Nonselective COX inhibitors	-0.35	0.39	0.64	-1.28	0.58
	Preferential COX-2 inhibitors	-1.39*	0.39	0.002	-2.32	-0.47

a based on observed means, the error term is mean square (error)=2.510, * – the mean difference is significant at the 0.05 level

Preferential COX-2 inhibitors exhibit a considerably greater frequency than Non-selective COX inhibitors and selective COX-2 inhibitors. Notably, preferential COX-2 inhibitors expressed a significantly greater prevalence of ADRs compared to both nonselective COX inhibitors (mean difference=1.05, p=0.023) and selective COX-2 inhibitors (mean difference=1.39, p=0.002) (Table 6).

Discussion

The reporting frequency of adverse effects identified encompasses a multitude of ocular and systemic consequences, with variable ranges observed through various studies. A greater quantity of research corresponds to a higher predominance of corneal complications such as corneal perforation (rank 33), decreased corneal sensation (rank 32), epithelial defects, and corneal melt (both rank 30). Inflammatory conditions like corneal infiltration (rank 27), keratitis, tissue loss, and eye pruritus (all rank 23.5) additionally display with significant frequency. Conversely, an assortment of less frequently reported adverse effects (all rank 11) consists epithelial wound, superficial punctate keratitis, delayed corneal wound healing, stromal thinning, reduced corneal responsiveness, lower Schirmer values, scleral melt, conjunctival injection, edematous swelling of the eyelids, periorbital dermatitis, iritis, posterior capsule opacification, iris prolapse, neurotrophic keratopathy, and shrunken eye. Remarkably, systemic observations were also incorpo-

rated in the assessment, like low concentration of breast milk, dilated ventricle, tricuspid regurgitation, pulmonary insufficiency, closure of the ductus arteriosus, prenatal ductal constriction (all rank 11), and asthma (rank 30), reflecting an expanded spectrum of feasible adverse outcomes taken into consideration in the study. The substantial positive association indicates that a greater frequency of findings is related to a higher probability of identifying and documenting these adverse consequences, particularly the more significant ocular issues. Preferential COX-2 inhibitors, particularly for topical applications, may be a "gift and a burden" in clinical administration, considering the realization that they are often conceived of as exhibiting significantly severe adverse effects as opposed to non-selective NSAIDs.

NSAIDs are progressively being formulated for topical ophthalmic administration, driven by compelling scientific evidence recommending their therapeutic potential in ophthalmic pathologies like diabetic retinopathy, age-related macular degeneration, and other ocular tumors.[51-55] Their mechanism of action essentially is based on the dominant inhibition of cyclooxygenase (COX) enzymes, crucial catalysts in the biosynthesis of eicosanoids, including prostaglandins (PGs) and thromboxanes, obtained from arachidonic acid.[52,56-58] Encased in the ocular province, PGs devote substantially to inflammatory activities by stimulating vasodilation, yielding the blood-ocular barrier, and promoting leukocyte migration.[59-63] NSAIDs' efficacy stems from their capability to conquer these pernicious PG-mediated consequences.[64] The pharmacokinetic portrait of NSAIDs, regardless of their division (salicylates, indole acetic acid derivatives, aryl acetic acid derivatives, aryl propionic acid derivatives, enolic acid derivatives, and fenamates), effectively implies admirable gastrointestinal absorption, triggering peak serum concentration within 1 to 3 hours.[64-65] An important property is their extensive plasma protein binding, ordinarily immense 95%, particularly to albumin, which restricts their capacity for distribution to plasma. This systemic absorption, even considering topically administered NSAIDs via mucosal surfaces of the nasolacrimal outflow network, enhances the significance of conceiving systemic resonances.[66-71] Nevertheless, innovative topical approaches like 0.1% nepafenac and 0.09% bromfenac illustrate ameliorated retinal probing and efficacy in impeding retinal prostaglandin formation.[65] This reinforces the continuing expansion of preparation with intensified pharmacokinetics to optimize therapeutic advantages in posterior segment pathologies. Pharmacodynamically, NSAIDs comprehensively restrain COX enzymes, hence alleviating the overactive secretion of endogenous PGs (e.g., PGE2, PGD2, PGF2a, PGI2), which are involved in miosis, vasodilation, blood-ocular barrier breakdown, leukocyte movement, and pain sensitivity within the eye. This article also demonstrates the way topical NSAIDs permeate the vitreous, particularly their increasing application for the therapy of retinal diseases.[65,72-75] The findings of this study readily demonstrate that, in contrast to simultaneous application of non-selective and selective COX-2 inhibitors, they are associated with a higher occurrence of adverse treatment outcomes. The following intricate pharmacological pattern may be a possible explanation for the observed hypersensitivity and higher frequency of complications, despite topical therapy.[64,76] Despite preferential COX-2 inhibitors concentrating on the stimulated COX-2 enzyme in inflammatory regions, a certain level of COX-1 inhibition is assumed, considering their "preferential" instead of "selective" trait.[64,78] The sensitive physiological equilibrium that COX-1 sustains may still be disrupted by this partial inhibition of intrinsically obtained COX-1, through systemic absorption employing topical application. More specifically, a disruption in the delicate balance within the production of pro-thrombotic thromboxane (primarily COX-1 facilitated) and anti-thrombotic prostacyclin (primarily COX-2 transmitted) may trigger the identified higher ADR frequency.

Study limitations

Although the topic has been extensively reviewed, the nonexistence of subgroup analyses reveals an important research space, particularly when it comes to different age groups or population-focused data that can advance clinical application with potentially different reactions and adverse consequences, and also, the majority of the included studies did not disclose comprehensive information on NSAID dosage. To have a more thorough grasp of the effects of NSAIDs, future studies should investigate dose-dependent and population-specific effects.

Conclusion

The diversified behavior and different intensity of the documented adverse effects underline the critical importance of proactive approaches to lessen ADRs in clinical activities. A comprehensive outlook to risk evaluation, attentively monitoring individual patient factors such as age, comorbidities, polypharmacy, and genetic predispositions, may increase their susceptibility to ADRs. Continuous medication reconciliation, comprising over-the-counter drugs and supplements, is appropriate to evaluate probable drug interactions. Administering the lowest effective concentration and dose for the shortest span of time is a promising option to mitigate the complications. Constant observation and follow-up for early signs and symptoms of ADRs, coupled with patient education on potential ad-

verse events, are important. As an instance, whenever reduced corneal responsiveness or lower Schirmer values are stated, close monitoring for corneal health is justified. Equivalently, comprehending the potential for systemic effects like pulmonary insufficiency or changes in neonatal circulation necessitates prudent consideration when prescribing medications to pregnant women or breastfeeding mothers. The evidence revealed indicates that in order to effectively reduce ADRs, subsequent studies must concentrate on prolonged safety profiles and tailored individualized therapy. Longitudinal studies with frequent follow-ups are essential to completely constitute the incidence, severity, and long-term effects of the reported adverse effects, particularly the less frequent but potentially harmful ones, such as neurotrophic keratopathy or the impact on the health of the infant, even though the current analysis shows associations.

Acknowledgments

We express our heartfelt gratitude to all our supporters and well-wishers for their invaluable counsel and encouragement throughout the preparation of this evaluation.

Declarations

Funding

This study did not receive any grant and/or funding.

Author contributions

Conceptualization, S.S and M.D.; Methodology, S.S.; Software, S.S.; Validation, S.S., and M.D.; Formal Analysis, M.D.; Investigation, S.S.; Resources, M.D.; Data Curation, M.D.; Writing – Original Draft Preparation, S.S.; Writing – Review & Editing, M.D.; Visualization, M.D.; Supervision, M.D.; Project Administration, S.S.; Funding Acquisition, M.D.

Conflicts of interest

The authors declare no competing interests.

Data availability

The datasets generated during and/or analyzed during the current study are available from the corresponding author on reasonable request.

Ethics approval

This article reviews existing research and does not include any investigations involving human volunteers or animals done by the authors. Consequently, ethical approval and informed consent were not required for this study.

References

1. Bettman JW. Seven hundred medicolegal cases in ophthalmology. *Ophthalmology*. 1990;97(10):1379-1384. doi:10.1016/s0161-6420(90)32406-5
2. Brick DC. Medication errors result in costly claims for ophthalmologists. *Surv Ophthalmol*. 1995;40(3):232-236. doi:10.1016/s0039-6257(95)80031-x
3. Fernandez E, Phillips E, Saeed HN. Ocular involvement in allergic drug reactions. *Curr Opin Allergy Clin Immunol*. 2023;23(5):397-408. doi:10.1097/ACI.0000000000000932
4. Dhingra D, Kaur S, Ram J. Illicit drugs: Effects on eye. *Indian J Med Res*. 2019;150(3):228-238. doi:10.4103/ijmr.IJMR_1210_17
5. Gaynes BI, Fiscella R. Topical nonsteroidal anti-inflammatory drugs for ophthalmic use: a safety review. *Drug Saf*. 2002;25(4):233-250. doi:10.2165/00002018-200225040-00002
6. World Health Organization (WHO). *Safety of medicines: adverse drug reactions-key facts*. https://www.who.int/docs/default-source/medicines/safety-of-medicines--adverse-drug-reactions-jun18.pdf?sfvrsn=4fcaf40_2. Accessed October 20, 2025.
7. Tandon VR, Mahajan V, Khajuria V, Gillani Z. Under-reporting of adverse drug reactions: a challenge for pharmacovigilance in India. *Indian J Pharmacol*. 2015;47(1):65-71. doi:10.4103/0253-7613.150344
8. Manu MS, Mehta K, Das M, et al. Ocular adverse events in drug sensitive TB patients on daily fixed dose combination anti-TB drugs: A record review study from Kerala, India. *Indian J Tuberc*. 2020;67(2):216-221. doi:10.1016/j.ijtb.2020.02.008
9. Qureshi O, Dua A. COX Inhibitors. In: StatPearls. Treasure Island (FL): StatPearls Publishing. https://www.ncbi.nlm.nih.gov/books/NBK549795/. Published February 28, 2024. Accessed December 3, 2025.
10. Shanbhag SS, Sangwan VS, Singh A, et al. Clinical Aspects of Stevens-Johnson Syndrome/Toxic Epidermal Necrolysis With Severe Ocular Complications in India. *Front Med (Lausanne)*. 2021;8:643955. doi:10.3389/fmed.2021.643955
11. Li J, Tripathi RC, Tripathi BJ. Drug-induced ocular disorders. *Drug Saf*. 2008;31(2):127-141. doi:10.2165/00002018-200831020-00003
12. Patel TK, Barvaliya MJ, Sharma D, Tripathi C. A systematic review of the drug-induced Stevens-Johnson syndrome and toxic epidermal necrolysis in Indian population. *Indian J Dermatol Venereol Leprol*. 2013;79(3):389-398. doi:10.4103/0378-6323.110749
13. Zimmerman D, Dang NH. Stevens-Johnson Syndrome (SJS) and Toxic Epidermal Necrolysis (TEN): Immunologic Reactions. *Oncologic Critical Care*. 2019;267-280. doi:10.1007/978-3-319-74588-6_195
14. Peponis V, Kyttaris VC, Chalkiadakis SE, Bonovas S, Sitaras NM. Ocular side effects of anti-rheumatic medications: what a rheumatologist should know. *Lupus*. 2010;19(6):675-682. doi:10.1177/0961203309360539
15. Rigas B, Huang W, Honkanen R. NSAID-induced corneal melt: Clinical importance, pathogenesis, and risk mitigation. *Surv Ophthalmol*. 2020;65(1):1-11. doi:10.1016/j.survophthal.2019.07.001

16. Haddaway NR, Page MJ, Pritchard CC, McGuinness LA. *PRISMA2020*: An R package and Shiny app for producing PRISMA 2020-compliant flow diagrams, with interactivity for optimised digital transparency and Open Synthesis. *Campbell Syst Rev*. 2022;18(2):e1230. doi:10.1002/cl2.1230
17. Kim SJ, Flach AJ, Jampol LM. Nonsteroidal anti-inflammatory drugs in ophthalmology. *Surv Ophthalmol*. 2010;55(2):108-133. doi:10.1016/j.survophthal.2009.07.005
18. Nichols J, Snyder RW. Topical nonsteroidal anti-inflammatory agents in ophthalmology. *Curr Opin Ophthalmol*. 1998;9(4):40-44. doi:10.1097/00055735-199808000-00007
19. Flach AJ. Corneal melts associated with topically applied nonsteroidal anti-inflammatory drugs. *Trans Am Ophthalmol Soc*. 2001;99:205-212.
20. Lin JC, Rapuano CJ, Laibson PR, Eagle RC Jr, Cohen EJ. Corneal melting associated with use of topical nonsteroidal anti-inflammatory drugs after ocular surgery. *Arch Ophthalmol*. 2000;118(8):1129-1132.
21. Guidera AC, Luchs JI, Udell IJ. Keratitis, ulceration, and perforation associated with topical nonsteroidal anti-inflammatory drugs. *Ophthalmology*. 2001;108(5):936-944. doi:10.1016/s0161-6420(00)00538-8
22. Isawi H, Dhaliwal DK. Corneal melting and perforation in Stevens Johnson syndrome following topical bromfenac use. *J Cataract Refract Surg*. 2007;33(9):1644-1646. doi:10.1016/j.jcrs.2007.04.041
23. Asai T, Nakagami T, Mochizuki M, Hata N, Tsuchiya T, Hotta Y. Three cases of corneal melting after instillation of a new nonsteroidal anti-inflammatory drug. *Cornea*. 2006;25(2):224-227. doi:10.1097/01.ico.0000177835.93130.d4
24. Jesus J, Almeida I, Soares R, Geraldes R, Chibante-Pedro J. Corneal perforation associated with the use of ketorolac tromethamine after cataract surgery. *J EuCornea*. 2020;6:1-3. doi:10.1016/j.xjec.2019.12.002
25. Murtagh P, Comer R, Fahy G. Corneal perforation in undiagnosed Sjögren's syndrome following topical NSAID and steroid drops post routine cataract extraction. *BMJ Case Rep*. 2018;2018:bcr2018225428. doi:10.1136/bcr-2018-225428
26. Congdon NG, Schein OD, von Kulajta P, Lubomski LH, Gilbert D, Katz J. Corneal complications associated with topical ophthalmic use of nonsteroidal antiinflammatory drugs. *J Cataract Refract Surg*. 2001;27(4):622-631. doi:10.1016/s0886-3350(01)00801-x
27. Mikropoulos DG, Kymionis GD, Chatzea MS, et al. Acute Corneal Melting Induced by the Concomitant Use of a Non-steroidal Anti-inflammatory Agent with an Antiseptic Eye Drop. *Ophthalmol Ther*. 2024;13(2):645-649. doi:10.1007/s40123-023-00864-0
28. Sun R, Gimbel HV. Effects of topical ketorolac and diclofenac on normal corneal sensation. *J Refract Surg*. 1997;13(2):158-161. doi:10.3928/1081-597X-19970301-12
29. Donnenfeld ED, Donnenfeld A. Global experience with Xibrom (bromfenac ophthalmic solution) 0.09%: the first twice-daily ophthalmic nonsteroidal anti-inflammatory drug. *Int Ophthalmol Clin*. 2006;46(4):21-40. doi:10.1097/01.iio.0000212134.83513.11
30. Fossati G, Bartoli E, Montericcio A, et al. Neurotrophic Keratopathy after wide retinal endolaser and postoperative Ketorolac eye drops: A case series. *Eur J Ophthalmol*. 2024;34(3):NP18-NP21. doi:10.1177/11206721241228005
31. Aragona P, Stilo A, Ferreri F, Mobrici M. Effects of the topical treatment with NSAIDs on corneal sensitivity and ocular surface of Sjögren's syndrome patients. *Eye (Lond)*. 2005;19(5):535-539. doi:10.1038/sj.eye.6701537
32. Aragona P, Tripodi G, Spinella R, Laganà E, Ferreri G. The effects of the topical administration of non-steroidal anti-inflammatory drugs on corneal epithelium and corneal sensitivity in normal subjects. *Eye (Lond)*. 2000;14(Pt 2):206-210. doi:10.1038/eye.2000.55
33. Seitz B, Sorken K, LaBree LD, Garbus JJ, McDonnell PJ. Corneal sensitivity and burning sensation. Comparing topical ketorolac and diclofenac. *Arch Ophthalmol*. 1996;114(8):921-924. doi:10.1001/archopht.1996.01100140129002
34. Szerenyi K, Sorken K, Garbus JJ, Lee M, McDonnell PJ. Decrease in normal human corneal sensitivity with topical diclofenac sodium. *Am J Ophthalmol*. 1994;118(3):312-315. doi:10.1016/s0002-9394(14)72954-x
35. Acosta MC, Berenguer-Ruiz L, García-Gálvez A, et al. Changes in corneal sensitivity after topical NSAIDs. *Invest Ophthalmol Vis Sci*. 2005;46(1):282. doi:10.1167/iovs.04-0884
36. Shimazaki J, Saito H, Yang HY, Toda I, Fujishima H, Tsubota K. Persistent epithelial defect following penetrating keratoplasty: an adverse effect of diclofenac eyedrops. *Cornea*. 1995;14(6):623-627.
37. Hsu JK, Johnston WT, Read RW, et al. Histopathology of corneal melting associated with diclofenac use after refractive surgery. *J Cataract Refract Surg*. 2003;29(2):250-256. doi:10.1016/s0886-3350(02)01702-9
38. Tomas-Barberan S, Fagerholm P. Influence of topical treatment on epithelial wound healing and pain in the early postoperative period following photorefractive keratectomy. *Acta Ophthalmol Scand*. 1999;77(2):135-138. doi:10.1034/j.1600-0420.1999.770203.x
39. Assouline M, Renard G, Arne JL, et al. A prospective randomized trial of topical soluble 0.1% indomethacin versus 0.1% diclofenac versus placebo for the control of pain following excimer laser photorefractive keratectomy. *Ophthalmic Surg Lasers*. 1998;29(5):365-374.
40. Chen X, Gallar J, Belmonte C. Reduction by antiinflammatory drugs of the response of corneal sensory nerve fibers to chemical irritation. *Invest Ophthalmol Vis Sci*. 1997;38(10):1944-1953.
41. Rodríguez NA, Abarzuza R, Cristóbal JA, Sierra J, Mínguez E, Del Buey MA. Eyelid contact allergic eczema

caused by topical ketorolac tromethamine 0.5%. *Arch Soc Esp Oftalmol*. 2006;81(4):213-216. doi:10.4321/s0365-66912006000400007

42. Rajpal RK, Ross B, Rajpal SD, Hoang K. Bromfenac ophthalmic solution for the treatment of postoperative ocular pain and inflammation: safety, efficacy, and patient adherence. *Patient Prefer Adherence*. 2014;8:925-931. doi:10.2147/PPA.S46667
43. Demarinis G, Tatti F, Taloni A, et al. Treatments for Ocular Diseases in Pregnancy and Breastfeeding: A Narrative Review. *Pharmaceuticals (Basel)*. 2023;16(10):1433. doi:10.3390/ph16101433
44. Auer M, Brezinka C, Eller P, Luze K, Schweigmann U, Schwärzler P. Prenatal diagnosis of intrauterine premature closure of the ductus arteriosus following maternal diclofenac application. *Ultrasound Obstet Gynecol*. 2004;23(5):513-516. doi:10.1002/uog.1038
45. Sitenga GL, Ing EB, Van Dellen RG, Younge BR, Leavitt JA. Asthma caused by topical application of ketorolac. *Ophthalmology*. 1996;103(6):890-892. doi:10.1016/s0161-6420(96)30591-5
46. Sharir M. Exacerbation of asthma by topical diclofenac. *Arch Ophthalmol*. 1997;115(2):294-295. doi:10.1001/archopht.1997.01100150296037
47. Polachek J, Shvartzman P. Acute bronchial asthma associated with the administration of ophthalmic indomethacin. *Isr J Med Sci*. 1996;32(11):1107-1109.
48. Sheehan GJ, Kutzner MR, Chin WD. Acute asthma attack due to ophthalmic indomethacin. *Ann Intern Med*. 1989;111(4):337-338. doi:10.7326/0003-4819-111-4-337
49. Donnenfeld ED, Holland EJ, Stewart RH, et al. Bromfenac ophthalmic solution 0.09% for postoperative ocular pain and inflammation. *Ophthalmology*. 2007;114(9):1653-1662.e1.
50. Wright JM. The double-edged sword of COX-2 selective NSAIDs. *CMAJ*. 2002;167(10):1131-1137.
51. Agrahari V, Mandal A, Agrahari V, et al. A comprehensive insight on ocular pharmacokinetics. *Drug Deliv Transl Res*. 2016;6(6):735-754. doi:10.1007/s13346-016-0339-2
52. Ahmed S, Amin MM, Sayed S. Ocular Drug Delivery: a Comprehensive Review. *AAPS PharmSciTech*. 2023;24(2):66. doi:10.1208/s12249-023-02516-9
53. Jitendra SP, Banik A, Dixit S. Ocular drug delivery system: a new trend. *PharmaSci Monit*. 2011;2:1-25.
54. Worakul N, Robinson JR. Ocular pharmacokinetics/pharmacodynamics. *Eur J Pharm Biopharm*. 1997;44(1):71-83. doi:10.1016/S0939-6411(97)00064-7
55. Urtti A. Challenges and obstacles of ocular pharmacokinetics and drug delivery. *Adv Drug Deliv Rev*. 2006;58(11):1131-1135. doi:10.1016/j.addr.2006.07.027
56. Farkouh A, Frigo P, Czejka M. Systemic side effects of eye drops: a pharmacokinetic perspective. *Clin Ophthalmol*. 2016;10:2433-2441. doi:10.2147/OPTH.S118409
57. Marino M, Jamal Z, Zito PM. Pharmacodynamics. In: StatPearls. Treasure Island (FL): StatPearls Publishing. https://www.ncbi.nlm.nih.gov/books/NBK507791/. Published January 29, 2023. Accessed December 3, 2025.
58. Park Y, Ellis D, Mueller B, Stankowska D, Yorio T. Principles of Ocular Pharmacology. *Handb Exp Pharmacol*. 2017;242:3-30. doi:10.1007/164_2016_25
59. Novack GD, Robin AL. Ocular Pharmacology. *J Clin Pharmacol*. 2024;64(9):1068-1082. doi:10.1002/jcph.2451
60. Gaudana R, Ananthula HK, Parenky A, Mitra AK. Ocular drug delivery. *AAPS J*. 2010;12(3):348-360. doi:10.1208/s12248-010-9183-3
61. Foster CS. The pathophysiology of ocular allergy: current thinking. *Allergy*. 1995;50(21):6-38. doi:10.1111/j.1398-9995.1995.tb04250.x
62. Solomon A, Pe'er J, Levi-Schaffer F. Advances in ocular allergy: basic mechanisms, clinical patterns and new therapies. *Curr Opin Allergy Clin Immunol*. 2001;1(5):477-482. doi:10.1097/01.all.0000011063.28808.cc
63. Baudouin C. Allergic reaction to topical eyedrops. *Curr Opin Allergy Clin Immunol*. 2005;5(5):459-463. doi:10.1097/01.all.0000183112.86181.9e
64. Russo A, Costagliola C, Delcassi L, et al. Topical nonsteroidal anti-inflammatory drugs for macular edema. *Mediators Inflamm*. 2013;2013:476525. doi:10.1155/2013/476525
65. Ahuja M, Dhake AS, Sharma SK, Majumdar DK. Topical ocular delivery of NSAIDs. *AAPS J*. 2008;10(2):229-241. doi:10.1208/s12248-008-9024-9.
66. Tripathy KD. *Essentials of Medical Pharmacology*. 8th ed. New Delhi: The Health Science Publisher; 2019.
67. Carreño E, Portero A, Galarreta DJ, Herreras JM. Update on twice-daily bromfenac sodium sesquihydrate to treat postoperative ocular inflammation following cataract extraction. *Clin Ophthalmol*. 2012;6:637-644. doi:10.2147/OPTH.S23381
68. Dwivedi AK, Gurjar V, Kumar S, Singh N. Molecular basis for nonspecificity of nonsteroidal anti-inflammatory drugs (NSAIDs). *Drug Discov Today*. 2015;20(7):863-873. doi:10.1016/j.drudis.2015.03.004
69. Heier J, Cheetham JK, Degryse R, et al. Ketorolac tromethamine 0.5% ophthalmic solution in the treatment of moderate to severe ocular inflammation after cataract surgery: a randomized, vehicle-controlled clinical trial. *Am J Ophthalmol*. 1999;127(3):253-259. doi:10.1016/s0002-9394(98)00413-9
70. Mahmoodi AN, Kim PY. *Ketorolac*. In: StatPearls. StatPearls Publishing. https://www.ncbi.nlm.nih.gov/books/NBK545172/. Published 2022. Accessed Decembre 3, 2025.
71. Markham A, Faulds D. Ganciclovir. An update of its therapeutic use in cytomegalovirus infection. *Drugs*. 1994;48(3):455-484. doi:10.2165/00003495-199448030-00009
72. Gupta SK, Velpandian T, Mathur P, Sengupta S. Comparative analgesic activity of nimesulide and diclofenac by intramuscular route: correlation with pharmacokinetic profile of nimesulide. *Pharmacology*. 1998;56(3):137-143. doi:10.1159/000028191

73. Cohen B, Preuss CV. *Collectible*. In: StatPearls. StatPearls Publishing. https://www.ijbls.org/images/IJBLS_2_2023_Full_issue_with_bookmarks.pdf. Published 2024. Accessed Decembre 3, 2025.
74. Botting RM. Mechanism of action of acetaminophen: is there a cyclooxygenase 3?. *Clin Infect Dis*. 2000;31(5):S202--S210. doi:10.1086/317520
75. Gerrett D. Pharmacology. In: *Clinical Skills in Treating the Foot*. 2nd ed. Turner W, Merriman LM, ed. Churchill Livingstone: Elsevier; 2005:161-191.
76. de Ladoucette A. Management of perioperative pain after TKA. *Orthop Traumatol Surg Res*. 2023;109(1S):103443. doi:10.1016/j.otsr.2022.103443
77. Chawla J, Le Guern ME, Alquier C, Kalhorn TF, Levy RH. Effect of route of administration on the pharmacokinetic behavior of enantiomers of nefopam and desmethylnefopam. *Ther Drug Monit*. 2003;25(2):203-210. doi:10.1097/00007691-200304000-00010
78. Pillans PI, Woods DJ. Adverse reactions associated with nefopam. *N Z Med J*. 1995;108(1008):382-384.

Rzeszów University Press 2026
ISSN 2544-1361 (online)
doi: 10.15584/ejcem.2026.1.3

http://www.ejcem.ur.edu.pl
European Journal of Clinical and Experimental Medicine
Eur J Clin Exp Med 2026; 24 (1): 201–209

CASE REPORTS

From diagnosis to therapy – mixed hyperkinetic-hypokinetic dysarthria – a comprehensive case study

Isha Wosti

Audiology and Speech Language Pathology, BASLP Audiology Officer, Pokhara Academy of Health Sciences, Pokhara, Nepal

ABSTRACT

Introduction and aim. Progressive dysarthria and dysphagia pose substantial diagnostic and therapeutic challenges. This case report aims to describe the assessment and intensive structured management of a patient with chronic, functionally limiting dysarthria and dysphagia.

Description of the case. The patient was a 38-year-old male with neuroacanthocytosis syndrome. Dysarthria diagnosis was established through auditory-perceptual profiling and acoustic analysis, confirming a mixed hyperkinetic-hypokinetic pattern. Clinical bedside evaluation of swallowing was done, which revealed severe oral dysphagia. Speech therapy was conducted using the hierarchy of motor speech treatment, targeting various motor speech bases. Additionally, severe oral phase dysphagia was managed using rehabilitative, compensatory, and modified diet approaches.

Results. Improvements were noted across all motor speech bases, supported by subjective reports and objective data. The patient's self-reported measures, as well as the improvement in voice quality (AVQI score decreased from 4 to 2.95), improved intelligibility (from 30 to 75%), and decreased speech rate (4.36 to 2.53 syllables/second) showed substantial improvement in dysarthria. Similarly, safe swallowing was achieved at IDDSI Levels 4–6 with compensatory strategies.

Conclusion. This case illustrates that even rare and chronic forms of dysarthria can respond positively to structured, intensive speech-language therapy, underscoring the importance of individualized, comprehensive intervention approaches.

Keywords. dysphagia, mixed dysarthria, movement disorder, neuroacanthocytosis, progressive dysarthria, speech therapy

Introduction

Dysarthria and dysphagia frequently occur in progressive neurological disorders, including amyotrophic lateral sclerosis, multiple sclerosis, myasthenia gravis, and Parkinson's disease (PD).[1,2] Dysarthria is a collective name for a group of neurologic speech disorders that reflect abnormalities in the strength, speed, range, steadiness, tone, or accuracy of movements required for the breathing, phonatory, resonatory, articulatory, or prosodic aspects of speech production.[3] On the other hand, dysphagia is difficulty in swallowing, characterized by an abnormal delay in the transit of liquid or solid bolus from the oral cavity to the stomach.[4] Since dysarthria is marked by impaired voluntary oromotor control, it frequently co-occurs with dysphagia.[5] While the incidence of dysarthria varies in different neurological conditions, some degenerative conditions have an incidence of up to 90%.[6]

This case report aims to describe the comprehensive assessment and speech therapy intervention for a patient with chronic progressive dysarthria and dysphagia secondary to neuroacanthocytosis (NA) syndrome, a rare neurological disorder.. NA syndromes represent a group of rare, genetically distinct disorders marked by the presence of red blood cell acanthocytosis and progressive

Corresponding author: Isha Wosti, e-mail: ishawosti@gmail.com, isha.764402@mmc.tu.edu.np

Received: 4.06.2025 / Revised: 24.07.2025 / Accepted: 19.08.2025 / Published: 30.03.2026

Wosti I. From diagnosis to therapy – mixed hyperkinetic-hypokinetic dysarthria – a comprehensive case study. *Eur J Clin Exp Med.* 2026;24(1):201–209. doi: 10.15584/ejcem.2026.1.3.

basal ganglia degeneration.[7] NA presents with a diverse range of symptoms, including both hyperkinetic movement disorders such as chorea, dystonia, and tics, and hypokinetic features like Parkinsonism. NA syndromes are categorized into core forms and other related disorders.[8] Each subtype has an estimated prevalence of fewer than 1 to 5 cases per million individuals.[9] Speech and swallowing impairments are consistently observed in these disorders and result from the progressive deterioration of motor control.[10] The patient in this study has a diagnosis of NA syndrome, and not a subtype, given the clinical phenotype and MRI findings, in the absence of conclusive genetic results of the particular subtype at this stage.

The unpredictable and relentlessly progressive nature of the underlying movement disorder leads to a gradual decline in communication and swallowing abilities and increased social isolation. This experience is unique for each individual and family. A multidimensional clinical protocol that integrates both clinician-reported measures and patient-reported outcomes is essential in comprehensive dysarthria assessment and management.[11] Such a protocol helps select the diagnostic tools and determine the timing of interventions, including the implementation of augmentative and alternative communication.[12]

In regards to management, clinical decision-making in the progressive conditions warrants the sequencing or staging of interventions so that current problems can be addressed and future problems anticipated.[2] However, evidence-based management practices for dysarthria are still limited[13], and Speech-Language Pathologists (SLPs) are found to employ inconsistent and varied treatment techniques.[14,15] Furthermore, the efficacy of speech therapy in progressive dysarthria remains debated, as some studies report limited or inconsistent evidence for long-term speech improvements in neurodegenerative conditions[16–18], citing disease progression as a limiting factor. However, there are reports of contrasting evidence in the study of PD and related syndromes, which show that intensive behavioral interventions can mitigate motor speech decline.[19]

Aim

This case contributes to this discourse by examining the outcomes of intensive behavioral speech therapy in a case with progressive dysarthria and dysphagia.

Description of the case

This case report adheres to the ethical principles of the Declaration of Helsinki.[20] Ethical approval was not required due to the descriptive nature of the report; however, informed written consent for publication of anonymized clinical information was obtained from the patient and his family. The patient is a 38-year-old male. He presented to the Speech-Language Pathology Unit of Tribhuvan University Teaching hospital (TUTH) with clinical indications of imbalanced walking, and gross involuntary choreiform movement of the hand and leg, unclear speech, muscle atrophy, difficulty swallowing and chewing, drooling, weight loss, for 5 years. The problem had an episodic onset and was aggravated by anxiety. There was no significant family history of neurological or psychiatric disorders, head injury, or exposure to neurotoxins. He reported no issues with memory and language, and no family history of the disorder.

We utilized the International Classification of Functioning, Disability, and Health (ICF)[21] framework to understand the holistic impact of the condition. The involuntary movements of the trunk made it difficult to engage in activities of daily living. He lost his job at the bank, which was his sole source of income. He had been separated from his parents at a young age and was no longer on good terms with them. His pregnant wife was his sole caretaker. He had difficulty masticating, could no longer enjoy mealtimes, and had significant weight loss throughout the symptom progression. His disorder had isolated him from his friend circle, as he was no longer able to travel alone (Table 1).

Timeline

Table 1. Timeline of events

2015–2016	Onset of symptoms: episodic involuntary mouth movements, drooling, and sleep disturbances.
11/03/2019	First neurological consultation at a tertiary care hospital in Nepal; differential diagnoses included Tourette's syndrome and NA syndrome.
Mid-2019	Referred to an international referral center in Delhi, India, for further evaluation.
	Peripheral smear showed normocytic normochromic red blood cells with acanthocytosis
2023	Magnetic resonance imaging of the brain showed bilateral caudate atrophy, enlarged frontal horns of lateral ventricles, and T2 hyperintensities in the putamina. Nerve conduction velocity test indicated bilateral peroneal pure motor axonal loss. Electromyography revealed a neurogenic pattern. Huntington's disease was ruled out via genetic testing. Whole Exome Sequencing one genetic variant of uncertain significance in the optineurin gene. Uncertain diagnosis of amyotrophic lateral sclerosis 12.
Current	Patient is under pharmacological management with Revocon 25 mg, Bexol 2 mg, and Serenace 0.5 mg. The patient was relieved of duties from his previous position at a bank.

Diagnostic Assessment

Colorado Motor Speech Framework (CMSF)

CMSF was used for structured, subsystem-based assessment of the patient's motor speech profile.[22] Recorded speech samples of sustained vowel, reading, and conversational speech were used for perceptual analysis. 16 characteristics that correspond to hypokinetic dysarthria and 8 characteristics that correspond to hyperkinetic dysarthria were observed; thus, he was diagnosed to have hypokinetic-hyperkinetic mixed dysarthria. Subsequent therapy planning was conducted based on CMSF findings.

Articulation assessment

Done using Photo Articulation Test-3.[23] Findings revealed hypernasality in stop sounds, and deaffrication of affricates.

Voice assessment

Voice assessment was conducted using a voice proforma involving a detailed history, aerodynamic, and acoustic analysis. The perceptual voice analysis was done using the grade, roughness, breathiness, asthenia, strain (G1 R1 B0 A0 S1) rating scale.[24] Rapid fluttering tremor was intermittently present on vowel prolongation, and Maximum Phonation Duration (MPD) was reduced – 5 seconds. Acoustic analysis was done using PRAAT software version 6.4.34. Acoustic Voice Quality Index (AVQI) v.03.01[25] was used to objectively quantify the voice quality, which incorporates multiple parameters including shimmer, jitter, harmonic-to-noise ratio (HNR), cepstral peak prominence (CPP), and formant-based measures. The speech samples used were a vowel prolongation /a/ and a reading sample of a 100-syllable passage. Recording was done using a smartphone microphone (Infinix Hot 10s) placed at 10 cm distance from the patient's mouth. The recording was done in a sound-treated room. An AVQI score of 4 was obtained (Table 2, Fig. 1).

Table 2. Dysarthria assessment findings (AVQI – acoustic voice quality index, DDK – diadochokinetic rate)

Speech characteristics	Fast rate of speech
	Variable rate of speech
	Stutter-like dysfluencies
	Monoloudness
	Loudness decay
	Maximum phonation time: 5 seconds
	Telescoping
	Hypernasality
	Irregular rhythm in DDK
	Rapid vocal flutter
	Reduced stress
	Atypical silences
	Imprecise consonants
	Fast rate of speech
	Variable rate of speech
AVQI	4.00
Speech Rate	4.36 syllable/second
GRBAS	G1R1B0A0S1
Speech intelligibility	30%

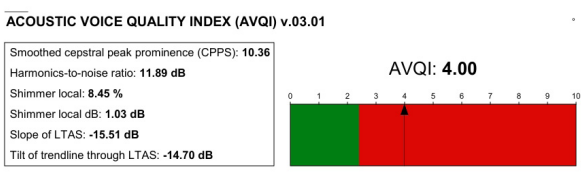

Fig. 1. Pre-Therapy AVQI analysis report

Speech intelligibility assessment

The patient was asked to read a passage in his native language to elicit the speech sample. The reading was audio-recorded in a quiet environment. To assess intelligibility, a blinded transcription task was carried out by an SLP who was unfamiliar with both the patient and the reading passage. Percentage intelligibility was calculated based on the number of intelligible words. Intelligibility was found to be 30%.

Speech rate

The rate of speech was calculated from the recorded speech sample. Speech rate was determined by dividing the total number of syllables spoken by the overall duration of the sample, including all pauses, and was expressed in syllables per second. The rate was 4.36 syllables/ second (81.6 words per minute).

Language assessment

Language assessment was done using the Frenchay Aphasia Screening test (FAST) to screen for aphasia, and the findings were normal.[26]

Cognitive-Communication assessment

The Montreal Cognitive Assessment (MoCA) test was administered for cognitive assessment, and the findings were normal with a score of 26.[27] The test was completed in 15 minutes.

Evaluation of swallowing function

A clinical non-instrumental evaluation of swallowing was performed. We followed the Comprehensive Assessment Protocol for Swallowing (CAPS) protocol.[28] Swallowing evaluation was done under the supervision of an SLT trained in dysphagia.

The patient was diagnosed with severe oral phase dysphagia. While hyolaryngeal elevation and airway protection were intact, the primary difficulties stemmed from impaired oral bolus control due to jaw dystonia, poor labial seal, and reduced tongue movement for bolus transit, limiting the safe and efficient oral intake to the International Dysphagia Diet Standardization Initiative (IDDSI) levels 4–6 (Table 3).[29]

Therapeutic intervention

In terms of management, speech therapy was done to establish intelligible communication skills across various communicative contexts relevant to the patient. Based on the findings from the initial assessment, therapeutic objectives were established for the rehabilitation of the five motor bases for speech, following the hierarchy of speech-motor treatment. This hierarchy includes prioritizing the recovery of breathing, resonance, prosody, phonation, and articulation, respectively.

Table 3. Swallowing evaluation findings using CAPS

Phase	Tasks	Clinical observations
Pre-testing	IDDSI levels trialed: 0 (water), 1 (thin milkshake), 2 (biscuit with water), 5 (pudding), 6 (banana), 8 (rice)	Determined safest bolus amounts for various IDDSI Levels: Level 0, 1, 2–5 ml (1 tsp) Level 3, 4–10 ml Level 5–≤5 mL or ½ tsp bite size Level 6–<15 mm^3 piece Levels 7 and 8 contraindicated due to poor chewing ability.
Dry swallowing	Asked to swallow saliva	Poor secretion management. Excessive drooling and compensatory lip smacking. proper, timely hyolaryngeal excursion.
Non-swallowing	Patient asked to clear throat, yawn, sniff, cough, hum, and pronounce vowels	A good, strong cough and throat clearing indicate an intact airway protection mechanism.
Wet swallowing	IDDSI levels trialed: 0 (water), 1 (thin milkshake), 2 (biscuit with water), 5 (pudding), 6 (banana),	Oral phase: Anterior spillage noted in levels 0-3 due to inadequate lip seal. The patient smacked his lips several times to prevent liquid from spilling. Level 4 – difficulty in oral transit of food to the back of the mouth due to reduced tongue Levels 5, 6 – inefficient chewing was noted. Jaw dystonia was present with extreme difficulty in closing the jaw once opened. He could not manage lateral jaw movement during chewing and used a munching pattern. Pharyngeal phase – normal hyolaryngeal excursion and timing. No signs of aspiration were noted. Thus, the patient was diagnosed with severe oral phase dysphagia. He had choking risks due to oral inefficiency

Table 4. Management of dysarthria

Target	Therapy goals	Techniques	Frequency and duration	Therapist involvement	Home practice
Respiration	To increase respiratory support and relax laryngeal muscles	1) Abdominal Diaphragmatic breathing 2) Correct posture 3) Cueing for complete inhalation and speaking immediately on exhalation	45 minutes per session, 6 sessions	Direct instruction, Modeling, Feedback	Abdominal breathing + counting aloud 30 minutes per day.
Resonance	To reduce nasal air emission on non-nasal stop sounds.	1) Decreasing the rate of speech 2) Open mouth posture during speech 3) Increasing loudness	45 minutes per session, 6 sessions	Feedback, Self-monitoring	Self-monitoring hypernasality while reading.
Phonation and Prosody	1) To reduce vocal tremor and promote easy phonation. 2) To vary pitch, loudness, and duration of speech to convey emotion, emphasis, and linguistic information.	1) Yawn-sigh 2) Easy onset phonation 3) Forward focus 4) Pitch range exercises 5) Contrastive stress drills	45 minutes per session, 6 sessions	Direct instruction, Modeling, Feedback, self-monitoring	Reading different sentence types and controlled conversations with wife.
Articulation	To improve articulatory precision and intelligibility of speech.	1) Intelligibility drills 2) Hand-tapping, rhythmic cueing 3) Minimal contrast drills	45 minutes per session, 6 sessions	Direct instruction, Modeling, Feedback	Intelligibility drills with difficult-to-pronounce words.

One-hour therapy sessions were conducted daily over a four-week period. Each session comprised 45 minutes focused on the targeted motor speech base, followed by 15 minutes of swallowing exercises. In addition, the patient was tasked with daily articulation exercises to be done at least 30 minutes at home each day. The exercises included intelligibility drills with a list of difficult-to-pronounce words and daily conversation in a controlled situation with a family member to generalize the articulatory gains to conversations (Table 4).

Dysphagia was managed side-by-side with speech therapy. A combination of rehabilitative and compensatory approaches was used for the management of dysphagia. SLP discussed tube feeding options with the patient, providing insight into the disease prognosis. Patient and family denied tube feeding, so a careful hand-feeding plan ensuring good nutrition intake was made. After consulting with the dietician, a feeding protocol was prepared that included a fully nutritional, pureed mixture for the patient. The mixture was to be orally fed to the patient every 2 hours to maintain bodily intake (Table 5).

Table 5. Management of dysphagia

Approach for therapy	Techniques and exercises
Rehabilitative approach	Exercises for oral structures: labial exercise- labial press, which entails holding a tongue depressor between the lips to improve the anterior seal. – Rapid labial opening and closing using the consonants /p, b/ Lingual exercises- with resistance which entails pushing the tongue out, up, and to each side against a tongue depressor. – Use the phonemes /t, d/ for rapid contact and release of the tongue tip to the alveolar ridge. Base-of-tongue exercises – yawning, simulating gargling, and pulling the tongue straight back in the mouth. Jaw opening against resistance – to increase the strength of the jaw Range of motion exercise for the jaw against resistance – chewing exercise using chewy tubes.
Compensatory approach	Postural techniques: Head extension – for more efficient oral transit.
Modified diet texture	A diet consisting of IDDSI levels – 4, 5, and 6 [29] was recommended for the patient considering the limited range of motion and strength of jaw for chewing.

Follow-up and outcomes

Re-evaluation of the objective as well as the subjective measures done after 4 weeks showed improvements across all motor speech bases. While there are no normative values for AVQI in the Nepali population, the decrease in AVQI score from 4 to 2.95 suggests significant improvement in voice quality. The decreased speech rate suggest increased control of articulatory movements and better coordination of the respiratory and phonatory systems. This improved the overall intelligibility. The patient had improved safety and efficacy of swallowing and better nutritional intake (Tables 6–8, Fig. 2 and 3).

Table 6. Patient self-reported outcome using the Colorado Motor Speech Framework after 4 weeks of therapy

Measure	Task	Score	
		Pre-therapy	Post-therapy
Self-Report	Ask the patient: "On a scale of 1-7, 1 being the worst and 7 being the best, how would you rate your speech right now?"	2/7	5/7
Intelligibility	Judge during running speech tasks. Estimate of the percentage of words correctly understood.	58%	80%
Naturalness	Judge during running speech how well speech matches normal stands of rate, pitch, and loudness.	Severe	Moderate
Efficiency	Judge during running speech tasks for how efficient message is conveyed (e.g., is it effortful? Slow?)	Severe	Mild

Table 7. Speech characteristics and objective outcomes of dysarthria management after 4 weeks of therapy. (AVQI – acoustic voice quality index, DDK – diadochokinetic rate)

	Pre-therapy	Post-therapy
Speech characteristics	Fast rate of speech	Slowed speech rate
	Variable rate of speech	uniform rate
	Stutter-like dysfluencies	Absent
	Monoloudness	Improved prosody
	Loudness decay	Absent
	Maximum phonation time: 5 seconds	Maximum Phonation time: 10 seconds
	Telescoping	Absent, Open mouth, over-articulation present
	Hypernasality	Reduced
	Irregular rhythm in DDK	Reduced rate, but uniform
	Rapid vocal flutter	Reduced
	Reduced stress	Better stress on stressed syllables
	Atypical silences	Natural speech phrasing
	Imprecise consonants	Improved articulatory precision
	Fast rate of speech	Slowed speech rate
	Variable rate of speech	Uniform rate
AVQI	4.00	2.95
Speech Rate	4.36 syllable/ second	2.53 syllable/second
GRBAS	G1R1B0A0S1	G0R0B0A0S0
Speech intelligibility	30%	75%

Table 8. Outcomes of dysphagia management

	Pre therapy	Post therapy
Nutrition intake	inadequate, severe weight loss	well-balanced nutrition
Diet consistency	tried all consistencies, risk of choking due to impaired chewing. limited success in oral transit	IDDSI levels 4, 5, 6 are recommended to be used with head extension posture to support oral transit
Lip seal	impaired, excessive drooling	better lip seal, decreased drooling
Chewing	jaw dystonia, extreme difficulty in chewing	no significant improvement

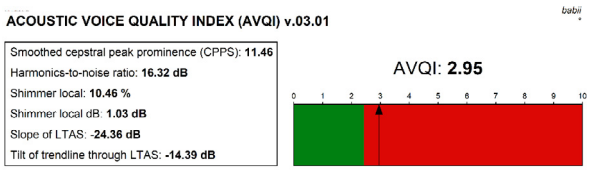

Fig. 2. Post-therapy AVQI analysis report – note the improvement in AVQI score, Smoothed Cepstral Peak Prominence, and Harmonics to Noise ratio compared to Fig. 1

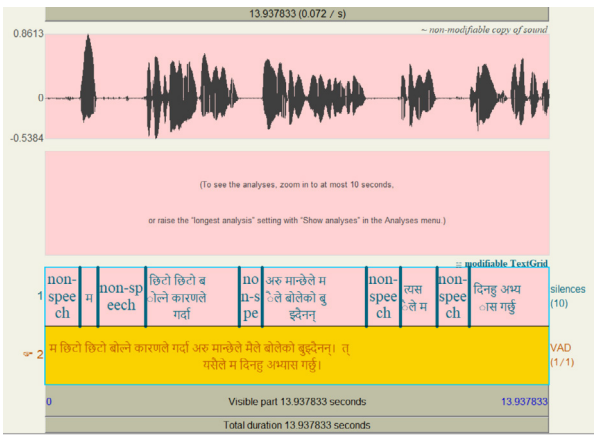

Fig. 3. Praat waveform with Textgrid annotation showing speech and non-speech segments in connected speech. This illustrates natural speech phrasing and prosody post-therapy (English translation: "People don't understand what I say because I speak very fast. So, I practice every day")

Discussion

There are a few case reports published on hyper-hypokinetic mixed dysarthria and no study on dysarthria and dysphagia management in NA syndrome to the best of our knowledge.[30] The findings in this study suggest that effective behavioral intervention can moderate the pace of functional and neurophysiological decline, even in progressive conditions.[31] We conducted a comprehensive set of objective and subjective evaluations, which included both descriptive and quantitative tests, that played a crucial role in reaching a diagnostic conclusion.[32] Specifically, characteristics such as rapid rushes of speech, inappropriate silences, variable speech rate, intermittent hypernasality, inaccuracies in consonants, and reduced speech intelligibility collectively delineate a perceptual and physiological profile consistent with mixed hyperkinetic-hypokinetic dysarthria.[33] Furthermore, we gained insight into the impact of the disorder on his daily functioning and participation using the ICF framework, and planned treatment best suited for the patient, and also approved by the patient.[2] The goal of any intervention is to change how the condition progresses over time.[34] In our case, where there was an ongoing decline in motor and potentially future cognitive functions, the aim was not restoration of function but to slow the rate of functional deterioration, preserve the remaining abilities, and support communication

through adaptive strategies.[10] We designed the therapy around specific, realistic, and functional goals, with a focus on maintaining the patient's communicative abilities through consistent and targeted activities.

Motor-based treatment, which aligns with the principle of neural plasticity, was selected for the patient. Initially, rehabilitation focused on enhancing breathing to establish strength, control, and respiratory support for speech. The coordination of respiratory function with speech production is crucial for achieving adequate loudness and speech phrasing. Therefore, treatment approaches that effectively target impaired or weakened respiratory drive and its coordination with speech production were employed.[35,36]

Progressing from breathing adjustments, attention was then directed toward addressing other motor bases of speech like resonance, phonation, articulation, and prosody. The phonatory and respiratory coordination improvement is shown by the reduced AVQI score. While there are no AVQI norms for the Nepali language, we used the same reading material to compare pre- and post-therapy measures.

One of the goals in therapy was to make speech more natural to compensate for intelligibility.[37] Speech therapy targeting a decrease in speech rate has been shown to improve speech intelligibility significantly in patients with hypokinetic dysarthria.[38] The patient's speech rate before therapy was 81.6 wpm, which is well below the normal speech rate, but it is perceived to be too fast because it is beyond the patient's neuromuscular control.[39] To reduce speech rate, we introduced a rigid rate reduction technique- hand tapping. However, hand tapping was difficult for the patient due to chorea. The metronome was used, set to a target speech rate of 46 wpm. After 3 sessions of metronome-induced slowed rate in reading and structured conversations, rhythmic cueing was used where the clinician guided natural speech pauses and phrasing in reading, followed by structured conversations. This allowed for more natural prosody, which again contributes to speech intelligibility.[40] The speech rate at the end of therapy was 64.61 words per minute, with appropriate speech phrasing.

All the therapy sessions were structured based on motor learning principles.[41] Each motor target was introduced with increasing complexity over time. During the initial three sessions, blocked and constant practice was used to support the learning of new skills. In later sessions, the approach shifted to random and variable practice to promote retention and generalization.[42] Similarly, feedback strategies evolved throughout the program. Early sessions involved frequent, knowledge of performance feedback, while later sessions incorporated less frequent, knowledge of results feedback to encourage independent monitoring. The clinician gradually reduced cueing to foster the patient's ability to engage in self-evaluation and internal feedback. A range of feedback methods was used, including auditory and visual modeling as well as phonetic placement cues.

For the swallowing assessment, we followed the CAPS protocol as it provides a structured, non-instrumental method to evaluate swallowing safety and efficiency. Instrumental evaluation could not be done due to a lack of services in the hospital. While it has limitations, clinical bedside evaluation remains a key component in assessing patients with dysphagia.[43,44] It is commonly used to identify the presence and severity of swallowing difficulties and to guide the development of appropriate rehabilitation strategies.[45] Our findings revealed the patient had severe oral dysphagia, with a normal pharyngeal phase of swallow. He had extreme difficulty in chewing secondary to jaw dystonia. Jaw dystonia, specifically precipitated by eating, is a characteristic feature of neuroacanthocytosis.[46] Our goals in dysphagia were to promote safe swallowing and improve nutritional status. It has been suggested that alternative means of nutrition, such as a feeding tube, should be considered early in NA, in light of the significant risk of aspiration and the characteristic marked weight loss.[10] The patient and family denied alternative feeding options, so we used a combination of rehabilitative and compensatory approaches.[47] Labial, lingual, and jaw-strengthening exercises were used to create changes in the patient's swallowing over time by improving the underlying physiological function. Lingual exercises have been shown to increase lingual strength and improve their role in swallowing function.[48] Studies report aspiration as a major risk in NA, as patients adopt dramatic maneuvers to swallow food, such as extending the head and throwing food into the back of the throat.[10] So, we worked on safe feeding strategies and consistencies. The patient and his wife were also given extensive information on monitoring the symptoms of aspiration and regular follow-up visits.

The head extension compensatory technique was used for efficient oral transit, but it reportedly does not create lasting functional change.[49] This chin-up posture may enhance oral bolus transport, as suggested by prior studies.[49] Additionally, this posture could potentially have a rehabilitative effect on pharyngeal swallow.[50] While there was a significant improvement in nutritional status post-therapy, the patient's swallowing difficulties persisted even after intervention, and there was no significant improvement in the patient's chewing ability.

Outcomes are influenced by both the timing and appropriateness of the therapeutic strategies employed. As Yorkston[51] said, "Instead of asking questions like, 'Does dysarthria treatment work?', it is more important to set intervention as a series of targeted steps and explore which specific treatments are effective at different stages of the condition. It is important to identify the signs that

indicate a speaker is ready to transition from one stage to the next. SLPs are invaluable team members in the rehabilitation of patients with extrapyramidal movement disorders, and speech therapy has the potential to diminish the impact of dysarthria on functional communication and alleviate the effort associated with speaking.[52]

Study limitations

As an individual case study, the findings of this study lack generalizability and do not allow for causal conclusions regarding treatment efficacy. Furthermore, the use of informal, non-standardized tools to assess activity and participation was necessitated by the lack of validated instruments in the local context, in the patient's native language. In addition, instrumental assessments for swallowing were not available, which restricted diagnostic precision in evaluating pharyngeal phase function.

Patient perspective

For a long time, I was confused, depressed, and angry about my situation, but I'm glad I'm getting treatment now, and I'm hoping for answers. What I want most is to be able to work again. I feel like my speech has improved a lot, and people understand me now. But it's still very difficult for me to chew.

Conclusion

This case study demonstrates that individualized, structured speech therapy can lead to measurable improvements in the functional communication of individuals with chronic, progressive dysarthria. Success of therapy depends on careful monitoring of the patient's current functioning, anticipating future changes, and managing symptoms accordingly. Realistic counseling, compensatory strategies, coupled with rehabilitative interventions, can significantly boost the patient's motivation and improve quality of life.

Declarations

Funding

The author received no funding for this study.

Author contributions

Conceptualization, I.W.; Methodology, I.W.; Software, I.W.; Formal Analysis, I.W.; Investigation, I.W.; Resources, I.W.; Data Curation, I.W.; Writing – Original Draft Preparation, I.W.; Writing – Review & Editing, I.W.

Conflicts of interest

The author declares no conflict of interest.

Data availability

The dataset generated and analyzed in this study consists of patient speech recordings and is not publicly available to protect patient confidentiality.

Ethics approval

Ethical approval was not required for this single case study from the Institutional Review Board of the Institute of Medicine, TUTH. Written informed consent was obtained from the patient for participation and publication of anonymized data.

Use of AI and AI-assisted technologies in the writing process

AI-assisted technology (ChatGPT, OpenAI) was used to paraphrase a few sentences to improve readability. The content was reviewed and verified by the author for accuracy.

References

1. Nishio M, Niimi S. Relationship between speech and swallowing disorders in patients with neuromuscular disease. *Folia Phoniatr Logop*. 2004;56(5):291-304. doi:10.1159/000080066
2. Yorkston KM, Beukelman DR. Dysarthria: Tools for Clinical Decision-Making. *ASHA Lead*. 2004;9(9):4-21. doi:10.1044/LEADER.FTR2.09092004.4
3. Duffy JR. *Motor Speech Disorders: Substrates, Differential Diagnosis, and Management*. 3rd ed. Elsevier Health Sciences; 2012.
4. Ovsiowitz M. Dysphagia. In: *Gut Instincts: A Clinician's Handbook of Digestive and Liver Diseases*. CRC Press; 2024:17-21. doi:10.1201/9781003524489-4
5. Wang BJ, Carter FL, Altman KW. Relationship between dysarthria and oral-oropharyngeal dysphagia: the present evidence. *Ear Nose Throat J.* Published online 2020. doi:10.1177/0145561320951647
6. Tjaden K. Speech and swallowing in Parkinson's disease. *Top Geriatr Rehabil*. 2008;24(2):115-126. doi:10.1097/01.TGR.0000318899.87690.44
7. Jung HH, Danek A, Walker RH. Neuroacanthocytosis syndromes. *Orphanet J rare Dis*. 2011;6(68). doi:10.1186/1750-1172-6-68
8. Walterfang M, Evans A, Looi JCL, et al. The neuropsychiatry of neuroacanthocytosis syndromes. *Neurosci Biobehav Rev*. 2011;35(5):1275-1283. doi:10.1016/j.neubiorev.2011.01.001
9. Walker RH, Jung HH, Dobson-Stone C, et al. Neurologic phenotypes associated with acanthocytosis. Neurology. 2007;68(2):92-98. doi:10.1212/01.WNL.0000250356.78092.CC
10. Walker RH. Management of neuroacanthocytosis syndromes. *Tremor Other Hyperkinet Mov (N Y)*. 2015;5:346. doi:10.7916/D8W66K48
11. Atkinson-Clement C, Letanneux A, Baille G, et al. Psychosocial Impact of Dysarthria: The Patient-Reported Outcome as Part of the Clinical Management. *Neurodegener Dis*. 2019;19(1):12-21. doi:10.1159/000499627
12. Chiaramonte R, Di Luciano C, Chiaramonte I, Serra A, Bonfiglio M. Multi-disciplinary clinical protocol for the

diagnosis of bulbar amyotrophic lateral sclerosis. *Acta Otorrinolaringol Esp*. 2019;70(1):25-31. doi:10.1016/j.otorri.2017.12.002

13. Mitchell C, Bowen A, Tyson S, Butterfint Z, Conroy P. Interventions for dysarthria due to stroke and other adult-acquired, non-progressive brain injury. *Cochrane Database Syst Rev.* 2017;2017(1):CD002088. doi:10.1002/14651858.CD002088.pub3
14. Conway A, Walshe M. Management of non-progressive dysarthria: Practice patterns of speech and language therapists in the Republic of Ireland. *Int J Lang Commun Disord*. 2015;50(3):374-388. doi:10.1111/1460-6984.12143
15. MacKenzie C, Muir M, Allen C. Non-speech oro-motor exercise use in acquired dysarthria management: Regimes and rationales. *Int J Lang Commun Disord*. 2010;45(6):617-629. doi:10.3109/13682820903470577
16. Fox CM, Ramig LO. Vocal sound pressure level and self-perception of speech and voice in men and women with idiopathic Parkinson disease. *Am J Speech-Language Pathol*. 1997;6(2):85-94. doi:10.1044/1058-0360.0602.85
17. Connor N, Abbs J, Cole K, Gracco V. Parkinsonian deficits in serial multiarticulate movements for speech. *Brain.* 1989;112(4):997-1009. doi:10.1093/brain/112.4.997
18. Helm-Estabrooks N, Yorkston KM, Spencer KA, Duffy JR. Behavioral management of respiratory/phonatory dysfunction from dysarthria: a systematic review of the evidence. *J Med Speech Lang Pathol.* 2003;11(2):xiii.
19. Robertson SJ, Thomson F. Speech therapy in Parkinson's Disease: A study of the efficacy and long term effects of intensive treatment. *Int J Lang Commun Disord*. 1984;19(3):213-224. doi:10.3109/13682828409029837
20. World Medical Association. World Medical Association Declaration of Helsinki: ethical principles for medical research involving human subjects. *JAMA*. 2013;310(20):2191-2194. doi:10.1001/jama.2013.281053
21. World Health Organization. *Framework for Action on Interprofessional Education & Collaborative Practice.* World Health Organization website. https://www.who.int/publications/i/item/framework-for-action-on-interprofessional-education-collaborative-practice. Published 2010. Accessed January 26, 2024.
22. Dunne-Platero K, Cloud C, Hilger A. Colorado Motor Speech Framework. Published online 2023. doi:10.17605/OSF.IO/PM936
23. Lippke BA, Dickey SE, Selmar JW, Soder AL. *PAT-3: Photo Articulation Test—Third Edition.* PRO-ED; 1997. https://www.proedinc.com/Products/8370/pat3-photo-articulation-testthird-edition. Accessed April 21, 2024.
24. Hirano M. Psycho-acoustic evaluation of voice. *Clin Exam Voice Disord Hum Commun.* Published online 1981:81-84. Accessed April 21, 2024.
25. Maryn Y, Weenink D. Objective dysphonia measures in the program praat: Smoothed cepstral peak prominence and acoustic voice quality index. *J Voice*. 2015;29(1):35-43. doi:10.1016/j.jvoice.2014.06.015
26. Enderby PM, Wood VA, Wade DT, Hewer RL. The Frenchay Aphasia Screening Test: A short, simple test for aphasia appropriate for non-specialists. *Disabil Rehabil*. 1986;8(4):166-170. doi:10.3109/03790798709166209
27. Nasreddine ZS, Phillips NA, Bédirian V, et al. The Montreal Cognitive Assessment, MoCA: A Brief Screening Tool For Mild Cognitive Impairment. *J Am Geriatr Soc*. 2005;53(4):695-699. doi:10.1111/J.1532-5415.2005.53221.X
28. Lim HJ, Lai DKH, So BPH, et al. A Comprehensive Assessment Protocol for Swallowing (CAPS): Paving the Way towards Computer-Aided Dysphagia Screening. *Int J Environ Res Public Health*. 2023;20(4). doi:10.3390/IJERPH20042998
29. Cichero JAY, Lam P, Steele CM, et al. Development of International Terminology and Definitions for Texture-Modified Foods and Thickened Fluids Used in Dysphagia Management: The IDDSI Framework. *Dysphagia*. 2017;32(2):293-314. doi:10.1007/S00455-016-9758-y
30. Rusz J, Megrelishvili M, Bonnet C, et al. A distinct variant of mixed dysarthria reflects parkinsonism and dystonia due to ephedrone abuse. *J Neural Transm*. 2014;121(6):655-664. doi:10.1007/S00702-014-1158-6
31. De Angelis EC, Mourão LF, Ferraz HB, Behlau MS, Pontes PAL, Andrade LAF. Effect of voice rehabilitation on oral communication of Parkinson's disease patients. *Acta Neurol Scand*. 1997;96(4):199-205. doi:10.1111/J.1600-0404.1997.tb00269.x
32. Chiaramonte R, Vecchio M. A Systematic Review of Measures of Dysarthria Severity in Stroke Patients. *PM R*. 2021;13(3):314-324. doi:10.1002/pmrj.12469
33. Darley FL, Aronson AE, Brown JR. Differential diagnostic patterns of Dysarthria. *J Speech Hear Res*. 1969;12(2):246-269. doi:10.1044/JSHR.1202.246
34. Ludlow CL, Hoit J, Kent R, et al. Translating principles of neural plasticity into research on speech motor control recovery and rehabilitation. *J Speech, Lang Hear Res*. 2008;51(1). doi:10.1044/1092-4388(2008/019)
35. Spencer KA, Yorkston KM. Evidence for the treatment of respiratory/phonatory dysfunction from dysarthria. *Perspect Neurophysiol Neurogenic Speech Lang Disord.* 2002;12(4):4-16. doi:10.1044/nnsld12.4.4
36. Lester-Smith RA, Miller CH, Cherney LR. Behavioral therapy for tremor or dystonia affecting voice in speakers with hyperkinetic dysarthria: a systematic review. *J Voice.* 2023;37(4):561-573. doi:10.1016/j.jvoice.2021.03.026
37. Yorkston KM, Beukelman DR. Ataxic dysarthria: treatment sequences based on intelligibility and prosodic considerations. *J Speech Hear Disord*. 1981;46(4):398-404. doi:10.1044/JSHD.4604.398
38. Martens H, Van Nuffelen G, Dekens T, et al. The effect of intensive speech rate and intonation therapy on intelligibility in Parkinson's disease. *J Commun Disord*. 2015;58:91-105. doi:10.1016/J.JCOMDIS.2015.10.004

39. Yorkston KM, Miller RM, Strand EA, Britton D. *Management of Speech and Swallowing in Degenerative Diseases*. Pro-Ed Inc.; 2013.
40. Patel R. Prosodic Control in Severe Dysarthria. *J Speech, Lang Hear Res*. 2002;45(5):858-870. doi:10.1044/1092-4388(2002/069)
41. Schmidt RA, Lee TD, Winstein C, Wulf G, Zelaznik HN. *Motor Control and Learning: A Behavioral Emphasis*. 6th ed. Champaign, IL: Human Kinetics; 2018.
42. Maas E, Robin DA, Hula SNA, et al. Principles of motor learning in treatment of motor speech disorders. *Am J Speech-Language Pathol*. 2008;17(3):277-298. doi:10.1044/1058-0360(2008/025).
43. O'Horo JC, Rogus-Pulia N, Garcia-Arguello L, Robbins J, Safdar N. Bedside Diagnosis of Dysphagia: A Systematic Review. *J Hosp Med*. 2015;10(4):256. doi:10.1002/jhm.2313
44. Ricci Maccarini A, Filippini A, Padovani D, Limarzi M, Loffredo M, Casolino D. Clinical non-instrumental evaluation of dysphagia. *Acta Otorhinolaryngol Ital*. 2007;27(6):299.
45. Lim SHB, Lieu PK, Phua SY, et al. Accuracy of bedside clinical methods compared with fiberoptic endoscopic examination of swallowing (FEES) in determining the risk of aspiration in acute stroke patients. *Dysphagia*. 2001;16(1):1-6. doi:10.1007/s004550000038
46. Peikert K, Dobson-Stone C, Rampoldi L, et al. VPS13A Disease. *Encycl Mov Disord Three-Volume Set*. Published online March 30, 2023:V1-217-V1-219. doi:10.1016/b978-0-12-374105-9.00396-8
47. Adult Dysphagia. American Speech-Language-Hearing Association website. https://www.asha.org/Practice-Portal/Clinical-Topics/Adult-Dysphagia. Accessed April 25, 2024.
48. Robbins JA, Kays SA, Gangnon RE, et al. The Effects of Lingual Exercise in Stroke Patients With Dysphagia. *Arch Phys Med Rehabil*. 2007;88(2):150-158. doi:10.1016/j.apmr.2006.11.002
49. Sollazo A, Monaco L, Vecchio L Del, et al. Investigation of compensatory postures with videofluoromanometry in dysphagia patients. *World J Gastroenterol*. 2012;18(23):2973-2978. doi:10.3748/wjg.v18.i23.2973
50. Calvo I, Sunday KL, Macrae P, Humbert IA. Effects of chin-up posture on the sequence of swallowing events. *Head Neck*. 2017;39(5):947-959. doi:10.1002/hed.24713
51. Yorkston KM. The degenerative dysarthrias: A window into critical clinical and research issues. *Folia Phoniatr Logop*. 2007;59(3):107-117. doi:10.1159/000101769
52. Ford CN, Roy N, Bless DM. Muscle tension dysphonia and spasmodic dysphonia: The role of manual laryngeal tension reduction in diagnosis and management. *Ann Otol Rhinol Laryngol*. 1996;105(11):851-856. doi:10.1177/000348949610501102

Rzeszów University Press 2026
ISSN 2544-1361 (online)
doi: 10.15584/ejcem.2026.1.6

http://www.ejcem.ur.edu.pl
European Journal of Clinical and Experimental Medicine
Eur J Clin Exp Med 2026; 24 (1): 210–216

CASE REPORTS

Occipital necrotizing fasciitis – a case report of diagnostic and surgical challenges from an atypical anatomical presentation

Koespriyandito [1], Laurensia Evita [2], Kalyana Maharani [2]

[1] Department of Surgery, Universitas Indonesia Hospital, Jl Prof. Dr Bahder Djohan, Depok, Indonesia
[2] Faculty of Medicine, Universitas Indonesia, Salemba Raya No 6, Jakarta Pusat, Indonesia

ABSTRACT

Introduction and aim. Necrotizing fasciitis (NF) is a rapidly progressive soft tissue infection with high mortality. While most cases involve the extremities or perineum, isolated occipital scalp NF is exceptionally rare, often leading to delayed recognition. We present a case describing its unusual site, diagnostic pitfalls, and surgical challenges.

Description of the case. A 48-year-old man presented with one week of progressive swelling and pain following rupture of a boil-like lesion on the occipital region. Examination revealed a 20×20 cm erythematous, tender, and swelling. The primary survey was unremarkable. Laboratory results showed hyperglycemia (490.6 mg/dL), hyponatremia (122.0 mEq/L), and leukocytosis (26.72×10^9/L). Imaging suggested a localized abscess, initially managed with incision and drainage. Rapid necrosis progression necessitated emergent wide debridement, confirming NF. Intraoperative bleeding complicated tissue assessment. Negative pressure wound therapy was attempted but discontinued due to anatomical limitations. The patient improved with repeated debridements, antibiotics, and reconstructive surgery.

Conclusion. This case highlights the rarity of occipital NF and the risk of low clinical suspicion in atypical locations, emphasizing the importance of early recognition and tailored surgical management.

Keywords. case report, diabetes mellitus, necrotizing fasciitis, occipital, posterior neck

Introduction

Necrotizing fasciitis (NF) is a rare but devastating soft tissue infection with reported in-hospital mortality rates as high as 30%.[1] It is a rapidly progressive and life-threatening condition that can lead to septic shock and multiorgan failure if not promptly treated.[2,3] Early diagnosis and surgical debridement are critical, yet initial presentations can be subtle and deceptively benign. While NF typically involves the extremities, perineum, or abdominal wall, head and neck involvement accounts for only 1–10% of cases.[4,5] Occipital involvement is particularly uncommon, with only isolated reports in the literature. One previously published case described occipital NF arising in the setting of psoriasis.[6]

Aim

We report a case of NF confined to the occipital scalp and posterior neck in a clinically stable patient with newly diagnosed diabetes mellitus, initially mistaken for a localized abscess. Our case expands on the limited literature by highlighting diagnostic uncertainty and technical challenges unique to this location. Suspicion is often low when NF occurs outside the typical sites, and subtle early features may further obscure recogni-

Corresponding author: Koespriyandito, e-mail: koespriyandito@gmail.com, koespriyandito@rs.ui.ac.id

Received: 9.07.2025 / Revised: 26.08.2025 / Accepted: 31.08.2025 / Published: 30.03.2026

Koespriyandito, Evita L, Maharani K. Occipital necrotizing fasciitis – a case report of diagnostic and surgical challenges from an atypical anatomical presentation. *Eur J Clin Exp Med.* 2026;24(1):210–216. doi: 10.15584/ejcem.2026.1.6.

tion. Management is also complicated because no established guidelines exist, and intraoperative decisions rely heavily on clinical judgment. In the scalp, abundant vascularity blurs the distinction between necrotic and granulating tissue and makes hemostasis more difficult. Furthermore, applying negative pressure wound therapy in this region requires special consideration of neck flexion and patient comfort.

Description of the case

A 48-year-old man presented with a one-week history of progressive occipital swelling. Two weeks earlier, he had noticed a small, boil-like lesion approximately 0.5 cm in diameter on the occipital scalp that ruptured three days later, discharging purulent material. Believing it to be a minor superficial infection, he did not seek medical attention. Over the next few days, he developed neck stiffness, subjective fever, localized throbbing pain, and swelling that interfered with sleep. He self-medicated with paracetamol.

On day seven, his wife observed spreading erythema and multiple nodules. A week later, he sought care at our emergency department. On arrival, his primary survey was unremarkable, and he appeared clinically stable without signs of sepsis. Local examination revealed a 20×20 cm erythematous, fluctuant mass extending from the occiput to the posterior cervical region with edema, superficial bleeding, and yellowish crusting (Fig. 1).

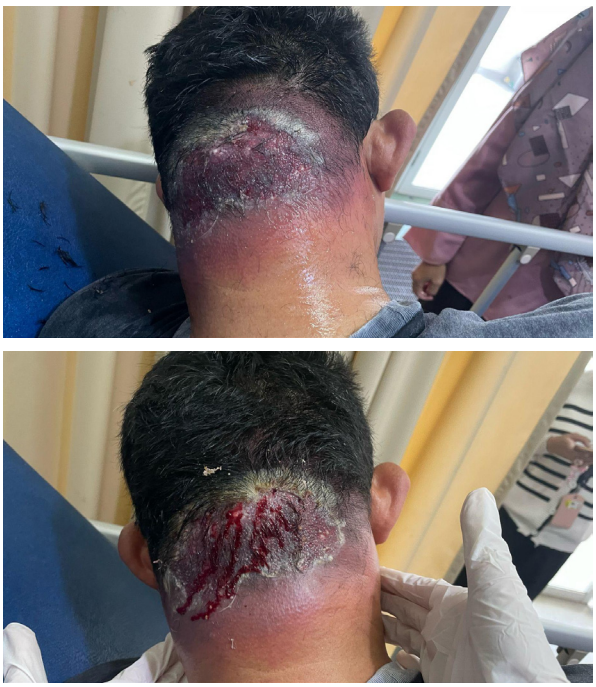

Fig. 1. Posterior view of the occipital and cervical region at initial presentation

Initial labs showed marked hyperglycemia (random blood glucose: 490.6 mg/dL), corrected hyponatremia (122.0 mEq/L), leukocytosis (26.72×10^9/L, 87.4% neutrophils), and partially compensated metabolic acidosis. Blood ketones were mildly elevated. The surgical team assumed care and requested a contrast-enhanced MRI of the brain and cervical spine, performed using a Philips Ingenia 1.5T. Internal medicine was consulted for glycemic and metabolic stabilization.

The MRI revealed an abscess in the subgaleal and subcutaneous layers of the posterior parietal and occipital regions, extending into the posterior cervical paravertebral soft tissues (C1–C4), involving multiple muscles (semispinalis capitis, splenius capitis, splenius cervicis, longissimus capitis, superior sternocleidomastoid, trapezius) with no spinal or bone involvement (Fig. 2).

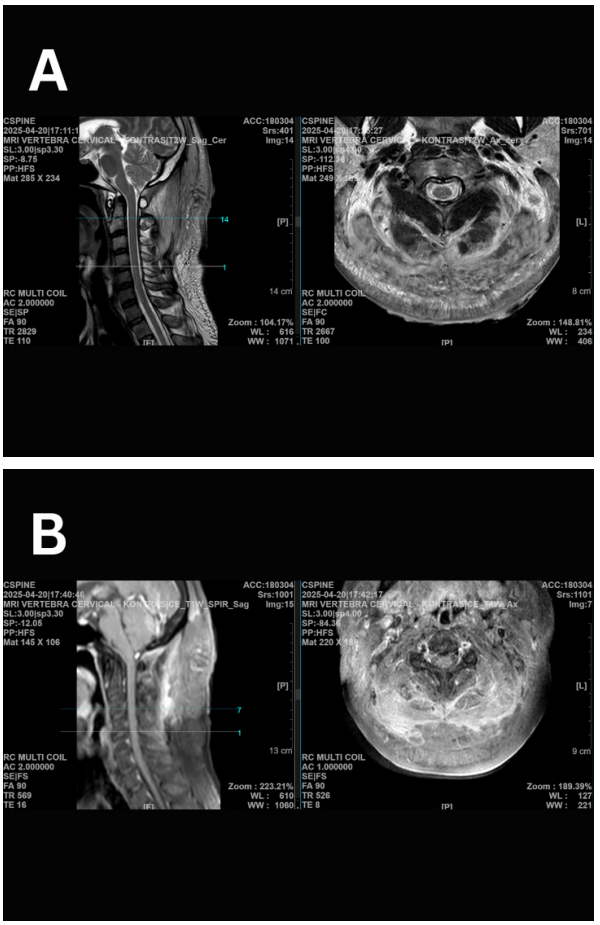

Fig. 2. MRI of the occipital and cervical region, A: Sagittal and axial T_2-weighted images, B: Sagittal and axial T_1-weighted images

Based on clinical and radiologic findings, the patient was diagnosed with a localized occipital abscess. Initial management included wound care with 0.9% saline-soaked gauze, intravenous fluids, and analgesics. On hospital day two, following glycemic stabilization, he underwent urgent incision and drainage under general anesthesia. A 10 cm transverse incision released purulent, blood-tinged fluid. A secondary 5 cm incision was

made inferiorly to access a second, septated collection (Fig. 3). Both cavities were irrigated and packed with iodine-soaked gauze for secondary intention healing and then transitioned early to daily honey-impregnated gauze dressings. The patient was started empirically on ampicillin-sulbactam and metronidazole. Tissue cultures grew *Staphylococcus aureus,* and antibiotics were adjusted to ceftriaxone and metronidazole based on sensitivities. He was monitored in the ICU for two days before transfer to the ward and was discharged on postoperative day four with outpatient follow-up.

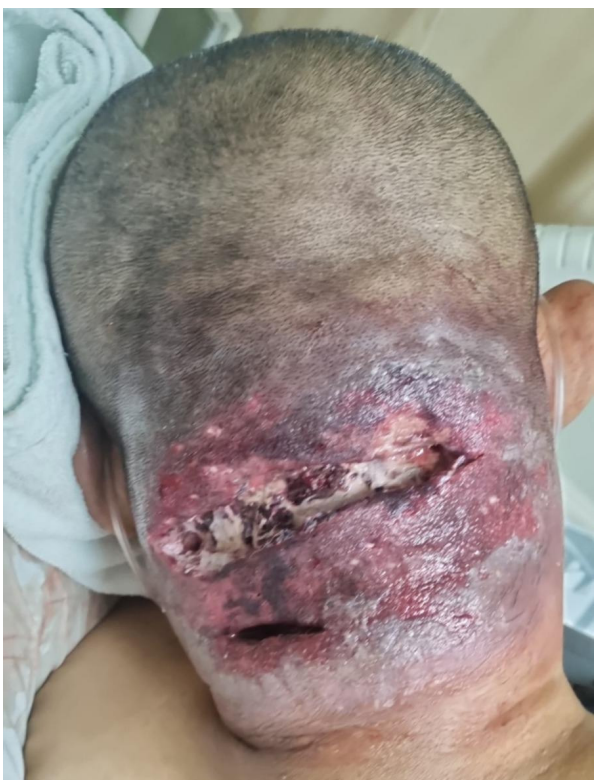

Fig. 3. Postoperative appearance following initial incision and drainage

Three days later, the patient was readmitted due to worsening necrosis and purulent discharge. Examination revealed undermined tissue planes and rapid spread beyond the prior surgical site, raising strong suspicion for NF. Emergent necrotomy and fasciotomy were performed. Debridement revealed a 10×12 cm area of necrotic scalp with spongy, septated subcutaneous tissue and necrotic fascia. The proximal cervical muscles showed friable, granulation-like tissue that bled easily, complicating differentiation between viable and nonviable tissue due to the scalp's rich vascularity. A tissue specimen was submitted for culture and histopathology. Estimated blood loss was 800 mL, and the patient received 230 mL of packed red blood cells. Hemostasis was achieved. The wound was left open and packed (Fig. 4). Microscopic examination showed necrotic skin overlaid by epidermis, with dense infiltration

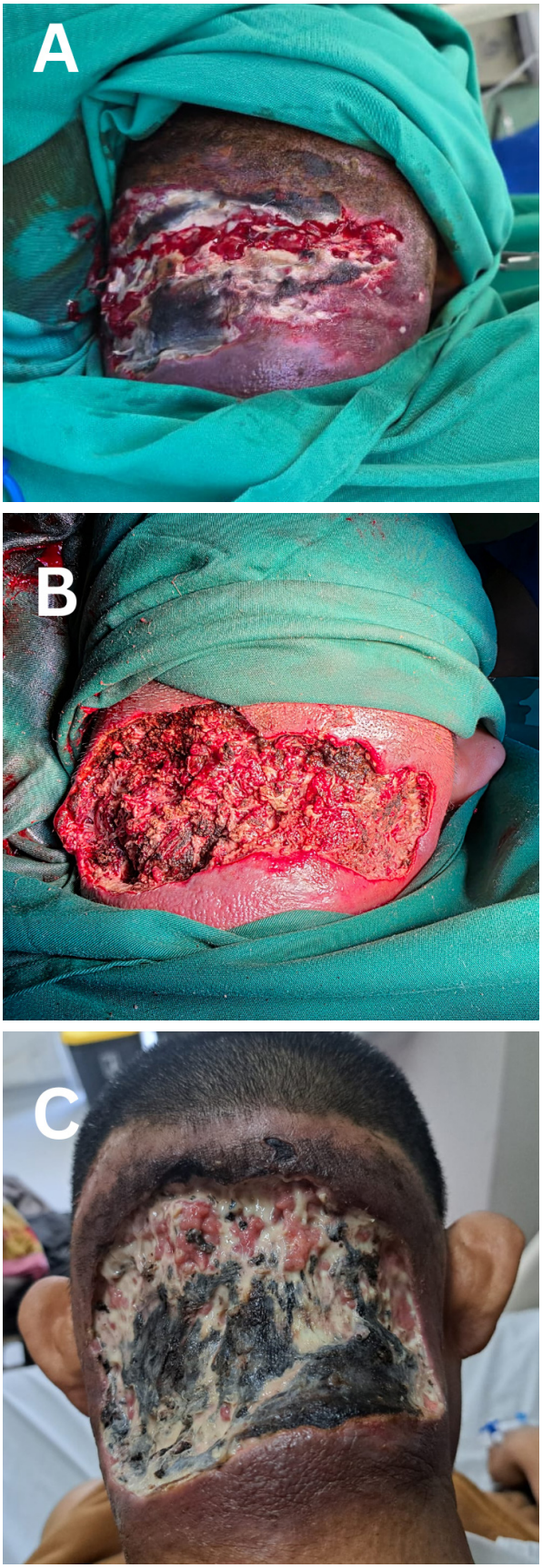

Fig. 4. Sequential images for the second debridement procedure, A: Preoperative view showing necrosis, B: Intraoperative view revealing devitalized fascia, C: Postoperative wound with eschar

of lymphocytes, histiocytes, and neutrophils extending into the dermis and subcutaneous tissue. Areas of hemorrhage and fibrin deposits were also present. These findings support the clinical and operative diagnosis of NF, with evidence of extensive soft tissue necrosis and mixed acute and chronic inflammation. Postoperatively, wound care with daily honey-impregnated gauze dressings continued. He remained on the same antibiotics regimen and was monitored in the intensive care unit for two days before transfer to the general ward.

Six days after the second surgery, a final debridement was performed in preparation for negative pressure wound therapy (NPWT). The patient was positioned prone with limited cervical flexion. Residual necrotic tissue was excised, and blood loss was estimated at 15 mL (Fig. 5). Tissue samples were obtained for culture, with the antibiotic regimen maintained. NPWT was initiated using the Renasys Touch system by Smith & Nephew, with intermittent suction set at 40 mmHg for two minutes and 120 mmHg for four minutes.

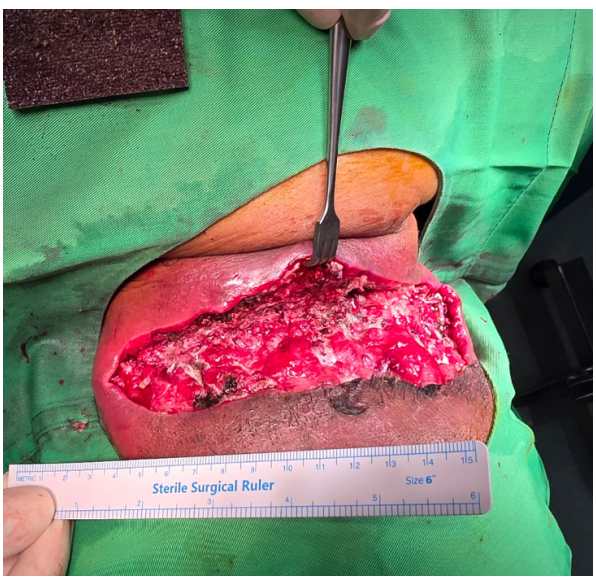

Fig. 5. Intraoperative view during the third debridement demonstrating a clean wound bed

On the second day of NPWT, the system appeared to leak due to dressing dislodgement caused by cervical flexion during daily activity. Sounds from the tubing suggested a problem, but the device did not display any failure notifications. Attempts to restore suction were unsuccessful, and the device ultimately developed a mechanical obstruction. Consequently, the decision was made to discontinue NPWT and resume conventional open wound management. The wound healed well without new infection or need for further debridement. The patient stabilized clinically and was discharged the next day with outpatient follow-up. Plastic surgery was consulted, and definitive reconstruction was performed 20 days after the final debridement (Fig. 6).

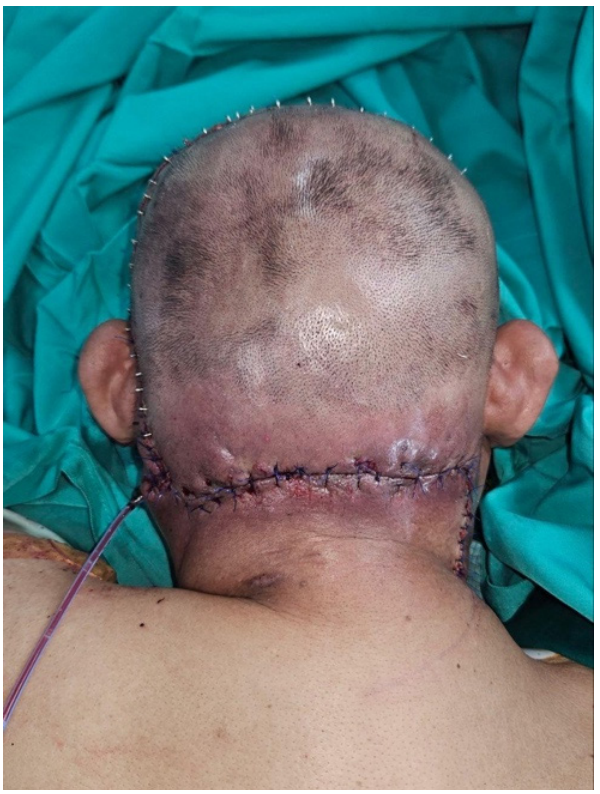

Fig 6. Post-reconstruction view showing the scalp and posterior neck

During the reconstruction, a 12×4.5 cm granulating defect was identified. After tumescent infiltration, the wound edges were refreshed, and the granulation tissue was shaved. A double rotation flap was then designed. The superior left flap was rotated superiorly with a defect-to-flap ratio of 1:8, while the inferior right flap was rotated inferiorly using a cut-as-you-go technique. The scalp flap was elevated in the loose areolar plane, and the neck flap in the subcutaneous plane. Both were mobilized sufficiently for tension-free closure. A vacuum drain was placed. Intradermal suturing was performed with Vicryl (Ethicon) 2-0 and 3-0. The scalp skin was closed with a skin stapler, and the remaining incisions with Prolene (Ethicon) 2-0 and 3-0. The wound was dressed in tulle and sterile gauze. The procedure was completed uneventfully. Figure 7 presents a concise chronological overview of the events related to this case.

Discussion

NF is a rare, aggressive soft tissue infection that requires early recognition and surgical intervention to prevent mortality. Although advanced disease may present with sepsis, shock, or multiorgan failure, the early course is often nonspecific and easily mistaken for cellulitis or other soft tissue infections. Clinical features considered atypical, including absence of fever, stable vital signs, minimal skin changes, or subtle pain, are in fact encountered in the initial phase and contribute to diagnostic delay.[2,3]

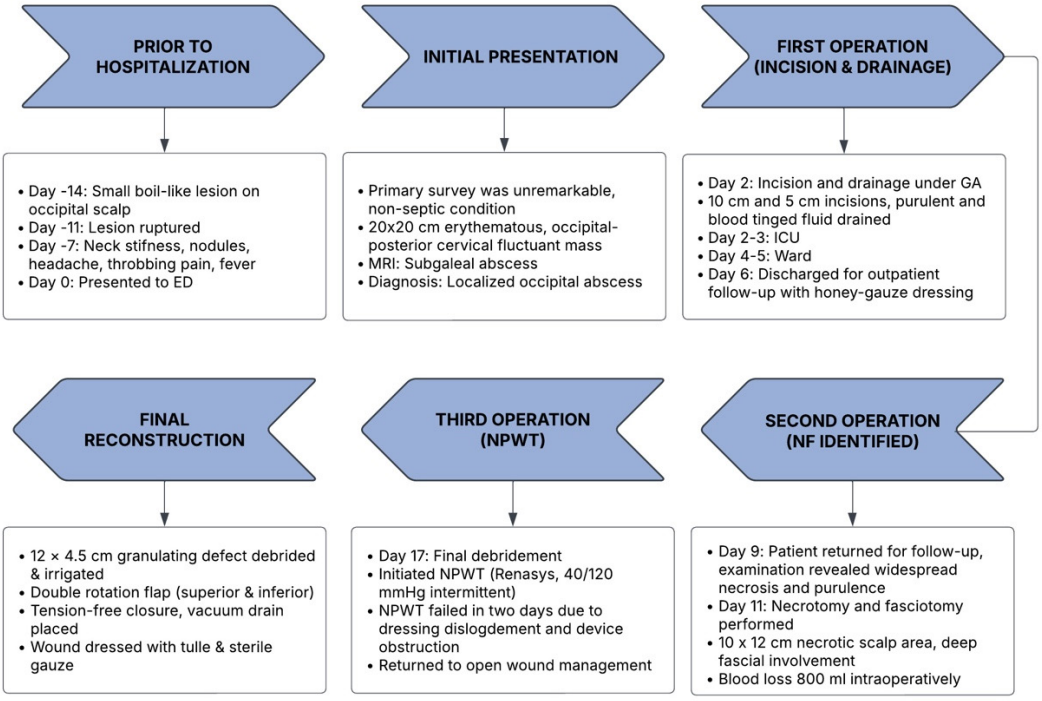

Fig. 7. Clinical timeline summarizing symptom progression, interventions, and recovery

In our case, the patient appeared stable and afebrile, with only localized swelling that initially suggested a simple abscess. Laboratory results showed hyperglycemia, hyponatremia, and neutrophilic leukocytosis. Although diabetes had not been previously diagnosed, it likely increased both susceptibility and diagnostic delay. Diabetes impairs neutrophil function and reduces tissue perfusion, blunting inflammatory responses and obscuring early signs of NF.[7]

The occipital scalp is an exceptionally rare site of involvement, in contrast to the extremities, trunk, or perineum, where NF is more commonly reported.[4] This atypical location contributed to diagnostic delay and conservative initial management. In addition to such rare anatomical sites, NF has also been described after cosmetic procedures and in uncommon mycotic etiologies, reflecting its expanding spectrum.[8,9] These variations highlight the need for clinicians to maintain a heightened index of suspicion when evaluating soft tissue infections.

With no established guidelines for occipital or posterior neck NF, the team opted for limited drainage, consistent with 2015 World Society of Emergency Surgery recommendations for stable patients without signs of necrosis.[10] The posterior neck is also thought to resist deep infection due to thicker skin, unlike anterior infections like descending necrotizing mediastinitis, which require early, wide debridement.[11–13] In such cases, decisions must rely on anatomical reasoning and clinical judgment.

The scalp's rich vascularity, supplied by branches of both the external and internal carotid arteries, is thought to support a strong immune response and promote healing.[14,15] This has led some to favor conservative management in scalp infections.[16] In our case, this presumed protection contributed to delayed debridement. However, the loose areolar tissue beneath the galea aponeurotica provides a potential space for rapid horizontal spread, which likely facilitated the disease's unexpectedly aggressive course.[15]

Paradoxically, this same vascularity complicates intraoperative assessment. In hypervascular regions like the scalp, bleeding is not a reliable indicator of viability. Intraoperative evaluation typically relies on visual and tactile cues such as color, bleeding, and texture, but an inflamed, friable cervical muscle mimicked granulation tissue, making it difficult to distinguish necrotic from viable structures.[17] This led to extended dissection and significant blood loss requiring transfusion. Thus, vascular density may obscure necrosis, adding complexity to surgical decision-making in scalp NF.

NPWT has demonstrated favorable outcomes in head and neck wounds across various settings.[18] However, its use in the occipital scalp and posterior neck presents a unique anatomical challenge. In our case, routine cervical flexion during daily activities and salat caused the NPWT dressing to dislodge. The dressing had been applied with the neck only partially flexed. Applying it in maximal flexion from the start would have better accommodated the patient's range of motion. While NPWT is increasingly used for complex wounds, occipital application requires specific precautions that remain under recognized in the literature.

Finally, the limitation of our study is that it reports a single patient, which inherently restricts its generalizability and precludes comparison with alternative treatment strategies. Nonetheless, it offers useful guidance for clinicians facing similar diagnostic and operative challenges.

Conclusion

This report describes a rare case of NF confined to the occipital region, an anatomical site with little prior documentation. From a clinical perspective, its atypical location and initially subtle presentation delayed recognition, emphasizing the need to consider NF even when systemic signs are preserved. The case also highlights how the scalp's vascularity may obscure necrosis, how subgaleal spread accelerates progression, and how posterior neck anatomy complicates wound management, including negative pressure therapy. Greater awareness of these features can guide timely diagnosis and surgical decisions, ultimately improving outcomes in similarly uncommon presentations.

Acknowledgements

The authors wish to express sincere gratitude to Anne L. Lashbrook from the Department of Physics, University of Washington, for her invaluable assistance in proofreading this article.

Declarations

Funding

Not applicable.

Author contributions

The following statements should be used:
Conceptualization, K. and L.E.; Methodology, L.E. and K.M.; Formal Analysis, K., L.E., and K.M.; Investigation, K.; Resources, K.; Data Curation, L.E. and K.M.; Writing – Original Draft Preparation, L.E.; Writing – Review & Editing, K., L.E., and K.M.; Visualization, K.M.; Supervision, K.

Conflicts of interest

The authors declare that they have no competing interests.

Data availability

No datasets were generated or analyzed during this study.

Ethics approval

The authors confirmed that informed consent was obtained from the patients, including consent for publication of photographs and clinical details. Patients were assured that their identities and confidentiality would be protected.

References

1. Sartelli M, Coccolini F, Kluger Y, et al. WSES/GAIS/WSIS/SIS-E/AAST global clinical pathways for patients with skin and soft tissue infections. *World Journal of Emergency Surgery*. 2022;17(1):3. doi:10.1186/s13017-022-00406-2
2. Yu X, Guo Z, Zhang M, Fu Q, Zhou J. Clinical analysis of diagnosis and treatment of necrotizing fasciitis. *Eur J Inflamm*. 2022;20. doi:10.1177/1721727X221141822
3. Howell GM, Rosengart MR. Necrotizing soft tissue infections. *Surg Infect (Larchmt)*. 2011;12(3):185-190.
4. Green R, Dafoe DC, Raffin TA. Necrotizing Fasciitis. *Chest*. 1996:110:219-229. doi:10.1378/chest.110.1.219
5. Gupta V, Sidam S, Behera G, Kumar A, Mishra UP. Cervical Necrotizing Fasciitis: An Institutional Experience. *Cureus*. 2022;14(12):e32382. doi:10.7759/cureus.32382
6. Țenț PA, Juncar M, Mureșan O, Arghir OC, Iliescu DM, Onișor F. Post-traumatic occipital psoriatic plaque complicated by extensive necrotizing fasciitis of the head and neck: a case report and literature review. *J Int Med Res*. 2018;46(8):3480-3486. doi:10.1177/0300060518788490
7. Berbudi A, Rahmadika N, Tjahjadi AI, Ruslami R. Type 2 Diabetes and its Impact on the Immune System. *Curr Diabetes Rev*. 2019;16(5):442-449. doi:10.2174/1573399815666191024085838
8. Gilardi R, Parisi P, Galassi L, Firmani G, Bene M Del. Candida albicans necrotizing fasciitis following cosmetic tourism: A case report. *JPRAS Open*. 2023;38:129-133. doi:10.1016/j.jpra.2023.10.004
9. Gilardi R, Galassi L, Del Bene M, Firmani G, Parisi P. Infective complications of cosmetic tourism: A systematic literature review. *J Plast Reconstr Aesthet Surg*. 2023;84:9-29. doi:10.1016/j.bjps.2023.05.021
10. Sartelli M, Malangoni MA, May AK, et al. World Society of Emergency Surgery (WSES) guidelines for management of skin and soft tissue infections. *World J Emerg Surg*. 2014;9(1):57. doi:10.1186/1749-7922-9-57
11. Micheels P, Besse S, Elias B, Viski S. A Comparison of Skin Thickness Data from Ultrasonography with Literature Data Obtained via Histology and Magnetic Resonance Imaging: Posterior Neck, Lumbar Back, Lateral Epicondyle, and Posterior Knee. *J Clin Cosmet Dermatol*. 2020;4(3):153. doi:10.16966/2576-2826.153
12. Micheels P, Besse S, Rouijel J, Viski S. A Comparison of Skin Thickness Data from Ultrasonography with Literature Data Obtained via Histology and Magnetic Resonance Imaging: Cheek, Anterior Neck, and Décolleté. *J Clin Cosmet Dermatol*. 2020;4(3):152. doi:10.16966/2576-2826.152
13. Sugio K, Okamoto T, Maniwa Y, et al. Descending necrotizing mediastinitis and the proposal of a new classification. *JTCVS Open*. 2021;8:633-647. doi:10.1016/j.xjon.2021.08.001
14. Moore KL, Dalley AF, Agur AM. *Clinically Oriented Anatomy*. 7th ed. Wolters Kluwer Health; 2013.

15. Ellis H, Mahadevan V. The surgical anatomy of the scalp. *Surgery (Oxford)*. 2014;32:e1-e5.
16. Baek S, Park JH. Negative Pressure Wound Therapy (NPWT) after Hybrid Reconstruction of Occipital Pressure Sore Using Local Flap and Skin Graft. *Medicina (Lithuania)*. 2023;59(7). doi:10.3390/medicina59071342
17. Dima A, Gateau J, Claussen J, Wilhelm D, Ntziachristos V. Optoacoustic imaging of blood perfusion: Techniques for intraoperative tissue viability assessment. *J Biophotonics*. 2013;6(6-7):485-492. doi:10.1002/jbio.201200201
18. Liebman RM, Hanubal KS, Dziegielewski PT. Negative Pressure Wound Therapy in the Head and Neck: A Summary of Uses and Application Techniques. *Semin Plast Surg*. 2023;37(01):009-018. doi:10.1055/s-0042-1759562

Rzeszów University Press 2026
ISSN 2544-1361 (online)
doi: 10.15584/ejcem.2026.1.7

http://www.ejcem.ur.edu.pl
European Journal of Clinical and Experimental Medicine
Eur J Clin Exp Med 2026; 24 (1): 217–221

CASE REPORTS

Carcinosarcoma of the uterus and its monoclonal behavior – a case report with review of literature from rural India

Seema Dayal

Department of Pathology, Uttar Pradesh University of Medical Sciences, Saifai, Etawah, India

ABSTRACT

Introduction and aim. Carcinosarcoma of the uterus is a rare and aggressive monoclonal tumor composed of both epithelial and mesenchymal components. It is associated with poor prognosis and shows a marked tendency for early metastasis and recurrence, posing a significant challenge in gynecological oncology. This study aimed to identify the precise clinicopathological features of uterine carcinosarcoma that may facilitate accurate diagnosis and, ultimately, timely patient management.

Description of the case. A 53-year-old nulliparous woman presented with vaginal bleeding and an abdominal mass. Clinically, the case was initially diagnosed as leiomyoma uteri. The patient underwent hysterectomy, and the specimen was submitted for histopathological examination. Histopathology suggested a malignant mixed Müllerian tumor (homologous type). Immunohistochemistry was performed to confirm the diagnosis and to exclude differentials such as endometrial carcinoma. The tumor was positive for cytokeratin, vimentin, cyclin D1, and CD10, while negative for p53 in both components. The coexistence of epithelial and mesenchymal elements of common embryonic origin, together with the absence of p53 expression, confirmed the monoclonal nature of the tumor.

Conclusion. Accurate diagnosis of uterine carcinosarcoma requires the combined use of clinical evaluation, histopathology, and immunohistochemistry, which are essential for guiding optimal therapeutic interventions and determining prognosis.

Keywords. carcinosarcoma, corpus uterus, hysterectomy, immunohistochemistry, mixed Mullerian tumor

Introduction

Malignant mixed Müllerian tumor is also defined as carcinosarcoma, which means a tumor with a combination of both carcinoma and sarcoma simultaneously. It is an extremely uncommon malignant tumor of the uterine corpus, leading to scanty contribution to gynecological malignancies.[1] The frequent mutations are TP53, PTEN, PIK3CA, PPP2RIA, FBXW7, and KRAS. Regarding the origin of carcinosarcoma, the primitive Müllerian duct develops from the mesenchyme of the urogenital ridge and the lining of the coelomic epithelium. These ducts undergo differentiation into the body of the uterus, fallopian tubes, and cervix. This analogy gives rise to myometrial smooth muscle, endometrial stroma, and endometrial glands. So, the mixed Müllerian tumor consists of both elements.[2] These tumors are common in the uterus because epithelial and mesenchymal components both arise from the common embryonic origin.[3] It is commonly seen in women of the postmenopausal age group but has also been reported in younger women.[4] This tumor has bilateral components. On the basis of components, it is bifurcated into two subtypes and is called homologous when sarcomatous components are composed of fibrous or smooth muscle tissue, such as fibrosarcoma, endometrial stromal tumors, or leiomyosarcomas. Similarly, it is named heterologous when

Corresponding author: Seema Dayal, e-mail: seemadayal5@gmail.com

Received: 22.06.2025 / Revised: 23.08.2025 / Accepted: 10.09.2025 / Published: 30.03.2026

Dayal S. Carcinosarcoma of the uterus and its monoclonal behavior – a case report with review of literature from rural India. *Eur J Clin Exp Med.* 2026;24(1):217–221. doi: 10.15584/ejcem.2026.1.7.

the sarcomatous components are composed of cartilage, skeletal muscle, and bone, therefore rhabdomyosarcoma, chondrosarcoma, osteosarcoma, and liposarcoma.[1] In both types, the carcinomatous component is mainly composed of endometrioid, serous, or clear cell type adenocarcinoma.

Aim

The aim of this study was to identify the diagnostic significance of histopathology and immunohistochemistry in uterine carcinosarcoma with homologous elements.

Description of the case

A 53-year-old nulliparous postmenopausal woman presented with abdominal pain, bleeding per vaginam, and an abdominal mass. There was no history of tamoxifen use or pelvic radiation therapy.

Ultrasonography revealed an intramural tumor mass that did not extend beyond the uterus. Clinically and radiologically, it was diagnosed as a fibroid uterus. Therefore, a hysterectomy with bilateral salpingo-oophorectomy was performed, and the surgically resected specimen was sent in 10% formal saline to the Department of Pathology for histopathological examination. The uterus with bilateral adnexa measured 7×9×10 cm grossly (Fig. 1).

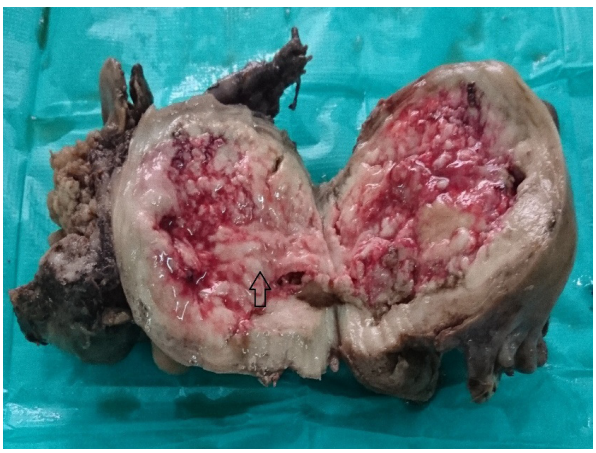

Fig. 1. Gross section of hysterectomy specimen showing endometrium and myometrium, the endometrium and myometrium were replaced by tumor mass, the tumor was grey/white in color, fragile with hemorrhagic and necrotic areas

After macroscopic examination, the specimen was sectioned, processed, and embedded in paraffin. Subsequently, 4 µm sections were prepared and stained with hematoxylin and eosin (H&E).

On histopathological examination, the endometrium and myometrium were replaced by glandular components showing marked atypical features. This was accompanied by a cellular stroma exhibiting pronounced pleomorphism and frequent mitoses. These findings were suggestive of a malignant mixed Müllerian tumor (homologous type). The cervix, ovaries, and fallopian tubes were free of invasion.

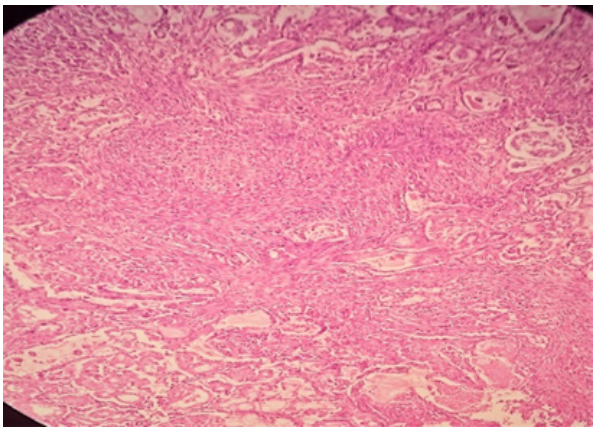

Fig. 2. H&E stained section of carcinosarcoma showing both epithelial and mesenchymal components (200x)

Immunohistochemistry was performed to confirm the diagnosis, to determine the nature of the tumor, and to exclude differential diagnoses. The procedure included tissue preparation, deparaffinization with rehydration, antigen retrieval, blocking, antibody incubation, detection, counterstaining, mounting, and visualization. The antibodies applied were cyclin D1, cytokeratin, vimentin, CD10, and p53. Cytokeratin (Fig. 3), vimentin (Fig. 4), and cyclin D1 (Fig. 5) were strongly positive, whereas CD10 was weakly positive (Fig. 6) and p53 was negative in both components (Fig. 7).

Endometrial carcinomas usually show positive immunoexpression for cytokeratin AE1/AE3, cyclin D1, and p53, while being negative for vimentin and often negative for CD10.

Based on histomorphology and immunohistochemistry, the diagnosis of carcinosarcoma of the uterine corpus (homologous variant) was established.

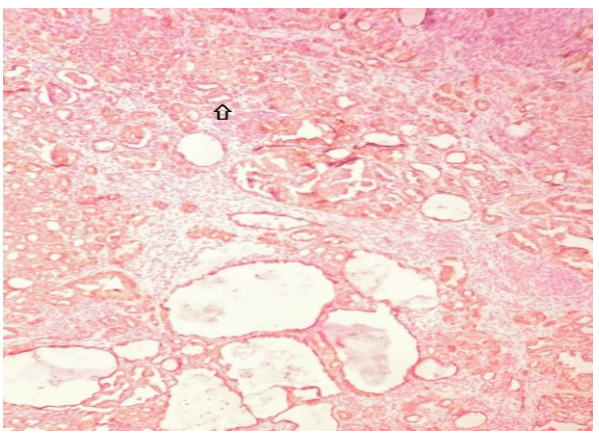

Fig. 3. Strong immunopositivity of cytokeratin AE1/AE3 in the epithelial component of carcinosarcoma (200×)

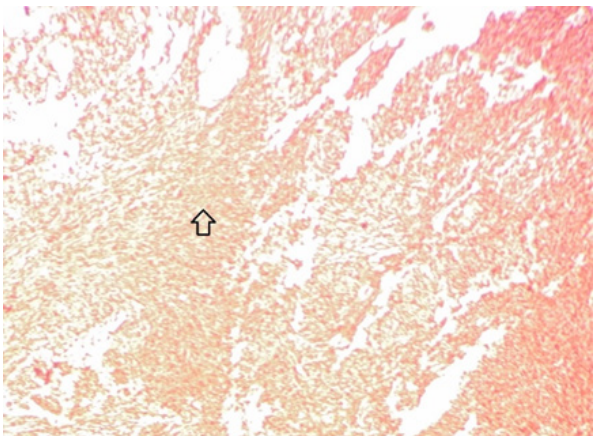

Fig. 4. Strong immunopositivity of vimentin in the sarcomatous component of carcinosarcoma (200×)

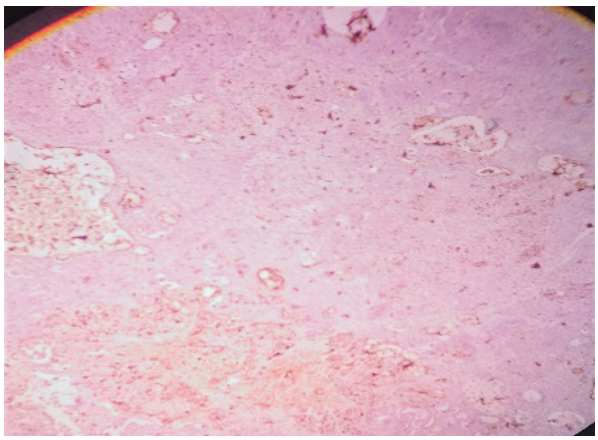

Fig. 6. Section of carcinosarcoma showing CD10 focal positivity in mesenchymal components (100×)

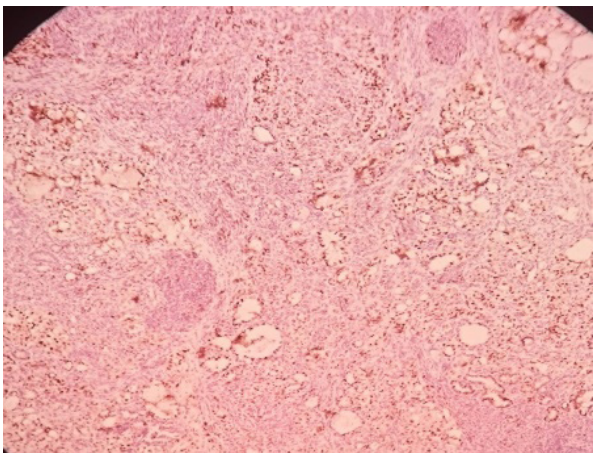

Fig. 5. Section of carcinosarcoma (100×) showing cyclin D1 positivity in epithelial components

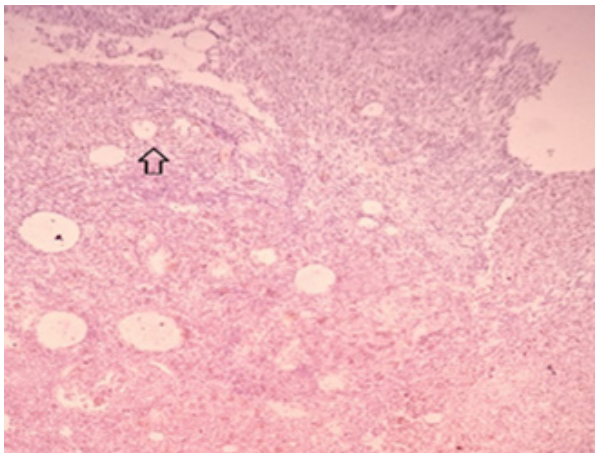

Fig. 7. Section of carcinosarcoma showing p53 immunonegativity in both components (100×)

Discussion

Mixed Müllerian tumors are classified by the WHO as carcinosarcomas, consisting of both carcinomatous and sarcomatous components. The first case was reported by Gerhardt in 1989 and later confirmed by Meyer.[5] The majority of patients diagnosed with carcinosarcoma are in the 5th decade of life. In the present study, the patient was a 53-year-old nulliparous woman.

The locations of mixed Müllerian tumors include the uterine corpus, other parts of the uterus, and extragenital sites. The most common site is the uterine body (corpus uteri), which was also the case in this study. Clinical symptoms include pain, bleeding per vaginam, and the passage of necrotic debris or material.[6] In this case, the patient presented with pain, abdominal mass/growth, and postmenopausal bleeding. There was no history of tamoxifen use or pelvic radiation therapy.

Regarding histogenesis, four theories have been proposed:

a. Collision theory – both elements originate separately and later collide.
b. Combination theory – both components arise from the same stem cell, which later undergoes divergent differentiation.
c. Composition theory – the spindle cell element represents a pseudosarcomatous reaction to carcinoma.
d. Conversion theory – the sarcomatous elements develop from the carcinomatous elements via a metaplastic process.[7]

On gross examination, the tumor may present as a polypoid, fleshy, bulky, and fragile growth, with necrosis and hemorrhage being common findings. In the present case, similar features were observed (Fig. 1).

Mixed Müllerian tumors are classified into two subtypes: homologous and heterologous.[8] The tumor is considered homologous when the sarcomatous component consists of nonspecific malignant stroma, while it is termed heterologous if the sarcomatous component contains tissues not native to the uterus, such as cartilage. The most frequent glandular component is adenocarcinoma, while the most common mesodermal component is undifferentiated sarcoma in homol-

Table 1. Comparison of immunohistochemical characteristics of carcinosarcoma reported by different researchers

S no.	Authors	Epithelial elements	Sarcoma elements	Cytokeratin	p53	Vimentin	CD10	Cyclin D1
1	Adachi Y et al.[11]	serous adenocarcinoma	homologous	positive (epith)	positive (both)	positive (sarcoma)	positive (sarcoma)	
2	Al Dallal HA et al.[12]	endometroid ca	heterologous	positive (epith)	positive (both)	-	negative (both)	
3	Dragusin RC et al.[13]	endometriod ca	homologous	positive (epith)		positive (sarcoma)	positive	positive
4	Kord A et al.[14]	endometroid ca	homologous	positive (epith)	positive (both)	positive (sarcoma)		-
5	Current study	endometroid ca with serous ca	homologous	positive (epith)	negative (both)	positive (sarcoma)	positive (sarcoma)	positive (epith)

ogous tumors and rhabdomyosarcoma in heterologous tumors.[9] The present case was diagnosed as a homologous carcinosarcoma of the uterine corpus. Immunohistochemical markers cytokeratin AE1/AE3, vimentin, CD10, cyclin D1, and p53 were applied to confirm the diagnosis.

Ahmed reported that cytokeratin, cyclin D1, and CD10 are significant immunomarkers in determining carcinosarcoma.[9] Cyclin D1, a member of the cyclin family of cell cycle regulators, is involved in tumorigenesis when mutated, and its immunohistochemical expression is useful for prognostic evaluation.[9,10] Vimentin is a cytoplasmic intermediate filament characteristic of cells of mesenchymal origin.[11] CD10 is an antibody that identifies neprilysin, useful in the diagnosis of female genital tract tumors, particularly endometrial stromal neoplasms.[9,11-13]

Mutation in the p53 tumor suppressor gene represents a common genetic alteration in human tumors. The altered mutant protein has a much longer half-life and can be detected by immunohistochemistry.[11,12,14]

Among the immunomarkers applied, AE1/AE3 cytokeratin, vimentin, and cyclin D1 were strongly positive, whereas CD10 was weakly positive. p53 was analyzed and found to be negative in both components. Several studies have shown homogeneous p53 staining in both components of uterine sarcomas. p53 immunostaining usually yields similar results in both components – it may be positive or negative in both – which supports the hypothesis of a common origin of the two components (Tab. 1).[11,12,14]

Carcinosarcoma is a rare malignant neoplasm. If a postmenopausal woman presents with bleeding per vaginam, the possibility of malignant mixed Müllerian tumor should be considered. Histopathology together with immunohistochemistry is essential to establish the correct diagnosis, which is also crucial for optimal therapeutic interventions and prognosis. Our findings further support the most widely accepted histogenesis theory, which suggests that carcinosarcoma originates through transdifferentiation of uterine carcinoma into sarcoma.

Conclusion

Carcinosarcoma of the uterus is a rare and aggressive neoplasm that primarily affects postmenopausal women. Early diagnosis is pivotal for effective management. Histopathological examination combined with immunohistochemistry is essential to exclude differential diagnoses and to confirm the tumor variant; therefore, these investigations should be performed in every case of carcinosarcoma.

Declarations

Funding

The author received no external funding.

Author contributions

Conceptualization, S.D.; Methodology, S.D.; Software, S.D.; Validation, S.D.; Formal Analysis, S.D.; Investigation, S.D.; Resources, S.D.; Data Curation, S.D.; Writing – Original Draft Preparation, S.D.; Writing – Review & Editing, S.D.; Visualization, S.D.; Supervision, S.D.; Project Administration, S.D.; Funding Acquisition, S.D.

Conflicts of interest

The author have no conflict of interest to declare.

Data availability

The data that support the findings of this study are available from the author.

Ethics approval

Not required for a case report but ethical clearance on histopathology evaluation of hysterectomies specimens was already taken (reference no.30/UPUMS/Dean/2017-18).

References

1. Tuan HX, Duc NM, Tri CM, Quyen HD, Dung PX. Carcinosarcoma of uterus. *Radiol Case Rep*. 2023;18(3):1297-1301. doi:10.1016/j.radcr.2022.12.070
2. Toboni MD, Crane EK, Brown J, et al. Uterine carcinosarcomas: From pathology to practice. *Gynecol Oncol*. 2021;162(1):235-241. doi:10.1016/j.ygyno.2021.05.003
3. Efared B, Koura HH, Bako ABA, etal . Uterine carcinosarcomas: A case series of 9 cases from a low income country. *Medicine* 2024;103:40(e39773). doi:10.1097/MD.0000000000039773
4. Garg G, Shah JP, Kumar S, Bryant CS, Munkarah A, Morris RT. Ovarian and uterine carcinosarcomas: a comparative analysis of prognostic variables and survival outcomes. *Int J Gynecol Cancer* 2010;20(5):888-894. doi:10.1111/IGC.0b013e3181dc8292.

5. Siva RD, Surendar J, Rama AS , Manjunatha HK. Malignant mixed mullerian tumor of the uterus: A case report. *IOSR Journal of Pharmacy* 2013;3(9):49-52. doi:10.9790/3013-0309-49-52
6. Tekwani DT, Joshi SR, Pathak S, Nagare M, Bihade A, Kendre D. Malignant mixed mullerian tumor of the uterus: A case report. *Ind J Basic Appl Med Res.* 2013;3:33-36.
7. McCluggage WG. Malignant biphasic uterine tumours: carcinosarcomas or metaplastic carcinomas? *J Clin Pathol.* 2002;55(5):321-325. doi:10.1136/jcp.55.5.321
8. Ho SP, Ho TH. Malignant mixed mullerian tumours of the uterus- a ten years experience. *Singapore Med J.* 2002;43(9):452-456.
9. Ahmed T, Selvi SK, Muthaiyah M, Kannan S, Arnold JAP. Uterine carcinosarcoma with heterogeneous chondrosarcomatous differentiation and bone formation: a rare case report. *IP J Diagn Pathol Oncol.* 2024;9(3):161-164. doi:10.18231/j.jdpo.2024.033
10. Montalto FI, De Amicis F. Cyclin D1 in cancer: a molecular connection for cell cycle control, adhesion, and invasion in tumor and stroma. *Cells.* 2020;9(12):2648. doi:10.3390/cells9122648
11. Adachi Y, Nonogaki H, Minamiguchi S, Li M, Ikehara S. Carcinosarcoma of the uterus: a case report. *Mol Clin Oncol.* 2016;4(4):571-573. doi:10.3892/mco.2016.744
12. Al Dallal HA, Jacobs TH, Bergman CL, et al. Uterine carcinosarcoma with heterogeneous osseous elements: a case report of an extremely rare clinical occurrence with literature review. *Front Oncol.* 2025;14(15):1505504. doi:10.3389/fonc.2025.1505504
13. Dragusin RC, Dinu M, Hodorog AD, Cismaru AFS, Tudorache S, Aron RM. Uterine carcinosarcoma: case report. *Obstetrica si Ginecologia.* 2023;4(71):174. doi:10.26416/ObsGin.71.4.2023.9130
14. Kord A, Rabiee B, Elbaz Younes I, Xie KL. Uterine carcinosarcoma: a case report and literature review. *Case Rep Obstet Gynecol.* 2020;2020:8816348. doi:10.1155/2020/8816348

Rzeszów University Press 2026
ISSN 2544-1361 (online)
doi: 10.15584/ejcem.2026.1.24

http://www.ejcem.ur.edu.pl
European Journal of Clinical and Experimental Medicine
Eur J Clin Exp Med 2026; 24 (1): 222–226

CASE REPORTS

Simultaneous cardiac and cerebral infarction – a case report

May Thu Kyaw [1,2]

[1] Heart and Vascular Center, Victoria Hospital, Yangon, Myanmar
[2] University of Medicine 2, Yangon, Myanmar

ABSTRACT

Introduction and aim. Concurrent cardiocerebral infarction (CCI) is a rare condition defined by the simultaneous presentation of acute myocardial infarction (AMI) and acute ischemic stroke (AIS). This case report aims to illustrate the clinical presentation, diagnostic challenges, and treatment considerations in a patient with CCI.

Description of the case. We describe the case of a 61-year-old Asian patient with symptoms of AMI, which was successfully treated with primary percutaneous coronary intervention (PCI). Six hours after the initial presentation, the patient developed symptoms of AIS. Imaging revealed an acute infarct in the left globus pallidus and small lacunar infarcts in the left thalamus region. Due to the location of the cerebral infarct, the patient was managed conservatively for AIS. The patient showed a positive response to the treatment, with no recurrence of chest pain or neurological symptoms observed at the six-month follow-up.

Conclusion. This case emphasizes the importance of prompt brain imaging to distinguish between different types of stroke and highlights the challenges in managing CCI, a condition linked to high mortality and morbidity. Early recognition and tailored therapy are crucial for improving prognosis.

Keywords. acute ischemic stroke, acute myocardial infarction, cardio-cerebral infarction, percutaneous coronary intervention

Introduction

Acute myocardial infarction (AMI) is diagnosed based on the presence of elevated cardiac enzymes, ischemic symptoms, ECG changes, loss of viable myocardium on non-invasive testing, or the presence of a coronary artery thrombus on angiography. Acute ischemic stroke (AIS) is characterized by the sudden onset of a focal neurological deficit caused by an acute focal injury to the central nervous system caused by arterial occlusion or thromboembolism.[1] Cardio-cerebral infarction (CCI) is a rare condition that occurs when AMI and AIS happen simultaneously. The overall prevalence of CCI is low, with few cases having been reported in the literature.[2-4]

Aim

This case report aims to illustrate the clinical presentation, diagnostic challenges, and treatment considerations in a patient with CCI.

Description of the case

A 61-year-old patient with a history of hypertension, diabetes mellitus, and stage 3A chronic kidney disease (CKD) presented to our emergency department with two hours of left-sided constricting chest pain and profuse sweating. He had no previous history of stroke or ischemic heart disease. Upon admission, vital signs were stable, with a blood pressure of 160/100 mmHg and a heart rate of 50 beats per minute. ECG showed ST elevation in leads II, III, and aVF, with reciprocal ST depression in V1–V3 (Fig. 1).

Corresponding author: May Thu Kyaw, e-mail: maythu.mtk517@gmail.com

Received: 20.06.2025 / Revised: 23.08.2025 / Accepted: 18.09.2025 / Published: 30.03.2026

Kyaw MT. Simultaneous cardiac and cerebral infarction – a case report. *Eur J Clin Exp Med.* 2026;24(1):222–226. doi: 10.15584/ejcem.2026.1.24.

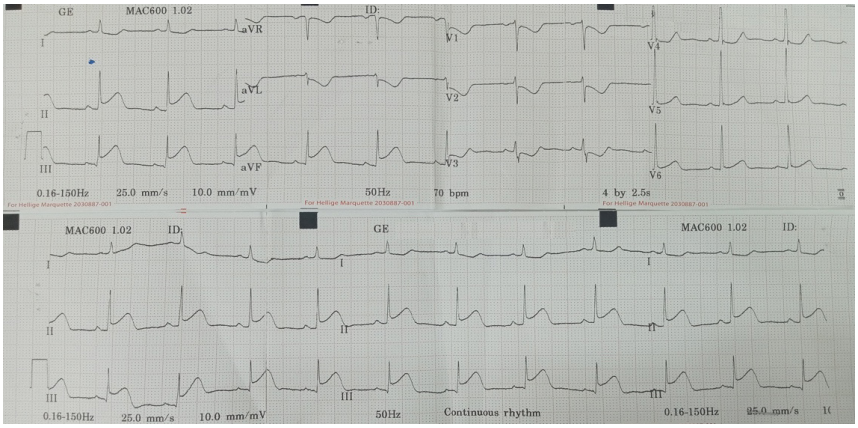

Fig. 1. ECG showed ST elevation in II, III and aVF with reciprocal ST depression in V1–V3

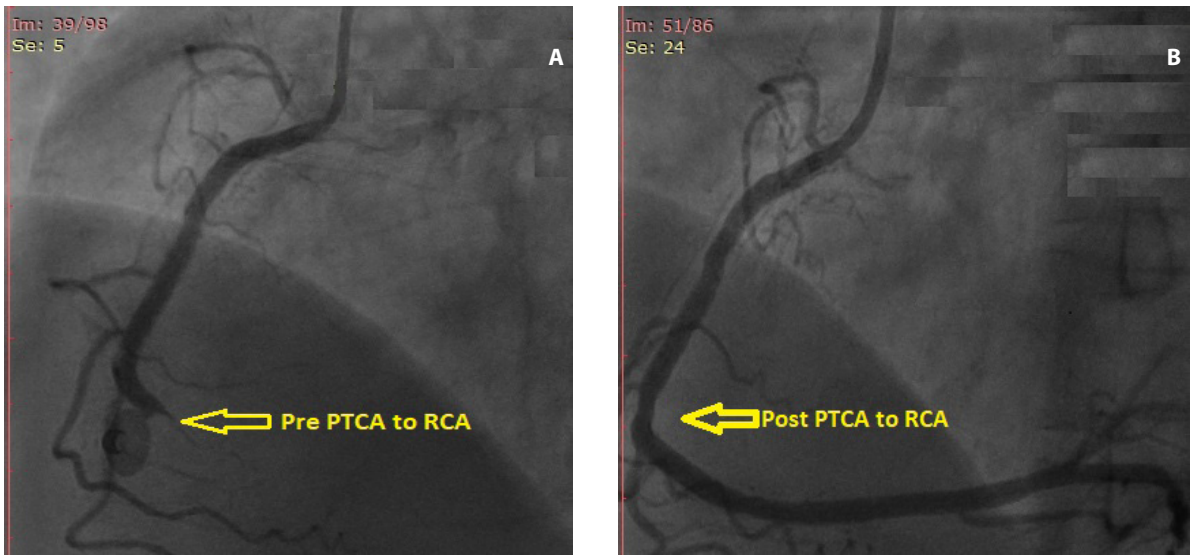

Fig. 2. A: Total occlusion of the dominant right coronary artery with thrombus, 2B: PCI to RCA-PDA with 2 DES resulting in TIMI 3 flow distally

Troponins were elevated (540 ng/mL). Coronary angiogram revealed total occlusion of the dominant right coronary artery with thrombus, while the left coronary system was normal. A JR4 6F guiding catheter and a Fielder FC 0.014-inch wire were used to access the right coronary artery, followed by balloon angioplasty using a 2.5×15 mm coronary balloon inflated to 14 atm for 5 seconds. Two sirolimus-eluting stents (DES) (3.5×27 mm and 2.75×37mm) were implanted, followed by post-dilation with an NC Accuforce 3.5×15 mm balloon at 18 atm. A final angiogram confirmed successful PCI to RCA-PDA with two DES, resulting in complete distal flow (Fig. 2A, 2B).

Six hours post- PCI, the patient suddenly developed neurological symptoms, including memory impairment, reduced consciousness, disorientation, right-sided hemiparesis, right upper motor neuron facial palsy, and a right extensor plantar response, with a National Institutes of Health Stroke Scale (NIHSS) score of 15. A magnetic resonance imaging (MRI) revealed acute ischemic lesions in the left globus pallidus and multiple small acute lacunar infarcts in the left thalamus region and lenticulostriate branches of the left middle cerebral artery (MCA) territory (Fig. 3A–D).

Given the recent AMI and infarct location, a conservative approach was taken for AIS. The patient was discharged on the seventh post-procedure day, showing gradual improvement in memory and orientation. Continuous ECG monitoring during hospitalization showed no atrial fibrillation or arrhythmias. At three- and six-month follow-ups, the patient remained well, with no recurrence of chest pain or neurological symptoms. The modified Rankin Scale (mRS) at six months was 1, indicating slight disability but overall favorable functional recovery. Serial ECGs demonstrated normal sinus rhythm without new ischemic changes.

Discussion

The term "concurrent cardio-cerebral incident (CCI)" was first introduced by Omar et al. in 2010 to describe the co-occurrence of AMI and AIS.[5] CCI can manifest as either synchronous, where both events occur simul-

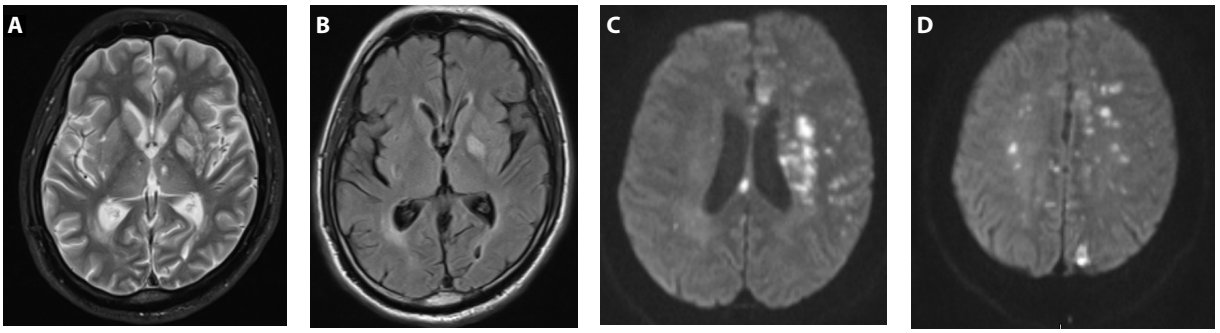

Fig. 3. A and B: Acute lacunar infarct in left globus pallidus, C and D: Small acute lacunar infarcts in left thalamus

taneously, or metachronous, where one precedes the other.[6] Type 1 CCI refers to simultaneous or within 12 hours of each other, with subcategories: type IA (cardiac factors responsible), type IB (brain-related factors), and type IC (neither cardiac nor brain-related factors). Type 2 involves AIS within 4.5 hours of recent AMI, but more than three hours after onset. Type 3 CCI involves AMI within 12 hours of recent AIS, but more than 4.5 hours after AIS.[7] Our case fits into Type 1 CCI, with symptoms of AIS six hours after MI onset.

The prevalence of CCIs varies from 0.009% to 0.29% with AIS following AMI occurring in 0.7% to 2.2% of hospitalized patients with peak occurrence in the early days post-AMI, but remains elevated for up to 12 weeks post-MI.[1,2,7,8] A single-center study by Olivier Hachet found that most stroke and TIAs occur within the first five days post-AMI, with 52.8% occurring on the first day and 87% within five days.[9] In our case, the development of neurological symptoms within six hours post-PCI highlights this early period and emphasizes the need for vigilance in the immediate post-revascularization phase. In addition, studies by Chin et al. and Yeo et al. have demonstrated that 6-12.7% of patients with acute stroke have a history of recent AMI.[6,10] A retrospective study revealed that among over 11 million patients hospitalized for AMI between 2000 and 2017, 1.6% developed AIS within 24 hours.[3] CCIs are associated with high mortality; meta-analyses report in-hospital mortality of 33.3% and a three-month mortality of 49.2%.[11]

The overlap of risk factors such as hypertension, hypercholesterolemia, smoking, diabetes, and advanced age contributes to both conditions via inflammation and atherosclerosis.[12] Our patient's hypertension, diabetes, and CKD likely contributed both coronary and cerebral artery disease. The pathophysiology of CCI involves mechanisms like intra-cardiac thrombogenesis due to coronary vasospasm, ventricular dysfunction, atrial fibrillation, and type A aortic dissection, as well as thrombotic viral infections, like COVID-19.[1,4,13] Cardiomyopathies, such as left ventricular non-compaction, predispose to intra-cardiac thrombus and systemic embolization.[14] Furthermore, right ventricular infarction or extensive MI complicated by cardiogenic shock can rapidly compromise hemodynamics, leading to watershed brain infarction (hemodynamic stroke) in patients with a prolonged history of hypertension.[5]

Management of CCIs requires a multidisciplinary approach. Prompt brain imaging is essential to determine stroke type; MRI is often necessary when CT is inconclusive, as seen in our case.[15] In metachronous CCIs, treatment focuses on the initial event. Both conditions carry high mortality and narrow therapeutic windows, so delays can worsen outcomes. Furthermore, thrombolytic therapy for AIS may increase the risk of cardiac rupture post-MI, although two large studies (SMART and SITS-MOST) show no significant difference.[16] The use of anticoagulants and antiplatelet agents during PCI may also increase the risk of thrombolysis-associated hemorrhagic conversion in AIS. Therefore, individualized treatment plans are vital.

The American Heart Association/American Stroke Association (AHA/ASA) recommends that stable patients with hyperacute CCI without contraindications receive IV alteplase followed by PCI (Class IIa: level of evidence C).[17] However, the 2019 European Stroke Organization (ESO) guidelines advise against IV alteplase within 4.5 hours in patients with recent MI; instead, mechanical thrombectomy and PCI are recommended.[18] Our conservative approach was guided by infarct location, size, and bleeding risk, with mechanical thrombectomy contraindicated due to the infarct's deep location, and thrombolysis avoided because of recent MI. Instead, we prioritized dual antiplatelet therapy and supportive care, leading to neurological improvement.

In CCIs, dual antiplatelet therapy (DAPT) should continue for 12 months, then transition to single antiplatelet therapy (SAPT) for life. When cardioembolic stroke accompanies CCI, especially with atrial fibrillation, triple therapy (aspirin, clopidogrel, and a non-vitamin K oral anticoagulant, NOAC or warfarin) is recommended for one week, then dual therapy (SAPT and NOAC) for 6–12 months, depending on bleeding risk. Long-term, single-agent therapy is advised. The MIRACL study and GRACE registry have shown that early high-intensity statins reduce recurrent non-fatal

ischemic stroke in AMI, by lowering low-density lipoprotein cholesterol (LDL-C) by over 50%, aiming for levels below 1.4 mmol/L (55 mg/dL).[7]

Key clinical messages

- CCI needs timely recognition and a team-based approach due to the challenges posed by simultaneous AMI and AIS.
- Immediate brain imaging, especially MRI, is crucial for diagnosing AIS after AMI, guiding treatment decisions and outcomes.
- Treatment should be personalized based on the timing and type of infarcts, while carefully weighing thrombolysis risks.
- Ongoing monitoring and follow-up are important as patients may gradually improve in neurological function after CCI despite initial severity.
- Increasing clinician awareness of CCI can enhance early detection and improve management, reducing mortality and morbidity rates.

Conclusion

Concurrent CCI is a rare and complex condition requiring a multidisciplinary approach. Prompt brain imaging is critical for accurate diagnosis. In this case, conservative stroke management was chosen due to cerebral infarct location, which contraindicated mechanical thrombectomy. The patient was maintained on DAPT for 12 months, then transitioned to SAPT. Early recognition and management are vital to reduce high mortality and morbidity. Despite progress, gaps remain in evidence-based guidelines for managing CCI, particularly concerning the timing and choice of thrombolytic and revascularization strategies. Further research should focus on establishing standard guidelines through large-scale prospective studies for better patient outcomes.

Declarations

Funding

This study received no financial support.

Author contributions

Conceptualization, M.T.K.; Validation, M.T.K.; Formal analysis, M.T.K.; Investigation, M.T.K.; Resources, M.T.K.; Data curation, M.T.K.; Writing – Original Draft Preparation, M.T.K.; Writing – Review & Editing, M.T.K.

Conflicts of interest

There are no conflicts of interest.

Data availability

No new data generated.

Ethics approval

This case report does not require ethical approval because it is not considered human subject research.

References

1. Habib M. Cardio-Cerebral infarction syndrome: definition, diagnosis, pathophysiology, and treatment. *J Integr Cardiol*. 2021;7. doi:10.15761/JIC.1000308
2. Lee J, Choi WY, Park GT, Park KT, Jeong HB, Won H. Concurrent Acute Ischemic Stroke and Myocardial Infarction Associated With Atrial Fibrillation. *JACC Case Rep*. 2024;29(1):102145. doi:10.1016/j.jaccas.2023.102145
3. Bao CH, Zhang C, Wang XM, Pan YB. Concurrent acute myocardial infarction and acute ischemic stroke: Case reports and literature review. *Front Cardiovasc Med*. 2022;9:1012345. doi:10.3389/fcvm.2022.1012345
4. Khairy M, Lu V, Ranasinghe N, Ranasinghe L. A case report on concurrent stroke and myocardial infarction. *Asp Biomed Clin Case Rep*. 2021;4(1):42-49. doi:10.36502/2021/ASJBCCR.6227
5. Bao CH, Zhang C, Wang XM, Pan YB. Concurrent acute myocardial infarction and acute ischemic stroke: Case reports and literature review. *Front Cardiovasc Med*. 2022;9:1012345. doi:10.3389/fcvm.2022.1012345
6. Yeo LLL, Andersson T, Yee KW, et al. Synchronous cardiocerebral infarction in the era of endovascular therapy: which to treat first?. *J Thromb Thrombolysis*. 2017;44(1):104-111. doi:10.1007/s11239-017-1484-2
7. Habib M. Cardio-Cerebral Infarction Syndrome: An overview. *Int J Clin Case Rep Rev*. 2021;8(1). doi:10.31579/2690-4861/140
8. Merkler AE, Diaz I, Wu X, et al. Duration of Heightened Ischemic Stroke Risk After Acute Myocardial Infarction. *J Am Heart Assoc*. 2018;7(22):e010782. doi:10.1161/JAHA.118.010782
9. Hachet O, Guenancia C, Stamboul K, et al. Frequency and predictors of stroke after acute myocardial infarction: specific aspects of in-hospital and post-discharge events. *Stroke*. 2014;45(12):3514-3520. doi:10.1161/STROKEAHA.114.006707
10. Chin PL, Kaminski J, Rout M. Myocardial infarction coincident with cerebrovascular accidents in the elderly. *Age Ageing*. 1977;6(1):29-37. doi:10.1093/ageing/6.1.29
11. Habib M, Alhout S. Concurrent cardio-cerebral infarction: Meta-analysis. *Mathews J Case Rep*. 2023;8(2):87. doi:10.30654/MJCR.10087
12. Lichtman JH, Krumholz HM, Wang Y, Radford MJ, Brass LM. Risk and predictors of stroke after myocardial infarction among the elderly: results from the Cooperative Cardiovascular Project. *Cir-*

culation. 2002;105(9):1082-1087. doi:10.1161/hc0902.104708
13. Chiang CH, Hung WT, Huang WC, et al. The risk of stroke after acute myocardial infarction in patients with and without atrial fibrillation: A nationwide cohort study. *J Chin Med Assoc*. 2021;84(12):1126-1134. doi:10.1097/JCMA.0000000000000631
14. Abdi IA, Karataş M, Abdi AE, Hassan MS, Yusuf Mohamud MF. Simultaneous acute cardio-cerebral infarction associated with isolated left ventricle non-compaction cardiomyopathy. *Ann Med Surg (Lond)*. 2022;80:104172. doi:10.1016/j.amsu.2022.104172
15. Powers WJ, Rabinstein AA, Ackerson T, et al. 2018 Guidelines for the Early Management of Patients With Acute Ischemic Stroke: A Guideline for Healthcare Professionals From the American Heart Association/American Stroke Association. *Stroke*. 2018;49(3):e46-e110. doi:10.1161/STR.0000000000000158
16. Akinseye OA, Shahreyar M, Heckle MR, Khouzam RN. Simultaneous acute cardio-cerebral infarction: is there a consensus for management?. *Ann Transl Med*. 2018;6(1):7. doi:10.21037/atm.2017.11.06
17. Powers WJ, Rabinstein AA, Ackerson T, et al. Guidelines for the Early Management of Patients With Acute Ischemic Stroke: 2019 Update to the 2018 Guidelines for the Early Management of Acute Ischemic Stroke: A Guideline for Healthcare Professionals From the American Heart Association/American Stroke Association. *Stroke*. 2019;50(12):e344-e418. doi:10.1161/STR.0000000000000211
18. Berge E, Whiteley W, Audebert H, et al. European Stroke Organisation (ESO) guidelines on intravenous thrombolysis for acute ischaemic stroke. *Eur Stroke J*. 2021;6(1):I-LXII. doi:10.1177/2396987321989865

Rzeszów University Press 2026
ISSN 2544-1361 (online)
doi: 10.15584/ejcem.2025.1.25

http://www.ejcem.ur.edu.pl
European Journal of Clinical and Experimental Medicine
Eur J Clin Exp Med 2026; 24 (1): 227–233

CASE REPORTS

Floating-Harbor syndrome – case report with literature review

Trifon T. Popov [1], Natasha Y. Yaneva [2]

[1] Medical Faculty, Medical University, Sofia, Bulgaria
[2] Clinic for Endocrinology, Diabetes and Metabolism, University Children's Hospital, Medical University of Sofia, Sofia, Bulgaria

ABSTRACT

Introduction and aim. Floating-Harbor syndrome (FHS) is a very rare disease, whose typical characteristics include short stature, facial dysmorphic features and significant speech delay. We aim to present the first reported case of FHS with discordant growth hormone tests and confirmed hypoplasia of the pituitary gland.

Description of the case. We report a case of a boy aged 8 years and 3 months with a height constantly below the 3rd percentile, delayed bone age in comparison to chronological age, typical dysmorphic triangular face and a high-pitched voice. Whole-exome sequencing (WES) detected a heterozygous pathogenic variant in SRCAP gene – a confirmation of the diagnosis Floating-Harbor syndrome (FHS). Recombinant human growth hormone (rhGH) therapy at a dose of 0.033 mg/kg/day (0.65 mg/day) was initiated at the age of 7 years and 10 months. Because of the insufficient growth velocity at the time of manuscript preparation a dose increase was made to 0.035 mg/kg/day (0.80 mg/day).

Conclusion. In children presenting with short stature (especially when GH deficiency is confirmed), facial dysmorphism and developmental delay, Floating-Harbor syndrome should be considered as a possible diagnosis. A multidisciplinary approach involving pediatric endocrinologists, geneticists and developmental specialists is essential for timely etiological diagnosis and optimal management.

Keywords. Floating-Harbor syndrome, recombinant human growth hormone treatment, short stature

Introduction

Floating-Harbor syndrome (FHS) is a rare genetic disorder, with approximately one hundred documented cases in the scientific literature worldwide.[1] This syndrome derives its name from the names of the hospitals in the United States (Boston Floating Hospital and Harbor General Hospital in California), where the first cases were reported (unlike the majority of the genetic diseases that are named after the physicians who initially described them).[1] FHS is attributed mainly to a point mutation (frameshift or nonsense mutation) in the SRCAP gene, which is located on the short arm of 16 chromosome 16p11.2 and encodes the central catalytic subunit of the SNF2-Related CBP Activator Protein (SRCAP).[2] This protein is an ATPase that modulates gene expression by chromatin remodeling and interaction with transcription activators (CREBBP/CBP).[2] Pathogenic variants in SRCAP gene are located in exons 33 or 34 and, in the most cases, arise de novo, although rare examples of autosomal dominant inheritance have been reported in familial cases.[3]

The clinical phenotype of FHS is the characteristic triad: short stature, severe language developmental delay, as well as typical facial dysmorphologies.[1] Height is persistently below the 3rd percentile and is attributed to the growth hormone (GH) deficiency.[1] Bone age lags

Corresponding author: Trifon T. Popov, e-mail: 102268@students.mu-sofia.bg

Received: 25.09.2025 / Revised: 30.11.2025 / Accepted: 10.12.2025 / Published: 30.03.2026

Popov TT, Yaneva NY. Floating-Harbor syndrome – case report with literature review. *Eur J Clin Exp Med.* 2026;24(1):227–233. doi: 10.15584/ejcem.2026.1.25.

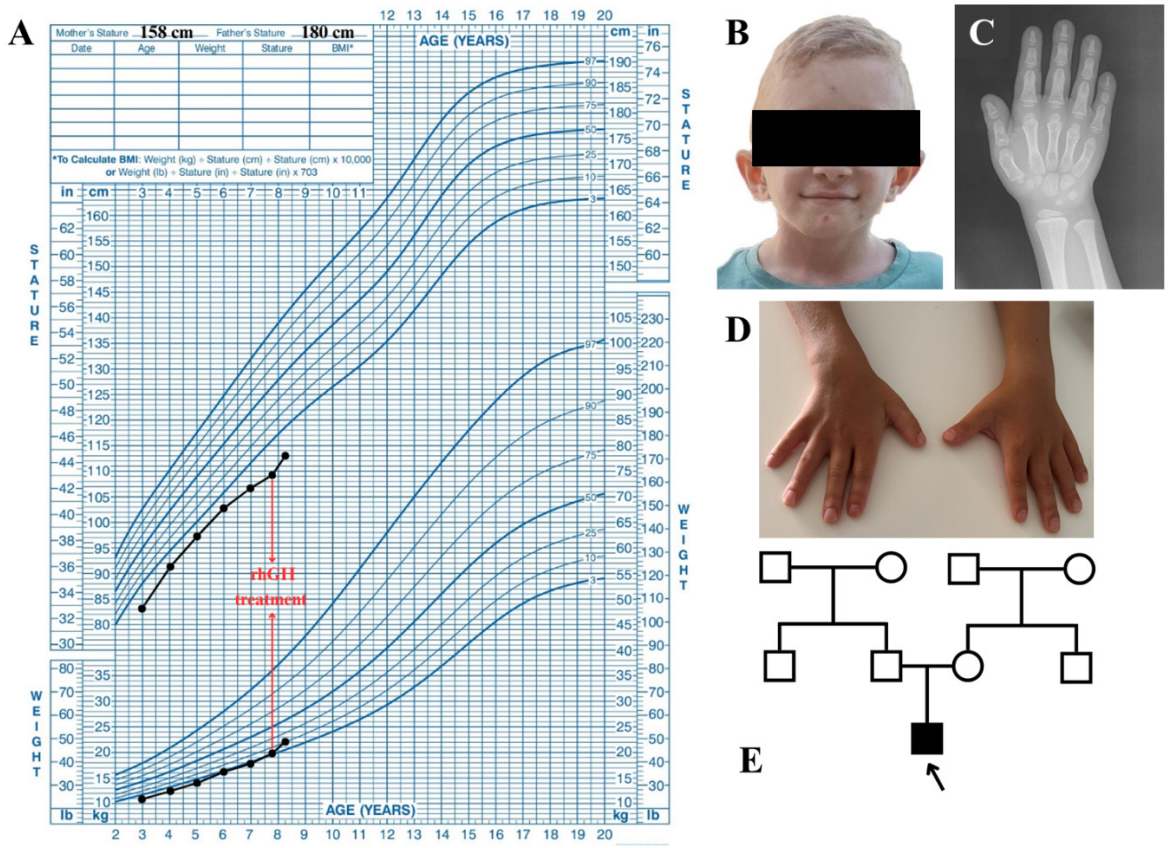

Fig. 1. Characteristics of the patient: A: Growth chart from the age of 3 years to present, B: Triangular dysmorphic face of the child, C: Radiography of the left forearm – a bone age of 4 years and 6 months (2 years and 7 months behind patient's chronological age), D: Small hands with hypertrophy of the distal phalanges of the fingers and prominent nail plates, E: Family tree confirming the de novo emergence of the pathogenic variant

behind chronological age.[1] The typical facial features of FHS patients are a triangular facial shape, deep-set eyes, a prominent nasal bridge with a broad nose and enlarged nostrils, a short philtrum, and a wide mouth with thin upper and lower lips. Some patients may also have dental anomalies, such as delayed eruption of primary and permanent teeth, microdontia and others.[1] While motor development is generally normal, neuro-psychic and language development are delayed. The voice is also specific – screaming (more pronounced during laughing or crying). Skeletal abnormalities – such as brachydactyly, clinodactyly, vertebral anomalies, additional rib, short neck, etc. – can be seen in some patients with FHS.[4] Another less common clinical manifestations may include cardiac, sensory (hearing, eye), genitourinary, gastrointestinal anomalies.[4] This rare disease may present with behavioral challenges, including attention-deficit/hyperactivity disorder (ADHD) and learning difficulties.[4] The diagnosis of Floating-Harbor syndrome is based primarily on clinical evaluation and can be confirmed through molecular genetic analysis, specifically whole exome sequencing (WES) or targeted sequencing of SRCAP gene, which reveals a heterozygous pathogenic variant in exon 33 or 34.[2,4]

Aim

The purpose of this case report is to describe the first reported case of Floating-Harbor syndrome with discordant GH tests and MRI confirmed pituitary hypoplasia.

Description of the case

The patient is a male aged 8 years and 3 months, born from a first, complicated pregnancy of a mother with type 1 diabetes and Hashimoto's thyroiditis, with inadequate glycemic control during pregnancy and under therapy with L-thyroxin. A course of indomethacin was administered in the 7th lunar month due to polyhydramnios. Delivery occurred at term via cesarean section. The newborn's weight was 4170 g (+1.23 SDS) and length of 56 cm (+2.16 SDS), in asphyxia requiring resuscitation in the delivery room, oxygen therapy, antibiotics and phototherapy. A persistent foramen ovale with left-to-right shunt was established. The patient is regularly immunized.

Since the age of 3 years, the patient has constantly grown below the prognostic stature (175,5 cm, -0.37 SDS), calculated as (mother's height + father's height + 13)/2. As shown on the height and weight growth charts (Fig. 1A), the growth curve lies below the 3rd percen-

tile. At the age of 3 years and 2 months, he was evaluated by a psychologist who reported slightly delayed speech development and coefficient of development 86 (low-normal range) was reported. Due to the dysmorphic features and delays in physical and cognitive development, karyotyping and MLPA testing for microdeletions, subtelomeric deletions, and duplications were performed, with no abnormalities found. At 4 years and 5 months, the patient's height and weight were (-3.07 SDS), his bone age was 2 years and 6 months (delay of 1 year and 11 months from calendar) and the level of insulin-like growth factor-1 (IGF-1) was 118.0 ng/mL (-0.08 SDS). Hypermetropia was identified and corrected with spectacles: right eye +4.5 diopters spherical, left eye +4.5 diopters spherical.

Table 1. Laboratory analyses before and 6 months after rhGH treatment

Parameter	Results before rhGH therapy	Results after rhGH therapy	Units	Reference range
Fasting glucose	4.89	4.76	mmol/L	4.11–5.89
HbA_{1c}	5.27	5.20	%	4.0–5.7
Total cholesterol	4.14	3.79	mmol/L	<5.2
LDL	2.60	2.00	mmol/L	<3.5
HDL	1.19	1.09	mmol/L	>0.9
ASAT	23.0	20.9	U/L	10–46
ALAT	17.0	13.2	U/L	5–37
GGT	15.0	12.0	U/L	5–31
Albumin	45.24	45.3	g/L	32–55
TSH	3.51	3.82	mIU/L	0.58–4.1
fT4	16.7	17.2	pmol/L	9.5–16.5
MAT	<10.0	<10.0	IU/mL	<35.0
TAT	<20.0	<20.0	IU/mL	<40.0
IGF-1	84.8	208.0	ng/mL	40–255

The patient was not followed up until the age of 7th year 1 month, when he was admitted to the Endocrinology Department. During the physical examination, a typical facial phenotype was observed: triangular, with a sharp chin, convergent strabismus, deep-set eyes, broad bridge and root of the nose, smooth glabella, prominent forehead, sparse hair with thin strands; low-set and dysmorphic ears (Fig. 1B). His height was 106.4 cm (–2.98 SDS), while his weight was 17.6 kg (–2.26 SDS). Bone age, determined via wrist X-ray, was 4 years and 6 months – even a greater delay of 2 years and 7 months (Fig. 1C). Despite ongoing support from a speech and language therapist, psychologist and special education teacher, the patient's language and speech development remained delayed. The child's hands and feet appeared slightly small with hypertrophy of the distal phalanges of the fingers and prominent nail plates (Fig. 1D). A slightly screaming voice can be detected during crying and laughing. From laboratory tests (CBC, biochemistry, thyroid hormones, morning and evening cortisol, electrolytes), all values were within reference range (Table 1), only the IGF-1 concentration was 84.8 ng/mL (–1.41 SDS).

Two stimulation tests (Fig. 2) for growth hormone were performed (with arginine hydrochloride 8.8 g i.v. for 30 minutes and glucagon 0.6 mg i.m.) with opposite results. In the arginine test, the peak GH level at 60 minutes was 16.5 ng/mL (normal response), whereas in the glucagon test, the peak GH plasma concentration at 90 minutes was 5.67 ng/mL (insufficient response).

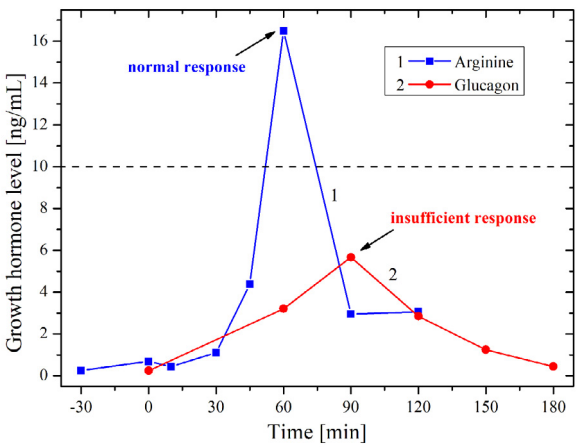

Fig. 2. Plasma concentration of growth hormone (ng/mL) over the time (min) during the stimulation tests with arginine hydrochloride (blue curve 1) and glucagon (red curve 2), the results are discordant: normal response in the arginine test (with peak GH value over 10.0 ng/mL) and insufficient response in the glucagon test (peak GH level below 10.0 ng/mL)

Therefore, MRI of the hypothalamus-pituitary were performed, revealing mild hypoplasia of the pituitary gland – a height of ≈4.6 mm (norm 6 mm), without any hypointense areas suspected for adenomas. Considering the short stature, combined with significant bone age delay, the dysmorphic facies as well as the speech and language delay, the decision for whole-exome sequencing (WES), using the next-generation sequencing (NGS) platform NovoSeq6000/Illumina, was undertaken. The results disclosed a heterozygous pathogenic variant c.7330C>T (pArg2444Ter) in exon 34 of the SRCAP gene on short arm of chromosome 16. This is the most common pathogenic variant in SRCAP gene in the literature and along with the typical clinical presentation confirmed the diagnosis Floating-Harbor syndrome (FHS). The pathogenic variant emerges de novo like in the majority of the already described cases (Fig. 1e). Considering the short stature, notable delayed bone age, as well as the MRI finding and the results from the glucagon stimulation test, a treatment with 0.033 mg/kg/day (0.65 mg/day) of recombinant human growth hormone (rhGH) subcutaneously in the evening was initiated at the age of 7 years and 10 months. At the time of preparation of

the manuscript, the child has been under this treatment for 6 months and has increased his height by 3.3 cm and gained weight by 3 kg (Table 2). The dose of the rhGH has been increased to 0.035 mg/kg/day (0.80 mg/day) s.c. During ophthalmologic evaluation, visual acuity was 0.3 in the right eye (VOD) and 0.3 in the left eye (VOS). Fundoscopy revealed normal findings in both eyes. The optic discs appeared vital with clear margins; retinal vessels and retina showed no abnormalities. Abdominal ultrasonography showed no abnormalities.

Table 2. Dynamics of patient's height, weight, IGF-1 levels and bone age[a]

Calendar age (years months)	Height		Weight		IGF-1 levels before application		Bone age (years months)
	(cm)	(SDS)	(kg)	(SDS)	(ng/mL)	(SDS)	
3y 2m	83.5	–3.54	11.0	–2.79	–	–	–
4y 5m	91.5	–3.07	12.6	–2.88	118.0	–0.08	2y 6m
5y*	96.0	–2.74	14.0	–2.42	–	–	–
6y*	102.5	–2.54	15.7	–2.31	–	–	–
7y 1m	106.4	–2.98	17.6	–2.26	84.8	–1.41	4y 6m
7y 9m	109.2	–3.14	19.5	–1.91	188	+0.23	5y 2m
8y 3m	112.5	–2.99	22.5	–1.11	208	+0.52	5y 10m

[a] * – these values are given from the patient's parent, not measured by a physician

Discussion

FHS is a rare genetic disease that is associated with a short stature (usually below the 3rd percentile), lag in the bone age (often 1–3 years compared to chronological age), triangular dysmorphic face, as well as skeleton abnormalities such as short arms and legs, brachydactyly or clinodactyly, deficit in speech and language development. FHS is a result of frameshift or nonsense mutations in exons 33 or 34 of SRCAP gene, located on the short arm of chromosome 16 (16p11.2). SRCAP gene encodes an ATPase (catalytic subunit of SNF2-Related CBP activator protein), which plays a key role in chromatin remodeling and gene expression.

Management of FHS is symptomatic and multidisciplinary, involving growth hormone therapy for the short stature, language and speech support, as well as educational and developmental support. The use of recombinant human growth hormone (rhGH) dates back from 2001, and to date, there are 35 patients in the literature with FHS treated with rhGH, showing variable responses (Table 3). The typical dosage of rhGH is in the range of 0.025-0.060 mg/kg/day (most commonly 0.030–0.035 mg/kg/day). No clear correlation can be established between rhGH dose and final height, since the response to the treatment is highly individual. Most published cases report marked bone age delays, though the magnitude of delay varies widely. The duration of the treatment is also different in the reported patients, but almost everyone has a satisfactory response to the rhGH application which can be concluded from the increase in the growth velocity and concentration of insulin-like growth factor-1 (IGF-1), as well as the reduction in the difference between the calendar and bone age (which is again strongly individual and not directly connected to the dose and duration of the rhGH treatment).

In contrast to the published cases of patients with FHS, who are typically small for the gestational age, our patient was born large for the gestational age which is likely attributed to the maternal diabetes type 1 which was poorly controlled during the pregnancy. Maternal hyperglycemia results in increased fetal blood glucose, leading to fetal hyperinsulinemia and consequently increased growth. Another unusual finding in this case was the inconsistency of growth hormone stimulation test results – a normal response to the arginine test, and insufficient response to the glucagon test). As a result, an MRI of the hypothalamus-pituitary gland was performed to confirm GH deficiency.

In our patient, the growth velocity is 3.3 cm for the 6 months of rhGH treatment (6.6 cm/year), which is 44.1% higher than the speed velocity from patient's 3rd to 7th year (4.58 cm/year). The bone age at the start of the treatment was 5 years and 2 months (the difference (ΔA) between bone age (BA) and calendar age (CA): ΔA=BA–CA is minus (–) 2 years and 8 months), while this difference 6 months later is (–) 2 years and 6 months. The level of IGF-1 is an important marker whose levels must be monitored before and after the start of the rhGH treatment. Low level of IGF-1 combined with a pathological response to GH stimulation tests (such as arginine, clonidine, glucagon, etc.) are laboratory indicators for GH deficiency and initiation of substitution therapy. When IGF-1 concentration remains at the lower range during the rhGH treatment, the dosage must be elevated and if IGF-1 concentration remained low despite the dose increase, then IGF-1 resistance can be the reason. In case of elevated IGF-1 levels, the dosage must be reduced in order to prevent the onset of side effects.

Monitoring patients undergoing rhGH therapy requires clinical examinations approximately every 6 months to assess height, weight, and bone age. Additionally, IGF-1 levels, lipid profile (total cholesterol, LDL, HDL), glucose and glycated hemoglobin levels (HbA_{1c}), thyroid status (TSH, fT4), and blood pressure should also be monitored. Regular ophthalmological examinations (including visual acuity assessment and fundoscopy) are also recommended. In the present case, there were no changes in these parameters within 6 months of therapy (Table 1), nor did the patient have any subjective complaints about the treatment. The IGF-1 concentration on the 6th month after the initiation of rhGH treatment is 208.0 ng/mL (0.52 SDS), still well below the targeted around + 2.0 SDS and along with the suboptimal growth velocity (6.6 cm/year), still significant bone age delay

Table 3. Characteristics of patients with FHS treated with rhGH*

	Dosage of rhGH (mg/kg/day)	Age at rhGH treatment start (years months)	Height at rhGH treatment start		Bone age rhGH treatment start		Duration of rhGH application (months)	Height at the time of report		Bone age at the time of report		IGF-1 levels before application		IGF-1 levels at the time of report		Reference
			(cm)	(SDS)	(years months)	ΔA		(cm)	(SDS)	(years months)	ΔA	(ng/mL)	(SDS)	(ng/mL)	(SDS)	
1	0.040	5y 3m	77.0	–3.00	remarkably delayed		3y 7m	129.0	–1.90	7y 9m	–1y 1m	–	–	–	–	[5]
2	0.030	9y 1m	113.9	–2.90	5y 5m	–3y 8m	1y 6m	130.2	–1.90	8y 4m	–2y 3m	138	–0.60	395	+1.70	[6]
3	0.030	10y 1m	126.2	–2.23	9y 10m	–0y 3m	7y 4m	156.1	–1.20	–	–	99.8	–1.57	–	–	[7]
4	–	7y	–	–	–	–	6m	115.0	–4.32	–	–	–	–	–	–	[8]
5	–	4y	–	–	–	–	7y	129.0	–2.84	–	–	–	–	–	–	[8]
6	–	5y	–	–	–	–	2y	106.9	–2.90	–	–	–	–	–	–	[8]
7	–	10y	–	–	–	–	2y	154.5	–2.95	–	–	–	–	–	–	[8]
8	–	4y	–	–	–	–	12y	155.0	–2.89	–	–	–	–	–	–	[8]
9	–	5y	–	–	–	–	6y	117.0	–4.00	–	–	–	–	–	–	[8]
10	–	5y	–	–	–	–	3y	123.0	–0.90	–	–	–	–	–	–	[8]
11	0.035	5y 4m	99.0	–3.84	3y 0m	–2y 4m	2y 3m	112.5	–2.22	8y 0m	+0y 5m	–	–	–	–	[9]
12	0.025–0.050	3y 5m	85.0	–3.11	2y 0m	–1y 5m	5y 1m	116.4	–2.40	concordant with CA		68.0	–0.48	–	+1.0	[10]
13	–	3 y	–	–2.50	delayed		3y 0m	–	–2.00	–	–	–	–	–	–	[11]
14	–	5y	–	–3.20	delayed		9y 0m	154.0	–1.80	–	–	–	–	–	–	[11]
15	–	5y 4m	–	–3.40	delayed		–	–	–1.70	–	–	–	–	–	–	[11]
16	0.033	10 y	107.8	–4.90	5y 0m	–5y 0m	2y	137.0	–3.60	12y 0m	0	–	–	–	–	[12]
17	0.050	5y 2m	92.5	–4.52	3y 5m	–1y 10m	1y	98.0	–4.40	–	–	–	–	–	–	[13]
18	0.057	2y	74.7	–3.62	0y 9m	–1y 3m	0y 1m	–	–	–	–	–	–	49.2	–0.70	[13]
19	0.057	4y 10m	92.3	–4.12	2y 9m	–2y 1m	4y 2m	120.5	–2.56	–	–	–	–	–	–	[13]
20	0.025	5y	93.8	–3.84	2y 6m	–2y 6m	1y 7m	103.4	–3.49	–	–	–	–	163.0	+0.64	[13]
21	0.067	6y 6m	95.0	–5.30	2y 6m	–4y 0m	4y 3m	119.0	–3.86	–	–	–	–	343.0	+0.96	[13]
22	0.050	5y 2m	92.7	–4.47	delayed		4y 3m	118.0	–3.31	–	–	–	–	141.0	–1.01	[13]
23	0.050	1y 5m	68.5	–4.17	delayed		2y 2m	88.6	–2.96	–	–	–	–	56.5	–0.84	[13]
24	0.042	2y 3m	75.0	–4.17	1y 1m	–1y 2m	0y 3m	77.9	–3.81	–	–	–	–	86.5	+0.37	[13]
25	0.050	4y 11m	–	–3.10	2y 10m	–2y 1m	8y 1m	–	–1.10	–		–	+0.3	–	+1.7	[14]
26	0.050	4y 3m	–	–3.40	3y 1m	–1y 2m	2y 9m	–	–2.60	–	–	–	+1.6	–	+3.3	[14]
27	0.050	7y 11m	–	–3.00	3y 7m	–4y 4m	2y 6m	–	–2.00	–	–	–	+2.1	–	+2.6	[14]
28	0.050	10y 5m	–	–2.10	9y 4m	–1y 1m	4y 2m	–	–2.50	–	–	–	+4.2	–	+3.9	[14]
29	0.050	8y	112.8	–3.33	delayed		4y 7m	141.3	–2.70	concordant with CA		223.1	–0.52	–	–	[15]
30	0.043	6y 9m	100.0	–4.50	3y 9m	–3y 0m	0y 6m	106.3	–3.69	–	–	95.9	–1.15	257.0	+1.35	[16]
31	0.033	3y 6m	81.0	–3.60	1y 3m	–2y 3m	0y 6m	83.5	–4.11	–	–	108.0	+0.60	–	–	[17]
32	0.030–0.035	4y 5m	86.0	–4.11	1y 3m	–3y 2m	11y 10m	150.2	–3.28	concordant with CA		–	–	540.0	+1.0	[2]
33	0.030	2y 2m	78.2	–3.40	1y 3m	–0y 11m	3y 8m	104.0	–2.76	2y 11m	–2y 11m	–	–	–	–	[18]
34	0.045–0.060	4y	83.4	–4.63	delayed		9y 4m	141.9	–2.50	–	–	55.3	–1.02	–	–	[19]
35	0.040	2y 1m	73.0	–4.79	1y 0m	–1y 1m	3y 2m	100.0	–	–	–	172.0	+1.74	–	–	[20]
36	0.033–0.035	7y 9m	109.2	–3.14	5y 2m	–2y 8m	0y 6m	112.5	–2.99	5y 10m	–2y 6m	188.0	+0.23	208.0	+0.52	present case

* ΔA – difference between bone and calendar age (ΔA=BA–CA)

(ΔA=-2 years and 6 months) and the lack of any significant side effects from the rhGH treatment, a decision to slightly increase in the dose of rhGH is made: from 0.033 mg/kg/day (0.65 mg/day) to 0.035 mg/kg/day (0.80 mg/day) s.c. The patient will continue to be monitored every 6 months while being on rhGH treatment.

Patient perspective

The family expressed gratitude for reaching a definitive diagnosis and for the initiation of rhGH therapy. Since the beginning of the replacement therapy and with the help of the speech and language therapist, the physical and mental development of their child have improved noticeably. The patient feels better which makes the parents calmer. They report no difficulties with the therapy and acknowledge the importance of the regular follow-up.

Conclusion

FHS is a rare disorder, which must be considered in children presenting with proportional short stature, dysmorphic facial features (including a triangular face shape, deep-set eyes, and a prominent nose) and marked speech and language delay. In the presence of this classical clinical triad for FHS, target sequencing of the SRCAP gene can be suggested as the first-line molecular diagnostic test. In cases with atypical or incomplete clinical manifestations, a broader next-generation sequencing (NGS) panel must be considered, including SRCAP and other genes associated with short stature, language delay, and facial dysmorphism such as CREBBP, EP300, KMT2D, KDM6A, NIPBL, SMC1A, SMC3 and others, in order to differentiate FHS from other syndromes (such as Rubinstein-Taybi syndrome, Cornelia de Lange syndrome, Kabuki syndrome, and others).

Management of patients with FHS involves a multidisciplinary team consisting of endocrinologists, geneticists and developmental specialists. In cases with confirmed growth hormone deficiency, therapy with recombinant human growth hormone (rhGH) is indicated, typically at a dose between 0.030-0.040 mg/kg/day, with close monitoring of insulin-like growth factor-1 (IGF-1) levels both prior and during treatment.

Acknowledgements

We are thankful to the patient and his family for allowance to publish this case.

Declarations

Funding

The authors declare that the study received no funding.

Author contributions

Conceptualization, T.T.P.; Writing – Original Draft Preparation, T.T.P.; Writing – Review & Editing, T.T.P. and N.Y.Y.; Visualization, T.T.P.; Supervision, N.Y.Y.

Conflicts of interest

Both authors declare that there is no potential conflict of interest.

Data availability

All data during this study are included in this published article.

Ethics approval

The study was conducted following the regulations of the Hospital and Medical University – Sofia, as well as General Data Protection Regulation (GDPR). Written informed consent was obtained from the parent of the patient for publication of this article and any accompanying images.

References

1. Patton MA, Hurst J, Donnai D, McKeown CM, Cole T, Goodship J. Floating-Harbor syndrome. *J Med Genet*. 1991;28(3):201. doi:10.1136/jmg.28.3.201
2. Turkunova ME, Barbitoff YA, Serebryakova EA, et al. Molecular Genetics and Pathogenesis of the Floating Harbor Syndrome: Case Report of Long-Term Growth Hormone Treatment and a Literature Review. *Front Genet*. 2022;13:846101. doi:10.3389/fgene.2022.846101
3. Lacombe D, Patton MA, Elleau C, Battin J. Floating-Harbor syndrome: description of a further patient, review of the literature, and suggestion of autosomal dominant inheritance. *Eur J Pediatr*. 1995;154(8):658-661. doi:10.1007/BF02079072
4. Nikkel SM, Dauber A, De Munnik S, et al. The phenotype of Floating-Harbor syndrome: clinical characterization of 52 individuals with mutations in exon 34 of SRCAP. *Orphanet J Rare Dis*. 2013;8:63. doi:10.1186/1750-1172-8-63
5. Wieczorek D, Wüsthof A, Harms E, Meinecke P. Floating--Harbor syndrome in two unrelated girls: mild short stature in one patient and effective growth hormone therapy in the other. *Am J Med Genet*. 2001;104(1):47-52. doi:10.1002/ajmg.1585
6. Cannavò S, Bartolone L, Lapa D, et al. Abnormalities of GH secretion in a young girl with Floating-Harbor syndrome. *J Endocrinol Invest*. 2002;25(1):58-64. doi:10.1007/BF03343962
7. Stagi S, Galluzzi F, Bindi G, et al. Precocious puberty in a girl with Floating-Harbor syndrome. *J Pediatr Endocrinol Metab*. 2007;20(12):1333-1338. doi:10.1515/JPEM.2007.20.12.1333
8. White SM, Morgan A, Da Costa A, et al. The phenotype of Floating-Harbor syndrome in 10 patients. *Am J Med Genet A*. 2010;152(4):821-829. doi:10.1002/ajmg.a.33294
9. Galli-Tsinopoulou A, Kyrgios I, Emmanouilidou E, et al. Growth hormone deficiency: an unusual presentation of Floating-Harbor syndrome. *Hormones (Athens)*. 2011;10(3):236-240. doi:10.14310/horm.2002.1314

10. García RJ, Kant SG, Wit JM, Mericq V. Clinical and genetic characteristics and effects of long-term growth hormone therapy in a girl with Floating-Harbor syndrome. *J Pediatr Endocrinol Metab.* 2012;25(1-2):207-212. doi:10.1515/jpem.2011.406
11. Seifert W, Meinecke P, Krüger G, et al. Expanded spectrum of exon 33 and 34 mutations in SRCAP and follow-up in patients with Floating-Harbor syndrome. *BMC Med Genet.* 2014;15:127. doi:10.1186/s12881-014-0127-0
12. Nagasaki K, Asami T, Sato H, et al. Long-term follow--up study for a patient with Floating-Harbor syndrome due to a hotspot SRCAP mutation. *Am J Med Genet A.* 2014;164(3):731-735. doi:10.1002/ajmg.a.36314
13. Zhang S, Chen S, Qin H, et al. Novel genotypes and phenotypes among Chinese patients with Floating-Harbor syndrome. *Orphanet J Rare Dis.* 2019;14(1):144. doi:10.1186/s13023-019-1111-8
14. Homma TK, Freire BL, Honjo R, et al. Growth and clinical characteristics of children with Floating-Harbor syndrome: analysis of current original data and a review of the literature. *Horm Res Paediatr.* 2020;92(2):115-123. doi:10.1159/000503782
15. Son HW, Lee JE, Oh SH, Keum C, Chung WY. Effects of long-term growth hormone therapy in a girl with Floating-Harbor syndrome. *Ann Pediatr Endocrinol Metab.* 2020;25(2):126-131. doi:10.6065/apem.1938144.072
16. Bo H, Jiang L, Zheng J, Sun J. Floating-Harbor Syndrome treated with recombinant human growth hormone: a case report and literature review. *Front Pediatr.* 2021;9:747353. doi:10.3389/fped.2021.747353
17. Prosvirnina A, Bolmasova A, Melikyan M. A case of a Floating-Harbor syndrome in a child with severe short stature. *Horm Res Paediatr.* 2021;94(1):343.
18. Yang YC, Tang Q, Yan LJ, et al. A case of Floating-Harbor Syndrome with "growth and language development delay" as its clinical manifestation. *Pharmacogenomics Pers Med.* 2023;16:1091-1096. doi:10.2147/PGPM.S433444
19. Jeon J, Noh ES, Hwang IT. Floating-Harbor Syndrome in a Korean patient with short stature and early puberty: a case report. *J Clin Res Pediatr Endocrinol.* 2024. doi:10.4274/jcrpe.galenos.2024.2023-12-12
20. He Q, Deng Y, Xu L, et al. Recombinant human growth hormone treatment of Floating-Harbor syndrome: a case report and literature review. *BMC Pediatr.* 2025;25:97. doi:10.1186/s12887-025-05437-7

Rzeszów University Press 2025
ISSN 2544-1361 (online)
doi: 10.15584/ejcem.2026.1.27

http://www.ejcem.ur.edu.pl
European Journal of Clinical and Experimental Medicine
Eur J Clin Exp Med 2026; 24 (1): 234–235

LETTER TO THE EDITOR

Commentary on the use of D-dimer as a biomarker in chronic obstructive pulmonary disease

Sanjay Gabhale , Rishi Govind Orakkan

Department of Respiratory Medicine, Dr. D. Y. Patil Medical College, Hospital & Research Centre, Pimpri, Pune, Dr. D. Y. Patil Vidyapeeth, Pimpri, Pune (Deemed to be University), India

Dear Editor,

We read with great interest the article, "D-dimer as a potential biomarker in chronic obstructive pulmonary disease" by Patel et al.[1] published in the *European Journal of Clinical and Experimental Medicine*. Although the study explores a relevant clinical question, several methodological and interpretational issues merit consideration.

Methodological issues

The study aimed to evaluate D-dimer for COPD diagnosis and outcome prediction, yet no measures of diagnostic accuracy such as sensitivity, specificity, predictive values, or ROC analysis were reported. Given its cross-sectional design, the study is also not suitable for assessing prognostic outcomes.

The inclusion criteria specify "known cases of COPD", but the control group is not adequately described. It is unclear whether the 54 controls were COPD cases in remission or non-COPD subjects, and the rationale for their selection is not explained. Furthermore, several conditions that can increase D-dimer such as trauma, immobilization, cardiovascular disease, uncontrolled diabetes, autoimmune disorders, and smoking – were not excluded, raising the possibility of confounding.

GOLD classification inconsistencies

The study was conducted between 2023-2024, when the GOLD 2023 report was the valid guideline. Table 3 presents variable FEV1/FVC cutoffs across stages, which is inconsistent with GOLD 2023 definitions. By definition, GOLD requires FEV1/FVC <0.7 to define obstruction, irrespective of severity.[3] Such deviations may lead to misinterpretation of staging and affect the reliability of results.

Phenotyping issues

The study subdivides COPD into "chronic bronchitis, emphysema, and small airway disease." However, contemporary GOLD recommendations no longer emphasize such classifications, as these represent descriptive phenotypes rather than diagnostic categories.[3] Adhering to current standards may have improved the generalizability and comparability of the findings.

Other remarks

The clinical implications of elevated D-dimer in COPD are not fully discussed. Without addressing potential applications – such as exacerbation risk stratification or prognostic monitoring – the practical relevance of the findings remains uncertain. Additionally, typographical errors and incomplete reporting of control group details (e.g., Table 9) reduce overall clarity.

Corresponding author: Rishi Govind Orakkan, e-mail: rishigovindorakkan@hotmail.com

Received: 10.09.2025 / Accepted: 18.09.2025 / Published: 30.03.2026

Gabhale S, Orakkan RG. Commentary on the use of D-dimer as a biomarker in chronic obstructive pulmonary disease. *Eur J Clin Exp Med.* 2026;24(1):234–235. doi: 10.15584/ejcem.2026.1.27.

In conclusion, although the authors highlight an interesting association, limitations in study design, unclear control group definition, inconsistencies with GOLD classification, and reliance on outdated phenotypic categories restrict the clinical utility of the findings. At present, evidence does not justify the use of D-dimer for COPD diagnosis or phenotypic classification without further prospective validation in well-designed studies.

Declarations

Funding
The authors declare that no funding was received for the preparation of this letter to the editor.

Author contributions
Conceptualization: S.G. and G.O.; Methodology: S.G.; Software: R.G.O. Validation: S.G. and R.G.O.; Formal Analysis: S.G.; Investigation: R.G.O.; Resources: S.G.; Data Curation: S.G.; Writing – Original Draft Preparation: R.G.O.; Writing – Review and Editing: S.G.; Visualization: S.G.; Supervision: Dr. S.G.; Project Administration: R.G.O.

Conflicts of interest
The authors declare that there are no conflicts of interest related to this letter to the editor.

Data availability
No new data were generated or analyzed in support of this letter to the editor.

Ethics approval
Ethical approval was not required for this 'Letter to the Editor', as it does not involve any new research on human or animal subjects.

References

1. Patel AV, Sharma V, Maheshwari P, et al. D-dimer as a potential biomarker in chronic obstructive pulmonary disease. *Eur J Clin Exp Med*. 2025;23(2):408-414. doi:10.15584/ejcem.2025.2.20
2. Killeen RB, Kok SJ. D-dimer test. In: StatPearls [Internet]. Treasure Island (FL): StatPearls Publishing; January 2025. Updated June 22, 2025. Accessed September 10, 2025. https://www.ncbi.nlm.nih.gov/books/NBK431064/. Accessed September 10, 2025
3. Agustí A, Celli BR, Criner GJ, et al. Global Initiative for Chronic Obstructive Lung Disease 2023 Report: GOLD Executive Summary. *Arch Bronconeumol*. 2023;59(4):232-248. doi:10.1016/j.arbres.2023.02.009

Rzeszów University Press 2026
ISSN 2544-1361 (online)

http://www.ejcem.ur.edu.pl
European Journal of Clinical and Experimental Medicine
Eur J Clin Exp Med 2026; 24 (1): 236–247

Instructions for Authors

About the Journal

The European Journal of Clinical and Experimental Medicine (Eur J Clin Exp Med) is an open access journal, and all articles are free to access, download, share, and re-use. The Eur J Clin Exp Med is a peer-reviewed, scientific journal that publishes full-length articles on topics within medical science. The journal welcomes submissions of articles on current advances in life and health sciences, clinical and experimental medicine, and related disciplines.

Publication frequency

The Eur J Clin Exp Med publishes four issues per year with online-first publication. All accepted articles are published online promptly after completion of editorial production and subsequently assigned to an issue. The journal ensures regular publication according to the announced schedule.

Editorial structure and independence

The journal is led by the Editor-in-Chief and supported by an international Editorial Board and Scientific Advisory Board. Editorial decisions are based solely on the scientific merit of submissions and are independent of the publisher, sponsors, and institutional affiliations. Editorial roles and responsibilities are defined and publicly available on the journal website.

Open access and creative commons

Our open access policy is in accordance with the Budapest Open Access Initiative *(BOAI)* definition: this means that articles have free availability on the public Internet, permitting any users to read, download, copy, distribute, print, search, or link to the full texts of these articles, crawl them for indexing, pass them as data to software, or use them for any other lawful purpose, without financial, legal, or technical barriers other than those inseparable from having access to the Internet itself.

All articles are published with **free** open access under the CC-BY Creative Commons attribution license (the current version is *CC-BY,* ***version 4.0***). If you submit your paper for publication by the Eur J Clin Exp Med, you agree to have the CC-BY license applied to your work. Under this Open Access license, you, as the author, agree that anyone may download and read the paper for free. In addition, the article may be reused and quoted provided that the original published version is cited. This facilitates freedom in re-use and also ensures that Eur J Clin Exp Med content can be mined without barriers for the research needs.

All published articles include a clear license statement (CC BY 4.0) within the full text and PDF versions to ensure transparency, reuse, and machine-readable indexing. The CC BY 4.0 license applies to the article content except where otherwise indicated for third-party material.

Article processing charges

The Eur J Clin Exp Med is an open access journal and does not levy any article processing charges. There are no submission, color, or page charges for any article type.

Copyright statement

Authors of articles published in the Eur J Clin Exp Med retain copyright on their articles, except for any third-party images and other materials added by the Eur J Clin Exp Med which are subject to copyright of their respective owners. Authors are therefore free to disseminate and re-publish their articles, subject to any requirements of third-party copyright owners and subject to the original publication being fully cited. Visitors may also download and forward articles subject to the citation requirements. The ability to copy, download, forward or otherwise distribute any materials is always subject to any copyright notices displayed. Copyright notices must be displayed prominently and may not be obliterated, deleted or hidden, totally or partially.

Authors warrant that they hold the necessary rights to all content submitted for publication, including fig-

ures, tables, and supplementary materials, and that any required permissions have been obtained prior to submission. Any breach of copyright or licensing terms may result in editorial action, including rejection, correction, or retraction of the article.

Ethics in publishing

The Eur J Clin Exp Med is committed to rigorous peer review and strict ethical policies to ensure the publication of high-quality scientific work. Cases of plagiarism, data fabrication and falsification, inappropriate authorship practices, and other forms of publication misconduct may occur and are treated with utmost seriousness. The journal applies a zero-tolerance policy toward confirmed cases of ethical misconduct.

The Eur J Clin Exp Med is a member of and subscribes to the principles of the *Committee on Publication Ethics* ***(COPE)***. The journal uses plagiarism detection software, and by submitting a manuscript authors agree that their work may be screened for plagiarism against previously published content.

Handling complaints and allegations of misconduct

The journal follows COPE guidance for handling allegations of misconduct (e.g., plagiarism, data fabrication/falsification, unethical research, authorship manipulation, peer-review manipulation). Allegations may be reported to the Editorial Office. The Editor-in-Chief (or a delegated editor without conflicts of interest) will conduct an initial assessment and, when appropriate, request explanations and original data from authors, consult independent experts, and/or contact the authors' institutions. If concerns are substantiated, the journal may issue an Expression of Concern, Correction, or Retraction. All investigations are documented and handled confidentially.

Changes to authorship

Authors are expected to consider carefully the list and order of authors before submitting their manuscript and provide the definitive list of authors at the time of the original submission. Any addition, deletion or rearrangement of author names in the authorship list should be made only before a final acceptance decision, and only if approved by the journal Editor. To request such a change, the Editor must receive the following from the corresponding author: (a) the reason for the change in author list and (b) written confirmation (e-mail, letter) from all authors that they agree with the addition, removal or rearrangement. In the case of addition or removal of authors, this includes confirmation from the author being added or removed. Authorship change requests may pause editorial processing and will be evaluated to prevent inappropriate authorship practices.

After the article has been published, **no changes to the list of authors or the order of authorship will be permitted** under any circumstances. All authors must approve the final author list before publication.

Clinical trial registration

Clinical trials must comply with all policies related to research involving human subjects. Additionally, the Eur J Clin Exp Med adheres to the guidelines set by the *International Committee of Medical Journal Editors (ICMJE)*, which mandate the registration of clinical trials in a public trials registry prior to or at the time of the first patient enrollment as a prerequisite for publication consideration. The ICMJE defines a clinical trial as any research study that prospectively assigns individuals or groups to an intervention, with or without a concurrent control or comparison group, to examine the association between a health-related intervention and an outcome. Consequently, the term "clinical trial" extends beyond hospital-based studies or pharmaceutical research to include all investigations involving participant randomization and group classification in relation to the intervention being evaluated.

Authors must pre-register clinical trials in an internationally recognized clinical trials registry. Suitable databases include *ClinicalTrials.gov*, the *EU Clinical Trials Register*, and registries listed by the *World Health Organization's International Clinical Trials Registry Platform*. The registry name, trial registration number, and registration date must be stated in the Institutional Review Board (IRB) statement or the methods section of the manuscript. Purely observational studies (e.g., cohort studies, cross-sectional studies, and case–control studies) are exempt from registration requirements. However, in exceptional cases, editors may consider submissions without prior trial registration. If an exception is granted, authors must retrospectively register the trial and clearly specify the registration date and justification for the delayed registration within the methods section.

Approval from an independent local, regional, or national ethics review body does not substitute for prospective clinical trial registration. The journal reserves the right to reject manuscripts that lack appropriate trial registration. For systematic reviews, prospective protocol registration (e.g., PROSPERO) is strongly encouraged and should be reported in the Methods section. For other study types, preregistration is recommended when applicable.

Randomized clinical trial reporting guidelines

In addition to clinical trial registration, authors reporting results from randomized clinical trials must submit a completed *CONSORT 2010 checklist* and ***flow diagram*** as part of the manuscript submission. Templates for these documents are available on the *CONSORT website*, which

also provides extensions for various study designs and data types beyond two-group parallel trials. At a minimum, clinical trial reports must address all relevant items from the checklist and include a completed flow diagram.

Editorial and submission policies

When you submit a manuscript to the Eur J Clin Exp Med, we will take it to imply that the manuscript has not already been published or submitted elsewhere. If similar or related work has been published or submitted elsewhere, then you must provide a copy of this work with the submitted manuscript. You may not submit your manuscript elsewhere while it is under consideration in the Eur J Clin Exp Med. If the manuscript includes personal communications, please provide a written statement of permission from any person who is quoted. Permission by email is acceptable.

We reserve the right to reject a paper even after it has been accepted if it becomes apparent that there are serious problems with its scientific content, or our publishing policies have been violated.

Author responsibilities

Authorship provides credit for a researcher's contributions to a study and carries accountability. Authors are expected to fulfill the criteria below (adapted from McNutt et al., Proceedings of the National Academy of Sciences, 2018, 201715374; DOI: 10.1073/pnas.1715374115):

— Each author is expected to have made substantial contributions to the conception or design of the work; or the acquisition, analysis, or interpretation of data; or the creation of new software used in the work; or have drafted the work or substantively revised it
— AND to have approved the submitted version (and any substantially modified version that involves the author's contribution to the study);
— AND to have agreed both to be personally accountable for the author's own contributions and to ensure that questions related to the accuracy or integrity of any part of the work, even ones in which the author was not personally involved, are appropriately investigated, resolved, and the resolution documented in the literature.

The Eur J Clin Exp Med does not require all authors of a research paper to sign the cover letter upon submission, nor do they impose an order on the list of authors. Submission to the Eur J Clin Exp Med is taken by the publication to mean that all the listed authors have agreed to all of the contents. The corresponding (submitting) author is responsible for having ensured that this agreement has been reached, and for managing all communication between the publication and all co-authors, before and after publication.

Author contributions statements

Authors are required to include a statement of responsibility in the manuscript (at the end of the main text, before the 'References' section) that specifies the contribution of every author. For articles with several authors, a short paragraph specifying their individual contributions must be provided. The following statements should be used: "Conceptualization, X.X. and Y.Y.; Methodology, X.X.; Software, X.X.; Validation, X.X., Y.Y. and Z.Z.; Formal Analysis, X.X.; Investigation, X.X.; Resources, X.X.; Data Curation, X.X.; Writing – Original Draft Preparation, X.X.; Writing – Review & Editing, X.X.; Visualization, X.X.; Supervision, X.X.; Project Administration, X.X.; Funding Acquisition, Y.Y."

Corresponding author – responsibilities

The corresponding (submitting) author is solely responsible for communicating with the Eur J Clin Exp Med and for managing communication between co-authors. Before submission, the corresponding author ensures that all authors are included in the author list, its order has been agreed by all authors, and that all authors are aware that the paper was submitted.

A confidential process

The Eur J Clin Exp Med treats the submitted manuscript and all communication with authors and referees as confidential, although reviewers are aware of the authors' identities as part of the single-blind peer review process. Authors must also treat communication with the Eur J Clin Exp Med as confidential: correspondence with the Eur J Clin Exp Med, referee reports and other confidential material must not be posted on any website or otherwise publicized without prior permission from the Eur J Clin Exp Med publishing team, regardless of whether or not the submission is eventually published. Our policies about posting preprints and accepted manuscripts, and about previous communication of the work at conferences or as part of a personal blog or of an academic thesis, are described in the journal's Archiving policy. This confidentiality requirement does not restrict authors from sharing their own work as preprints or accepted manuscripts in accordance with the journal's Archiving policy.

Referee suggestions

During the submission process, please suggest three potential reviewers (names and institutional e-mail addresses) with the appropriate expertise to review the manuscript, but please keep in mind that we are not obliged to follow these recommendations. The proposed referees should neither be current collaborators of the co-authors nor have published with any of the co-authors of the manuscript within the last five years. Proposed reviewers should be from different institutions to the authors. You may suggest reviewers

from among the authors that you frequently cite in your paper. You may also name a limited number of scientists who should not review your paper (up to 3 named individuals or laboratories); these exclusions will be honored. The journal verifies reviewer identity and affiliation; the use of non-institutional e-mail addresses for suggested reviewers may be declined. The decision of the Editorial Board Member on the choice of referees is final.

Ethics, use of experimental animals, and human participants

For articles in the Eur J Clin Exp Med reporting experiments on live vertebrates and/or higher invertebrates, the methods section must include a statement: (i) identifying the institutional and/or licensing committee approving the experiments, including any relevant details; (ii) confirming that all experiments were performed in accordance with relevant guidelines and regulations. The ethics statement must include the name of the approving ethics committee, approval or decision number, and date of approval; studies involving human participants must confirm compliance with the Declaration of Helsinki, and animal studies must comply with the ARRIVE guidelines and the principles of the 3Rs (Replacement, Reduction, Refinement).

For research involving human participants, authors must identify the committee that approved the research, confirm that all research was performed in accordance with relevant guidelines/regulations, and include in their manuscript a statement confirming that informed consent was obtained from all participants and/or their legal guardians. Authors may be required to submit, on request, a statement from the research ethics committee or institutional review board indicating approval of the research.

Competing interests policy

In the interests of transparency and to help readers form their own judgments of potential bias, authors must declare any competing financial and/or non-financial interests related to the work described. Competing interests are defined as financial or non-financial relationships or circumstances that could directly influence, or be perceived to influence, the objectivity, integrity, or interpretation of the reported research.

Examples of potential competing interests include, but are not limited to, employment, consultancies, stock ownership or options, honoraria, paid expert testimony, patents or patent applications, and other personal or institutional relationships. Sources of research funding must be disclosed separately in the Funding statement, regardless of whether they are considered a competing interest.

Competing interests statement format guidelines

The statement included in the article file must be explicit and unambiguous, describing any potential competing interest (or lack thereof) for EACH contributing author.

Examples of declarations are:

— Competing interests: The author(s) declare no competing interests.

— Competing interests: Dr X's work has been funded by A. He has received compensation as a member of the scientific advisory board of B and owns stock in the company. He has also consulted for C and received compensation. Dr Y and Dr Z declare no competing interests.

Funding information must be reported in a separate Funding statement and should not be included in the Competing interests declaration.

Application to Editors or Editorial Board Members

Editors and Editorial Board Members of the *Eur J Clin Exp Med* are required to disclose any conflicts of interest and may be excluded from the peer review process if such conflicts exist. They should also recuse themselves from handling manuscripts where a conflict of interest is present. This may include, but is not limited to, having previously co-published with one or more of the authors or being affiliated with the same institution as one or more of the authors.

If an Editor or Editorial Board Member of Eur J Clin Exp Med is listed as an author on a manuscript, it is recommended that they declare this in the competing interests section of the submission. If they are an author or have any other conflict of interest regarding a specific manuscript, another editor will be assigned to oversee the peer review process. These submissions will undergo the same review process as any other manuscript.

Editors and Editorial Board Members of Eur J Clin Exp Med are welcome to submit their own papers to the journal. These submissions receive no special priority, and the status of the Editor or Editorial Board Member does not influence the editorial consideration.

Peer-reviewers

The Eur J Clin Exp Med invites peer-reviewers to exclude themselves in cases where there is a significant conflict of interest, financial or otherwise. However, just as financial interests need not invalidate the conclusions of an article, nor do they automatically disqualify an individual from evaluating it. We ask peer-reviewers to inform the editors of any related interests, including financial interests as defined above that might be perceived as relevant. Editors will consider these statements when weighing peer-reviewers' recommendations.

Availability of materials and data

In order to maintain the integrity, transparency, and reproducibility of research records, authors are encouraged to make their experimental and research data openly available either by depositing data in repositories or by publishing the data and files as supplementary information in this journal. The journal may request access to underlying data, protocols, or original materials for editorial assessment. Where data cannot be publicly shared due to privacy, ethical, or legal restrictions, authors must describe the restrictions and provide a mechanism for qualified access where feasible.

Data may be deposited with specialized service providers or institutional/subject repositories, preferably those that use the DataCite mechanism. Large datasets and files greater than 60 MB must be deposited in this way. For a list of other repositories specialized in scientific and experimental data, please consult re3data.org and DataCite resources. The data repository name, link to the dataset (URL) and accession number, DOI or handle number of the dataset must be provided in the paper. The journal Data also accepts submissions of dataset papers.

Data availability statement format guidelines

The statement should be provided as a separate section (titled 'Data Availability') at the end of the main text, before the 'References' section. Data availability statements should include, where applicable, accession codes, other unique identifiers and associated web links for publicly available datasets, and any conditions for access of non-publicly available datasets. Where figure source data are provided, statements confirming this should be included in data availability statements. Depending on the data described in the manuscript, data availability statements commonly take one of the following forms, or can be a composite of the statements below:

— The datasets generated during and/or analyzed during the current study are available in the [NAME] repository, [PERSISTENT WEB LINK TO DATASETS].
— The datasets generated during and/or analyzed during the current study are available from the corresponding author on reasonable request.
— All data generated or analyzed during this study are included in this published article (and its Supplementary Information files).
— The datasets generated during and/or analyzed during the current study are not publicly available due to [REASON(S) WHY DATA ARE NOT PUBLIC] but are available from the corresponding author on reasonable request.
— No datasets were generated or analyzed during the current study.
— The data that support the findings of this study are available from [THIRD PARTY NAME] but restrictions apply to the availability of these data, which were used under license for the current study, and so are not publicly available. Data are however available from the authors upon reasonable request and with permission of [THIRD PARTY NAME].

Declaration of use of AI and AI-assisted technologies in the writing process

Authors are required to disclose the use of generative AI in the writing of scientific papers upon submission. This guidance applies solely to the writing process and does not pertain to the use of AI tools for data analysis or drawing insights as part of the research process.

Generative AI and AI-assisted technologies should be used in the writing process solely to enhance the readability and language of the manuscript. These tools must be employed under human supervision, with authors thoroughly reviewing and editing the output, as AI can produce seemingly credible content that may be inaccurate, incomplete, or biased. Ultimately, authors are responsible and accountable for the content of the work.

Authors should not list generative AI and AI-assisted technologies as an author or co-author, nor cite AI as an author. Authorship entails responsibilities and tasks that can solely be assigned to and carried out by humans.

The Eur J Clin Exp Med does not allow the use of generative AI or AI-assisted tools to create or modify images in submitted manuscripts. This includes activities such as enhancing, obscuring, moving, removing, or introducing specific elements within an image or figure. Adjustments to brightness, contrast, or color balance are permitted as long as they do not obscure or remove any information present in the original. Image forensics tools or specialized software may be used to detect suspected irregularities in images within submitted manuscripts. Authors must not upload confidential, personal, or patient-identifiable information to generative AI tools.

The only exception to this policy is when AI or AI-assisted tools are integral to the research design or methods, such as in AI-assisted imaging approaches used to generate or interpret the underlying research data, particularly in fields like biomedical imaging. In such cases, the use of AI must be described in a reproducible manner within the methods section. This description should include details on how the AI or AI-assisted tools were applied in the image creation or alteration process, along with the name of the model or tool, version and extension numbers, and the manufacturer.

Authors must follow the AI software's specific usage policies and ensure proper content attribution. When applicable, authors may be required to provide pre-AI-adjusted versions of images and/or the composite raw images used to produce the final submitted versions for editorial assessment.

The use of generative AI and AI-assisted technologies in scientific writing should be disclosed by including a statement at the end of the manuscript when it is initially submitted.

— Title of new section: Use of AI and AI-assisted technologies in the writing process.
— Example of a statement: "During the preparation of this work the author(s) used [NAME TOOL/SERVICE] in order to [REASON]. After using this tool/service, the author(s) reviewed and edited the content as needed and take(s) full responsibility for the content of the published article."

The declaration does not apply to the use of basic tools, such as those used for checking grammar, spelling, and references. If there is nothing to disclose, no statement is required.

NOTE: to protect authors' rights and the confidentiality of their research, the Eur J Clin Exp Med does not currently allow the use of Generative AI or AI-assisted technologies such as ChatGPT or similar services by reviewers or editors in the peer review and manuscript evaluation process. Suspected breaches may result in reviewer removal and rejection of the manuscript or other editorial actions. Moreover, editors may decline to move forward with manuscripts if AI is used inappropriately.

Correction and retraction policy

The Eur J Clin Exp Med operates the following policy for making corrections to its peer-reviewed content.

Publishable amendments must be represented by a formal online notice because they affect the publication record and/or the scientific accuracy of published information. Where these amendments concern peer-reviewed material, they fall into one of four categories: Publisher Correction (formerly Erratum), Author Correction (formerly Corrigendum), Retraction or Addendum.

Publisher Correction (formerly Erratum). Notification of an important error made by the journal that affects the publication record or the scientific integrity of the paper or the reputation of the authors or the journal.

Author Correction (formerly Corrigendum). Notification of an important error made by the author(s) that affects the publication record or the scientific integrity of the paper, or the reputation of the authors or the journal.

Retraction. Notification of invalid results. All co-authors must sign a Retraction specifying the error and stating briefly how the conclusions are affected, and submit it for publication. In cases where co-authors disagree, the in-house editors may seek advice from independent referees and impose the type of amendment that seems most appropriate, noting the dissenting author(s) in the text of the published version.

Addendum. Notification of additional information. Addenda are published when the in-house editors decide that the addendum is crucial to the reader's understanding of a significant part of the published contribution.

Expression of Concern. A notice issued when serious concerns have been raised about a publication, but an investigation is ongoing and conclusive evidence is not yet available.

Corrections, retractions, and expressions of concern are published as separate notices and are permanently linked to the original article. The online article and PDF are clearly labeled to reflect the amendment status.

Archiving policy

Articles published in Eur J Clin Exp Med are long-term deposited in the repository of the University of Rzeszów. Authors of articles are permitted to self-archive the submitted (preprint) version of the article at any time, and may self-archive the accepted (peer-reviewed) version. The authors may also deposit the published version of the article. On submission of the manuscript, authors may deposit the submitted version in their personal, institutional, or online preprint repository. The first page of the manuscript must clearly display the following wording: *"This paper is a preprint of a paper submitted to European Journal of Clinical and Experimental Medicine (ISSN: 2544-1361)"*. If the paper is rejected, authors must remove all mention of the journal.

The author may deposit the accepted manuscript of the paper (accepted version of the manuscript after peer-review and content amendments, but before copyediting, typesetting and proof correction) to the author's personal website, provided that it is non-commercial, and to the repository of the author's institution with acknowledgement of the Journal (acknowledgement should be made as follows: *"This is an accepted peer-reviewed version of the paper. The published version of the article is available at European Journal of Clinical and Experimental Medicine (ISSN: 2544-1361), at https://doi.org/[DOI of the article]"*.

Published version of an open-access article. The author may deposit the published version of the paper (final edited and typeset version that is made publicly available by the Publisher and can be considered an article) to any institutional repository, and distribute and make it publicly available in any way with acknowledgement to the Journal (acknowledgement should be made as follows: *"This is a published version of the paper, available at European Journal of Clinical and Experimental Medicine (ISSN: 2544-1361), at https://doi.org/[DOI of the article]"*.

The journal ensures long-term digital preservation of the version of record through institutional repository archiving and persistent identifiers (DOIs).

Preprint policy

The Eur J Clin Exp Med permits the posting of manuscripts on recognized preprint servers prior to submission

or during the peer review process. Authors must disclose the existence of any preprint version at the time of submission and provide the preprint DOI or URL.
Preprints are not considered peer-reviewed publications and must not be cited as references in manuscripts submitted to the Eur J Clin Exp Med.
Following publication in the journal, authors are encouraged to update the preprint record by providing a clear link to the final published version of record (VoR), including the article DOI.

Sponsorship and advertising

As part of its publication policies, the Eur J Clin Exp Med does not accept commercial sponsorships or advertisements. However, the journal may post announcements on its website for non-profit scientific and educational events.

Peer-review process

Initial checks

Once submitted, your manuscript will be assigned to a member of our Editorial Board, who will read the paper and decide whether it is appropriate for the journal. Manuscripts that are within scope and seem, on initial assessment, to be technically sound and scientifically valid, will be sent to external reviewers. Copies of any papers containing similar or related work under consideration or in press at other journals must be included with the submission.
Manuscripts that do not fit the journal's ethics policy or do not meet the standards of the journal will be rejected before peer-review. Manuscripts may be rejected at the editorial screening stage due to: out-of-scope content, insufficient novelty or methodological rigor, ethical concerns, suspected misconduct, poor reporting quality, or failure to comply with author guidelines. Manuscripts that are not properly prepared will be returned to the authors for revision and resubmission.

Peer review

Once a manuscript passes the initial checks, it is assigned to at least two independent experts for peer review. The reviewers access the manuscript securely through our online system. The Eur J Clin Exp Med applies a single-blind peer review process, in which the reviewers are aware of the authors' identities, but the authors do not know the identity of the reviewers.
Reviewers are selected by the editorial team based on their subject expertise and the absence of any conflict of interest with the authors or the submitted work. Suggested reviewers must not have co-authored publications with the authors in the last five years or be affiliated with the same institutions.
All peer review comments are treated as confidential and will only be disclosed with the explicit consent of the reviewer. Reviewers are expected to evaluate manuscripts objectively, fairly, and constructively, and to refrain from any personal criticism of the authors.

Editorial Decision

After considering the reviewer reports the Editorial Board Member will make one of the following decisions:

— Accept outright,
— Request a minor revision, where authors revise their manuscript to address specific concerns, Request a major revision, where authors revise their manuscript to address significant concerns and perhaps undertake additional work,
— Reject outright.

The final decision is made by the Editor-in-Chief.

Revisions

In cases where the referees or Editorial Board Member has requested changes to the manuscript, you will be invited to prepare a revision. The decision letter will specify a deadline for submission of a revised manuscript. Once resubmitted, the manuscript may then be sent back to the original referees or to new referees, at the Editorial Board Member's discretion.
A revised manuscript should be submitted via the revision link provided in the decision letter, and not as a new manuscript. Authors should attach a cover letter to explain, *point by point*, the details of the revisions to the manuscript and responses to the referees' comments. The destination of the cover letter file in the submission system is 'Supplementary File for Review'. Please ensure that all issues raised have been addressed in the first round of revision. Where the authors disagree with a reviewer, they must provide a clear response. You can use a template for responding to the reviewers' comments

Final submission and acceptance

When all editorial issues are resolved, your paper will be formally accepted for publication. Once accepted, the manuscript will undergo professional copy-editing, English editing, final corrections, pagination, and publication on the https://www.ejcem.ur.edu.pl/. The Eur J Clin Exp Med reserves the right to make the final decision about matters of style and the size of figures.

Appeals

Even in cases where the Eur J Clin Exp Med does not invite resubmission of a manuscript, some authors may ask the Editorial Board to reconsider a rejection decision. These are considered appeals, which, by policy, must take second place to the normal workload. In practice, this means that decisions on appeals often take several weeks. Only one appeal is permitted for each manuscript, and appeals can only take place after peer review. Final

decisions on appeals will be made by the Editorial Board Member handling the paper.
Decisions are reversed on appeal only if the relevant Editorial Board Member is convinced that the original decision was a serious mistake. Consideration of an appeal is merited if a referee made substantial errors of fact or showed evidence of bias, but only if a reversal of that referee's opinion would have changed the original decision. Similarly, disputes on factual issues need not be resolved unless they were critical to the outcome.
If an appeal merits further consideration, the Editorial Board Member may send the authors' response and the revised paper out for further peer review.

ORCID

The Eur J Clin Exp Med supports the use of ORCID. The Eur J Clin Exp Med mandates ORCID iDs for all submitting authors; this is published on the final article to promote discoverability and credit. Please provide the ORCID iDs of the authors in the title page.

Submission guidelines

Submission process
Manuscripts for the Eur J Clin Exp Med should be submitted online at *https://mc04.manuscriptcentral.com/pmur*. The submitting author, who is generally the corresponding author, is responsible for the manuscript during the submission and peer-review process. The submitting author must ensure that all eligible co-authors have been included in the author list (read the criteria to qualify for authorship) and that they have all read and approved the submitted version of the manuscript. To submit your manuscript, register and log in to the submission website. All co-authors can see the manuscript details in the submission system, if they register and log in using the e-mail address provided during manuscript submission.

Cover letter

A cover letter must be included with each manuscript submission. It should be concise and explain why the content of the paper is significant, placing the findings in the context of existing work and why it fits the scope of the journal. Confirm that neither the manuscript nor any parts of its content are currently under consideration or published in another journal. The names of proposed and excluded reviewers should be provided in the submission system, not in the cover letter.

Accepted file formats

Use the Microsoft Word template to prepare your manuscript [**download**]
Authors must use Microsoft Word to prepare their manuscript. LaTeX submissions are not accepted. Please insert your tables, graphics (schemes, figures, etc.) in the main text after the paragraph of its first citation.
In most cases, we do not impose strict limits on word count or page number. However, we strongly recommend that you write concisely and stick to the following guidelines:

— We encourage not exceeding 20 pages for original and review papers, and 8 pages for case reports of standard computer text (1800 characters on a page).
— The main text should be no more than 4,500 words (not including Abstract, References and Figure legends).
— The title should be no more than 20 words.
— The abstract should be no more than 200 words.
— Recommended font: Times New Roman, 12 points.
— Manuscript text should be double-spaced. Do not format text in multiple columns.

Types of publications

Manuscripts submitted to the Eur J Clin Exp Med should neither be published previously nor be under consideration for publication in another journal. The main article types are as follows:
Original research manuscripts. The journal considers all original research manuscripts provided that the work reports scientifically sound experiments and provides a substantial amount of new information.
Reviews. These provide concise and precise updates on the latest progress made in a given area of research. Systematic reviews should follow the PRISMA guidelines.
The Eur J Clin Exp Med accepts also the following types of submissions: case reports, letters to the editor, commentaries, book reviews, and reports from scientific meetings and conferences.

Reporting guidelines

The guidelines listed below should be followed where appropriate. Please use these guidelines to structure your article. Completed applicable checklists, structured abstracts and flow diagrams should be uploaded with your submission.
Please refer to existing guidelines for reporting methodology; e.g.:

— *AGREE guidelines for clinical practice guidelines*
— ARRIVE guidelines for *in vivo* animal studies
— *CARE guidelines for clinical case reports*
— *CONSORT guidelines for clinical trials*
— *PRISMA guidelines for systematic reviews and meta-analyses*
— *SPIRIT for clinical trials*
— *STARD guidelines for studies of diagnostic accuracy*
— *STROBE guidelines for observational studies*

Manuscript preparation

Your paper should consist of the following parts.

Research manuscripts should comprise:

— Title page: Title, Author list, Affiliations.
— Research manuscript sections: Abstract, Keywords, Introduction, Aim, Materials and Methods, Results, Discussion, Conclusions.
— Back matter: Supplementary Materials, Acknowledgments, Funding Statement, Author Contributions, Conflicts of Interest, Data Availability, Ethics Approval, References.

Research manuscript sections:

— *Introduction*

State the objectives of the work and provide an adequate background, avoiding a detailed literature survey or a summary of the results.

— *Materials and methods*

Provide sufficient details to allow the work to be reproduced by an independent researcher. Methods that are already published should be summarized, and indicated by a reference. If quoting directly from a previously published method, use quotation marks and also cite the source. Any modifications to existing methods should also be described.

— *Results*

Results should be clear and concise. The section may be divided into subsections, each with a concise subheading. Tables and figures central to the study should be included in the main paper. Do not use the term "significant" unless p-values are provided. Show p-values to 2 or 3 decimal places. The Results section should be written in past tense.

— *Discussion*

This should explore the significance of the results of the work, not repeat them. Avoid extensive citations and discussion of published literature.

— *Conclusions*

Summarize the work's findings, state their importance, and possibly recommend further research.

Review manuscripts should comprise:

— Title page: Title, Author list, Affiliations.
— Abstract, Keywords, Literature review sections.
— Back matter: Supplementary Materials, Acknowledgments, Funding Statement, Author Contributions, Conflicts of Interest, Data Availability, References.

Structured reviews and meta-analyses should use the same structure as research articles and ensure they conform to the PRISMA guidelines.

Case reports should comprise:

— Title page: Title, Author list, Affiliations.
— Abstract, Keywords. Case reports should include a succinct introduction about the general medical condition or relevant symptoms that will be discussed in the case report; the case presentation including all of the relevant de-identified demographic and descriptive information about the patient(s), and a description of the symptoms, diagnosis, treatment, and outcome; a discussion providing context and any necessary explanation of specific treatment decisions; a conclusion briefly outlining the take-home message and the lessons learned.
— Back matter: Supplementary Materials, Acknowledgments, Funding Statement, Author Contributions, Conflicts of Interest, Data Availability, Ethics Approval, References.

Requirements for case reports submitted to Eur J Clin Exp Med:

— Patient ethnicity must be included in the Abstract under the Case Presentation section.
— Consent for publication is a mandatory journal requirement for all case reports. Written informed consent for publication must be obtained from the patient (or their parent or legal guardian in the case of children under 18, or from the next of kin if the patient has died).

The best way to ensure you have obtained appropriate consent for publication in Eur J Clin Exp Med is to *use our Eur J Clin Exp Med consent form.*

Language style

Manuscripts must be submitted in English (American or British usage is accepted, but not a mixture of these).

Title page

These sections should appear in all manuscript types:

Title: The title of your manuscript should be concise and informative. It should identify if the study reports (human or animal) trial data, or is a systematic review, meta-analysis or replication study. When gene or protein names are included, the abbreviated name rather than full name should be used.

Author List and Affiliations: Authors' full first and last names must be provided. We recommend adding as primary the affiliation where most of the research was conducted or supported, but please check with your institution for any contractual agreement requirements. For each affiliation provide the details in the following order: department, institution, city, country.

It is very important that author names and affiliations are correct. Incorrect information can mean a lack of proper attribution or incorrect citation and can even lead to problems with promotion or funding. After the publication of an article, updates or corrections to the author's address or affiliation may not be permitted.

At least one author should be designated as *corresponding author*, and his or her email address and other details should be included at the end of the affiliation sec-

tion. Please also provide the ORCID iDs of the authors in the title page.

Independent Researcher: If one or all the authors are not currently affiliated with a university, scientific institution or company, or have not been during the development of the manuscript, they should list themselves as an "Independent Researcher".

Abstract

The abstract should be a total of about 200 words maximum. The abstract should be a single paragraph and should follow the style of structured abstracts: *Introduction and aim*: Place the question addressed in a broad context and highlight the purpose of the study; *Materials and methods*: Describe briefly the main methods or treatments applied. Include any relevant preregistration numbers, and species and strains of any animals used. *Results:* Summarize the article's main findings; and *Conclusion*: Indicate the main conclusions or interpretations.

The abstract should not contain any undefined abbreviations or unspecified references.

Keywords

Three to six pertinent keywords need to be added after the abstract in alphabetical order. We recommend that the keywords are specific to the article, yet reasonably common within the subject discipline.

Back Matter

Supplementary materials: Describe any supplementary material published online alongside the manuscript (figure, tables, video, spreadsheets, etc.). Please indicate the name and title of each element as follows Figure S1: title, Table S1: title, etc.

Acknowledgments: Thank all of the people who helped with the research but did not qualify for authorship. Acknowledge anyone who provided intellectual assistance, technical help, or special equipment or materials.

Funding statement: Authors must disclose all sources of funding and the role of the funder(s) in study design, data collection, analysis, interpretation, and manuscript preparation. If the funder had no role, authors should explicitly state this.

Author contributions: Authors must supply an Author Contribution Statement as described in the *Author contributions statements* section

Conflicts of interest: Authors must supply a competing interests statement. For more details please see *Competing interests policy*.

Data availability: Authors must include a Data Availability Statement in all submitted manuscripts; see *Availability of materials and data* section for more information.

Ethics approval: Example of an ethical statement: "All subjects gave their informed consent for inclusion before they participated in the study. The study was conducted in accordance with the Declaration of Helsinki, and the protocol was approved by the Ethics Committee of XXX (Project identification code)."

Use of AI and AI-assisted technologies in the writing process: Example of a statement: "During the preparation of this work the author(s) used [NAME TOOL/SERVICE] in order to [REASON]. After using this tool/service, the author(s) reviewed and edited the content as needed and take(s) full responsibility for the content of the published article."

The declaration does not apply to the use of basic tools, such as those used for checking grammar, spelling, and references. If there is nothing to disclose, no statement is required.

References: References must be numbered in order of appearance in the text (including table captions and figure legends) and listed individually at the end of the manuscript. We recommend preparing the references with a bibliography software package, such as EndNote, Reference Manager or Zotero to avoid typing mistakes and duplicated references.

References style

In-text citations and references should be prepared according to the American Medical Association (AMA) style. Each item should be listed in numerical order.

In-text citations

Each reference should be cited in the text using superscript Arabic numerals. These superscript numbers should be outside periods. If you are citing sequential references, these should be indicated with a hyphen. Nonsequential references should be separated with commas. There should not be a space between numbers.

For example: The degree of respiratory muscles fatigue depends on the applied exercise protocol and the research group's fitness level.[1,2] The greatest load with which a patient continues breathing for at least one minute is a measure of inspiratory muscles strength.[3] Diabetes mellitus is associated with a high risk of foot ulcers.[4-6]

Sample reference

In listed references, the names of all authors should be given unless there are more than 6, in which case the names of the first 3 authors are used, followed by "et al.". If the source does not have any authors, the citation should begin with the title.

To find the proper abbreviation of a journal, go to the National Library of Medicine PubMed Journals Database at *https://www.ncbi.nlm.nih.gov/entrez/query.fcgi?db=Journals.*

Page number(s) should be inserted in full (for example: use 111–112, not 111–2). DOIs should be provided whenever available.

The following are examples of individual citations made according to the required rules of editing and punctuation:

— ***Article from a journal, number of authors from 1 to 6***

Author AA, Author BB, Author CC. Title of article. *Accepted Abbreviated Journal Title*. Year;Volume(Issue):Page-Page. doi (if available)

Lee JC, Seo HG, Lee WH, Kim HC, Han TR, Oh BM. Computer-assisted detection of swallowing difficulty. C*omput Methods Programs Biomed*. 2016;134(2):72-78. doi:10.1016/j.cmpb.2016.07.010

Morris A. New test for diabetes insipidus. *Nat Rev Endocrinol*. 2019;15(10):564-565. doi:10.1038/s41574-019-0247-x

— ***Article from a journal, number of authors more than 6***

Author AA, Author BB, Author CC, et al. Title of article. *Accepted Abbreviated Journal Title*. Year;Volume(Issue):Page-Page. doi (if available)

Gonzalez ME, Martin EE, Anwar T, et al. Mesenchymal stem cell-induced DDR2 mediates stromal-breast cancer interactions and metastasis growth. *Cell Rep*. 2017;18:1215-1228. doi:10.1016/j.celrep.2016.12.079

Jordan J, Toplak H, Grassi G, et al. Joint statement of the European Association for the Study of Obesity and the European Society of Hypertension: obesity and heart failure. *J Hypertens*. 2016;34:1678-1688. doi:10.1097/HJH.0000000000001013

— ***Websites***

Author AA (if indicated). Webpage title. Name of Website. URL. Published or Updated date. Accessed date.

Cholera in Haiti. Centers for Disease Control and Prevention Web site. *https://www.cdc.gov/haiticholera/*. Published October 22, 2010. Updated January 9, 2012. Accessed February 1, 2012.

Address double burden of malnutrition: WHO. World Health Organization site. *https://www.searo.who.int/mediacentre/releases/2016/1636/en/*. Accessed February 2, 2017.

— ***Book***

Author AA, Author BB. *Title of Work*. Location: Publisher; Year:Page-Page

Doane GH, Varcoe C. *Family Nursing as Relational Inquiry: Developing Health– Promoting Practice*. Philadelphia, PA: Lippincott Williams & Wilkins; 2005:25-28.

London ML, Ladewig PW, Ball JW, et al. *Maternal & Child Nursing Care*. Upper Saddle River, NJ: Pearson Education; c2011:101-103.

— ***Chapter in a book***

Chapter Author AA. Title of chapter. In: *Name of Book*. Edition Number. Editor AA, ed. Location: Name of Publisher; Year:Page-Page.

Grimsey E. An overview of the breast and breast cancer. In: *Breast Cancer Nursing Care and Management*. 2nd ed. Harmer V, ed. Chichester, UK: Wiley-Blackwell; 2011:35-42.

— Manuscripts "in press" may be included in the reference list if they have been accepted for publication in a peer-reviewed journal but have not yet been published in their final form, provided they are citable with a DOI (Digital Object Identifier) and the journal name is specified.

— Abstracts: If citing an abstract is necessary because it contains data not published elsewhere, it must be clearly designated as such in both the text and the reference list.

The following sources should not be included in the reference list

— Unpublished observations including personal communications

— Submitted manuscripts and manuscripts in preparation

— Preprints

NOTE: The Editorial Board requires consistent and carefully made references prepared according to the above-mentioned AMA standards. Otherwise, the work will be sent back to the authors.

Preparing Figures, Schemes and Tables

Figures and schemes must be provided during submission in sufficiently high quality (minimum 1000 pixels in either dimension or a resolution of at least 300 dpi). Common file formats are accepted; however, TIFF, JPEG, EPS, and PDF are preferred.

All figures, schemes, and tables must be embedded in the main manuscript file and placed next to the relevant text, not at the beginning or end of the document. Figure captions should be placed directly below the figure (not on the figure itself), and table titles above the table. All figures, schemes, and tables must be numbered consecutively according to their first appearance in the text (Figure 1, Scheme 1, Table 1, etc.) and must be cited in the text in numerical order.

Tables should present new information and must not duplicate content already described in the text. Each table must be understandable independently and include clear and explanatory column headings. Tables must be provided in an editable format and placed in the appropriate location within the manuscript. Tables submitted as image files (e.g., JPEG, TIFF) or as separate files will not be accepted. For large tables, smaller fonts may be used, but not smaller than 8 pt.

All text within figures and tables must be in English and remain clearly legible after reduction.

Any image manipulation that could misrepresent data (e.g., selective enhancement, splicing without disclosure) is prohibited; original/raw images may be requested for

verification. The journal may conduct image integrity checks and request original, unprocessed image files.

Copyright and Permissions

All figures, schemes, and illustrations must be original or legally reusable. Authors are fully responsible for ensuring compliance with copyright regulations. Simple citation of the source (e.g., "Source: [reference]") is not sufficient and does not constitute permission.

Figures reproduced or adapted from previously published works require explicit permission from the copyright holder, unless the original publication is licensed under a Creative Commons license permitting reuse. Reused figures must be clearly labeled in the caption as "Reproduced from" or "Adapted from", include the full reference, and specify the applicable license or confirm that permission has been obtained. Third-party material not covered by CC BY must be clearly indicated in the caption and may require separate permission for reuse.

Submission of identical figures previously published elsewhere without documented permission constitutes a serious breach of publication ethics and may result in rejection at the editorial screening stage.

The Editorial Office reserves the right to request modification, replacement, or removal of any figure, scheme, or table that does not meet technical, ethical, or editorial standards. By submitting a manuscript, authors confirm that all figures, schemes, and tables comply with copyright requirements and that all necessary permissions have been obtained.

Persistent identifiers and metadata

The journal assigns DOIs to all published articles and deposits metadata to support indexing, citation linking, and long-term discoverability. Authors are encouraged to provide ORCID iDs and funder information to ensure accurate attribution.

Abbreviations

The journal requires using only standard abbreviations. Common abbreviations such as DNA and RNA do not require definitions. Abbreviations should be defined in parentheses the first time they appear in the abstract, main text and in figure or table captions and used consistently thereafter. Ensure consistency of abbreviations throughout the article. Use the following abbreviations for measurement units: gram (g), litre (L), milligram (mg), kilogram (kg), seconds (s), minutes (min), and hours (h). Do not add 's' to indicate plural forms of units. Keep abbreviations to a minimum.

SI Units

SI Units (International System of Units) should be used. Imperial, US customary and other units should be converted to SI units whenever possible.